

AD 7 1-90 83

proceedings
of the
nineteenth international
wire and cable
symposium
first - second
and third
of
december
1970
shelburne
hotel
atlantic city
new jersey



SPONSORED BY U. S. ARMY ELECTRONICS COMMAND, FT. MONMOUTH,

19960405 030

REF 16154 - 16164

DISCLAIMER NOTICE



**THIS DOCUMENT IS BEST
QUALITY AVAILABLE. THE
COPY FURNISHED TO DTIC
CONTAINED A SIGNIFICANT
NUMBER OF PAGES WHICH DO
NOT REPRODUCE LEGIBLY.**

**PROCEEDINGS OF
19th INTERNATIONAL WIRE AND CABLE
SYMPOSIUM**

**Sponsored by Industry
and U. S. Army Electronics Command**

**Atlantic City, N. J.
December 1, 2, and 3, 1970**

DTIC QUALITY INSPECTED 1

THIS DOCUMENT HAS BEEN APPROVED FOR PUBLIC RELEASE AND SALE; ITS DISTRIBUTION IS UNLIMITED.

19th INTERNATIONAL WIRE AND CABLE SYMPOSIUM

SYMPOSIUM COMMITTEE

Jack Spergel, Co-Chairman (phone 201-535-1615)
Milton Tenzer, Co-Chairman (phone 201-535-1834)
Ferris Scoville, Assistant to Co-Chairman (phone 201-535-1934)
U. S. Army Electronics Command
ATTN: AMSEL-KL-EE
Fort Monmouth, New Jersey 07703
Frank Horn, Bell Telephone Laboratories
Jules Ruskin, Phillips Cables, Ltd.
Gerald A. Lohsl, Rural Electrification Administration
Fred M. Oberlander, RCA Corporation
Michael M. Suba, Union Carbide Corp.
E. Mark Wolf, Anaconda Wire and Cable Co.
Dan F. Stewart, Phillips Petroleum Co.

TECHNICAL SESSIONS

Tuesday, 1 December 1970

2:15 p.m. Session I — Panel Discussion on Flat Cable Design Characteristics and Fabricating Techniques

8:00 p.m. Informal Seminar on Flat Cable and Connectors

Wednesday, 2 December 1970

9:15 a.m. Session II — Cables, Conductors and Terminating Techniques

2:15 p.m. Session III — Multi-Pair and Coaxial Cable Characteristics

Thursday, 3 December 1970

9:15 a.m. Session IV — Wire and Cable Materials

2:15 p.m. Session V — Cable Manufacturing and Testing Techniques

PROCEEDINGS

Responsibility for the contents rests upon the authors and not the Symposium Committee or its members. After the symposium all the publication rights of each paper are reserved by their authors, and requests for republication of a paper should be addressed to the appropriate author. Abstracting is permitted, and it would be appreciated if the symposium is credited when abstracts or papers are republished. Requests for individual copies of papers should be addressed to the authors. Extra copies of the Proceedings may be obtained from the Symposium Co-Chairman (Requests should include a check for \$4.00 per copy made payable to the Shelburne Hotel). Copies may also be obtained for a nominal fee from the U. S. Department of Commerce, Clearinghouse for Federal Scientific and Technical Information, 2585 Port Royal Road, Springfield, Virginia 22151.

Copies of papers presented in previous years may also be obtained from the Clearinghouse. Papers from the first 15 years with their AD numbers are cataloged in the "KWIC Index of Technical Papers, Wire and Cable Symposia (1952-1966)," November 1967, AD-661308.

Highlights of 18th International Wire and Cable Symposium

3, 4, and 5 December 1969

Shelburne Hotel, Atlantic City, N. J.



AWARD FOR BEST TECHNICAL PAPER: H. Lubars and J. A. Olszewski, General Cable Co., receiving plaques from M. Tenzer for their outstanding paper entitled, "Analysis of Structural Return Loss in CATV Coaxial Cable," at the 17th IWCS.



AWARD FOR BEST PRESENTATION OF TECHNICAL PAPER: N. Dean, B.I.C.C., receiving plaque from M. Tenzer for best presentation of a significant technical paper entitled, "The Development of Fully Filled Cables for the Telephone Distribution Network," at the 17th IWCS.



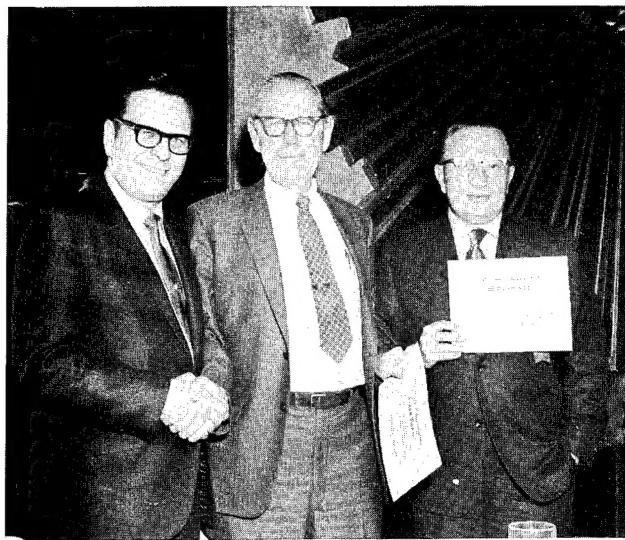
W. L. Doxey, Director of USAECOM R&D Directorate, delivering his address at the banquet.



Claude Buster, REA, delivering his keynote speech on "A Challenge and a Blueprint for a Total Telecommunications System."



Certificates of Appreciation presented by M. Tenzer (center) on behalf of the committee to J. R. Perkins, DuPont (left), and I. Kolodny, General Cable (right) for serving on the committee for three years.



I. Kolodny on behalf of the committee presents the permanent committee members F. Horn, Bell Telephone Labs, and M. Tenzer, USAECOM, with certificates of appreciation for their long service to the Symposium.

PROCLAMATION

The Committee of the International Wire and Cable Symposium, meeting in camera over light refreshments, considered the qualifications of the candidate, one Jack Spergel, who after five years of grueling graduate study and research has presented as his thesis:

"The successful operation of a conglomeration of motley and non-homogeneous specimens of humanity, assembled for short finite periods of time under high density conditions with exposure to high concentrations of alcohol, for the specific purpose of transferring superficial bits of information from one specimen to another, and secondarily for mellowing and neutralizing the generally acid surface character of some few specimens."

The Committee, acting under authority granted to it by itself, decrees that:

On the condition that the candidate, Jack Spergel, agrees to continue to act in the same fashion as Co-Chairman, that he be awarded the degree —

"DR. OF SYMPOSIA"

December 3, 1969

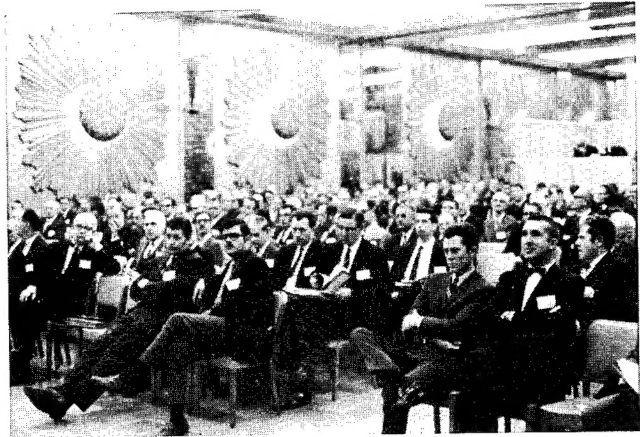


FINAL PRESENTATION: J. Spergel, Co-Chairman, accepting, in state of shock, a proclamation from J. Perkins with I. Kolodny and W. Doxey looking on.

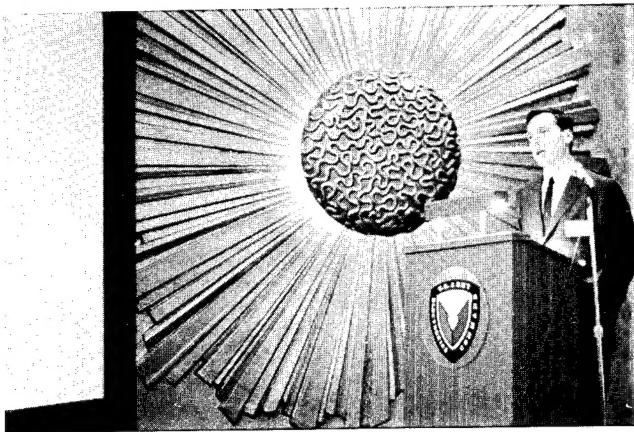
Miscellaneous Scenes During Symposium



Panel on Wideband Cable Transmission Systems (CATV). Left to Right — I. Kolodny, moderator, J. Norback, GT&E Services Co., H. J. Schlafley, Teleprompter Corp., J. Stillwell, Telesystems Service Corp., K. A. Simons, Jerrold Electronics, (J. Nevin, not shown).



Our wide awake attentive audience.



Bob Halperin of Raychem delivering his paper in his usual inimitable style.



Coffee Break — to help the audience keep awake.



A walk in the fresh air — on the boardwalk in Atlantic City.



Who said the symposium is all work and no play!

TABLE OF CONTENTS

TECHNICAL PROGRAM

Tuesday, 1 December 1970, 2:15 p.m.

SESSION 1 — Panel Discussion on Flat Cable Design Characteristics and Fabricating Techniques

Chairman: Joseph R. Perkins, E. I. DuPont de Nemours & Co., Inc.

"Digital Speeds Versus the Flat Cable Transmission Line," by D. Bossi, Ansley Corp.	1
"Characteristic Impedance of Unshielded Flat Multi-Conductor Cables," by S. M. Verma and P. E. Gamble, Burndy Corp., Tape Cable Div.	18
"System of Interface Matrix of Parallel Lines," by R. de Barros, SABENA-Belgium World Airlines	34
"Flat Conductor Cable Application for Airplane Power Feeders," by J. P. Morris, Boeing Co.	63
"Design and Fabrication Techniques for Flat Conductor Cable Harness," by A. L. Peters, Librascope Div., Singer Co.	81

Tuesday, 1 December 1970, 8:00 — 10:00 p.m.

Informal Seminar Discussion on Flat Cable and Connectors

"Digital Data Transmission in Shipboard Applications," by J F. Shiells, Jr., Ansley West Corp.	87
---	----

Wednesday, 2 December 1970, 9:15 a.m.

SESSION II — Cables, Conductors and Termination Techniques

Chairman: Fred M. Oberlander, RCA

"Aluminum Conductors in Paper Insulated Telephone Cables," by R. A. Clark, M. R. Rheinberger and A. W. Sisson, Australian Post Office	90
"Fundamentals of Establishing Reliable Connections to Small Gage Aluminum Wire," by I. F. Matthyse and S. M. Garte, Burndy Corp.	108
"New Techniques for Terminating Small Aluminum Wire to Connector Pins and Sockets," by M D. Lazar, Burndy Corp.	117
"Heat Aging Evaluation of Common Coated Copper Conductors," by T. B. McCune, Hudson Wire Co., J. H. Burns, G. A. Busch and D. J. Larson, Jr., Grumman Aerospace Corp.	122
"Electro-Tin Plating Copper Wire—When? 'Before or After Wire Draw?' " by P. E. Lawler and L. N. McKenna, Western Electric Co.	131
"New Italian Types of Cables for PCM and FDM Transmission," by S. Longoni, P. Calzolari and A. Portinari, Pirelli S.P.A.	136

Wednesday, 2 December 1970, 2:15 p.m.

SESSION III — Multipair and Coaxial Cable Characteristics

Chairman: E. Mark Wolf, Anaconda Wire and Cable Co.

"Estimation of Voice Frequency Noise in Communication Circuits," by E. W. Riley, Anaconda Wire and Cable Co.	144
---	-----

"Self Return Near-End Near-End Crosstalk of Multi-Pair Balanced Type Cable," by T. Hosono, Nippon Univ., H. Kaiden and S. Inao, The Furukawa Electric Co., Ltd.	155
"A Low Capacitance Cable for the T2 Digital Transmission Line," by D. E. Setzer and A. S. Windeler, Bell Telephone Laboratories	167
"Multi Pair Cable Shielding for PCM Transmission," by W. L. Roberts and F. N. Wilkenloh, Superior Continental Corp.	175
"Design and Applications of Coaxial Cable Carrier Systems," by S. J. Johnson and K. R. Bullock, Canada Wire and Cable Co., Ltd., and J. D. Adam, Manitoba Telephone System	182
"Leaky Coaxial Cable at VHF Band and Its Application to Vehicular Communi- cations," by T. Yoshiyasu, Ohsaka City Transit Authority, T. Hatta, K. Mikoshiba, S. Okada and T. Hanaoka, Hitachi Cable, Ltd.	200

Thursday, 3 December 1970, 9:15 a.m.

SESSION IV — Wire and Cable Materials

Chairman: Michael M. Suba, Union Carbide Corp.

"A Recently Developed Composite Insulation System Kapton/Polyimide," by R. E. Smith, Havg Industries, Inc.	208	16155
"Tefzel ETFE Fluoropolymer: A Versatile New Insulation for Wire and Cable," by E. A. Stecca, and E. W. Fasig, Jr., and J. C. Chevrier, E. I. DuPont de Nemours & Co., Inc.	217	16156
"Brittle Fracture of Polyethylene at Low Temperatures," by M. Okada and A. Utsumi, Dainichi-Nippon Cables, Ltd.	227	16157
"A New Flame Self-Extinguishing Hydrogen Chloride Binding PVC Jacketing Compound for Cables," by Dr. O. Leuchs, Kabel-und Metallwerke.	239	16158
"Photometric Determination of Carbon Dispersion Quality in Polyethylene," by J. B. Howard, Bell Telephone Laboratories	256	16159
"A Method for Manufacturing Polyolefin Insulated Communication Cable by Solvent Injection Foaming Process," by A. Asai, M. Jitsukawa, Y. Fujiwara, and A. Utsumi, Dainichi-Nippon Cables	259	16160

Thursday, 3 December 1970, 2:15 p.m.

SESSION V — Cable Manufacturing and Testing Techniques

Chairman: Dan F. Stewart, Phillips Petroleum Co.

"Manufacturing Waterproof Telephone Cable," by R. A. Conser, T. A. Heim and L. D. Moody, Western Electric	270	16161
"Compatability of Polyolefine Insulation and Hydrocarbon Fillers in Telephone Cable," by S. Verne, R. T. Puckowski and J. M. R. Hagger, B. I. C. C.	280	16162
"The Impact of Melting Theory on Screw Design," by R. A. Barr and L. Kovacs, Midland-Ross Corp., Waldron-Hartig Div.	288	16163
"An Analysis of Cooling Problems in Communications Cable Insulation," by R. L. Boysen, Union Carbide Corp.	294	
"New Dielectric Testing Methods for Insulated Wire," by R. S. Thayer, Tensolite Div. of Carlisle Corp.	302	
"A Foaming Process for Wire Insulation," by Y. Kato and H. Ohshima, Nippon Telegraph and Telephone Public Corp.	314	16164

DIGITAL SPEEDS VERSUS THE FLAT CABLE TRANSMISSION LINE

Author: Dennis F. Bossi

Company: Ansley Corporation
Old Easton Road
Doylestown, Pa. 18901

SUMMARY

It is the intent of this paper to describe the most important electrical and transmission properties in a flat cable system handling high speed digital pulses. The calculations and measurement of these properties in flat and round wire flat cable is an essential part in the evaluation of flat cable as a high quality transmission line system. In this respect a separate section is allotted for each of these electrical parameters.

- Section I - Characteristic Impedance and Propagation Velocity
- Section II - Capacitance
- Section III - Attenuation (Pulse and Sinewave)
- Section IV - Crosstalk (Coupling)

As pulse risetimes increase, testing procedures and terminations become more critical. Section V will involve termination techniques and adapters for flat cable testing, which assures the test engineer that he is observing the characteristics of his transmission line and not those of his termination.

Section VI compares attenuation and crosstalk results of flat cable with existing Coaxial and Twisted Pair Systems.

Characteristic Impedance and Velocity of Propagation

The input impedance of any electrical or electronic system is the effective combination of its internal components. This impedance is the actual resistive load seen by any external signal source. Therefore the input impedance to any type of cabling system can be considered to be made up of a continuous structure of resistors, capacitors, and inductors and is termed the cables' characteristic impedance (Z_0). As shown in Figure 1, if this cable system were infinitely long, and all the components defined per unit length, then;¹

$$Z_{in} = Z_0 = \sqrt{\frac{R + j\omega L}{G + j\omega C}} \quad (1)$$

The characteristic impedance of a flat cable is a function of the cables' geometry (its wire size, spacing, and dielectric) and its mode of operation. By mode of operation it is meant that a flat cable transmission line may be used as either a balanced pair or an unbalanced system. Since the majority of flat cable systems to date are operating as unbalanced lines (alternate Gnd. - Sig. - Gnd. configuration), this mode shall be illustrated for the transmission characteristics other than impedance. The first consideration in the calculation of the characteristic impedance of a flat cable is to determine the Impedance in Air (Z_{air}) for a given wire configuration, and then determine the effect of the surrounding dielectric.

Figure 2 shows various cabling systems and their corresponding characteristic impedance in air. These

formulas were adequate for most cabling systems until the innovation of the flat cable transmission line. In flat cable the field theory is quite involved and simple formulae are not readily available for a 3-wire unbalanced configuration. Figures 3 and 4 show graphs developed by Ansley Corp. for unbalanced characteristic impedance in air.

Figure 3 (for flat conductors) is a family of curves each defined by the wires' width to thickness ratio with Z_{air} plotted against the conductors' pitch to width ratio. Formulae developed for these curves are very complex, cumbersome to work with, involve elliptical integrals, and are only valid for certain sections of the curves.

Figure 4 (for round conductors) is far easier to formulate because there are only two dependent factors, the pitch and wire diameter. Since most flat transmission lines today use this wiring system, Ansley has devoted the majority of its research time to develop precise transmission properties in this configuration. This graph was obtained under accurately controlled laboratory conditions, and the formula (developed by Ansley Corp.) which best matches this curve is;

$$Z_{air} = 42 \cosh^{-1} \left[1.8x^2 - \sqrt{1.25x^2 - 1} \right] \quad (2)$$

where:

$$\begin{aligned} x &= \frac{p}{d} \\ p &= \text{Conductor Pitch (center to center)} \\ d &= \text{Conductor Diameter} \end{aligned}$$

Knowing the Z_{air} , the characteristic impedance of the cable is defined as;

$$Z_0 = Z_{air} / \sqrt{\epsilon_{eff}} \quad (3)$$

where:

$\sqrt{\epsilon_{eff}}$ = the effective propagation velocity of the cable in nanoseconds per foot or the square root of the effective dielectric constant of the insulation times 1.016, which is the velocity of propagation in air.

The determination of the effective dielectric constant by mathematical means is very difficult, and most relationships for this figure are based on test results. The manufacturing of Ansley flat cable produces a geometry unlike the majority of manufacturers. A cross-sectional view of our flat cable shows very little contouring around conductors. Because of this, a precisely controlled laboratory test was set up to find the amount of the electrostatic and electro-magnetic fields contained in the dielectric material as a function of the cables' overall thickness to pitch ratio. Figure 5 is a graph of these results and shows the Air effect on a flat cable or the percent of the field in Air plotted against the cables' thickness to pitch ratio. Using this curve the

calculation of the $\sqrt{\epsilon_{\text{eff}}}$ is easily obtained by:

$$\sqrt{\epsilon_{\text{eff}}} = 1.016 \left[\sqrt{\epsilon_d} \left(1 - \frac{\text{o/o AIR}}{100} \right) + \frac{\text{o/o AIR}}{100} \right] \quad (4)$$

where:

$\sqrt{\epsilon_d}$ = square root of the relative dielectric constant of the insulation.

Figure 6 shows in flow chart fashion the calculation of characteristic impedance for various wiring configurations.

The Z_0 and $\sqrt{\epsilon_{\text{eff}}}$ of a flat cable system can be expressed by a number of different parameters, and they can be measured by many different methods. The majority of these measurements are more tedious than they are worth, but the modern techniques of Time Domain Reflectometry have made Z_0 and $\sqrt{\epsilon_{\text{eff}}}$ readings directly observable. This technique is most widely used and provides the greatest speed and accuracy in measurements.

Time Domain Reflectometry, commonly called TDR, employs a step generator and an oscilloscope in a system best described as "Closed Loop Radar." The voltage output step from the generator is propagated down the transmission line under investigation and the incident and reflected voltage waves are monitored by the oscilloscope at a particular point along the line. (Figure 7). The TDR equipment commercially available today has output risetimes between 35 and 300 picoseconds into a 50 ohm output impedance. This impedance is used as the Calibrated Reference Level for all measurements. Figure 8 is a typical test setup using a Hewlett Packard 1415 TDR with a 180 picosecond risetime and an Ansley 50 ohm Double Strip Launcher to make Z_0 readings on flat cable. The cable here was made to the dimensions shown in item 3 of Figure 6, and a 10 foot sample is terminated at both ends as illustrated in Figure 9. As the trace is observed on the scope screen, the horizontal axis is distance along the line in feet or time, and the vertical axis is the reflection coefficient (ρ). ρ is the ratio of the reflected wave to the incident wave at the source, and averaged by the high frequency components of the pulse. This reflection coefficient (ρ) is related to the Z_0 of the cable by:

$$\rho = \frac{Z_0 - Z_s}{Z_0 + Z_s} \quad (5)$$

where:

Z_s = the calibrated output impedance of the TDR or 50 ohms.

Solving this for Z_0 with the 50 ohm substitution yields;

$$Z_0 = 50 \frac{1 + \rho}{1 - \rho} \quad (6)$$

The scope trace in Figure 10 shows the Z_0 of the sample at every point along its length. If there is any change in

pitch or the dielectric at a particular point along the cable, the Z_0 will change and the percentage of the wave reflected back from that point will cause a corresponding change in the scope trace. The resolution obtained with this system is dependent on the length of the sample or discontinuity along the sample compared to the output risetime of the system. The faster the risetime the better the resolution. As a rule of thumb, if the length of the sample or discontinuity is greater than 1/4 of a wavelength at the highest frequency component of the risetime, an absolute reflection will be seen. The accuracy obtained with TDR measurements is, of course, dependent on the initial calibration of the Reference Level, but changes in impedance as small as 0.05 ohms are readily visible on the oscilloscope.

The propagation time or delay can also be determined from the scope trace in Figure 10, but the accuracy of such measurements depends strongly on the ability to distinguish the termination points of the cable. The time shown on the TDR to reach any point on the cable or between any two points in the cable is always twice the actual delay between those points. The test setup used to obtain appreciable accuracy in $\sqrt{\epsilon_{\text{eff}}}$ measurements is shown in Figure 11. Two small pin point probes are forced through the cable insulation to make contact with the signal conductor. The distance between these probes is selected so that the delay will be approximately full screen on the TDR. With these probes in place there is an increase in capacitance at the point of contact along the signal line, and the impedance at that point becomes lower. The exact location of this Contact point becomes more evident as the risetime of the system is increased. A risetime of 180 picoseconds is sufficiently fast enough for most accuracy requirements. Figure 12 shows the scope trace obtained with this method, and the determination of the cables' $\sqrt{\epsilon_{\text{eff}}}$.

These two basic transmission properties, namely Characteristic Impedance and Propagation Velocity, are very important parameters in the evaluation of a complete flat cable system. They provide the building blocks for a complete flat cable analysis into areas like: Mismatch, VSWR, Attenuation, Radiation, Coupling, etc.

Capacitance

The capacitance between wires in a round or flat wire cable is related to the characteristics impedance for a given wire configuration by;

$$C = \frac{1016 \sqrt{\epsilon_{\text{eff}}}}{Z_0} \quad (7)$$

where:

C = Capacitance in picofarads per foot.

For unbalanced 3-wire systems (Gnd-Sig-Gnd), this is probably the simplest and most used expression for calculating the capacitance of a flat cable.

For wire above ground (microstrip) and stripline configurations the calculation of cable capacitance can be obtained by considering the following factors.

1. Parallel Plate Capacitance:

For microstrip configurations as shown in Figure 13A, the effective parallel plate capacitance in air dielectric is;

$$C_{pp} = 0.224 \frac{A}{h} \quad (8)$$

where:

- C_{pp} = Plate capacitance in picofarads
- A = Area of flat wire in sq. in. (length of wire x width)
- h = Separation between wire and gnd. plane

For a symmetrical stripline configuration as shown in Figure 13B, the parallel plate capacitance is twice the value given by equation (8). For non-symmetrical striplines the plate capacitance must be calculated for each gnd. plane.

2. Fringing Capacitance:

With respect to this area there has been a great deal of research compiled in an attempt to obtain a working knowledge for the edge capacitance relationship to the cables' physical parameters. Figure 14 is a graph of the fringing capacitance values for a symmetrical stripline plotted against the wire thickness to shield separation ratio. From the cross-sectional view of the stripline it can be seen that these values were obtained by summing the effective capacitances from each of the four edges of the flat wire. The mathematical expression for the capacitance in air at one of these edges is;²

$$C'_{ff} = 30.48 \left[\frac{0.0885}{\pi} \left[\frac{2}{1-\frac{t}{b}} \ln \left(\frac{1}{1-\frac{t}{b}} + 1 \right) - \left(\frac{1}{1-\frac{t}{b}} \right) \ln \left(\frac{1}{(1-\frac{t}{b})^2} - 1 \right) \right] \right] \quad (9)$$

where:

- C'_{ff} = edge capacitance in picofarads per foot
- t = wire thickness
- b = shield separation

The research into this area by Ansley Corp. has shown that this formula is also valid for microstrip configurations. The total fringing capacitance in this case is obtained by summing the capacitance from only 2 edges of the flat wire.

3. Composite Dielectric Constant

The effective dielectric constant of a stripline configuration is of course the total dielectric constant of the insulation, because there is no air effect or percentage of the field around the wire in air.

In microstrip configurations where the conductor is exposed and no cover insulation is added, the fractional part of the field surrounding the wire which is in air is shown in Figure 15. The composite dielectric constant for this configuration is obtained by;

$$K_{comp} = K_d (1 - \% \text{ AIR}) + \% \text{ AIR} \quad (10)$$

where:

- K_d = the Dielectric Constant of the insulation
- $\% \text{ AIR}$ = fractional part of the field around the wire in air

When a cover insulation is added the air effect diminishes as the insulation over the wire increases. For all practical purposes, 100% of the field is contained in the dielectric when the thickness of the cover coat is three times the wire to shield separation. This factor of change in the air effect is shown in Figure 16, and equation 10 is used to obtain the composite dielectric constant.³

Considering all the beforementioned factors the total capacitance for microstrip and stripline configurations is then;

$$\text{microstrip} \text{ ----- } C_{tot} = [C_{pp} + 2 C'_{ff}] K_{comp} \quad (11)$$

$$\text{stripline} \text{ ----- } C_{tot} = [2C_{pp} + 4C'_{ff}] K_{comp} \quad (12)$$

(symmetrical)

Capacitance measurements on flat cable using an unbalanced configuration or on striplines and microstrips between conductor and shield are easily obtained on most commercially available bridges. The test frequency should be between 100 KHz and 1 MHz. This allows the use of an I. F. type amplifier which has the desirable combination of high gain, low noise, and excellent harmonic rejection properties.

Capacitance measurements between 2 wires which are not associated with a common ground (balanced pairs) can be obtained by the following formula;

$$C_{tot} = \frac{2(C_a + C_b) - C_c}{4} \quad (13)$$

where:

- C_a = the measured capacitance between No. 1 conductor and No. 2 conductor connected to the common gnd.
- C_b = the measured capacitance between No. 2 conductor and No. 1 conductor connected to the common gnd.
- C_c = the measured capacitance between No. 1 and No. 2 conductors together and the common gnd.

Figure 17 shows various flat cable, microstrip, and stripline configurations with their associated

capacitance both calculated and measured.

Attenuation

The value of sine wave attenuation is a useful parameter in flat cable analysis. It can be used to determine important characteristics of the applied pulse as it travels down the transmission line. The effect that the copper and insulation losses have on a unit step input is a general degradation of the pulse risetime. This is usually first noticeable in the rounding-off of the high frequency corner of the pulse. Recently there has been an appreciable amount of work done to describe the shape of the output pulse of a system with a mathematical expression involving the sine wave attenuation.

The sine wave attenuation for most cabling systems is given in db per unit length and is calculated by the following equation:

$$A_o = \frac{1}{Z_o} + \frac{2}{2.78 \cdot \frac{0.2}{d} \cdot f \cdot F_p} \quad (14)$$

where:

A_o = total attenuation in db per 100 feet.

R_t = the equivalent wire resistance at frequency f .

For round wire; $R_t = \frac{0.2}{d} \sqrt{f}$

For flat wire; $R_t = \frac{0.1}{w} \sqrt{\frac{\pi f}{t_w}}$

For coaxial cable; $R_t = \left(\frac{1}{d} + \frac{1}{D} \right) \sqrt{f}$

d = wire diameter in inches (Coaxial-line center conductor)

D = diameter of inner surface of outer conductor in inches

t = thickness of flat wire

w = width of flat wire

f = frequency in MHz

F_p = dissipation factor of insulation

The first half of this equation, as noted above, depicts the losses in the cable due to the copper, and the second half shows insulation losses.

In order to relate sine wave attenuation values to pulse risetime degradation, there must first be a correlation between the sine wave frequency and the pulse risetime from 10% to 90%. Research compiled by Ansley Corp. has shown that by using the resonant frequency (f_o) which matches a particular pulse risetime (t_r) the relationship is;

$$t_r = \frac{0.295}{f_o} \quad (15)$$

Where t_r is in nanoseconds and f_o is in MHz.

Since most authors dealing with this output pulse shape use the upper frequency limit defined by the 3 db point (f_c) in describing the relationship between pulse risetimes and sine waves, equation (15) converted to this form by the equality $\frac{f_c}{f_o} = 1.448$ yields;

$$t_r = \frac{.425}{f_c} \quad (16)$$

Knowing this relationship the correspondence between sine wave and pulse attenuation is given by;⁴

$$T_o = (4.56 \times 10^{-7}) \left(\frac{A_o}{f_c} \right)^2 \text{ in seconds} \quad (17)$$

where:

T_o = the normalized output risetime at 50% of the input pulse level

l = cable length in feet

A_o = sine wave attenuation in db per 100 feet at frequency f_c .

With a theoretically ideal unit step input pulse " T_o " would be the time for the output pulse to reach one half the magnitude of the input. For practical pulses " T_o " is simply the time shift between input and output at the 50% level. The complete slope of the output pulse can be defined in terms of " T_o " according to Figure 18.⁵

Measurements of sine wave and pulse attenuation are relatively easy to make on most dual channel oscilloscopes. The only critical factor in these measurements is the termination. The cable must be resistively terminated in exactly its own characteristic impedance with the best match possible to eliminate reflections. On pulse measurements this is extremely important. If the resistive load is a different value than the cable impedance, it will cause variations in the height of the output pulse. This will evidently lead to erroneous readings in the pulse risetime. If there is a mismatch between the load and the cable, this will cause variations in the risetime itself as it passes thru this impedance change.

An alternate technique used with sine wave measurements which has proven successful, is to terminate the cable system in the same output impedance as the signal source. In other words if a 50 ohm generator is used for a 100 ohm cable, the cable is terminated in 50 ohms. Measurements with this system must be performed at multiples of the half wave length frequency of the cable sample. This makes certain that the initial mismatches at both input and output will cancel each

other out. The half wavelength frequency of the cable is determined by:

$$f_z = 492 / \sqrt{\epsilon_{\text{eff}}} l \text{ in MHz} \quad (18)$$

where:

f_z = half wavelength frequency

l = cable length in feet

Crosstalk

Crosstalk or Coupling is of major importance in almost every transmission line system. It is the electrical interference or voltage and current pickup introduced into a quiet signal line of a system by adjacent active or pulse driven lines. This coupling in transmission line systems has different characteristics when measured at different points along the line.

When a quiet line is observed at the signal source end or driven end of the system, the voltage pickup seen is a pulse having the same risetime as the driving pulse with a magnitude or lower DC value, and a duration of twice the delay time of the cable. This coupling is termed NEAR END or BACKWARDS CROSSTALK. When the pulse risetime is faster than twice the delay time in the cable, this coupling has also been called FAST CROSSTALK, and appropriately SLOW CROSSTALK occurs when the pulse risetime is less than twice the delay time. This Slow Crosstalk has a triangular shape, and reaches full DC magnitude when the risetime is equal to twice the delay. The Near End Crosstalk of a system is independent of pulse risetime and the length of the system as long as the requirements defining Fast Crosstalk are met. The only factors which effect the Near End crosstalk are the Z_0 of the system, the number of drivelines, and the amount of isolation from Signal to Signal (for unbalanced flat cable system this is dependent on the number of Gnds. between each signal).

When the quiet line is observed at the termination end of the cable, the pick-up is a spike of opposite polarity from the driving line and a time duration equal to approximately twice the output risetime. This coupling is termed FAR END, FORWARD, or DIFFERENTIAL CROSSTALK. In addition to those factors mentioned for Near End Crosstalk, the magnitude of the Far End coupling is dependent on the cable length and the pulse risetime.

Figure 19 shows typical scope traces depicting the Near and Far End Driving Pulses along with their corresponding Crosstalk traces.

The picture of the near end coupling is especially important in the analysis of a total cable system, because it shows the coupling which occurs at each point in the system. The crosstalk caused by different components of the system (connectors, jumper boards,

etc.) can be clearly observed if the testing risetime is fast enough. As mentioned before, if the equivalent frequency of the risetime is faster than the 1/4 wavelength frequency of the component (connector), then the maximum crosstalk caused by that component will be observed.

The picture of the far end crosstalk shows a complete summing of the crosstalk caused by each component and it is impossible to relate the major cause of this coupling to any one component part. For Far End crosstalk evaluations, it is necessary to measure the component parts of a system separately in order to evaluate or redesign a system efficiently.

Termination Techniques

Recently Ansley has designed and developed four types of testing adapters to insure reliability and reproducibility in measurements of important transmission characteristics. These adapters are shown in Figure 20 along with a general description of each one. With these adapters, testing is possible on a wide variety of flat cables. Almost any type of termination can be used with some success on mechanical or general wiring cable systems, but with sophisticated transmission lines with 60 to 70 wires per inch, termination techniques become extremely critical. For accurate and reliable attenuation and crosstalk measurements, impedance matching is essential. Since most commercially available pulse generating equipment uses a 50 ohm output impedance, these adapters were designed for use with this type equipment. Each of the four connectors will be discussed separately with emphasis placed on the most sophisticated design (P/N 604200).

Ansley's 50 ohm Double Strip Launcher (P/N 604197) is the simplest design and lends itself best to making accurate impedance measurements, although it can also be used for other measurements on 50 ohm cables only and at relatively slow risetimes of ≈ 10 nanoseconds. Impedance measurements on any impedance cable are accurately obtained because the transition point between connector and cable is relatively short and reflections from this area are small. Techniques using this connector can be seen in the previous discussion on Z_0 measurements.

The 50 ohm Coaxial Bar Adapter (P/N 604198) was designed specifically for use with the Hewlett Packard 1415 TDR. It is recommended for use with 50 ohm characteristic impedance cable systems. Figure 21 shows a 50 ohm cable terminated to this adapter. In the termination the two signal lines under test extend forward beyond on the ground termination to connect to the signal leads of the adapter. Even though this transition length is short, the higher impedance of these bare signal lines is readily noticeable with a pulse risetime of 1 nanosecond. The reason for this increase is that the signal line is separated from its adjacent grounds and the capacitance at this point from signal line to ground

is lower. To eliminate this problem, which will cause errors in attenuation and crosstalk measurements, a tuning plate is supplied to cover this transition area. Since the tuning plate is at ground potential, as it is lowered over the signal line it adds capacitance to lower the impedance in this area. This compensation to enable the use of faster pulse risetimes is shown in Figure 22. To illustrate the importance of a matched termination, measurements were made using this 50 ohm bar adapter with and without the tuning plate. The results of this comparison are shown in Figure 23. It can be seen from the scope trace of the Near End crosstalk, that there is a definite mismatch in the system which causes a more direct coupling between the two adjacent signal lines. This mismatch of course is not evident in the Far End crosstalk or the pulse attenuation traces. Without knowing how this mismatch effects these two parameters, even though the mismatch is known to be present by the Near End crosstalk, erroneous results are obtained for the Far End crosstalk and the pulse degradation.

The 100 ohm Coaxial Bar Adapter (P/N 604199) was designed for use with 100 ohm impedance cabling systems, and is very similar to the 50 ohm bar adapter. There is an internal resistive matching network to match a 50 ohm signal source to a 100 ohm transmission line. This adapter is fitted with probe receptacles to accept standard miniature probes common to commercially available high speed sampling oscilloscopes. Incorporated into the internal matching pad is a compensation for these types of miniature probes, because to obtain their fast pulse response they have relatively low load impedances, generally 500 ohms. The functions of this adapter are comparable with the 50 ohm adapter, but no tuning plate is required. The mismatch caused by the open signal wire is much smaller and is also reduced further by the effect of the matching pad.

The Universal Impedance Matching Adapter (P/N 604200) has the main distinction of matching any impedance cable up to 200 ohms to a 50 ohm signal source. Another main advancement of this adapter is that it has the facility for the termination of 5 signal lines. This enables the user to have four driven or active lines for crosstalk testing. For all practical purposes increases in crosstalk values due to the number of driven lines seems to diminish when more than four lines are active. The matching network consists of high frequency resistors which are individually interchangeable to accommodate a variety of flat cables. The matching of a flat cable for crosstalk testing driving four lines can cause numerous errors in measurement because of the relatively large amount of space needed for the components. Also, maintaining the same pulse characteristics on all four drivers is not simply obtained with ordinary matching techniques. The drivers must be matched in both directions along the transmission lines. When the initial drive pulse is reflected back from the load it must encounter no

impedance variations. Previous testing methods using L, T, or H matching pads, which require that all the driven lines be commoned and the signal source be matched to their parallel equivalent, proved to be insufficient for numerous reasons. There is a large mismatch as the pulse travels through the match pad. To eliminate this problem the components of the pad had to be housed in a common ground block which maintained the proper impedance through the resistors and did not add excessive capacitance to distort the pulse. When the lines of the cable were commoned to one terminal of the match pad excessive capacitance at this point was always present. The total termination was generally bulky and isolation between active lines and the quiet line at the termination was difficult to maintain. This caused a direct coupling at this point and the Far End crosstalk values were not reliable.

A sketch of the matching technique used on this universal impedance matching adapter is shown in Figure 24. Mismatch problems on the drive lines are greatly reduced because each line is connected separately. Also isolation between drive and quiet lines is very good due to the fact that they are terminated on opposite sides of the connector. A comparison of measurements between old techniques and this adapter is shown and described in Figure 25.

Conclusions

There are many reasons and advantages of flat cabling which have prompted its success in today's equipment. To date most of these were based on physical parameters and economic advantages. As a conclusion to this discussion on flat cable as a quality transmission line with high speed digital pulses, Figures 26 and 27 offer comparison crosstalk and attenuation values between flat cable, coaxial, and twisted pair systems.

REFERENCES

1. Hewlett Packard, Application Note #62 & 67
Time Domain Reflectometry.
2. Cohn, Seymour B., Problems in Strip Transmission Lines, "IRE transactions on microwave theory and techniques," March 1955.
3. Wheeler, Harold A., Transmission-Line Properties of Parallel Strips Separated by a Dielectric Sheet, "IEEE transactions on microwave theory and techniques." March, 1965.
4. Dreher, Thad, Cabling Fast Pulses? Don't Trip on the Steps, "The Electronic Engineer," August, 1969.
5. Botos, Bob, Precautions for Handling High Speed Digital Pulses, "The Electronic Engineer," October, 1967.

Dennis F. Bossi
Ansley Corporation
Old Easton Rd.
Doylestown, Pa. 18901

Attended West Virginia University from 1963 to 1966 in Electrical Engineering and continued studies in Electrical Engineering at Villanova University from 1968 till present.

AMP Incorporated 1966 - 1967 - Worked on design and development of Land and Sea Communications Systems.

Ansley Corporation 1967 to present - Job functions include design and development of flat cable transmission line systems, termination techniques both test and product and research into high frequency transmission characteristics.

Accepted the chairmanship in the I.P.C. for the EMI/RFI Shielding Sub-Committee as of September 1970.

Presented paper entitled "Characteristic Impedance Used for Dimensional Evaluation," at the I.P.C. Spring Meeting.

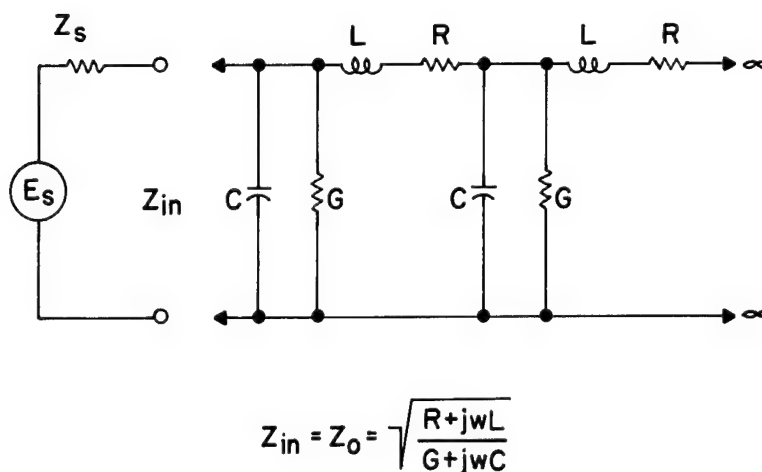
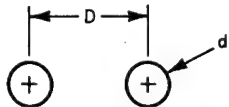
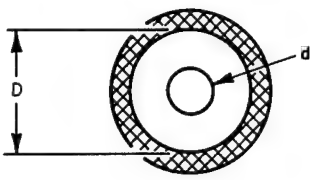
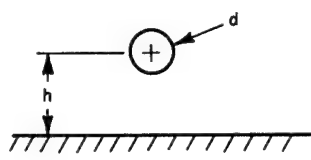
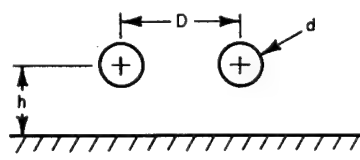
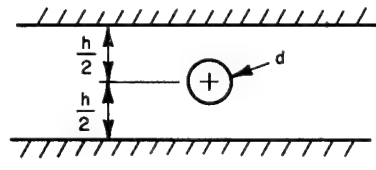
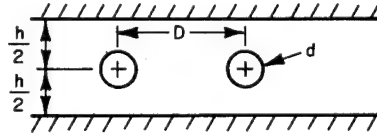


Figure 1. CLASSICAL MODEL FOR A TRANSMISSION LINE

Figure 2

Conductor Configuration	Characteristic Impedance in Air
<p>Open two-wire line</p> <p>D = pitch d = wire dia</p> 	$Z_{\text{air}} = 120 \cosh^{-1} \frac{D}{d}$ $\approx 276 \log_{10} \frac{2D}{d}$
<p>Single Coaxial Line</p> <p>D = Dia. of inside surface of outer Cond. or shield d = dia of Center Cond.</p> 	$Z_{\text{air}} = 138 \log_{10} \frac{D}{d}$ $= 60 \ln \frac{D}{d}$
<p>Single wire, near gnd.</p> <p>h = distance between Cond. and gnd. plane d = wire dia.</p> 	<p>For $d \ll h$,</p> $Z_{\text{air}} = 138 \log_{10} \frac{4h}{d}$
<p>Balanced Pair, near gnd.</p> 	<p>For $d \ll D, h$,</p> $Z_{\text{air}} = 276 \log_{10} \left[\frac{2D}{d} \sqrt{1 + \left(\frac{D}{2h} \right)^2} \right]$
<p>Single wire between grounded parallel planes</p> 	<p>For $\frac{d}{h} < 0.75$</p> $Z_{\text{air}} = 138 \log_{10} \frac{4h}{\pi d}$
<p>Balanced pair between grounded parallel planes</p> 	<p>For $d \ll D, h$,</p> $Z_{\text{air}} = 276 \log_{10} \left[\frac{4h \tanh \frac{D}{2h}}{\pi d} \right]$

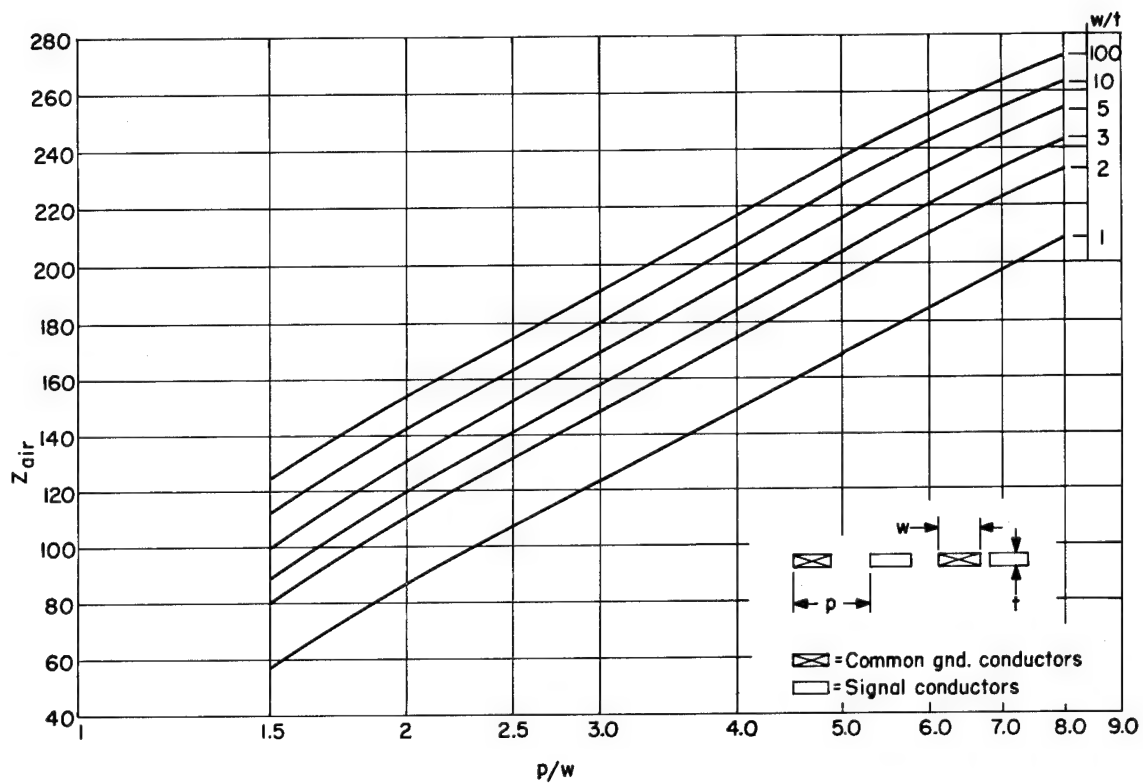


Figure 3

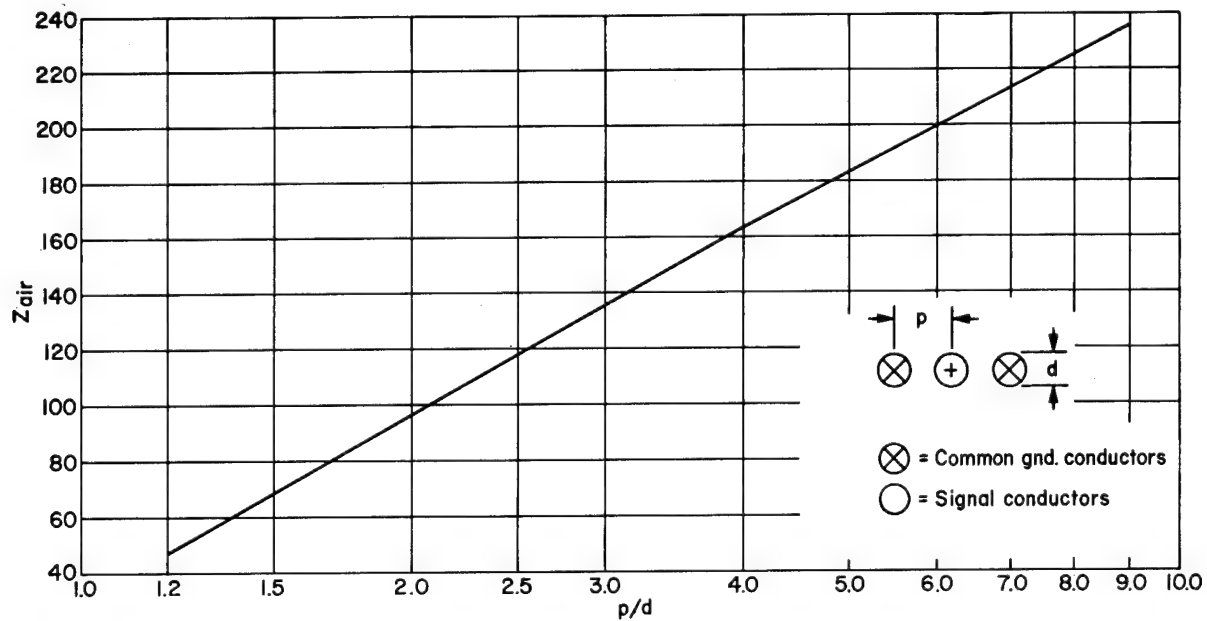


Figure 4

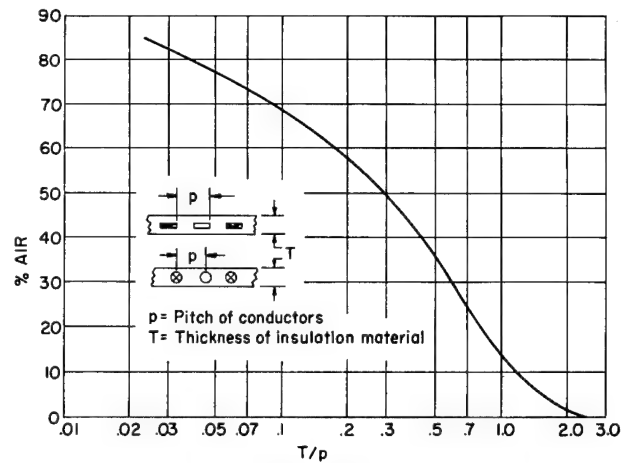


Figure 5 The % in air of the field surrounding adjacent conductors in flat cable

Wire Configuration	1.	2.	3.
w/t	5.0	N. A.	N. A.
$\frac{p}{w}$ or $\frac{p}{d}$	2.0	1.67	1.67
Z_{air}	132 ohms (from Graph in Fig. 3)	132 ohms (from Item 1 in Fig. 2)	80 ohms (from Graph in Fig. 4 or eq. 2)
$\sqrt{\epsilon_d}$	1.87	1.52	1.52
$\frac{T}{p}$	0.3	2.4	2.4
E. M. F. % Air	50% (Fig. 5)	$\approx 0\%$ (Fig. 5)	$\approx 0\%$ (Fig. 5)
$\sqrt{\epsilon_{eff}}$	1.51 (eq. 4)	1.52	1.52
Z_o (Cable)	87.4 ohms (eq. 3)	86.8 ohms (eq. 3)	52.6 ohms (eq. 3)

Figure 6

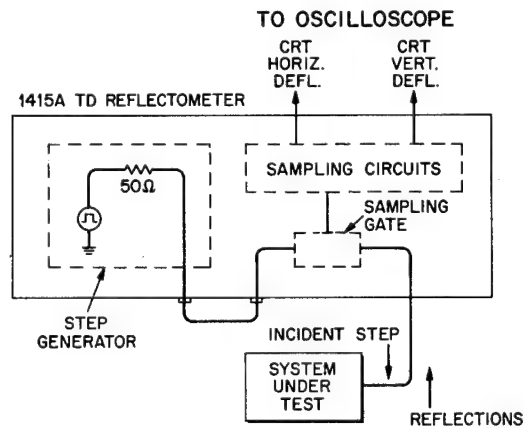


Figure 7. T.D.R. SYSTEM

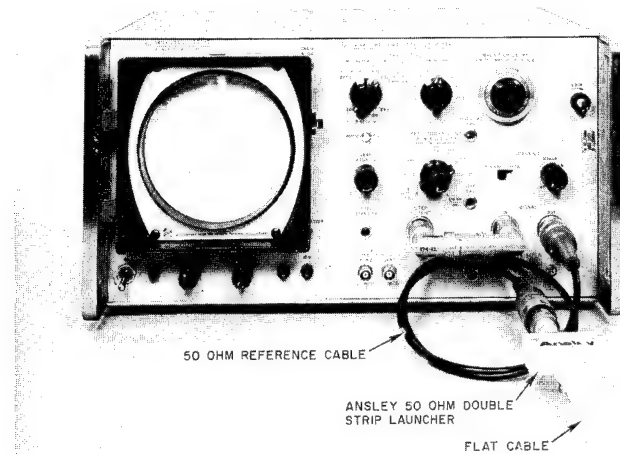


Figure 8. SET-UP FOR Z_0 MEASUREMENTS

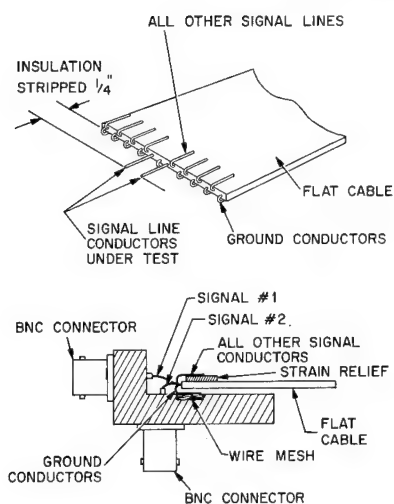
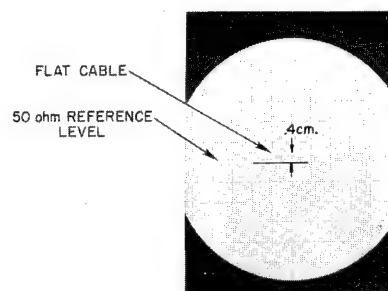


Figure 9. CABLE TERMINATION



VERTICAL DEFLECTION .05 μ /cm.
 HORIZONTAL DEFLECTION 4 ns./cm.
 μ FOR FLAT CABLE = .4cm. x .05 μ /cm. = .02
 $Z_0 = 50 \frac{1+\mu}{1-\mu}$
 $Z_0 = 50 \frac{1.02}{.98}$
 $Z_0 = 52$ ohms

Figure 10. FLAT CABLE CHARACTERISTIC IMPEDANCE

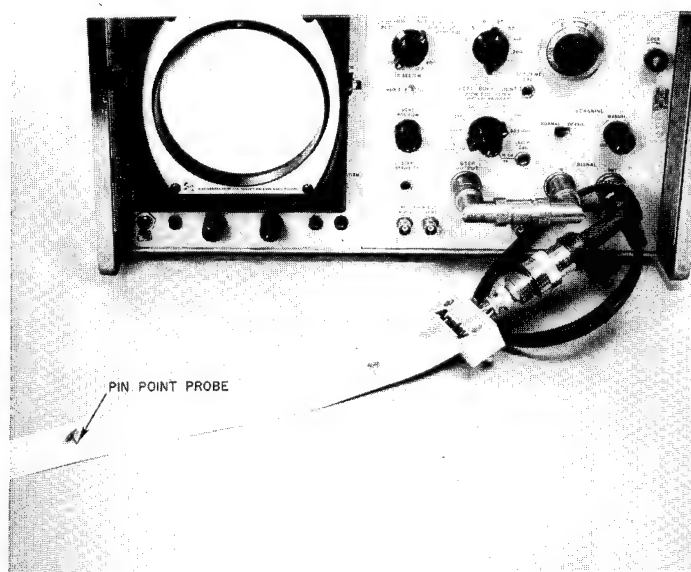
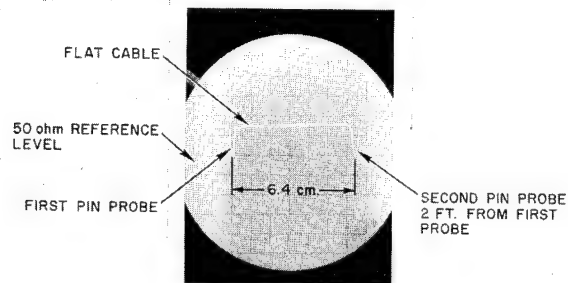


Figure 11. PROPAGATION DELAY SET-UP



VERTICAL DEFLECTION .02 p/cm.

HORIZONTAL DEFLECTION 1 ns./cm.

$$\text{TOTAL DELAY} = \frac{6.4 \text{ cm.} \times 1 \text{ ns./cm.}}{2} = 3.2 \text{ ns.}$$

$$\text{CABLE DELAY/FOOT} = \frac{3.2 \text{ ns.}}{2 \text{ ft.}} = 1.6 \text{ ns./foot}$$

$$\sqrt{\epsilon_{\text{eff}}} = 1.6 \text{ ns./foot}$$

Figure 12. PROPAGATION VELOCITY IN FLAT CABLE

Figure 13a.

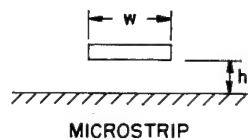


Figure 13b.

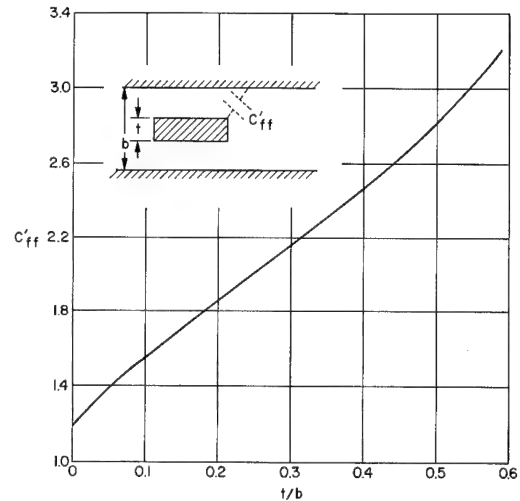
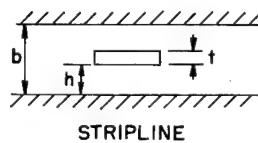


Figure 14. FRINGING CAPACITANCE

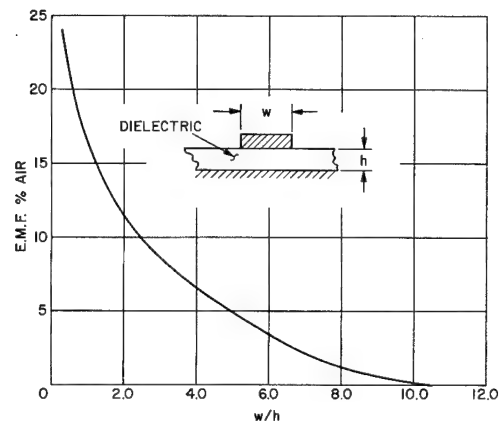


Figure 15. THE % IN AIR OF THE FIELD SURROUNDING A MICROSTRIP CONFIGURATION

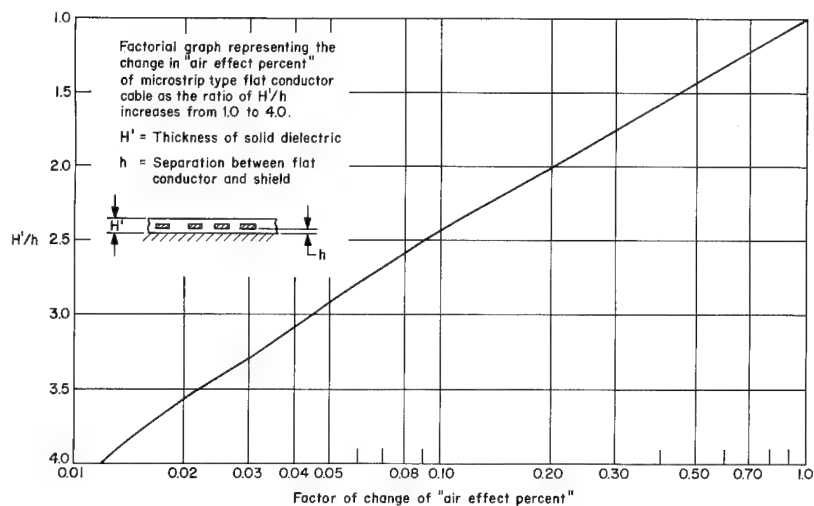



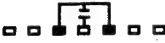




Figure 16. FACTOR OF CHANGE OF "AIR EFFECT PERCENT"


	Flat Cable	Microstrip	Stripline
			
Measurement Conditions & Values	 Cap. = 12.32 picofarads/foot	 Cap. = 43.7 picofarads/foot	 Cap. = 73.6 picofarads/foot
Capacitance Calculations	$Z_{air} = 147 \text{ ohms (from Fig. 3)}$ $\sqrt{\epsilon_d} = 1.73$ $\sqrt{\epsilon_{eff}} = 1.33 \text{ (from Fig. 5)}$ $Z_o = \frac{147}{1.33} = 110.5 \text{ ohms}$ $Cap. = \frac{1016 \sqrt{\epsilon_{eff}}}{Z_o}$ $Cap. = \underline{12.23}$	$C_{pp} = 8.57 \text{ (from eq. 8)}$ $C'_{ff} = 2.95 \text{ (from eq. 9)}$ $K_d = 3.0$ $\% \text{ AIR} = 8\% \text{ (from Fig. 15)}$ $\% \text{ AIR corrected} = 1.6\% \text{ (Fig. 16)}$ $K_{comp} = 2.96 \text{ (eq. 10)}$ $C_{tot} = \underline{42.83} \text{ (eq. 11)}$	$C_{pp} = 8.57 \text{ (eq. 8)}$ $C'_{ff} = 1.92 \text{ (eq. 9)}$ $K_d = 3.0$ $\% \text{ AIR} = 0$ $K_{comp} = 3.0$ $C_{tot} = \underline{74.46} \text{ (eq. 11)}$

 POLYESTER INSULATION

 ADHESIVE

 SHIELD

 FLOATING CONDUCTORS (IF UNCONNECTED)
 SIGNAL CONDUCTORS (IF CONNECTED)

 GROUND CONDUCTORS

CONDUCTOR SIZE - .022 x .004
 CONDUCTOR PITCH - .050

Figure 17. Capacitance Values

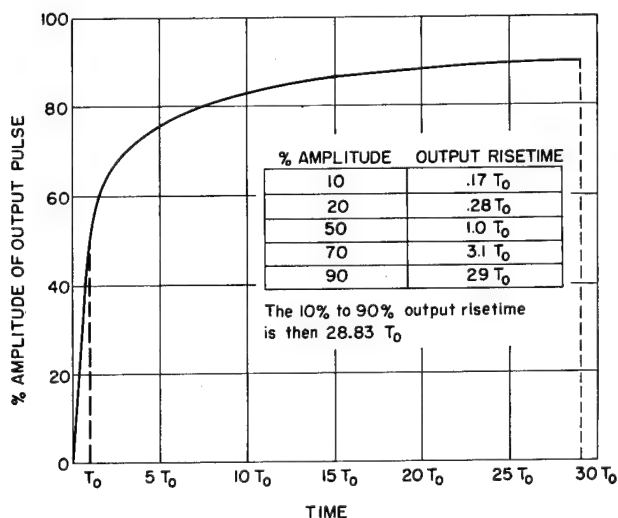


Figure 18

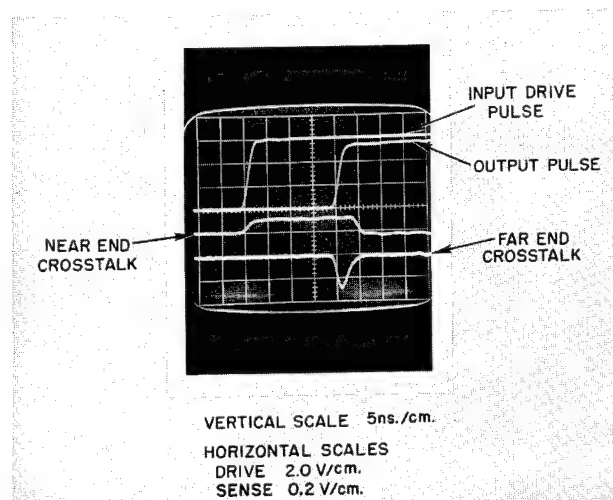


Figure 19. TYPICAL CROSSTALK TRACES

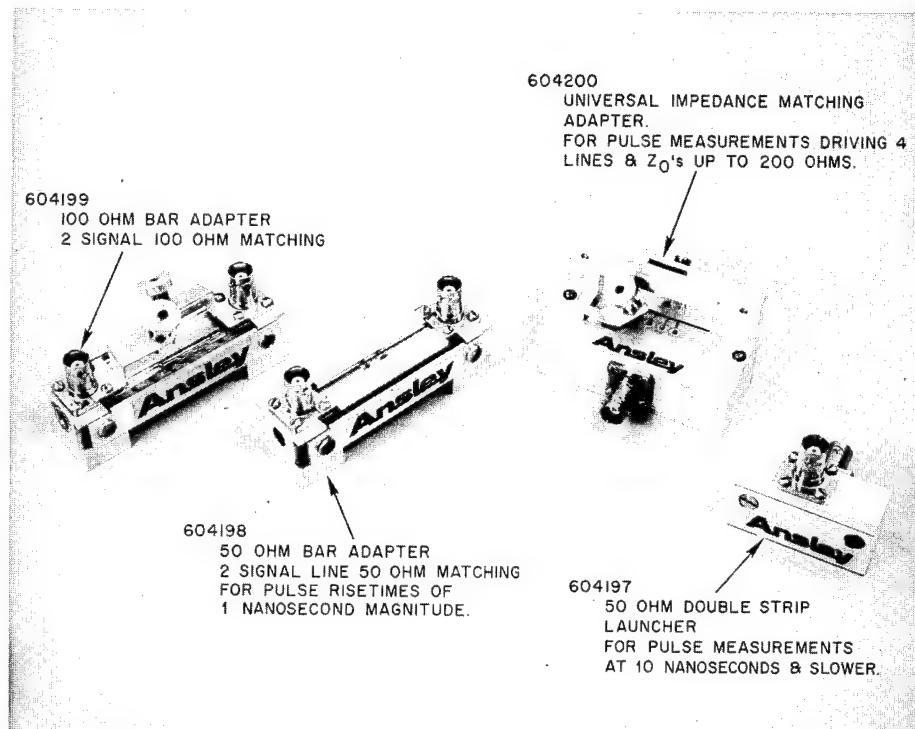


Figure 20.

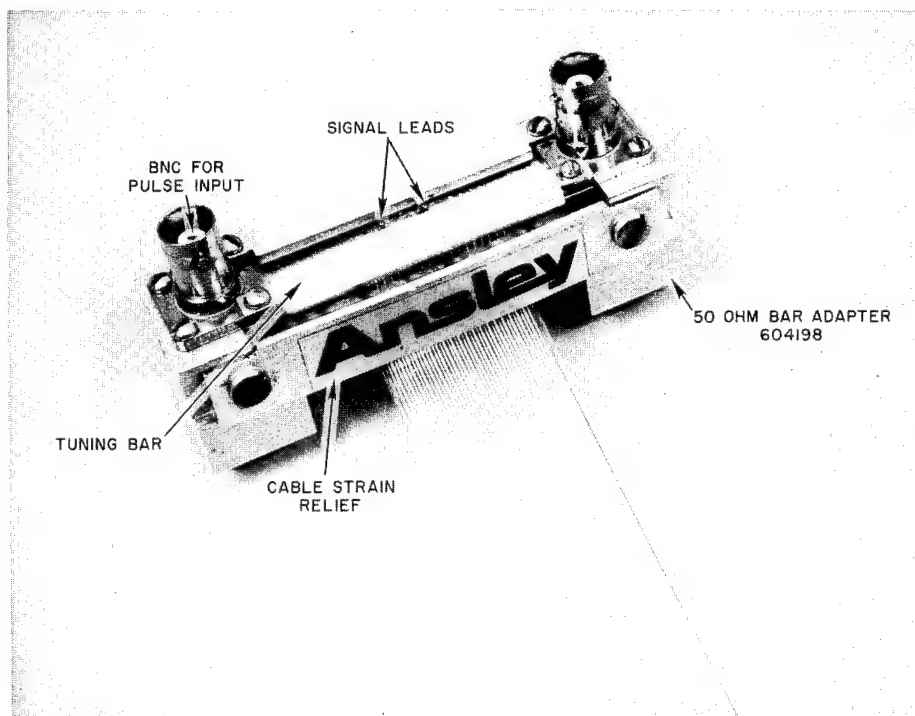


Figure 21.

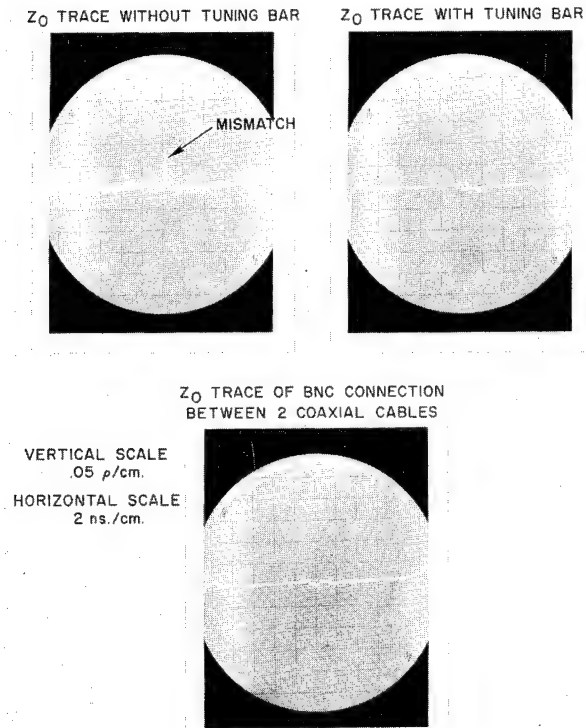


Figure 22. TUNING BAR COMPENSATION

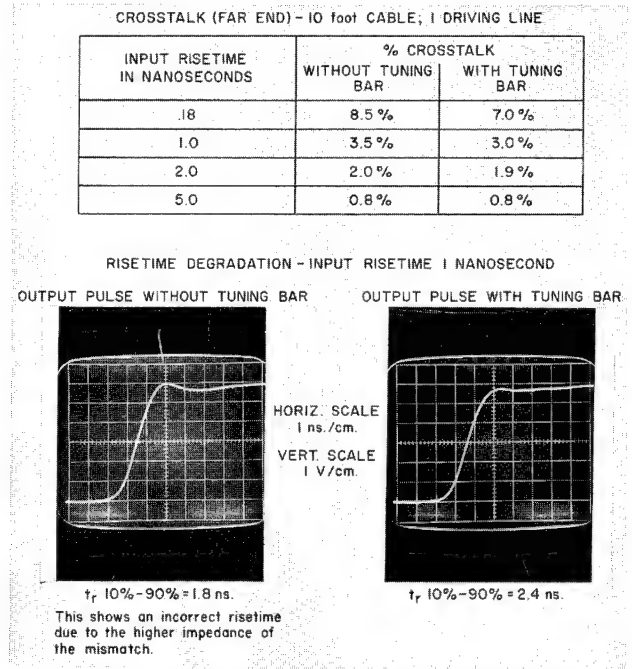


Figure 23. MISMATCH EFFECT ON CROSSTALK AND ATTENUATION

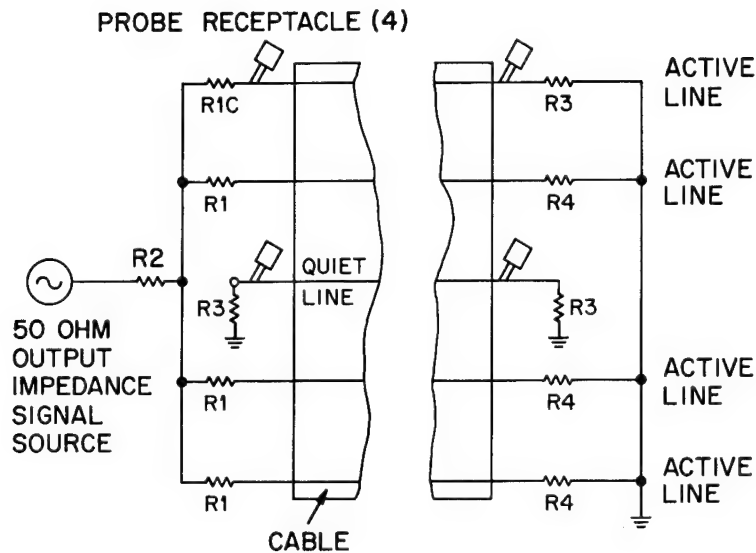


Figure 24. IMPEDANCE MATCHING TECHNIQUE

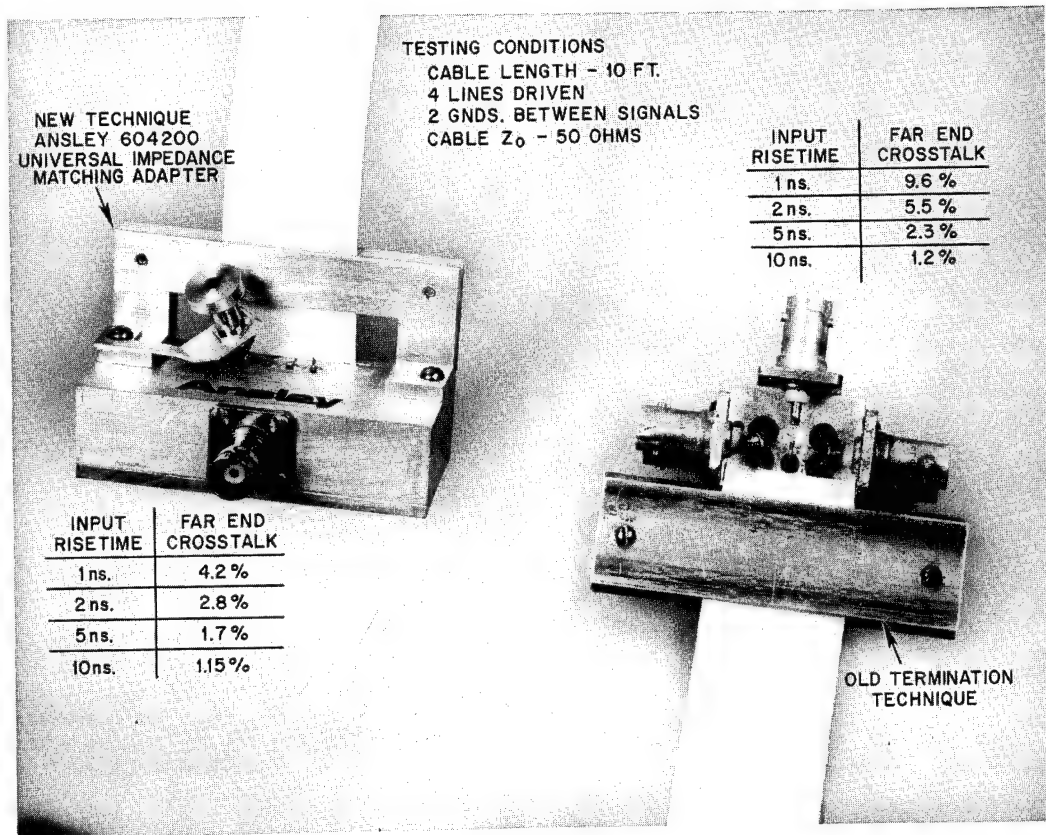


Figure 25. TERMINATION COMPARISON

"A" - RG 174, -50 ohm coaxial cable
 "B" - ANSLEY 50 ohm shielded flat cable
 "C" - ANSLEY 50 ohm standard flat cable
 "D" - Twisted pair, 52 ohm Belden 8745-100

Test conditions:
 Cable length - 25 feet
 Number of drive lines - 4
 Connector used - ANSLEY 650200

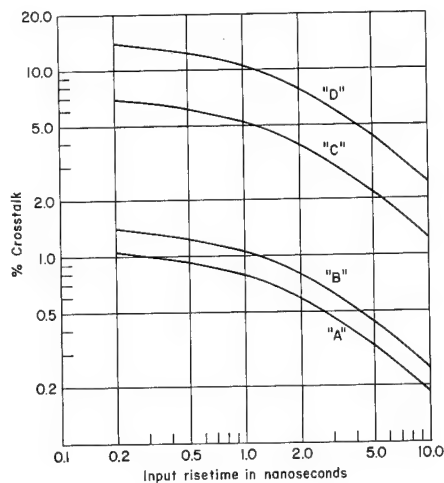


Figure 26. CROSSTALK COMPARISON

I = Input pulse (1ns., 10% to 90%)

A = RG 174 -50 ohm coaxial cable

B = ANSLEY 50 ohm shielded flat cable

C = ANSLEY 50 ohm standard flat cable

D = Twisted pair, 52 ohm Belden 8745-100 } cable length 25 feet

PULSE	MAX. SLOPE dv/dt	t _r 10%-60%
I	1.10	.55 ns.
A	.70	.95 ns.
B	.48	1.5 ns.
C	.30	2.6 ns.
D	.20	4.6 ns.

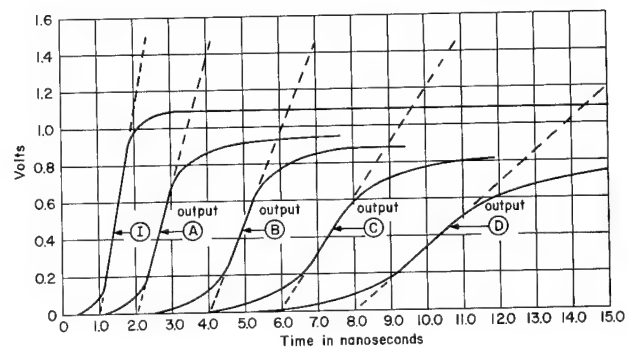


Figure 27. RISE TIME DEGRADATION COMPARISON

CHARACTERISTIC IMPEDANCE OF FLAT UNSHIELDED MULTI-CONDUCTOR CABLES

Surendra M. Verma and Paul E. Gamble

Burndy Corporation Tape Cable Division

Rochester, New York

Summary

Data for characteristic impedance of flat air-dielectric unshielded multi-conductor cables for any given conductor size and spacings is presented on the basis of a new theoretical equation derived for a basic module of three parallel coplanar round conductors in ground-signal-ground configuration. These results have been extended to cover flat conductors also. Comparison has been made with a large number of actual flat cables and the theoretical values are found very satisfactory.

Introduction

In recent years there has been a significant increase in the use of flat unshielded multi-conductor cables as multi-transmission line cables. In these applications, a single cable is used to transmit a number of signals over a set of signal conductors in the cable, the ground return being provided by separate conductors placed between the signal lines, (Fig. 1) these grounds being usually connected together at either end of the cable in the actual applications.

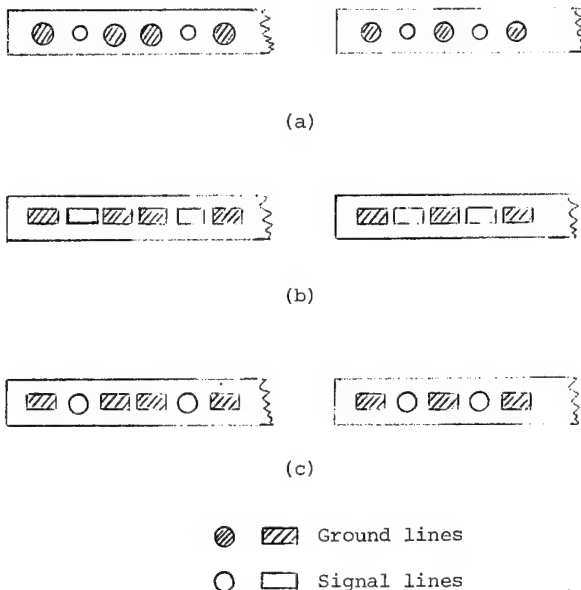


Fig. 1 Flat Cable Configurations

For any signal transmission application, the choice of a flat cable is governed by many considerations such as:

velocity of signal propagation,
extent of mutual interference between
neighboring signal lines,
levels of signal attenuation and distortion
over a line.

But, before any of the above mentioned characteristics are considered, the cable is required to have a specific characteristic impedance value between a signal line and the ground (formed by all the ground conductors connected together), in order to be compatible with the impedance levels of the system in which it is being used.

Therefore, it is of great importance to an unshielded flat cable designer or user to be able to predict the characteristic impedance of these cables from the physical parameters such as conductor size, inter-conductor spacing, cable thickness and the dielectric constant (s) of the insulating material(s) used. The prediction must take into account many features of the unshielded flat cables which are distinct from a normal two conductor transmission line such as a co-axial cable, e.g.

- a) Signal propagation takes place in the dielectric(s) of the cable insulation material(s) and the surrounding air. The effect of this on the characteristic impedance may be expressed by an effective dielectric constant ϵ_{eff} as follows:

$$Z = Z_0 \cdot 1/\sqrt{\epsilon_{eff}} \quad (1)$$

where Z and Z_0 are respectively the characteristic impedances in ohms of a signal line to ground in the actual cable configuration and in the same configuration with air as the only dielectric; ϵ_{eff} is some value between the relative dielectric constant values for air ($\epsilon_{air} = 1$) and the insulating material (ϵ_r). The magnitude of ϵ_{eff} depends upon the geometry of the cable and the type of insulation used.

- b) The signal and the ground conductors used may be round, flat or the one round and the other flat or vice versa (see Fig.1 (c)).

- c) A signal line in a flat cable has more than one ground return conductors

From equation (1) it follows that a complete solution to predict Z_0 will consist of two parts:

- d) Evaluation of Z_0 in the air dielectric for the given conductor size and spacings

- e) Evaluation of ϵ_{eff} when the conductors are encapsulated in a given insulation.

In this paper, a solution has been provided to the relatively easier problem of part (d) above i.e. prediction of Z_0 for a signal line in the flat cable configuration with only air dielectric. It is based on a new impedance equation derived originally for the round conductors flat cable and then extended to cover the case of flat conductors or a combination of flat and round conductors in the same cable. The results obtained have been found to yield Z_0 to a high degree of accuracy for round conductors and to a slightly lower accuracy for the flat conductors.

Derivation of Z_0 for Round Conductor Flat Cables

Consider a set of parallel co-planar lossless round conductors placed in air and forming a multi-transmission line cable with air dielectric. Let this cable be operated in the TEM mode of signal propagation, with all signal lines operating at the same potential. In such a cable, the characteristic impedance of any signal line can be related to the total capacitance C_0 between that line and all the ground conductors by the following equation

$$Z_0 = 120\pi / (C_0/\epsilon_0) \text{ ohms} \quad (2)$$

where $120\pi = 376.7$ ohms is the impedance of free space; ϵ_0 is the absolute permittivity of free space (2.7 pf/ft)

Thus (2) may be re-written as

$$Z_0 = 1017/C_0 \text{ ohms} \quad (3)$$

where C_0 is the capacitance value in pf/ft.

To develop an expression for C_0 and hence Z_0 we shall make the following assumptions:

- a) For each signal line the electric field is confined only to one neighbouring ground conductor on either side of the signal line and does not extend to the ground conductors beyond these.

- b) There is no inter-action between the fields due to the different signal lines.

These assumptions are not strictly accurate for the conductor spacings involved in flat cables. However, the results show that these assumptions may be made and still a satisfactory accuracy be obtained.

As a result of these assumptions, a flat cable may be considered to be made up of a number of co-planar three conductor modules each consisting of a signal conductor and two ground conductors, one on either side (See Fig.2).

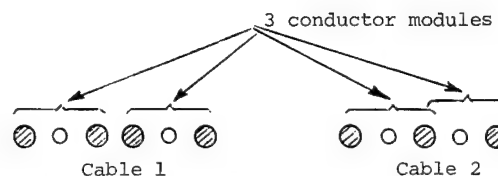


Fig. 2 Flat Cables as Series of 3 Conductor Modules

Having assumed this simplified model of a flat cable, C_0 of equations (2) or (3) then really becomes the capacitance between a signal conductor and the two grounds forming the basic module with it. We may now proceed to evaluate this C_0 as follows.

Let the three conductor transmission line module consist of cylindrical conductors A, B and A' placed with their centers at a distance S apart, with B as the signal line and A and A' as the returns (Fig.3). Let $D_1 = 2r_1$ and $D_2 = 2r_2$ be the diameters of A (and A') and B respectively.

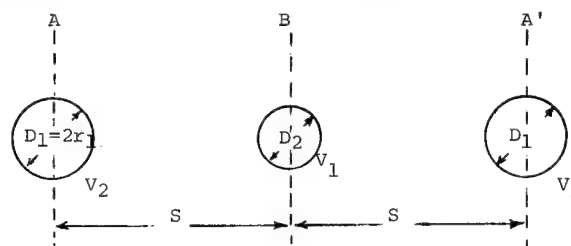


Fig. 3 Flat Transmission line with one Signal Line and Two Returns

Let the lines be charged with a charge $+Q$ on B and $-Q/2$ on each of A and A' giving rise to a potential V_1 on B and V_2 on A and A'. The potential surfaces of V_2 and V_1 are equi-potential cylinders.

Let us assume that it is possible to produce these equi-potential surfaces by replacing the charged lines by a set of line charges $-Q/2$, $+Q/2$, $+Q/2$ and $-Q/2$ located at points 1, 2, 2' and 3 respectively as shown in the Fig. 4 and such that the charges at 1 and 2 form one set of image charges, the other set being formed by the charges at 2' and 3.

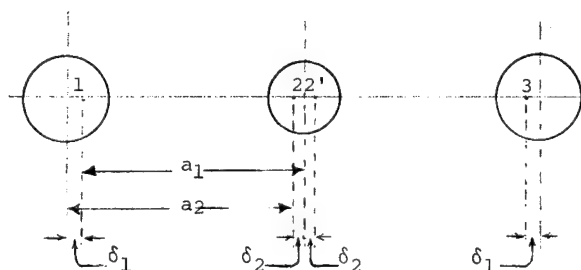


Fig.4 Distribution of Image Charges

With these two sets of image charges we can now derive the conditions for the existence of the equi-potential surfaces V_1 and V_2 and the mathematical expressions for the latter.

Consider a point p as shown in Fig.5. The potential at p may be written as follows; $R_{1x}, R_{2'x}, R_{2x}$ and R_{3x} in the equations are the distances of the line charges, 1, 2', 2 and 3 to a reference point x (not shown)

$$V_p = K \cdot \underbrace{\{\ln (R_{2x}/R_{2p}) - \ln (R_{1x}/R_{1p})\}}_{\substack{\text{Due to line charges} \\ \text{at 1 and 2}}} + K \cdot \underbrace{\{\ln (R_{2'x}/R_{2'p}) - \ln (R_{3x}/R_{3p})\}}_{\substack{\text{Due to line charges} \\ \text{at 2' and 3}}} \quad (4)$$

where $K = Q/2 \cdot (2\pi \cdot \epsilon_0)$

This simplifies to

$$V_p = K \cdot \{\ln (R_{2x}/R_{1x}) \cdot (R_{1p}/R_{2p})\} + K \cdot \{\ln (R_{2'x}/R_{3x}) \cdot (R_{3p}/R_{2'p})\} \quad (5)$$

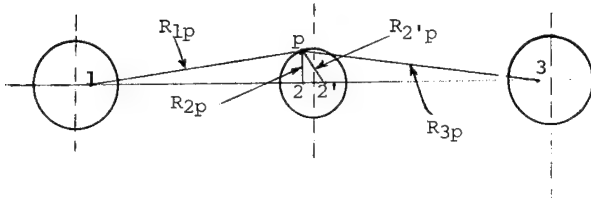


Fig.5 For Finding Potential at any point p on the Signal Line Boundary

Now, let the reference point x move to infinity, then R_{2x}/R_{1x} or $R_{2'x}/R_{3x}$ approaches 1 and (5) simplifies to

$$V_p = K \cdot \{\ln (R_{1p}/R_{2p}) + \ln (R_{3p}/R_{2'p})\} \quad (6)$$

If p is to be a point on an equi-potential surface of radius r_2 (i.e. coinciding with the boundary of conductor B), V_p should be constant for all positions of p on the boundary A. This can be achieved if in each set the image charges are placed at the inverse points, for then

$$R_{1p}/R_{2p} = R_{3p}/R_{2'p} = a_2/r_2 \quad (7)$$

which makes equation (6) independent of the position of p . The implication then is that each set of image charges produces an equi-potential cylinder of radius r_2 and the superimposition of the two results in the cylindrical surface of equi-potential V_1 .

With these substitutions in (6), V_p becomes V_1

$$V_1 = 2K \cdot \ln (2a_2/D_2) \quad (8)$$

Now, consider a point q as shown in Fig. 6

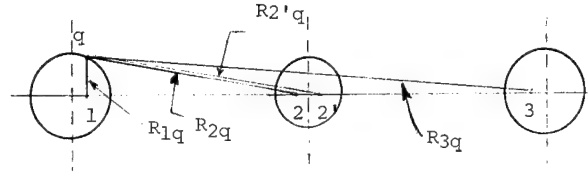


Fig.6 For Finding Potential at Any Point q on a Return Line

Then following the same reasoning as above, we can write

$$V_q = K \cdot \underbrace{\ln (R_{2q}/R_{1q})}_{\substack{\text{Due to charges} \\ \text{at 1 and 2}}} - K \cdot \underbrace{\ln (R_{2'q}/R_{3q})}_{\substack{\text{Due to charges} \\ \text{at 2' and 3}}} \quad (9)$$

Again, if the point q is to lie anywhere on an equi-potential surface of radius r_1 (i.e. coinciding with the boundary of conductor A) V_q should be constant for all positions of q on the boundary A. Since the image charges in each set are at the inverse points, we obtain $R_{2q}/R_{1q} = a_1/r_1$ which makes the first term on the right hand side of (9) a constant. To make the second term also a constant let us further make the assumption that $R_{2'q}/R_{3q} = \frac{1}{2}$. The validity of this approximation increases if the line charges (conductors in the actual cable) are widely apart.

Actually only charges at 1 and 2 can produce a cylindrical equi-potential surface of radius r_1 coinciding with the boundary of A. The set of charges at 2' and 3 cannot produce this cylindrical surface. However, by making the assumption $R_{2'q}/R_{3q} = \frac{1}{2}$ we have implied that 2' and 3 contribute only a fixed potential, which is added at all points to the equi-potential cylinder of radius r_1 due to charges 1 and 2, resulting in the equi-potential cylindrical surface of a potential V_2 .

With these substitutions in (9), V_q becomes V_2

$$V_2 = -2K \cdot \ln (a_1/D_1) \quad (10)$$

Therefore, the potential difference $V_1 - V_2$ is given by

$$V_m = V_1 - V_2 = 2K \cdot \ln \left\{ (a_1/D_1) \cdot (2a_2/D_2) \right\} \quad (11)$$

Now a_1 and a_2 can be evaluated by using the following relationships:

$$\begin{aligned} a_2 + \delta_1 &= S \\ a_1 + \delta_2 &= S \\ a_2 \delta_2 &= r_2^2 \\ a_1 \delta_1 &= r_1^2 \end{aligned} \quad (12)$$

The last two relations follow from the fact that points 1 and 2 (as 2' and 3) are the inverse points.

From (12) we can derive

$$\begin{aligned} a_1 - a_2 &= (r_1^2 - r_2^2)/S = (D_1^2 - D_2^2)/4S \\ a_1 + (r_2^2/a_2) &= S \\ a_2 + (r_1^2/a_1) &= S \end{aligned} \quad (13)$$

which gives

$$\begin{aligned} a_1 + (D_1^2/4a_1) &= S + (D_1^2 - D_2^2)/4S \\ a_2 + (D_2^2/4a_2) &= S - (D_1^2 - D_2^2)/4S \end{aligned} \quad (14)$$

from which a_1 and a_2 can be evaluated.

If all conductors are of the same size i.e. $D_1 = D_2 = D = 2r$ then $\delta_1 = \delta_2 = \delta$, $a_1 = a_2 = a$ and (11) becomes:

$$V_m = 2K \ln\{(a/D)^{1/2} \cdot (2a/D)\} \quad (15)$$

We may now calculate the capacitance C_0 and the impedance Z_0 of this 3-conductor module as follows:

$$\begin{aligned} C_0 &= Q/V_m \\ &= 2\pi \epsilon_0 / \ln\{(a_1/D_1)^{1/2} \cdot (2a_2/D_2)\} \end{aligned} \quad (16)$$

and

$$\begin{aligned} Z_0 &= 120\pi / (C_0/\epsilon_0) \text{ ohms} \\ &= 60 \ln\{(a_1/D_1)^{1/2} \cdot (2a_2/D_2)\} \text{ ohms} \end{aligned} \quad (17)$$

Adopting the notation

$D_g = D_1$ = Diameter of the ground conductor
 $D_s = D_2$ = Diameter of the signal conductor

We may re-write (17) as;

$$Z_0 = 60 \ln\{(a_1/D_g)^{1/2} \cdot (2a_2/D_s)\} \text{ ohms} \quad (18)$$

For equal size conductors $D_g = D_s = D$, $a_1 = a_2 = a$ and

$$Z_0 = 60 \ln\{(a/D)^{1/2} \cdot (2a/D)\} \text{ ohms} \quad (19)$$

Z_0 Graphs For Round Conductors

Using the equation (18), a set of impedance graphs has been drawn for the basic 3-conductor modules. The modules considered are of the type in which

- 1) the two ground conductors are of the same size
- 2) the ground conductor diameter D_g is either equal to or greater than the signal conductor diameter D_s .

The normalised impedance graphs of Fig. 7 & 8 give Z_0 vs. S/D_g , where S is the pitch, i.e. the center to center distance between two adjacent conductors. These figures consist of 10 curves, each drawn for a specific D_s/D_g ratio, such as 1, 0.89, 0.8 ... 0.31. All of these ratios are

so chosen that each corresponds to a certain specific AWG step difference between the ground and the signal conductors; e.g. the first curve for $D_s/D_g = 1$ implies same AWG size for the grounds and the signal, the next curve is for the ratio 0.89 and corresponds to one AWG size difference between the grounds and the signal, for example 30 AWG grounds and 31 AWG signal; $D_s/D_g = 0.8$ similarly stands for a two AWG's size difference between the grounds and the signal e.g. 30 AWG ground and 32 AWG signals.

Impedance graphs for a few commonly used wire sizes are also drawn directly in terms of pitch. Thus, Figs. 9, 10, 11 cover the cases of modules made with ground conductors of AWG's 30, 31 and 32 respectively and the signal lines with the same and higher AWG numbers.

Extension To Flat Conductors

Analytically, a flat conductor is not so easy to solve as a round conductor. A flat conductor has points of singularity at every re-entrant corner and simple equations of the type used to describe the field due to a cylindrical conductor are not available in its case. The easier way then is to somehow make use of the round conductors equation (18) for the flat conductors also. This can be done if for any given flat conductor we can think of an equivalent round conductor, such that for a given pitch the flat conductors or their equivalent rounds would both give the same Z_0 . Thus, in terms of the equivalent round conductor grounds and signal, the equation (18) becomes;

$$Z_0 = 60 \ln\{(a_1/D_{g\text{eq}})^{1/2} \cdot (2a_2/D_{s\text{eq}})\} \text{ ohms} \quad (20)$$

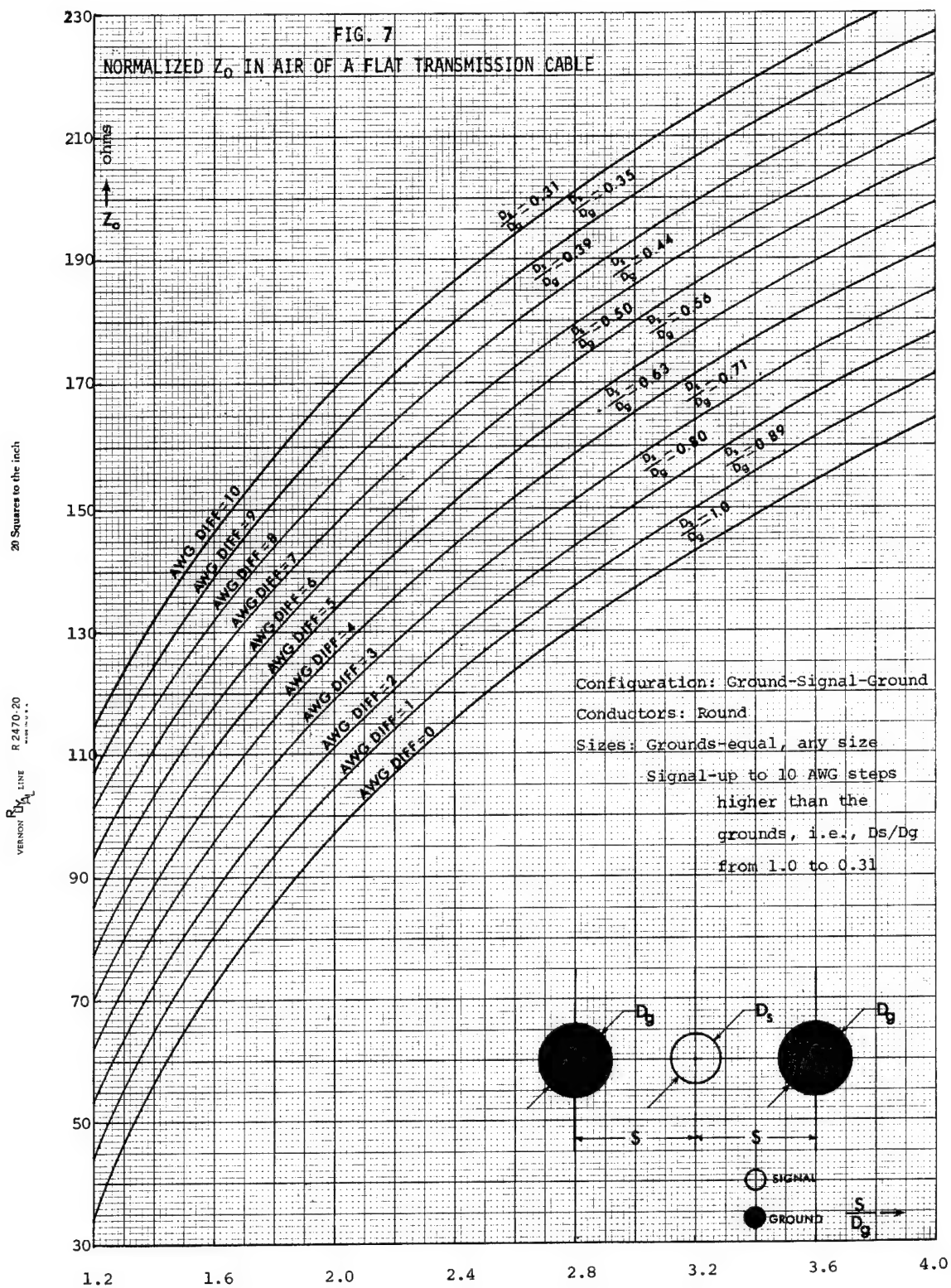
where $D_{g\text{eq}}$ and $D_{s\text{eq}}$ are the diameters of the equivalent round ground and signal conductors, respectively.

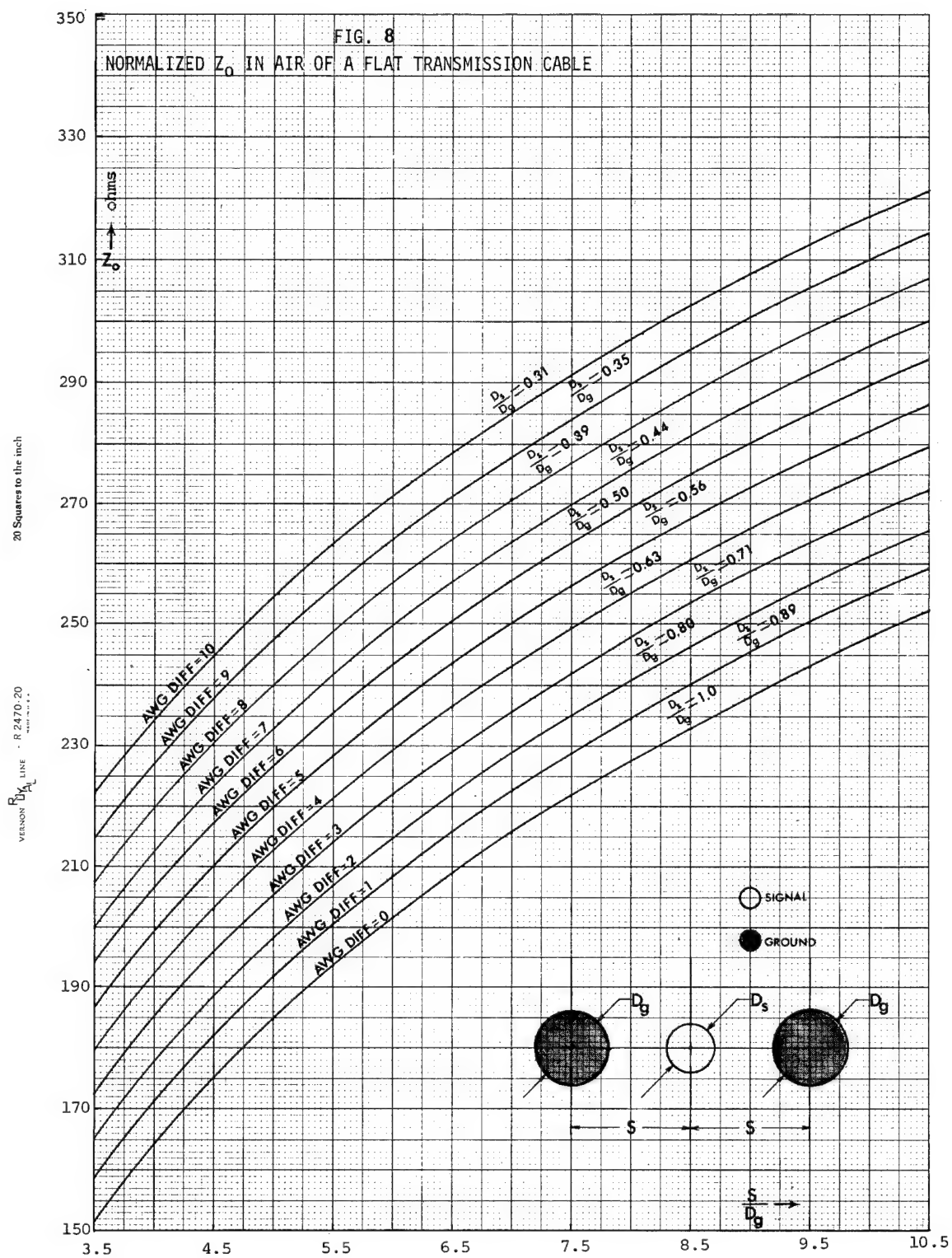
The concept of an equivalent round conductor for a given flat conductor to yield the same characteristic impedance is by no means new. Such flat-round equivalence has been studied by Marcuvitz¹ and Flammer² and has been used for predicting Z_0 of a strip transmission line with flat conductors from the values of a line with round conductors³.

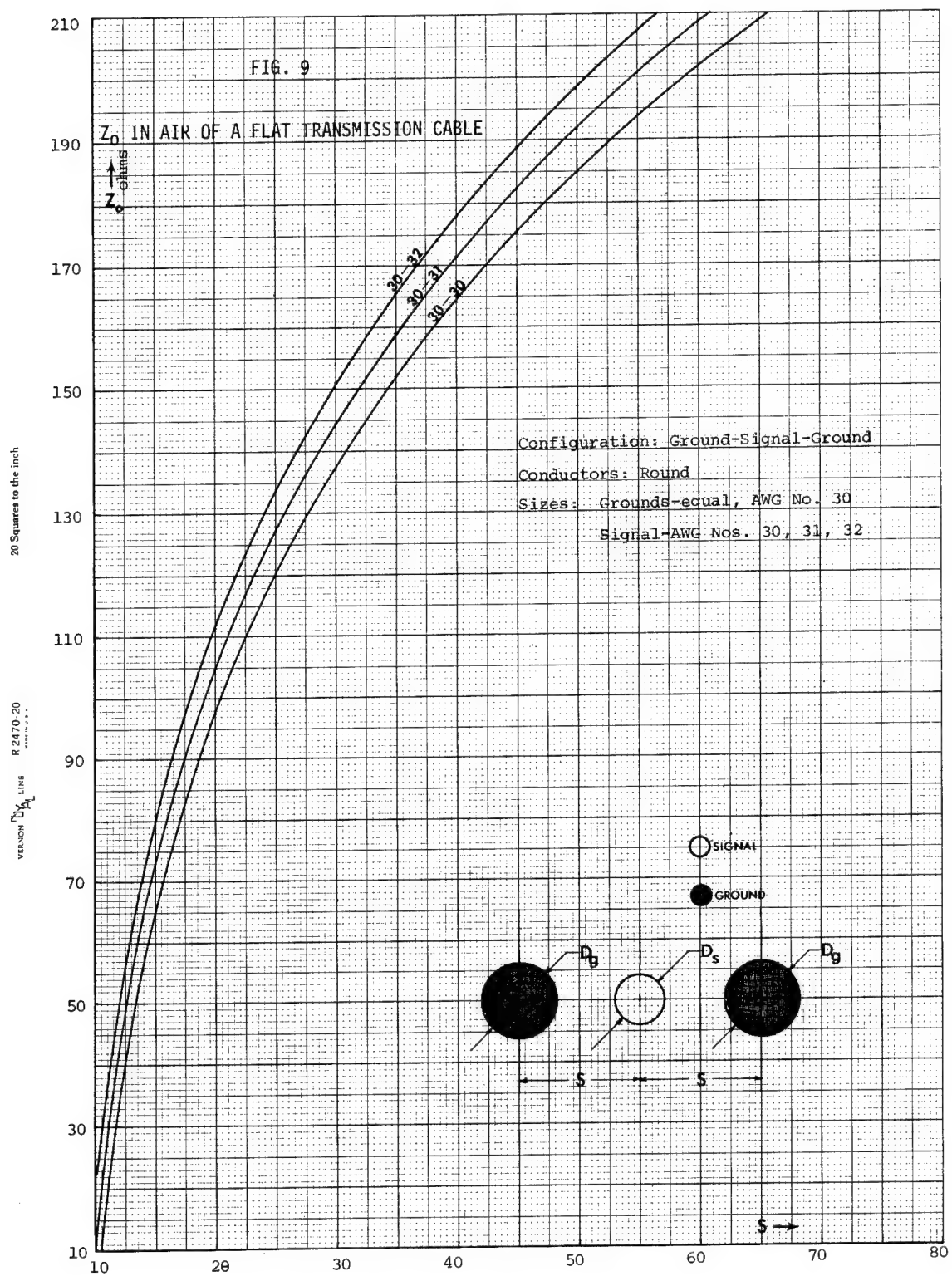
In the present case of the unshielded multi-conductor flat cables, it was decided to try the same equivalence relationship which is represented by Fig. 12.

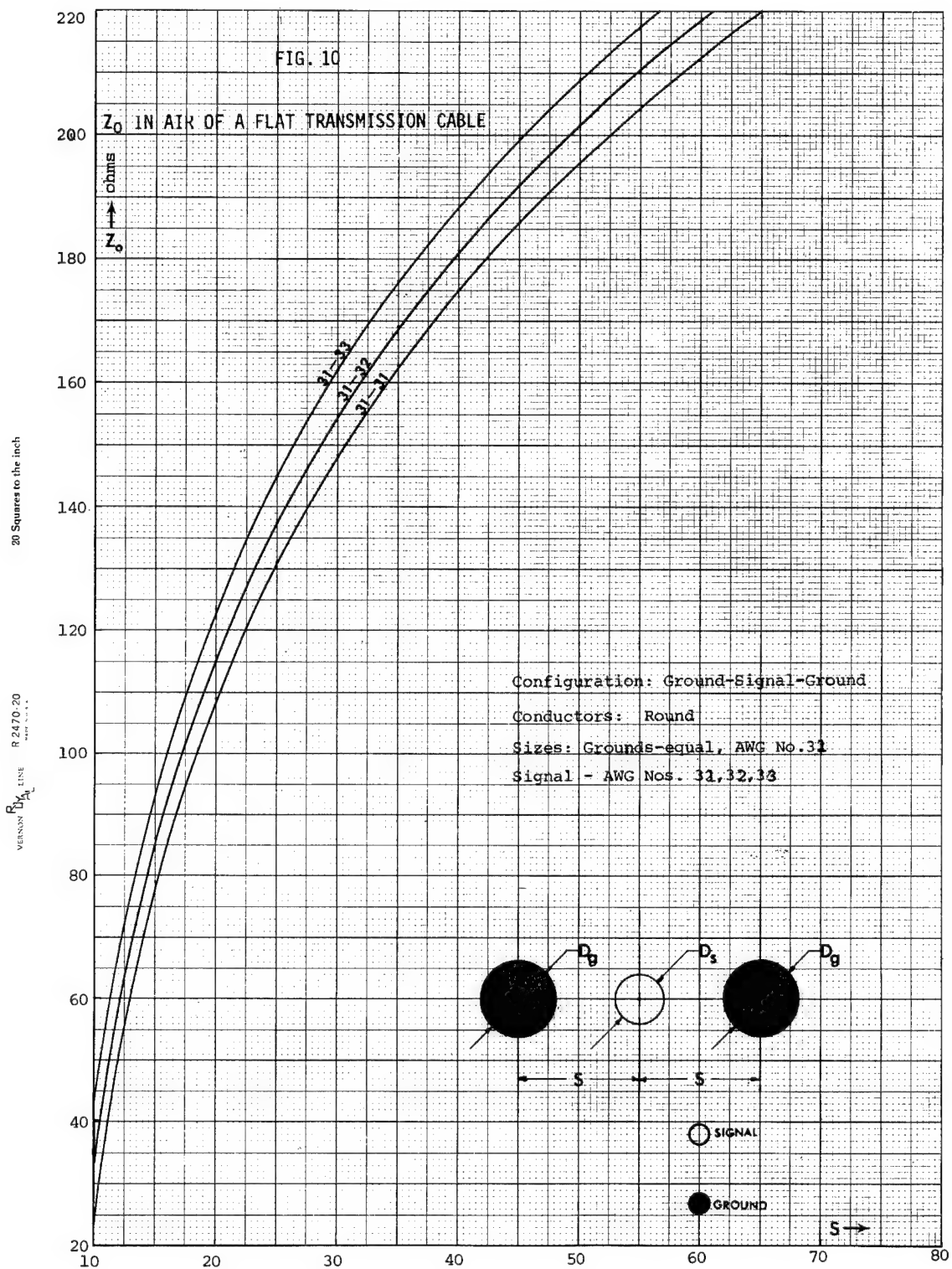
According to this the equivalent round conductors for a few commonly used flat conductors are shown in Table 1.

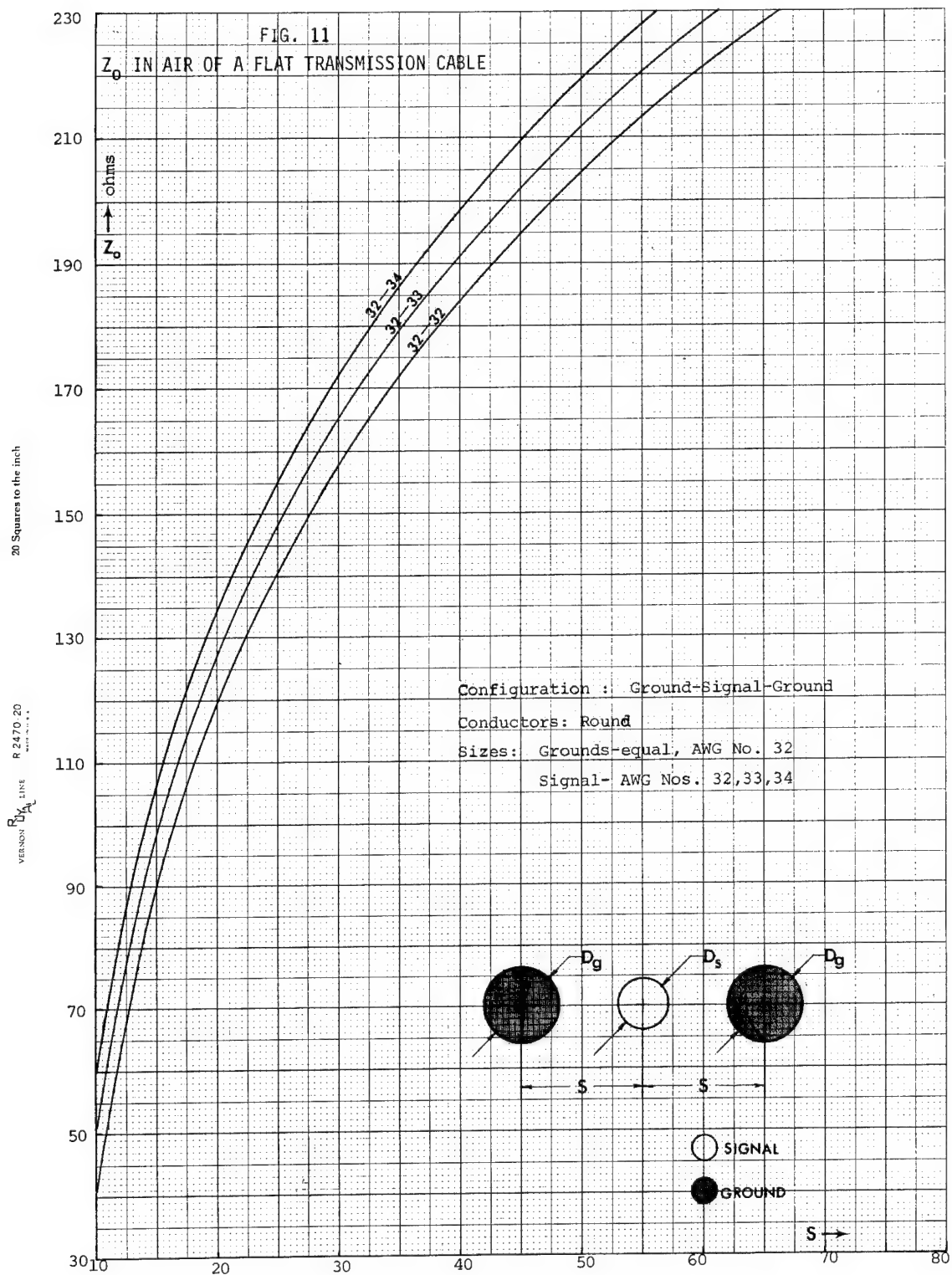
For flat conductor sizes not indicated in Table 1, the graph of Fig. 12 may be used to obtain the equivalent round conductor diameters. Fig. 12 and Table 1 both give the flat conductor sizes in terms of the ratio width/thickness (W/t). The equivalent round conductor is obtained in terms of the equivalent round conductor diameter per unit flat conductor width (D_{eq}/W). Thus, for a given flat conductor size, the quantity D_{eq}/W must be multiplied by the flat conductor width to obtain the D_{eq} .











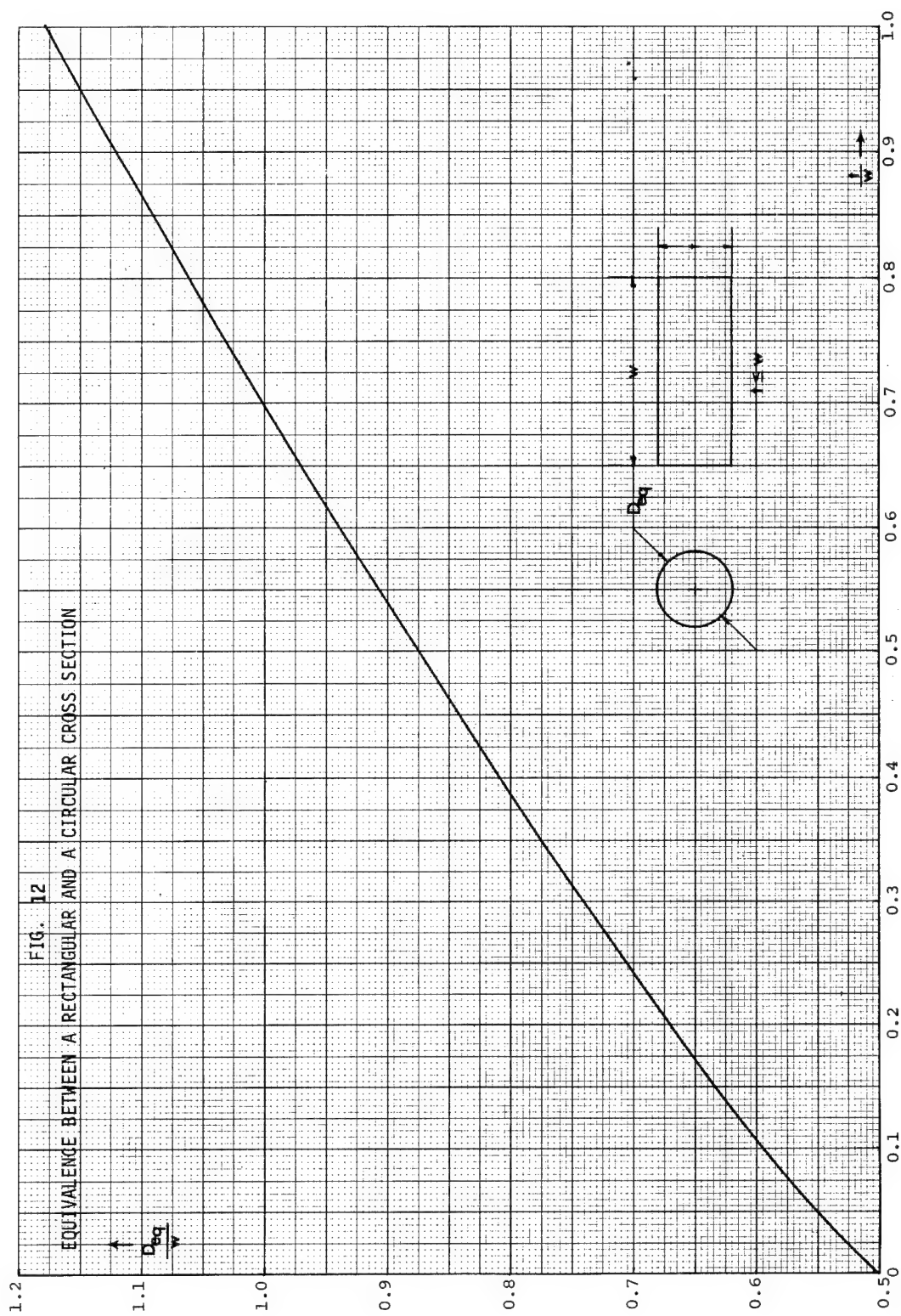
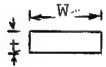


TABLE I

EQUIVALENT ROUND CONDUCTOR DIAMETERS

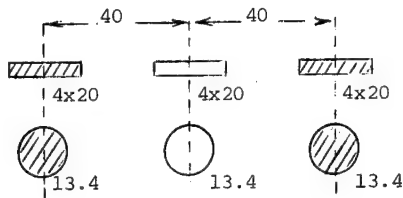
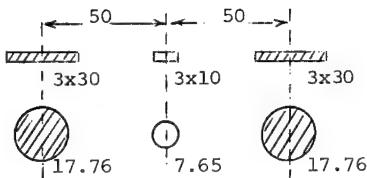
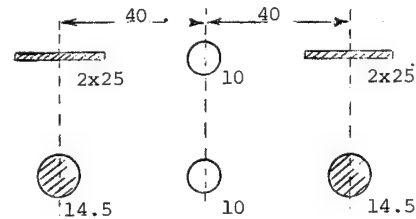
FOR A FEW FLAT CONDUCTOR SIZES

FLAT CONDUCTORS EQUIVALENT ROUND CONDUCTORS

RATIO $W:t$ D_{eq}/W 

1:1	1.18
3:1	0.76
4:1	0.71
5:1	0.67
6.25:1	0.64
8:1	0.615
10:1	0.592
12.5:1	0.58
16:1	0.56
20:1	0.55
25:1	0.54
32:1	0.53

Examples of flat-round equivalence. The use of Fig. 12 and Table I is illustrated by the following examples of conversions of flat conductor modules to their equivalent rounds. In the figures given below the flat conductor sizes are in terms of thickness x width and the equivalent round conductors are shown by their diameters. All values indicated are in mils.

Case 1Case 2Case 3

shaded conductors - grounds
unshaded conductors - signals

Fig. 13 Flat-Round Conversions

 Z_0 Curves For Flat Conductors

Using the equivalence values of Table I and the impedance graphs of Fig. 7 and 8, a set of curves has been drawn in Figs. 14 and 15 to give Z_0 in air of 3-conductor modules using three equal flat conductors of various width/thickness ratios. The Z_0 values are given in terms of the ratios pitch/conductor width.

For cases where a module uses different size flat conductors for the grounds and signal lines or has a combination of round and flat conductors, an equivalent round conductor module can first be derived and then an appropriate D_s/D_g curve of Figs. 7 and 8 used to obtain Z_0 for the particular value of S/D_g .

Examples: The above ideas can now be applied to the cases 1, 2 and 3 of the previous section.

Case 1 Here $S/W = 2$ and from Fig. 14
 $Z_0 = 137$ ohms.

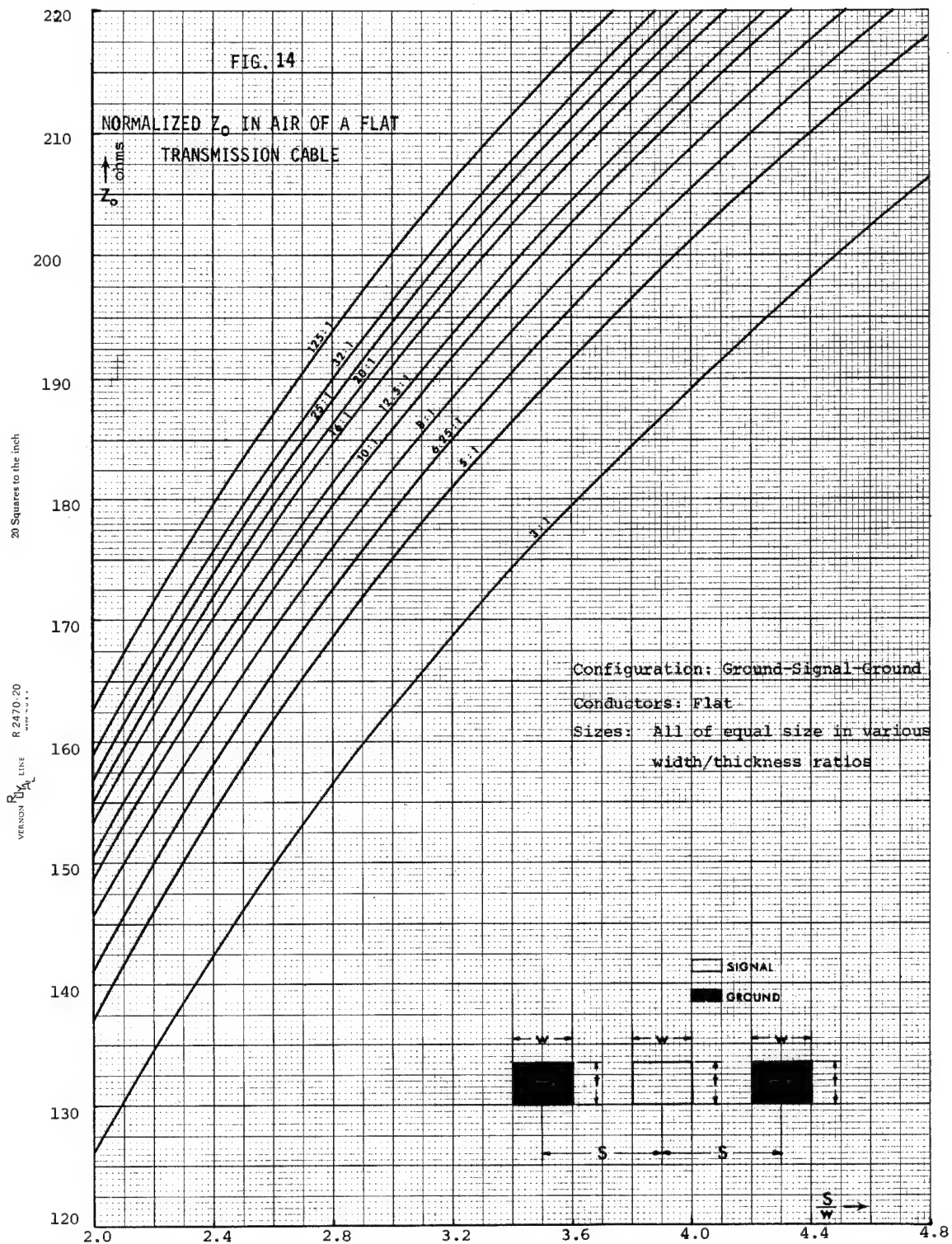
Case 2 From the equivalent round conductor module, we obtain $S/D_g = 2.82$ and $D_s/D_g = 0.43$. In Fig. 7 we do not have a Z_0 curve for this ratio of D_s/D_g , however, we may use the curve for the nearest ratio 0.44 and obtain $Z_0 = 180$ ohms.

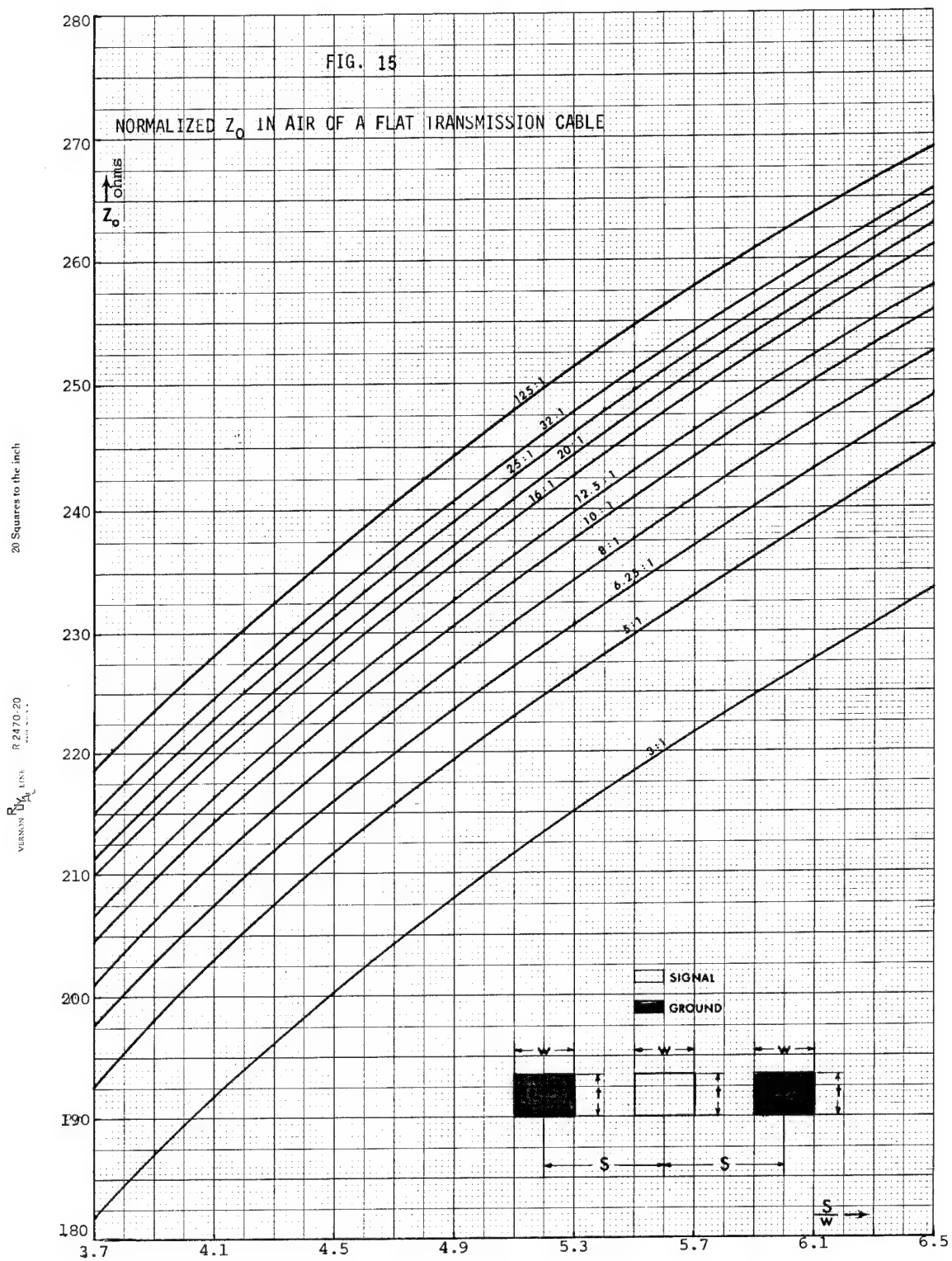
Case 3 As in case 2, we have here $S/D_g = 2.78$ and $D_s/D_g = 0.69$. Using the nearest $D_s/D_g = 0.71$ curve, we estimate Z_0 to be approximately 154 ohms.

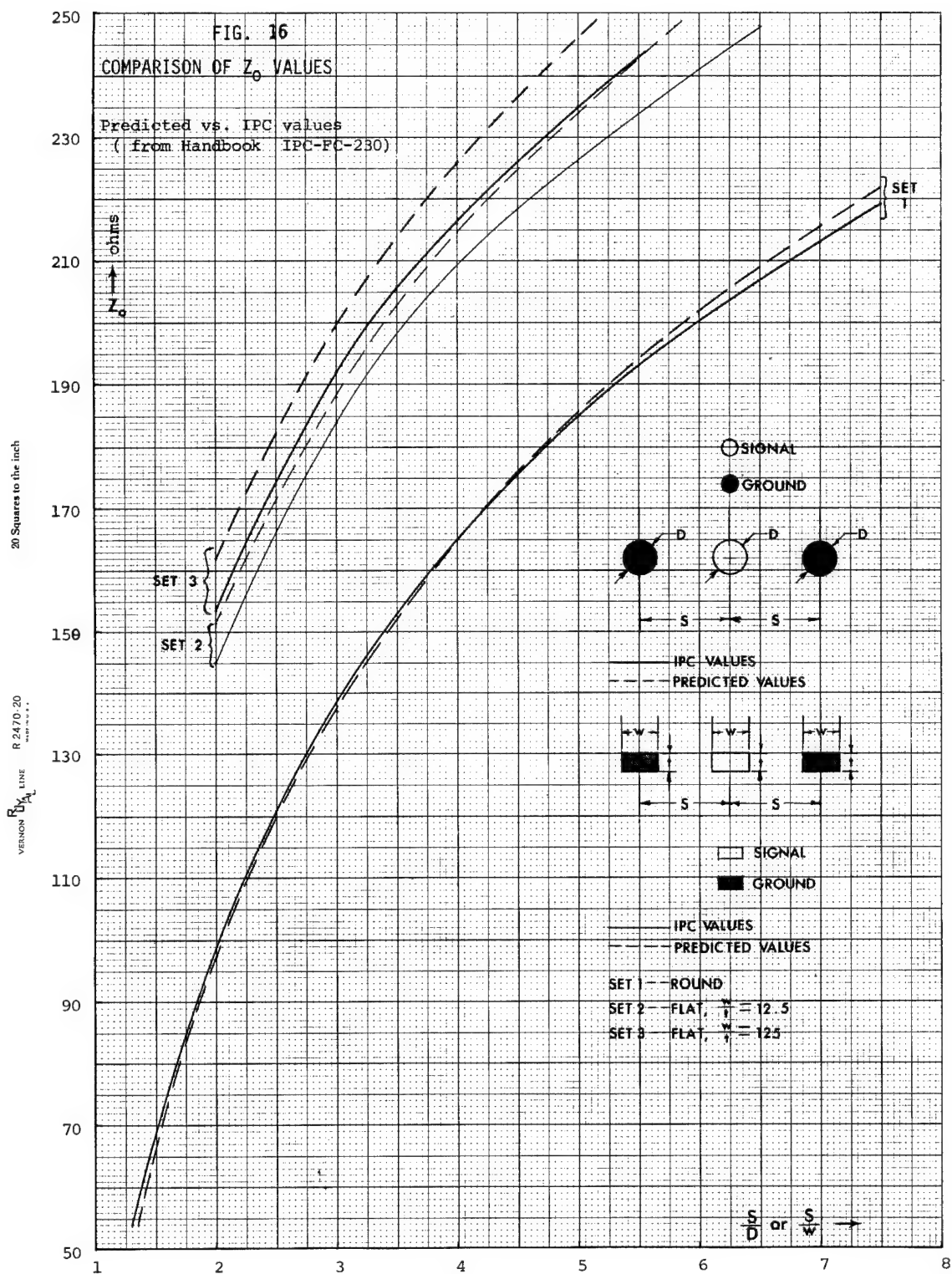
Verification

A comparison of the impedance values in air predicted by the equation (18) with the values obtained from other sources for identical conductor configurations is presented in Fig. 16 and Tables 2A and 2B.

The Fig. 16 shows the predicted Z_0 curves for the flat and round conductor configurations







vs. the empirical curves for the same configurations given in the "Proposal Handbook of Flat Conductor Cable and Flexible Printed Wiring," IPC-FC-230, pp. 54, April, '69.

Tables 2A and 2B show predicted Z_0 vs. average Z_0 calculated from measurements on a few actual multi-conductor flat cables with ground and signal conductors arranged in configurations of Fig. 1. The latter Z_0 values from the actual cables were obtained only indirectly by making the following two measurements with a time domain reflectometer:

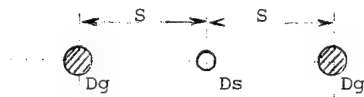
Characteristic impedance Z of actual cable and ϵ_{eff} of the insulation by measuring the velocity of signal propagation through the cable.

The calculated values of Z_0 are accurate to only ± 2 ohms.

TABLE 2A

COMPARISON OF PREDICTED Z_0
WITH Z_0 OBTAINED FROM ACTUAL

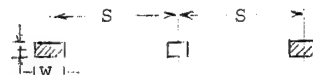
ROUND CONDUCTOR CABLES



S	Dg	Ds	Predicted Z_0	Computed from measured Z and ϵ_{eff}
mils	mils	mils	ohms	ohms
25	10	10	89	88
30	10	10	98	93
125	12.6	12.6	175	172
25	8	8	104	103
125	8	8	176	170
25	10	7.1	141	135
13	10	7.1	74	75
50	10	10	132	125

TABLE 2B

COMPARISON OF PREDICTED Z_0
WITH Z_0 OBTAINED FROM ACTUAL
FLAT CONDUCTOR CABLES



S	t x w (grounds)	t x w (signal)	Predicted Z_0	Computed from measured Z and ϵ_{eff}
mils	mils	mils	ohms	ohms
40	4x20	4x20	137	136
60	3x26	3x26	155	152
50	3x30	3x10	180	188
50	3x30	3x20	160	148
175	7x114	7x114	124	122
183	16x133	16x133	110	100

From the comparison data presented it may be observed that

- 1) For the round conductors the predicted Z_0 is within 5% of the empirical values of Fig. 16 or the calculated values of Table 2A.
- 2) For the flat conductors, the predicted Z_0 is not so accurate as in the case of the round conductors. This is to be expected since the flat-round equivalence is not exact. However, in most cases, the prediction is within 10% of the empirical or the calculated values.
- 3) From the empirical curves of Fig. 16, the % accuracy in prediction is observed to be very good for the higher S/Dg or S/W ratios and worsens as these ratios approach 1. This is due to the fact that the approximations used in the derivation of equation (18) are no longer valid as S/Dg approaches 1.

Conclusions

The characteristic impedance of multi-transmission line flat cables with air dielectric may be readily obtained by using the data presented in this paper. The basic impedance equation (18) derived for the round conductors and its extension

to flat conductors using the concept of flat-round equivalence may be applied to all conductor sizes and spacings and values obtained to an accuracy useful to the flat cable designer and user.

Acknowledgment

The authors wish to thank S.D. Bergman for his encouragement and help throughout the preparation of this work.

In addition, appreciation is extended to M.A. Fetcie for preparing illustrations for this paper.

References

- (1) N. Marcuvitz, "Waveguide Handbook" McGraw Hill, pp. 263-265; 1951.
- (2) C. Flammer, "Equivalent radii of thin cylindrical antennas with arbitrary cross-sections", Stanford Research Institute Technical Report, March 15, 1970
- (3) S.B. Cohn "Problems in Strip Transmission Lines", IRE Trans. Microwave Theory and Techniques, Vol. MTT-3, pp. 119-126; March 1955.

FOREWORD: This last decade, a great amount of engineering and design effort has been put into the electronic packaging art. Miniaturization of equipment and components has resulted in a significant improvement in reliability, together with a drastic reduction of hardware weight. However, the wiring and interconnecting devices are basically what they were some twenty years ago, and in complex systems the weight of the cable harness represents often more than 50% of the weight of the installed system. It is surprising to note that no more research and development has been devoted to improve this situation. In this paper, it is suggested that there is a possibility to use a wiring system that offers significant advantages over conventional wiring namely smaller volume, lighter weight, reduced cross talk, greater flexibility, higher tensile strength and error free installation.

0. INTRODUCTION.

The present study discloses a new concept of aircraft wiring based upon the use of the already well known flat cables, associated with special connectors and a so called "matrix box", the theory of which is developed hereafter.

The combination of these three elements enables a complete new way of wiring an aircraft with the following main advantages :

- wiring simplification
- increased flexibility
- weight saving
- volume reduction
- versatility
- better protection from the environment
- testability
- engineering efficiency
- improved maintainability.

1. THEORY OF THE INTERCONNECTION MATRIX.

Let A B C D be the elements of a system to be interconnected.

Let $a_1 \dots a_n$ be the terminals of element A

$b_1 \dots b_k$ be the terminals of element B

$c_1 \dots c_l$ be the terminals of element C

$d_1 \dots d_m$ be the terminals of element D.

The matrix can be established very easily if it is known what signal corresponds to each terminal in an unambiguous and well-defined manner.

It is not important to know which terminal is the source of a voltage or current and which ones are the receivers, since all that matters in an interconnection system is to establish a common line between terminals.

By this method, it is even possible to program a machine that will find the common terminals of a system composed of a determined number of elements and to foresee the possibility of optimum cable length by operational research.

Let us suppose for example that we have a listing of signals and terminals that have been established randomly.

LISTING OF SIGNALS.

a ₁ - VG Roll (X)	b ₁ - VG Roll (Z)
a ₂ - VG Roll (Y)	b ₂ - 28 Volt DC (-)
a ₃ - VG Roll (Z)	b ₃ - Signal (M)
a ₄ - 28 Volt DC (+)	b ₄ - Signal (K)
a ₅ - 28 Volt DC (-)	b ₅ - Signal (L)
a ₆ - Signal (K)	b ₆ - 28 Volt DC (+)
a ₇ - Signal (L)	b ₇ - Signal (N)
a ₈ - Signal (M)	b ₈ - Ground
a ₉ - Signal (N)	b ₉ - VG Roll (X)
a ₁₀ - Ground	b ₁₀ - VG Roll (Y)
c ₁ - Signal (M)	d ₁ - VG Roll (Y)
c ₂ - Signal (N)	d ₂ - VG Roll (X)
c ₃ - Signal (L)	d ₃ - Ground
c ₄ - 28 Volt DC (+)	d ₄ - Signal (N)
c ₅ - VG Roll (Z)	d ₅ - VG Roll (Z)
c ₆ - 28 Volt DC (-)	d ₆ - Signal (K)
c ₇ - Signal (K)	d ₇ - 28 Volt DC (-)
c ₈ - Ground	d ₈ - Signal (N)
c ₉ - VG Roll (X)	d ₉ - Signal (L)
c ₁₀ - VG Roll (Y)	d ₁₀ - VG Roll (Y)

From the listing, a matrix can be established, in which the lines represent the terminals that have to be interconnected by a common line. The columns represent the terminals of each element, that are involved in the interconnection.

ELEMENTS COMMON LINES	A		B		C		D	
	a ₁	a ₁₀	b ₁	b ₁₀	c ₁	c ₁₀	d ₁	d ₁₀
1	a ₁		b ₉		c ₉		d ₂	
2	a ₂		b ₁₀		c ₁₀		d ₁ d ₁₀	
3	a ₃		b ₁		c ₅		d ₅	
4	a ₄		b ₆		c ₄			
5	a ₅		b ₂		c ₆		d ₇	
6	a ₆		b ₄		c ₇		d ₆	
7	a ₇		b ₅		c ₃		d ₉	
8	a ₈		b ₃		c ₁			
9	a ₉		b ₇		c ₂		d ₄ d ₈	
10	a ₁₀		b ₈		c ₈		d ₃	

The SIMPL solution is provided by the materialization of the matrix in an interconnection box, and by joining the elements A B C D to the interconnection box with parallel geometry lines.

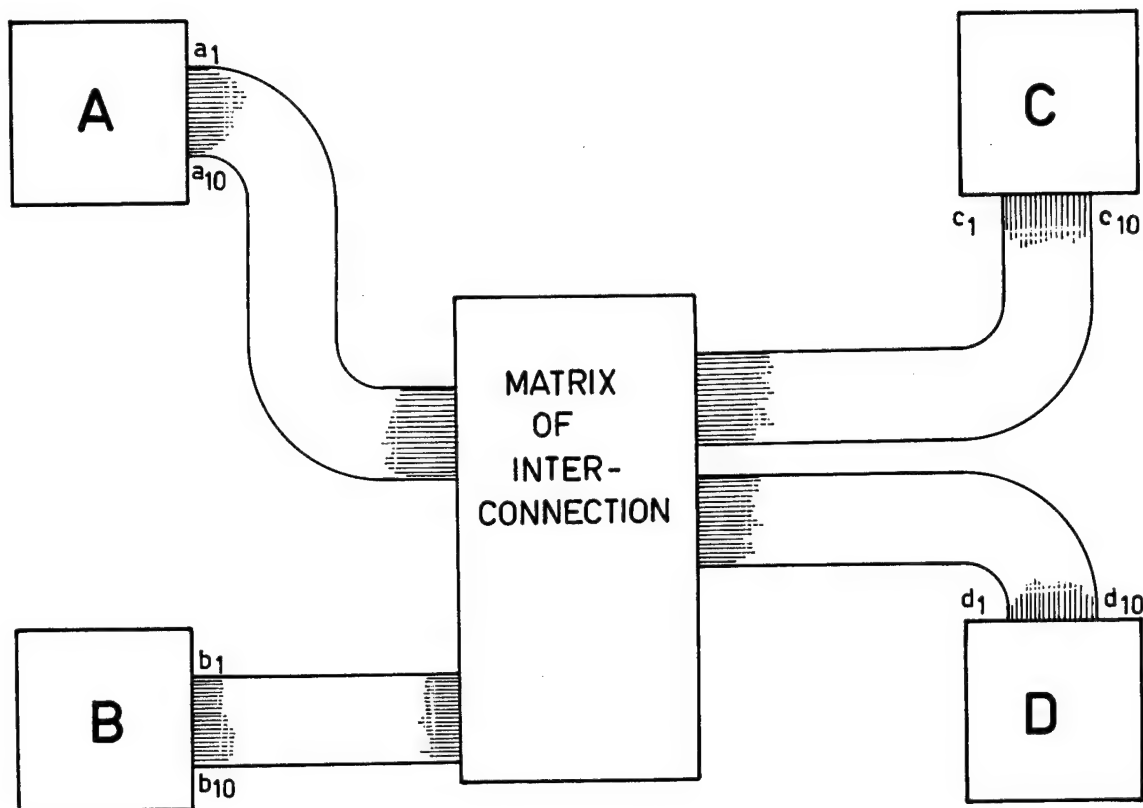


Fig. 1.1

In this manner, there are only rectilinear segments of lines between boxes. The parallel line geometry of the cables eliminates the necessity of numbering the wires.

In order to materialize the matrix, the interconnections that are the lines of the matrix, are transposed on a printed circuit board, double face.

The whole wiring diagram is now concentrated on the small surface of the printed circuit, leaving outside a parallel geometry, simple to implement as shown in fig. 1.1.

Everything happens as if we had scanned through the wiring with a comb, going from A, B, C, D to the center. The resulting group of knots represents the wiring diagram that can be replaced by the printed circuit board. This board becomes the element that "links" the parallel lines among them in accordance with a pre-established program or "matrix".

In fig. 1.2. we have shown the conventional diagram and the resulting cable harness. On the left of fig. 1.3. we have shown the equivalent circuit using flat cables. But in order to make the printed circuit a plug-in module, it is more practical to bring the three connectors in line by rotating the two side connectors by 90 degrees as shown on the right.

CONVENTIONAL DIAGRAM AND AIRCRAFT HARNESS

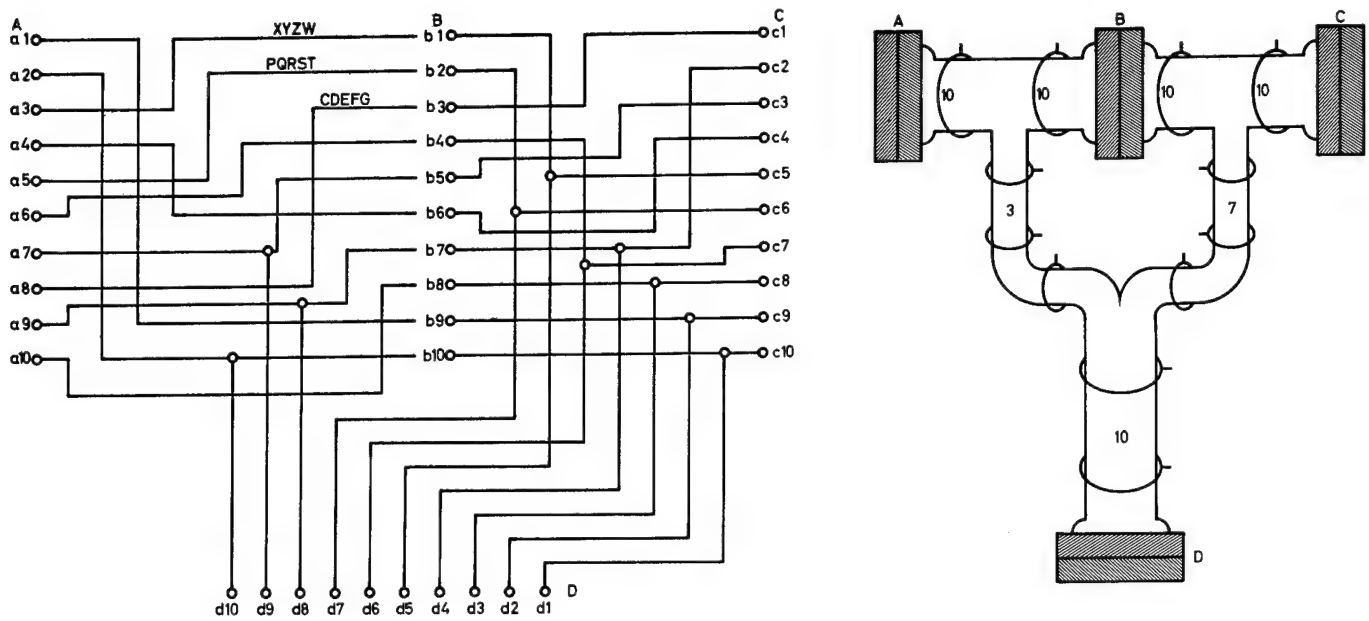


fig.1.2

PARALLEL LINE GEOMETRY AND PRINTED CIRCUIT BOARD INSTALLATION

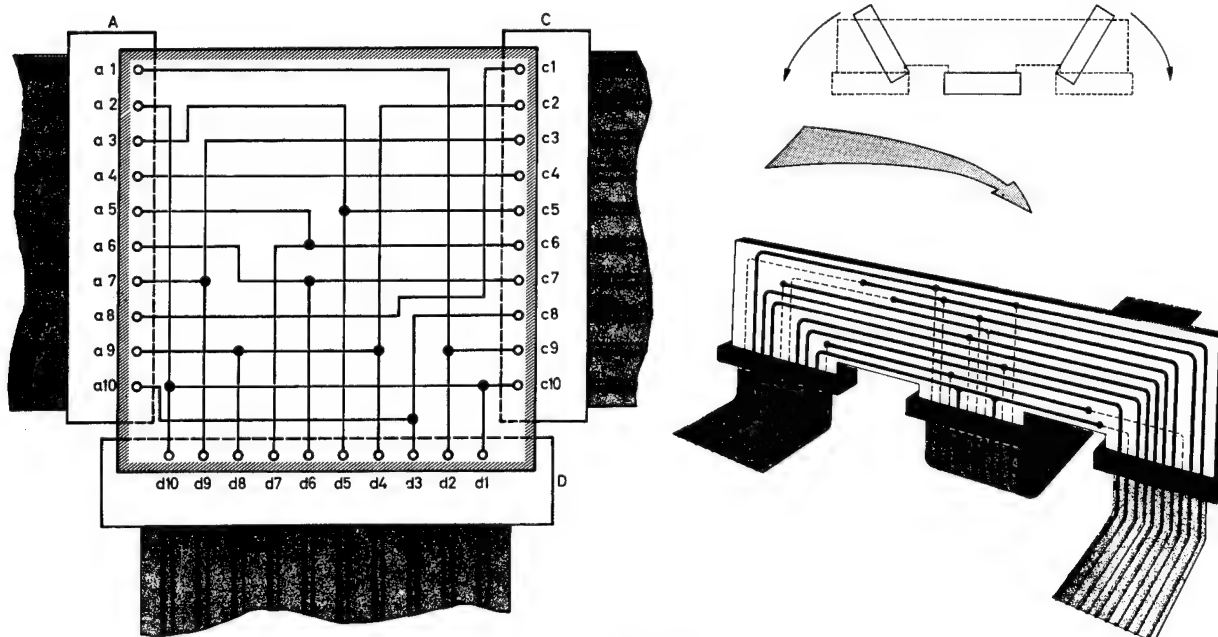


fig.1.3

The materialization of the matrix of interconnection through the printed circuit card offers many advantages :

The printed circuit board :

1. can be made or modified outside of the airplane.
2. is a plug-in element.
3. is replaceable and easy to test.
4. if introduced in a box, it can be completely isolated from the environment.

With respect to the environmental conditions, the following can be stated :

1. The wires, in ribbon cable or flat cable, can be specified and made to satisfy the most severe criteria in the following areas :
 - mechanical strength,
 - temperature,
 - vibration,
 - humidity and corrosion.
2. The box containing the interconnection matrix, like any avionics box, can be specified and manufactured to any desired standard.

Since all the cards and even the connectors are inside the box, the problem becomes one of an avionics box, the design of which has reached a high degree of integrity.

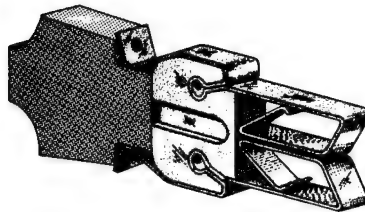
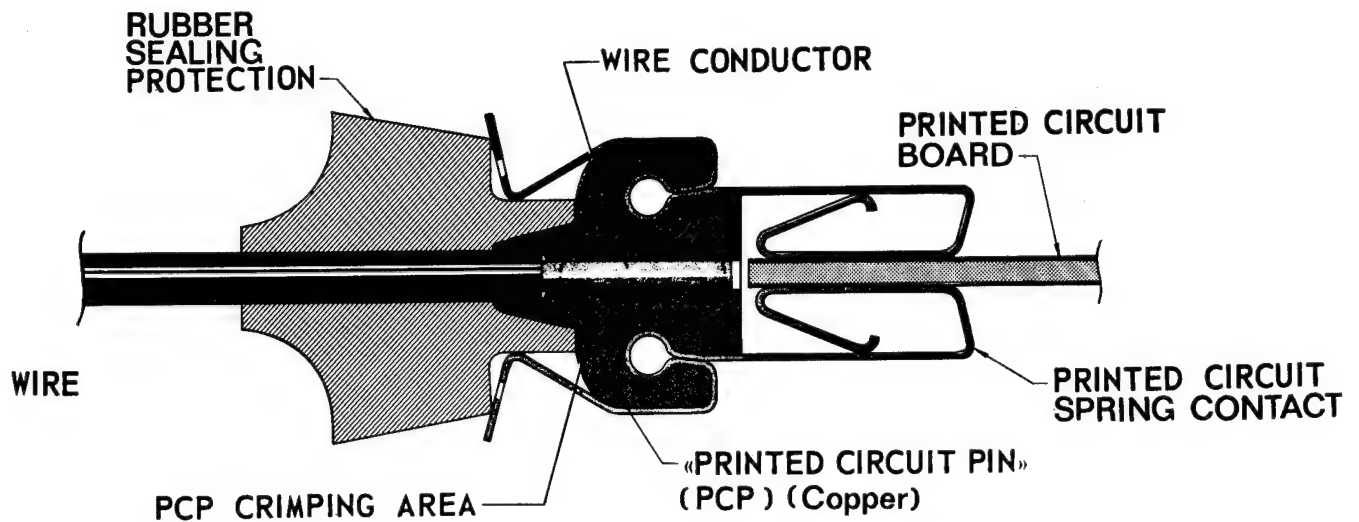
2. THE TERMINATION PROBLEM.

The lack of appropriate termination is the major reason for the flat or ribbon cable unsuccessful utilization in aircraft wiring.

The terminations proposed by the industry for the flat or ribbon cables, although at first sight attractive, cannot be considered here mainly due to lack of adaptability. Consequently, a connector was developed for the SIMPL system that provides a direct link between the ribbon cable and the printed circuit. It complies with the following requirements :

- The electrical resistance path between the wire copper and the printed circuit conducting surface should be minimum.
- Each contact assembly (wire-to-printed circuit) should be an entity within the connector independant from adjacent contact assemblies.
- Sufficient protection against the environment at the wire insertion side should be provided in order to prevent contamination of the contact assembly.
- Only simple and quick assembly operations should be necessary to terminate the ribbon cable in order to provide the flexibility required for production as well as field operation.

Figure 2.1. shows the SIMPL connector concept. It is composed of three elements assembled and inserted in individual housing compartments within the connector plastic shell whose outlines are typical of any standard straight edge connector for printed circuit cards.



WIRE TO PRINTED CIRCUIT CONNECTOR

Fig. 2.1

The three elements of the connector are :

1. The PCP (printed circuit pin) is a conductive metal piece having on one side the crimped terminal for the wire and on the other side the holder of the printed circuit spring contacts.

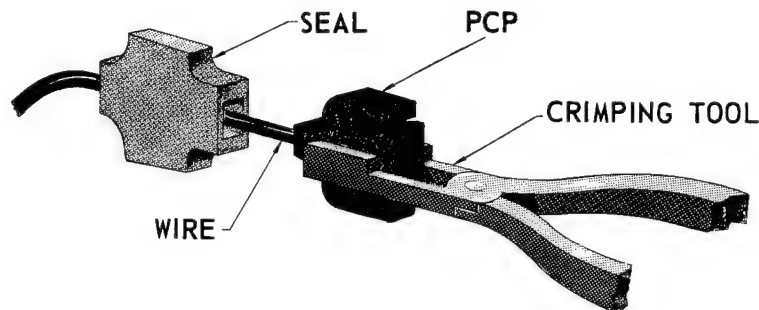
NOTE : Crimping is becoming more generally used in modern aircraft.

A recent analysis indicates that non-engine soldered and engine soldered connectors have respectively a failure rate 5.2 and 2.1 times that of a crimped connector.

Moreover, in the proposed connector, the PCP is a solid machined metal piece into which the wire is squeezed without possibility of poor contact.

The quality of the crimping can effectively be checked by the strength test.

Noise generation is unlikely since the conductor, either stranded or solid, completely fills the cylindrical hole adjusted to the wire gauge.



CRIMPING WIRE TO CONNECTION

Fig.2.2

2. The printed circuit spring contacts, whose particular shape provides a positive pressure on the printed circuit being symmetrically inserted in the PCP, can be removed and replaced whenever necessary.

The replaceability of the spring contacts is important since these are usually the parts that are likely to be deteriorated after many printed circuit insertions.

The installation of the spring contacts in the PCP insures a good contact between the PCP and the printed circuit.

3. The rubber sealing protects the connector against contamination by corrosive substances that could be carried along the wire insulation.

The ribbon cable termination is being made through only three simple and quick operations. The three operations are : the cutting of the ribbon, the wire stripping and the crimping. All the operations can be automated for production purposes or realized very simply in the field with adequate tooling, with appreciable reduction in time and labor, compared with what it takes with present wiring systems.

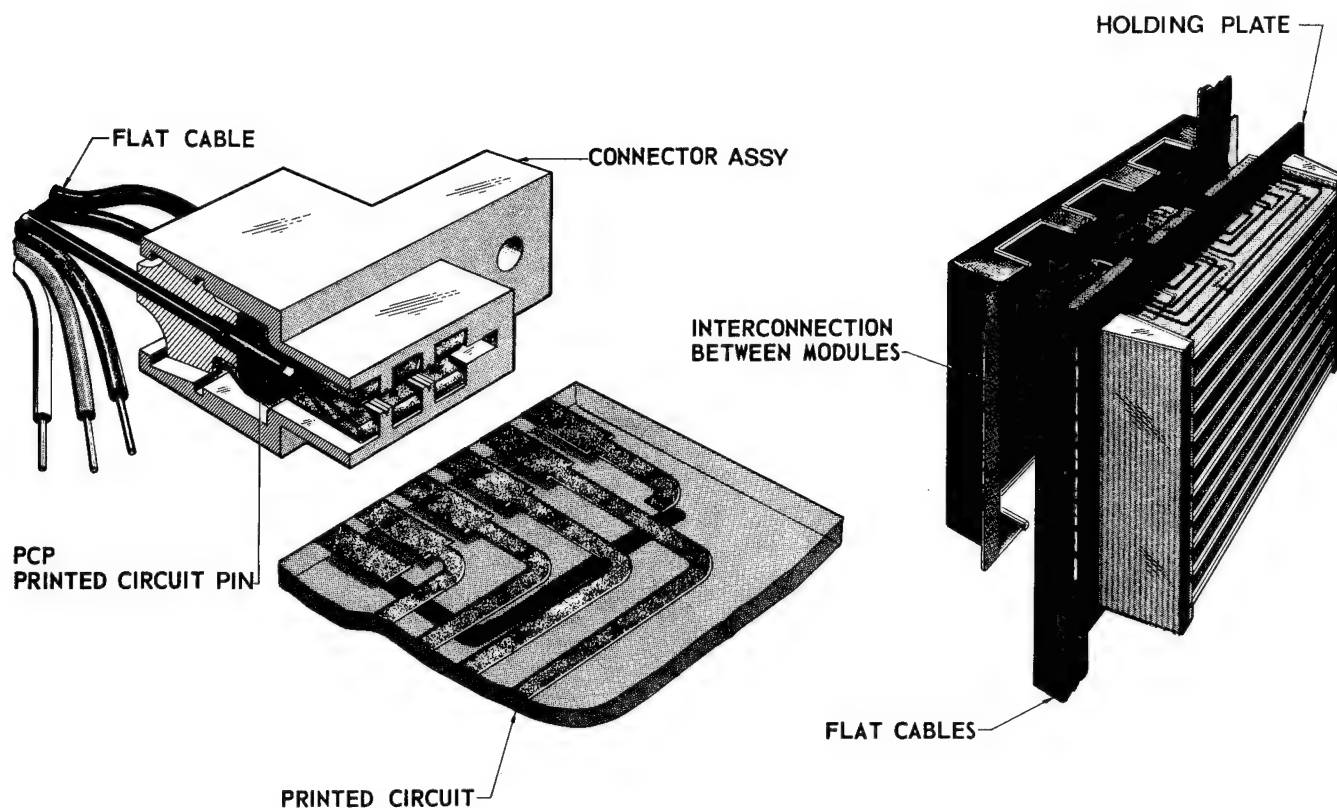


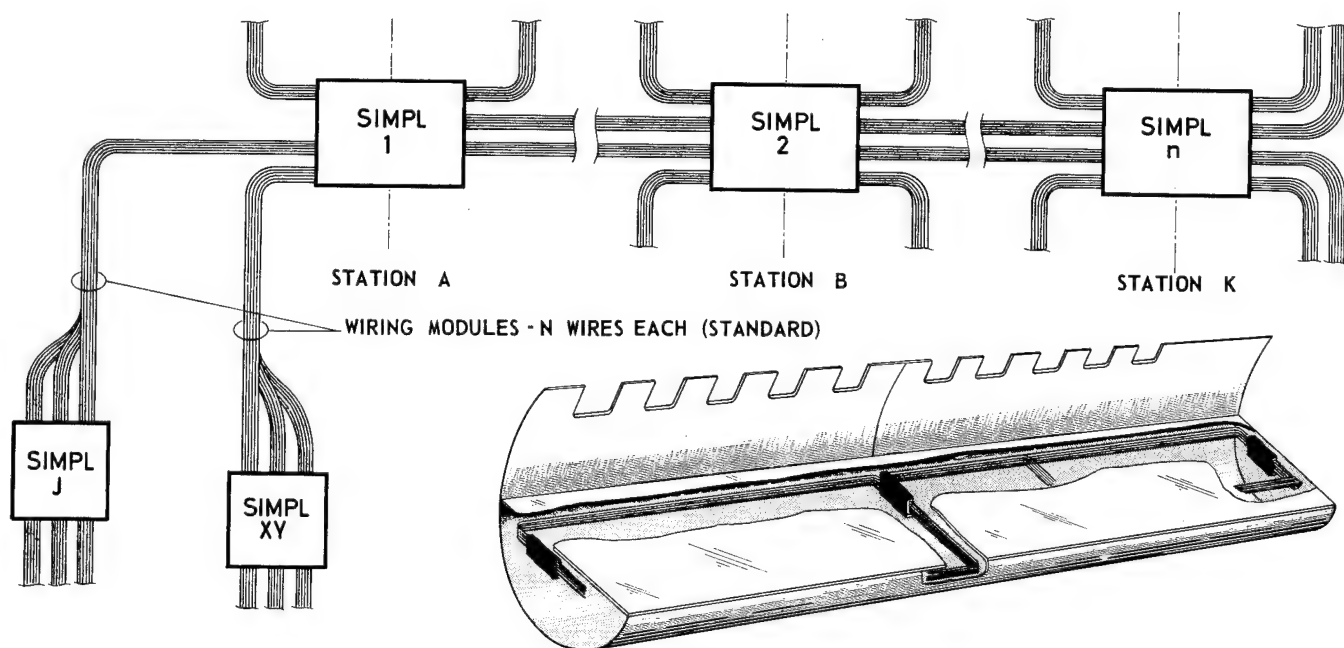
Fig.2.3

Fig. 2.3. shows how the ribbon cable termination and the printed circuit prefabricated in the workshops can be installed in the interconnection box - SIMPL box. It constitutes a means for error-free installation of a complete avionics system composed of a large number of distinct units.

Intermediate outputs in the printed circuit cards enable cross-connections from one card to another through connectors and jumpers located underneath the holding plate of the connectors.

3. APPLICATION OF THE SIMPL CONCEPT TO AIRPLANE AVIONIC INSTALLATIONS.

Among the advantages offered by the application of the SIMPL concept to the aircraft wiring, let us note in particular the elimination of complex harnesses and junction boxes and their replacement by small interface units consisting of flat cable segments and matrix boxes containing the printed circuits. The whole interconnection system allows a neat, easy and error-free installation and constitutes a truly integrated connective system.



FLEXIBILITY

Fig.3.1

Figure 3.1. illustrates the flexibility provided by the SIMPL concept. The wiring is composed of a number of "flat cables" designated as wiring modules routed between stations. An interface unit of SIMPL box is to be located at each point of derivation. The versatility of the system is obviously due to the ease of modification of the interconnections. All it takes is the change of cards and possibly the addition of wiring modules between the matrix boxes.

Figure 3.2. shows a suggested distribution for future airplanes in which the size of the airplane and the electrical complexity of the interconnection justify the installation of two electronic bays, one forward, near the cockpit, and the other aft. The pilot and flight engineer panels determine the number and location of the SIMPL interface units.

MODULE CONCEPT IN AIRCRAFT WIRING

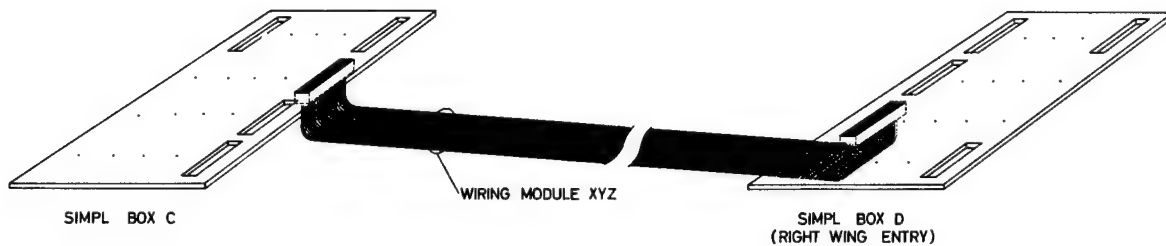
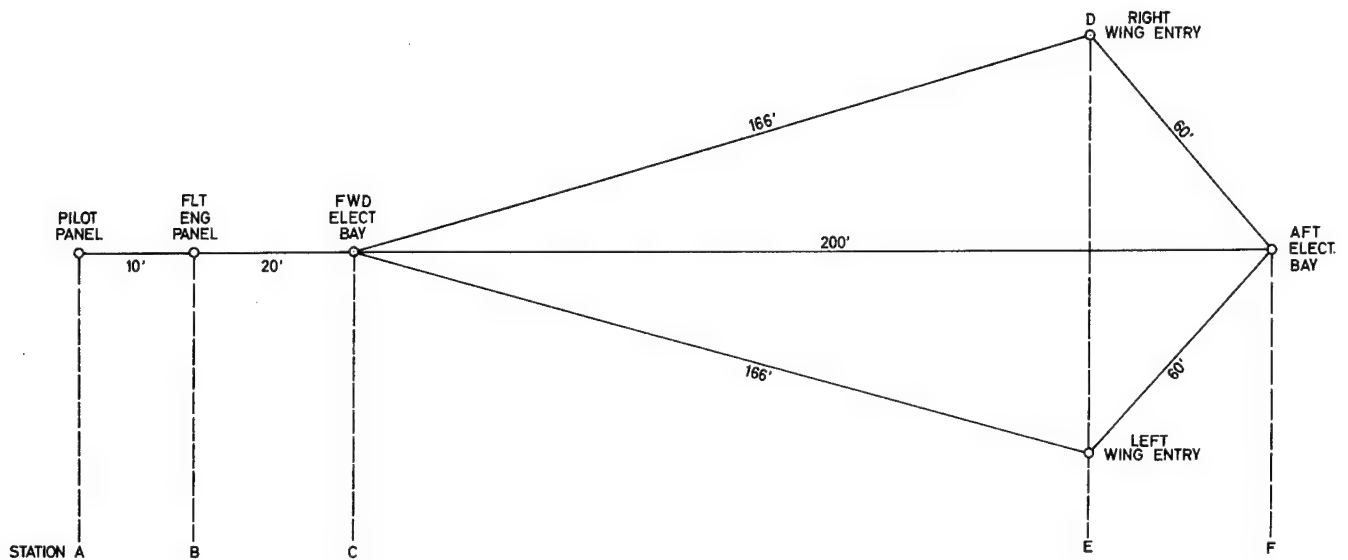


fig.3.2.

The wiring modules run between these stations, they are stacked and clamped to the airplane structure at appropriate locations. Figure 3.3. illustrates an interface unit at station "C" from which four layers of wiring modules (flat cables) are interconnected to three other groups of wiring modules. The lateral groups are routed to the wing entries while the central group interconnects the forward electronic bay to the aft one.

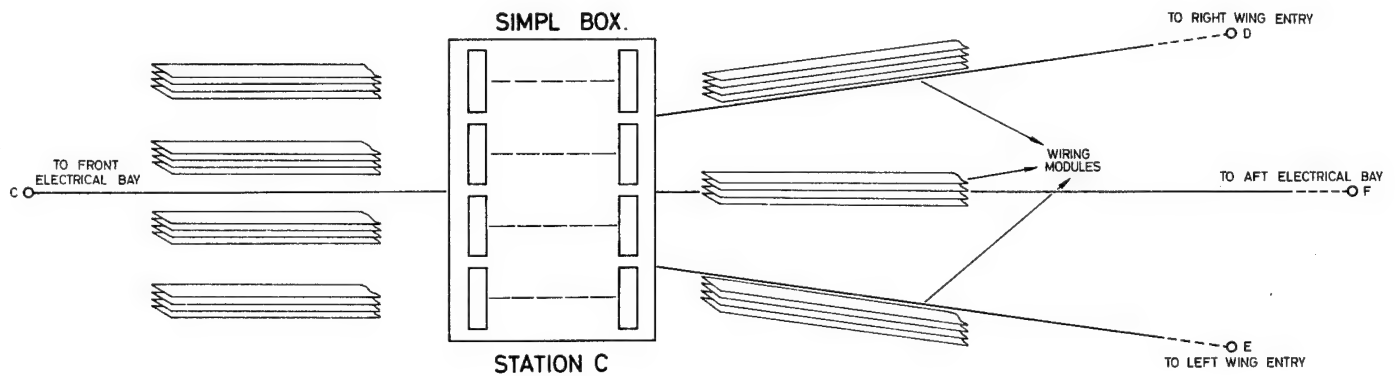


Fig.3.3

A modification of any complexity is a straight forward operation which can be performed in the field because it only requires either the activation of existing spares in wiring modules or, for a more complex modification, the addition of another wiring module. In both cases, changes in printed circuit boards are necessary, but they are manufactured and readied in the workshops.

In essence, the modifications consist either of a change of PC cards in the SIMPL interface units, which can even be done during a turn-around, or the addition of wiring modules plus the replacement of PC cards in SIMPL units can be performed during a line maintenance check. A complete fleet can be modified overnight and thus avoiding unwanted transition period.

The installation versatility results essentially from the inherent growth capability of the system and comes up to the airframe and airline expectations in providing substantial production and operational benefits.

4. WEIGHT AND VOLUME REDUCTION.

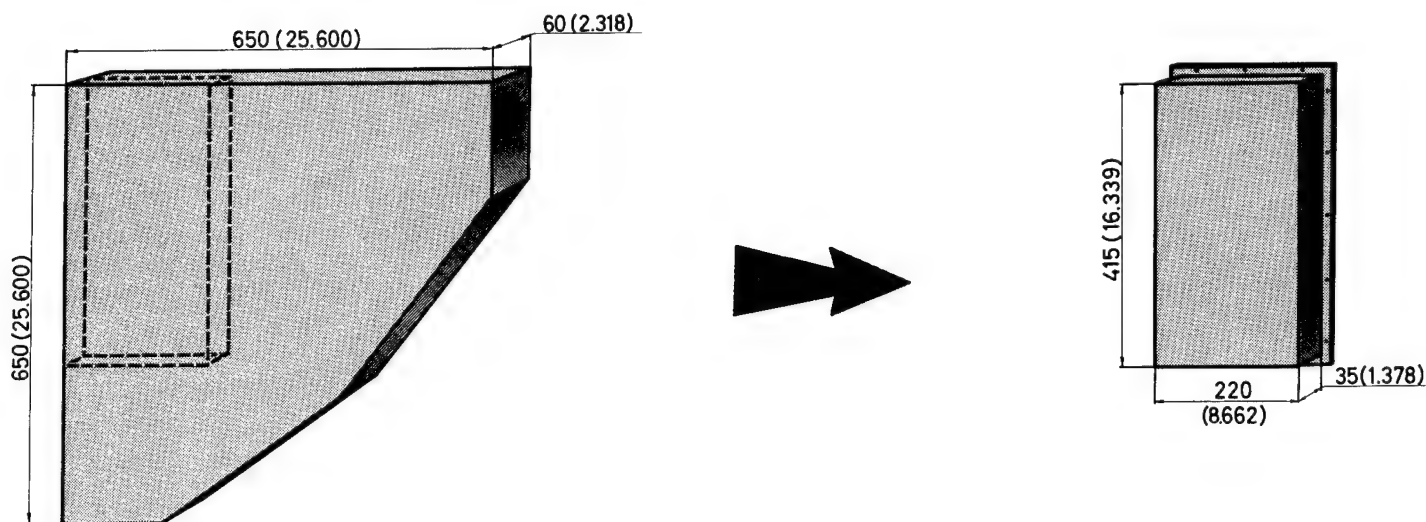
Significant weight savings are obtained by the introduction of SIMPL in airplane wiring. There are essentially two main areas in which important weight and volume savings can be achieved.

4. 1. Weight and volume reduction in the interconnection boxes.

An exercise has been carried out in which the Boeing 707 PB-20 autopilot junction box RJ-3 has been replaced by a SIMPL interface unit. Although the full benefit of the SIMPL system cannot be obtained by merely replacing a junction box of an existing system by a SIMPL box, it nevertheless demonstrates the weight and volume reductions that can be realized in the interconnection.

FIG. 4.1. WEIGHT SAVING

REDUCTION IN VOLUME AND WEIGHT OF THE J-BOXES
TYPICAL EXAMPLE OF SIMPLIFICATION OF THE BOEING 707 AUTOPILOT SYSTEM RJ-3



RJ - 3

Nbr of IN & OUT WIRES	Weight	Volume
823 wires from 47 System Components	Strips : 3.5 lb	Total : 1002 cu in
	Screws } 2.75 lb	
	Washers }	
	Nuts }	
	Jumpers 4.6 lb	
	Box 2.4 lb	
	Total : 13.25 lb	

WEIGHT REDUCTION 50%

SIZE REDUCTION 66%

SIMPL RJ - 3

Nbr of IN & OUT WIRES	Weight	Volume
1020 wires Subdivided in wiring modules of 10 wires each	Connectors 4.5 lb	Total : 338 cu in
	Base 1.1 lb	
	Cover 0.9 lb	
	Jumpers 0.6 lb	
	Total : 7.1 lb	

Figure 4.1. shows, as a result of the exercise, a reduction of 50% in weight and 66% in volume. Moreover, the application of SIMPL provides 20% of spare wires that can be used for later modification as required. The analysis shows that the economy results from the complete elimination of strips, screws, nuts and other parts that are out of place in to-day's electronic interconnection systems.

4.2. Weight reduction in the wiring.

The use of ribbon cables in the SIMPL system leads to a substantial reduction of the conductor cross section since the wire gauge is determined only by the electrical requirements as opposed to the individual wire where gauge 22 corresponds to the smallest acceptable size compatible with the mechanical stress that it has to withstand. For instance, when a bundle of individual wires is bended, the wires on the outside have to withstand a heavier stress and are likely to break if not of the required size.

The parallel line geometry cable in which a number of insulated wires are bonded in a single layer constitutes a mechanically strong material which satisfies the stress criteria and makes it possible to consider the unique electrical specification for the systems interconnection.

Attachment 1 highlights the main factors characterizing the weight reduction in wiring. The tables of attachment 2 extracted from a remarkable study made by Mr. Elmer F. Godwin, U.S. Army Electronics Command, Fort Monmouth, and published in IEEE Transactions of December 1967, permits an evaluation exercise of weight savings to be made with 17 or 8 round/flat conductor flat cables. For instance, if 1000 feet of unshielded flat cable, 17 round wires gauge 22, were to be replaced by a flat cable of 17 round wires gauge 30, admitting that the electrical requirements are satisfied, would result in a saving of $51,5 - 13,5 = 38,0$ lbs, which is 70 %.

Another enlightening exercise on the same subject is described in attachment 3 where a safety circuit of the mach trim coupler 707 PB-20 autopilot was simulated with five different wire gauges from $\neq 20$ to $\neq 30$. The maximum voltage drop measured was 1 volt with gauge $\neq 30$. Since the safety relay is still energized with 16 volts and the DC power source is 28 volts nominal, there is no objection in using gauge $\neq 30$ instead of gauge $\neq 22$. This results in a 74% reduction in weight.

On the same attachment, a table shows that the utilization of flat cable for Saturn S-TVB by Douglas Missile & Space Division permitted a saving of 76% in weight and 76% in manufacturing time.

5. TEST ABILITY.

Future airplanes will be equipped with increasingly complex electronic systems. The problem associated with their functional test becomes difficult to solve. The application of SIMPL to airplane interconnections brings a considerable simplification of the test operations ranging from the check at manufacturing stages to in-flight surveillance. This is a consequence of the availability of an accessible interface unit materializing an interconnection "matrix" which by essence contains all the signals existing in a system. Therefore, either by using available outputs in the printed circuit cards or by introducing special purpose test cards, every test operation can be performed. This is illustrated in figures 5.1. and 5.2. which are self-explanatory.

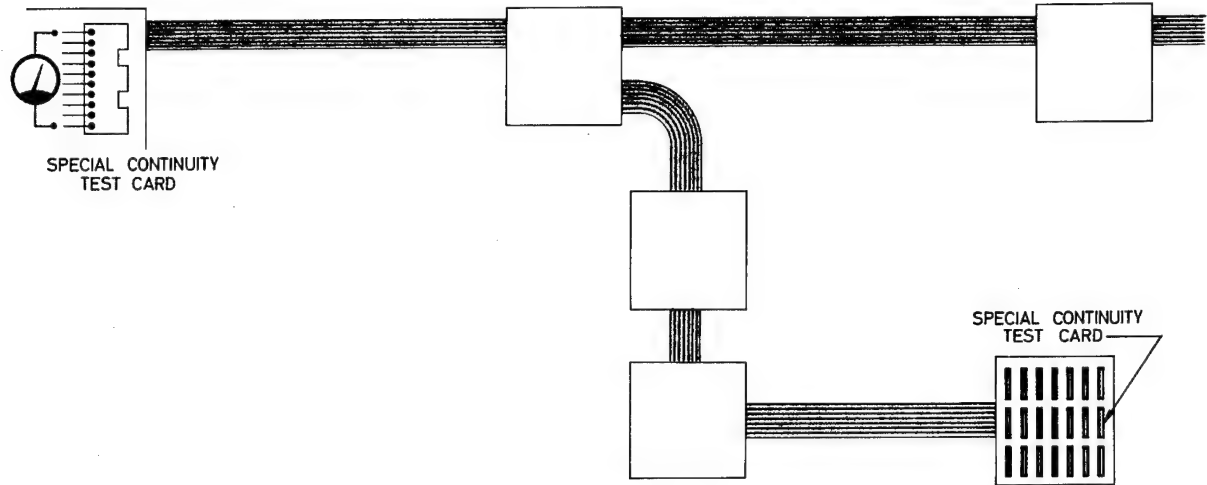
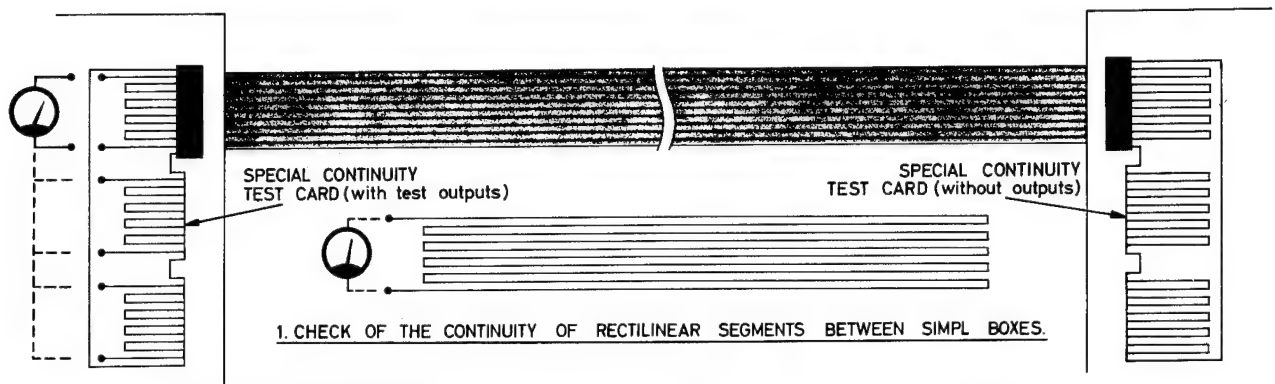


fig.5.1

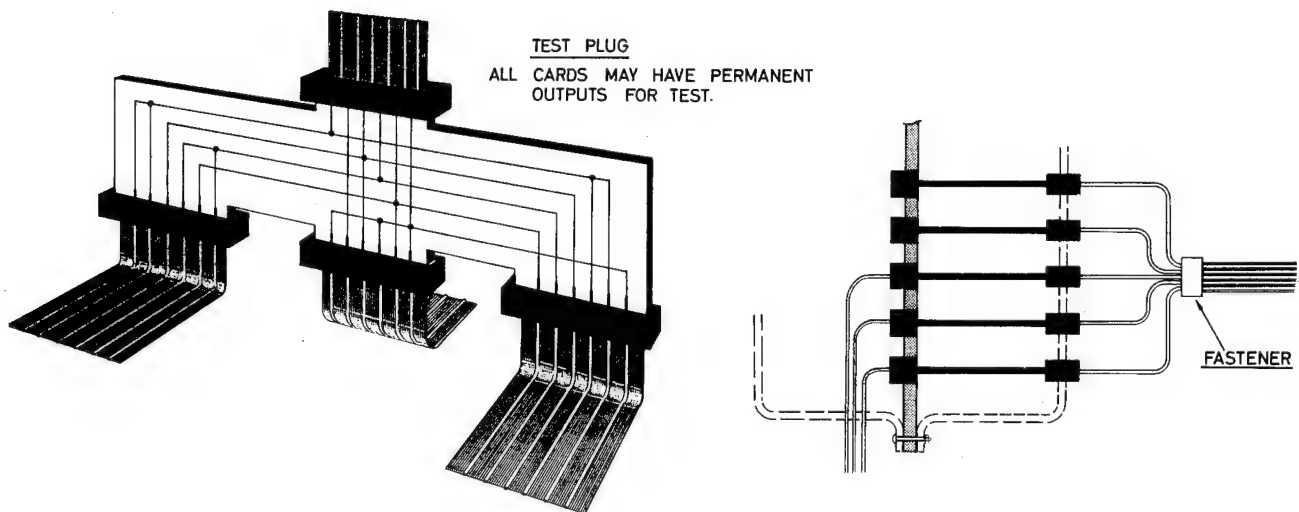


fig.5.2

It should be noted that an interface unit or SIMPL box can also be rack-mounted. Under such configuration all the test points of a system may become available in the electronic bay (fig. 5.3.).

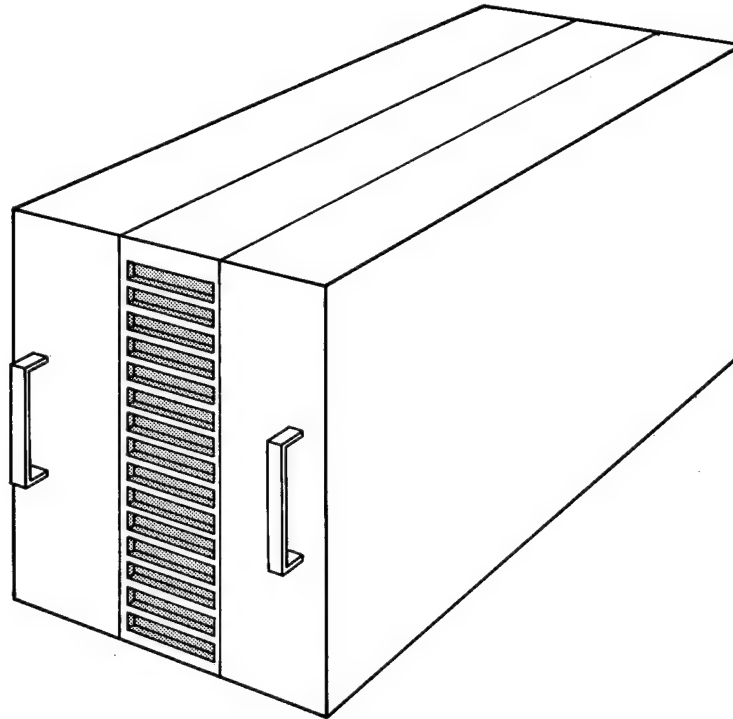


Fig.5.3

6. INSTALLATION ENGINEERING.

The unique characteristic of the SIMPL system opens new fields in the development of engineering and design methods for electronic equipment packaging and installation in airplanes.

There are two main areas in which the repercussions are easily foreseeable.

6.1. Engineering repercussions.

Figures 6.1. illustrate the considerable simplicity in data presentation for all purposes, i.e. manufacturing, testing, operation and field trouble shooting. It is shown, as an example, how a cumbersome set of thick books and wiring diagrams, broken up into small and difficult to follow schematics, are reduced to a set of listings, an interconnection "matrix" and few pages of wiring module routings in the airplane. It should be noted that the lines of the "matrix" correspond to the lines of interconnections in the printed circuit cards.

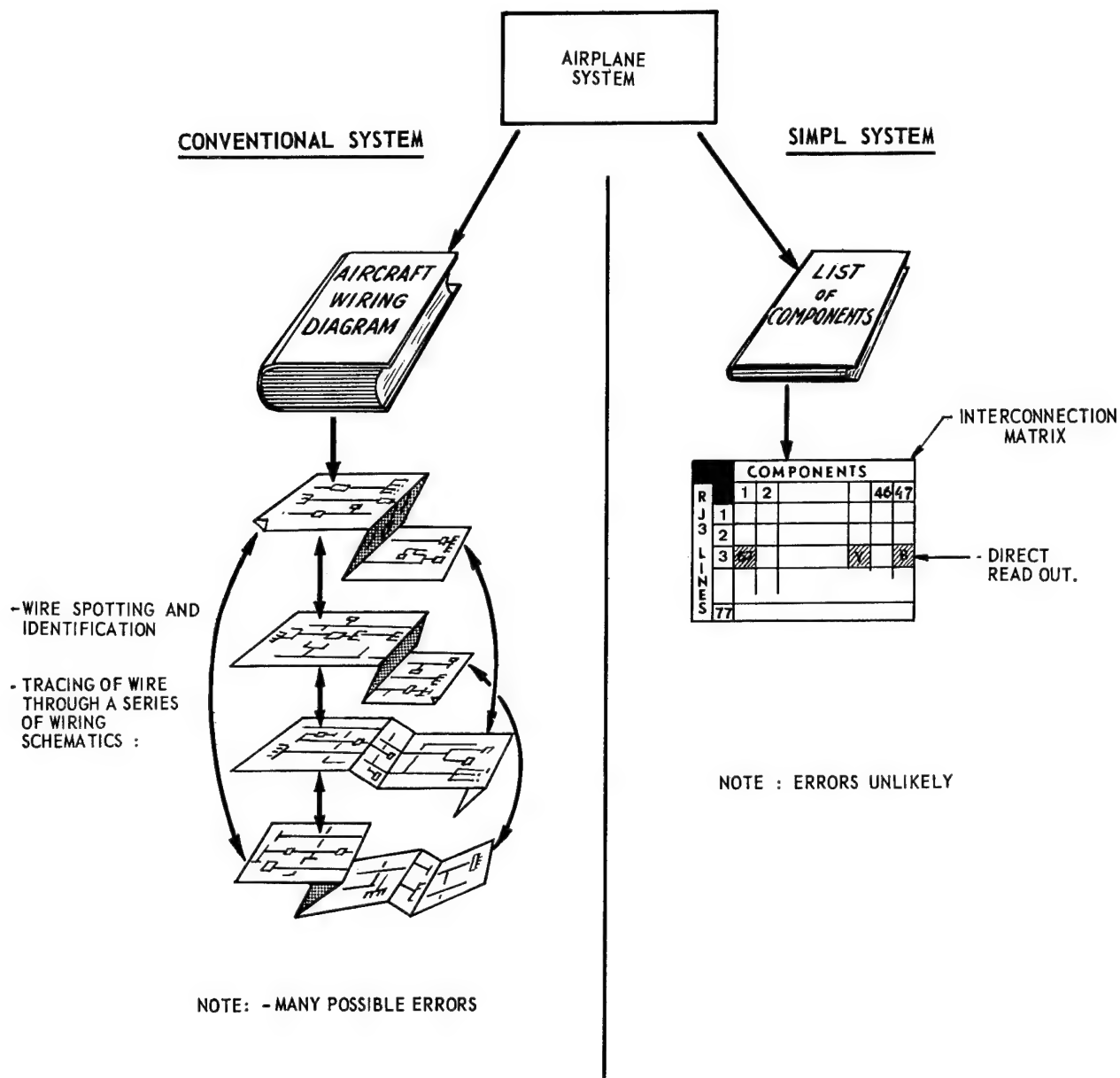


Fig. 6.1. a. - TROUBLE SHOOTING - CIRCUIT TRACING

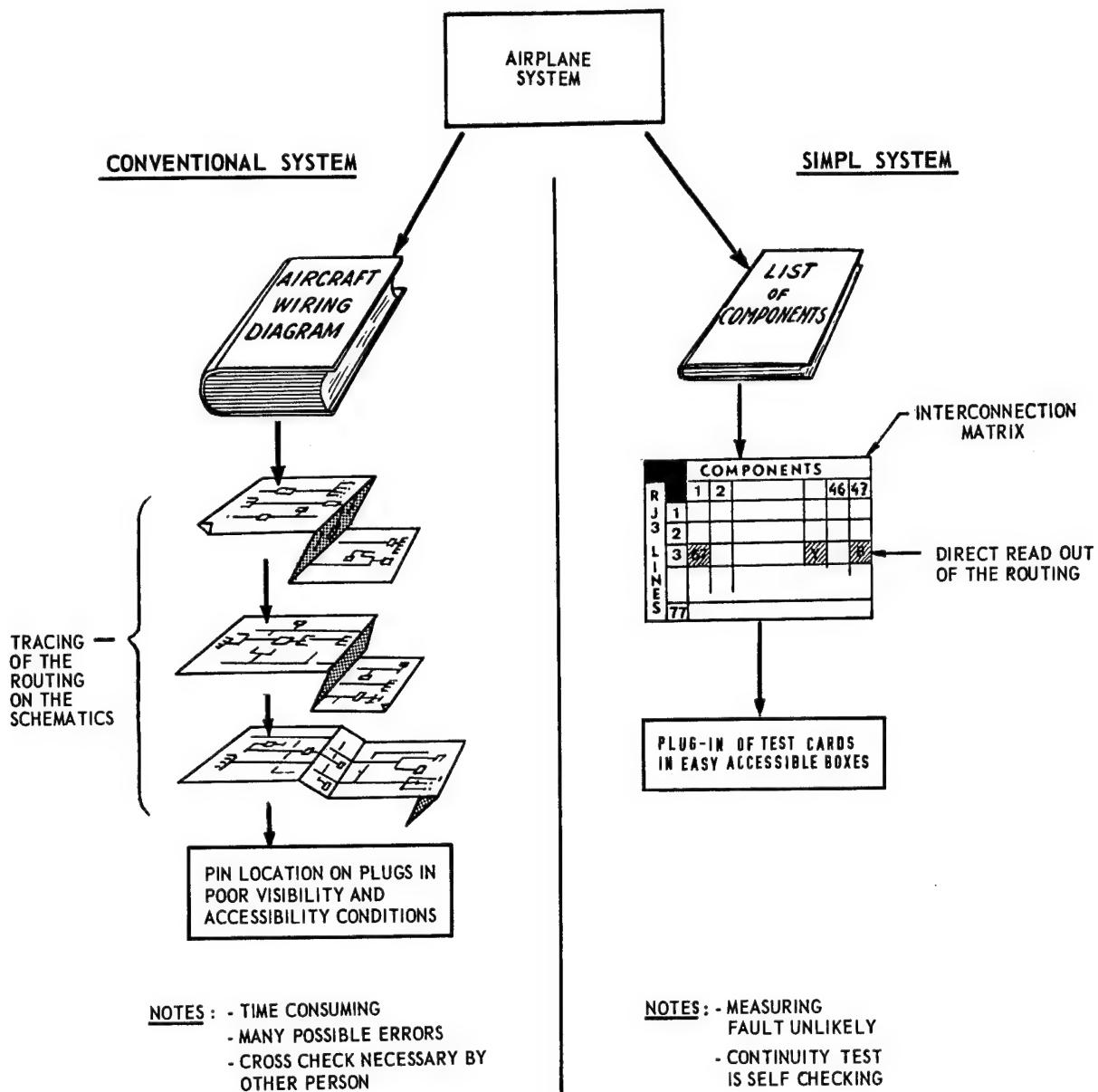


Fig.6.1.b. - SYSTEM WIRING CONTINUITY TEST

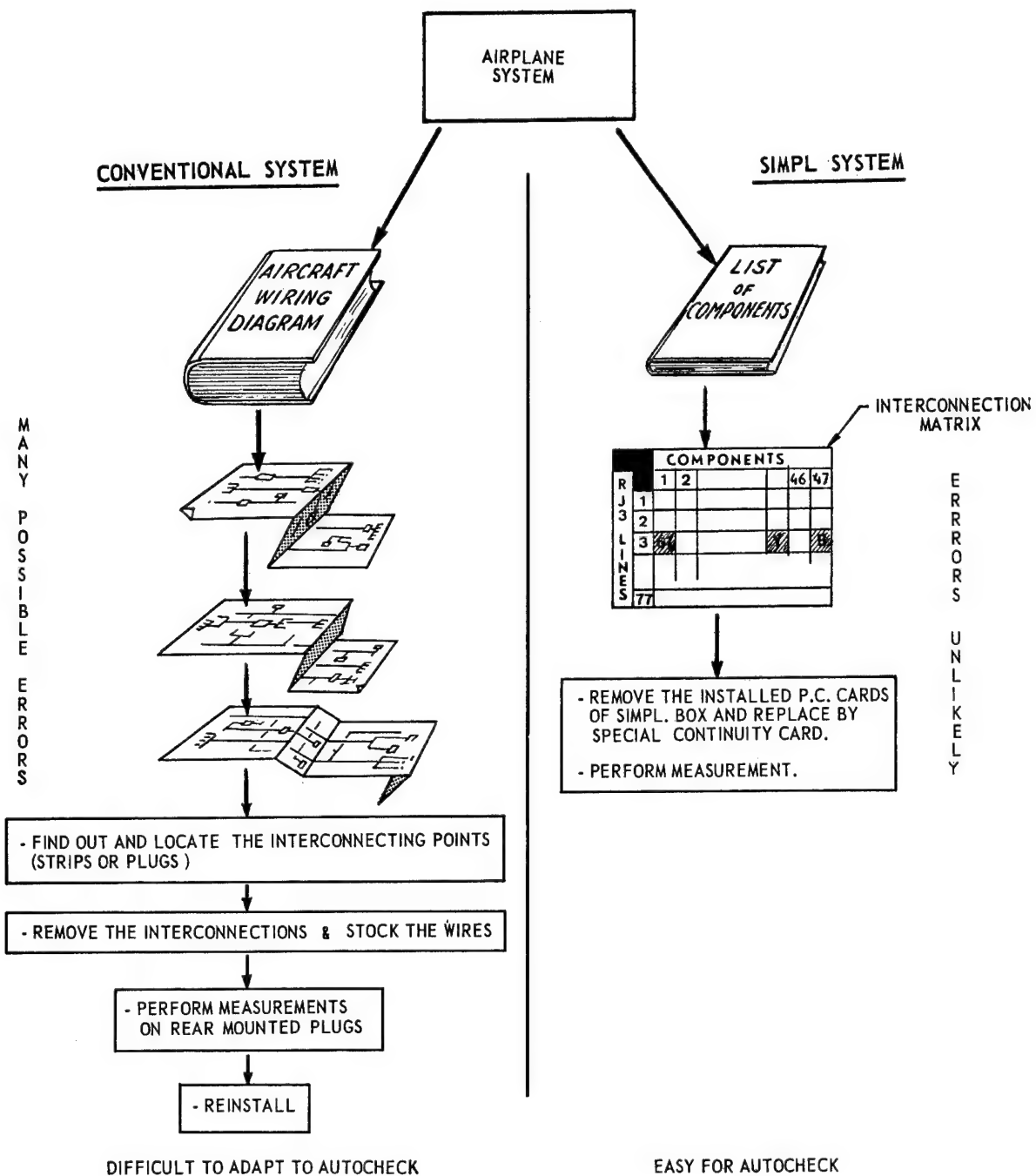


Fig- 6.1. c. — IF INTERCONNECTION INTERFERENCES MUST BE AVOIDED WHILE TESTING CONTINUITY

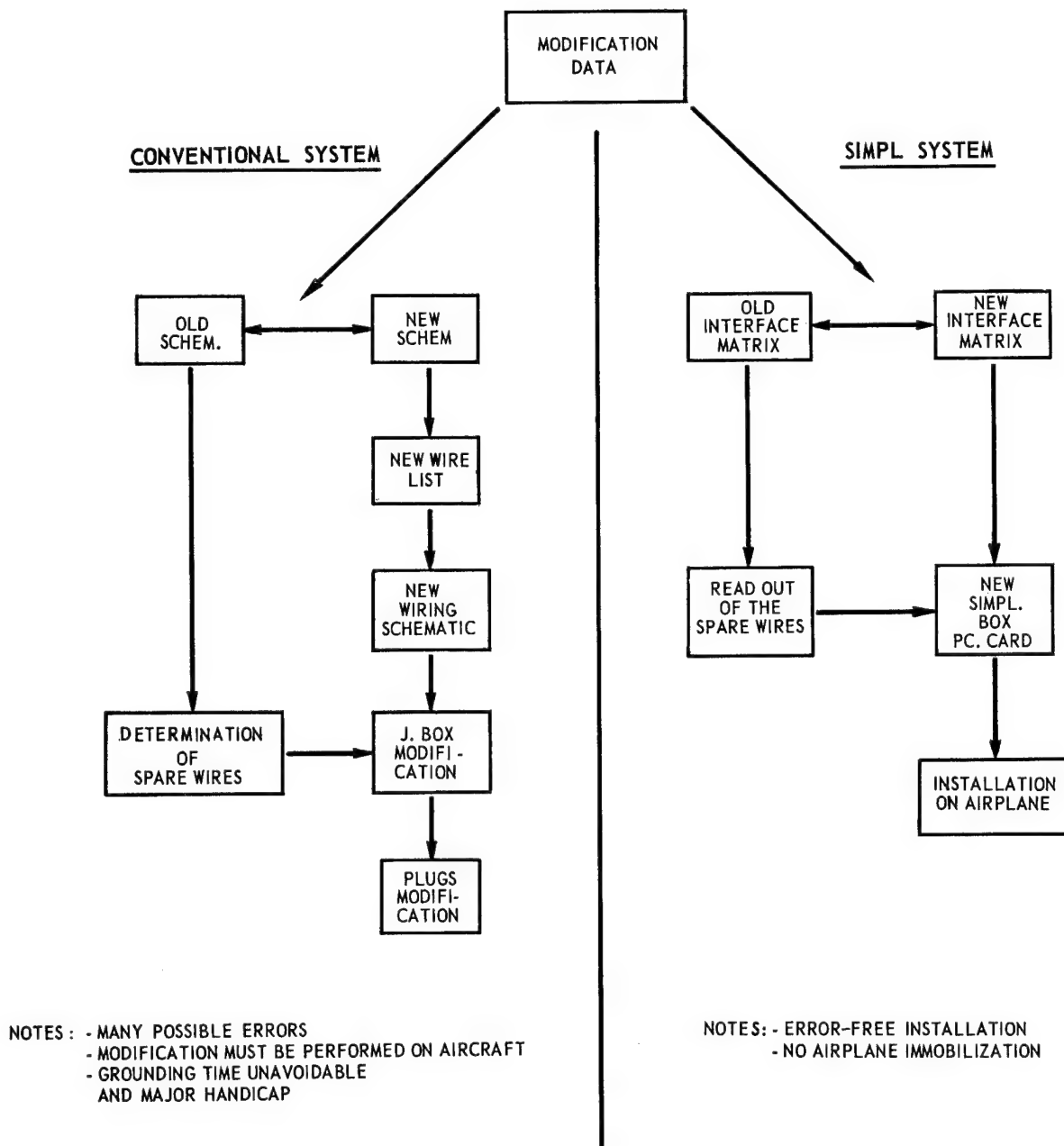


Fig. 6.1.d. - WIRING MODIFICATION

We can predict that a considerable time saving in maintenance and trouble shooting will be obtained. But also aircraft manufacturers will appreciate the simplicity of SIMPL. Master changes and individual operators change requests will be easy to implement with resulting benefits to both manufacturers (less engineering and wiring shops load) and customers (lower costs of changes).

6.2. RACK ENGINEERING.

The main problems in present rack engineering are :

1. The alarming increase in the number of pins required by the ever increasing number of signals and functions in avionics equipment and the insertion force needed in high density connectors will demand a substantial improvement in the interface between the wiring and the units.
2. In order to plug-in the avionic boxes with rear mounted connectors and to be sure that all the contacts are made, tight tolerances are required in the shelf trays, the box dimensions and the fastening mechanisms. These are difficult to obtain and to maintain.

In consideration of these factors, installation of wiring during airplane production as well as maintainability by the operators will require improved accessibility of the rack rear ends.

A trend towards a rack configuration with rear accessibility is noticeable in some of the newer aircrafts.

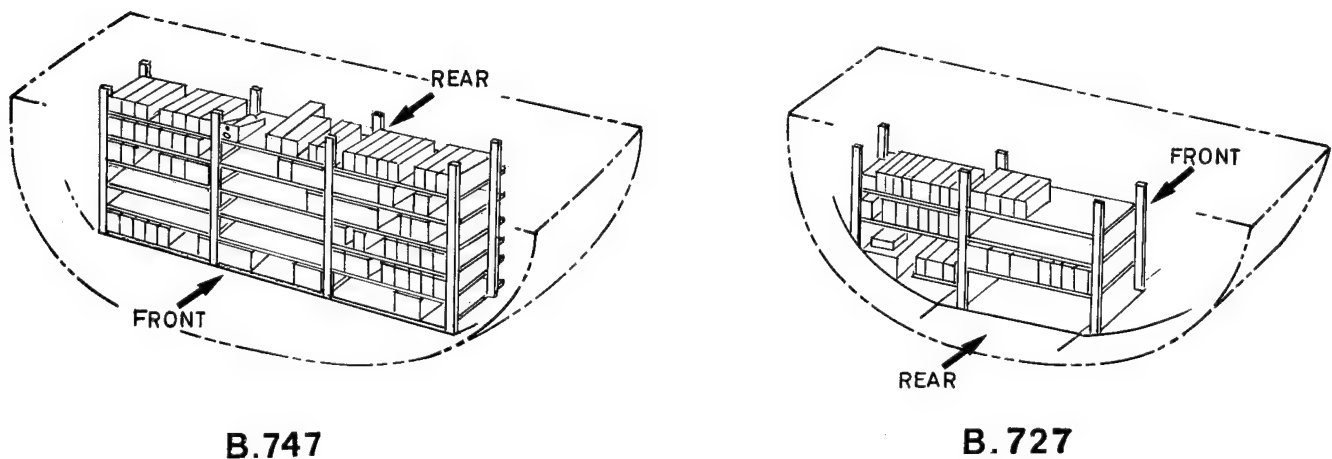


fig.6.2

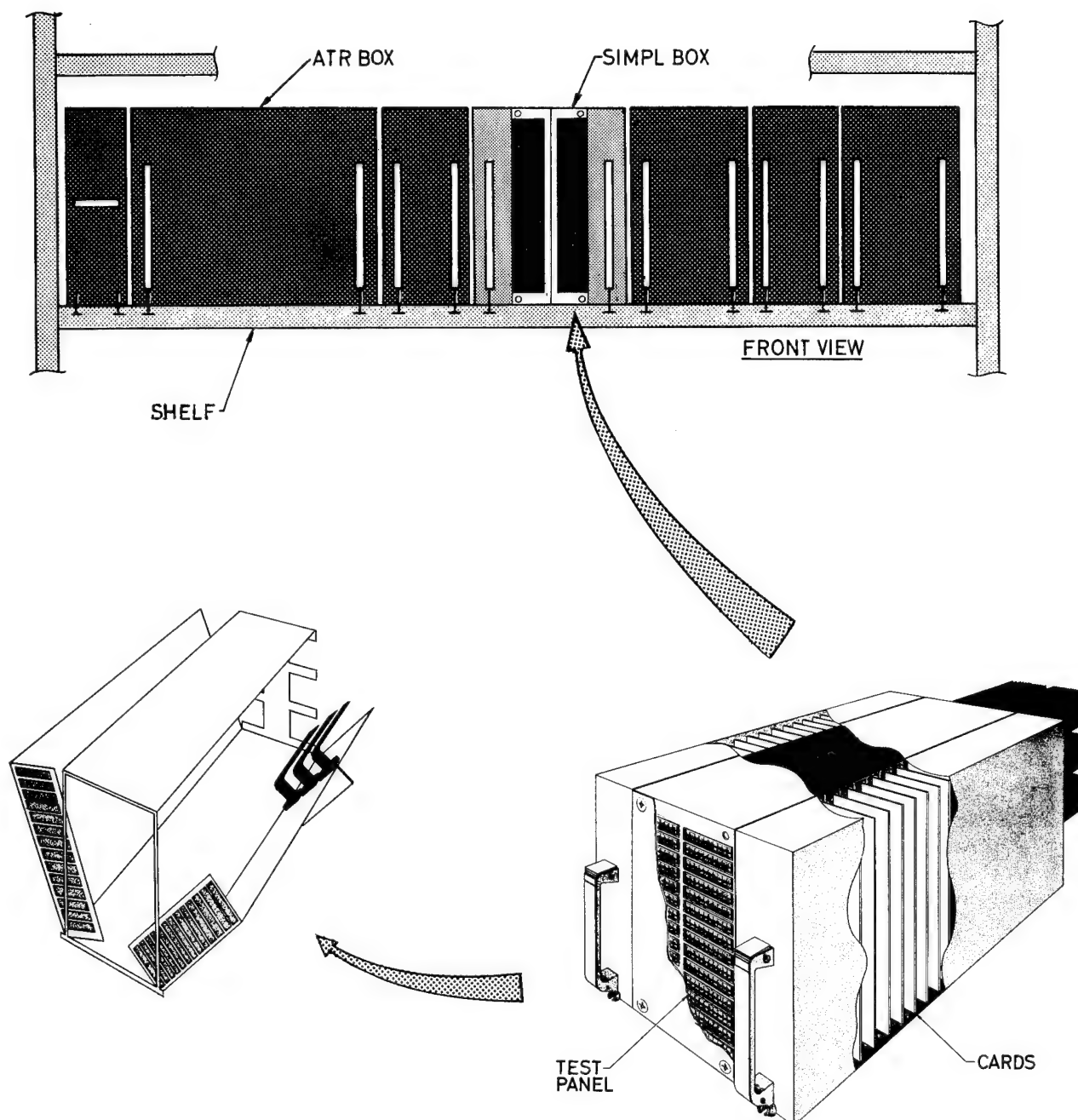
In rack systems with rear accessibility, the SIMPL wiring can be interconnected very easily using rack mounted SIMPL boxes as shown in fig. 6.3. Of course, non rack mounted matrix boxes can be interconnected to the units without difficulty.

A complete system can be shelf mounted as indicated in fig. 6.3.

In fig. 6.4. , cards are replaceable on the aircraft.

In fig. 6.3. , adjacent units to the SIMPL box have to be removed to open the SIMPL box and replace cards.

These are only suggested configurations indicating the improvement that can be obtained by making the radio rack and the wiring accessible from the rear. The SIMPL system can, however, be adapted to existing types of rack configurations where units are installed in the conventional manner.



RACK MOUNTED R-J SIMPL BOX
ARINC STANDARD

fig.6.3

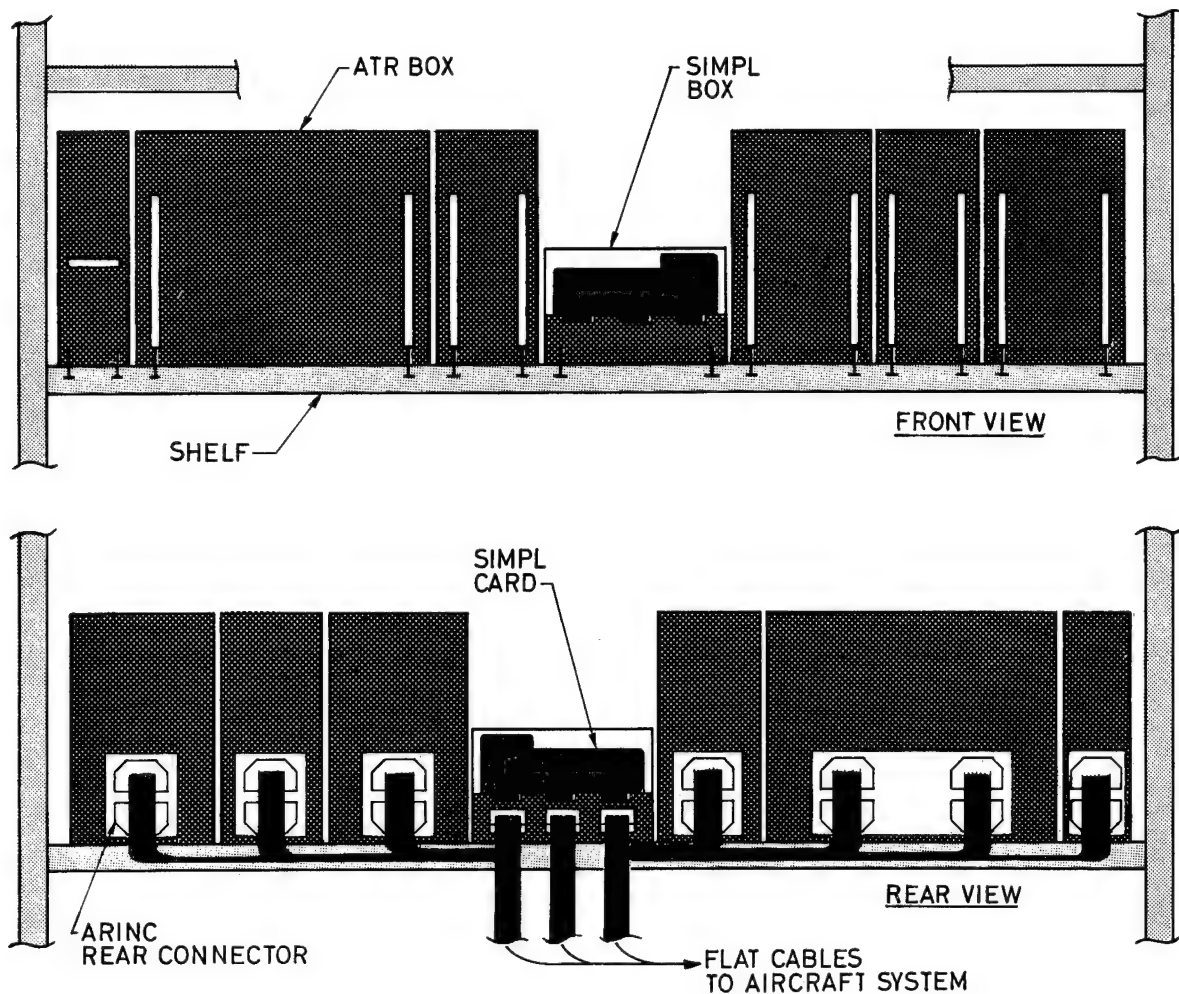


Fig. 6.4

CONCLUSION.

The application of SIMPL to aircraft wiring provides :

1. Wiring simplification.

- Elimination of wire identification (numbering).
- Elimination of bundles assembled "in loco" or "prewired".
- Reduction of Time and Labor in aircraft wiring. With few exceptions the wiring can be installed in the last phases of airplane manufacturing and assembly lines instead of early stages.

2. Versatility.

- By the adoption of SIMPL the wiring becomes "modular" which means that the modules can be "standardized" (wiring module Nbr XY).
- The addition of connections has no incidence on the wiring. It becomes a simple utilisation of existing spares in "Wiring Modules" or the addition of more "Wiring Modules" rather than to have to unbundle and/or modify complex harnesses.
- Modifications of wiring routing has no incidence upon the wiring itself.
- Modifications of connections results in replacing one P. C. board by a modified one, prepared in this shop without grounding the aircraft.

3. Weight Saving and space reduction.

- Considerable reduction in volume and weight of the junction boxes. Figures of 30 to 60% reduction can easily be attained.
- The adoption of SIMPL permits a substantial reduction in cabling weight. Weight reductions from 30 to 60% can be obtained through copper reduction as a function of the true electrical requirements (current rating).

4. Environment isolation.

- The SIMPL concept enables the wiring and the interconnecting devices to comply with the same criteria as the airborne black boxes. This means that the specifications of the Interface Wiring can meet the most severe existing specifications.
- It should be pointed out that none of the present day commercial aircraft have wiring and junction boxes that are adequately protected against temperature, humidity and vibration.

5. Testability.

- Considerable simplification of wiring tests at assembly stages and in operation.
- The continuity check is reduced to an extremely simple operation requiring a minimum of labor and time.
- A major consequence of the SIMPL concept is that the test of any box or complex system comprising a great number of subcomponents can be made at any point, at any time (ground or in flight) or on a permanent basis without any problem of accessibility or extra wiring.
- SIMPL reduces all the interconnection problems associated with automatic testing and solves most of AIDS problems.

6. Engineering efficiency.

- The SIMPL concept simplifies and reduces in a revolutionary manner the wiring schematics and diagrams, at all stages, from design to line operation and trouble shooting of any electronic system.
- The SIMPL concept eliminates all the existing obstacles for the computerization of the interface wiring. In other words, the utilisation of ground computers for the design, modification and storage of wiring information becomes practical which means a significant step forward in the aircraft wiring industry.

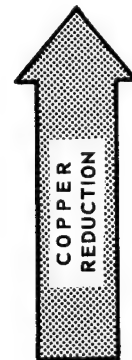
7. Limitations.

There may be some limitations in the application of the SIMPL concept.

The system is presently limited to the interface and interconnection of electronic and low power electrical systems. However, this represents more than 80% of the total wiring. It is not readily applicable for the transmission of HF, VHF and UHF signals for which the coaxial cable is still the most adequate.

Normal power lines can be accommodated through the SIMPL system provided that functional design and layout are applied.

SIMPL PERMITS A SUBSTANTIAL REDUCTION IN CABLING WEIGHT.



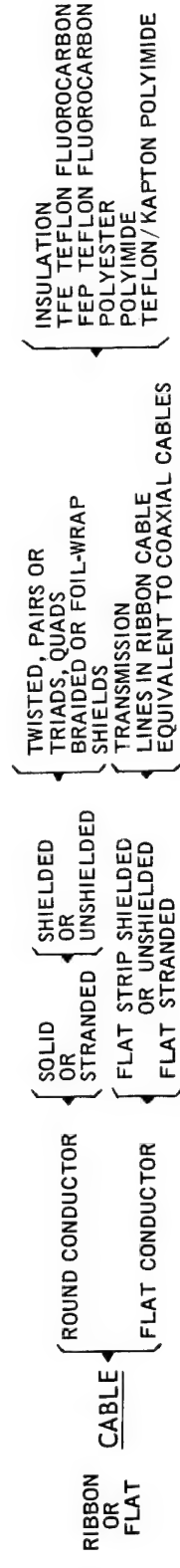
INSTEAD OF USING A LARGE WIRE SIMPLY TO WITHSTAND MECHANICAL STRESS, INDIVIDUAL CONDUCTORS CAN BE SPECIFIED IN TERMS OF ELECTRICAL REQUIREMENTS. SPECIFICALLY, SIGNAL LEADS NOW SPECIFIED AS AWG 22 CAN BE REDUCED ELECTRICALLY TO AWG 30. IN RIBBON CABLE FORM, THE LEADS WOULD WEIGH ONLY 25 TO 30 % AND OCCUPY 1/3 THE SPACE.



THE FLEXIBILITY OF THE CONDUCTOR IS INCREASED IN THE FLATTENED PLANE AND THE STIFFNESS IS INCREASED IN THE ORTHOGONAL PLANE. INCREASED FLEXIBILITY ALLOWS THE CONDUCTOR TO BE BENT AND FOLDED AND THE BENDING RADIUS CAN BE SMALLER. THE INCREASED STIFFNESS IN THE ORTHOGONAL PLANE TURNS THE CABLE INTO A TWO-DIMENSIONAL STRUCTURE BUT BY FOLDING OR BY TWISTING IT INTO AN HELIX IT CAN BE ROUTED IN ALL THREE DIRECTIONS.



MECHANICALLY 10 CONDUCTOR AWG 30 RIBBON IS IN SOME RESPECTS STRONGER THAN A BUNDLE OF 10 AWG 22 WIRES. EXAMPLE: WHEN PULLED, THE SHORTEST 22 GAUGE WIRE IN THE BUNDLE BREAKS AT 19 POUNDS, THE 30 GAUGE RIBBON BREAKS AT MORE THAN 30 POUNDS.



STANDARDS : NAS 729 AND NASA SPECIFICATION 220 B
MIL-C-55543 AND - 55544 (IN PREPARATION)

REMARKS :

FLAT CABLE ROUND CONDUCTOR : STANDARD TERMINATIONS, GREATER VERSATILITY IN INTERWIRING INDUCTANCE AND CAPACITANCE PATTERN IN A STANDARD KNOWN FORM. YEARS OF EXPERIENCE-TABLES EXISTING.

FLAT CABLE FLAT CONDUCTOR : NON STANDARD TERMINATIONS - SOURCE OF PROBLEMS PRESENTLY. (BUT NOT A FUTURE PROBLEM FOR SIMPL) NEW ELECTRICAL CHARACTERISTICS. BETTER TEMPERATURE RISE CHARACTERISTICS THAN ROUND CONDUCTOR. NOT ENOUGH EXPERIENCE TODAY. EXTENSIVE TESTS AND R & D STILL IN PROCESS. - WIRING OF TOMORROW.

CONDUCTOR EQUIVALENT

FLAT CONDUCTOR	EQUIVALENT DIMENSIONAL	ROUND WIRE (AWG) CURRENT RATING
0.025 × 0.002	# 32	# 30
0.025 × 0.003	# 30	# 28
0.075 × 0.003	# 26	# 23

COMPARISON OF 17 CONDUCTOR CABLES

CONDUCTOR TYPE AND SIZE	UNSHIELDED			SHIELDED			
	DIAMETER over INSULANT	CABLE O.D.	CABLE AREA	WEIGHT lb _s / 1000 Ft	CABLE O.D.	CABLE AREA	WEIGHT lb _s / 1000 Ft
FLAT 0.025 × 0.002		1.0 × 0.010	0.010	9.4	1.0 × 0.020	0.020	13.3
FLAT 0.025 × 0.003		1.0 × 0.010	0.010	10.4	1.0 × 0.020	0.020	14.3
ROUND # 32 AWG	0.031	0.170	0.023	12.8	0.195	0.030	24.0
“ # 30 “	0.033	0.180	0.026	13.5	0.205	0.033	29.0
“ # 28 “	0.036	0.200	0.032	18.0	0.230	0.042	35.0
“ # 26 “	0.040	0.220	0.038	25.0	0.250	0.049	44.0
“ # 24 “	0.046	0.255	0.051	35.0	0.285	0.064	56.0
“ # 22 “	0.053	0.295	0.068	51.5	0.325	0.083	74.0

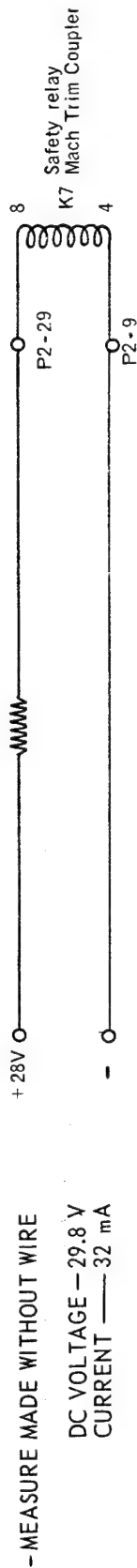
COMPARISON OF 8 CONDUCTOR CABLES

FLAT 0.075 × 0.003		1.0 × 0.010	0.010	11.8	1.0 × 0.020	0.020	15.7
ROUND # 26 AWG	0.040	0.175	0.025	12.0	0.200	0.032	25.0
" # 23 "	0.050	0.220	0.038	20.0	0.250	0.049	39.0
DIMENSIONS IN INCHES AREA IN ² ROUND CONDUCTOR ARE STRANDED INSULATION 0.007 TO 0.010 IN WALL THICKNESS							

EXTRACT FROM « MATERIALS FOR FLAT CABLE, THE INTERCONNECTING SYSTEM OF TOMORROW »
By Elmer F. Godwin - US. Army Electronics COMMAND, FORTH MONMOUTH, N.J.

TWO SIGNIFICANT EXAMPLES :

I. INTERLOCK RELAY CIRCUIT OF THE BOEING 707 AUTOPILOT SYSTEM.



MEASUREMENTS MADE WITH 100 meters OF ROUND WIRE.

Conductor Type and Size	Voltage Drop (volts)	Weight lbs./100 m	Weight Savings Relative to #22 AWG	Percent Weight Savings Relative to #22
AWG #30	29.8-28.8=1V	0.26	0.734	74 %
#28	0.80	0.347	0.647	65 %
#26	0.60	0.48	0.514	52 %
#24	0.40	0.67	0.324	32.5 %
#22	0.20	0.994	-	-

REMARK : 1. IT IS RECOGNISED THAT MANY CIRCUITS RARELY OPERATE AT FULL LOAD, AND LOADS ARE FREQUENTLY DISTRIBUTED RATHER THAN CONCENTRATED AT THE END OF THE CIRCUIT, SO THAT THE VOLTAGE DROP UNDER AVERAGE CONDITIONS IS NOT A LIMITING FACTOR.

2. THE WIRING CAN BE FUNCTIONAL. THIS MEANS THAT THE SELECTION OF THE FLAT CABLE WIRE GAUGE MUST BE MADE TAKING INTO ACCOUNT THE I MAX, R MAX, AND R MIN. ALLOWED FOR THE FUNCTIONS THAT IT HAS TO PERFORM.

II. SATURN S-IV-B BEFORE AND AFTER MODIFICATION FROM AWG" 19 TO FLAT CABLE DOUGLAS MISSILE AND SPACE DIVISION UNDER CONTRACT TO NASA-MSFC.

		Round Wire	Flat Cable	Savings	%
WEIGHT LBS	MOUNTING HARDWARE HARNESS	413 1010 1423	46 297 343	367 713 1080	89 70 76
	TOTAL				
TIME (HOURS)	CABLE ASSY INSTALLATION	2125 1113 3238	400 364 764	1725 749 2474	80 67 76
	TOTAL				
COST US \$	WIRE PLUGS FASTENERS	1430 4730 3207 9367	5195 700 404 6299	-3765 4030 2803 3068	-260 85 88 33
	TOTAL				

ATTACHMENT 4.

Flat cable round conductor and flat cable flat conductor.

The present report refers only to flat cables with round conductors. However two types of parallel line geometry cables exist : the flat ribbon cable with round conductors and the flat ribbon cable with flat conductors. For a given conductor cross-section, the flat conductor has a greater heat dissipation capacity but the cable termination problems and increased cable width are such that a further reduction of weight by using flat conductors is offset by installation difficulties. Furthermore, the flat cable round conductor can be used without any change in installation design methods since existing specifications concerning current rates, capacitance, voltage breakdown and resistance are applicable, whereas for the flat cable or flat conductor, the geometry of the conductor is radically different and the data required for system design are not fully known. There is no doubt however, that the necessary tables will be available in the future, enabling the use of the flat conductors where their application is profitable.

In both cases, round or flat, all the characteristics of the interconnecting wiring, such as capacitance crosstalk, are readily predictable due to the fixed and uniform position of the conductors in the cable. This constitutes an important step forward in connective systems allowing full control of each individual wire position at any point in the airplane. The significance of the advantage becomes clear when considering the present sensitivity of electronic equipment to interference and the effort being made to minimize and control such effects.

APPENDIX

STANDARDISATION OF FLAT CABLE WIRING :

There are already a number of military specifications for flat multiconductor cables of the type round wire conductor (RWC) and flat conductor (FCC).

The current carrying capability in air or vacuum of single and stacked cables is defined in charts of maximum current versus temperature rise for different types of insulation.

APPLICABLE MIL SPECIFICATION, FOR FLAT CABLES :

MIL-W-5086 Type II (RWC).

MIL-W-16878 Type E (RWC) 10 mil Teflon.

MIL-W-81381/2 (RWC) 7 mil Kapton.

MIL-C-55543 (FCC) H/FEP standard density.

MIL-C-55543 (FCC) H/FEP High density.

These specifications are the basic material to lay the foundations of standardisation of interconnecting wiring systems.

An important task has to be carried out by organisations such as SAE to modify and adapt existing wiring standards to cover modern types of flat multiconductor cables which will be used in conjunction with rational interconnecting devices such as SIMPL interface boxes.

FLAT CONDUCTOR CABLE APPLICATION FOR AIRPLANE POWER FEEDERS

Julian P. Morris
Electrodynamics Technology
Commercial Airplane Group
The Boeing Company

Abstract

The use of flat conductor cable (FCC) in place of conventional round wire will provide more effective power feeders for airplane applications. This paper presents a design approach and the supporting laboratory results for determining the flat conductor cable configuration to meet requirements of a 200-ft-long, 90 kVA, three-phase, airborne power feeder system. Electrical and thermal parameters affecting conductor size are: resistance, reactance, voltage drop, current, temperature, surface area, heat dissipation, and condition of the surroundings. Conductor configuration, i.e., width and thickness for a given area, will affect both electrical and thermal parameters. In addition to electrical considerations, a discussion is included in the selection of conductor and insulation materials and methods for terminating the FCC feeders.

Introduction

Weight reduction in airplane design is a constant goal because it allows increased performance in either extended range, increased speed, greater payload, lower operating cost, or a combination of all of these benefits.

The economic operation of advanced technology airplanes like the widebodied jets requires aggressive weight control programs in all areas. While several airplanes in service today take advantage of lighter weight aluminum instead of copper conductor round wire power feeders, research is being conducted at Boeing to develop flat conductor cable feeder systems that will achieve even greater weight reduction for the same electrical loads. This can be accomplished because the geometry of FCC is more conducive to heat dissipation and contributes to a lower net impedance by causing less inductive reactance than round wire.

Power Feeder System Description

Power feeders are used on commercial transport airplanes to interconnect generators and electrical/electronic system loads through power distribution centers as illustrated in figure 1. The design of auxiliary power unit (APU) feeders has been selected for this study as a typical application. These feeders are routed from generators in the aft fuselage to power shields located near the cockpit. The 200-ft-long feeders are installed for 170 ft at an effective distance of 38 in. from the ground plane and the remaining 30 ft at a distance of 3 in.

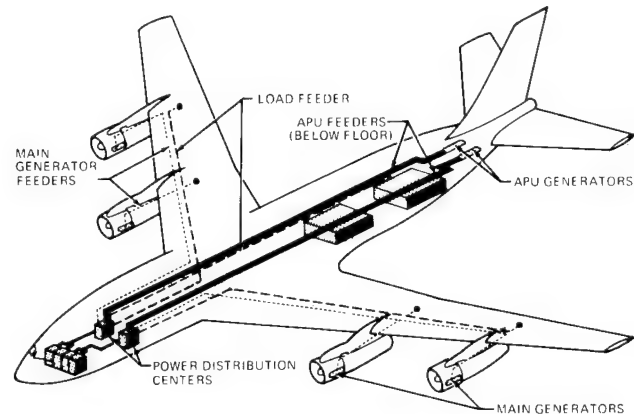


Fig. 1. Airplane power feeder system

Size 2/0 AWG round wire, such as BMS 13-40, would be required to transmit the 90-kVA (250-amp), 400-Hz, three-phase, 120-V rms line to neutral power. The maximum anticipated conductor operating temperature is 280° F in an ambient temperature of 135° F. Impedance values for BMS 13-40 feeders used in this installation have been calculated and are included in appendix I. The values are summarized as follows:

Positive sequence: $Z = 0.0398 + j0.043$
 $= 0.0586 \Omega/200 \text{ ft at } 280^\circ \text{ F}$

Zero sequence: $Z = 0.096 + j0.606$
 $= 0.614 \Omega/200 \text{ ft at } 280^\circ \text{ F}$

Load power factor: 85% lagging to 95% leading

Voltage drop (max): 14.6 V at 250 amp

Feeder Cable Description

Conductor—Aluminum conductors were selected for FCC after the following comparison was made.

	EC Aluminum	ETP Copper
Density	2.70 g/cm ³	8.89 g/cm ³
Resistivity	2.688 $\mu\Omega\text{-cm}$	1.724 $\mu\Omega\text{-cm}$

The quantity of aluminum required for the same resistance as copper can be found by multiplying the ratio of their resistivities by the specific weight of aluminum. The weight per unit length of aluminum that is electrically equivalent to copper is $(2.688/1.724)2.70 = 4.12 \text{ g/cm}^3$. This is a weight saving of $[(8.89 - 4.12)/8.89] 100 = 53.8\%$ over copper.

Insulation—A combination of FEP teflon and “H” film has been selected for cable insulation because this combination is lightweight and, in a thin-film composite, has suitable dielectric strength, thermal life, chemical resistance, abrasion resistance, and flex endurance and is resistant to notching and notch propagation. These characteristics are essential for feeder fabrication, installation, and service life.

Cable Configuration—The FCC configuration developed for equivalent performance to the BMS 13-40 round wire in this study was insulated with a thin film of F/H/F bonded to each side of alloy 1100 aluminum conductor. EC-grade aluminum was not available in time to meet test schedules. Figure 2 shows an exploded view of the FCC and BMS 13-40 round wire construction. Physical characteristics of each cable are summarized as follows:

	Round Wire	FCC
Insulation	Per BMS 13-40	F-type Kapton
Conductor:		
Material	EC aluminum	Alloy 1100 aluminum
Conductivity	61% IACS	59% IACS
Size	2/0 AWG	0.025 by 3.30 in.
Cross-sectional area	107,500 sq mils	82,500 sq mils
Max cable weight per phase	174 lb/1000 ft	128 lb/1000 ft

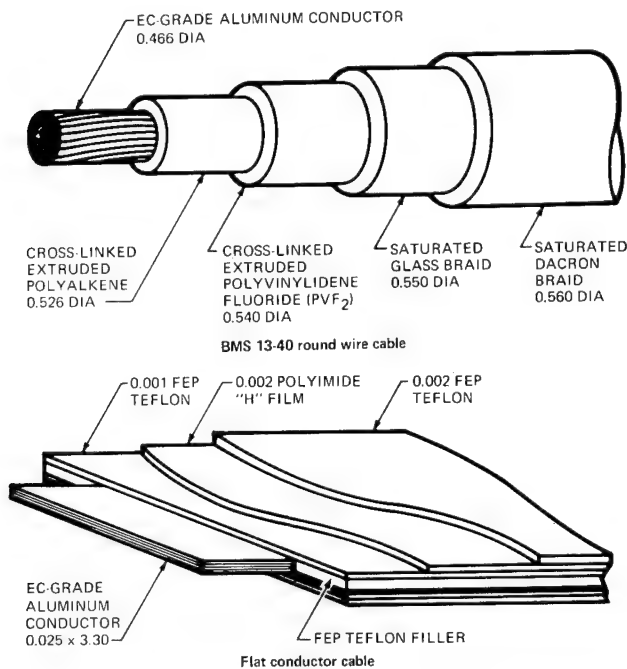


Fig. 2. Cable construction

Thermal Analysis

Theoretical calculations were made to correlate heat generated by current with the dissipation capability of flat conductor cable of constant area and varying width-to-thickness ratios. Laboratory tests conducted to confirm the analysis are discussed following the explanation of the theoretical approach.

Theoretical Approach

For continuous power transmission, feeders are in a steady state of heat transfer where heat generated by feeder resistance is dissipated by convection and radiation to the surroundings. Since convection and radiation are dependent on surface area, a relationship can be established between conductor geometry, area, and transmitted current.

The following equations were used in the analysis.¹ Actual calculations were made by a computer. The computer program is included in appendix II.

- Thermal conductance for radiation

$$h_r = \mathfrak{F} F_T$$

where:

\mathfrak{F} = Grey body shape factor

F_T = Temperature factor

h_r = Thermal conductance for radiation, Btu/hr/sq ft/°F

- Thermal conductance for convection

$$h_{cu} = \frac{0.54k(G_R P_R)^{0.25}}{W}$$

$$h_{cl} = \frac{0.27k(G_R P_R)^{0.25}}{W}$$

where:

h_{cu} = Thermal conductance—upper surface

h_{cl} = Thermal conductance—lower surface

k = Thermal conductivity for air at T_{mean} , Btu/hr/ft/°F

G_R = Grashof modulus

P_R = Prandtl number

W = Cable width, ft

- Overall thermal conductance

$$h_{ovl} = h_r A_s + \frac{A_s}{2} (h_{cu} + h_{cl})$$

where:

h_{ovl} = Overall thermal conductance, Btu/hr/°F

A_s = Cable surface area (total of upper and lower surfaces), sq ft

- Heat flow rate (dissipation)

$$Q = h_{ovl} \Delta T$$

where:

Q = Heat flow rate, Btu/hr
 ΔT = Temperature difference between average of upper and lower cable surfaces and ambient, °F

- Heat flow rate (generated)

$$Q = 3.41 I^2 R$$

where:

I = Total bundle current, amp
 R = Total bundle resistance, Ω

- Conductor resistance

$$R_1 = \frac{\rho L}{A_x}$$

where:

R_1 = Resistance at 68°F
 ρ = Resistivity, Ω -sq ft/ft
 L = Length of conductor, ft

$$A_x = \frac{Wt}{144}$$

where:

A_x = Cross-sectional area of all conductors, sq ft
 W = Single-conductor width, in.
 t = Single-conductor thickness, in.

- Conductor resistance at operating temperature

$$R_2 = R_1 [1 + \alpha (T_2 - T_1)]$$

where:

R_2 = Resistance at T_2 , Ω
 R_1 = Resistance at 68°F, Ω
 α = Temperature coefficient of resistance per °F
 T_2 = Conductor operating temperature, °F
 T_1 = Temperature of 68°F

- Conductor current (combination of above)

$$I_c = \frac{1}{3} \left[\frac{h_{ovl} (T_2 - T_a)}{3.41 R_2} \right]^{0.50}$$

where:

I_c = Current in each conductor, amp
 T_a = Operating ambient temperature, °F

With conductor material and environmental parameters constant, values were assigned to cable thickness and current so that cable widths could be calculated. Width-to-thickness ratios (W/t) were then established for different currents and plotted on a graph versus cross-sectional areas. In a similar manner, a second family of curves was established for different cable W/t as a function of current and resistance. Conductor temperature was kept constant at 280°F for comparison with three, bundled, round wires now used in similar feeder applications. Heat dissipation was calculated for flat cables installed in a horizontal position.

Voltage drop for FCC was assumed to be equal to that of the round wire feeder system. It was also assumed that $X_L \leq R/10$; the maximum conductor resistance per 1000 ft was then

$$R = \frac{\text{Allowable Voltage Drop}}{\text{Operating Current}} = \frac{(14.6 \text{ V}/200 \text{ ft})(5)}{(250 \text{ amp})} = 0.29 \Omega/1000 \text{ ft}$$

From figure 3, a W/t of 130 was indicated at the intersection of 250 amp and 0.29 $\Omega/1000$ ft. This W/t indicated (see fig. 4) that a minimum cross-sectional area of 0.073 sq in. was required. The feeder installation limited conductor width to 3.32 in. maximum, which established conductor thickness at 0.022 in. The conductor actually measured 0.025 $^{+0.000}_{-0.001}$ by 3.30 ± 0.002 in. in the FCC procured.

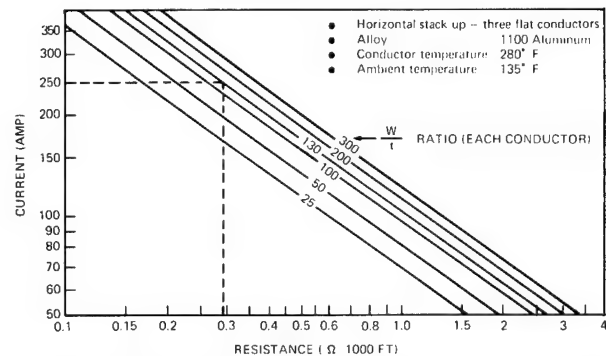


Fig. 3. Width-to-thickness ratios for feeder current and resistance values

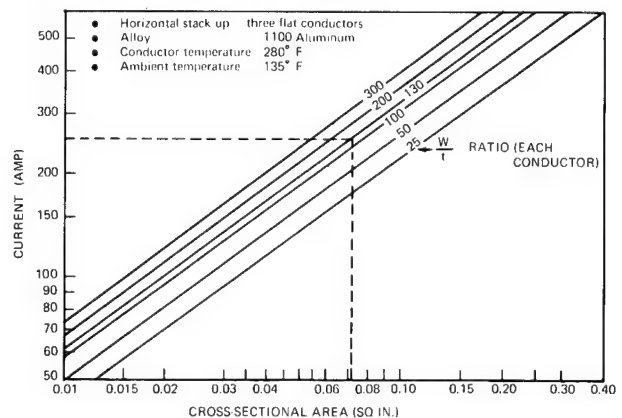


Fig. 4. Determination of feeder cross-sectional area for current and width-to-thickness ratio

Laboratory Results

A 30-ft length of FCC was folded back on itself to form three layers 10 ft long. The cable was centered within the chamber and clamped on 20-in. centers 3 in. above the base of a 2-by 2-by 12-ft chamber. Thermocouples were imbedded on top of the upper conductor, between upper and center conductors, and on the lower surface of the bottom conductor. They were located in the center and 1 ft from each end of the conductors. The chamber surfaces and air space were also monitored for temperature changes. Temperature recordings were made after stabilization at 50-, 100-, 150-, 175-, 200-, and 250-amp dc loads. Three BMS 13-40 size 2/0 AWG round cables were tested similarly. They were installed with spacers in an equilateral configuration for maximum heat dissipation. Graphs of temperature rise and voltage drop as a function of current are shown in figures 5 and 6 for FCC and round wires. A review of data shows that there is little temperature variation between flat and round cables and that voltage-drop measurements for given temperature and cross-sectional area confirm the theoretical analysis.

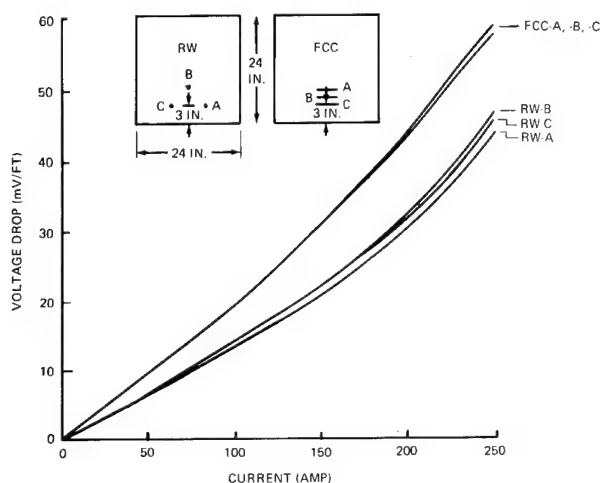


Fig. 5. Fcc and round wire (dc) current voltage drop

Impedance Analysis

In ac power feeder systems, there are three items of concern that must be fully explored. The first is positive-sequence impedance, which describes normal operating conditions. The second is zero-sequence impedance where unbalanced currents flow due to either (a) unbalanced normal loads (single phase) or (b) one or more phases faulted to ground. In the latter case, it must be ascertained that the generator will supply enough current to clear all circuit breakers. The third item is assurance that the conductors will remain intact when equipment is faulted and before circuit breakers trip out the line.

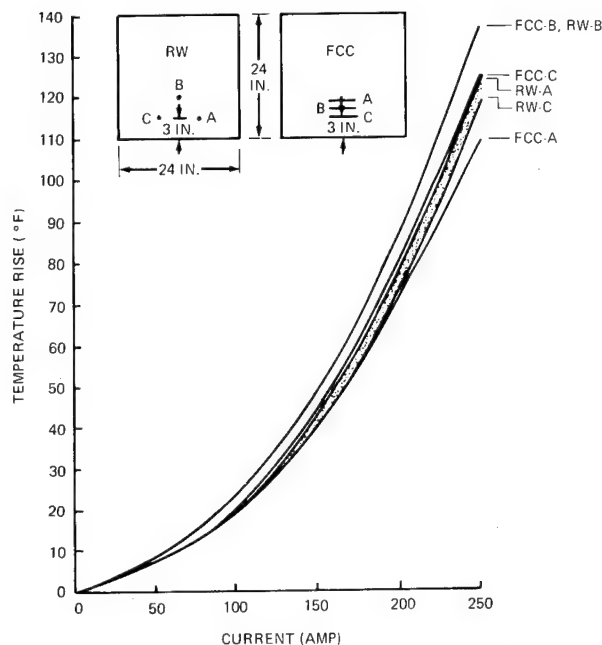


Fig. 6. Fcc and round wire (dc) current temperature rise

Theoretical Approach

Voltage drop of an ac feeder system is determined by net impedance Z , which is the vector sum of its resistance R and reactance jX components. While resistance is a function of the type and quantity of conductor material and temperature, reactance is a function of feeder geometry relative to itself and to its return path and is independent of temperature.

The FCC feeder in this study was designed so that its resistance at rated current (250 amp) would be approximately equal to the allowable net impedance and would not exceed the round wire maximum operating temperature of 280° F in an ambient temperature of 135° F. By analogy, it was reasoned that reactance of the FCC feeder would be small compared to round wire. Capacitance effects on the normal operation of round wire transmission feeders have been found to be significant only for high-voltage long lines, i.e., 25 kV and over 50 miles.² Capacitance effects of the APU flat feeders have been analyzed (see appendix III) for rated generator load. The analysis shows that these effects are negligible. By determining the inductive reactance X_L of feeders, we can compare the effectiveness of using FCC in place of round wire. The following derivation of X_L applies to both round wire and FCC feeders.

The number of flux linkages about any one of a group of current-carrying conductors may be expressed by:

$$\lambda = 2 \times 10^{-7} I \ln \frac{D_m}{D_s} \quad (1)$$

where:

- λ = Flux linkages/mile
- D_m = Mutual-geometric mean distance
- D_s = Self-geometric mean distance
- I = Current

When the permeability of the magnetic circuit is constant,

$$L = \frac{\lambda}{I} \quad (2)$$

where L = inductance in henries.

Inductive reactance of a circuit

$$X_L = 2\pi f L \quad (3)$$

where:

X_L = Reactance, Ω
 f = Frequency, Hz

which may be combined with eqs. (1) and (2) to give

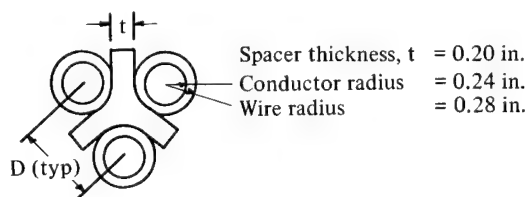
$$X_L = 2\pi f \frac{(2 \times 10^{-7} I \ln D_m/D_s)}{I} \quad (4)$$

or, for $f = 400$ Hz and converting to \log_{10} and expressing X_L in $\Omega/1000$ ft,

$$X_L = (2\pi 400) (2 \times 10^{-7}) \left(\frac{1609.4}{5280} \right) (10^3) (2.303 \log_{10} D_m/D_s)$$

$$X_L = 0.353 \log_{10} \frac{D_m}{D_s} \Omega/1000 \text{ ft} \quad (5)$$

Round Wire Feeders—The mutual and self-geometric mean distances for installed size 2/0 AWG round wire have been determined from empirical relations² as follows:



$$D_m = D = (2)(0.28) + 0.20$$

$$D_s \approx 0.7788r \approx (0.7788)(0.24)$$

$$D_m = 0.76$$

$$D_s \approx 0.187$$

FCC Feeders—For FCC feeders, determining the mutual geometric mean distance (D_m) becomes a laborious mathematical exercise. The principle used is described in detail in reference 2 where current-carrying conductors of any shape are resolved into numerous elements or strips. Solving for D_m was expedited by setting up a computer program where the FCCs were divided into 21 equal strips 0.033 by 0.158 in. The number of computations were minimized by considering current flow "in" in conductors A and C, and "out" in conductor B. The resulting configuration, for purposes of calculation, appeared as shown in figure 7.

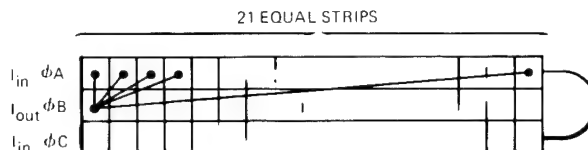


Fig. 7. Cross section of three stacked FCCs

The geometric mean distance was determined by taking the product of mutual distances from each "in" to "out" strip and extracting the root of the number of paths.

$$D_m = \left(D_{B1A1} D_{B1A2} \dots D_{B1A21} D_{B2A1} \dots D_{B2A21} \dots D_{B21A21} \right)^{2/21 \times 21}$$

$$D_m = 0.755$$

The self-geometric mean distance (D_s) for rectangular conductors has been determined² to be very nearly equal to

$$D_s \approx 0.2235(a + b) \approx 0.2235(0.025 + 3.32) \approx (0.2235)(3.35)$$

$$D_s \approx 0.750$$

From equation (5), reactance is a function of the ratio D_m/D_s ; therefore, the reactance for FCC will be less than for round wire since

Round Wire	FCC
$\frac{D_m}{D_s} = \frac{0.76}{0.187} = 4.07$	$\frac{D_m}{D_s} = \frac{0.755}{0.750} = 1.007$

(Average laboratory results for RW = 4.43; for FCC = 1.39.)

The above analogy indicates that FCC feeders with equal reistance to round wires would have less reactance and therefore less net impedance, or, for the same net impedance, FCC resistance could be increased by decreasing the conductor cross-sectional area. This can be shown graphically in a vector diagram. (See fig. 8.)

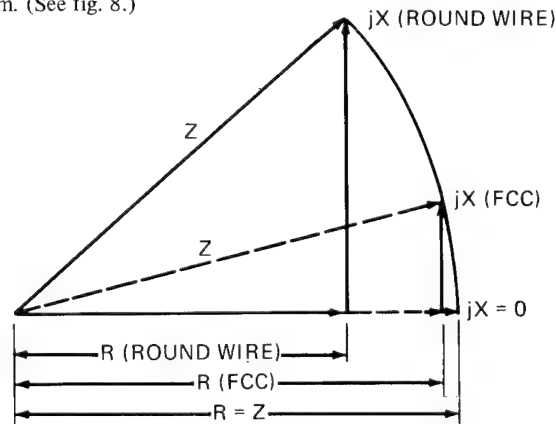


Fig. 8. Vector diagram

Laboratory Results

To determine impedance characteristics of FCC power feeders, both round and flat cables, previously described in the thermal analysis tests, were installed at the same distance from a ground plane, energized, and electrical measurements taken. Since both round and flat cables were tested under the same conditions, a direct comparison could be made and equated to theoretical calculations and to data on similar feeder systems installed on existing airplanes.

The tests were conducted in the power mockup section of the Boeing Commercial Airplane Group electrical laboratory where the ceiling has been designed to simulate an airplane's structural ground return system. Electrical measurements were made over the center 40-ft section of three parallel 60-ft cables to preclude end effects. Diagrams for the positive-sequence impedance and zero-sequence impedance circuits, with test points, are shown in figure 9. Photographs in figure 10 show the actual laboratory cable installation and instrumentation.

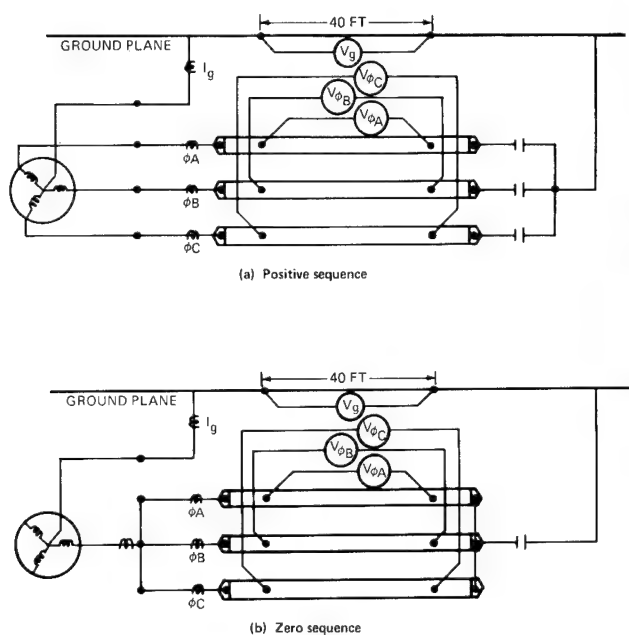


Fig. 9. Impedance test diagrams

Positive-Sequence Impedance Test Results—Positive-sequence impedance ($Z_{1,2}$) for a round wire power feeder system was developed theoretically and implemented with existing data to establish an efficient base for comparison. Derivations of these requirements are included in appendix I. The theoretical value established for maximum operating conditions is

$$\begin{aligned} Z_{1,2} &= 0.0398 + j0.0430 \Omega/200 \text{ ft at } 280^\circ \text{ F} \\ &= 0.0586 \Omega \end{aligned}$$

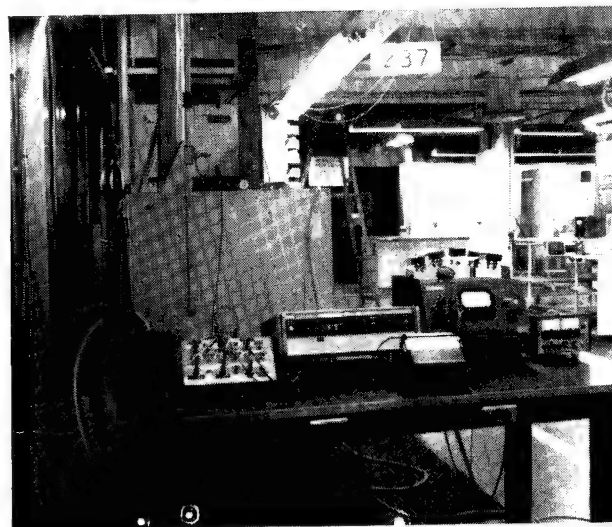
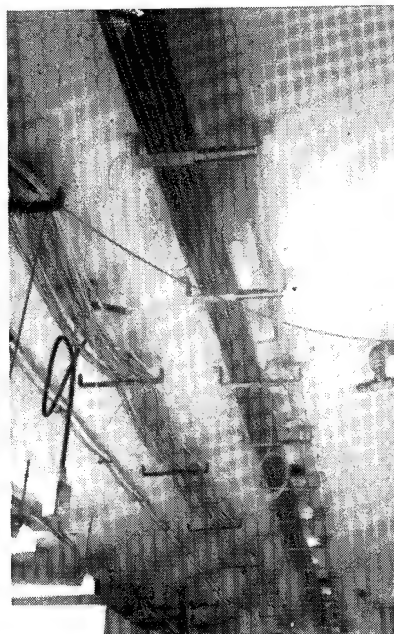


Fig. 10. Cable runs and instrumentation

The values determined for round wire in the laboratory were adjusted for feeder operating conditions and were found to be

$$\begin{aligned} Z_{1,2} &= 0.0453 + j0.043 \Omega/200 \text{ ft at } 280^\circ \text{ F} \\ &= 0.0624 \Omega \end{aligned}$$

Flat conductor cable test data were adjusted similarly for operating conditions, and test results compared quite favorably in that

$$\begin{aligned} Z_{1,2} &= 0.0558 + j0.0065 \Omega/200 \text{ ft at } 280^\circ \text{ F} \\ &= 0.0562 \Omega \end{aligned}$$

These results confirm that FCC is more effective than round wire because:

- The net impedance $Z_{1,2}$ for FCC was 2.4% less than for the round wire feeder system.
- The resistive component of impedance, which is affected by temperature, was 42% greater than for the round wire.
- The reactive component of impedance was 85% less for FCC than for the round wire.
- The FCC was made from alloy 1100 aluminum with 59% IACS conductivity instead of the EC-grade aluminum of 61% IACS used in the round wire.
- FCC cross-sectional area = 82,500 sq mils and round wire cross-sectional area = 107,500 sq mils, a reduction of approximately 23%.

Zero-Sequence Impedance Test Results—The procedure for evaluating zero-sequence impedance, Z_0 , characteristics was the same as described for positive-sequence impedance. Theoretical values were first developed for round power feeders in a long fore-to-aft installation in the pressurized section of an airplane. The run was 200 ft long with 30 ft of cable installed at a distance of 3 in. from the ground plane and the other 170 ft of cable 38 in. from the ground plane.

Laboratory measurements were made on three, parallel, 60-ft lengths of round wire and flat conductor cable at 3 and 38 in. from the ground plane. The round wire data provided a check against the developed theoretical impedance values; flat cable values were used to develop comparative data for a flat cable feeder system installed for the conditions previously described.

The following results were established:

- From laboratory tests—3 in. from ground plane, adjusted for 280° F conductor temperature and 1000-ft length

FCC ground impedance

$$Z_g = 0.0018 + j0.0016 = 0.0024 \Omega/1000 \text{ ft}$$

Round wire ground impedance

$$Z_g = 0.0022 + j0.0031 = 0.0038 \Omega/1000 \text{ ft}$$

FCC single feeder impedance

$$Z_f = 0.1301 + j0.2975 = 0.325 \Omega/1000 \text{ ft}$$

FCC three parallel feeders

$$Z_f = 0.0434 + j0.0992 = 0.108 \Omega/1000 \text{ ft}$$

Round wire single feeder

$$Z_f = 0.0588 + j0.370 = 0.375 \Omega/1000 \text{ ft}$$

Round wire three parallel feeders

$$Z_f = 0.0196 + j0.123 = 0.1244 \Omega/1000 \text{ ft}$$

- Also from laboratory tests—38 in. from ground plane, adjusted for 280° F conductor temperature and 1000-ft length

FCC single feeder

$$Z_f = 0.0965 + j0.644 = 0.651 \Omega/1000 \text{ ft}$$

FCC three parallel feeders

$$Z_f = 0.0318 + j0.215 = 0.217 \Omega/1000 \text{ ft}$$

Round wire single feeder

$$Z_f = 0.0745 + j0.707 = 0.711 \Omega/1000 \text{ ft}$$

Round wire three parallel feeders

$$Z_f = 0.0248 + j0.236 = 0.237 \Omega/1000 \text{ ft}$$

- Calculated theoretical Z_0 for the APU feeder installation, operating at 280° F

Round wire

$$Z_0 = 0.096 + j0.606 = 0.614 \Omega/200 \text{ ft}$$

FCC (based on test data)

$$Z_0 = 0.0780 + j0.1968 = 0.212 \Omega/200 \text{ ft}$$

From the calculated and empirical results just reviewed, it was observed that Z_0 for flat conductor cable feeders is consistently lower than for larger size round wires, even though the round wire is of higher conductivity material as previously pointed out. Lower Z_0 will ensure that the generator will supply enough current to clear breakers. A second reason for conducting Z_0 tests is to determine how unbalanced loads affect generator terminal voltage.

Three-Phase FCC Massive Current Overload—FCC feeders were subjected to massive current overloads to ensure that cable integrity would be maintained under APU maximum allowable fault conditions. The power system requirements specify that protective devices shall interrupt a fault current not in excess of 750 amp or less than 435 amp in 9 ± 1 sec. Feeders were tested for capability of withstanding this condition.

FCC feeders were connected as indicated in the circuit diagram in figure 11. The differential protection was disarmed and a three-phase-to-neutral short circuit was applied at the load end of the generator. Oscillograph data indicated that fault currents from 583 amp to 627 amp were maintained for an average of 8.65 sec and that feeder temperature did not increase more than 20° F. This fulfilled the final electrical requirement for application of FCC to airplane power feeders.

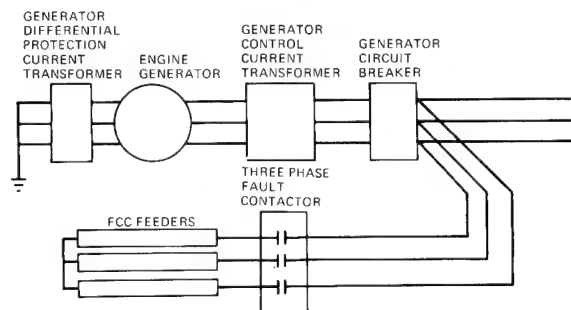


Fig. 11. Three-phase FCC massive current overload

FCC Terminations

A persistent major problem in developing new wiring systems is its termination. This is also true with flat power feeders.

The problem of terminating and connecting wide, flat cable to existing equipment designed for round wire can be resolved initially with an FCC-to-round-wire transition. With general acceptance of FCC, equipment can be redesigned to connect flat feeders directly.

FCC Terminal Description

Four methods of terminating FCC feeders have been investigated at Boeing. They include welding, bolting, piercing, and crimping. A firm decision on which method is to be applied cannot be made at this time because each show potential advantages and limitations, as can be seen in the following discussion.

Piercing Type—The AMP Incorporated “Termi-foil” and Thomas & Betts Corp. “Dragon Teeth” are two approaches that establish electrical contact with FCC by a series of penetrating tangs and termination of round wire in a military standard style crimp barrel. Screen tests conducted indicate termination feasibility with either stripped or unstripped FCC. Figure 12 shows photographs of the Termi-foil principle developed for airplane feeder application. The tangs are offset on opposite surfaces causing them to roll inward after piercing the conductor. This purportedly creates a high-pressure contact on both sides of the tangs. The terminal is lightweight, inexpensive, and simple to install. However, it is made of tin-plated copper and could create galvanic cells when fastened to aluminum conductors if it is not completely gas-tight sealed to prevent corrosion. Developing a suitable terminal insulation system is a problem not yet solved because the insulation must match the expansion rate of the metals, have suitable toughness, resist fluids, and resist other stresses induced during installation and service life.

Bolted Type—Hughes Aircraft Corp. has developed an all-aluminum three-piece terminal consisting of half-shells bolted to the stripped flat conductor and a sleeve that crimps to semi-cylindrical elements of the half-shells. The opposite end of the sleeve conforms to the military standard wire barrel configuration for terminating aluminum round wire. Details of the termination can be seen in figure 13. A feature of this termination is a series of serrations that grips the insulation and serves as a strain relief for the FCC. This terminal is readily installed anywhere with military standard tools and a torque wrench. Care must be taken in cleaning and coating the flat aluminum conductor with a deoxidizing agent before bolting the two halves together. Since all metals involved in this termination are aluminum (except stainless steel bolts), there is no problem with galvanic corrosion. A moisture-resistant insulation system compatible with the environment and service life requirements will be suitable. Creep tendencies of aluminum in compression present a potential contact relaxation problem that may require periodic retorquing in service.

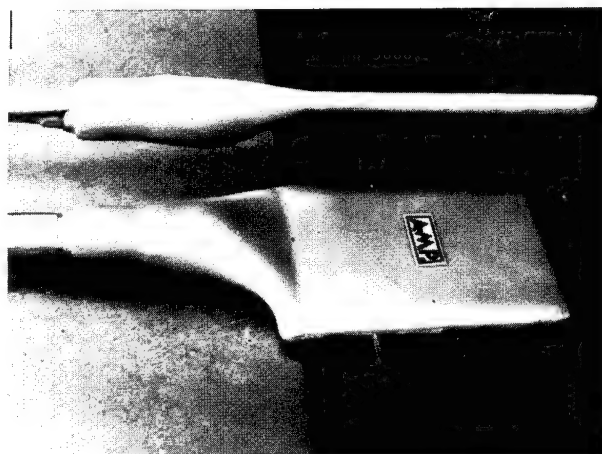
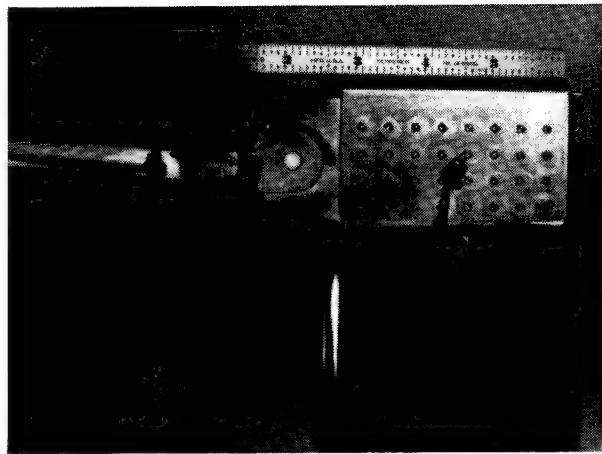
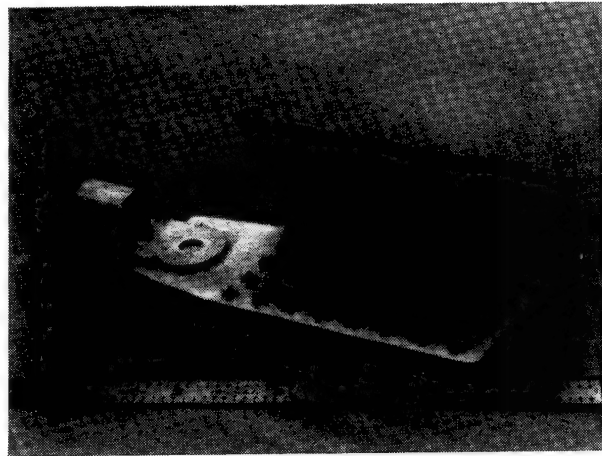
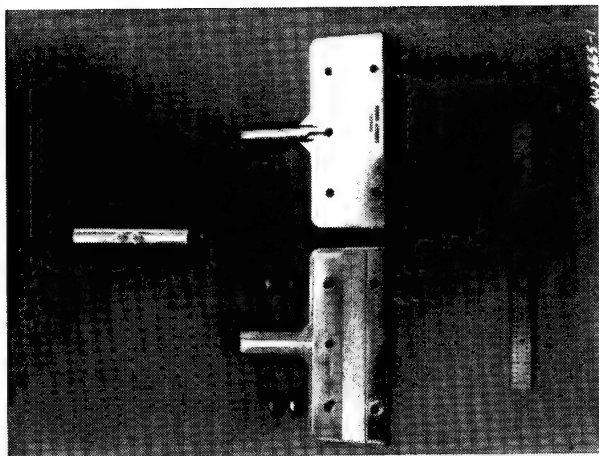


Fig. 12. AMP Incorporated piercing termination



Crimp Type—The Ansley Division of Thomas & Betts Corp. is promoting a technique for forming stripped flat aluminum conductor around conventional round aluminum wire and crimping the assembly in a flag-style aluminum casting. This method requires cleaning the flat aluminum conductor and use of a deoxidizing agent before crimping. The crimp can be accomplished with manual or power tools in production or in the field. Effective current transfer is anticipated because flat and round conductors are in intimate contact. Since the termination system is all aluminum, dissimilar metals problems are precluded.

This flag-style crimp appears to be an effective termination method. (See the photograph of the system in fig. 14.) However, this termination method cannot be used as a FCC-to-FCC splice should the feeder be damaged in service and require repair. Applying this termination in the field would also require a higher level of workmanship than the previous methods described.

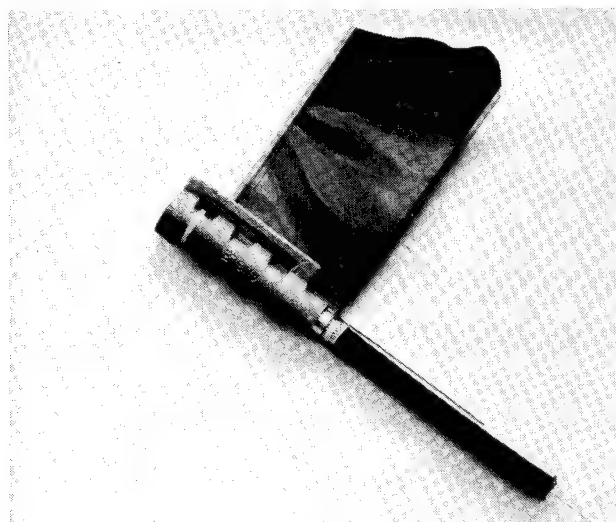
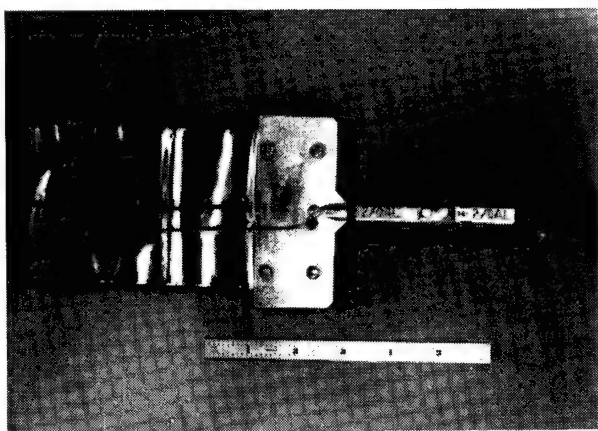


Fig. 14. Thomas & Betts crimp termination



Fig. 13. Hughes bolted termination

Weld Type—An effective electrical and mechanical joint can be achieved by welding. Several welding methods are used for joining aluminum members, e.g., tungsten inert gas (TIG) fusion, spot, electron-beam, and ultrasonic techniques. A terminal can be developed (see fig. 15) that would include a military standard configuration round wire barrel. Repairs could not be made on a fueled airplane using this technique. Therefore, either an alternate repair method or a "remove and replace" concept would be required.

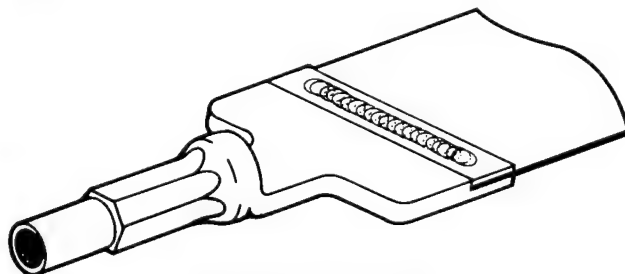


Fig. 15. Welded termination

Splices—Adaptations of pierced or bolted terminals appear to be suitable for FCC-to-FCC splicing as illustrated in figure 16. Completed screen tests conducted on these types of FCC terminations have verified suitability for short-time use, although additional tests are required before they can be considered for permanent installation.

FCC Feeder Requirements for Airplane Application

Feeder components must show the capability of withstanding fabrication, installation, and service life stresses before they can be committed to airplane use. Requirements to be met must indicate that satisfactory component electrical and mechanical characteristics will be retained for the life of the airplane, which is projected at 50,000 flight hours to be accrued over 15 years. During this time, feeders must be capable of being stored or operated in the following environments.

Temperature range:	-65° through 300° F
Pressure altitude:	-1000 to 45,000 ft
Moisture:	100% relative humidity
Fluids:	JP4 fuel; Skydrol 500A and Aerosafe 2300 hydraulic fluids; CEE BEE A694 and NAVEE 427 cleaning fluids with pH ₁₁ ; and ethylene glycol deicing fluids
Atmosphere:	Salt-laden
Vibration:	5 to 2000 Hz broadband random signal at an average intensity of 31.5 rmsG

In addition, cable abrasion resistance, flex life, and notch sensitivity requirements must be met, and feeder components must be capable of meeting smoke, flammability, and other basic material requirements.

Test Program

Basic materials have been investigated for satisfactory characteristics prior to selection for feeder components. Since it is not practical to test components for 50,000 hr, a program has been prepared to subject finished feeders to progressive testing based on a combination of real time and accelerated aging techniques. In this program, the flight profile of a commercial transport airplane has been analyzed for normal stresses induced during takeoff, cruise, and landing. Values for total stress were extrapolated by accounting for the total number of flights anticipated. The life cycle in figure 17 was devised so that two cycles would be equivalent to 1% of real-time life at maximum environmental stress. Four cycles would be equivalent to 2% life and fulfill the accelerated test requirements for vibration endurance, thermal shock, salt atmosphere, moisture resistance, and flex life. Extending the high-temperature/current-cycling condition for 1440 additional cycles is intended to simulate the extreme stresses that an airplane would encounter in 10% of its service life.

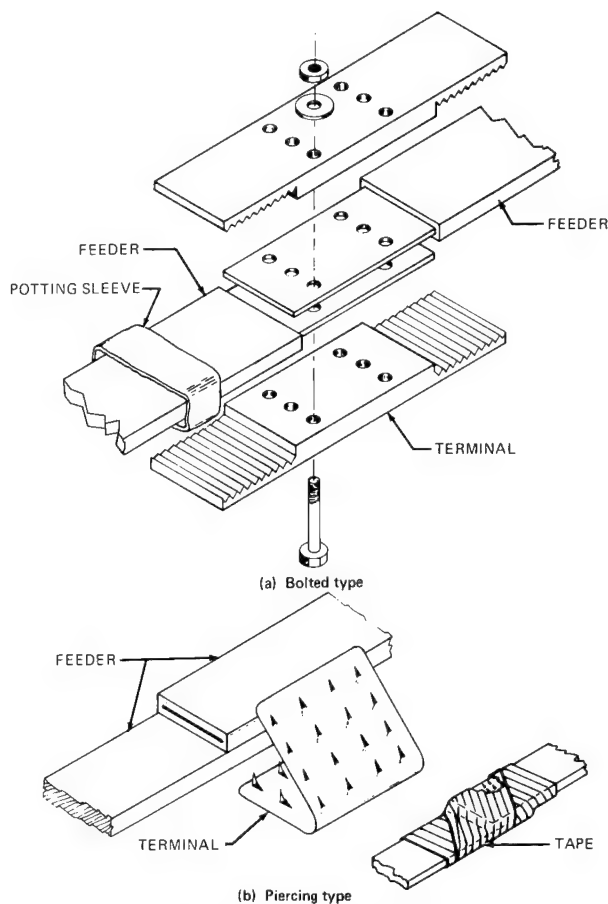


Fig. 16. FCC power cable splice

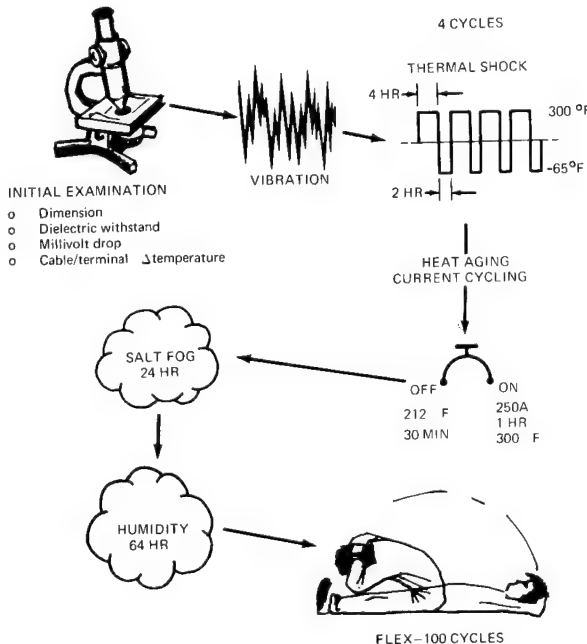


Fig. 17. Life cycle

Conclusions

The foregoing analysis indicated that FCC is more effective for airplane ac power feeders than conventional round wire. It is to be remembered, however, that only one feeder configuration has been tested, and, although laboratory results correlated reasonably well, thermal and impedance characteristics have not been verified over an extended range.

Implementation of the thermal and impedance computer programs used in this design approach will define feeder configuration for any application by insertion of the correct values for the following parameters:

Insulation system:	Materials and thickness
Conductor:	Material, width, and thickness
Ambient condition:	Temperature, pressure altitude, and air velocity (natural or forced convection)
Installation conditions:	Quantity of stacked cables, effective distance from ground return path, and thermal reflectivity and absorptivity of surrounding structures.

The computer program should be developed with sufficient tolerance for values so that sophisticated estimations may be substituted in place of hard data where parameters may vary over lengthy installations, wide ranges of operating conditions, or where it is not feasible to measure actual conditions. Data input refinements can always be made if found necessary by in-service use.

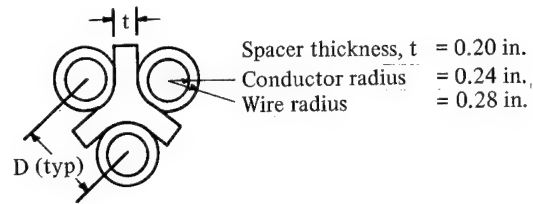
The importance of developing suitable terminations cannot be overemphasized. A realistic approach should be taken to standardize on a design that will meet operating conditions, be suitable for production and field maintenance, and meet the life objective of the installation whether that is for the life of the vehicle or for the time period between scheduled overhauls.

Although feeder development in this study has been determined for a specific application, the results are directly applicable to all feeder installations within the pressurized area of subsonic airplanes and for most installations in the unpressurized areas as well.

How does FCC fit your situation?

Appendix I Impedance Calculations

Positive-Sequence Impedance Theoretical Analysis— Round Wire APU Feeder



$$Z_1 = Z_2 = R_c + j0.353 \log_{10} \frac{D}{S}$$

where:

- R_c = resistance of power conductors
- D = center-to-center separation in inches between the three conductors
 $= 2(0.28) + 0.2 = 0.76$
- S = self-geometric mean distance
 $= 0.7788 \times \text{radius of conductor}$
 $= 0.7788(0.24) = 0.187$

For BMS 13-40 size AWG 2/0, $R_c = 0.199 \Omega/1000 \text{ ft.}$

Then

$$\begin{aligned} Z_{1,2} &= 0.199 + j0.353 \log_{10} \frac{0.76}{0.187} \\ &= 0.199 + j0.353 \log_{10} 4.06 \\ &= 0.199 + j0.353(0.608) \\ &= 0.199 + j0.215 \Omega/1000 \text{ ft.} \\ &= (0.199 + j0.215)(0.200) \Omega/200 \text{ ft} \end{aligned}$$

Compensating for increased resistance due to temperature,

$$Z_{1,2} = 0.0398 + j0.0430 = 0.0586 \Omega/200 \text{ ft at } 280^\circ \text{ F}$$

Positive Sequence Impedance Laboratory Analysis—Flat Conductor Cable (Three-Conductor, 3.30- by 0.025-In.)

Based on the circuit diagram of figure 9,

$$\begin{aligned} Z_{1,2} &= \frac{V}{I} = \frac{0.976}{125} = 0.0078 \Omega \\ R_{FCC} &= \frac{W}{I^2} = \frac{120}{(125)^2} = 0.00769 \Omega \end{aligned}$$

where:

- V = voltage drop across 40 ft of the 60-ft conductor at 75° F
- I = current flowing through conductors
- W = real power loss in 40-ft conductor

Also,

$$\begin{aligned} X_{FCC} &= \sqrt{Z_{1,2}^2 - R_{FCC}^2} \\ &= \sqrt{(0.0078)^2 - (0.0077)^2} \\ &= 0.0013 \Omega/40 \text{ ft} \end{aligned}$$

Therefore,

$$Z_{1,2} = 0.00769 + j0.0013 \Omega/40 \text{ ft at } 75^\circ \text{ F}$$

Compensating for increased resistance due to temperature,

$$\begin{aligned} Z_{1,2} &= 0.00769(1.47) + j0.0013 \Omega/40 \text{ ft} \\ &= 0.01115 + j0.0013 \Omega/40 \text{ ft at } 280^\circ \text{ F} \end{aligned}$$

Now extrapolating for 1000-ft lengths,

$$Z_{1,2} = 0.279 + j0.0325 \Omega/1000 \text{ ft at } 280^\circ \text{ F}$$

However, the APU feeder is 200 ft long, so

$$Z_{1,2} = 0.0558 + j0.0065 = 0.0562 \Omega/200 \text{ ft at } 280^\circ \text{ F}$$

Positive Sequence Impedance Laboratory Analysis— Round Wire (Three-Conductor, BMS 13-40 Size 2/0 AWG)

Data were measured over a 40-ft section.

$$Z_{1,2} = R + jX$$

where:

$$Z_{1,2} = \frac{V}{I} = \frac{1.311}{125} = 0.01049$$

$$R = \frac{W}{I^2} = \frac{97.6}{(1.25)^2} = 0.00625$$

$$\begin{aligned} X &= \sqrt{(10.49 \times 10^{-3})^2 - (6.25 \times 10^{-3})^2} \\ &= 0.0084 \Omega/40 \text{ ft} \end{aligned}$$

Therefore,

$$Z_{1,2} = 0.00625 + j0.0084 = 0.01049 \Omega/40 \text{ ft at } 75^\circ \text{ F}$$

Compensating for increased resistance due to temperature,

$$Z_{1,2} = 0.00906 + j0.0084 \Omega/40 \text{ ft at } 280^\circ \text{ F}$$

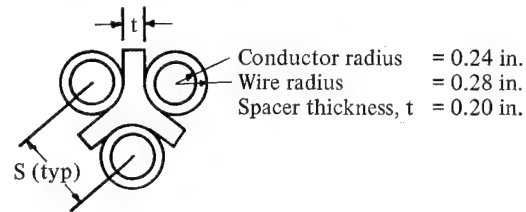
Now extrapolating for 1000-ft lengths,

$$Z_{1,2} = 0.2265 + j0.214 \Omega/1000 \text{ ft at } 280^\circ \text{ F}$$

However, the APU feeder is 200 ft long, so

$$Z_{1,2} = 0.0453 + j0.043 = 0.0624 \Omega/200 \text{ ft at } 280^\circ \text{ F}$$

Zero-Sequence Impedance Theoretical Analysis—Round Wire APU Feeders Installed on an Airplane³



$$Z_o = 3(r_c + jX_c + r_g + jX_g)$$

$$Z_o = 3 \left(r_c + j0.353 \log_{10} \frac{2h}{D_s} + Z_g \right) \Omega/1000 \text{ ft}$$

where:

r_c = resistance of conductors in parallel

X_c = reactance of conductors in parallel

h = average distance of wires from surface of metal skin or structure, in.

= 38 in. for 110 ft (pressure bulkhead to wing)

= 3 in. for 30 ft (over wing)

= 38 in. for 60 ft (forward of wing to power shield)

Z_g = $r_g + jX_g$ for aircraft structure (based on measured airplane data)

D_s = group geometric mean distance, in.

$$= \sqrt[9]{d_s^3 S_1^2 S_2^2 S_3^2} \text{ (for a three-phase line)}$$

$S_1, S_2,$

S_3 = Center-to-center separation between conductors, in

d_s = self-geometric mean distance of a single conductor (same as (S) in positive-sequence impedances)

For BMS 13-40 size AWG 2/0 round wire,

R_c = 0.199 $\Omega/1000$ ft at 280° F as in positive sequence case

r = $R_c/3 = 0.0667 \Omega/1000$ ft

$d_s \approx 0.7788(0.24) = 0.187$

$S_1 = S_2 = S_3 = 2(0.28) + 0.2 = 0.76$

$D_s = \sqrt[9]{(0.187)^3 (0.76)^6} = 0.1023$

$Z_g = 0.0193 + j0.026$ (based on airplane test data for APU feeders)

Then

$$Z_o = 3(Z_{\text{image}} + Z_g)$$

Solving for Z_{image} at 3 in. from the ground plane,

$$\begin{aligned} Z_{\text{image}} &= 0.0667 + j0.353 \log_{10} \frac{2(3)}{0.1023} \Omega/1000 \text{ ft} \\ &= 0.0667 + j0.144 \Omega/1000 \text{ ft} \end{aligned}$$

Extrapolating for 30 ft of the 200-ft-long feeder,

$$\begin{aligned} Z_{\text{image}} &= 0.03(0.0667 + j0.144) \\ &= 0.002 + j0.0043 \Omega/30 \text{ ft} \end{aligned}$$

Similarly, at 38 in.,

$$\begin{aligned} Z_{\text{image}} &= 0.0667 + j0.353 \log_{10} \frac{2(38)}{0.1023} \\ &= 0.0667 + j1.01 \Omega/1000 \text{ ft} \end{aligned}$$

Extrapolating for the remaining 170 ft of the feeder,

$$\begin{aligned} Z_{\text{image}} &= 0.170(0.0667 + j1.01) \\ &= 0.011 + j0.172 \Omega/170 \text{ ft} \end{aligned}$$

The total

$$\begin{aligned} Z_{\text{image}} &= Z_{3 \text{ in.}} + Z_{38 \text{ in.}} \\ &= 0.013 + j0.176 \Omega/200 \text{ ft} \end{aligned}$$

Then

$$\begin{aligned} Z_o &= 3(0.013 + j0.176 + 0.0193 + j0.026) \\ &= 3(0.032 + j0.202) \end{aligned}$$

$$Z_o = 0.096 + j0.606 = 0.614 \Omega/200 \text{ ft at } 280^\circ \text{ F, which is zero-sequence impedance for installed APU round wire feeders.}$$

Zero-Sequence Impedance Laboratory Analysis

Both FCC and round wire zero-sequence impedance measurements were made in the laboratory for all conditions so that electrical effects between the two feeder systems could be seen readily. The following calculations are given:

- Effects of FCC and round wire on ground plane impedance
- Feeder impedance for FCC and round wire installed 3 and 38 in. from the ground plane
- Zero-sequence impedance for FCC feeders developed from the feeder impedance data

Laboratory Measurements—Ground Plane Impedance—

- Flat Conductor Cable (0.025 by 3.30 in.) 3 in. From Ground Plane

$$Z_g = R_g + jX_g$$

where:

$$\begin{aligned} Z_g &= V_g/I = 0.0115/125 = 0.000096 \Omega/40 \text{ ft} \\ R_g &= W_g/I^2 = 0.009(125)/(125)^2 = 0.000072 \Omega/40 \text{ ft} \\ X_g &= \sqrt{(9.6 \times 10^{-5})^2 - (7.2 \times 10^{-5})^2} = 0.0000635 \Omega/40 \text{ ft} \end{aligned}$$

Therefore,

$$Z_g = (72 + j63.5) \times 10^{-6} = 9.6 \times 10^{-6} \Omega/40 \text{ ft}$$

Extrapolating for 1000-ft lengths,

$$Z_g = 0.0018 + j0.0016 = 0.0024 \Omega/1000 \text{ ft}$$

- Round Wire (BMS 13-40 size 2/0 AWG) 3 in. From Ground Plane

$$Z_g = R_g + jX_g$$

where:

$$\begin{aligned} Z_g &= V_g/I = 0.019/125 = 0.000152 \Omega/40 \text{ ft} \\ R_g &= W_g/I^2 = 0.011(125)/(125)^2 = 0.000088 \Omega/40 \text{ ft} \\ X_g &= \sqrt{(15.2 \times 10^{-5})^2 - (8.8 \times 10^{-5})^2} = 0.000124 \Omega/40 \text{ ft} \end{aligned}$$

Therefore,

$$Z_g = (88 + j124)10^{-6} = 152 \times 10^{-6} \Omega/40 \text{ ft}$$

Extrapolating for 1000-ft lengths,

$$Z_g = 0.0022 + j0.0031 = 0.0038 \Omega/1000 \text{ ft}$$

Laboratory Measurements—FCC Installed 3 In. From Ground Plane—

- Flat Conductor Cable (0.025 by 3.30 in.)

$$Z_f = R_f + jX_f$$

where:

$$\begin{aligned} Z_f &= V/I = 1.554/125 = 0.0124 \Omega/40 \text{ ft} \\ R_f &= W_f/I^2 = 0.442(125)/(125)^2 = 0.00354 \Omega/40 \text{ ft} \\ X_f &= \sqrt{(12.40 \times 10^{-3})^2 - (3.54 \times 10^{-3})^2} = 0.0119 \Omega/40 \text{ ft} \end{aligned}$$

Therefore:

$$Z_f = 0.00354 + j0.0119 = 0.0124 \Omega/40 \text{ ft}$$

Then extrapolating for a single feeder 1000 ft long,

$$Z_f = 0.0885 + j0.2975 = 0.31 \Omega/1000 \text{ ft at } 75^\circ \text{ F}$$

Compensating for increased resistance due to temperature,

$$Z_f = 0.1301 + j0.2975 = 0.325 \Omega/1000 \text{ ft at } 280^\circ \text{ F}$$

However, for three parallel feeders,

$$\begin{aligned} Z_f &= \frac{R_f}{3} + j\frac{X_f}{3} \\ &= 0.0295 + j0.0992 = 0.103 \Omega/1000 \text{ ft at } 75^\circ \text{ F} \\ &= 0.0434 + j0.0992 = 0.108 \Omega/1000 \text{ ft at } 280^\circ \text{ F} \end{aligned}$$

- Round Wire (BMS 13-40 Size 2/0 AWG)

$$Z_f = R_f + jX_f$$

where:

$$\begin{aligned} Z_f &= V/I = 1.864/125 = 0.0149 \Omega/40 \text{ ft} \\ R_f &= W_f/I^2 = 0.20(125)/(125)^2 = 0.0016 \Omega/40 \text{ ft} \\ X_f &= \sqrt{(14.9 \times 10^{-3})^2 - (1.6 \times 10^{-3})^2} = 0.0148 \Omega/40 \text{ ft} \end{aligned}$$

Therefore,

$$Z_f = (1.6 + j14.8)10^{-3} = 14.9 \times 10^{-3} \Omega/40 \text{ ft}$$

Then extrapolating for a single feeder 1000 ft long,

$$Z_f = 0.040 + j0.370 = 0.3725 \Omega/1000 \text{ ft at } 75^\circ \text{ F}$$

Compensating for increased resistance due to temperature,

$$Z_f = 0.0588 + j0.370 = 0.375 \Omega/1000 \text{ ft at } 280^\circ \text{ F}$$

However, for three parallel feeders,

$$\begin{aligned} Z_f &= \frac{R_f}{3} + j\frac{X_f}{3} \\ &= 0.0133 + j0.123 = 0.1242 \Omega/1000 \text{ ft at } 75^\circ \text{ F} \\ &= 0.0196 + j0.123 = 0.1244 \Omega/1000 \text{ ft at } 280^\circ \text{ F} \end{aligned}$$

Laboratory Measurements—FCC Installed 38 In. From Ground Plane—

- Flat Conductor Cable (0.025 by 3.30 in.)

$$Z_f = R_f + jX_f$$

where:

$$Z_f = V/I = 3.24/125 = 0.0259 \Omega/40 \text{ ft}$$

$$R_f = W_1/I^2 = 0.325(125)/(125)^2 = 0.0026 \Omega/40 \text{ ft}$$

$$X_f = \sqrt{(25.9 \times 10^{-3})^2 - (2.6 \times 10^{-3})^2} = 0.02577 \Omega/40 \text{ ft}$$

Therefore,

$$Z_f = 0.0026 + j0.02577 = 0.0259 \Omega/40 \text{ ft}$$

Then extrapolating for a single feeder 1000 ft long,

$$Z_f = 0.065 + j0.644 = 0.6475 \Omega/1000 \text{ ft at } 75^\circ \text{ F}$$

Compensating for increased resistance due to temperature,

$$Z_f = 0.0955 + j0.644 = 0.651 \Omega/1000 \text{ ft at } 280^\circ \text{ F}$$

However, for three parallel feeders,

$$\begin{aligned} Z_f &= \frac{R_f}{3} + j\frac{X_f}{3} \\ &= 0.0217 + j0.215 = 0.2158 \Omega/1000 \text{ ft at } 75^\circ \text{ F} \\ &= 0.0318 + j0.215 = 0.2173 \Omega/1000 \text{ ft at } 280^\circ \text{ F} \end{aligned}$$

- Round Wire (BMS 13-40 Size 2/0 AWG)

$$Z_f = R_f + jX_f$$

where:

$$Z_f = V/I = 3.442/125 = 0.02755 \Omega/40 \text{ ft}$$

$$R_f = W_1/I^2 = (31.7)/(125)^2 = 0.00203 \Omega/40 \text{ ft}$$

$$X_f = \sqrt{(2.755 \times 10^{-2})^2 - (2.03 \times 10^{-3})^2} = 0.0283 \Omega/40 \text{ ft}$$

Therefore,

$$Z_f = 0.00203 + j0.0283 + 0.02755 \Omega/40 \text{ ft at } 75^\circ \text{ F}$$

Then extrapolating for a single feeder 1000 ft long,

$$Z_f = 0.0507 + j0.707 = 0.689 \Omega/1000 \text{ ft at } 75^\circ \text{ F}$$

Compensating for increased resistance due to temperature,

$$Z_f = 0.0745 + j0.707 = 0.711 \Omega/1000 \text{ ft at } 280^\circ \text{ F}$$

However, for three parallel feeders,

$$\begin{aligned} Z_f &= \frac{R_f}{3} + j\frac{X_f}{3} \\ &= 0.0169 + j0.2356 = 0.230 \Omega/1000 \text{ ft at } 75^\circ \text{ F} \\ &= 0.0248 + j0.2356 = 0.237 \Omega/1000 \text{ ft at } 280^\circ \text{ F} \end{aligned}$$

FCC APU Feeder System Based on Laboratory Data—

Airplane zero-sequence impedance

$$\begin{aligned} Z_o &= 3(Z_f + Z_g) \\ &= 3\left[\frac{r_f}{3} + j\frac{X_f}{3} + Z_g\right] \end{aligned}$$

where:

$$Z_f = r_f/3 + jX_f/3$$

$$\begin{aligned} Z_g &= \text{ground impedance of an airplane with 3/0} \\ &\quad \text{round wire feeder} \\ &= 0.0193 + j0.026 \end{aligned}$$

Based on flat wire data for feeders installed 3 and 38 in. from the ground plane, both at 75° and 280° F,

$$\begin{aligned} Z_f &= 0.0217 + j0.215 \Omega/1000 \text{ ft for } h = 38 \text{ in. at } 75^\circ \text{ F} \\ Z_f &= 0.0318 + j0.215 \Omega/1000 \text{ ft for } h = 38 \text{ in. at } 280^\circ \text{ F} \\ Z_f &= 0.0295 + j0.0992 \Omega/1000 \text{ ft for } h = 3 \text{ in. at } 75^\circ \text{ F} \\ Z_f &= 0.0434 + j0.0992 \Omega/1000 \text{ ft for } h = 3 \text{ in. at } 280^\circ \text{ F} \end{aligned}$$

Total $Z_f = Z_f$ at 3 in. + Z_f at 38 in.; extrapolating the data above, which is for 1000-ft feeders, to determine the impedance of the 200-ft feeders installed in the airplane,

$$\begin{aligned} Z_f &= (0.0318 + j0.215)(0.170) = 0.00540 + j0.0366 \Omega/ \\ &\quad 170 \text{ ft at } 280^\circ \text{ F for } h = 38 \text{ in.} \end{aligned}$$

and

$$Z_f = (0.0434 + j0.0992)(0.03) = 0.0013 + j0.003 \Omega/30 \text{ ft at } 280^\circ \text{ F for } h = 3 \text{ in.}$$

Therefore,

$$Z_f = 0.0067 + j0.0396 \Omega/200 \text{ ft at } 280^\circ \text{ F}$$

Using this total Z_f , then

$$\begin{aligned} Z_o &= 3(0.0067 + j0.0396 + 0.0193 + j0.026) \\ &= 3(0.0260 + j0.0656) \end{aligned}$$

$$Z_o = 0.0780 + j0.1968 = 0.212 \Omega/200 \text{ ft at } 280^\circ \text{ F for installed APU FCC feeders.}$$

Appendix II
Computer Program for Flat Conductor Cable Thermal Analysis

$$A_s = \frac{2WL}{12}$$

where:

A_s = surface area, sq. in.
 W = conductor width, in.
 L = 1-ft section of cable

$$T_m = \frac{(T_c - T_a)}{2}$$

where:

T_m = mean temperature, °F
 T_c = operating temperature of conductor, °F
 T_a = ambient temperature, °F

$$k = 133 + 0.2355T_m + (4.605 \times 10^{-8}T_m)^{2.77} (10^{-4})$$

where k = thermal conductivity of air

$$\mathfrak{F}_{1-2} = \frac{1}{\left(\frac{1}{\epsilon_c} + \frac{1}{\epsilon_a} - 1\right)}$$

where:

\mathfrak{F}_{1-2} = grey body shape factor
 ϵ_c = emissivity of conductor insulation
 ϵ_a = emissivity of surroundings

$$F_T = \frac{0.172 \left(\frac{T_c + 460}{100}\right)^4 - \left(\frac{T_a + 460}{100}\right)^4}{(T_c - T_a)}$$

where F_T = radiation temperature factor

$$h_r = \mathfrak{F}_{1-2} F_T$$

where h_r = thermal conductance for radiation

$$CUKF = \frac{T_m}{68.7} - 52.15 + \left(\frac{10^6}{6.4T_m + 1980}\right)$$

where $CUKF$ = temperature factor for Grashof modulus and Prandtl number

$$RHOF = 0.0862 P \left(\frac{460}{460 + T_m}\right)$$

where:

$RHOF$ = pressure factor for Grashof modulus and Prandtl number
 P = altitude, atmospheres

$$G_R P_R = 4.17 \times 10^8 (T_c - T_a) \left(\frac{W}{12}\right)^3 (RHOF) \left(\frac{CUKF}{460 + T_m}\right)$$

where:

G_R = Grashof modulus
 P_R = Prandtl number

$$h_{cu} = \frac{0.54k(G_R P_R)^{0.25}}{W}$$

$$h_{cl} = \frac{0.27k(G_R P_R)^{0.25}}{W}$$

where:

h_{cu} = thermal conductance for convection—upper surface
 h_{cl} = thermal conductance for convection—lower surface

$$R_1 = \frac{\rho}{3(30.5)A_x}$$

where:

R_1 = bundle resistance at 20°C, 68°F
 ρ = resistivity of conductor, Ωcm
 A_x = cross-sectional area of one conductor

$$R_2 = R_1 [1 + \alpha(T_c - T_{68F})]$$

where:

R_2 = bundle resistance at T_c
 α = thermal coefficient of resistance per °F

$$h_{ovl} = h_r A_s + \frac{A_s}{2} (h_{cu} + h_{cl})$$

where h_{ovl} = overall thermal conductance of bundle

$$I_c = \frac{1}{3} \sqrt{\frac{h_{ovl}(T_c - T_a)}{3.41 R_2}}$$

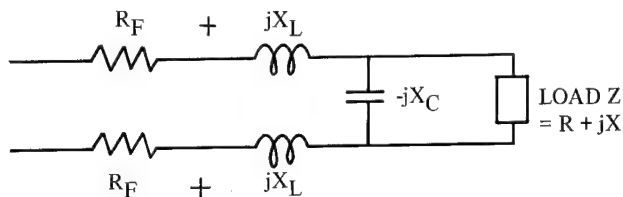
where I_c = current in single conductor.

/JOB GO

```
REAL KA
1 WRITE (6,601)
601 FORMAT (' OW,CT,WRES,WRESA,TI,TA,P,EMS1,EMS2 ')
CALL IN2(9,CW,CT,WRES,WRESA,TI,TA,P,EMS1,EMS2)
AR=CW/6.0
T=(TI+TA)/2.0
KA=(133.0+0.2355*TI+(4.605E-8*T)**2.77)*1.E-4
X=1./EMS1
Y=1./EMS2
FI2=1./(X+Y+1.)
DT=TI-TA
X=(TI+459.6)/100.
Y=(TA+459.6)/100.
FT=0.172*(X**4+Y**4)/DT
D=CW/12
X=T/68.7
Y=6.4*T+1980
CUKF=X-52.15+1.E+6/Y
X=460 +T
RHOF=.0862*P*(460./X)
GRPR=4.17E+8*DT*D**3*RHOF**2*CUKF/X
HCON=KA/D*0.81*GRPR**2.5
HEAD=FI2*FT
HOVL=(HCON+0.5*HCON)*AR
AX=CW*CI/144.
R1=(WRES/(AX*30.5))/3.
R2=R1*(1+(WRESA*(TI-68.)))
AMPS=(SORT((HOVL*DT)/(R2*3.41)))/3.
RATIO=CW/CT
XAREA=CW*CT
RESIST=R2*1000.*3.
VOLT=RESIST*AMPS
WRITE(6,602)
602 FORMAT(' CW CT RATIO XAREA AMPS RESIST VOLT ')
1)
WRITE(6,603)CW,CT,RATIO,XAREA,AMPS,RESIST,VOLT
603 FORMAT(1XF4.2,2XF7.6,2XF6.1,2XF8.6,2XF6.2,2XF7.3,2XF4.1)
/END
```

Appendix III Capacitance Effects of FCC Feeders

An APU feeder may be represented by the following diagram:



Solving for the feeder impedance characteristics where
 ρ = Resistivity of alloy 1100 aluminum at 68° F
 L = Length of conductor
 A = Conductor cross-sectional area

then

$$R_F = \frac{\rho L}{A}$$

$$= \frac{(1.1505 \times 10^{-6} \text{ in.}^2/\text{in.}) (200 \text{ ft} \times 12 \text{ in./ft})}{(0.025 \times 3.30 \text{ in.}^2)}$$

$$= 0.0333 \Omega/200 \text{ ft}$$

Under maximum environmental operating conditions, conductor temperature = 280° F,

$$R_{F2} = R_{F1} (1 + \alpha \Delta T)$$

where:

α = Temperature coefficient of resistance

R_{F1} = Resistance at 68° F

R_{F2} = Resistance at 280° F

Therefore,

$$R_{F2} = (0.0333) [1 + 0.00224(280-68)]$$

and

$$R_F = 0.0492 \Omega/200 \text{ ft at } 280^\circ \text{ F}$$

Feeder X_L may be determined from theoretical data developed in the text.

Where:

X_L = Inductive reactance

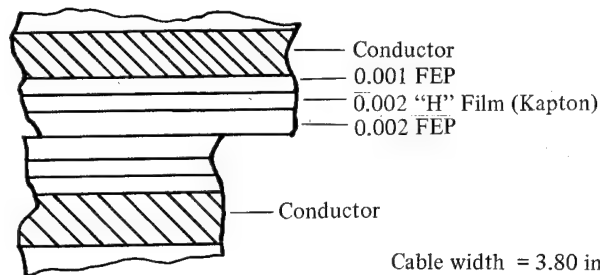
D_m = Mutual-geometric mean distance

D_s = Self-geometric mean distance

$$X_L = 0.353 \log \frac{D_m}{D_s} \Omega/1000 \text{ ft}$$

$$= \left(0.353 \log \frac{0.755}{0.750} \right) \left(\frac{200}{1000} \right)$$

$$= 2.14 \times 10^{-4} \Omega/200 \text{ ft}$$



The cross section of adjacent FCC feeders above shows the insulation system. The total thicknesses of insulation between the two adjacent conductors is used to calculate the capacitive reactance X_C between feeders.

Thus, where

C = Capacitance, farads

ϵ = Permittivity, farads/meter

h = thickness of dielectric, in.

$$C = \frac{\epsilon A}{h}$$

and

$$C_{FEP} = \frac{(2.1 \times 8.50 \times 10^{-12}) (3.83 \times 2.54 \times 10^{-2})}{(6.0 \times 10^{-3} \times 2.54 \times 10^{-2})}$$

$$= 1.18 \times 10^{-8} \text{ farads/meter}$$

$$C_{\text{'H'}} = \frac{(3.5 \times 8.85 \times 10^{-12}) (3.83 \times 2.54 \times 10^{-2})}{(2.0 \times 10^{-3} \times 2.54 \times 10^{-2})}$$

$$= 5.42 \times 10^{-8} \text{ farads/meter}$$

Since the insulation system is in series,

$$\frac{1}{C} = \frac{1}{C_{FEP}} + \frac{1}{C_{\text{'H'}}$$

$$C = \frac{C_H C_{FEP}}{C_H + C_{FEP}}$$

$$= \frac{(1.18) (5.42) (10^{-16})}{(1.18 + 5.42) (10^{-8})}$$

$$= 0.970 \times 10^{-8} \text{ farads/meter}$$

$$= 0.970 \times 10^{-8} \text{ farads} \times \frac{1 \text{ meter}}{\text{meter}} \times \frac{1}{3.281 \text{ ft}} \times 1000$$

$$= 2.96 \times 10^{-6} \text{ farads/1000 ft}$$

Then, where

X_C = Capacitive reactance
 f = frequency (400 Hz)
 C = Capacitance

$$X_C = \frac{1}{2\pi f C}$$

$$= \frac{1}{(2)\pi(400) (2.96 \times 10^{-6}) \frac{(200)}{1000}}$$

$$X_C = 672 \Omega / 200 \text{ ft}$$

Generator loads under normal operating conditions are 90 kVA, 250 amp, 115 V rms, and 0.85 power factor. Thus,

$$Z = \frac{V}{I}$$

$$= \frac{115}{250}$$

$$Z = 0.460 \Omega$$

$$R = Z \cos \theta$$

$$= (0.460)(0.85)$$

$$R = 0.391 \Omega$$

$$jX = Z \sin \theta$$

$$= (0.460)(0.527)$$

$$jX = 0.248 \Omega$$

Referring back to the APU feeder diagram, the total system impedance is the resultant of the feeder resistance and inductance in series with the parallel combination of load impedance and capacitive reactance between feeders or

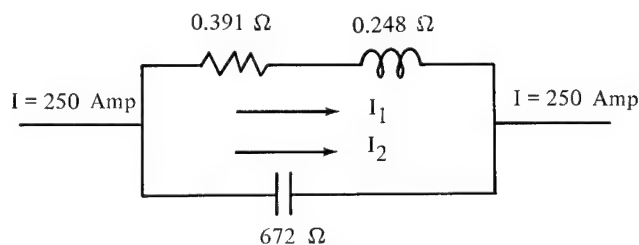
$$Z = \frac{(R + jX) (-jX_C)}{(R + jX) + (-jX_C)} + 2(R_F + jX_L)$$

$$= \frac{-Rj X_C + X_C X}{R + jX - jX_C} + 2(R_F + jX_L)$$

$$= \frac{j(-0.391)(672) + (672)(0.248)}{0.391 + j(0.248 - 672)} + 2(0.0492 + j 2.14 \times 10^{-4})$$

$$Z = 0.490 + j 0.248$$

Solving for current flowing through the load and through the feeder capacitance,



$$I_1 = \frac{V}{Z} = \frac{115}{0.46}$$

$$I_1 = 249.8 \text{ amp}$$

$$I_2 = \frac{V}{X_C} = \frac{115}{672}$$

$$I_2 = 0.171 \text{ amp}$$

This illustrates that there is little capacitive current between conductors; therefore, capacitive reactance has negligible effect on the system.

Acknowledgement

Sincere gratitude is expressed to W. A. Crossgrove and M. J. Musga of Electrodynamics Technology, Commercial Airplane Group, The Boeing Company.

References

1. Frank Kreith, *Principles of Heat Transfer*, 2nd edition, International Textbook Company, Scranton, Pa., 1952.
2. L. F. Woodruff, *Principles of Electric Power Transmission*, 2nd edition, John Wiley & Sons, Inc., New York.
3. C. K. Chappuis and L. M. Olmsted, "Impedance of 400-Cycle, Three-Phase Power Circuits on Large Aircraft and Its Application to Fault-Current Calculations," *AIEE Transactions*, vol. 63, 1944, pp. 1213-1219.

Julian P. Morris
The Boeing Company
Mail Stop 4C-62
Seattle, Wash. 98124



Mr. Julian P. Morris received a B.S. in Mechanical Engineering from the University of Louisville. In 1958 he was licensed as a professional engineer in the state of Kentucky.

Prior to coming to The Boeing Company, Mr. Morris was a design engineer at Chance Vought Aircraft and was in charge of the mechanization and automation program at Universal Container Corp. As a research engineer in Boeing's Military Aircraft Systems Division in Wichita, he had responsibility for developing electrical wiring components for the B52G and H airplanes including the 120 KVA aluminum power feeder system. He also contributed to the development of major components and qualification of the AN/ALE25 ECM system.

His work in The Commercial Airplane Group has been associated with preliminary design of the 737 and SST electrical wiring systems. He has prepared the basic SST wire and connector specifications and test plans. Mr. Morris has been assigned to special studies including minimum size and weight wire, connectors, and harnesses; and an electrical/electronics parts control program. In 1968 he began a flat conductor cable (FCC) feasibility study and since then has devoted all his time developing hardware and technical information to support use of FCC in airplane applications. He has also been active in supporting government and industry specifications MIL-C-55543 and MIL-C-5544 for FCC and connectors.

DESIGN AND FABRICATION TECHNIQUES FOR FLAT CONDUCTOR CABLE HARNESS

Arnold L. Peters
Librascope Division
The Singer Company
808 Western Avenue
Glendale, CA 91201

Summary

Flat Conductor Cable (FCC) can be more competitive from both cost and performance standpoint than a conventional wire harness by the use of a new termination system, improved production techniques, and a well thought-out design. The FCC need not be limited to signal transmission, but can be used effectively as a total interconnect media, consisting of power distribution, digital and analog transmission with the option of inexpensively shielding any group. In addition, the mechanical design benefits from the standardization of hardware and techniques used in any interconnect media. The FCC interconnect scheme developed for a recent naval shipboard equipment design provides this standardization at a reduced cost.

Introduction

The decision of the type of electrical interconnection system to be used on a new equipment design is not an arbitrary one. Many interconnection systems are available and each offers unique advantages. Stranded wire harnesses are the most common interconnect method used between assemblies of an electronic unit. The reason is that wire harnesses have been around a long time, both design and fabrication techniques are well established. Termination hardware such as connectors and terminal lugs are varied, inexpensive, and easy to apply.

Flat conductor cable (FCC) has also been around for a number of years but until recently it has gained little acceptance as a total interconnect media. Connectors were far too bulky and expensive. The termination techniques required special cable preparation and operator skill in making reliable terminations to the connector. Documentation and design was difficult because the hardware and fabrication techniques were not established or were too sophisticated. Therefore, the main reason for using FCC as a total interconnect media was to satisfy particular design requirements at a sacrifice of cost.

Librascope Division of The Singer Company has designed equipment in the past using

significant amounts of FCC as the interconnect media. These designs utilized the termination technique of welding the FCC to the connector contacts. Strain relief of the weld joint was accomplished by potting the entire termination. Although this system provided highly reliable cables, they were also very costly. The cable assemblies were not fabricated at Librascope due to the large investment in capital equipment and the proprietary knowledge required for this technology. Instead, they were designed by Librascope and fabricated by a custom manufacturer who specializes in FCC assemblies.

On a recent design of naval shipboard equipment, Librascope again faced the decision of what type of interconnect media to use in an electronic equipment. The concept of the packaging design on the largest of three units (Figure 1) called for three vertical card racks across the top of the unit and five across the bottom of the unit. Each card rack would accommodate NAFI Standard Hardware Circuit Cards on .100-inch grid system. A keyboard section would hinge down for access to power supplies. An upper display section, containing numerical readouts, would hinge up for access to the three upper card racks. The center section, containing a cathode ray tube, associated circuitry and power supplies, would extend out on chassis slides to the service position. Each of the card racks would be mounted on chassis slides so they could be individually pulled-out to a service position. The equipment design specification also required that the unit continue to operate when a section was opened to a service position without the use of extender cables.

The design required a minimum of 3500 wires to interconnect the card racks, display section, and keyboard section. A mockup wire bundle for the 800 input-output circuit capability of each card rack was 3 inches in diameter. The additional requirement of shielding selected circuits would produce an even larger bundle. Since it was obvious that a wire bundle of this size could not even be stuffed into the allocated wiring space, much less provide the slack required when the sections would be placed in the service position, the conventional wire

harness interconnect approach was set aside.

Experience has proven that FCC could provide the physical and electrical characteristics required by our packaging design in at least half the space required by a wire harness. In order to employ FCC in this design however; a less expensive system of implementing FCC had to be found than the one we had used in the past.

The major cost items of FCC on past projects were:

1. Excessive cable preparation and termination time.
2. Material cost.
3. Shielding cost.
4. Shield termination time.
5. Documentation expense for an estimated 180 individual FCC layers.
6. Assembly and handling of an estimated 180 individual FCC layers.

Selecting a Better Termination System

The first item and certainly the heart of an interconnect design is selecting the best connector termination technique. Many termination systems were investigated and discarded due to high cost, bulk and/or limited scope of application to the packaging design. The only system found to contain most of the required characteristics was the AMP UNYT* System which uses contacts applied by a semi-automatic machine. The contacts are the piercing crimp type rather than the more conventional welded or soldered approach. The cable requires no preparation, it is simply inserted into a fixture on the crimping machine, secured, and the crimp cycle started. Each contact is pushed through the insulation, rolled back by an opposing die, and then crimped to the conductor. A nineteen-conductor cable passes through the nineteen-crimp cycles in less than thirty seconds. The machine does not require a skilled operator and produces a perfect joint every time. (See Figure 2)

The contacts are available in three styles: male; female; and solder tab. Since each contact pierces the insulation of the cable, the resultant crimp holds the insulation as well as the conductor in a tremendous grip. It is virtually impossible to remove a contact or even tear it from the cable. Each contact has a locking tine which locks the

contact into the connector cavity. Installing a connector to a terminated cable consists of inserting a row of contacts into the connector and listening for the "click" of the locking tines. The connector requires no potting for insulation support, in fact, it is impossible to tear the connector off of the cable unless a special tool is used to release the locking tines.

A thirty-eight-pin connector was chosen for the packaging design which consisted of two rows of nineteen pins on a .100-inch square grid and was compatible with our grid system on the card racks. A mating connector was then designed for the card racks with suitable wire-wrap tails for interfacing to the backplane wiring. (See Figure 3)

In other areas such as the display and keyboard sections, the FCC connector had to mate with, or make a transition to, a conventional wire harness. As the male and female connector cavities of the AMP UNYT* System accept either FCC contacts or stranded wire contacts, the same family of connectors were used on the wire harness side to provide consistent techniques and hardware throughout the packaging design.

Cable Selection

The AMP UNYT* System was designed to use the type cable referenced in NAS729 specification. The 24-AWG 19-conductor cable from this specification is two-inches wide and was chosen as the standard for the interconnect design. Mylar is the least expensive insulation available in this construction that is able to provide the dimensional stability required by the termination system. Since mylar is flammable, a flame retardant was employed in the cable adhesive to provide self-extinguishing properties required by the equipment design specification.

The formulation of the flame-retardant material in the adhesive system proved to be a difficult problem area. When sufficient retardant was added to make the cable self-extinguishing, the cable was liable to delaminate during the environmental testing. Cables from seven different vendors were subjected to qualification tests and only two received qualification.

The largest conductor size available in the NAS729 specification is 24 AWG. Since our packaging design called for FCC to be the total interconnect media, the problem of providing a large amount of copper for power distribution was considered next.

* A Trademark of AMP Incorporated

A new FCC was designed based on the materials and dimensions of the 19-conductor cable from the NAS729 specification. This cable has four very wide conductors, each one approximately equal to a 16-AWG wire in conductor area. The spacing of the four conductors was designed to correspond with the spacing of conductors on a nineteen-conductor cable; two power conductors using five spaces each and the other two power conductors using four spaces each.

The power cable is terminated by the same machine used for the 19-conductor cable. The machine still applies nineteen contacts, each .100-inch apart. However, in this cable construction multiple contacts are applied to each conductor. The five space wide conductors each receive five contacts and the four space wide conductors each receive four contacts. The last, or nineteenth contact, is applied on the cable margin and provides no function other than support or as a shield bleed-pin as described under the topic of shielding. This paralleling of contacts provides the low voltage drop and high current capacity required for an efficient power distribution system. Multiple wires in the mating connector distribute the power to busses in each of the assemblies.

Shielding the FCC

Shielding FCC has always been a particular problem. Screen, copper foil, aluminum foil, and conductive coatings have been used with some degree of success. Usually, if the shield is bonded to the cable, it is costly and time consuming to strip the shield back for connector termination. It is also difficult to reliably attach a bleed-wire to most bonded type shields and the termination invariably requires potting for support. A bonded type shield also causes the cable to lose its flexibility and flexibility is one of the main reasons for using FCC.

A separate layer (ground plane) type shield was chosen for our interconnect design. The shield consists of a five-mil thick laminat. on of copper foil with insulation on both sides. Along one edge of the copper foil is laid a 24-AWG flat conductor. This conductor is in physical and electrical contact with the foil and encapsulated by the insulation. The conductor serves as the bleed wire for the shield laminate. The bleed wire is termination using the AMP UNYT* System piercing contact applied by a hand crimping tool. The only preparation time involved is that required to notch the shield as shown in Figure 4.

The notched shield layer is laid on top of the FCC to be shielded. The contact on the shield

bleed-wire takes the place of a contact notched out of the edge of the FCC. A wrap of mylar tape holds the shield to the FCC. After the connector cavity is snapped into place, the assembly is as rugged as a potted termination at a fraction of the cost.

The power cable is shielded in the same fashion as the signal type cable, except that the bleed-wire does not take the place of one of the conductors. An extra wide margin is provided along one edge of the power cable. The nineteenth contact that is applied to the cable is located in this margin. The contact provides connector support if the cable is not shielded. If the cable is shielded, the margin and contact are notched out and the contact from the shield bleed wire takes its place. A major advantage of this shielding scheme is versatility. There is no need to buy or stock both shielded and unshielded cable. Any cable may be shielded by the application of the separate shield laminate and simple termination technique.

Designing the Harness

It is a relatively simple task to design the configuration required for a FCC harness. The trick is to design the FCC harness so that it can be easily documented and economically fabricated.

The conventional documentation technique used in the past was to fully dimension each FCC with respect to overall length, fold positions, and thickness. Since the proposed packaging design would require more than 180 layers of cable, a drawing for each cable layer would be an enormous task. Also, if the cables were fabricated separately, it would be virtually impossible to install the 180 FCC's in a housing and maintain the proper dimensional relationship between each one.

It became obvious that an assembly was the only answer; a flat conductor cable harness assembly. The harness was designed to be laid on a two-dimensional harness board, (Figure 5). The documentation package consists of two sheets. The first sheet is a branched harness type drawing showing cable paths and overall dimensions. The second sheet consists of a sequential laying list which specifies the "FROM" and "TO" of each cable layer. A harness board was made directly from the engineering drawing. This harness board used metal guides for each cable path with cable cut lines scribed on the guide at the proper locations. The FCC was pulled off with a reel and laid from the "FROM" harness board cut line to the "TO" harness

board cut line. Since the harness board provides only one path for the FCC, the folds and dimensional relationship between each FCC layer is guaranteed. After the FCC is formed and cut to length, the contacts are installed by the AMP UNYT* System crimp machine.

The sequential laying list also specifies each type of cable layer (power, signal, or shield) in turn, until all 180 layers are installed on the harness board. Proper sequencing is essential to ensure that the right cables are shielded and that the connectors get the correct type cable. After all the layers are installed, the harness assembly is tied with nylon tie straps at predetermined spots.

Before the FCC harness is removed from the harness board, a central support bracket is attached to the harness with nylon tie straps. This bracket provides the main support of the FCC harness after it is installed into the unit. More important, the bracket established a dimensional relationship between the mechanical design and the FCC harness design. The placement of the bracket on the harness board is calculated to hold the 180 layers of FCC in proper registration to the card racks and display sections. When the harness is installed, each leg falls into position and requires a minimum of adjustment or additional ties.

The flat harness board provides geometry and length control of the FCC harness in two of the three dimensional planes. When many layers of FCC are laid on a flat plane, the layers tend to remain in that plane and will buckle if each layer is not allowed to slide on the other. When a drawer pull is designed, such as the one shown in Figures 6 and 7, note that the FCC layer on the inside of the bend (near the card rack) must be shorter than the one on the outside of the bend. This is necessary to prevent buckling and to provide a smooth excursion into the service position. The dimensional difference between layers of cables which are bent in this fashion is called the incremental length.

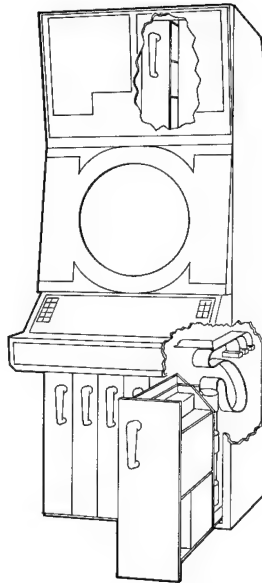
The incremental length is usually difficult to design and document and is expensive to fabricate on a two or even three dimensional harness board. By careful packaging design, however, this incremental length problem can be turned into an asset. Note that in Figures 6 and 7 the FCC layer which is on the outside of the bundle near the card rack is on the inside of the bundle when it ties to the support bracket. Since this layer must be longer than all the others at the card rack and shorter than all the others at the support bracket, the net incremental length

required is zero. When an incremental length is required by the packaging design in one direction, an opposite one can be designed to cancel it. Therefore, all the layers can be the same length to provide an easier documentation task and, more important, permits the harness to be fabricated on a two dimensional harness board. (See Figures 8 and 9)

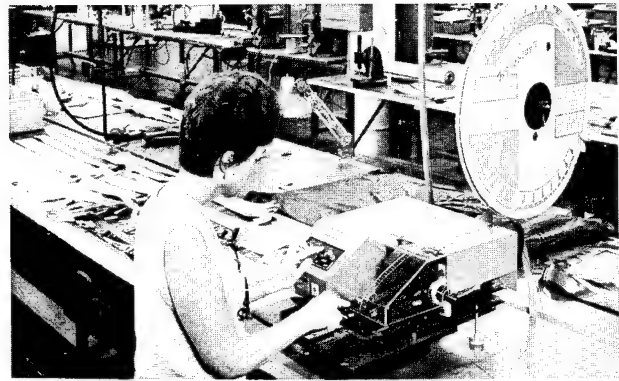
When the FCC harness is installed, care is exercised that it is not nicked by sharp corners. Each drawer pull is checked for proper cable adjustment. A properly built and installed FCC harness assembly should last indefinitely, even with thousands of operations to the service position. This is certainly more than can be used for a conventional wire harness.



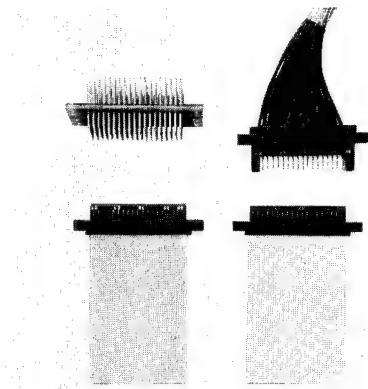
Arnold L. Peters was born in Hollywood, California, on May 5, 1935. He attended Los Angeles Valley College and West Coast University in his work toward a degree in Electrical Engineering. Joining Librascope Division of the Singer Company in 1958, he has worked in Manufacturing, Industrial Engineering and Design Engineering. At present he is the Packaging Design Engineer responsible for interconnect systems design, including harnesses, cables, and back plane wiring on naval shipboard equipment.



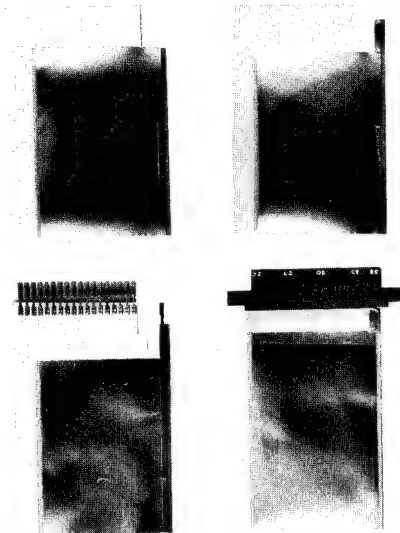
1. Conceptual packaging drawing.



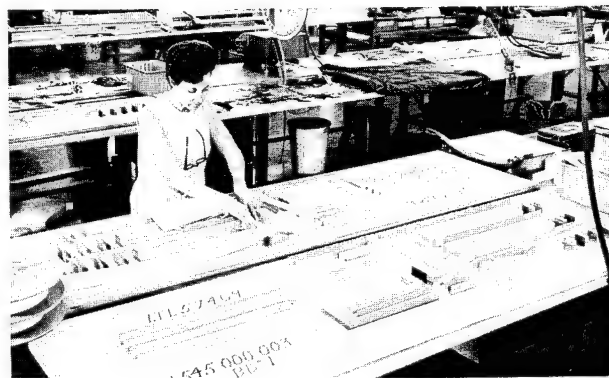
2. FCC being terminated in the AMP UNYT* System semi-automatic crimping machine.



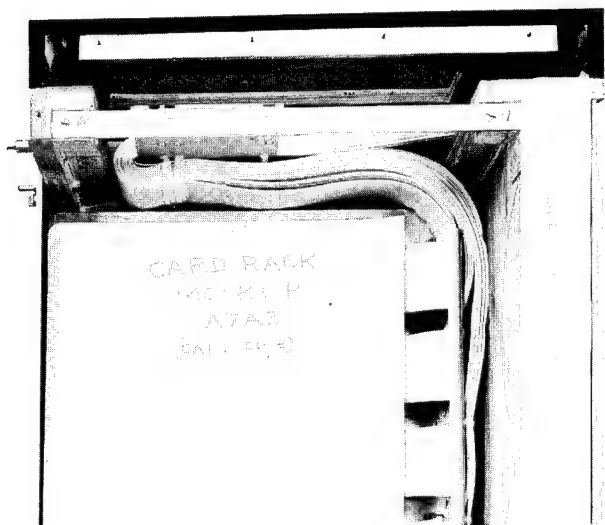
3. A power cable interfacing with a wire wrap connector and a signal cable interfacing with a wire harness.



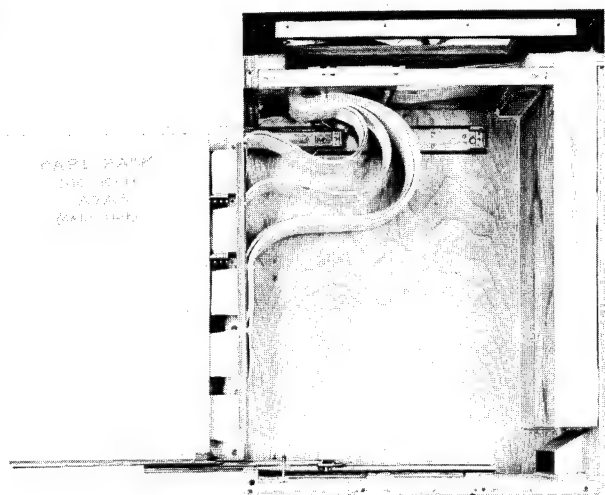
4. Four steps in terminating a signal cable and shield.



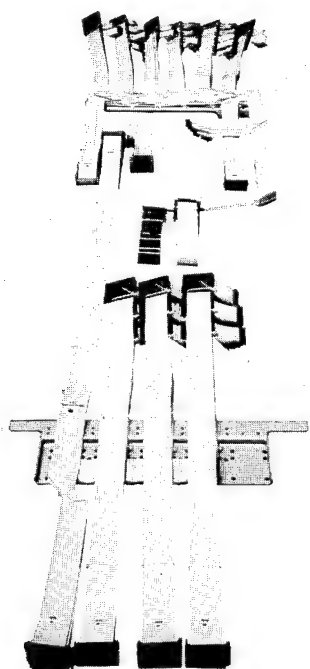
5. Laying a FCC harness on the harness board.



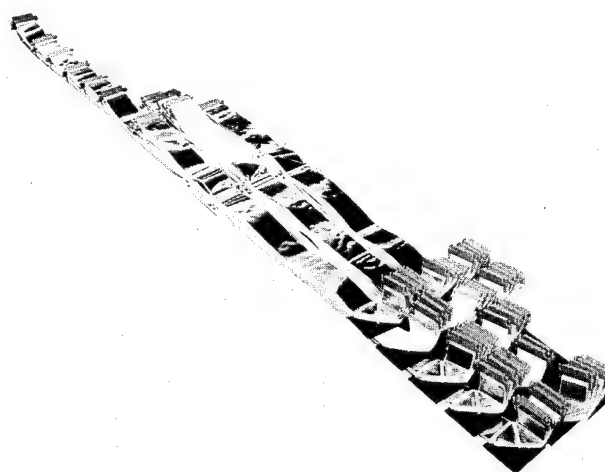
6. Mockup of a typical drawer in closed position.



7. Mockup of a typical drawer in service position.



8. A completed nine-foot long 180 layer FCC harness.



9. A completed six-foot long 80 layer FCC harness 100% shielded.

DIGITAL DATA TRANSMISSION IN SHIPBOARD APPLICATIONS

James F. Shiells, Jr.

Ansley West Corporation
Los Angeles, California

Summary

Today's electronic systems are not able to use yesterday's interconnection systems because they don't fit mechanically, won't work electrically and are often prohibitively expensive. Flat cable when designed into a system at an early stage will fit mechanically, will work electrically and is frequently low in installed cost. Integrated circuits force us to live in a miniaturized electronic world, whether we like it or not. The mechanical density and electrical sensitivity of the integrated circuits created a whole new family of interconnection problems. Flat cable is uniquely able to provide the flexible interconnections required in this densely packed and electrically complex situation.

The number of interconnections increased tenfold when analog systems were upgraded to digital systems. The mechanical problems were severe since these were usually military systems that went into consoles that were already full before they decided to increase the number of lines in them. The electrical problems were equally severe since one cable was frequently called upon to carry both sensitive signals and noisy switching and power circuits. The drawers were intended to be frequently opened for servicing and they had to do so without interrupting normal operation. Shielded flat cables were able to fit into the restricted space available and satisfactorily perform all the required electrical and mechanical functions.

Today's electronic industry has made demands upon the interconnection industry that has created what some people have termed the Interconnection Revolution. A comparison with the Industrial Revolution brings to light some interesting facts that are helpful to understand how flat cable allows the wire and cable industry to interface with today's complex electronic packages. Certainly flat cable is one of the active participants in this Interconnection Revolution.

Electrical Interconnections Past and Present

The first electrical interconnections were very simple and provided nothing more than an insulated path from one point to another. If the conductor was the right size and the insulation would hold up for a reasonable period of time, everyone was happy. A handful of wires could hook up the most complex electrical device. They were usually installed in a semi-permanent condition with no need for connectors to assist in the servicing of the devices. Gradually, the electrical systems became

more complex and when electronic devices came into being, a whole new family of problems was created. Now instead of being concerned only about temperature rise and voltage drop, things like characteristic impedance, crosstalk and propagation velocity became the engineering problems of the day. Connectors became increasingly important to allow the fabrication, check-out and servicing of sub-systems and modules. With the advent of integrated circuits miniaturization became a fact of life. Literally thousands of microscopic elements had to be interconnected with previously unattainable precision. It was not economically possible to build large size integrated circuits that could be terminated into the wire and cable that was being used prior to that time.

Printed circuit and multi-layer boards developed at a fantastic rate since they readily accepted the miniaturized electronic elements. Back plane wiring became highly automated in a short period of time to eliminate the high cost of hand termination and its resulting errors. More connectors were used to allow increased modularization and ease of servicing. Flat cable fit very nicely into this new situation because it could efficiently interconnect the boards, panels, drawers and consoles. The high cost of flat cable was more than offset by the performance that it provided and the labor savings that resulted from its use.

The Industrial Revolution of History

The Interconnection Revolution that is taking place today promises to have a greater effect on the wire and cable industry than the Industrial Revolution had on the lives of 18th and 19th century Americans and Europeans. Some of the key factors in the Industrial Revolution can give us a better understanding of what is happening today. Prior to 1770 almost all cloth was made in small household type manufacturing enterprises. The yarn was spun by hand and then woven into the fabric on small looms. When the flying shuttle was invented an imbalance was created in the distribution of work since it allowed one weaver to use more thread than a number of spinners could make. James Hargreaves patented the spinning jenny in 1770 to solve this problem. Little did he know that he had started the Industrial Revolution that would change the way of life of almost everyone in the modern world. The spinning jenny allowed one person to operate a number of spindles mounted side by

side. Now the balance had shifted and the weaver couldn't keep up with the spinner. Bigger and better spinning and weaving machines followed in rapid succession until textile manufacturing was forced to move into factories designed to efficiently use these new machines. The high-quality, low cost cloth from these factories was purchased in unprecedented quantities thereby encouraging new invention and rapid technological changes. A new way of life had been created for the consumer, the factory worker, and the factory owner. The concept of industry had been discovered. The specialist working on a machine could be many times more productive than his more versatile counterpart. Hand labor was too expensive to remain competitive and the numerous small businesses went out of existence. Although it was an evolutionary process by modern standards, history calls it the Industrial Revolution.

The Interconnection Revolution

Electronic devices are being produced by modern, automated techniques that are low in price because they are small. The number of active devices in a typical system has skyrocketed. The cost of interconnecting these devices has become an increasingly important percentage of the cost of the entire system. The interconnection design must be an integral part of the package design, almost from the initial inception of the system if it is to be successful. The old ways will not work and new ways are being developed to keep up with the need.

The Interconnection Revolution has taken place at a fantastic pace in order to keep up with the Electronic Age in which we are living. In this rapidly changing technology it is important that we keep track of those forces and trends that will influence tomorrow's business. It is interesting to note that almost all the thread spinning inventions were applicable to cotton but not flax. In spite of large government subsidies, the linen industry died a technological death because inventions to make thread from flax did not come soon enough.

Modern Trends in Interconnections

Several features of today's complex electronic systems are clearly defined and favor the use of flat cable.

Miniaturization - The integrated circuit has the advantages of reduced size and low power dissipation. All modern systems must adjust the concept of size to make use of these devices. Flat cable provides an efficient interconnection mechanism that can be scaled down to small center distances without a cost penalty. Being thin and flat it uses a minimum of space.

Machine fabrication - Manual assembly has become prohibitively expensive as systems have become more complex. One layer of flat cable can be handled almost as easily as a single conductor. It is virtually impossible to make a wiring error. Miniaturization makes manual

assembly even more difficult.

Electrical performance - Impedance, crosstalk and propagation velocity have become increasingly important for the proper operation of any system. Flat cable is able to provide stable electrical characteristics because of its precise mechanical orientation. They will repeat from system to system to allow the use of interchangeable modules, an important concept in servicing any large system.

Mechanical performance - Flexible interconnections are required in complex systems to allow installation and servicing. Flat cable represents the most compact cable configuration known. It can be flexed with a small bend radius and it can be creased or folded without damage. Flat cable is almost immune to vibration problems. Perhaps most important is the fact that the insulation provides the strength and the conductor is securely protected from all tensile and abrasive forces as long as the insulation remains intact.

Connectors - As systems have become more complex, the modular philosophy has become more widely accepted. In addition to the input/output connectors, there are increasing numbers of connectors required to install and service these modules. These interior connectors must match the geometry of the printed circuit boards and back plane wiring panels. Flat cable is ideally suited to interface with this connector geometry or even eliminate the need for the connector.

Installed cost - Great emphasis must be put on holding the cost of a system to a minimum, if it is to be sold in today's competitive market. The skill of the packaging engineer in using the most modern techniques will spell the difference between success and failure in many cases. Flat cable is one of the new tools that is available to solve his problems. Flat cable must be designed in at an early stage to take full advantage of its many well defined features. New hardware is being designed and built to make it easier for the packaging engineer to use flat cable at minimum installed cost.

Digital Data Transmission in Shipboard Applications

As a result of upgrading shipboard electronic equipment from analog to digital measurements, a severe electrical cable requirement was presented. The shipboard systems were fixed in size by the consoles that had been used by the analog systems. In converting to the greatly sophisticated digital system, the volume occupied by the electronic equipment was increased only slightly while the number of interconnections between drawers increased tenfold. The pulses used in data transmission presented difficult problems of electrical isolation that required shielding. It was important to consistently isolate the noise generating lines with respect to the sensitive signal circuits. The drawers were regularly opened and closed for servicing and had to remain

operational at all times.

Ships Inertial Navigation Systems

The Ships Inertial Navigation Systems (SINS) manufactured by Autonetics is a high performance set of equipment that has made it possible for the atomic submarines to navigate all over the world. Every motion of the submarine is measured and integrated to provide the precise position for both navigation and missile launching purposes.

Difficult mechanical and electrical problems were presented in designing the cables coming from the backs of the drawers to the console interconnection matrix. MS connectors with a cylindrical configuration were mandatory on the back of the drawers. The space from the back of the connector to the back of the console was very restricted. The clearance between the side of the drawer and the console was quite limited. The restricted front panel space made it necessary to include some of the meters and adjustments on the side of the drawers so that the drawers went through frequent opening and closing cycles. The equipment had to be operational at all times. Great emphasis was put on reliability under severe operating conditions.

The electrical problems were equally demanding. The pulsed digital signals had to be carried in a consistent manner whether the drawer was opened, closed, or being moved. Noise generating lines were dispersed with sensitive signal lines in a random manner in almost all the connectors. The power levels were relatively high on a number of lines and in the milliamp range on others. Many of the signal lines needed co-axial cable performance.

Due to the restrictive mechanical problems, Autonetics made the decision to use flat conductor cable at an early design stage. A special cable was developed which had the required electrical and mechanical characteristics. All layers were shielded on both sides with a solid copper shield. Flexibility was achieved by developing a special corrugating process that gave a smooth, rolling action as the drawer was opened and closed. Polyurethane was molded in special shapes on the back of all connectors to properly support the cables since no space was available for cable retractors. All conductors were terminated by a unique new process of welding through the insulation. The shields were welded to a ground conductor periodically along their length to provide redundancy in case of field damage.

Lengths were carefully adjusted to give a smooth rolling action even when 8 or more layers were stacked on top of one another. Electrical parameters were analyzed to determine the isolation between any conductor and all adjacent conductors. A very stable, controlled impedance was achieved with very high isolation. TFE Teflon insulation was selected for its low dielectric character-

istics to assure minimum conductor to shield capacitance.

The cost of this SINS cabling system was low even when compared to alternate constructions that would not work mechanically. The high material costs were offset by the savings in labor. As a result of the reasonable cost and outstanding mechanical and electrical performance all SINS systems were retrofitted with similar flat cable systems.

MK 48 Torpedo Fire Control System

The MK 48 Torpedo Fire Control System manufactured by Librascope faced the same sort of upgrading to allow the use of digital systems that provided more functions and greater accuracy. Thanks to the packaging skill of a number of engineers, every nook and cranny in the entire console was full of electronic components. All the areas had a large number of interconnections required and each section needed to be available for servicing while operational. It would be difficult to say whether the electrical or the mechanical problems were more severe.

The shielded, flat conductor was selected as the only one suitable for the application at an early design stage. Grooves were machined inside the console to create raceways. Some areas required extreme flexure since some sections had to move both in and out and pivot to allow service accessibility. All cables had to be self-retracting due to space limitations.

Two new types of connectors were developed to terminate the cables. One type of connector had wire wrap contacts mounted in a plate. Jack screws pulled the connector firmly in place against the wire wrap plate to withstand the open and closing forces imposed by the cable. A hybrid block connector was developed that allowed stacking of a large number of cable ends in a small area. The cable conductors were terminated by welding. Taper pin jumpers were used to interconnect the hybrid blocks.

The majority of the cables had 20 conductors. Due to the high current requirement, some of the cable layers had a smaller number of very wide conductors. Both types of cable had the same mechanical characteristics as far as width, thickness and flexing ability. Shielding was applied to both sides of the inner Teflon insulated flat conductor cable. All the 90° folds were molded with epoxy to guarantee a perfect fit in the mechanical console casting.

In the MK 48 system there were extremely difficult mechanical and electrical requirements that adversely influenced the cabling cost. The outstanding features of flat cable could have been realized at a much lower cost if additional freedom of design had been available.

James F. Shiells, Jr., Ansley West Corp.,
4100 N. Figueroa St., Los Angeles, Cal. 90065

ALUMINIUM CONDUCTORS IN PAPER INSULATED TELEPHONE CABLES

R.A. CLARK, M.A. RHEINBERGER, and A.W. SISSON

Australian Post Office
Melbourne, Victoria, Australia.

Summary

The Australian Post Office believes that there is an economic application for paper insulated aluminium conductor cable in the city networks. The basis for this belief and the particular installation and maintenance practices applicable in such a network are discussed in this paper. The manufacture of cables and the results of field installations are also reported on.

Introduction

Copper Prices and Shortages

The price of copper has fluctuated over the last twenty years. It has twice shown marked increases for lengthy periods, firstly from 1950 to 1959, and secondly from 1964 till the present time. The more stable price level from 1958 to 1964 was substantially higher than that prior to 1950 and the prices in 1970, whilst dropping from the record highs, are substantially above those in 1964, and may be expected to remain so. The Australian consumer prices for both copper and aluminium¹ are shown in Figure 1. The trends are similar in other countries and reflect a world market situation.

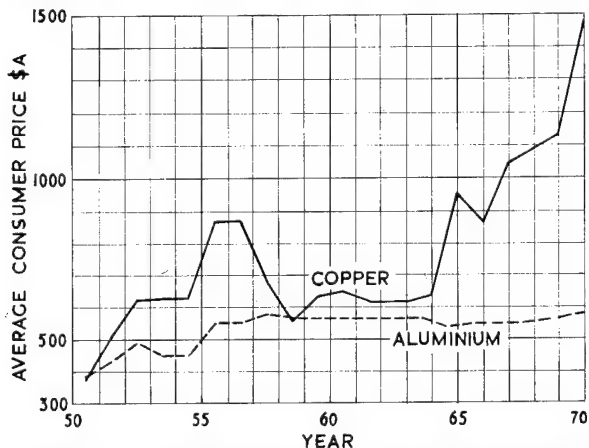


FIG. 1. ANNUAL AVERAGE OF AUSTRALIAN CONSUMER PRICES FOR COPPER AND ALUMINIUM.

On both occasions that copper prices have shown marked upward trends, the A.P.O. (Australian Post Office), the only telephone administration in Australia, has directed development effort toward substitute materials, principally aluminium. Figure 1 shows that aluminium has also increased in price, but the change has been small compared to copper and the future price is predicted to

remain more stable. The development effort during the 1950-1958 period was minimal and proceeded no further than the manufacture of trial lengths of plastic insulated and sheathed cables which were never installed. Some knowledge of manufacturing was gained but jointing and servicing problems were not really confronted. However, in 1964, industrial problems at Mt. Isa Mines temporarily forced Australia to import rather than export copper. This, and the coincident price increases, meant the A.P.O. had to restrict its installation of new cables. The result was an enforced programme to develop aluminium as a substitute for copper conductors to the point, at least, where substitution could be made in the event of future shortages of copper.

Initial A.P.O. Decisions

Simultaneous studies of the economics of aluminium conductor cable, including duct penalty costs and service problems, led the A.P.O. to concentrate initial development effort in the field of large size paper insulated underground cables. The maintenance practices in Australia, where the paper insulated subscribers main cables and junction cables are protected from moisture entry by gas pressure, seemed adequate to avoid the disasters of the 1950's experienced by the American Bell System in their extensive installations of paper insulated aluminium conductor cables^{2 3 4}. Reports on the British Post Office experience with the Dover-Deal experimental cable installed in 1955, tended to support this⁵.

Network Economics

Cable Costs

The manufacturing conditions and processes in Australia for aluminium and copper conductor cables with moisture-barrier sheaths have been studied. Approximate costs for cables containing 200 pairs or more are compared in Figures 2 and 3. Figure 2 generalises the cost comparison for copper prices ranging from \$A600 to \$A1400 per ton (2240 lbs.) and aluminium prices from \$A400 to \$A700 per ton. Figure 3 gives the comparison for the same range of copper prices and the specific aluminium price current in Australia (\$A586 per ton for Properzi quality EC. grade ingots). These comparisons reveal, for example, that with copper at \$A1400 per ton, (a price that has been exceeded in Australia for most of 1970), cables with aluminium conductors electrically equivalent to 0.9 mm (approx. 19 AWG) copper are 46% cheaper than copper

conductor cables. Or, in another measure, the savings exceed \$A10 per thousand pair yards (\$A1.67 million per bcf.).

Similar graphs could be prepared for other sheath types, but moisture-barrier sheaths constitute about 80% of current Australian usage of large sized paper insulated cables. In most cases other sheaths are more expensive than moisture-barrier and both the percentage difference in cost and the gross difference in cost are reduced.

Duct Costs

Large sized paper insulated cables in Australia are usually installed in 4" diameter ducts. These ducts are considered suitable for cables up to 3½" external diameter. The pair capacity of ducts when used with aluminium conductor cables is only 2/3rds of that achievable with copper conductors or cables of the same resistance and mutual capacitance. Depending on the achieved pair occupancy of ducts, savings in cable costs could be more than offset by the costs of the additional duct space required.

In Australia, duct costs vary widely depending on the installation situation. Typical costs are:-

Cost per 1000 yards in "easy" conditions = \$A(5600 + 2650 D)

Cost per 1000 yards in "average" conditions = \$A(7100 + 3250 D)

Cost per 1000 yards in "difficult" conditions = \$A(10100 + 4500 D)

where D is the number of ducts provided.

Cable Installation and Maintenance Costs

In assessing the economics of aluminium it has been assumed that the installation and maintenance costs of aluminium conductor cables are not substantially different from those of copper conductor cables. However, these costs are a function of both sheath length and conductor yardage and the sheath length factor predominates. In a typical network the greater diameter of aluminium conductors causes a greater sheath length of aluminium to be required. Hence the total installation and maintenance costs debited against aluminium in the economic comparisons are greater than debited against copper.

City Junction Plant

Provisioning Periods. City junction cables in Australia are usually provided by v.f. loaded 0.9 mm or 0.63 mm (approx. 19 A.W.G. or 22 A.W.G.) copper conductor cables. Most of these are maximum-sized, 600/0.9 or 1200/0.63. With present circuit growth rates such cable sizes normally cater for 4 to 10 years development. These provisioning periods are close to the optimum indicated by economic analyses. Smaller cable sizes are used only where maximum-sized cables lead to substantial diseconomy.

To adopt the maximum-sized aluminium conductor alternatives, 400/1.15 mm (approx. 17 A.W.G.) and 800/0.81 mm (approx. 20 A.W.G.), would reduce the average provisioning period by one-third and increase the duct requirements by a half. Studies of the economics of such substitutions have been conducted using the Present Value of Annual Charges (P.V. of A.C.) method of economic comparisons for two typical circuit growth rates and a series of installation situations.

The results, based on an interest rate of 7½% and a duct provisioning period of 20 years, inclusive of a standard allowance of 25% for unforeseen requirements, are summarised in Table 1.

Duct Laying Conditions	Ducts Available on Route	Break-even Copper Cost (\$A/ton)	
		High Growth Rate*	Medium Growth Rate**
Average	0	1060	840
	1	1150	990
	2	1150	840
	many	below 600	below 600
Difficult	0	1280	970
	1	1400	1190
	2	1400	980
	many	below 600	below 600

* High Growth rate is 240 pairs per year for 0.63 mm copper or 120 pairs per year for 0.9 mm copper.

** Medium Growth rate is 120 pairs per year for 0.63 mm copper and 60 pairs per year for 0.9 mm copper.

Table 1. Break-even Copper Costs for Various Duct Situations.

Theoretically, the duct provisioning period should differ for the two conductor types, for the two growth rates and for the two laying conditions. For minimum P.V. of A.C., it should be less than 20 years, being 10 years for the aluminium conductor high growth rate/average duct cost situation. The use of duct provisioning periods based on minimum P.V. of A.C. reduces the "break-even" copper cost considerably.

Duct costs can usually be expressed in the form $\text{Cost} = \$ (A + B.D)$, where A and B are constants, and D is the number of ducts. In the determination of optimum provisioning periods the costs of both the first and the subsequent installations should be taken into account as the period depends on the ratio of the "B" of the first installation to the "A" of the subsequent installation. Field engineers often foresee grave difficulties and high costs in future duct works and favour long provisioning periods. However, a 2 : 1 change in the B to A ratio alters an optimum of 10 years by only

about 3 years. In Australia the use of provisioning periods below 20 years is not accepted practice.

Negative Impedance Repeaters (NIRs). The effect of aluminium conductors on the economics of using NIRs has also been studied. Here the circuit bearer cost difference between conductor gauges, duct costs included, is important. The P.V. of A.C. difference between 0.9 mm and 0.63 mm copper bearers is \$A23 per mile for copper at \$A950 per ton. It increases to \$A26 per mile for copper at \$A1350 per ton. For aluminium at \$A586 per ton the difference between the equivalent gauges, 1.15 mm and 0.81 mm is \$A26. For higher duct costs these differences rise but the rise is greater for aluminium as the duct component of the difference is 70% whereas for copper it is about 40%. Hence NIRs continue to be applicable with aluminium conductor cables.

Pulse Code Modulation (P.C.M.) Systems. The interaction of 24 channel P.C.M. systems on the relative economics of aluminium and copper conductor cables has been broadly assessed. P.C.M. can expand the circuit capacity of unit twin cables by about 6 times, and as a result for a given circuit growth rate, the cable pair provision rate can be reduced. As indicated by Table 1, the "break-even" copper price is lower with reducing pair provision rates. Thus P.C.M. improves the case for aluminium. However, the converse does not always apply because the lower cost of aluminium increases the circuit length at which P.C.M. proves in on new cables, i.e. there are circuit lengths and copper prices for which P.C.M. is economic on copper conductor cables but is not economic on aluminium conductor cables.

City Subscribers Plant

Most of the large sized cables used in Australia for city subscribers have 0.4 mm (approx. 26 A.W.G.) copper conductors; some 0.63 mm copper is used but 0.5 mm (approx. 24 A.W.G.) is no longer installed.

In 0.4 mm, sizes up to 2,700 pair are used and the distribution of usage over the size range is:-

Size	2700	2400	1800	1200	800	600	400	300
Percentage of Sheath Length	1	4	13	17	12	14	22	17

The aluminium equivalent to 0.4 mm copper, 0.5 mm, can be installed in sizes up to 1800 pair, i.e. direct size-for-size substitution is possible for 95% of the length purchased. Pair sizes 1800, 1200 and 800 in copper virtually fill a 4" duct and use of aluminium in these sizes does not incur duct penalty costs. Occasionally a second cable is installed, or planned for installation, in ducts carrying 600, 400 and 300 pair copper cables and second cables could be placed with 400, 300 and 200 pair aluminium cables. Hence it is only for a proportion, perhaps 50%, of the 600 pair requirement and all of the 2700 and 2400 requirement that the duct penalty is significant. The "break-even"

copper cost for these sizes has not been assessed in detail but would be dependent on duct costs and growth rates and would be typically in the range \$A1000-\$A1200. Where there are no duct penalties, i.e. for over 80% of our usage, the "break-even" copper cost is below \$A600.

For 0.63 mm copper subscribers cables, most of the usage is in sizes 800 pair and smaller and direct size-for-size substitution is practicable with the "break-even" copper cost again below \$A600.

Installation and Maintenance Aspects

The A.P.O. Cable Network

In the early 1950's the A.P.O. commenced a programme of gas pressurisation of underground cables. The underground cable network at that time was entirely lead sheathed and a static pressurisation system was adopted and applied to the more important trunk cables. The system has been extended to include all trunk and junction cables and almost all subscriber main cable. The static concept, which relied on a completely defect-free sheath, has been substantially retained, but compressor-drier installations are now common and small flow rates are tolerated without corrective action. At an exchange, a flow of up to 2 cu. ft. per hour is classified as acceptable for any one cable.

The subscriber main cables are those from the exchange to the pillar (a cross-connecting flexibility point) and are essentially paper insulated. Prior to 1968 these cables were lead sheathed but the majority of new cables are now moisture-barrier sheathed. The tails to the pillars incorporate a gas seal and the distribution cables beyond the pillar to the subscribers are generally polythene insulated and sheathed and not placed under gas pressure.

The pressure system is connected to an alarm which operates if the pressure at any of the remote contactors falls below a given value (about 8 lbf/in²) or the flow rate at the exchange to any one cable exceeds 2 cu. ft. per hour. An alarm is treated as urgent and will involve staff recall if it occurs outside normal working hours. The gas used is dry air and the driers applied at compressor installations ensure that the air enters the cable at less than 5% R.H. at the ambient temperatures experienced in Australia.

Corrosion

Laboratory Studies. During 1966 the Research Laboratories of the A.P.O. investigated the corrosion of paper insulated aluminium conductors under different humidity conditions with and without d.c. voltage on the wires.⁶ This work showed that below 40% R.H. at 30°C the corrosion rate becomes small, and a figure for the corrosion threshold in a paper insulated cable has been taken as that amount of distributed moisture represented by 30% R.H. at 30°C. This temperature is seldom exceeded as far as buried cables in Australia are concerned.

Moreover, the insulation resistance of paper with this quantity of distributed moisture is below that normally classified as acceptable. Also the conditions are much worse than those which could occur while the cable remains under dry air pressure protection. Whilst the threshold figure was not completely established by laboratory testing the margin of safety was such that complete confidence could be held in paper insulated aluminium conductor cables provided that the cables were maintained under dry air pressure and the aluminium-copper joint to the terminating tails kept within the pressure system.

The investigations in 1966 covered the rate of corrosion, the characteristics of the by-products of corrosion which would occur if moisture actually entered the cable, as well as the drying-out of wet cables. Above the corrosion threshold aluminium conductors corroded faster than copper conductors and corrosion continued after the removal of applied potential. The cathodic wire in the case of aluminium was also seriously corroded due to the amphoteric character of the metal. An aluminium to copper joint produced one of the worst situations for corrosion under high relative humidity conditions. The insulation resistance of paper insulated aluminium conductors could not be restored to an original value after corrosion occurred and the drying time was longer than the drying time for paper insulated copper conductor cable, since the hydrated aluminium oxide does not lose all combined water at temperatures normally used for drying cables.

Fault Statistics. The conclusion that aluminium conductor cables would almost always necessitate replacement rather than repair in the event of actual water entry did not seriously affect their suitability for application to the A.P.O. network when considered in relation to the effectiveness of the gas pressure protection system. The service-affecting fault probability of cables under gas pressure is determined by the incidence of mechanical damage and experience has shown that only a small percentage of cases of mechanical damage lead to water entry. A study of fault statistics from 1958-1964 showed that about 10 faults per year per 100 sheath miles of installed cable occurred in cables over 54 pair, both gassed and non-gassed. Unfortunately the statistics do not distinguish between main subscriber and junction cables under gas pressure (generally above 100 pair) and distribution cables, but since most main subscriber and junction cables are located in multi-way duct runs, one can be fairly sure that the mechanical damage faults in gas-pressured cables would be below that quoted above for general cables over 54 pair. With only a small percentage of these cases presenting a worse hazard because of water entry when compared to copper conductor cables, the metallurgical penalty of aluminium from a corrosion viewpoint was considered insignificant.

Conductor Jointing

Inherent Difficulties

Both aluminium and copper form oxide films on clean surfaces but the speed of formation and the nature of the film is significantly different in each case. The aluminium oxide film (Al_2O_3) reforms almost instantaneously after cleaning and rapidly thickens until it reaches a depth of about 100\AA (0.0000004 inches). The film is hard and adherent, amorphous and non-conducting. It is for this reason that the simple twist joints used with copper conductors are unsatisfactory with aluminium and any jointing method used must include a method for oxide removal whilst jointing is proceeding.

The aluminium oxide film is insoluble in liquid or solid aluminium metal and can be removed by purely mechanical means. It will, however, reform immediately with perfect continuity, unless the underlying pure metal is protected by moisture-free petroleum jelly or some other agent which excludes air. Chemically, the film is remarkably inert but is attacked by chlorides and fluorides, which are therefore used in special soldering and welding fluxes. Once the oxide film has been successfully removed, the contact resistance between aluminium surfaces is no larger than in the case of copper.

Many Administrations have already replaced twist joints in copper conductor cables with more reliable techniques such as connector jointing or soldering. When aluminium conductors were first examined in this country the only well-developed connector system appeared to be the B-wire which was classified as being generally unsuited to the helically-lapped paper insulation used in Australia. In addition, there were complications regarding availability and special tool requirements when considered in relation to small-scale trials. For these reasons, initial investigations were confined to soldering, welding and pressure joints which could be made with available tools.

Table 2 gives some of the more important physical properties of aluminium and copper. The specific heat of aluminium is high compared to copper but due to its much lower density, roughly equivalent amounts of energy are required to heat equal volumes of both metals to a given temperature such as is required in soldering or welding. Aluminium is softer than copper and this characteristic affects the design of connector joints, especially when aluminium to copper connections are required. The difference in melting temperature gives rise to difficulties in welding aluminium to copper conductors.

Initial Trials

Several methods of conductor jointing were examined and of these, crimped sleeves and tip welding were chosen for initial field trials. Available tools for cold pressure welding, though giving satisfactory joints in a laboratory environment, were found to be completely impracticable

Property	Annealed Aluminium	Annealed Copper	Al/Cu Ratio
Resistivity (micro ohm-cm)	2.803	1.724	1.625
Tensile Strength (lbf/in ²)	10000-14500	33500-36000	0.35
Minimum Elongation (%)	35	50	0.7
Brinell Hardness	23	45	0.5
Melting Point (° C)	660	1083	0.61
Density (gm/cm ³)	2.7	8.9	0.304
Specific Heat (cal/gm) at 20°C	0.214	0.092	2.32
Thermal Conductivity (cal/sec/cm ² cm/°C)	0.54	0.92	0.59
Temperature Coefficient of Resistance at 20°C/°C	0.0040	0.0039	1.03
Standard Electrode Potential			
to Copper	-2.17V		
to Iron	-1.26V	+0.91V	
to Lead	-1.58V	+0.60V	

Table 2. Some Physical and Electrical Properties of Aluminium and Copper.

for field use. Soldering techniques were also investigated in initial developmental work. The fluxes used are highly corrosive and the joint requires very thorough post-cleaning. Ultrasonic soldering methods were considered but were rejected, as the requirement for a 230 V a.c. source could not always be met in the field. It was concluded that, in general, soldering was not a preferred method, particularly when its low productivity was considered.

Tip Welding. This method had already been used by the British Post Office (B.P.O.) in the experimental Dover-Deal cable installation of 1955⁵. A pair of conventional pliers connected to the negative terminal of a 24 V battery is used to grip the twisted wires near the tip. The positive terminal is connected to a carbon rod which is briefly touched to the tip of the wires, the rod being enclosed in an insulating holder. The passage of the high current melts the ends of the aluminium wires, producing a blob of metal at the tip which can make a satisfactory joint. Special preparation of the wires is not necessary as the temperature generated is high enough to produce fusion of the aluminium and at the same time destroy the oxide film.

The B.P.O. experience indicated that this method was quite satisfactory for aluminium-aluminium joints. However, the method is unsatisfactory for aluminium-copper jointing owing to the formation of a brittle zone at the metal junction due to the differing melting points of the two metals. The results of comparative laboratory testing of this method are given subsequently in this paper.

Crimped Sleeve Jointing. This method consists essentially in fitting a sleeve over the conductors which have been previously stripped of their insulant, and crimping this sleeve onto the conductors with a specially designed tool. The joints produced using a sleeve designed to be crimped by a standard nicopress tool are simple pressure joints and differ from cold pressure welding in that no fusion of metal occurs. Initial A.P.O. tests on 1.15 mm conductors showed that two methods were feasible - a joint with untwisted wires and a joint made by twisting the wires together and then crimping a sleeve over the twisted tail.

Comparative Results. In both crimped sleeve and tip welding techniques, a considerable amount of laboratory work was carried out to evaluate the anticipated lifetime performance of joints made between aluminium-aluminium in 0.63 mm and between aluminium-copper in various copper conductor gauges. All joints were submitted to accelerated heat-ageing tests at 105°C for a total of 12 weeks with intermediate measurements at 1, 3 and 6 weeks. It was considered that this test would simulate the relaxation in a joint which is in service for a period of 20 - 30 years. For a jointing method to be considered satisfactory, the contact resistance of all samples had to vary by less than 10 milliohms over the full test period.

Metallurgical tests showed that the jointing of aluminium-aluminium wire using a crimped aluminium sleeve produced a good metal flow, breaking the oxide film, provided the inside and outside diameters of the sleeve were carefully chosen. The results were equally satisfactory with $\frac{3}{4}$ H or fully annealed wire, but in both cases, with 0.63 mm conductors, twisting was necessary before crimping. The early results with aluminium-copper joints were not as satisfactory, however, and it was shown that improvements were possible using copper instead of aluminium sleeves. Furthermore, in the case of aluminium-copper jointing, a number of different copper conductor sizes were involved compared to a single aluminium size. This necessitated the use of several different sized copper sleeves. After considerable experimentation, three sizes were chosen. Although initial results displayed variability among different joints made by the same operator, results improved with operator practice. Tables 3 and 4 give results of resistance measurements on trial joints using these techniques.

Tip Welding appeared a preferable method of making aluminium-aluminium joints. Laboratory results, as given in Tables 3 and 4, showed the majority of these joints to be of excellent quality. Poor joints were readily recognisable as they were

Wire Combination		Crimped Sleeve Details				No. of Samples	Occurrences of Resistance Increase (milliohms)			
		Mat.	Ext. Diam mm	Int. Diam mm	Crimp		>10	>100	>1000	Max.
.63	.63	Al	3.18	1.32	X	40*	25	1	1	>2500
"	"	"	"	"	X	20	0	0	0	<1
"	"	"	"	"	XP	45	0	0	0	9.5
"	"	Cu	"	1.27	X	10+	5	4	1	>2500
"	"	"	"	"	X	10Ø	5	2	2	"
"	"	"	"	"	XX	10+	9	5	5	"
"	"	"	"	"	XX	10Ø	8	4	2	"
"	"	"	4.78	1.70	XX	10+	6	5	5	"
"	"	"	"	"	XX	10Ø	8	8	5	"
"	"	Al	3.66	1.59	X	10+	5	2	1	"
"	"	"	"	"	XX	10+	2	1	0	266
"	"	"	"	"	X	10Ø	5	0	0	64
"	"	"	"	"	XX	10Ø	0	0	0	3
"	"	"	3.25	"	X	10+	3	1	0	151
"	"	"	"	"	XX	10+	3	0	0	17
"	"	"	"	"	X	10+	3	0	0	37
"	"	"	"	"	XX	10Ø	1	0	0	36
"	"	"	3.66	"	XE	10Ø	0	0	0	3
"	"	"	"	"	XXE	10Ø	0	0	0	7.5
.63	.63	Tip Welded				40	0	0	0	4
"	"	" "				100	0	0	0	1
"	"	" "				66-	0	0	0	8

Code: *field joints, all others being laboratory joints; + fully annealed wire; Ø 3/4 H wire; X standard Nicopress tool; XX undersize tool; P Alconac paste; E epoxy dipped; - 2 open circuits not included.

Table 3. Results of Laboratory Tests (Aluminium - Aluminium Conductors)
Crimped Sleeve and Tip Welded Joints (after ageing for 2000 hours at 105°C).

Wire Combination		Crimped Sleeve Details				No. of Samples	Occurrences of Resistance Increase (milliohms)			
		Mat.	Ext. Diam mm	Int. Diam mm	Crimp		>10	>100	>1000	Max.
.63	.51	Al	3.18	1.32	X	40*	37	16	5	>2500
"	"	"	"	"	"	50*	47	34	15	"
"	"	"	"	"	"	30	13	1	0	124
"	"	"	"	1.25	"	40	14	1	0	203
"	"	Cu	"	1.27	"	30	0	0	0	9.7
"	"	"	"	"	"	40	17	7	1	1100
"	"	"	"	"	"	22	7	1	0	117
"	.4	Al	"	1.32	"	12	12	8	8	>2500
"	###	"	"	"	"	12	5	2	0	179
"	.5	"	3.18	1.32	"	57	56	31	6	>2500
"	.4##	"	"	"	"	62	54	22	3	"
"	.5	Cu	"	1.27	"	33	24	7	0	172
"	.4	"	"	"	"	20	15	7	0	68
"	###	"	"	"	"	20	16	3	1	>2500
"	.5	"	2.67	1.19	"	40	2	0	0	16
"	.63	"	3.18	1.42	"	35	2	0	0	10.5
"	.4	"	2.67	1.19	"	40	28	11	0	492
"	.5	"	3.18	1.42	"	40	6	0	0	17
.63	.5	Tip Welded				20	1	0	0	24
"	.4	" "				40-	1	0	0	73

Code: *field joints, all others being laboratory joints; #two wires used; ## wire doubled; -3 open circuits not included.

Table 4. Results of Laboratory Tests (Aluminium-Copper Conductors)
Crimped Sleeve and Tip Welded Joints (after ageing for 2000 hours at 105°C).

invariably open circuit. This differed from the behaviour of a potentially poor crimped joint which could have an initial low resistance, but over a period deteriorate slowly to a high resistance condition. As previously indicated, it was found that tip welding of aluminium-copper wires was most unsatisfactory and could not be recommended for field use.

During 1965-66, the initial trial installations of aluminium conductor cables were undertaken. These trials are discussed in detail later. The jointing methods used were tip welding for aluminium-aluminium and crimped copper sleeves for aluminium-copper. The field results for crimped sleeve joints were generally very good although jointing productivity was very low compared to A.P.O. standard copper jointing. The major proportion of all tip-welded joints appeared to be sound, but it was evident that further work was required to evaluate the tip-welding process in terms of voltage and current requirements and weld-times, in order to remove the subjective aspects present in the rudimentary method employed.

The general conclusion reached from the trials was that, whereas the jointing methods produced adequate joints, they were by no means optimum nor entirely practicable for use on a large scale. Further developmental work was continued on the jointing problem, for although the methods adopted had fulfilled the aim of providing an alternative in the case of shortage, it was clear that improvements were necessary before aluminium could be considered an economic substitute.

Later Experiments

Overseas experience indicated that connector-type joints made with a special tool offered an economic solution for a simple, high quality joint necessary in a modern network. By the time initial cable trials were completed, investigations in this country had confirmed that similar practices should be adopted by the A.P.O. and offers were being sought to establish the most suitable type of connector.

Several types of connector joints were available for initial experimentation. Of these the B-Wire connector (originally developed in the U.S.A.) was not really satisfactory with the ribbon paper insulant used in Australia. It was considered that the most suitable connector would be one applied from a magazine-fed, power-driven tool and which preferably pierced, as well as clamped, ribbon insulation. Initial tests up to mid 1967 indicated that the A-MP connector appeared promising although at least two sizes were necessary to satisfy all common conductor gauges that could be encountered in a field situation. The standard copper conductor connectors were evaluated by the A.P.O.⁷ for jointing aluminium conductors. Though not recommended by the suppliers for field use with aluminium, they were chosen for use in the subsequent field trials of 0.5 mm aluminium conductor cables. Results of laboratory tests on these connectors are given in Table 5.

Cable Manufacture

Metallurgical Considerations and Choice of Hardness

There are some metallurgical characteristics of aluminium which require a modification to established techniques used in cable manufacture. For electrical conductivity, fully-annealed wire is the best choice. High conductivity enables a smaller wire to be used thereby reducing cable insulation and sheathing costs, but the lower tensile strength of fully-annealed wire is a disadvantage when cable hauling is considered. Furthermore, manufacturing processes impose minimum tensile strength properties. However, wires of intermediate temper with high values of tensile strength have caused wire handling problems in Australia. Hence, an important initial problem is to determine the best economic compromises between conductivity and tensile strength for available wire-drawing processes.

An early problem in A.P.O. investigations lay in the fact that cable manufacturers in Australia receive aluminium wire supplies from different sources. It was observed when selecting the wire for use in initial trial cable installations, that the harder tempers exhibited a "kinking" phenomenon. This "kinking" was characterised by an initial bend of sharp angle, which, when bending was repeated, always occurred at the same point with the result that failure took place after very few cycles. H16 wire ($\frac{3}{4}$ hard) from one manufacturer manifested this phenomenon but wire of similarly designated temper from the other supplier was satisfactory. These findings indicated that specifications mainly intended for power applications were unsuitable for communication cable requirements. In these specifications the requirements for tensile strength and elongation are too broad and result in wires which, whilst meeting these requirements, may nevertheless still exhibit "kinking".

The conductor of a telephone cable must possess sufficient strength for hauling purposes and this necessity was pronounced in early developmental work undertaken in Australia where a heavy lead sheath was used. More relaxed requirements were foreseen for cables provided with a moisture-barrier sheath. Cable hauling practices for copper conductor cables were based on a maximum hauling tension given by the formula:-

$$\text{Maximum Hauling Tension (lbf)} = \frac{\text{Conductor Weight per mile (lbs)}}{\text{Number of Pairs}} \times$$

or 6000 lbf, whichever was the smaller and it was considered possible that, if fully annealed wire were used, the tensile strength at yield of the cable could be exceeded, particularly in long lengths of small size cables.

Conductors		R ₁							R ₂							ΔR						
Mat.	Diam	N ₁ for R(mΩ)					Value (mΩ)		N ₂ for R(mΩ)					Value (mΩ)		N ₃ for R(mΩ)					Value (mΩ)	
	mm	2	5	10	20	50	Max.	Mean	2	5	10	20	50	Max.	Mean	2	5	10	20	50	Max.	Mean
Cu	.91	2	-	-	-	-	2.31	1.51	17	9	4	2	-	28.6	6.81	9	8	2	2	-	26.9	5.3
"	.63	16	-	-	-	-	4.00	2.37	20	10	9	6	3	1000	75.9	11	9	8	4	3	996	73.5
"	"	16	-	-	-	-	4.40	2.27	20	8	6	2	1	51.0	9.32	13	7	5	2	-	46.6	7.00
"	.41	20	-	-	-	-	4.80	4.27	20	1	-	-	-	5.30	4.47	-	-	-	-	-	0.80	0.16
Al+	.63	20	-	-	-	-	3.60	2.99	20	-	-	-	-	4.50	3.38	-	-	-	-	-	1.80	0.44
AlØ	"	20	-	-	-	-	3.40	2.97	20	2	-	-	-	6.30	3.71	2	-	-	-	-	3.10	0.69
Al+	.51	20	6	-	-	-	8.20	4.89	20	18	1	1	1	9000	479	2	1	1	1	1	8990	474

Conductors		R ₃							R ₄							ΔR						
Cu	.91	-	-	-	-	-	1.41	1.17	2	-	-	-	-	2.15	1.47	-	-	-	-	-	0.81	0.32
"	.63	4	-	-	-	-	2.23	1.87	20	3	-	-	-	7.60	2.98	3	1	-	-	-	5.53	1.38
"	"	3	-	-	-	-	2.07	1.88	18	-	-	-	-	2.75	2.38	-	-	-	-	-	0.88	0.37
"	.41	19	-	-	-	-	4.10	3.72	19	-	-	-	-	4.70	4.28	-	-	-	-	-	1.20	0.61
Al+	.63	20	-	-	-	-	2.90	2.61	19	-	-	-	-	3.90	3.03	-	-	-	-	-	0.60	0.07
AlØ	"	20	-	-	-	-	2.73	2.46	20	-	-	-	-	4.20	3.26	-	-	-	-	-	1.70	0.80
Al+	.51	18	-	-	-	-	4.70	4.31	18	15	-	-	-	8.90	6.01	5	-	-	-	-	4.20	1.71

Code: + fully annealed wire

Ø $\frac{3}{4}$ H wire

R₁ Resistance before Heat Ageing

R₂ Resistance after 20 hours at 105° C

R₃ Resistance before Temperature Cycling

R₄ Resistance after 25 Temperature Cycles

ΔR Change in Resistance

N₁, N₂ No. of connector with joint resistance > R

N₃ No. of connectors with change in joint resistance > R

Note: 20 samples for each conductor type.

Table 5. Results of Laboratory Tests (Heat Ageing and Temperature Cycling)
on wire joints with A-MP Connectors.

Data was not available on general hauling tensions experienced with local-type cables and to obtain comparative information on this aspect, as well as manufacturing and jointing, as a basis for later decisions, it was resolved that initial trials should be carried out with cables of both $\frac{3}{8}$ " H wire (without "kinking") of tensile strength approximately 21000 lbf/in² and elongation 1.5% and fully-annealed wire of tensile strength approximately 12000 lbf/in² and elongation 16%. By this approach it was hoped to determine whether the fully annealed wire could be satisfactory for processing and subsequent cable hauling and if not, whether the $\frac{3}{8}$ " H wire, which appeared the maximum hardness permissible for wire jointing in pure aluminium, would prove adequate. In terms of wire costs, fully hard wire was the cheapest, followed by fully-annealed wire with intermediate tempers of higher cost. Consequently, if it could be shown that annealed wire was satisfactory, then an economically attractive solution would be available since recourse would not be needed to the $\frac{3}{8}$ " H wire.

As is discussed, in the next section, the initial trials with 0.63 mm conductor indicated the suitability of fully-annealed wire from a field viewpoint. The hauling tension encountered did not result in excessive wire breaks and the handling characteristics of the fully annealed wire were satisfactory. It was concluded that the same would apply for 0.5 mm conductors with a moisture-barrier sheath and factory trials were arranged to ensure the suitability of these finer conductors from a manufacturing viewpoint. It was found in these trials, that with slight modifications of the tension of pay-off and take-up stands at the paper-lapping and twinning stages, no undue difficulties would be experienced. Some details are given later in this section. It should be borne in mind that in Australia helical paper insulation is used wherein low tensions (1-2 lbf) are encountered.

Wire Drawing and Annealing

In Australia, the aluminium rod is produced from 99.7% purity ingots using the Properzi process. The 9.5 mm rod is reduced to 2.1 mm wire at which point it is annealed and then finally drawn to the required diameter, the final speeds being approximately 1500 metres/minute with a controlled tension of 0.75 lbf. The final wire is delivered to spools holding some 70 lb.

Continuous annealing is not available in this country for aluminium conductors as the problems of arcing at the conducting pulleys and adequate conduction through the aluminium oxide film have not been satisfactorily solved. This limitation has not been serious up to the present time since only limited quantities of aluminium have been processed for telephone cable manufacture. Furthermore, the choice of a fully-annealed wire, rather than some intermediate temper, means that the real economic demand for continuous annealing has been avoided. However, it is realised that a continuously annealed wire has better metallurgical characteristics than batch annealed and furthermore, the loss of production in the event of power failure to the

annealing ovens, dictates continuing attempts to develop continuous annealing in readiness for increased aluminium usage. Batch annealing is carried out at 270°C for 15 minutes in 800 lb. lots. This produces a wire of maximum tensile strength 14000 lbf/in² and a minimum elongation of 15%. Strict attention to adequate tension control at the final wire drawing stage has been found necessary to ensure free-flaking to the paper-lapping machines.

Paper Lapping

The machines formerly used for copper conductors have been found suitable with some modifications to the tension control of the pay-off spools and the die components. Most of these machines operate at about 3000 rpm. Factory joints in the wire are made by cold pressure welding with a "Koldweld" machine.

Twinning and Stranding

A variety of machines is used for twinning; most of these are double twist and produce up to 1000 metres per minute of twinned conductors. Some modification was required to the supply and take-up tensions to compensate for the lower tensile strength of the aluminium conductors.

Unit twin cable has recently been adopted as standard for all cable in the exchange area network. The machines used for unit construction are of the drum-twister design with stationary pay-off stands and rotating cpstans. For unit cabling the pay-off stands have 100% back-twist. The largest machine in use can handle finished core on drums of flange diameter 96 inches, and operate at about 50 rpm.

In early developmental work, the effect of the paper lapping, twinning and stranding operations on the metallurgy of the cable conductors was assessed by measurement of tensile strength and elongation characteristics at various stages throughout the manufacturing process. The results indicated a very slight increase in tensile strength (from 14400 to 14800 lbf/in²) due to work hardening but no significant reduction in elongation. This work led to the modification of the British Standard, B.S. 2627, for the specification of the annealed aluminium wire to be used. A maximum tensile strength of 15000 lbf/in² with a minimum elongation of 10% is now specified for samples taken from the completed cable.

Sheathing, Drying and Electrical Testing

Moisture-barrier sheath has now been satisfactorily developed in Australia and is rapidly replacing lead as the standard sheathing material for large size exchange area telephone cable. For this operation, the paper-wrapped cable core is electrically dried to meet an insulation resistance requirement of 25000 megohms mile.

In cooling the cable sheath, extra horizontal rollers must be fitted along the cooling trough to force the light-weight cable below the surface of the water since this cable has an average specific gravity of less than unity.

Another problem peculiar to aluminium conductors was associated with the operation of electrical cable core drying. Here it was found that special high pressure clamps were necessary to break the oxide film and guarantee a satisfactory electrical connection for the high amperage drying current.

Aluminium conductor cables did not present any special difficulties in electrical testing. It was originally thought that conductor ends might require soldering for electrical tests but twist joints and standard clips were found to be adequate.

Typical Factory Test Results

The results of factory tests on typical manufactured lengths of cable are given in Tables 6 and 7. These are provided for cables supplied for both series of trials (see next section), and in addition some results are provided for more recent cables of 0.81 mm and 1.15 mm gauges.

Table 6 gives results for the cables of 0.63 mm gauge manufactured for trial installation in 1965. These cables were electrically equivalent to 0.5 mm copper conductor cables. Table 7 shows results for cables manufactured for the trial series commencing in 1969 where the conductor gauge was 0.5 mm, electrically equivalent to 0.4 mm copper. In both cases the cables satisfied the specification. The cables of 0.5 mm gauge were manufactured with insulant paper of 0.06 mm thickness and this resulted in a mutual capacitance lower than specified. Investigations are proceeding aimed at determining the best method of increasing the mutual capacitance by decreasing the paper thickness or by the use of smaller closing dies at the paper lapping and unit wrapping stages.

Table 7 also provides factory results of cables with conductors of 0.81 mm and 1.15 mm. Again, the only difficulties appear to lie in the achievement of a mutual capacitance closer to the nominal 0.072 microfarads per mile. To meet this figure with 1.15 mm conductors, and also the specified external diameter, it will probably be necessary to use strings under the insulating paper. To maintain the high speed operation of the lapping machines, a polythene string is favoured.

Field Experience (1965 - 70) - Initial Trials (0.63 mm)

The first trials were commenced in 1965 with the installation of some 8000 KPY (Kilo pair yard) of cable in sizes ranging from 400 to 1200 pairs. These lead-sheathed cables were installed between exchange main distribution frames and cabinet or cable distribution points. At the time of these installations concentric quad

cable was generally in use for the larger (0.63 mm and 0.9 mm) gauge copper conductor subscriber cables. However, a unit quad design was chosen for the trial aluminium cables to facilitate the use of slack-splice jointing if this became desirable.

Conductors of 0.63 mm diameter were chosen since they presented the least developmental problems for cable manufacturers while at the same time proving their processes. Because the 0.63 mm gauge was also a standard copper conductor diameter, use could be made of the same insulation paper, strings, lay lengths of quadding and stranding, and other manufacturing processes.

Control of Trials

The main purpose of these trials was to determine at installation and throughout its service life, the performance of paper insulated, aluminium conductor cable under normal operating conditions. Data was gathered on hauling, jointing and electrical characteristics at installation together with a continuing appraisal of the in-service performance of the cable through regular tests and fault reports. The electrical tests made were of insulation resistance, loop resistance and resistance un-balance on all pairs. Other field reports provided opportunity for the separate recording of service aspects, e.g. quarterly tests of loop resistance and resistance unbalance readings on selected test pairs and a service history of any faulty pairs, sheath failures or other cable faults.

The aluminium-aluminium joints were generally made by tip welding with a small percentage being performed by placing 3.66 mm external diameter aluminium sleeves of bore 1.70 mm over a twisted aluminium joint and applying two crimps. Aluminium-copper joints were made with copper sleeves of 3.18 mm external diameter and 1.42 mm bore or 2.67 mm external diameter sleeves with 1.19 mm bore depending on the combination of conductors to be jointed, and in both cases applying three crimps.

Results of Trials

This cable was placed in five locations over the period May, 1965 - January, 1968. Standard hauling techniques were used except that two types of attachment were employed - a cast epoxy resin eye and an end spike with standard hauling grip (as used by the British Post Office).

Cable Hauling. The trials indicated that there were no undue difficulties in the handling and hauling of the cable when compared with an equivalent diameter copper conductor cable. The hauling eye, which is the A.P.O. preferred method, was found to be satisfactory with aluminium conductor provided that a change was made to the method of removing the paper. With copper an oxy-acetylene burning method is used but this proved unsuitable for aluminium and manual stripping was necessary.

Pair Size	Average Mutual Capacitance ($\mu\text{F}/\text{mile}$)	Capacitance Unbalance for 500 yard lengths (pF)				Mean Conductor Resistance (ohms/mile) (60°F)	External Diameter (inch)
		Side - Side		Side - Earth			
		Av.	Max.	Av.	Max.		
600	0.0715	191	720	237	1096	131.4	2.17
800	0.0714	182	716	229	1775	132.0	2.50
1200	0.0717	150	554	229	1174	134.8	2.96
<u>Recommended Limits</u>							
	0.075	350	1400	500	2400	138.2	

Table 6. Factory Results (0.63 mm Unit Quad).

Conductor Gauge (mm)	Pair Size	Average Mutual Capacitance (μF/mile)	Capacitance Unbalance for 500 yard lengths (pF)		Mean Conductor Resistance (ohms/mile) (60°F)	External Diameter (inch)
			Adj. Pr.-Pr.	Adj. Pr.-Pr.		
			Av.	Max.		
0.5	200	0.0660	22	72	213.2	1.24
"	300	0.0629	18	60	208.8	1.47
"	600	0.0653	22	92	208.0	2.00
"	1200	0.0658	22	71	213.7	2.76
"	1800	0.0657	19	71	213.5	3.39
<u>Recommended Limits</u>		0.0750		220	220.4	
			Adj. Pr.-Pr.	Pr.-E.		
			Max.	Max.		
1.15	100	0.0718	71	453	42.90	1.80
	400	0.0644	80	648	43.65	3.43
<u>Recommended Limits</u>		0.0750	140	1500	44.20	
0.81	100	0.0671	69	648	84.34	1.34
	800	0.0673	71	876	88.46	3.36
<u>Recommended Limits</u>		0.0750	180	1500	89.00	

Table 7. Factory Results (0.5, 0.81, 1.15 mm Unit Twin).

Hauling tensions experienced during the trials were comparable with those for copper conductor cables. Details of hauling tensions encountered with these lead sheathed cables are given in Table 8 together with the cable lengths and weights/foot.

Jointing. Apart from the actual wire jointing methods used, which were tedious and time consuming, no other difficulties were encountered during cable jointing.

The tip welding method provided a mechanically and electrically acceptable joint but had several disadvantages:-

- (i) it was difficult to control the weld;
- (ii) the carbon electrode required continual cleaning;
- (iii) the welding flash was severe on the eyes;
- (iv) batteries required frequent charging;
- (v) productivity was low, typically 50% of that for joints in copper conductor cables.

The crimped sleeve method of jointing was electrically and mechanically satisfactory but difficult to perform in the field. Several disadvantages were noted:-

- (i) it was sometimes difficult to insert the twisted conductors into the sleeve;
- (ii) there were difficulties in sliding a paper insulating sleeve over the crimped metallic sleeve because of the lugs formed on the latter during the pressing operation;
- (iii) the crimping tool was awkward to use in confined spaces;
- (iv) in aluminium-copper joints when using fully annealed aluminium wire, there was a tendency for the aluminium wire to "wrap around" the copper wire rather than the two forming a uniform twist;
- (v) once again the productivity was about 50% of that for joints in copper conductor cables.

Electrical Measurements. At the completion of each installation, measurements were made of Loop Resistance, Resistance Unbalance and Insulation Resistance. Periodic measurements were continued on selected test pairs for the following five years. Test pairs were selected to include working and non-working circuits, and both tip welded and crimped sleeve conductor joints. The results of resistance unbalance measurements from the date of installation to the end of 1967 are included in Table 9 and show that little difference can be observed with either time or between the two methods of jointing used.

Water Damage to Installed Cables. In one location a partially completed cable joint was found to be damp. Attempts were made to dry the cable by applying heat at the duct mouths, and working it towards the joint area, as dry air was blown into the cable from adjacent joint positions. After attempts to improve the insulation resistance by this method were made for some days, a bag sleeve fitted with an air valve was used to close the joint. Air was then introduced at adjacent joint positions until a pressure of 10 lbf/in² was measured at the damaged joint. This air was then released and the procedure repeated with dry air and the insulation resistance was thereby sufficiently improved to allow jointing to be resumed at the damaged joint. At the completion of all jointing, dry air was fed into the cable at the exchange pot head until the insulation resistance reached a satisfactory value.

At another location a partially completed joint was immersed as a result of water entering a manhole following a flash flood. The water flowed in both directions from the open joint. Attempts were made to dry the cables by passing dry air through them from the other ends of the cable lengths. After the consumption of twenty cylinders of dry air, insulation resistance had not risen above 200 ohms between wires of a pair. Both lengths had to be replaced.

Conclusions from Early Trials

Notwithstanding the difficulties experienced in the conductor jointing process and the confirmation of expected difficulties in drying out water-damaged aluminium conductor cable, the first trial installation was considered a success. Since 1965, these cables have continued to operate without faults that can be added directly to the use of aluminium conductors.

It was decided to proceed with a second series of trials in 0.5 mm gauge. This gauge, the most frequently used in subscriber main cable networks, accounts for some 50% of the total paper insulated cable requirements. Fully annealed wire was found satisfactory from a field viewpoint in the early trials and it was confidently expected that light-weight moisture-barrier sheath (by this time adopted as standard for duct cable) would remove any cable hauling difficulties due to the smaller gauge. Factory experiments undertaken in late 1966 revealed very few problems in manufacture. There was no significant change in the tensile strength or elongation characteristics of the aluminium, and the wire breaks which did occur were associated with mechanical damage to the conductor prior to the paper-lapping stage. Two grades of wire were used, one of tensile strength 14000 lbf/in², the other of 12000 lbf/in².

Pair Size	Weight (lb/yd)	Length (yds)	Tension (lbf)	Remarks	Pair Size	Weight (lb/yd)	Length (yds)	Tension (lbf)	Remarks
1200	23	148	3500	3½" duct "	1800	8	90	1200	Exchange entry
		258	2000		"		206	5000	Offset manhole
		265	5000		"		300	6000	"
		288	3250		"		300	6000	S bend
		305	2500		"		196	3000	Exchange entry
		104	1000		"		98	1000	
		172	3500		"		208	4500	Severe bends
		212	5500		"		213	1000	
		97	1000		"		108	800	
		107	1500		"		270	4000	
		152	800	Exch. entry " "	1200	6	63	1800	3½" duct
		233	1800		"		330	800	
		238	1500		"		287	600	
		163	5000		"		266	800	Vertical bend
		163	4000		"		254	600	
		170	5100		"		219	750	
		276	2800		"		281	800	Vertical bend
					"		183	250	
1000	19	122	650		600	3	63	600	3½" duct
		200	1000		"		134	1500	right angle bend
		293	1500		"		110	1000	
		304	1300		"		296	250	
		330	1400		"		217	50	
		398	1700		"		250	NR	
800	18	150	3725		"	2	139	"	
		235	2500		300		301	NR	
		380	2500		"		165	"	
		401	1500		"		139	1000	See Note 1
		453	5500						
600	14	221	500		200	1	310	1000	" " "
		253	500						
		416	1300						
		472	1400						
		480	1400						
400	10	300	4800	See Note 1					
		300	3000	" " "					

Note 1. Cables hauled over another cable in the same duct.

Table 8. Field Installations - Lengths, Cable Weights, and Hauling Tensions.

Cable Experiment	Date	Resistance Unbalance (mean)					
		Welded Joints			Sleeved Joints		
		No. of Pairs	Ohms Unbal.	% Unbal.	No. of Pairs	Ohms Unbal.	% Unbal.
No. 17 A (0.63 mm Conductors)	16.8.65	14	1.30	.25	10	1.05	.20
	21.9.65	14	0.99	.19	10	0.92	.17
	24.11.65	14	1.05	.20	10	0.54	.18
	25.1.66	14	1.05	.20	10	0.56	.18
	18.7.66	14	1.11	.21	10	1.00	.19
	18.7.67	14	1.00	.19	10	1.15	.22
No. 17 B (0.63 mm Conductors)	17.11.66	32	0.20	.10	32	0.64	.13
	4.4.67	32	0.13	.07	32	0.17	.09
No. 16 A (0.63 mm Conductors)	4.7.66	40	0.46	.18	9	0.56	.22
	18.10.66	40	0.31	.12	9	0.33	.13
	16.2.67	40	0.42	.16	9	-	-
	17.5.67	40	0.32	.12	9	0.22	.08
	20.10.67	40	0.92	.35	9	0.89	.34
No. 16 B (0.63 mm Conductors)	18.5.66	5	0.51	.20	5	0.57	.22
	25.8.66	5	0.66	.26	5	0.50	.19
	21.11.66	5	0.45	.18	5	0.52	.20
	21.2.67	5	0.44	.17	5	0.58	.23
	24.5.67	5	0.43	.16	5	0.54	.21
	25.8.67	5	0.42	.16	5	0.54	.21
No. 30 A (0.5 mm Conductors)		Connector Joints					
	21.12.69	40	0.72	.16			
	3.2.70	40	0.75	.16			
	15.5.70	40	0.68	.13			

Table 9. Field Installations - Resistance Unbalance.

Consequently it was decided to proceed with installations of 0.5 mm conductor cables with two main objectives:-

- (i) to establish a technique which would enable 0.5 mm conductor to be quickly introduced should the copper supply position deteriorate;
- (ii) to gain additional field information so as to permit finer economic comparisons of aluminium and copper cables to be made.

It was also decided to commence developmental work on the larger gauges, i.e. 0.81 and 1.15 mm.

The poor productivity of the jointing methods used in the first installations made the decision to use connector jointing, as already mentioned, more readily acceptable although the A-MP connectors chosen had not been designed for use with aluminium, nor have they been adopted in Australia for copper conductors.

Field Experience (1969-70) - Subsequent Trials (0.50 mm)

These were begun in 1969 and comprised 6000 KPY of cable in sizes ranging from 200 - 1800 pair in the subscribers' main cable network. These polythene/aluminium moisture-barrier sheathed cables were of unit-twin construction.

From these trials only limited information is available. However, the hauling tensions, lengths, and unit weights are shown in Table 8 and the available measurements of loop resistance and resistance unbalance are given in Table 9. Subjective reports from the field have commented favourably on the combination of a lightweight moisture-barrier sheath with aluminium conductors, particularly with regard to the ease of handling.

The fact that the cable floats necessitated the fitting of cable clamps at each manhole. Factory-fitted hauling eyes cast in epoxy resin were used in this trial and were satisfactory in most cases. The only difficulties were experienced in the largest cable sizes where the increase in cable diameter due to the casting made hauling more difficult. Subsequent developmental work has enabled a hauling eye to be produced which is almost flush with the cable sheath surface.

The trial cables were installed at four locations. The final electrical tests at installation at the first location indicated a completely acceptable jointing technique, but the tests at the next installation revealed 43 faults in 1800 pairs and of these all but 8 were open circuit faults. After testing with a pulse-echo set, the faults were found to be spread over most of the joints in the cable and subsequent examination showed them to be at the entrance to the connector. These faults were repaired by fitting new connectors and during this process a further 17 broken wires were detected and repaired. The joints were closed and the cable re-tested. It was then found that 25 new faults still existed of which 23 were open circuits. It seemed evident that further attempts to clear

the cable would only produce more faults, so it was decided to leave these faults uncleared. Complete test results are not yet available for the third and fourth locations.

An examination of faulty conductor joints removed from the second location indicated that the primary cause of the open circuit faults was due to heavy notching of the 0.5 mm aluminium conductor during pressing. This occurred due to misalignment of the conductor with respect to the insulation securing tang. Subsequent lateral movement of the conductor with respect to the connector body caused its failure in shear. In one case the misalignment was such as to cause direct shearing of the conductor by the tang. It is now necessary to determine whether the misalignment of the conductors during pressing is the result of

- (i) incorrect adjustment of the jointing machine
- (ii) operator error in positioning the wires
- (iii) the inability of the jointing machine to handle wires of 0.5 mm diameter of fully-annealed aluminium without damage.

Future Installations

At the present time, 10000 and 2000 KPY in 0.5 mm and 1.15 mm gauges respectively are being manufactured for further field installations. The jointing of 0.5 mm conductors will be effected with A-MP connectors. However, no suitable connectors are available for the larger gauge and these conductors will be jointed by an improved method of welding. The welding tool operates on the principle of two closely controlled currents, switched by transistors; a pre-heat current followed by a welding or fusing current. The electrodes are continually cleaned. These installations are scheduled to take place during 1970-71.

Concluding Remarks

Optimum Mutual Capacitance

The Australian Post Office decision to substitute aluminium for copper in paper insulated cables, whilst retaining a pure electrical equivalence, has been made with the knowledge that paper insulated cables will comprise the bulk of large size balanced pair subscribers main and junction cables installed in this country over the next decade.

The question of an optimum mutual capacitance design to accompany such a significant change in the proportionate costs of cable, duct and labour, as clearly demonstrated in the work of H.J.C. Spencer⁸ of the British Post Office, has not been overlooked. However, the practical implications of a complete change in mutual capacitances for different cable types and usage situations, and the implications of increasing high frequency operation in such cables, makes a study of optimum mutual capacitance for the future go far beyond the scope of this paper.

It would include comparative studies of different insulation types, including plastics, which will play an increasingly important role in the future.

Future Plans

The A.P.O. will be extending its installations of paper insulated aluminium conductor cables over the full range of conductor gauges, particularly the 0.5 mm subscribers main cable field, where extensive installations are already planned. It is hoped, that from January 1972 onwards, the choice between aluminium and copper conductor cables will be based mainly on network economic desiderata.

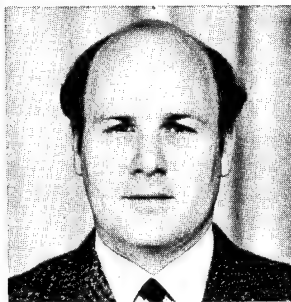
Acknowledgements

The Authors wish to thank the Australian Post Office for permission to publish this paper, and Austral Standard Cables Pty. Ltd. and Olympic Cables Pty. Ltd. for their assistance in supplying details of the manufacturing aspects. They also wish to thank Australian Amp Pty. Ltd. for the supply of connectors for laboratory testing with aluminium conductors.

References

1. Subocz, V. - "The Marketing of Non-Ferrous Metals in Australia - A Case to Answer?" The Australian Accountant, June 1970. pp. 241 - 247.
2. Herbert, J.S. - "Manufacture of Aluminium Conductor Telephone Cable". Wire and Wire Products, February 1956 p. 178 ff.
3. Horn, F.W. and Bleinberger, W.E. - "Design and Manufacture of Plastic Insulated Aluminium Conductor Telephone Cable". 15th Annual Wire and Cable Symposium. December 1966.
4. Horn, F.W. and Bleinberger, W.E. - "Aluminium Conductor Cable An Alternative to Copper?" Bell Laboratories Record, November 1967. pp. 314-319.
5. Hayes, H.C.S. - "The Dover-Deal Experimental Cable" P.O.E.E.J. Vol. 48, p. 224, Jan. 1956. and Vol. 49, p. 22, Apr. 1956.
6. Der, J. and McKelvie, D. - A.P.O. Research Laboratory Report No. 6188 (1966).
7. Stoddart, J. - A.P.O. Research Laboratory Report No. 6394 (1969).
8. Spencer, H.J.C. - Optimum Design of Local Twin Telephone Cables with Aluminium Conductors". Proc. I.E.E. (Electronics), Vol. 116, No. 4, April 1969. pp. 481 - 488.

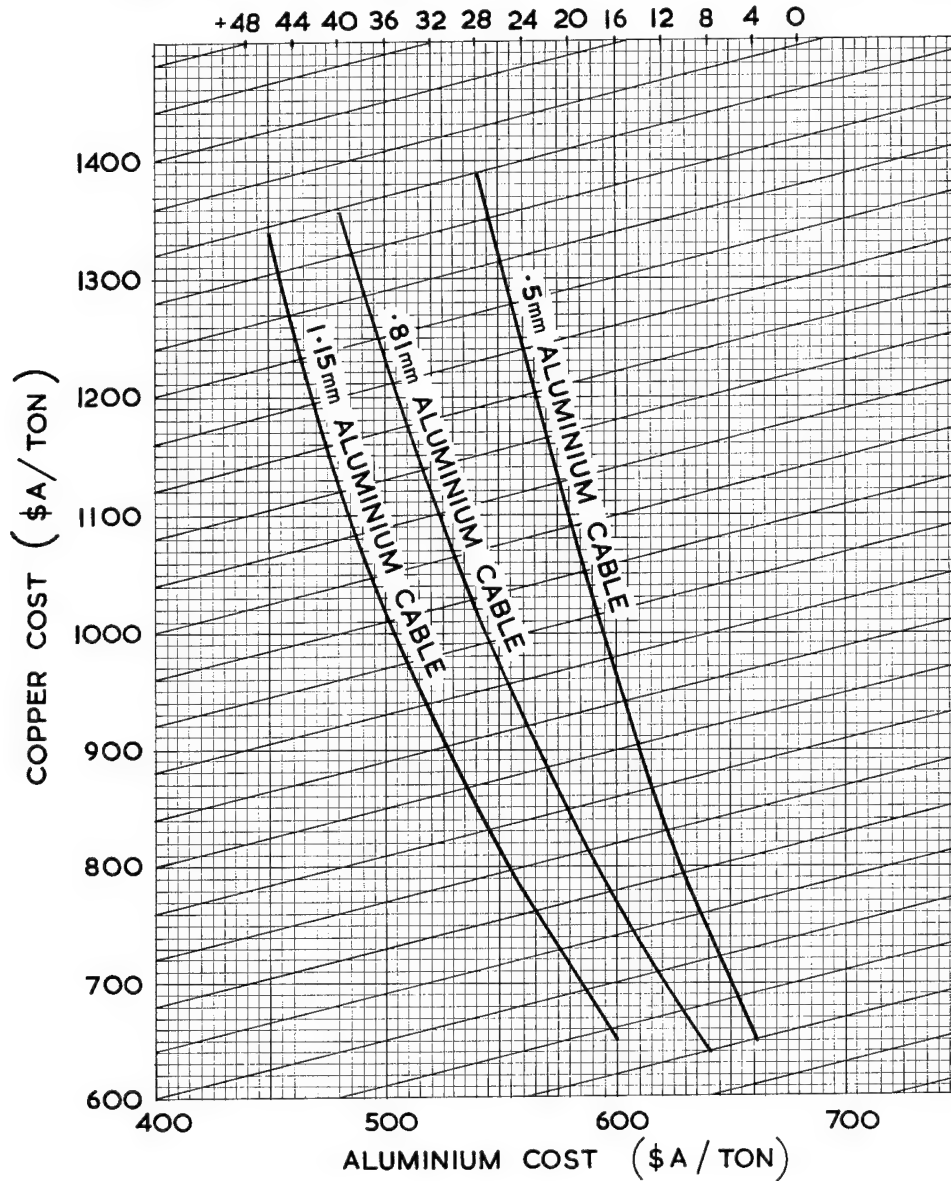
M. A. Rheinberger - Postmaster-General's Dept.
(Speaker)
Australian Post Office
Communication House
199 William St.
Melbourne, Victoria 3000
Australia



Mr. Rheinberger attended the University of New South Wales in Sydney, Australia. Upon graduation as Bachelor of Engineering (Electrical) in 1962, he joined the Postmaster-General's Department and was employed for three years in the planning, installation and acceptance testing of coaxial and other large scale trunk cable projects. Mr. Rheinberger then spent two years in the Central Laboratories of Siemens A.G. in Munich, W. Germany, where he was mainly engaged in broadband radio and carrier system design. Returning to Australia in 1967 he joined the Headquarters staff of the Australian Post Office in Melbourne, Victoria, where he is currently Divisional Engineer, Cable Design.

Mr. Rheinberger has the Bachelor of Arts Degree from the University of Melbourne and is an Associate Member of the Institution of Engineers (Australia).

PERCENTAGE BY WHICH ALUMINIUM CONDUCTOR CABLE IS
CHEAPER THAN EQUIVALENT COPPER CONDUCTOR CABLE



KEY: PLOT THE POINT OF RELEVANT COPPER & ALUMINIUM COST; PROJECT THE POINT ALONG THE DIAGONAL TILL IT INTERSECTS THE RELEVANT CONDUCTOR LINE THEN PROJECT IT VERTICALLY TO THE TOP SCALE TO FIND THE PERCENTAGE BY WHICH ALUMINIUM CONDUCTOR CABLE IS CHEAPER THAN THE EQUIVALENT COPPER CONDUCTOR CABLE

FIG.2 GENERAL PRICE COMPARISON OF COPPER & ALUMINIUM CONDUCTOR CABLES. (MOISTURE-BARRIER SHEATHS)

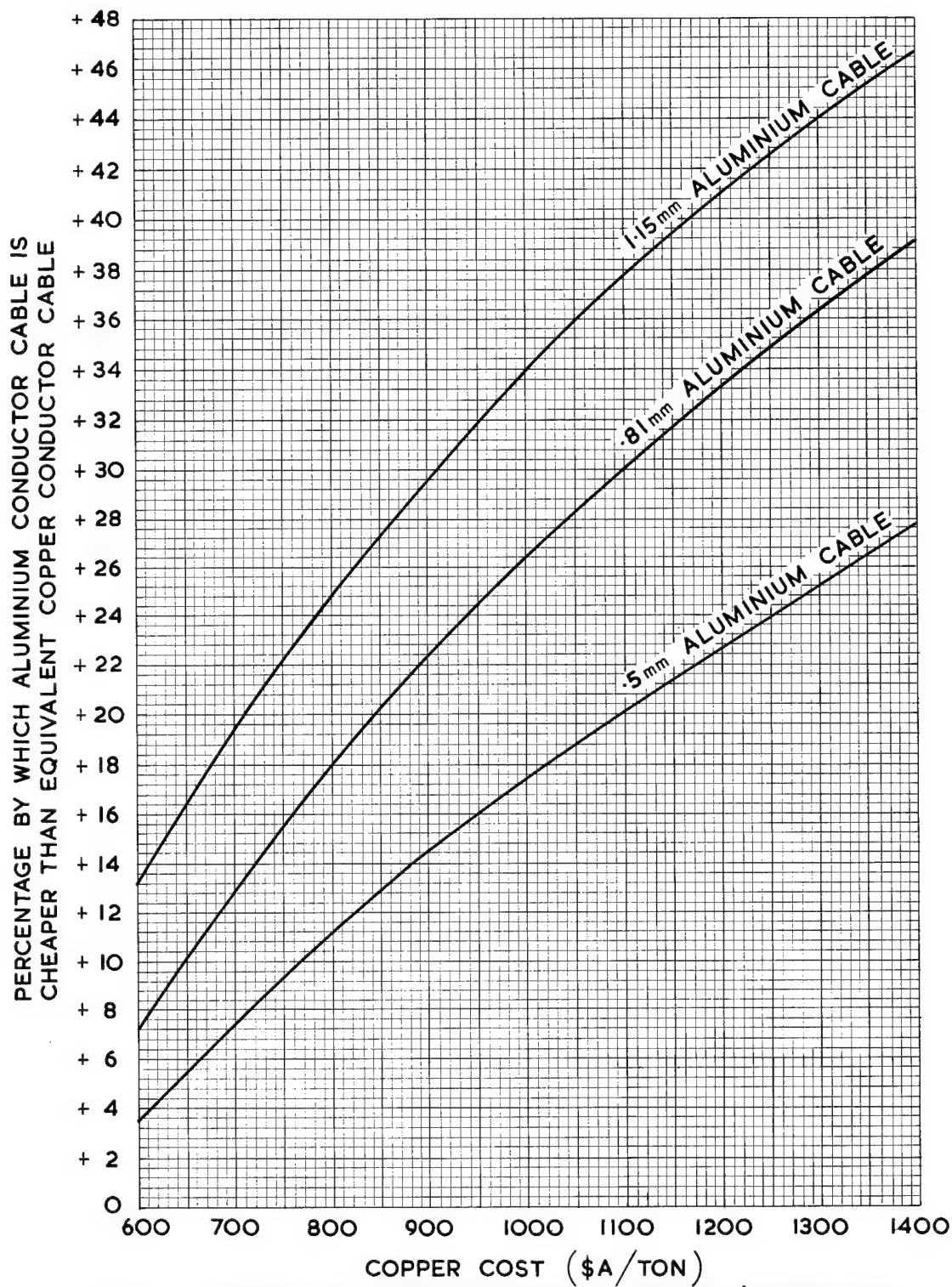


FIG.3 - EFFECT OF COPPER COST ON COPPER/ALUMINIUM CABLE PRICE RELATIVITIES. (ALUMINIUM \$A586/TON)

FUNDAMENTALS OF ESTABLISHING RELIABLE CONNECTIONS TO SMALL GAGE ALUMINUM WIRE

I. F. Matthyse and S.M. Garte
Burndy Corporation
Norwalk, Connecticut

Summary

Reliable connections can now be made to small gage aluminum wire as the result of fundamental research on the contact interface. The stability of the connection results from the development of a combination of contact surface topography that effectively locks the contact interface between the wire and the terminal, and protective finish that effectively inhibits corrosion.

Trend to Small Gage Aluminum Wire

Aluminum has been used successfully as an electrical conductor for many years. Particularly because of its light weight, it has become the principal conductor material for overhead transmission of electric power starting before the turn of the century. However, economy became the principal reason for adopting aluminum in place of copper for many electrical conductor applications beginning 20 to 25 years ago. The economic pressure resulting from the growing scarcity of copper and the relative abundance of aluminum ore (bauxite) was first felt in the larger conductor sizes used for electric power distribution. Much research and development was required to provide trouble free connectors and installation techniques, so that today the use of aluminum conductor for electric power distribution is universally accepted by the electric utility industry, and a standard of performance for connectors for aluminum cable adopted by the Edison Electric Institute¹ has become the industry standard.

Although the cost ratio of aluminum to copper has fluctuated widely over the years, the general trend has increasingly favored aluminum, so that now the economic advantage of aluminum cannot be ignored even for the smaller gage wires used for communications, signal circuits, and the low power applications. However, the use of aluminum in the smaller gages, such as #8 AWG and smaller, has been retarded by problems that were not entirely resolved by the research and development that led to the successful use of the larger aluminum conductor sizes. Until recently, little effort was devoted to resolving these problems, partly because of the lack of economic incentive in these sizes, and partly due to the lack of suitable aluminum alloys as the conductor materials. This paper shows how recent studies have resolved these problems and have enabled the user of small gage wire to realize the present economic advantage of aluminum conductor.

There are many factors that influence the design and performance of conductor terminations whether the conductor is aluminum or copper, but the influence of these factors is of much greater significance for aluminum

conductor terminations than for copper. Over the last 25 year period, much research has been carried out to understand these factors, and connector designs and installation techniques have been developed to provide trouble free terminations for aluminum conductors, for combinations of aluminum and copper conductors, and for universal terminations that may be used whether the conductor is aluminum or copper. It is not the purpose of this paper to review this work since a significant body of knowledge exists in the literature, some of which is listed in the bibliography of this paper. However, it is an objective of this paper to show the difference in the nature of the factors influencing the design and performance of terminations for small aluminum wire sizes, as distinct from the larger sizes, and to review the recent work that has made reliable terminations available for small aluminum wire sizes.

Improved Aluminum Conductor Alloy for Small Gage Wire

A major deterrent to the use of small gage aluminum wire sizes has been the lack of a suitable aluminum alloy for the conductor. Although EC grade aluminum wire has much poorer physical properties than copper, proper connector design and installation techniques resulting from extensive research and development efforts has overcome this disadvantage and permitted reliable use of this conductor in the larger sizes. Obviously, some of the physical limitations of EC grade aluminum present insurmountable obstacles to its use as small gage wire. One cannot risk broken wires as a result of tensile and flexural stresses imposed in normal operation and maintenance of equipment. Similarly, broken wires in the small sizes can be anticipated as a result of the excessive notch sensitivity of EC grade aluminum wire. These factors become of serious concern in the size range of #8 AWG and smaller with which this paper is concerned.

But there are more subtle factors regarding the poor physical properties of EC grade aluminum wire that present problems difficult to resolve for small gage aluminum wire although they have been successfully overcome in the larger sizes. These are related to the creep characteristics and relatively poor thermal stability of EC grade aluminum. For the larger sizes, terminations can be economically designed with adequate contact area to avoid excessive creep, and with the necessary resilience to maintain contact pressure despite creep and thermal instability of the wire. For the larger sizes, the most successful connector designs are made from aluminum or aluminum alloy even when they are universal, accepting either copper or aluminum wire. These connectors employ the "Massive Anode Principle"² in which a

relatively massive aluminum connector can be used successfully in contact with copper or brass equipment terminals, and can accept copper wire as well. For small wire terminations this is not always permissible, and at the present state of development, it is not economically feasible. Present requirements, therefore, often demand that the terminations be made of copper or brass which increase the difficulties of making stable connections under thermal cycling, due to the different temperature coefficients of expansion of aluminum and copper and the resulting loss of contact pressure as a result of the poor creep characteristics and thermal instability of EC grade aluminum wire.

Fortunately, at this time, manufacturers are making available new aluminum alloys suitable for small gage aluminum wire. For example, Southwire "Triple E" wire, an aluminum iron electrical conductor alloy, is reported to have significantly improved physical properties while retaining the high conductivity of EC grade wire. Figure 1 shows the greatly improved elongation relative to tensile strength of this alloy. Note that in the temper having a tensile strength of 16,000 p.s.i. suitable for small gage wire, its elongation is 20% as compared to only 5% for EC grade aluminum. In addition, these excellent physical properties are retained almost unaffected up to 200° C with very little change even after four hours at 275° C.³ Such thermal stability is of considerable importance for reliable small wire gage terminations.

The availability of such aluminum wire enabled Burndy to proceed with its research and development program to develop terminations for small gage aluminum wire with the confidence that the wire and cable industry, together with such specification agencies as the Underwriters' Laboratories, the S.A.E., the ASTM and perhaps others, will provide minimum performance requirements for aluminum for small gage wire, assuring the desired improvements over EC grade aluminum.

Selection of Connector Material

Terminations for small gage aluminum wire must be compatible with present day equipment designed for use with copper wire. The tangs or studs on such equipment are almost exclusively of copper or brass, and it is unlikely that they will be changed to another metal, such as aluminum, in the near future, and there is no assurance that such a change will ever prove to be practical. In addition, it is highly desirable that the terminations be compatible with copper wire as well as aluminum wire, since most users will find the need for both kinds of wire, and a universal terminal will simplify stocking problems and reduce installation machine set up time.

These requirements suggest that the terminals be made of copper or brass since the problems associated with dissimilar metals in contact (reviewed later in the paper) are eliminated at the equipment end of the terminal (front end), and when the wire is copper, they are eliminated at

wire receiving end of the terminal (back end) as well. This reduces the problem essentially to one of developing a copper or brass terminal that is compatible with aluminum wire under all the environmental conditions met in service. This paper will show how, starting with fundamental research on electrical contacts, this was accomplished.

The Contributions of Basic Research

The nature of contact resistance has been studied in considerable depth by many experimenters⁴⁻¹⁰ and the quantitative relationships have been determined for a fairly complete understanding of the phenomena. This work has shown that current flowing across the contact of metals under pressure passes through numerous tiny contacting asperities called "A" spots as shown in Figure 2. Only those contact spots to which actual metallic contact is made with no intervening nonmetallic film will actually carry current, and at those spots there will be no electrical resistance other than that offered by the conducting metal itself. Contact spots having unbroken non-metallic films intervening will carry no appreciable current.

Because of the very high current densities at the "A" spots, locally high temperatures, supertemperatures, are generated in the immediate vicinity of these contact spots. Normally, these temperatures are not excessive since the heat generated is dissipated through the surrounding metal. However, as chemical reaction proceeds, as the result of encroaching oxides and other non-conducting films, the "A" spots begin to disappear. The remaining "A" spots then carry the total current resulting in an increase in the supertemperatures at these spots. Since the "A" spots are, in effect parallel conductors, the initial effect of the disappearance of some of them is not noticeable. Toward the end of the lifetime of the connector, the cumulative effect of "A" spot erosion, rising supertemperatures, and increasing chemical reaction rates, results in a rapidly increasing rate of deterioration leading to sudden catastrophic failure.

The predictions made by a mathematical model are illustrated in Figures 3 and 4. These show the manner in which connector lifetimes will be related to current load and to the initial resistance of the connection. The prediction that the relatively small difference in initial resistance will be associated with large lifetime differences is well borne out by experience. However, the theory has predicted a much greater effect on lifetime than actually occurs. This "failure" of the theory is in itself instructive, since it arises from the assumption, made in constructing the model, that there is an unlimited supply of corrosive atmosphere to the "A" spots in the joint.

This assumption is incorrect as can be seen from consideration of the ingress of corroding gases into a metal-to-metal interface.¹⁰ In Figure 5 the progressive deterioration of the "A" spots is illustrated. These

pictures were made with a glass-metal interface and they are representative of the nature of ingress in an actual metal-to-metal interface. In a subsequent experiment two blocks of metal were clamped together at high pressure. One of the blocks had a small hole in the center through which air was aspirated, and the flow rate measured as a function of time. Within relatively short times, for both copper and aluminum, no more air could be aspirated. The growth of oxide around the "A" spots effectively blocked further access of air to these spots and acted to seal them against further chemical deterioration.

In another experiment with metal-to-metal, with the joints held in various corrosive atmospheres, it was found that after the joints were separated and then remated, the resistance immediately upon remating was very much higher than that just prior to separation.

As a result of these studies it can be expected that a high pressure joint will last a very long time provided that no relative movement between the contacting surfaces is allowed to occur. This finding was of major importance in the development of high reliability connections, and in particular in relation to the problem of providing stable terminations of a small gage aluminum wire to copper or brass terminals.

Development of Locked Contact Interface

The research described in the previous section clearly established the need to prevent relative movement at the contact interface in a connector and it led to the development of a connector contact surface that provides a locked contact interface between the connector and the conductor. The purpose of such locking action is to prevent relative movement that would otherwise occur at the contact interface during the life cycle of the connection due to mechanical stresses and metallic creep. The tendency for such relative movement can arise from many conditions such as tensile and bending stresses imposed on the conductor, and relative movement at the interface caused by mechanical shock and vibration. However, in the case of a connection between dissimilar metals such as aluminum wire in a copper or brass terminal, with which this paper is concerned, relative motion can be expected as a result of the different temperature coefficients of expansion of the dissimilar metals.

An objective sought in the development of terminals for small aluminum wire was to develop a surface topography, or controlled roughness, in the connector at the conductor contact surface that would, in effect, lock the conductor to the connector contact surface in such a manner as to prevent the relative movement that would otherwise occur due to the reasons noted above. In effect, this objective was to provide the connector contact surface with permanent "A" spots whose location would be specifically determined in the manufacturing process

of the terminal rather than to rely on random, and frequently temporary, "A" spots normally associated with pressure contacts.

The first experiments for this purpose were performed using thin shims of copper alloy having specific surface topographies placed between flat conductors of copper and aluminum, and resistance was measured between the flat conductors as a function of applied pressure. The resistance decreased with contact force in these joints in the manner usually found with pressure connections. However, the actual resistance-force relationship was dependent on the nature of the surface topography. A surface topography having sharp crater-like asperities as shown in Figure 6 was found that gave surprisingly low resistance values with increasing force, and what is of much greater significance, the resistance remained at the low value even after the external force was completely removed. Figure 7 shows the comparison of the resistance-force relationship between two flat aluminum surfaces with and without this shim between the surfaces. Note the very much higher values of contact resistance without the shim, and that with the shim the low contact resistance remains after the force is completely removed. These results indicated that a locked condition was achieved between the asperities on the contact shim and the conductor into which these asperities became embedded. This was further confirmed by the fact that considerable tension was required to separate the two conductors after the external pressure was removed.

In view of the great interest in the potential savings of using aluminum wire shown by the manufacturers of household appliances and other commercial equipment, it was decided to apply the results of these tests to the type of terminal used in great volume by the appliance industry. These terminals use "U" shaped elements as shown in Figure 8 into which the wire is crimped and the insulation is gripped. They will be referred to in this paper as "open barrel" connectors to distinguish them from "closed barrel" connectors having tubular shaped members into which the wire is crimped. The wire may be readily laid into the open barrel permitting machine installation of such connectors at very high rates. Such terminals are made of relatively thin brass material for further economy.

This led to the development of terminals as shown in Figure 9 in which the open barrel wire contact surface is made with the specially shaped, sharp, crater-like, contact asperities formed by piercing tiny holes through the terminal with properly shaped dies to extrude the sharp and rough crater shapes on the contact surface. Figure 10 shows a typical section through these asperities, showing how they pierce into the aluminum conductor breaking through the aluminum oxide and entrapping portions of the conductor in such a manner that the conductor becomes locked to the contact surface of the connector providing a permanent low resistance contact. These

asperities must be designed to be very small in comparison to the conductor size and the dimensions of the terminal, and a sufficient number of them must be distributed over the contact surface to lock the entire area of the contact interface and provide the desired low resistance.

The crimping die shape used to install these terminals is of the standard "B" shape commonly used on open barrel terminals, and produces the configuration shown in cross-section in Figure 11. The optimum die shape is designed to produce less compression at the wire entrance of the crimped barrel and deeper compression at the opposite end. This provides strain relief at the wire entrance for greater mechanical secureness and pullout strength of the wire, while providing more intimate electrical contact at the opposite end.

In current heat cycle tests on aluminum wire, these terminals having the new contact topography show a vast improvement over the same type of terminals with conventional contact surfaces. In addition, the new terminals perform equally well on copper wire giving them the desired universal character. Figure 12 shows the results of a typical heat cycle test comparing samples of both types of terminals installed on #18 gage, 7 strand, Triple E aluminum wire using a current required to reach a stable temperature of 105° C. In this test, the current-on and current-off periods were each 1/2 hour and the test was continued for 500 cycles.

The graph shows the relative resistance of the joints over the measuring distance shown, compared to the resistance of an equal length of wire. The initial relative resistances of all samples were close to 100% with the samples having the new topography showing excellent stability over the 500 cycles of the test. In contrast the resistances of the samples having conventional contact surfaces rose rapidly after the first few cycles, and their resistances and temperatures were so high by the 50th cycle that they had to be disconnected from the heat cycle loop to continue the test.

The results strongly supported the theory that good electrical contact can be maintained by providing locking action to prevent relative motion at the contact interface. As a result of this action, good contact was maintained despite the differences in the coefficients of expansion of the dissimilar metals and despite the creep tendency of aluminum under the cyclical forces and the elevated temperature during the test.

Similar heat cycle tests run on copper wire showed the same stability of performance in the new terminals as that shown for aluminum wire in Figure 11, thus confirming the universal nature of the new terminals.

Protection of Termination from Deteriorating Influences of the Environment

Having resolved the problem of maintaining stable contact of an aluminum wire in a brass or copper terminal

despite the mechanical forces tending to destroy the points of contact, it remained to provide the terminal with a suitable protective coating to prevent deterioration of the termination due to chemical activity. The predominating factor is, of course, galvanic corrosion as a result of contact between dissimilar metals. Aluminum wire in a bare brass or copper terminal would be severely attacked due to electrolytic action resulting from moisture and other elements, such as salt fog, in the atmosphere. The attack on the wire itself would sever strands where they enter the terminal, and it might destroy the connection by ingress into the contact area.

The usual manner of protection that has been practiced on copper alloy connectors for use with the larger sizes of aluminum conductor has been to plate the connector with a metal that is much closer to aluminum in the electrolytic series than copper, thereby reducing the galvanic action resulting from the dissimilar metals. Tin, zinc, and cadmium plating have been used for this purpose with some success, with tin being most commonly used. In addition, for these larger connectors, it has been common practice to use a grease-like joint compound, having several advantages when connecting aluminum conductor, one of which is to provide a degree of sealing against the corrosive elements in the environment.

However, the use of such a joint compound for small aluminum wire terminations is impractical and costly especially for the very inexpensive, high speed, machine installed terminations. Without the benefit of such joint compounds, platings which are effective for the larger terminations have been found inadequate for brass or copper terminals for small gage aluminum wire. In addition, small size terminations, as compared to the larger ones, suffer a greater rate of attack in a corrosive environment simply because there is not a sufficient aluminum mass of a sacrificial nature to retard the destruction of the termination.

As the result of an exhaustive investigation of plating and coating systems for brass or copper terminals for small gage aluminum wire, a proprietary surface protective finish was developed that gave consistently superior protection in extensive laboratory tests involving salt spray, humidity and thermal shock testing. The performance of terminations having this new protective finish together with the new contact surface topography is described in the next section.

Performance Testing

Although at the present time there are industry specifications^{1,11,12} for laboratory performance testing of the larger sizes of aluminum wire terminations, they exist only for copper wire in the small gage sizes. Industry standards are now being prepared for terminations for small gage aluminum wire by such agencies as the Underwriters' Laboratories, S.A.E. and governmental

agencies in cooperation with manufacturers of wire and connectors. It seems likely at this time that such specifications will have to recognize more than one level of reliability, since open barrel terminals made from thin wall brass for use in household appliances may not be required to have the full reliability of closed barrel terminals designed for the more critical aircraft and military applications. In fact, still another level may be required for especially severe environmental conditions, as for example, conditions of operating temperatures of 200° C or greater.

In the absence of industry-wide performance specifications, it was essential to prepare complete performance test specifications as part of this aluminum wire termination development program. Test series were selected using significant portions of existing specifications, appropriately modified for small aluminum wire on the basis of an understanding of contact failure mechanisms found through fundamental research. The specifications have been prepared recognizing the three levels of reliability and environmental conditions mentioned previously. All three require tests of similar character except for their different requirements and the severity of their testing conditions.

At the time of preparation of this paper, considerable confidence has been attained by experience with one of these specifications, namely that for the performance of terminations for applications such as those in household appliances and commercial equipment requiring the economy of the thin wall brass open barrel terminals. Confidence in this specification has been enhanced by the correlation of performance found for terminals tested by the new specification compared with their performance installed in household appliances operated under severe service conditions for extended periods. For example, in an extensive series of tests in household washing machines wired with aluminum wire, after 5000 cycles of extremely severe operating conditions, designed to assure satisfactory operation over the life of the equipment, the terminations gave entirely satisfactory performance, confirming the performance found on the same terminals that passed the testing specification.

The test specification adopted to qualify this class of terminations consists of three separate test sequences. In the first one, tests consisting of thermal shock, vibration, humidity, and tensile strength, are conducted sequentially on the same set of specimens. The second sequence is a salt spray corrosion test, and the third is a current heat cycle test.

The first sequence is shown in Figure 13. The corrosion test sequence is a 96 hour salt spray test per MIL-STD-202D.

The current heat cycle sequence calls for 500 cycles, each cycle having the specified current on for 15 minutes and off for 15 minutes; these times being sufficient

to reach temperature stability with current on, and return to ambient temperature with current off. In view of the critical nature of small wire aluminum terminations, it was decided to use 500 cycles for this test following the broadly accepted practice in accordance with the EEI-NEMA specification¹ for power connectors instead of the 42 cycle test in the present Underwriters' Laboratories Standard. On the other hand, because of the lighter duty class of these terminals, the current values selected are proportionally much less than those in the EEI-NEMA specification, but they are, nevertheless, 2 1/2 times the continuous test current interpolated from the Underwriters' Laboratory standard.

Qualification to this specification requires that all specimens show no more than a 30% increase of millivolt drop across the specimen lengths in each test sequence. The brass open barrel terminals having the new contact topography and the new protective finish have been qualified to this specification, and Figure 14 shows the test results obtained on these terminals installed on #16, 37 strand Triple E aluminum wire. Similar results were obtained on these terminals with copper wire for which the performance is even somewhat better than conventional tin plated terminals designed for copper wire only. Thus the universal applicability of these terminals was again confirmed. Figure 15 shows three forms of these universal open barrel terminals after crimping on the wire.

Performance Specifications and Terminations for Other Duty Classes

In the previous section it was indicated that the lack of any industry wide specifications for terminations for small gage aluminum wire required the development of performance specifications as part of this termination development program. The specification was developed for the duty class for terminations in household appliances and in other commercial equipment subject to similar duty requirements, and requiring a similar degree of reliability. This specification served, in effect, as an extension of the Underwriters' Laboratories Standard¹¹ to the small sizes of aluminum wire. It enabled the completion of the development of the new, thin wall brass open barrel terminals for this duty class.

It was also mentioned that a performance specification had been prepared for duty classes requiring terminations of higher reliability in the more critical applications such as for aircraft, for military applications and for other critical applications. This specification is for the duty class corresponding to the military specification MIL-T-7099D¹² for terminals for aluminum aircraft wire, and in effect, may act as its extension to the small aluminum wire sizes. In addition a performance specification has been prepared for a third duty class involving more severe environmental conditions, especially for higher temperature applications.

At the time of preparation of this paper, these additional specifications are somewhat tentative since the termination development program and the associated testing for these duty classes is not yet complete.

The terminations now under development for these duty classes employ closed barrel crimping contacts for the wire, similar to those now being used for copper wire as shown in Figure 16, and will include splices as well as terminals of the insulated as well as uninsulated varieties. The principles that led to the successful development of the brass, open barrel terminals for small aluminum wire, have been found equally successful for the closed barrel terminals; namely, the use of a surface topography that provides a locked contact interface with the wire, and a surface protective finish to prevent attack by the corrosive and oxidizing effects of the environment. However, copper is being used for these terminals instead of brass to provide the higher electrical conductivity for the more critical duty requirements.

Like the open barrel terminals, these closed barrel terminals are universal, performing satisfactorily with either copper or aluminum wire.

Conclusions

The economy of small size aluminum wire may now be realized for many applications as a result of the recent availability of high conductivity aluminum alloy wire having the required physical properties, and as a result of an extensive development program for suitable terminations. The following conclusions regarding terminating small aluminum wire can be drawn from this program.

1. Stability of a crimped connection to aluminum wire in a copper or brass terminal may be attained by the use of a contact surface topography that effectively locks the contact interface to prevent relative movement resulting from thermal stresses, creep and external forces, and by providing a surface protective finish on the terminal to prevent deterioration due to the corroding and oxidizing influences of the environment.
2. Terminals made according to these principles are universal, accepting either aluminum or copper wire.
3. Industry-wide performance specifications are not yet available for small aluminum wire terminations, and to qualify the terminals in this development program performance specifications have been prepared recognizing the severity of the environmental conditions and the degree of reliability required for three different duty classes.
4. The open barrel brass terminals that have been developed for such applications as household appliances, have qualified to the specification prepared for this duty class, and their good performance has been verified in accelerated life tests of appliances wired with aluminum wire.

5. The development of closed barrel terminations required for the more severe service applications, and requiring a higher degree of reliability, for applications such as those for aircraft wiring, is nearing completion, and preliminary testing to the performance specifications for this duty class shows very satisfactory performance.

References

1. "EEI-NEMA Standards for Overhead Distribution Connectors for Aluminum Conductors," Edison Electric Institute Publication No. TDJ-162, NEMA Publication No. SG14.10-1962, October, 1962.
2. "Basic Connection Principles, Second Edition," I.F. Matthisse, Burndy Corporation Publication, September, 1965.
3. "A Review of the Characteristics and Performance of 'Triple E' Aluminum in Laboratory Testing," G.E. Lenaeus, Non-Ferrous Metals Division Meeting of The Wire Association, Inc., April 15-16, 1970.
4. "Electric Contacts Handbook," Ragnar Holm, Springer-Verlag, Berlin, 1967.
5. "The Making and Testing of High Performance Electrical Connections; a Problem for the Surface Scientist," J.B.P. Williamson, Second Symposium on Connectors, Ballistics Systems Division of Space Technology Laboratories, Los Angeles, February, 1964. (Research Report No. 4, Burndy Research Division, March 23, 1964.)
6. "The Contact of Nominally Flat Surfaces," J.A. Greenwood, J.B.P. Williamson, Second International Symposium on Electric Contact Phenomena, Graz, Austria, May, 1964. (Research Report No. 15, Burndy Research Division, July 24, 1964.)
7. "Elastic Contact of Rough Spheres," J.A. Greenwood and J.H. Tripp, Research Report No. 21, Burndy Research Division, February 25, 1965.
8. "The Area of Contact Between a Rough Surface and a Plane," J.A. Greenwood, Research Report No. 25, July 30, 1965, presented at the ASME-ASLE Lubrication Conference, San Francisco, California, October, 1965.
9. "Significance of Non-Destructive Tests of Compression Joints," J.B.P. Williamson, Conference on Non-Destructive Testing in Electrical Engineering, Institution of Electrical Engineers, London, November, 1961. (Research Memorandum No. 18, Burndy Research Division, October 9, 1964.)
10. "Ingress-Limited Corrosion of Contacting Surfaces," R.F. Snowball, J.B.P. Williamson, and R. C. Hack, IEEE Transactions on Parts, Materials and Packaging, Vol. PMP-3, Number 3, September 1967.
11. Underwriters' Laboratories, Inc., Standard for Wire Connectors and Soldering Lugs, UL 486, June 27, 1969.

12. U.S. Department of Defense, Military Specification MIL-T-7099D, "Terminals; Lug and Splice, Crimp Style Aluminum, for Aluminum Aircraft Wire," January 2, 1964.



I. F. Matthyse, Burndy Corporation
Norwalk, Conn. 06852

I. F. Matthyse, Fellow of IEEE, holds the degree of B.S. in Electrical Engineering from both Cooper Union and New York University, and the degree of M.S. in Physics from the latter. He has been with Burndy Corp. since 1928, responsible for the design, development and research associated with electrical connectors, special fuses, and switching devices. He holds over 45 U.S. Patents and has been the author of over 30 technical papers. He has been active on technical committees of IEEE, EEC and NEMA, and has been influential in the development of industry-wide performance standards for electrical connections for aluminum conductors.

ALUMINUM WIRE STRENGTH AND DUCTILITY

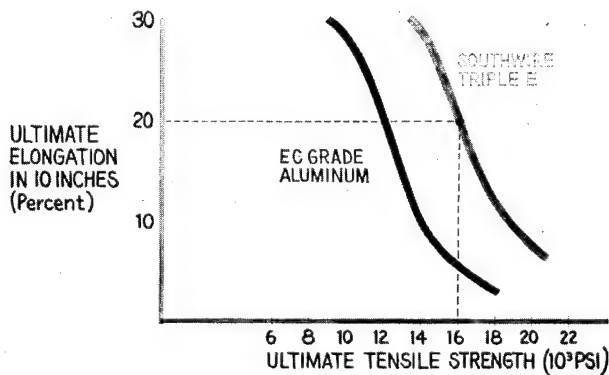
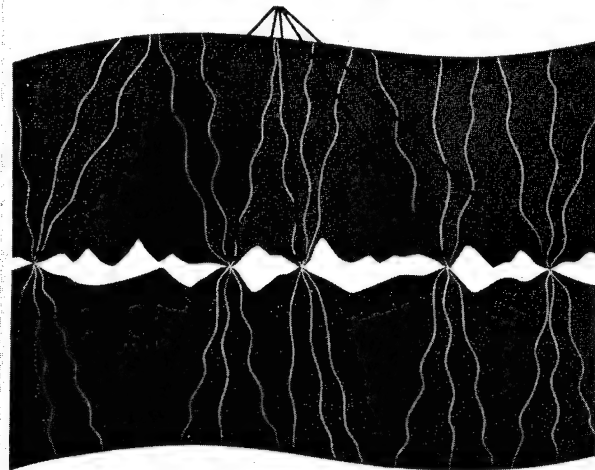


Fig. 1 Comparison of Improved Aluminum Alloy with EC Grade

"A" SPOTS



ENLARGED 5,000 X APPROXIMATELY

Fig. 2 "A" Spots at Contact Interface

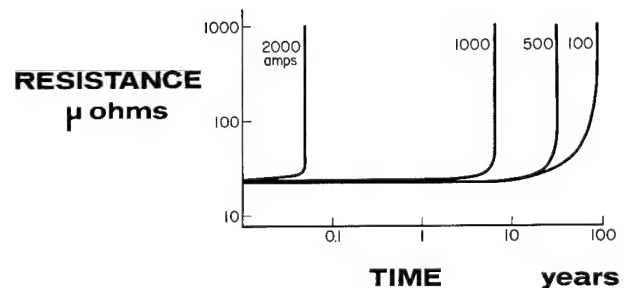


Fig. 3 Connector Lifetime as a Function of Current

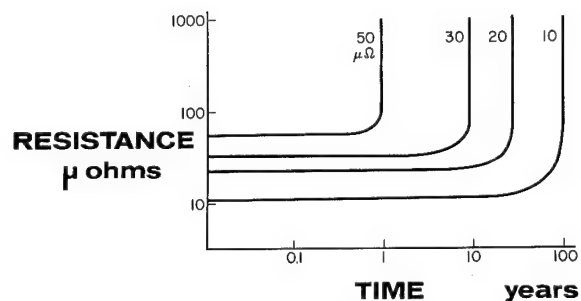


Fig. 4 Connector Lifetime as a Function of Initial Resistance

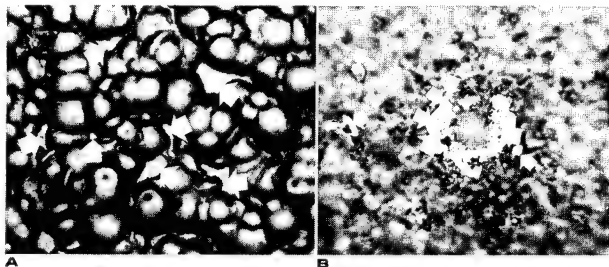


Fig. 5 Progressive destruction of "A" spots by ingress of corrodants. (a) Mated surface showing contacting "A" spots, indicated by arrows. (b) Surface after exposure to moist SO_2 . Small arrows indicate corrosion film on "A" spot; large arrows show clean metal areas.

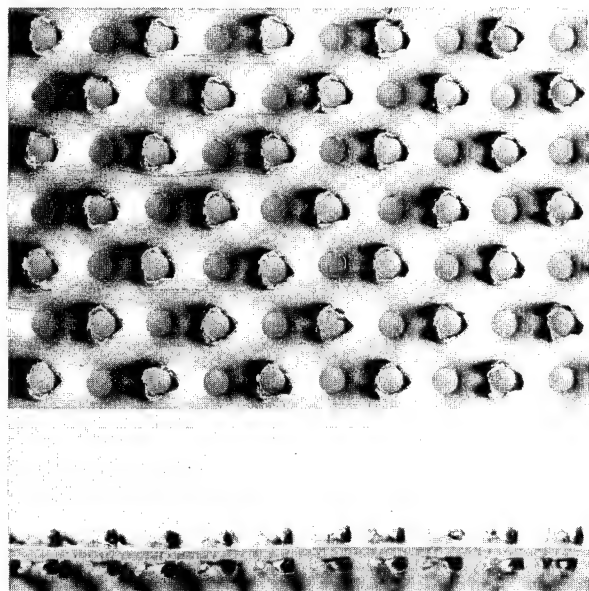


Fig. 6 Contact Shim with Topography for Locked Contact Interface

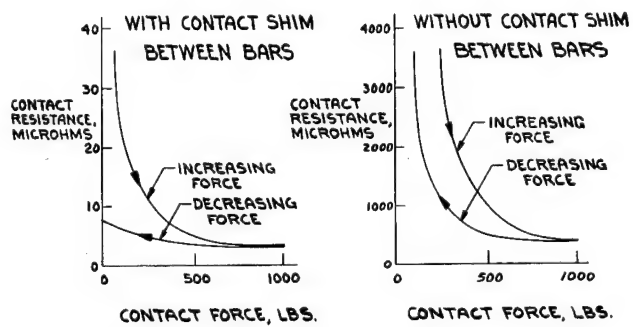


Fig. 7 Contact Resistance Between $1/8" \times 1"$ Aluminum Bars

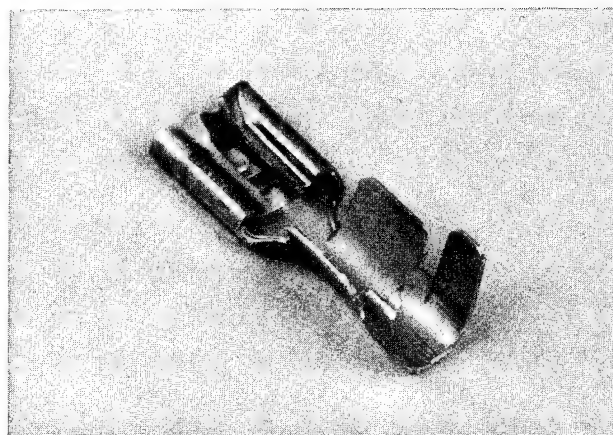


Fig. 8 Standard Open Barrel Terminal for Copper Wire

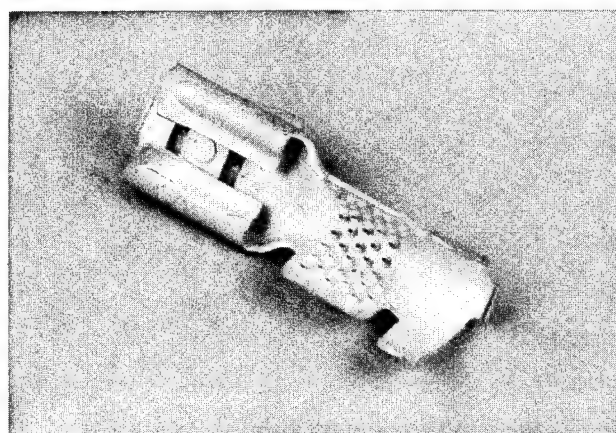


Fig. 9 Universal Open Barrel Terminal

ENLARGED VIEW OF ASPERITIES

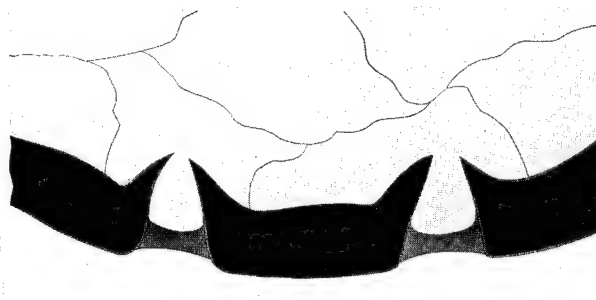


Fig. 10 Cross-Section through Asperities of Locked Contact Interface

MAGNIFIED CROSS SECTION OF CRIMPED UNIVERSAL TERMINAL



Fig. 11 Cross-Section of Crimped Universal Open Barrel Terminal

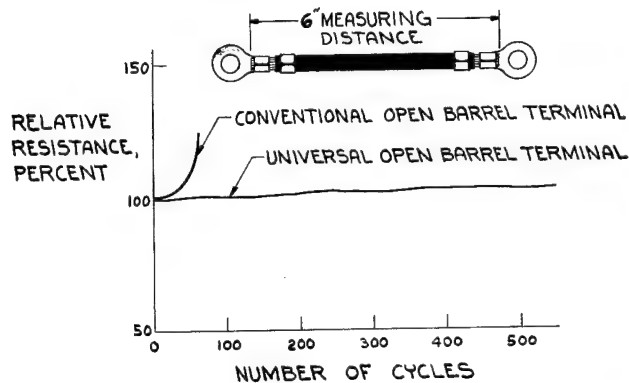
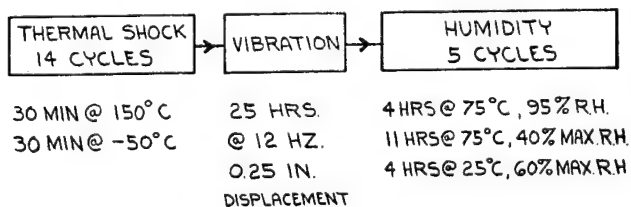


Fig. 12 Current Heat Cycle Tests on Terminals on #18, 7 Strand "Triple E" Aluminum Wire

PERFORMANCE SPECIFICATION FIRST SEQUENCE

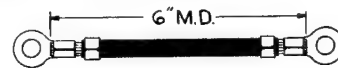


TENSILE STRENGTH TEST FOLLOWS FINAL
M V DROP MEASUREMENT

Fig. 13 Performance Specification, First Sequence, for Open Barrel Universal Terminals

PERFORMANCE OF UNIVERSAL OPEN BARREL TERMINALS

* 16, 37 STRAND
"TRIPLE E" ALUM. WIRE



SEQUENCE	PERCENT INCREASE OF M V DROP		
	HIGH	LOW	AVERAGE
THERMAL SHOCK VIBRATION HUMIDITY	18.1	6.4	12.2
SALT SPRAY CORROSION	21.1	8.2	12.6
CURRENT HEAT CYCLE	7.8	1.4	5.1

Fig. 14

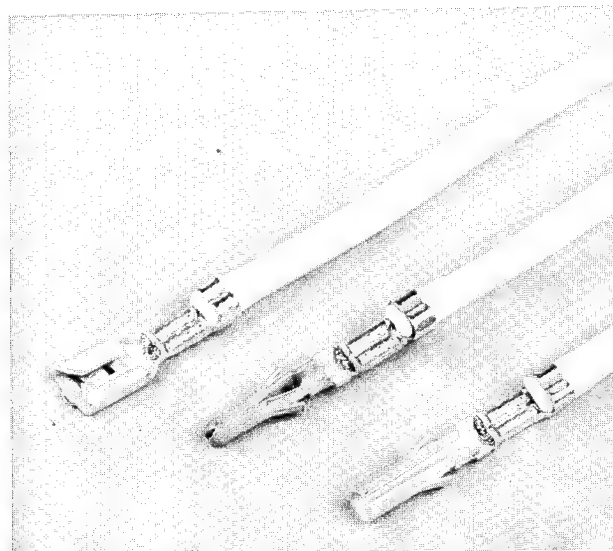


Fig. 15 Universal Open Barrel Terminals Crimped to the Wire

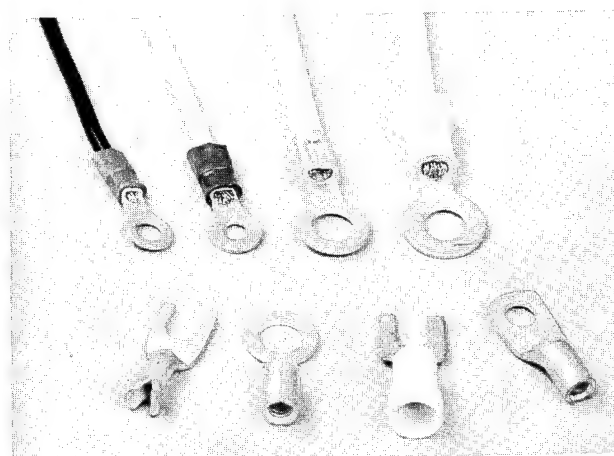


Fig. 16 Closed Barrel Terminals, Bare and Insulated

NEW TECHNIQUES FOR TERMINATING SMALL ALUMINUM
WIRE TO CONNECTOR PINS AND SOCKETS

Michael D. Lazar
Director, Advance Development
Electronic Products
Burndy Corporation
Norwalk, Connecticut

Introduction

Economics, the great motivator, has provided the impetus for converting copper conductors to aluminum, in applications heretofore considered undesirable. Savings averaging 25% typically result from such a change. With conditions as they are in the world copper market, and with demand growing faster than supply, all indications are that this cost trend will continue and become even more pronounced with time. For some applications the weight reduction is also a significant advantage as well.

It remains, therefore, only to provide solutions to the outstanding technical and reliability problems, before aluminum conductors as small as #22 gage will be used in all types of electrical and electronic equipment, both military and commercial.

This paper will summarize work done at the Burndy Corporation on one major aspect of this problem: namely, that of providing simple, reliable techniques for terminating stranded aluminum wires to connector pins and sockets.

Background

Aluminum wire in large gage sizes has been used successfully for many years in fields such as overhead transmission, distribution and service entrance cable. More recently, the replacement of copper with aluminum building wire has proceeded at a rapid pace. Aircraft also have used aluminum stranded wire in wire sizes #10 and larger. In all such cases the wire is made from electrical conductor (EC) alloy. The properties of EC alloy, however, leave much to be desired in terms of ultimate tensile strength, ultimate elongation, ductility, effect of temperature, and termination ability before it can be used reliably in the smaller wire sizes. Major innovations in new aluminum alloy development have recently taken place, and more work continues to be done. One such example is the new 'EEE' aluminum iron alloy. EEE aluminum alloy has illustrated that the cable alloy problems are well on their way towards resolution. Other alloys soon to be announced also hold out similar promise.

In the area of terminations, the major problems are as follows:

- (1) The tough, insulating, aluminum oxide film on the aluminum wire.
- (2) The difference in the coefficient of thermal expansion of the aluminum wire and the material from which the pin and socket contacts are normally made.
- (3) Galvanic corrosion between the aluminum wire and the metals and finishes normally used on pins and sockets, i.e., gold over silver, gold over nickel, gold over copper, or rhodium over silver, nickel or copper, silver, and tin.

Most terminations on aluminum wire up to the present time make use of a grease-like or "tacky" compound such as Burndy Penetrox, ^R in the interface of the wire and surrounding crimp barrel.² The crimp barrel is most often made of aluminum. The function of the compound is twofold. First, by using powder size metallic particles suspended in the compound, the particles serve to "puncture" the aluminum oxide and second, to create a multiplicity of current "bridges" between the two conductors. The compound is also effective in helping to seal the joint from attack by gases and other corrosive media. Our judgment, however, is that the use of such compounds is not desirable nor practical or economical for use with pin or socket terminations.

Therefore, industry is facing the problem of making a termination from a copper alloy (usually brass or bronze) pin or socket to an unplated aluminum conductor. There are two possible directions in which to proceed: (1) to find a successful termination technique to make the suitably plated copper alloy contact work, directly on the aluminum or; (2) to make a suitably plated aluminum barrel work well when crimped to the aluminum conductor, and to find a reliable, inexpensive means for joining the aluminum barrel to the copper alloy pin or socket.

In our work at Burndy, both approaches were developed simultaneously in order that we could be sure that the final selection made would be the best possible. This enabled the best of each to be compared. Factors such as performance, cost, logistics, compatibility with copper conductors, ease of use, and possible confusion by service personnel, were considered.

Copper Alloy Termination

The Burndy Corporation has pursued the prospect of making reliable crimp connections to aluminum conductors directly with copper alloy crimp elements, without the use of compounds for many years. A practical solution to this problem has evolved. It is established that if the following fundamental principles are practiced, a good connection would result.

1. Mechanically penetrate the oxide film at a multiplicity of points, encouraging relative motion during the crimping operation between the terminal and conductor.
2. Maintain the gas-tight, oxide free junctions by preventing any movement at the interface after the joint is made. This, of course, must take into account the different expansion rate of the two metals, and the resulting creep of the aluminum.
3. Coat the terminal with appropriate materials to avoid galvanic corrosion.

The paper given by Mr. Matthysse at this session amply explains and supports these fundamentals and one presented previously by Mr. Suffredini illustrates practical applications of these principles in one type of terminal design.

Utilizing these same fundamentals, but altering the geometry to suit the special size, shape, metals, and manufacturing methods associated with pins and sockets, a successful design was developed. It consisted of cutting multiple slots into the circumference of the crimp portion of the pin in such a manner as to make contact with each external strand of the conductor. Crimping was done with a set of dies shaped as semi-circles so that when closed, they made a complete circle. The only breaks in the true circle were two pockets on each side where the dies butted to allow for some flashing of the metal when it was compressed. (See Figure 1) Cross sections of the joint showed a great deal of movement on the part of the aluminum conductor, with the metal actually flowing up into the slots in the crimp barrel. This assured the meeting of the first requirement, to mechanically shear the aluminum oxide. An enlargement of the joint at one of the slots also shows that the aluminum was subsequently trapped in the slot, as the crimping action caused the normally parallel sides of the slot to change to

a keystone shape, so that relative motion between the aluminum and copper alloy parts was eliminated. (See Figure 2) In this way, the good contact established all along both sides of the slots was maintained gas-tight, and no opportunity for re-oxidation or corrosion existed. In addition, thermal shock tests illustrated the point that even the differential expansion of the copper and aluminum through a temperature gradient of 180°C. did not cause shifting of the contact areas. This was verified by the fact that the contact resistance did not significantly change.

While the joint itself also did not show any serious degradation due to salt spray testing, serious corrosion did occur on the aluminum wire itself where it emanated from the gold plated barrel of the contact. Testing with the contacts outside of the connector body (the results would be much better inside the protective housing of a sealed connector) established that the small space which would be commonly expected between the end of the wire insulation and the end of crimp barrel would be a serious corrosion site. Therefore, the crimp end of the contact would have to be plated with a heavy layer of a compatible material such as tin. Since the pin or socket end would have to remain gold in order to suitably perform its function, this required the contacts to be selectively plated at each end.

Aluminum Alloy Barrel Termination

The concurrent development of an aluminum barrel properly joined to a copper alloy pin or socket also produced a satisfactory design. (See Figure 3) Breaking down the oxide was accomplished by causing severe deformation of all strands of the wire, changing their shape and increasing the distance around their perimeter so that it would be impossible for the aluminum oxide to remain intact due to the fact that it is hard, brittle and its ductility is very low. Let us examine a typical crimp joint. (See Figure 4) We can observe that the perimeter of each strand has been increased as much as 12%. The oxide will separate at one or more locations since it simply cannot stretch that much. In addition, it is clear that the original round strand shape has been altered to irregular shapes with relatively sharp corners with included angles as small as 28°. Here, also, the oxide cannot bend in conformance with such corners and will crack here as well. A third factor in breaking up oxide is the extrusion of the aluminum strands along the axis of the crimp joint. Measurements of the area of each crimped strand show a reduction in the order of 38% from the undistorted area. Whereas the aluminum will readily extrude, the oxide will not, again forcing the oxide to break up. All three conditions expose fresh unoxidized aluminum which is simultaneously in contact with the crimp barrel inside surface and is made gas-

tight by the high compressive forces at the interface. Excellent low contact resistance values result from this action.

Eliminating motion at the interface with an aluminum crimp element is relatively easy compared to one of copper alloy. In the case of the aluminum, the rate of expansion is the same for the crimp barrel as it is for the conductor. This also minimizes stresses during the test, thereby minimizing creep. Tests have indicated that thermal shock cycling from -55°C . to $+125^{\circ}\text{C}$. does not cause significant changes in contact resistance. It therefore becomes unnecessary to create a special topography on the inside of an aluminum crimp element, whereas it is essential for one made of copper alloy.

For corrosion protection, we surveyed all possible electroplatings which are close to aluminum in the galvanic series, and which also would be suitable for a mass-produced reliable fused joint with the gold-plated pin or socket. Such a plating also had to give good results as a contact material since it would be in direct contact with the aluminum wire in the crimp joint. None of the commonly used electroplatings fulfilled all three requirements. Several special, composite platings were developed and sequential environmental tests are currently underway. A decision on the final choice of plating has not been made as of the time of publication in order to determine the plating with the best compatibility with the method and materials used in the fused joint.

Fused Joint

The joint between the aluminum crimp barrel and the pin or socket must have the following attributes:

1. Reliability equal to solid metal (no joint).
2. Automated production methods to eliminate variables (to achieve the reliability) and to minimize cost.
3. Elimination of metallurgical faults, such as a high concentration of intermetallic compounds, formed either by the fusing process or by subsequent long-term high temperature exposure.

A survey of all current joining techniques for plated aluminum to plated copper alloys was performed. The processes considered included brazing, resistance welding, thermo-compression bonding, diffusion bonding, friction welding, cold welding and soldering. It is not possible, in the interest of brevity, to go into all the considerations on each process. Our conclusion was that soldering offered the best prospect for achieving the three objectives above. Our work therefore concentrated itself on the various soldering techniques available within the

current state-of-the-art.

In addition to the plating variables mentioned on the aluminum crimp barrel, our program also is considering the plating variables found on Military Standards and Commercial Standards for pins and sockets. They include:

gold over copper
gold over silver

gold over nickel
rhodium over silver
rhodium over nickel
silver
tin

All of the above also are specified in different thicknesses for different connectors. Insofar as possible, our attempt is to provide a solder joint which is compatible with all of the above platings. Test programs are currently underway to determine whether this will be possible and if so, what materials and processes are required. If it turns out that there is some incompatibility, then we will probably recommend that some pin and socket platings be abandoned in favor of others in order to achieve the desired results. It is safe to say, at this point, that a suitable solder joint can be provided which will be compatible with a sufficient variety of plating to cover most, if not all of the connectors and applications foreseen. A further report will be made on this topic in the near future.

Compatibility with Copper Wire (Universal Contact)

All of the work reported above also included screening tests consisting of mechanical pullout, voltage drop before and after thermal cycling, and salt spray, utilizing standard MIL-W-16878 tin plated copper wire. Results to date are very promising in that all tests have been passed with values well within MIL-Spec limits. Crimping in the slotted copper alloy barrels with the semi-circular dies produced excellent results and good appearance. Crimping in the aluminum barrels with MIL-STD four indent tools showed surprisingly good results to date. The explanation is that the differential rate of expansion is now working in favor of lowering the residual stresses in the crimp at elevated temperatures instead of increasing those stresses as would normally occur when the aluminum is on the inside and the copper is on the outside. The net result is that the aluminum is not forced to creep under increased stress, and therefore the aluminum to copper contact junctions are not forced to shift and degrade. Also working for us is the fact that the plated aluminum barrel means that we do not have any

aluminum oxide problem to contend with. Since the plating on the aluminum crimp barrel and on the copper wire will be compatible, corrosion will not be a problem either.

Crimping Tool Compatibility

As described, specially designed crimping dies were needed to make the copper alloy crimp barrel work satisfactorily. On the other hand, the Military Standard four indent MS 3191 crimping tool worked well without any changes, on the aluminum barrel design. The only difference was that a different setting was used on copper and aluminum wire. A simple example is shown below:

MS 3191 Selector Setting		
wire size	for copper wire	for aluminum wire
20	7	5
22	6	5

The important thing is that it is no more complex to select the proper setting for aluminum wire than it is today for copper, providing that the contacts are clearly distinguishable from one another. This is easily done because the plating on the barrel end will contrast markedly with the gold or rhodium plated front end and is clearly different from any of the contacts currently in use. Even color blindness would not be a serious problem due to the difference in reflective properties of the dull plating used on the aluminum barrel.

Connector and Insertion/Extraction Tool Compatibility

Studies made on all currently popular types of contacts, including all those covered by MIL-SPECS assure that there will be no problem of compatibility between the contacts for aluminum wire and the connectors, and insertion/extraction tools with which they are used. All overall dimensions and those concerned with retention, etc., will be maintained.

Conclusion

Screening testing to date has established that suitable pin and socket type contact designs can be provided for crimp-type termination to the new-high strength aluminum alloy conductors. Both all copper alloy contacts, and copper-aluminum designs can do the job, but for logistics reasons, the copper-aluminum design is favored because it enables the use of MIL-STD crimping tools. Materials and platings have been developed which are compatible for the crimping on aluminum and on copper wire, providing a "Universal Contact". Compatibility with connectors and tools is also assured. Complete sequential testing programs are underway to verify the total performance of the new "Universal Contact", and will be reported on early in 1971.

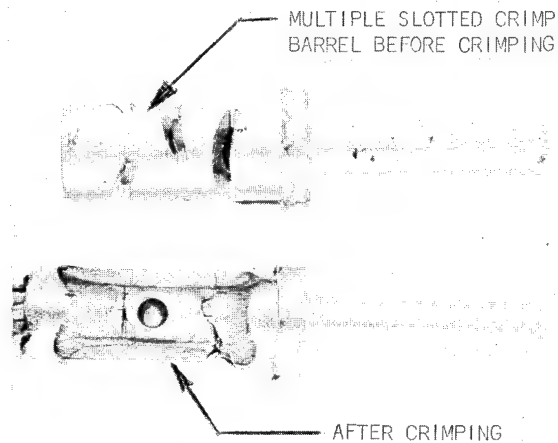


FIG. 1. PIN CONTACT FOR MIL-C-38999 CONNECTOR DESIGNED FOR CRIMPING ON ALUMINUM ALLOY WIRE

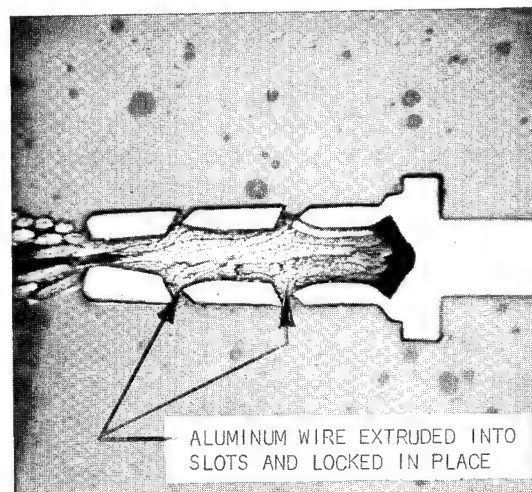


FIG. 2. CROSS SECTION OF MULTIPLE SLOTTED CRIMPED PIN

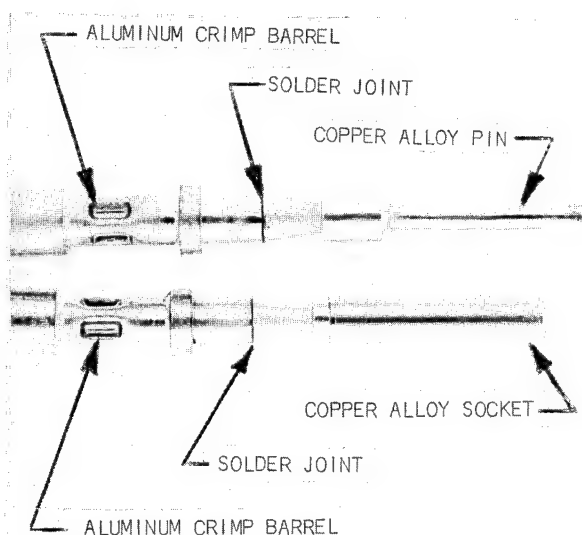


FIG. 3. PIN AND SOCKET CONTACTS FOR MIL-C-26482 OR MIL-C-26500 CONNECTOR SHOWN CRIMPED TO ALUMINUM WIRE

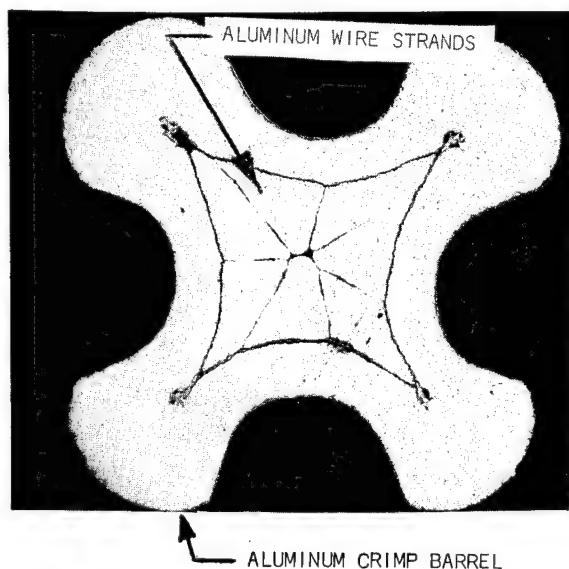


FIG. 4. CROSS SECTION OF CRIMPED ALUMINUM BARREL ON 7 STRAND ALUMINUM 'EEE' #20 GAGE WIRE. NOTE EXTENSIVE DEFORMATION OF EACH STRAND.

References

1. "A Review of the Characteristics and Performance of EEE Aluminum in Laboratory Testing", G. E. Lenaeus, Southwire Company, Non-Ferrous Metals Division meeting of the Wire Association Inc., April 15 - 16, 1970.
2. "Basic Connection Principles, Second Edition", I. F. Matthyse, Burndy Corporation, Norwalk, Connecticut, Publication September 1965.
3. "Fundamentals of Establishing Reliable Connections to Small Gage Aluminum Wire", Dr. S. Garte and I. F. Matthyse, Burndy Corporation, International Wire and Cable Symposium, Atlantic City, New Jersey, December 1970.
4. "Terminating Technique for Small Gage Aluminum Wire", N. R. Suffredini and W. R. Bowden, Burndy Corporation, National Electronic Packaging and Production Conference, New York Coliseum, New York, June 16, 1970.



Michael D. Lazar - Burndy Corporation
Norwalk Conn. 06852

Mr. Lazar is Director of Advance Development of Electronic Products for the Burndy Corporation. He has been with Burndy for 26 years, mostly involved with new connector and electronic packaging development. He is the author of many papers and articles and holds over 50 U.S. and foreign patents on this subject. He received his education at the Cooper Union and New York City University, both in New York City.

HEAT AGING EVALUATION OF
COMMON COATED COPPER CONDUCTORS

by

T. B. McCune
Hudson Wire Company
Ossining, New York

J.H. Burns, G.A. Busch, D.J. Larson, Jr.
Grumman Aerospace Corporation
Bethpage, New York

Introduction

Although there are generally accepted service temperature limits for commonly used conductor coatings, questions are frequently raised as to the performance of the conductor at or near these limits. There is even doubt as to the actual service temperature limit of the most commonly used coated conductor, tinned copper. These questions have become more significant in the last few years with the introduction of insulating materials that satisfy flexibility, durability, strippability, and dielectric criteria, while withstanding service temperatures within and above the range normally allowed the conductors.

Much attention, then, has been given to performance of the insulation in contemporary applications and much effort has been devoted to developing insulating materials to meet the design criteria of these applications. However, designers are now becoming aware of the service temperature limitations of the conductor. Assuming the conductor is capable of withstanding the mechanical and thermal requirements of the insulating process without degradation of the properties necessary for proper termination, and assuming proper installation and termination of the conductor, what can one expect of the performance of the conductor in service? The parameters that are particularly important in contemporary applications are conductivity and flexibility. The degradation of these parameters in service are critical when considering possible variability or discontinuity of electrical transmission. This is particularly true when safety margins for conductors are decreased to save weight, as now being done in the aerospace industry.

The original purpose of this evaluation was to determine the effects of aging at normal elevated service temperatures upon electrical conductivity and mechanical flexibility of commonly used coated conductors. The environment of testing was a circulating air atmosphere at selected temperatures of testing with the assumption that degradation of desired properties occurs in two ways: oxidation of the protective coating at exposed termination points and diffusion or alloying of the coating metal with the base metal. The occurrence of oxidation and diffusion have been generally recognized in the industry, but the effects have never been fully explained.

During the course of the general investigation at Hudson Wire Company, it became evident that tin coated conductors exhibited erratic behaviour at all testing temperatures. Because of production Problems, Grumman Aerospace Corporation had been performing an intensive study of heavily tinned insulated wires to determine causes and effects of the formation of oxides and/or intermetallic compounds.

The purpose of this paper, then, is to describe the effects of heat aging of commonly used coatings with a particular emphasis on tin coated conductors.

Test Procedure

Prior to any testing, a laboratory plan had to be established to determine methods of aging the wire samples. Samples for testing included various sizes of uninsulated solid and stranded wires and insulated stranded wires, including hot tinned copper, electrotinned copper, silver plated copper and nickel plated copper. Included in this test plan were insulated samples of heavily tinned copper stranded wire.

The samples were heat aged in air circulating ovens with calibrated temperature controls. The uninsulated samples were tested at steady state temperatures of 125, 150, 175 and 200°C for a period of at least 2000 hours (twelve weeks). The samples of insulated wire were tested at 150° for 1200 hours, the projected in service operating parameters for which the wire was purchased (in accordance with the governing military specification).

The uninsulated samples were heat aged on small spools. At selected intervals, samples were removed from the spools, the electrical resistance tests were performed, and the remaining material was replaced in the oven. At the end of the 2000 plus hours of the heat aging period, electrical resistance, flexibility, and solderability tests were performed. The insulated samples were heat aged with the ends exposed, so that electrical resistance measurements could be made at selected intervals.

Samples of the heavily tinned insulated wire were removed every 100 hours for metallographic examination and both an x-ray diffraction and electron microprobe analysis. Solderability, electrical

resistance, and bend tests were performed before and after 1200 hour heat aging periods.

X-ray Diffraction Analysis: The x-ray diffraction measurements were made on a Picker Theta-Theta diffractometer with nickel filtered copper radiation. Typical power settings were 36 KV and 16 MA.

The wire samples were held in a specimen holder such that the axis of rotation of the diffractometer was parallel to the axis of the wire and coincident with the outermost surface of the wire. Every effort was made to insure that the x-ray sampled volume was constant and any measureable differences were corrected by normalizing the data with an internal standard. In this fashion, the data may be compared on a relative basis, with a high degree of confidence, but no absolute numbers can be assumed. In order to do this, an external standard must be used, and this was accomplished by utilizing the metallographic data at three time intervals.

Electron Microprobe Analysis: The electron microprobe studies were made using the beam scanning technique. In this operation, an electron beam is electromagnetically deflected across the sample in both the x and y direction. An image of the area being investigated is simultaneously generated on an oscilloscope. The signal that is displayed is generated in the following manner:

First: Some of the high energy incident electrons are backscattered, the number of electrons emitted from any sample being a function of the average atomic number of the area which the beam strikes.

Second: The electrons that are captured by the object being investigated pass through it and are registered as sample current. The amount of current that will pass through any given portion of the sample is a function of its chemistry; that is, the greater the conductivity, the higher the sample current. The image generated by this method will indicate areas of different chemistries.

Third: The incident electrons striking the sample produce x-rays characteristic of the elements present, by interacting with the electronic structure of the individual atoms. The spectrometer and electronics of the microprobe are set up to receive the radiation from a particular element; when a pulse of this radiation is received, it is displayed as a point of light. The higher the percentage of an element in an area, the greater the number of dots and the closer their spacing.

Metallographic Examination: Samples removed from the oven were stripped of their insulation and a layer of copper was electrolytically deposited on the surface of the samples for edge preservation. The samples were then mounted and polished using standard metallographic techniques. Examination of the samples were performed with a Reichert metallograph and measurement of the thickness of any intermetallic phases and the free

tin were made. Five measurements were made on each strand and at least six strands were examined for each time period.

Solderability Test: The solderability tests were performed using two independent methods. Method #1 used on the insulated samples consisted of stripping a two inch piece of insulation from each end of the test specimen. Solid 60/40 solder was used to tin both ends of the test specimen, one end prepared with Type A acidic flux and the other end unprepared. The evaluation consisted of recording the ease with which the solder flowed and the amount of solder coverage.

Method #2 used on the uninsulated samples consisted of performing a standard solder immersion test using both white resin treated and untreated surfaces. The same 60/40 solder was used at a temperature of 475°F with an immersion time of seven seconds. The solderability was judged on the amount of solder coverage.

Flexibility Test: The flexibility test was performed on all uninsulated stranded samples in accordance with the method specified in ASTM B-470. This test consists of cycling the samples over two parallel mandrels causing the specimen to be bent in alternating directions in an arc of 60° on both sides of the vertical centerline until complete failure. The stress placed on the wire during this test was 1500 PSI.

Bend Test: The bend test which was performed on the heavily tinned insulated wire samples consisted of placing the wire in a vise and repeatedly bending 90° in alternating directions until wire failure was recorded. No external stress was placed on the wire during this test.

Electrical Resistance Test: All resistance measurements were made using a standard laboratory Kelvin bridge. However, two methods of contacting the specimens were used. Method #1, used on the uninsulated and insulated samples, consisted of using a normal four point contact fixture. Method #2, used on the heavily tinned insulated samples consisted of using needle point probes firmly inserted into the stranded conductors.

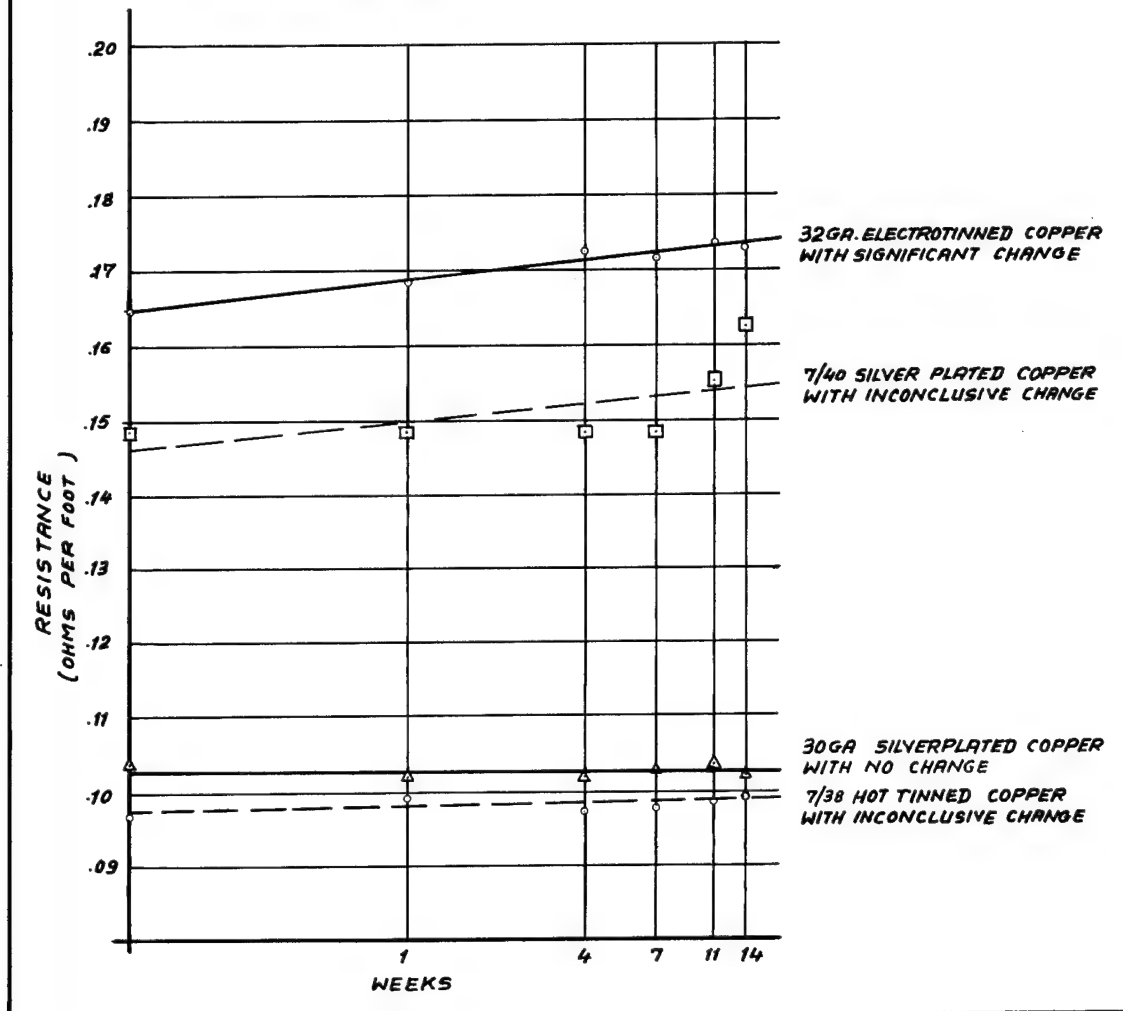
Results

Results of Tests Performed on Uninsulated Wires: The raw data generated by resistance readings from the four temperature testing levels were handled in the following manner:

1. The resistance readings were adjusted to a 68°F (20°C) level (from ambient room temperature) using standard temperature correction factors.
2. The corrected resistances for a given sample were analyzed using a linear regression correlation analysis technique with the basic assumption that the time variable is logarithmic. The concept of a logarithmic time function is common in metallurgical phenomena such as oxidation and diffusion rates. The expression of

FIGURE ONE

COMPARISON OF ACTUAL DATA WITH CALCULATION
RATE OF RESISTANCE CHANGE DURING
HEAT AGING AT 175°C.



resistance change, then, is:

$$R = R_0 + K \log t/t_1$$

where R is the resistance in ohms per foot, R_0 is the initial resistance reading, K is the rate of resistance change in ohms per foot per week, t is the time in weeks, and t_1 is an arbitrary initial time of 0.1 weeks.

In examining the data, it became evident that the first readings of the test represented a fast increase in resistance, with subsequent readings leaving a slower increase, which strengthened the desirability of a logarithmic time function.

In analyzing the results of the correlation analysis, the rate of resistance change was compared with the standard deviation of resistance read-

ings. If the deviation of the readings was too great, the results were judged to be insignificant or inconclusive. In figure 1, examples of true readings are compared with the correlation line. Included are a sample with no change in resistance, a sample with a significant change and two samples with inconclusive results. The 7/40 silver plated copper sample is particularly interesting in that it appears that very rapid deterioration is occurring after eight weeks of testing at 175°C. However, there is insufficient evidence to verify this with the parameters of this analysis.

In Table I, the results of the resistance study are shown for the samples and temperatures listed. Some deletions are noted because of the absence of the sample during that particular test. The table also has some size ranges, rather than a particular size. The deletions and size ranges are due to the

TABLE I

Effect of Heat Aging Upon ResistanceAfter 2000 Hours of Testing

	HEAT AGING TEMPERATURE			
	125°C	150°C	175°C	200°C
Silver Plated Copper				
40-42 Ga.	0	0	11.8%	13.5%
38 Ga.	x	I	I	11.8%
30-32 Ga.	0	0	0	I
27-29 Ga.	0	0.6%	I	0
7/40	0	0	I	5.1%
7/36	0	0	0	I
7/26	0	0	0	0
19/40 Unilay	0	0	0	I
19/36 Unilay	0	0	0	0
19/30 Unilay	0	0	0	0
Nickel Plated Copper				
34-36 Ga.	0	0	0	0
29-32 Ga.	0	0	0	0
25-27 Ga.	0	0	I	1.6%
7/25	0	0	0	0
19/34 & 36	0	0	0	0
Tinned Copper				
38 Ga. Hot	14.2%	4.4%	2.1%	3.8%
36 Ga. Hot	0	2.6%	I	3.3%
32-34 Ga. Hot	1.3%	1.8%	0	2.4%
29-32 Ga. Elec.	x	0.8%	5.3%	4.9%
24-26 Ga. Elec.	I	0	0	0
7/38 Hot	3.8%	0.7%	0	0
7/36 Hot	I	1.4%	0	0
7/36 Elec.	2.4%	x	2.3%	2.0%
19/32-36 Elec.	2.1%	1.2%	0	0
x = no sample I = inconclusive				

availability of recently produced materials. By using recently produced material for each test, the effects of "shelf life" were minimized. The rate of resistance change is expressed in percentage increase for a 2000 hour period. The inconclusive results are so noted so that one can differentiate between no real change and inconclusive change.

In analyzing Table I, the nickel plated copper samples withstand the heat temperatures very well, with only one sample having any increase in resistance. The nickel plated samples had virtually no discoloration after testing at any

temperature.

The silver plated copper samples withstand the heat aging temperatures fairly well, with definite increases in resistance in the finer sizes at 200°C. The samples were slightly tarnished at 125°C and heavily tarnished at higher temperatures. An additional test was performed to evaluate the surface effect of the resistance testing by carefully removing the tarnished layer using fine grit paper, and retesting. The results were that most of the resistance increase is due to the tarnished layer, with the resistance decreasing to within two percent of the original level with the outer

layer removed.

The performance of the tin coated copper samples, both hot tinned and electrotinned, is erratic, with no apparent predictability of performance. The surface of the wire had a yellowish discoloration after aging at 125°C and had a dark gray to black discoloration after aging at higher temperatures. Again, the effect of the surface layer upon electrical resistance testing was evaluated by carefully removing the discolored layer and re-testing. In this case, the resistance would change, but in both directions, with no significant changes noted.

In Table II, the effect of heat aging upon flexibility of the conductor is shown. Flexibility tests were only performed upon 19 strand constructions. The silver or nickel plated conductors did not show significant changes in flexibility. The flexibility of the tin coated conductors was consistently less after heat aging at all temperatures.

In Table III, the effect of heat aging upon solderability is shown for the main groups of samples.

The figures are the percentage of samples that passed the solderability criteria previously explained. The silver plated conductors became increasingly difficult to solder with increasing temperatures, probably due to the degree of tarnishing. The nickel plated conductors were generally difficult to solder, which is usually true without an acidic flux. The tin coated conductors were erratic as to solderability in relation to the method of tinning and to heat aging temperatures.

Results of Tests Performed on Insulated Wires:

The electrical resistance data generated from the samples of the 20 gauge stranded insulated wires, heat aged at 150°C, was evaluated in the same manner as that previously described for the uninsulated samples.

Results of these tests showed that both nickel and silver plated insulated conductors displayed a relatively stable resistance as previously discussed for uninsulated samples. The solderability characteristics of these insulated conductors were also found to be the same as that of the uninsulated samples as shown in Table III.

TABLE II

Effect of Heat Aging Upon Flexibility
on 19 Strand Constructions.

Type	125°C	150°C	175°C	200°C
Silver Plated Conductors	109%	91%	100%	94%
Nickel Plated Conductors	99%	97%	99%	102%
Tin Coated Conductors	70%	71%	70%	85%

Based on unaged flexibility of 100%.

TABLE III

Effect of Heat Aging Upon Solderability
Percentage of Samples Passing Test

Type	Flux*	125°C	150°C	175°C	200°C
Silver Plated Conductors	Without	100%	50%	20%	0%
	With	100%	70%	50%	10%
Nickel Plated Conductors	Without	60%	20%	0%	0%
	With	80%	20%	0%	0%
Hot Tinned Conductors	Without	100%	0%	0%	0%
	With	100%	20%	40%	20%
Electrotinned Conductors	Without	25%	0%	0%	0%
	With	75%	0%	50%	75%

* A standard white resin flux was used.

The tests performed on the insulated tin coated conductors were inconclusive. The resistance measurements on this were performed according to Method #1 explained in the test procedure portion of this paper. No correlation of these measurements could be made.

Results of Tests Performed on the Heavily Tinned Insulated Wire: The purpose of this portion of the analysis was to establish a basis for evaluating the wire. Examination of test sample properties in the as received condition would allow a comparison to be made from subsequent test results. The first step in this portion of the evaluation consisted of an extensive microscopic examination of the wire samples. This examination revealed that most of the samples exhibited a yellowish discoloration on the surface of the tin coating. These samples were then submitted to solderability tests. The wire samples soldered without fluxing did not wet sufficiently to solder easily, but they did solder. When flux was used however, soldering was apparently much easier.

The electron microprobe analysis performed next revealed that a thin, but detectable, oxide content was present on the surface of the tin coating. This was followed by a metallographic examination which revealed a nonuniformity of the tin coating. The nonuniformity was most pronounced on the outermost strands, i.e. those nearest the insulation. The tin layer was thinnest on the side of the wire strands closest to the insulation and thickest in the interstrand region. Figure 2 shows this agglomeration of tin between adjacent strands.



Figure 2: Agglomeration of Tin Between Adjacent Strands.

Also found on the wire during this portion of the analysis was a thin intermetallic sandwiched between the tin coating and the copper conductor. This is expected because the metallurgical basis for obtaining satisfactory tin coatings usually results in a formation of a thin intermetallic. This compound or intermetallic consisted of two layers identified as Cu_6Sn_5 (ζ) and Cu_3Sn (ϵ). The ϵ intermetallic of which there was only a trace was sandwiched between the copper and ζ intermetallic layer. Figure 3 shows the initial percent concentrations of tin and intermetallics.

The resistance measurements performed next revealed that in the as received condition the wire had a resistance of 1.88 ohms per 1000 feet. This test was followed by a bend test which showed the wire capable of withstanding 14 to 18 90° bends before complete rupture. The wire samples were then placed in the air circulating oven and the heat aging tests were begun.

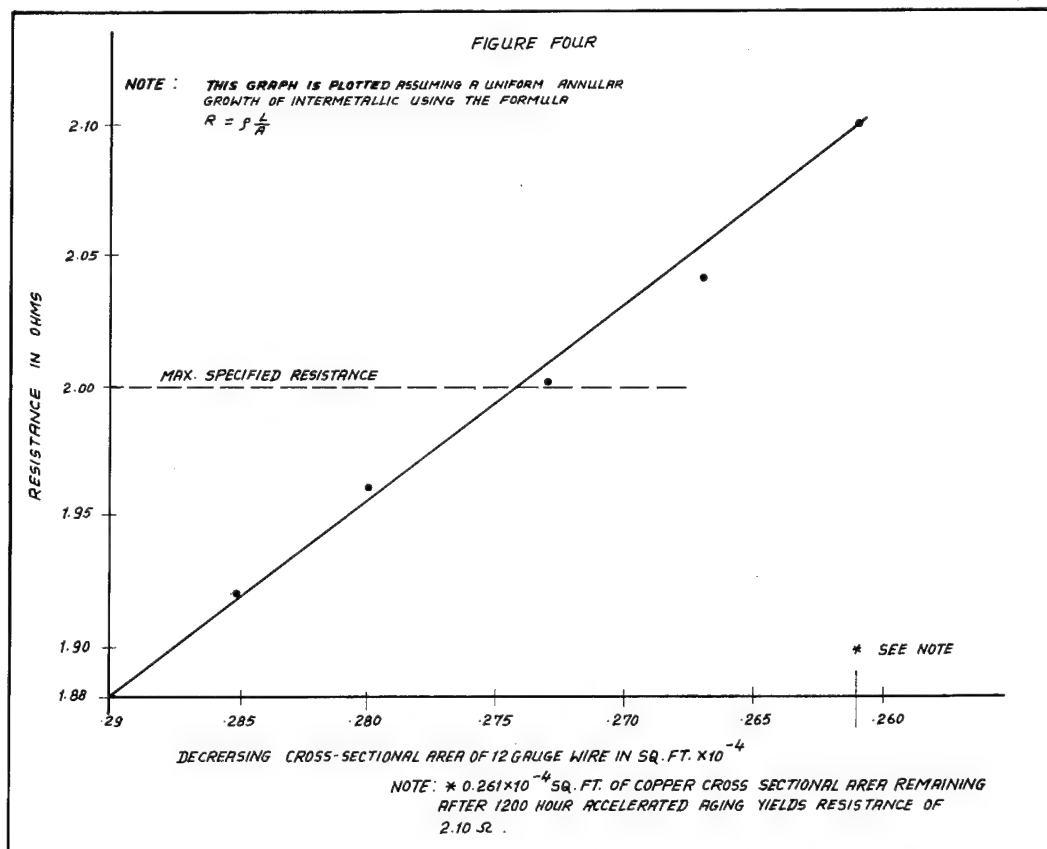
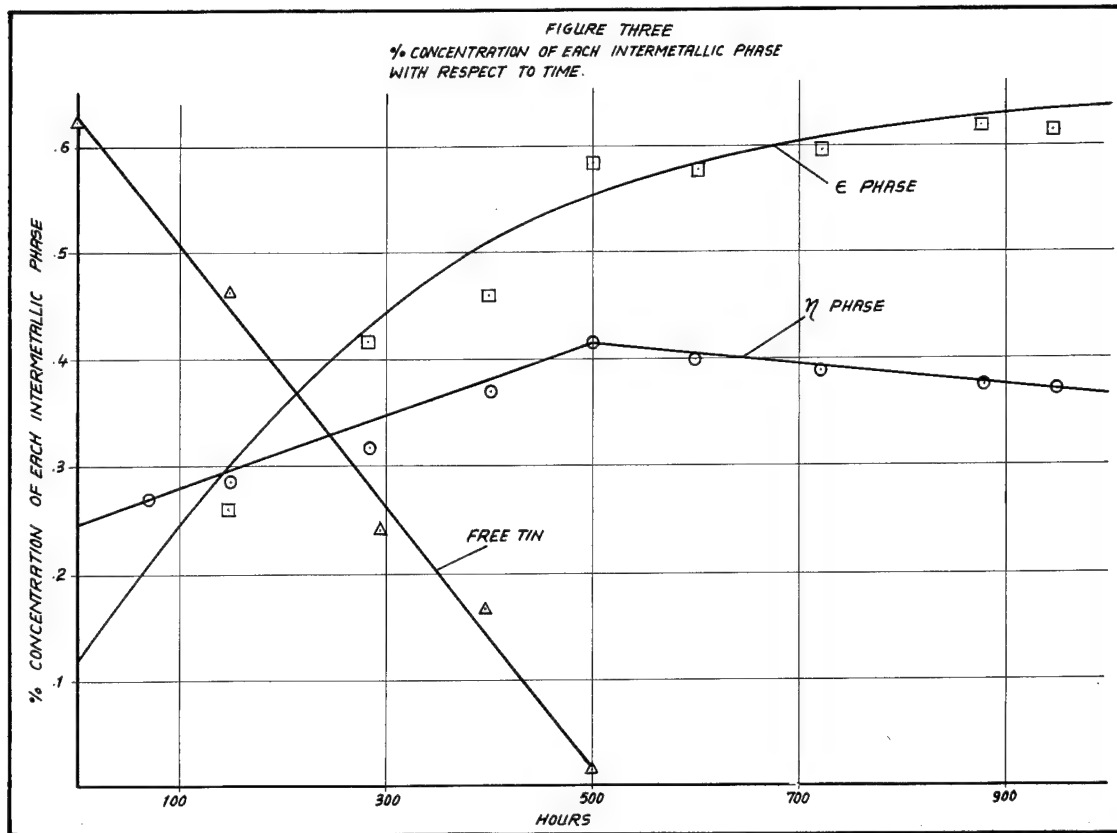
After 300 Hours at 150°C: An optical microscope examination was performed which showed the wire exhibited a very dark yellowish hue in appearance. An attempt to solder these samples revealed that, without prefluxing, soldering was almost an impossibility without overheating and damaging the insulation.

Samples of the aged wire were then submitted to the electron microprobe and x-ray diffraction tests. This analysis revealed no further oxide buildup but it was apparent that an interaction was occurring between the copper conductor and the tin coating. More clearly visible on these samples, were the 5 distinct layers of material. These layers, from the outermost surface, were: oxide, tin, two intermetallics, and copper. Measurements of the intermetallic layers revealed that the total intermetallic had grown at the expense of both the tin and the copper (refer to figure 3.)

Analytical measurements performed at this point revealed the intermetallic had grown, and approximately 0.5 mils of copper was lost from the diameter of each 28 gauge strand of wire in the copper conductor. This is a decrease of 7.55% in the copper cross-sectional area.

After 500 Hours at 150°C: The visual and microscopic analysis performed here revealed the wire had darkened considerably in color. The best description which can be given is to say it was turning dark gray. Solderability tests performed on these samples clearly indicated the necessity of conduct- or pretreatment prior to soldering.

A detailed metallographic analysis was performed on these samples and a precise measurement of the remaining free tin was made. These x-ray diffraction and electron microprobe tests showed there was effectively no free tin remaining on the samples. The ϵ and ζ intermetallic phases had continued to grow at the expense of the copper and tin.



After 1200 Hours at 150°C: After the full heat aging cycle was completed, the remaining samples were removed from the oven. Visual examination of these samples showed them to be black in color and very brittle to the touch. Simple bending caused the wire to emit loud cracking sounds which could be heard at arms length (this was done both with the insulation on the wire and with it removed). Investigations into the properties of the intermetallics formed indicated that they are very brittle and prone to cracking and flaking, i.e. the probable cause of the cracking sound. Soldering as expected was impossible without fluxing.

The x-ray diffraction and electron microprobe analysis performed on these samples revealed that the intermetallic buildup continued to form. (See figure 3). The absence of free tin, however, resulted in a decrease in the rate of the intermetallic growth, since now the governing factor was a non-equilibrium between the two phases of intermetallics (η and ϵ) and the remaining pure copper. Each of these phases containing a different concentration of tin to copper ($\eta = \text{Cu}_6\text{Sn}_5$; $\epsilon = \text{Cu}_3\text{Sn}$) reacted with each other and with a portion of the remaining pure copper.

The effects of the formation of the intermetallic on the resistance of the wire was examined next. Measurements on two specimens after the total 1200 hour heat aging tests revealed the resistance per thousand feet of 12 AWG (37/28) wire was approximately 2.5 ohms. Although this is only 0.5 ohms above the specification limit, it must be pointed out that the initial resistance reading upon receipt was approximately 1.88 ohms per thousand feet. This indicates the resistance increased by

a factor of 33%

It should also be noted here that this higher resistance reading was probably caused by an increase in contact resistance, the higher resistance of the new intermetallic formation and the decrease in cross-sectional area of copper. The change in resistance due to the decrease in cross-sectional area can be calculated to be 2.1 ohms as shown in Figure 4. The difference between the calculated resistance (2.1 ohms) and the measured value (2.5 ohms) can then be attributed to the combined resistance of the intermetallic formation and the contact resistance. While the individual value of each of these resistances cannot be determined, the net effect will be that the resistance due to the intermetallic formation will increase the calculated resistance from figure 4 to somewhat more than the 2.1 ohms. Therefore, the actual value of the measured resistance of the wire will exceed the maximum 2 ohm specification limit after aging.

The properties of the intermetallics were then examined. It was found that the intermetallic was very brittle and prone to cracking. This can be seen in Figure 5 which shows cracks which developed in the intermetallic after accelerated aging. These cracks did not, however, migrate into the copper but appeared to be blunted by the ductile copper.

Samples of the aged wire were then placed in a vise and bent 90°. Referring back to this test as performed on the new unaged wire, it was found that these samples withstood 14 to 18 bends. The same test performed on the aged samples revealed the wire had become embrittled and could only withstand

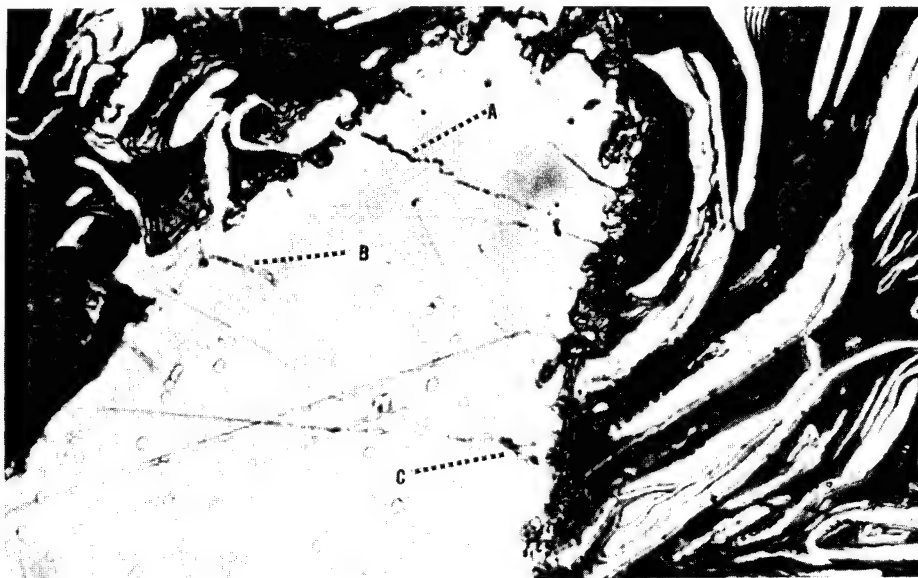


Figure 5: Shows the cracks (labeled A, B & C) which propagated through the intermetallic during normal handling after wire was aged for 1200 hours at 150°C.

3 to 7 bends.

Conclusion

In reviewing the results of the heat aging tests it is apparent that no one plating system performs flawlessly. Nickel, for instance, performed very well with stable electrical resistances at all temperatures tested. The flexibility of this system also remains unchanged throughout the test period. However, nickel surfaces present termination problems, particularly during soldering operations.

Silver, unlike nickel, displayed the best solderability characteristics initially. The effect of heat aging does, however, reduce the soldering characteristics with increasing temperature. Like nickel, the flexibility characteristics were very good after the heat aging period, remaining within 10% of the initial values. The resistance parameter of the silver plating system, unlike nickel, was found to vary. The resistance of the finer gauge wires became questionable at temperatures approaching 200°C. This resistance increase was shown to be caused by a surface chemical reaction, which could be easily removed resulting in the resistance returning to within 2% of original level. This surface film was also shown to be the cause of the solderability degradation.

The tin coating system, unlike nickel and silver, displayed during initial tests, numerous inconclusive performance characteristics at elevated temperatures. Flexibility, for instance, was found to decrease moderately on all samples, while solderability tests proved inconsistent. The resistance characteristics also showed no correlation to time parameters. This behaviour resulted in the more detailed analysis.

It was found that when heavily tinned copper wire was exposed to elevated temperatures, a metallurgical change consisted of the formation of two intermetallic compounds, Cu_6Sn_5 and Cu_3Sn . These compounds were formed at the expense of the tin coating and the copper conductor.

Results of the tests performed on the heavily tinned conductors revealed that, after 500 hours of heat aging at 150°C, no free tin remained on the conductor. The growth of the intermetallics continued throughout the 1200 hour heat aging period, resulting in a 10% loss in the cross-sectional area of the copper conductor. The combined effects of this copper loss, coupled with the growth of the intermetallic, resulted in a 33% increase in the effective resistance of the 12 gauge wire. Also, the brittleness of the intermetallic compounds was found to reduce the ability of the conductor to withstand severe bending by more than 50%.

The concept of a decreasing cross-sectional area as mentioned above, can be projected to occur in any tin coated copper system, being most severe on the finer gauge conductors where the tin to copper ratio is larger. This could result in the necessity of using larger gauge wires in areas where the resistance and conductance parameters are critical, thus defeating any attempts to save weight by using finer gauge wires. The effects of the intermetallic formation in the tin-copper system could also seriously affect the in service operation of the wire, especially in modern aerospace applications. When using a tin copper system at elevated temperatures, problems could develop under in service repair conditions. For instance:

1. The application of a crimp contact could result in a significant voltage drop through the intermetallic layers.
2. The application of solder is severely hampered.
3. Simple handling during repair conditions could result in wire fracturing.

As can be seen from the findings described in this paper, the cliché "We've been using it for years" can no longer be effectively applied to a choice of conducting systems, particularly in view of contemporary applications. Certainly, each user must perform his own evaluation prior to making a choice of which conducting system best fits his needs.

Thomas B. McCune - Manager of Product Engineering
(Speaker)
Conductors and Alloys
Hudson Wire Company
Ossining, New York 10562



Mr. McCune has been with Hudson Wire Company for two years. Prior to that he was a Senior Engineer in the Research and Engineering Laboratories of the Parts Division of Sylvania Electric Products, Inc., in Warren, Pennsylvania, where he was employed for seven years.

Mr. McCune was educated at Lehigh University in Bethlehem, Pennsylvania, where he earned a Bachelor of Arts, a Bachelor of Science in Metallurgical Engineering, and a Masters in Business Administration.

ELECTRO TIN PLATING OF COPPER WIRE - WHEN? "BEFORE OR AFTER" WIRE DRAW

P. E. Lawler
Western Electric Company
Omaha, Nebraska
L. N. McKenna
Western Electric Company
Buffalo, New York

A comparison is presented of the merits and disadvantages based upon production experiences of two types of Electro Tin Plating facilities for copper wire production insulating lines.

In 1962, a paper of "New Developments in the Manufacture of Communication Cable at Omaha" was presented to the 11th Symposium by a number of our colleagues. At that time, the subject of tinning methods was being studied. Since operating results have clearly shown an economically sound manufacturing environment, we now feel a report of the merits and disadvantages of two types of Electro Tin Plating facilities might be of informational value to the wire and cable industry.

The objective of this paper will be to present a brief resume of experiences of two Western Electric Cable Manufacturing Plants with two methods of electro tin plating of copper wire used in vinyl insulated wire products. The two methods are referred to as the Tin Before Wire Draw and the Tin After Wire Draw.

Both types of plating are accomplished on Tandem Vinyl Wire Insulating line facilities in a continuous operation with wire drawing, annealing, and plastic extrusion.

The Western Electric Cable Plants at Omaha, Nebraska and Buffalo, New York have used both methods of tinning. It is well known that both tin plating techniques are in use at many wire manufacturing plants and certainly a discussion of the merits of each process can include a variety of opinions.

Wire Insulating Line Process

In order that a suitable reference and comparison between tinning methods in the wire insulating processes can be understood, a brief description of each of the wire insulating line processes is presented. The tandem order of the machine components noted as the wire travels from left to right through the two processes is shown below:

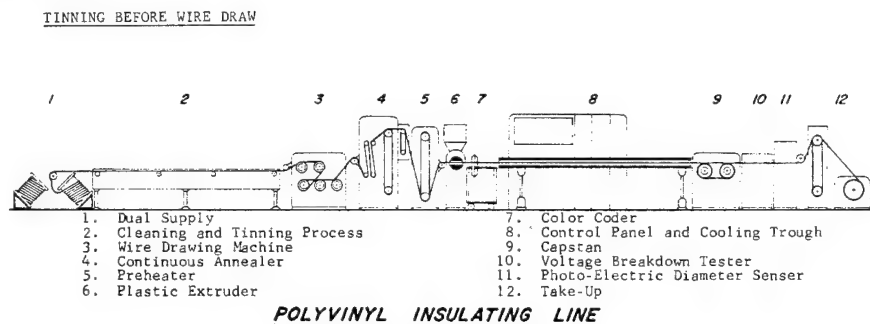


Figure 1

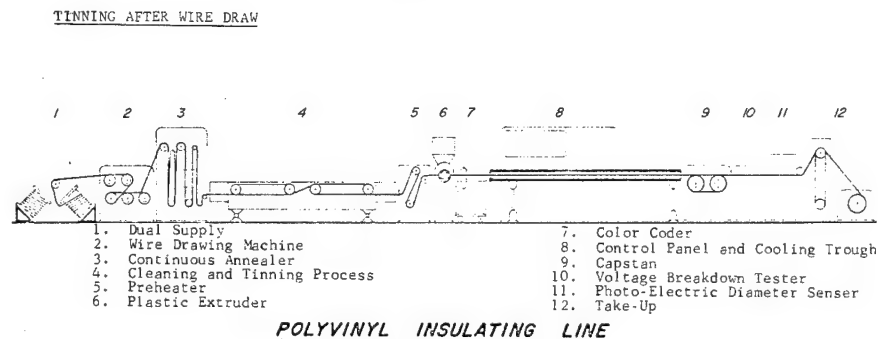


Figure 2

In Figure 1, 14 gage wire passes from the supply reel (position 1) through an alkali cleaning tank where it is cleaned of wire drawing compound residue, then through water rinses and into the plating tank (position 2) for the electro tinning of the copper wire. (Tin coating on copper wire is used on certain vinyl insulated communication cable codes to provide improved shelf life for conductor solderability and to assure electrical stability of solderless wrapped connections). After the tinning operation, the wire is drawn (position 3) to the finish AWG sizes 20, 22, 24, or 26. The wire must then be annealed in the annealer (position 4) to remove the hardness which has developed through the wire drawing operation. After preheating (position 5) the wire is ready for plastic insulation at (position 6) the plastic extruder, which applies the jacket to the wire. The hot insulated wire is then color code marked (position 7) and advances into the water cooling trough (position 8). The water in the trough solidifies the insulation before it gets to the wet capstan (position 9). The wet capstan is electrically locked to the wire draw and pulls the wire through the process. From this point, the wire is dynamically tested (position 10) for insulation breakdown and then spooled on the continuous take-up (position 12).

When Figure 2 is compared with Figure 1, it is evident that from the plastic extruder (position 6) on, both processes are alike. In Figure 2, however, the wire draw and annealer are before the cleaning and tinning process rather than after, hence the process names of Tin Before Draw Figure 1 and Tin After Draw Figure 2.

Tin Plating Facility

The tin plating facilities for the two tinning processes are very different. The schematics Figure 3 and Figure 4 show these differences.

BEFORE WIRE DRAW PLATING

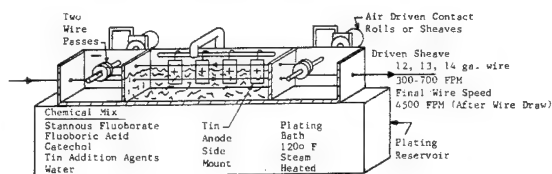


Figure 3

AFTER WIRE DRAW PLATING

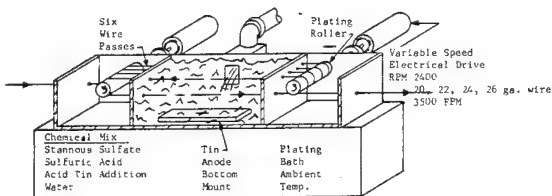


Figure 4

A number of points of particular differentiation and importance in the two types of plating tanks are:

1. The Plating Bath used in the Tin Before Draw process is Stannous Fluoborate while the bath used in the Tin After Draw process is Stannous Sulfate.
2. The wire conductor gage size is 14 gage, Figure 3 versus 22, 24, or 26 gage (Figure 4).
3. The wire speed through the bath is 300-700 FPM (Figure 3) versus approximately 3500 FPM (Figure 4).
4. The number of wire passes is two in Figure 3 and six in Figure 4.
5. In Figure 3 the electrical contact rolls are air driven versus a variable speed electrical drive in Figure 4.
6. The temperature of 1200° F for the Tin Before Draw Bath, Figure 3, versus ambient room temperature for the Tin After Draw Bath, Figure 4.

The above points of difference in the plating baths and the respective bath positions relative to the wire drawing and annealing operation are responsible for the merits and disadvantages of the two tinning processes.

Operation Experience
Advantages of Tin Before Draw Plating Versus Tin After Draw

Tin Before Draw

1. Less Wire Breaks

Data reflects negligible or no breaks per million conductor feet wire produced (chargeable to the tinner with 14 gage wire).

2. Less Line Capacity Loss/Wire Break

By measurement .12 hours are lost per wire break. This is the time required to restring the line if a wire break occurs in the supply position with two passes of wire.

3. Higher Line Speeds

Higher line speeds are possible because of the higher current density capability and slower wire speeds in the plating sections before wire drawing. The availability of higher current density (2,000 amp/sq. ft.) allows for shorter tank lengths and/or less wire passes.

4. Less Wire Tension Control Problems

Since 14 gage wire is run through the plating tank the wire can be used to actually pull the contact rollers if necessary. Therefore, tension control is not a problem. However, it usually is necessary to apply back tension to straighten large diameter wire.

5. Better Bath Chemical Solubility

Stannous Fluoborate has a high electrical conductivity and is very soluble in the plating solution. These properties combined with the High Current Density Capability (previous Item 3) account for the high plating efficiency of 98%.

6. Better Future Outlook For Tin Lead Plating

Tin lead (60-40) plating of copper wire for improved solderability and shelf life is possible with the Tin Fluoborate equipment.

Tin After Draw

Data shows .08 breaks per million conductor feet of wire produced (chargeable to the tinner with 24 gage wire).

By measurement .29 hours are lost per wire break. This is the time required to restring the line when a wire break occurs in the tinner with six passes of wire.

Because of the limiting current densities of the stannous sulphate bath (800-900 amp/sq. ft.) increase in wire speeds will require more wire passes and/or longer plating tank lengths. Mechanically, wire speeds in excess of 3500 ft/min. present some difficulties in synchronizing the contact rolls with the fragile 22, 24, and 26 AWG wires.

Since the wire is tin plated in the finish wire 22, 24, or 26 gage, the wire tension must be closely controlled or the wire will break. This requires close attention by the line operators and electricians.

Stannous Sulfate requires considerable mixing effort with other plating materials because it is not readily soluble. This, in turn with lower conductivity, lowers the plating bath efficiency to an 80% level.

Advantages of Tin After Draw Plating Versus Tin Before Draw

Tin After Draw

1. Chemical Bath Cost Are Less

Lower chemical concentrations permit the sulfate bath to operate with a chemical cost 1/5 that currently used for the fluoborate bath.

2. Lower Facility Maintenance Cost

The severity of corrosive attack of the bath chemicals on pumps, tanks, rollers, etc., is less than that of the fluoborate bath.

Tin Before Draw

Bath chemical costs are higher because of the initial bath make-up concentrations and higher chemical ingredient costs.

Recent development of engineered plastic components, with strengths approximating that of metal, have eliminated tank corrosion. Also, certain metals, ceramics and corrosion inhibitors have been developed that make wear parts serviceable for much longer periods than materials used in older designs.

Tin After Draw

3. Lower Tin Cost On Certain Wire Coatings

On wires requiring light coatings (2 MSI) the tin copper alloy formed is very small and the light weight tin metal coatings (16 millionths thick) will cost about one third less than with the Tin Before Draw method. However, if this wire is not used within a 4-6 month period the free tin will be tied up as copper tin alloy and this adversely affects wire solderability.

4. No Contamination of Wire Draw Solution

Since the wire does not pass through the wire tin plating tank before it is drawn to finish gage size there is no chance for the moving wire to contaminate the wire draw compound. Airwipes must be in good condition and properly adjusted to prevent solution drag out losses.

5. Less Wire Draw Capstan Care

Ball bearing steel wire draw capstans are satisfactory and can be re-cut to new size after wear grooves appear.

6. Less Operator Attention To Tin Coat Quality

After the wire exits the plating tank, it has little chance to incur tin coating damage or scoring.

Tin Before Draw

On wires requiring heavy tin coatings 6 MSI or greater, it is a matter of consideration as to when the tin copper alloy is formed, either at the time of manufacture (Tin Before Draw) or in storage (Tin After Draw). The final tin copper alloy will be about the same for the two processes after long aging periods and in many cases the customer use time. The total amount of tin plated will, therefore, be approximately the same.

If the tinned wire is not free of all tin plating residues before it goes into the wire draw, it will contaminate the wire draw lubricant and destroy lubricity which will result in wire breaks in the draw. Extreme care must be exercised that all wire wipes are in good order and working properly.

Chrome plated or ceramic wire draw capstans are required. The initial cost of these is high and the surfaces and/or capstans are fragile. Care must be exercised in their use and maintenance.

If care is not exercised in the tin before draw lines with respect to strand annealer heat settings and in the maintenance of the wire drawing capstans and wire drawing dies, there will be excessive tin-copper alloy formed and copper streaking in the tin plated wire product.

Tin Coating Quality

It should be noted that when correctly applied the tin coatings of both processes should be of approximately equal quality and no great difference should be expected in the end use of the tinned copper wire products. Both tinning methods are good processes with each having its own special advantages and each possessing certain disadvantages.

Generally speaking the Tin Before Draw process as applied to tandem plastic wire extrusion allows higher insulating line speeds of 4500 ft./min. with heavy tin coating capability. The Tin After Draw tinning adapts itself more readily to the medium gage sizes of 22 to 26 at wire speeds of 3500 ft./min. and tin deposits of six milligrams per square inch.

Further developments for both types of tinning methods are being considered by Western Electric. One interesting application will be the use of the stannous fluoborate solution for the Tin After Draw process. This will require the use of the previously mentioned corrosion resistant materials for plating equipment construction. It is expected that the benefits inherent to the stannous fluoborate bath will apply to the Tin After Draw process.

Another version of the Tin Before Draw method is the use of a central plating installation. At this installation 12-14 gage supply wire would be tin plated on one or two large electro tinning units. Then the large supply packages of tinned wire would be fed to the wire drawing and extrusion lines.

My colleagues and I appreciate the opportunity of highlighting our tinning experiences using both tinning techniques. We submit them for your consideration for a better understanding of Electro Tin Plating of Copper Wire Processes.

Acknowledgements

The authors would like to acknowledge the valuable contributions to this paper by D. F. Metzen of Western Electric Company, Buffalo, New York.

P. E. Lawler - Western Electric Co., Omaha Works
(Speaker) P. O. Box 14000 W. Omaha Station
Omaha, Nebraska 68114



Philip E. Lawler is a Senior Engineer with the Western Electric Company at Omaha, Nebraska. Since joining Western Electric in 1957, he has worked in the Wire and Cable Plant in the wire drawing annealing and wire insulating areas. He is presently engaged in process and product engineering in the tandem wire insulating line area for vinyl insulated wire products. He received his Bachelor of Science Degree in General Engineering from the South Dakota School of Mines and Technology in 1947 and a Masters Degree in Business Administration in 1968 from Creighton University. He is a registered Nebraska Professional Engineer and a member of the Wire Association.

NEW ITALIAN TYPES OF CABLES FOR PCM AND FDM TRANSMISSION

by S. Longoni, P. Calzolari, A. Portinari of Pirelli S.p.A., Milan, Italy.

SUMMARY

A broad application has recently been found in Italy for two new types of telephone cables. The first type, with small coaxial pairs, has been designed for PCM transmission; the second one, with polyethylene insulated quads, has been developed for FDM transmission. However, due to their characteristics, both cables could be used for PCM and FDM transmission as well.

Electrical and mechanical characteristics, manufacturing process sequence and some installations for these types of cables are outlined in this paper.

INTRODUCTION

The ever growing demand for telephone communications and data transmission in Italy, has enhanced the need for cables of good quality performances and designed to carry the very highest number of simultaneous calls, while still providing a possible economical advantage.

The results so far achieved have also been made possible by the continuous improvement of the available equipment.

In view of the progresses foreseen in Italy in the field of FDM and PCM system transmission, the cables hereinafter described have been developed. They have been designed for a distance in the range of some tens of kilometers.

Their use can be subject of further and interesting developments.

COAXIAL PAIR CABLES FOR PCM TRANSMISSION

Description of the cable.

The coaxial pair cable has been designed to provide an economical carrier capable of transmitting PCM signals at a sufficiently high speed; due to its transmission characteristics it is also suitable for FDM signals.

The coaxial pair used, when compared with those standardized by the C.C.I.T.T. (see

Livre Bleu, Avis G334 and Avis G342), has reduced dimensions, approximately half those of the 1.2/4.4 mm coaxial pair. It is made of a 0.65 mm diameter cellular polyethylene insulated inner copper conductor and of a 0.1 mm thick outer copper tape conductor, longitudinally applied with overlapped edges as to form a tube having an inner diameter of 2.8 mm.

In order to limit the influence of cross-talk at low frequencies, the outer conductor is screened with a 0.1 mm thick steel tape, longitudinally applied with overlapped edges.

The application of the copper and steel tapes is carried out in tandem with an outer lapping, made with paper or synthetic tapes.

Cables with this type of coaxial pair are of current production in Italy and consist of several coaxial pairs, up to a maximum of 60, laid up in concentric layers or in units.

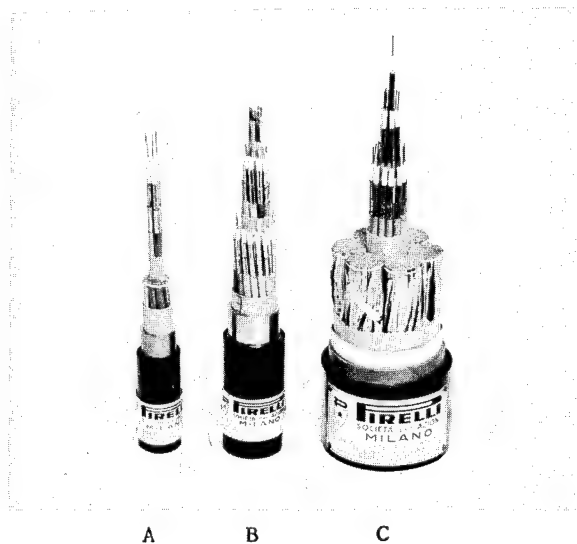


Fig. 1 - A) Cable with 10 coaxial pairs plus 2 star quads. B) Cable with 24 coaxial pairs plus 3 star quads. C) Cable with 20 coaxial pairs plus 222 multiple twins.

The standard sizes are 10, 12, 24, 36 and 48 coaxial pairs, those of 12 and 24 being the most commonly used. In the latter case

the make-up is generally concentric, while for cables with 36 or 48 coaxial pairs a unit make-up, composed of 6 coaxial pairs each, is to be preferred for mechanical reasons (handling and bending characteristics).

A homogeneous make-up is usually adopted for these cables with the addition of few alarm and/or service symmetric circuits.

The reduced outer diameter of the coaxial pair allows to obtain cables having rather small overall diameters; for instance, for a cable with 24 coaxial pairs and 3 service 0.9 mm quads the diameter over the laid up core is approx. 24 mm.

The dimensions of the coaxial pair are comparable to those of the multiple twin and the star quad as used in local and trunk cables (for example the 0.7 mm multiple twin, 38.5 nF/km capacitance, and the 0.9 mm star quad, 45 nF/km capacitance). This makes possible in cables with symmetric circuits to substitute some of these circuits with the described coaxial pairs without affecting the basic make-up of the cable.

As an example of this application, a cable consisting of 222 multiple twins 0.7 mm around a central core of coaxial pairs is shown in Fig. 1.

No. of 0.65/2.8 mm coaxial pairs	No. of service quads	Overall dia- meters (*) mm
10 (concentric)	2	20
12 (concentric)	5	26
24 (concentric)	3	32
36 (unit)	5	46
48 (unit)	5	50
Shipping lengths 500 m.		
(*) Approx. diameters for lead and polyethylene sheathed cables.		

Table 1 - Coaxial pair cables: standardized make-ups and overall diameters.

The protection of the coaxial cables consists of an extruded lead alloy or aluminium sheath and of a thermoplastic over-sheath.

The insulation between the core and the

metallic sheath is generally made of a paper tape lapping, capable of withstanding a 2000 V a.c. voltage test on finished cable lengths.

The standardized make-ups and the overall diameters are listed in Table 1.

Electrical characteristics of the cable

Up-to-date, cable lengths ranging from 200 to 500 m have been manufactured. On these finished cable lengths, a pulse echo test at 0.05 usec pulses was carried out in addition to the usual electrical measurements at low frequency (e.g. conductor ohmic resistance, capacitance, insulation resistance, voltage tests).

The corona level was also measured on the coaxial pairs.

Ohmic resistance at 20°C (av. values):	
- inner conductor	: 55 ohm/km
- outer conductor	: 15 ohm/km
Capacitance (av. value)	: 55 nF/km
Dielectric strength (d.c. voltage)	: 1500 V
Corona level at 50 Hz	: 1000 V

Table 2 - 0.65/2.8 mm coaxial pair : electrical characteristics.

Frequency kHz	Cross-talk worst value (dB)	
	near-end	equal-level far-end
60	80	70
250	110	100
500	120	110
1000	>120	>120

Table 3 - Coaxial pair cables: cross-talk worst values as a function of frequency (length 4000 m).

On some 4000 m cable sections, the attenuation versus frequency was determined and cross-talk measurements were car-

ried out at 60, 250, 500, 1000 kHz.

The results currently obtained on these cables are listed in Table 2 and 3 and plotted in diagrams 1, 2 and 3.

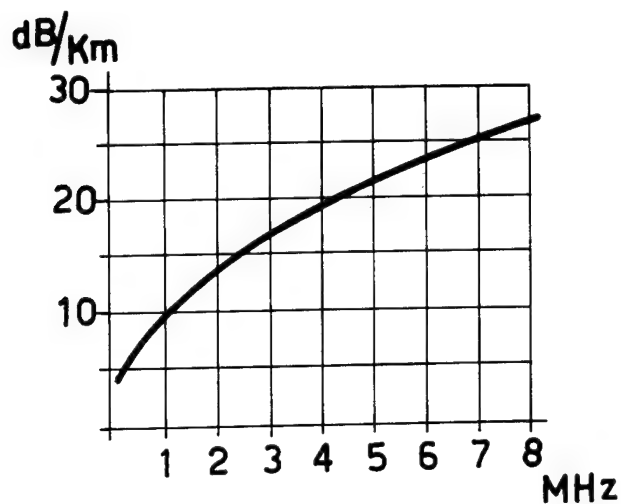


Diagram 1 - 0.65/2.8 mm coaxial pair: attenuation versus frequency (at 10°C).

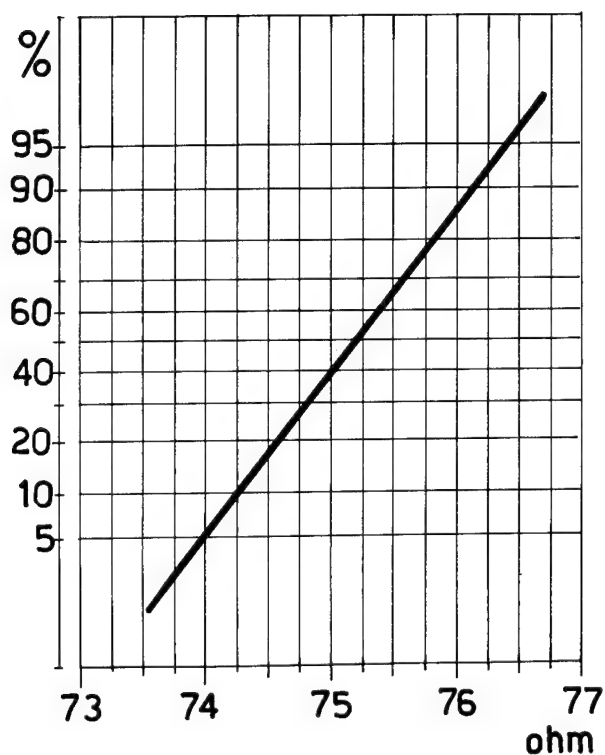


Diagram 2 - 0.65/2.8 mm coaxial pair : pulse-echo impedance distribution (0.05 usec pulse).

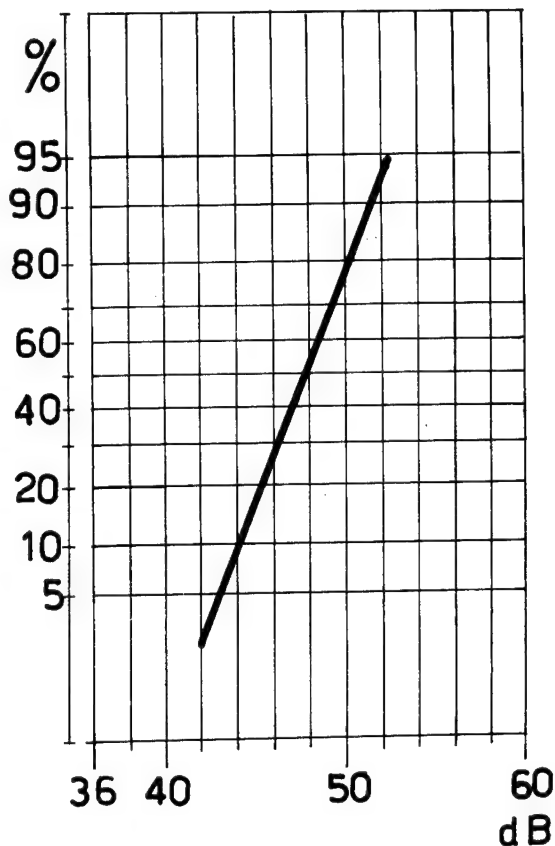


Diagram 3 - 0.65/2.8 mm coaxial pair: distribution of the pulse-echo worst values with distance correction (0.05 usec pulse)

Manufacturing line

The manufacturing line of these cables consists of the cellular polyethylene insulating line (Fig. 2), the coaxial pair forming line, the stranding machine (Fig. 3) and the conventional machinery for the application of the outer protective coverings.

Considerable work was done in solving the main problems of the setting up of the insulating line, associated with the temperature stabilization in the extruder heating areas and with the automatic control of the insulation diameter.

Special attention was paid to the capacitance of the cellular polyethylene insulated core and by improving the extrusion

conditions uniform values of capacitance were achieved.

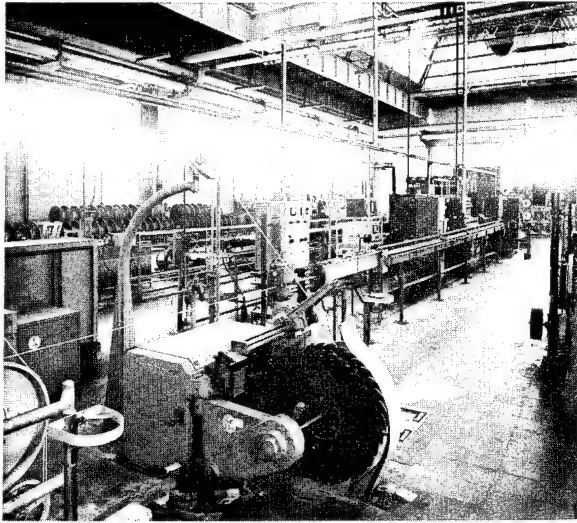


Fig. 2 - Cellular polyethylene core insulating line.

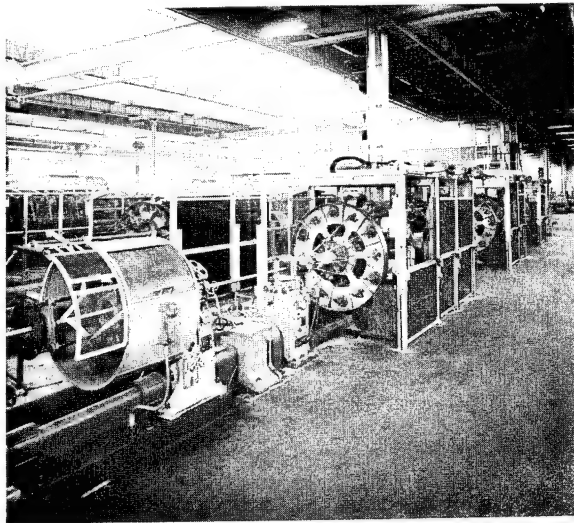


Fig. 3 - Stranding machine with 37 floating cradles.

The coaxial pair line includes the two forming tools for the application of the outer conductor and screen and the paper tape lapping head. Great care was given to the accurate setting up of the forming tools and of the paper tape lapping head,

in order to minimize impedance variations due to secondary effects (outer conductor slackening, ovalization, and so on).

The laying up of the coaxial pairs was carried out using a conventional laying up machine, suitably arranged for this process, and having 37 parallel floating cradles.

Performances

The coaxial pair above described has been designed to carry 120 PCM channels at a maximum frequency of 8 Mbit/sec, with regenerative repeaters every 4 km. With regenerative repeaters every 2 km only, it is possible to carry four times this number of channels.

The uniformity of the impedance and the good values of cross-talk at frequencies above 60 kHz, ensured by the screening as above described, let foresee the possibility of extending the use of these cables also to FDM transmission, for links of rather small length (approx. some tens of kilometers).

The exploitation of this cable has been made possible because of its low manufacturing cost; as a matter of fact, the cost of a single 0.65/2.8 mm coaxial pair does not considerably differ from that of the conventional circuits used in trunk cables, namely in Italy the paper insulated 0.9 mm multiple twin having capacitance 38.5 or 35 nF/km.

The saving is much more emphasized when this basic cost is compared with that of the 1.2/4.4 mm coaxial pair when used in systems with 120 to 480 channels, due to the very high electrical characteristics and consequent high cost of this pair.

QUAD CABLES FOR FDM TRANSMISSION

Description of the cable

This second type of cable consists of symmetric circuits with polyethylene insulated quads, 0.9 mm copper conductor. Each quad is bound with a synthetic tape; all the quads are laid up in concentric make-ups.

The cable identification code is as follows: white and red coloured insulation for the pairs in each quad; numbered binders for the quads.

The cable has an inner sheath of low melt flow index polyethylene (less than 0.3), a longitudinally applied 0.3 mm thick corrugated steel screen, protected by a special bituminous compound, and a polyethylene oversheath with at least a 2% carbon black content.

The standardized make-ups consist of 5 or 10 quads, but larger sizes up to 19 quads may also be manufactured.

A polyethylene insulated service quad is fitted into the interstices. The insulation of one of the two pairs of this quad is perforated as to provide an alarm circuit in case of water entering the cable.

In order to check the correct functioning of the alarm pair, a test is carried out in which the insulation resistance is measured after a given time interval, the alarm circuit being immersed in a few centimeters of water.

Other types of cables, consisting of 4 or 8 units of 5 quads each, have recently been developed and manufactured for the simultaneous transmission of 60 channels supergroups, i.e. for a total of 2400 channels.

Each unit is polyethylene sheathed and copper or aluminium tape screened and then lapped with a plastic tape, as to ensure the insulation among screens. After the laying up of the units, a lead alloy and/or a thermoplastic oversheath are applied.

No. of quads	No. of service quads	Overall diameters mm
5 (concentric)	1	20 (*)
10 (concentric)	1	30 (*)
20 (unit)	at least 1	52 (**)
40 (unit)	at least 1	70 (**)

Shipping lengths 500 m.

(*) Approx. diameters of double polyethylene sheathed cables with an interposed longitudinal steel screen.

(**) Approx. diameters of lead and polyethylene sheathed cables.

Table 4 - Quad cables: standardized make-ups and overall diameters.

Some types of the above described cables are shown in Fig. 4 and their standardized sizes and relevant overall diameters are listed in Table 4.

Electrical characteristics of the cable

Cable lengths of current production are usually 500 and 1000 m long for the concentric type, whereas for unit cables lengths may be shorter.

In addition to the usual electrical measurements at low frequency, which are performed on the finished cable lengths (conductor ohmic resistance, mutual capacitance, capacitance unbalances), cross-talk measurements at a frequency of 110 kHz are also made.

The electrical characteristics of the star quads of this cable are listed in Table 5,

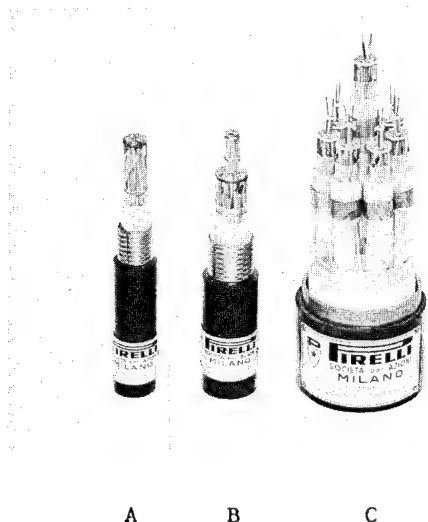


Fig. 4 - A) Concentric cable with 5 star quads.

B) Concentric cable with 10 star quads.

C) Unit cable with 40 star quads.

- Conductor ohmic resistance at 20°C	: 28.4 ohm/km (maximum)
- Core mutual capacitance at 800 Hz	: 35 nF/km (average)
- Conductor insulation resistance	: 15,000 Mohm per km (minimum)
- Near-end cross-talk attenuation at 110 kHz	: 65 dB (minimum)
- Equal-level far-end cross-talk attenuation at 110 kHz *	
100% values	: 70 dB (minimum)
90% values	: 78 dB (minimum)

* For lengths of 500 M

Table 5 - Electrical characteristics of the 0.9 mm copper conductor star quads (values derived from present Italian specifications).

together with the cross-talk limits prescribed by the present Italian specifications.

The values of cross-talk on cables of current production generally exceed the limits by approx. 5 dB.

In diagram 4 the attenuation versus frequency curves are plotted.

The near-end cross-talk attenuation between circuits of the different units was measured at 200, 400 and 600 kHz on some cable sections of approx. 700 m.

The results obtained are plotted in diagram 5.

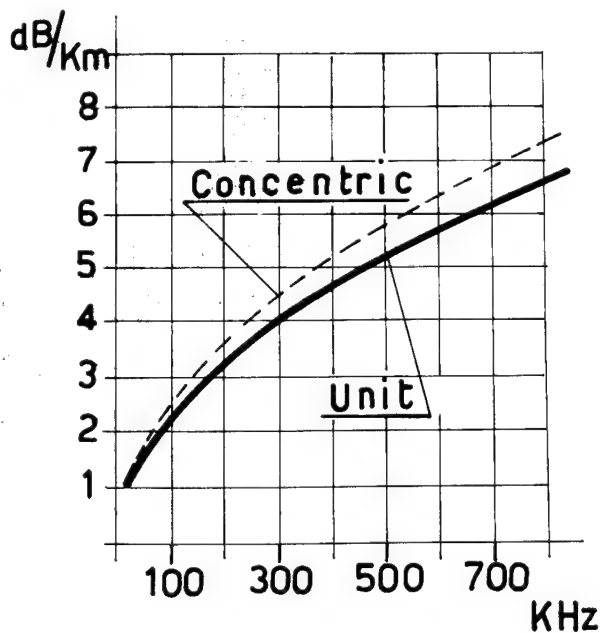


Diagram 4 - Star quad cables: attenuation versus frequency (at 10°C).

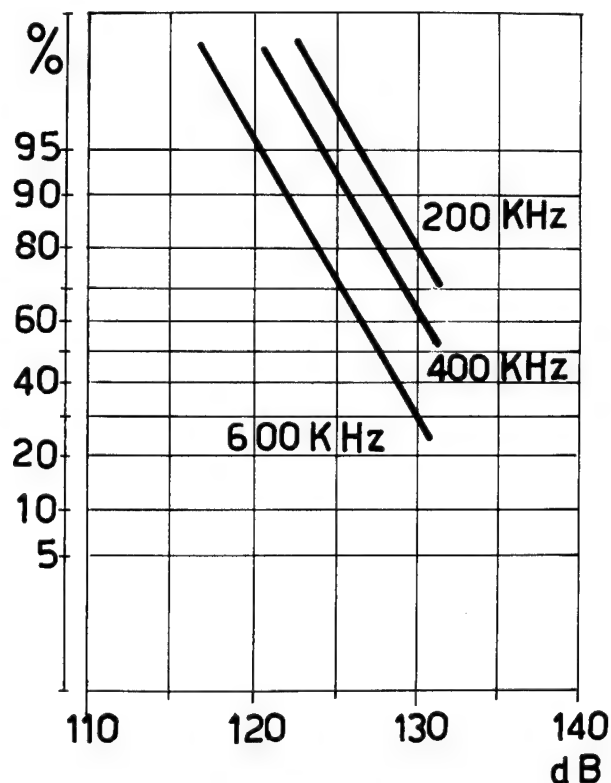


Diagram 5 - Unit quad cables: distribution of the near-end cross-talk attenuation between circuits of the different units (length 700 m).

Manufacturing line

In addition to the conventional machinery for the solid polyethylene insulation, laying up and covering, the manufacturing line of these cables includes special quadding machines and the line for the longitudinal application of the corrugated steel screen.

The floating cradles quadding machines provide a large number of lays, as requested to match the theoretical quadding lays determined for every make-up by means of a particular calculation process.

The line for the longitudinal application of the corrugated steel screen is in tandem with the line for the application of the outer thermoplastic sheath, the two lines being shown in Fig. 5

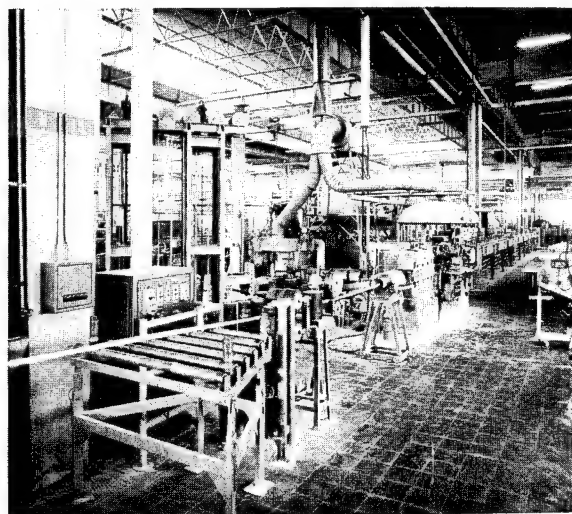


Fig. 5 - Corrugated steel screen and thermoplastic sheath application lines.

The sequence of the process is as follows: the corrugated tape is fed into the forming tool which shapes it to a tube with overlapped edges (overlapping of 5 to 10 mm); then a special bituminous compound, having anticorrosive and mechanical protection action, is applied and followed by a thermoplastic oversheath.

The corrugation profile of the steel tape has pitch of 2.5 mm and overall depth of 1 mm.

Performances

The concentric type cables have found broad application in Italy in the field of H.F. transmission, for aerial as well as for underground installations, owing to their good electrical characteristics, lightness and high mechanical resistance.

In these cables the cross-talk average values are so good that the balance adjustment is considerably facilitated and the adoption of terminating equipments is also simplified.

In addition, the excellent dielectric strength values measured between conductors and screen (the strength measured on cable sample is higher than 30 kV, breakdown occurring at 50 to 60 kV) allow a large application of this cable also in networks where a probable damage due to high induced voltages is to be feared, such as in aerial networks in parallel with high voltage power connections and links which must withstand lightning high voltages.

These cables have also been successfully used in links requiring d.c. or a.c. signals and telephone transmission, as for example along railways, oil and gas pipelines.

The steel screen gives the cable an effective longitudinal and radial mechanical protection which makes the laying operations easier (no rotation, slight elongation even with an applied load of some hundreds of kilograms) and reduces the possibility that the cable might be mechanically damaged, e.g. by hunter's shots, rodents' attack, squeezing due to roots of trees, and so on.

The screen, having a low mutual impedance value, provides also a good protection against noises at high frequencies; for instance, a considerable reduction of the noises caused by radiobroadcasting stations situated near the cable can be obtained.

The cables of the concentric type, are currently used in conventional systems with 12 + 12 channels (max. frequency 110 kHz); successful results have also been achieved by recent applications in bi-directional systems handling 48 + 48 channels (max. frequency 552 kHz).

It should be noted that networks including these cables may be gas pressurized.

Unit cables are generally used for H.F. systems and in particular for the transmission of supergroups (312 - 552 kHz),

for instance for connections of radio links to city telephone exchanges: in this case, different units in the cable are provided for the two transmission directions.

Tests have proved that either concentric or unit cables may also be used for PCM transmission up to a maximum of 120 channels with full exploitation of the cable circuits.

In the case of 120 PCM channels, the calculated distance between regenerative repeaters is approx. 4 km, that is in the same range of distances as for the 0.65/2.8 mm coaxial pair cables.

INSTALLATIONS

With reference to the 0.65/2.8 mm coaxial pair cables, a first experimental link of 12.6 km between Turro and Monza (near Milan) was made in 1969. The cable had a central core of 20 coaxial pairs, surrounded by 222 multiple twins with 0.7 mm conductors (overall diameter approx. 67 mm, weight per kilometer approx. 10,000 kg).

Some other installations are planned, for which about 100 km of homogeneous cables with 12 and 24 coaxial pairs will be manufactured during 1970.

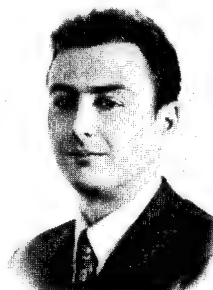
As to the quad concentric type cables, some thousands of kilometers are already in service, their application being primarily the aerial installation along valleys for FDM system transmission.

It is worth noting that these cables were adopted even when particular severe working conditions had to be faced, for instance in links having a serious danger of induced voltages or laid in high mountains, water channels, etc.

On the other hand, the quad unit type cables are of a more recent application. Several tens of kilometers have already been manufactured and a massive increase in production is foreseen for these cables. They are commonly used in networks laid in ducts and pressurized.

REFERENCES

- F. Camerone, G. Paladin: "Considerazioni tecnico-economiche sul dimensionamento delle coppie coassiali per la trasmissione dei segnali numerici", Istituto Internazionale Comunicazioni, Genova, 1969, XVII Convegno.
- G. Paladin: "Impostazione del problema della trasmissione di segnali PCM su portante fisico", LXIX Riunione annuale A.E.I., 1968.
- F. Bigi, G. Paladin: "Trasmissione di segnali PCM su cavi a coppie simmetriche e speciali", LXIX Riunione annuale A.E.I. 1968.
- G. Paladin, A. Savino: "Trasmissione di segnali PCM su cavi coassiali normali e speciali", LXIX Riunione annuale A.E.I., 1968.
- G. Paladin: "Nuovi portanti fisici per la trasmissione di segnali PCM a media velocità", Istituto Internazionale Comunicazioni, Genova, 1967, XV Convegno.



Pietro Calzolari - c/o Pirelli
(Speaker) 245 Park Ave.
New York, New York 10017

Mr. Pietro Calzolari, 38, has a Masters Degree in Electrical Engineering achieved at the University of Bologna, Italy. He has been with Pirelli since 1956 and presently is the Director of the Telephone Cable Planning and Development Department.

ESTIMATION OF VOICE FREQUENCY NOISE IN COMMUNICATION CIRCUITS

Eugene W. Riley
Anaconda Wire and Cable Company
Sycamore, Illinois 60178

ABSTRACT

Engineering considerations required for the development of a computer program to calculate expected measured noise on communication circuits exposed to nearby power lines are discussed. Using these concepts a computer program was developed to provide solutions for exposures involving single phase and three-phase, four-wire power circuits and one or more shielding conductors up to a maximum of five. Situations wherein no shielding is provided also are applicable.

The program has been written for the IBM 1130 System. An example of the output is included. A useful application of the procedure is that of determining, for given susceptiveness and coupling conditions, the maximum permissible influence (i.e., the maximum value of harmonic current) at some one frequency to ensure that a prescribed noise level will not be exceeded, assuming the contribution from other frequencies to be negligible.

INTRODUCTION

The field of inductive coordination is one of considerable scope. In a paper of this type one can hope to discuss, in a meaningful way, only some small segment of the problem. This paper relates to noise induced into communication circuits by harmonics of the fundamental power system current in nearby power lines. While it is true that many aspects of this subject already have been discussed in considerable detail in the literature, it now is receiving renewed attention and emphasis. The reasons are many; to name but a few there are: 1) extension of maximum voltages used in power transmission and distribution systems, 2) joint buried application including use of random separation, and 3) analog transmission of video signals over paired telephone cables.

If predictions for power system complexes of the future are realized, construction of new overhead transmission lines will continue throughout the next two decades with transmission voltages reaching the 1000 KV ac level.¹ Distribution voltages will reach 230 KV by the year 1990; but beginning in the 70's the trend toward underground plant for distribution systems will accelerate. By the year 2000 virtually all distribution plant will be underground. However, during this same period aerial construction of communication circuits also will be virtually eliminated.

With right-of-way at a premium and soaring construction costs, joint use of underground right-of-way will expand rapidly, and, considering the higher voltages which will be employed inductive coordination of joint buried facilities will require considerable attention. The problems associated with the relatively new concept of joint burial using random separation have been under investigation for the past few years, and recommended procedures have been established to avoid creating unsatisfactory noise conditions on telephone wires.^{2,3}

The application of balanced telephone cable pairs for the transmission of video information in the not-too-distant future will impose more stringent requirements on inductive coordination of power and communication facilities. To provide adequate picture quality the interfering signals from power lines must be at least 45 dB below the desired signal on each trunk carrying video information.⁴

Some additional developments which have led to increased cognizance of inductive coordination problems are improved sensitivity and efficiency of receiving devices, increased use of physical circuits for data transmission, application of gain devices to voice communication circuits, and, application of load devices on the power system, such as silicon controlled rectifiers for example, which have a very high potential for generating harmonics.

Although all this may lead to new approaches to the problems of coordination, the fundamental electromagnetic relationships which determine the noise levels induced into communication circuits from nearby power lines will not change. In the material which follows we will discuss these fundamental concepts and their application to the development of a computer program designed to compute the expected measured noise in a communication circuit exposed to a nearby power line. We first will define some terms and present an illustrative example to establish a basis for the subsequent material.

DEFINITIONS AND UNITS

The reference used to define noise in a communication circuit is one picowatt (10^{-12} watts) of 1000 Hertz power. This is equivalent to 24.5 microvolts across 600 ohms. Noise power (or voltage) is expressed relative to this reference power (or voltage). Thus, a particular noise level is said to be so many "decibels above reference noise" abbreviated dBrn.

A noise voltage V_n measured across 600 ohms is converted to dBrn by the expression:

$$\begin{aligned} \text{Noise in dBrn} &= 20 \log_{10} \frac{V_n}{24.5 \times 10^{-6}} \\ &= 20 \log_{10} V_n + 92.2 \end{aligned} \quad (1)$$

In the discussions which follow we will be concerned with two types of noise - noise metallic and noise-to-ground. Noise metallic, designated V_m , is a noise voltage which exists between the two conductors of a metallic circuit; it appears across the terminals of the receiver and hence is an interference voltage. Noise-to-ground, designated V_g , refers to a voltage existing between one conductor of a communication circuit and ground. It does not appear across the terminals of the receiving device; therefore, it is not, of itself an interference voltage. However, the voltage-to-ground produces the metallic voltage described above to an extent dependent upon the balance of the communication circuit with respect to ground which is defined:

$$\text{Balance (dB)} = 20 \log_{10} \frac{V_m}{V_g} \quad (2)$$

The noise measuring sets in use today measure metallic noise voltages across 600 ohms. Therefore, as indicated above, the noise metallic in dBrn is,

$$N_m = 20 \log_{10} V_m + 92.2 \quad (3)$$

When used in the noise-to-ground mode these same measuring sets provide a longitudinal drain of approximately 100,000 ohms between the input terminals and ground. Therefore, the noise-to-ground is attenuated 40 dB before being applied to the input terminals of the noise measuring set. Taking this into account we arrive at the following expression for the measured noise-to-ground (in dBrn) in terms of the open-circuit voltage-to-ground.

$$N_g = 20 \log_{10} V_g + 52.2 \quad (4)$$

Combining equations (2), (3) and (4) we obtain:

$$N_m = (N_g + 40) + \text{Balance} \quad (5)$$

For numerical expression of noise magnitude to be meaningful, two noise voltages which are equally interfering should be assigned the same numerical value. However, the human ear does not respond to all frequencies in the same way. Two noise voltages, one at frequency f_1 and one at frequency f_2 , may be equal in magnitude (i.e., have the same value of dBrn) but be quite different in interfering effect. Therefore, noise voltages at different frequencies must be weighted in some way to ensure that equally interfering noises will be assigned equal numerical values. This process, referred to as "message weighting", is described below.

MESSAGE WEIGHTING

Most of the power systems in the United States have a fundamental frequency of 60 Hertz. However, the current flowing on the power line is never a pure 60 Hertz sine wave; harmonics of the fundamental are present to some degree. Although the magnitudes of the harmonic currents are small compared to the magnitude of the fundamental, they are of greater importance from a noise standpoint. The human ear responds to frequencies in the range from 20 to 20,000 Hertz, but for practical purposes the usable range in voice communication circuits may be assumed to extend from about 180 Hertz to 4000 Hertz.

Moreover, the ear does not respond to all frequencies in the same way. Subjective tests performed by the Bell System using the modern "500 series" telephone set have led to a message weighting curve which expresses the relative importance of the various frequency components present in a received signal. This curve, termed "C-message weighting" is shown in Figure 1. It will be noted, for example, that an interference voltage at 180 Hertz would have to be 29.5 dB higher than one at 1000 Hertz to be equally annoying. This C-message weighting curve is the standard for evaluating noise in communication circuits.

When C-message weighting is applied to a noise voltage expressed in the units described above (dBrn) a suffix of C is attached to indicate the adjustment. Thus, noise levels normally are expressed in dBrnC. At a given frequency the noise in dBrnC may be obtained from the expression:

$$\text{Noise in dBrnC} = \text{Noise in dBrn} + C. \quad (6)$$

where C is the ordinate of the C-message weighting curve at the given frequency.

Although the individual noise voltages induced into a communication circuit at each harmonic frequency are of interest, it is the combined effect of all the frequency components throughout the usable voice band that is of greatest interest. This is what the listener hears. The noise measuring set sums the individual frequency components on a power summation basis to give a single noise figure for a whole band of frequencies. An example of a typical noise objective used in telephone application is "A noise metallic of 20 dB above reference noise, C-message weighted" which is abbreviated to "20 dBrnC". There is no reference to frequency; the objective refers to the combined effect of all frequency components added on a power summation basis. Thus,

$$\text{Overall Noise in dBrnC} = 10 \log_{10} (R_1 + R_2 + R_3 + \dots + R_n) \quad (7)$$

where $R_1, R_2, R_3 \dots R$ are the power ratios corresponding to the value of N_m at each frequency and are obtained from the equation,

$$R_k = \log_{10}^{-1} (N_m/10) \quad (8)$$

AN ILLUSTRATION

To illustrate the principles discussed in the foregoing sections, let us assume that we have induced voltages between a communication conductor and ground of 1.5 volts at 180 Hertz and 0.5 volts at 300 Hertz. Let us also assume that the circuit has a balance of -50 dB. Then the noise metallic in dBrnC is obtained as follows:

- 1) Calculate noise-to-ground in dBrn using equation (4).

At 180 Hertz:

$$N_g = 20 \log_{10} (1.5) + 52.2 = 55.7 \text{ dBrn}$$

At 300 Hertz:

$$N_g = 20 \log_{10} (0.5) + 52.2 = 46.2 \text{ dBrn}$$

- 2) Convert to dBrnC using equation (6) and Figure 1.

At 180 Hertz:

$$N_g = 55.7 - 29.5 = 26.2 \text{ dBrnC}$$

At 300 Hertz:

$$N_g = 46.2 - 16.5 = 29.7 \text{ dBrnC}$$

- 3) Calculate noise-metallic using equation (5).

At 180 Hertz:

$$N_m = (26.2 + 40) - 50 = 16.2 \text{ dBrnC}$$

At 300 Hertz:

$$N_m = (29.7 + 40) - 50 = 19.7 \text{ dBrnC}$$

- 4) Sum individual components using equation (8).

At 180 Hertz:

$$R_1 = \log_{10}^{-1} (16.2/10) = 41.7$$

At 300 Hertz:

$$R_2 = \log_{10}^{-1} (19.7/10) = 93.4$$

Sum 135.1

- 5) Calculate combined noise using equation (7):

$$\text{Overall Noise} = 10 \log_{10} 135.1 = 21.3 \text{ dBrnC}$$

We have used two frequencies to illustrate the procedure. If these same steps were carried out for all of the significant harmonics of the fundamental power frequency, the final figure obtained in step 5 would be the expected measured noise. We have assumed values of voltage-to-ground and circuit balance. The illustration clearly shows that if reasonable estimates of these two quantities can be obtained in an actual situation, then a reasonable estimate of the expected measured noise may be calculated. The following section discusses circuit balance; subsequent sections will describe a procedure for estimating the induced voltage-to-ground.

COMMUNICATION CIRCUIT BALANCE⁵

There are three basic factors which determine the noise level on a communication circuit exposed to a nearby power circuit. They are: 1) the inductive susceptiveness of the communication circuit, 2) the inductive coupling between the power and communication circuits, and 3) the inductive influence of the power circuit. The last two of the above will be considered subsequently when the procedure for determining the induced voltage-to-ground is taken up. The first is expressed in terms of the balance of the communication circuit.

A perfectly balanced metallic communication circuit is one for which the series impedances of both sides of the line are equal, the admittances of both sides of the line to ground are equal, and the impedances of both sides of any other metallic communication circuit on the same pole line are equal. As we have seen the degree of circuit balance is determined by the difference between the induced noise-to-ground and the noise metallic. Therefore, in order to calculate the expected measured noise on a yet-to-be-built communication circuit one must estimate the expected circuit balance. In reference 5 the degree of circuit balance is rated as follows:

Degree of Circuit Balance (DB)	Rating
> -40	Poor
-40 to -50	Fair
-50 to -60	Good
< -60	Excellent

It seems reasonable then to assume a circuit balance of -50 dB for calculating the expected measured noise. Should the actual value be less than this, the measured noise should be less than the expected measured noise. On the other hand, should the actual value be greater than the assumed value steps should be taken, as a matter of good engineering practice, to improve the balance. Reference 5 also gives an excellent survey of the causes of unbalance in communication circuits and the means by which they may be improved upon or eliminated.

We now will consider the second item in our list of factors: inductive coupling between the power and communication circuits.

INDUCTIVE COUPLING⁶

An interference problem must involve at least two conductors - a disturbing line and a disturbed line - as shown in Figure 2A. In this instance the current I_7^* in the disturbing line induces a voltage in the disturbed line measur-

able at the terminal between conductor and ground at V_6 . This induced voltage-to-ground is the product of the current in the disturbing circuit and the mutual impedance Z_{67} between the disturbing and disturbed circuits. Thus,

$$V_6 = I_7 Z_{67} \quad (9)$$

If one or more grounded conductors are placed in the vicinity of the disturbing and disturbed lines, they react upon the system in such a way as to lower the induced voltage between the disturbed conductor and ground. In a typical installation there usually will be several well grounded conductors present. For example, if the disturbed conductor is one side of a balanced pair in a shielded communication cable which parallels a grounded neutral power system, shielding will be provided by 1) the power neutral, 2) the communication cable shield, 3) the messenger strand to which the communication cable is attached, and 4) the shields of other communication or power cables installed on the same pole line.

To illustrate the principles involved in calculating the induced voltage-to-ground when shielding conductors are present, we shall first consider the elementary case involving a single shield as shown in Figure 2B. The shielding conductor takes on the role played by the disturbed conductor in the preceding discussion; that is, the current in the disturbing circuit induces a voltage in the shielding conductor which is measurable at the terminal between the conductor and ground as E_1 . Again, this voltage is equal to the product of the disturbing current and the mutual impedance between the disturbing and shielding conductors:

$$E_1 = I_7 Z_{17} \quad (10)$$

Since the shielding conductor is closed through ground, the induced voltage drives a current I_1 through the self-impedance Z_{11} of the shielding conductor producing a voltage drop $E_1' = I_1 Z_{11}$. This voltage is, of course, equal in magnitude and opposite in phase to that produced by the disturbing current since the voltage drop around the shield-ground circuit must be zero. Therefore,

$$0 = I_1 Z_{11} + I_7 Z_{17} \quad (11)$$

The voltage induced in the disturbed circuit no longer is a function only of the current in the disturbing circuit as given by equation (9). It now has a component due to the current flowing in the shielding circuit which is approximately counter to the original voltage. This component is equal to the product of the current in the shielding circuit and the mutual impedance between the shielding and disturbed conductors. Thus,

* The equations employed herein have been incorporated into a computer programming system which is applicable to a power/communication complex having from 1 to 5 shielding conductors. For consistency the shielding conductors are referred to as conductors 1 through 5, the disturbed conductor as conductor number 6 and the disturbing conductor as conductor number 7 throughout the paper.

$$V_6 = I_1 Z_{16} + I_7 Z_{67} \quad (12)$$

Equations (11) and (12) may be solved simultaneously to obtain the induced voltage-to-ground in terms of the disturbing current and the self and mutual impedances. We obtain,

$$V_6 = I_7 Z_{67} \left[1 - \frac{Z_{17} Z_{16}}{Z_{67} Z_{11}} \right] \quad (13)$$

The disturbing current and the self and mutual impedances vary with frequency; therefore, a separate calculation must be made for each frequency of interest.

As additional shielding circuits are added to the system the complexity increases. In general, if n shielding conductors are present, $(n + 1)$ simultaneous equations must be solved to obtain the induced voltage. These equations involve the mutual impedances between each of the conductors present in the system and the self impedances of the shielding conductors, all of which must be calculated for each frequency of interest.

When more than one disturbing conductor is present, as for example when the induced voltage is due to harmonics in a three phase-power system, the complexity of the calculations is further increased. The voltage induced by each disturbing conductor must be calculated separately; the total voltage-to-ground then is obtained by vector addition of the individual values. The formidable nature of the problem precludes a manual solution in all but the very simplest of situations; but the use of a computer reduces the problem to one of manageable proportions.

A computer program has been developed to provide solutions for exposures involving single phase and three-phase, four-wire power circuits and one or more shielding conductors up to a maximum of five. Situations wherein no shielding is provided also are applicable. The sets of simultaneous equations describing the system in each case are shown in Table I. The procedure for calculating the self and mutual impedances is described in the following section.

SELF AND MUTUAL IMPEDANCES

The self and mutual impedances required for the solution of the equations shown in Table I are calculated from formulas developed by J. R. Carson.⁷ A complete discussion of these formulas is beyond the scope of this paper;

they are stated formally in Appendix A and our discussion is limited to those points which are essential to an understanding of their use in a computer program.

In order to compute the self and mutual impedances using equations (15) and (16) the computer must be furnished with certain information about the system. This includes:

- 1) The approximate height of each conductor above ground in meters. For buried facilities the height is taken as zero.
- 2) The radius of each shielding conductor in centimeters.
- 3) The horizontal separations (center-to-center) between conductors in centimeters.

In addition the following information is required:

- 4) The resistance of each shielding conductor in ohms per kilometer.
- 5) Earth resistivity in meter-ohms. Typical values of earth resistivity fall within a range from 10 to 10,000 meter-ohms. The value used is not critical provided the separation between conductors is not too large (say less than 30 meters). In the absence of specific information about the earth resistivity in a given area a value of 100 meter-ohms may be assumed.⁸
- 6) Length of the exposure in kilometers.

The data described above are obtained and recorded on a suitable form, such as that shown in Figure 3, ready for key punching. When the program is executed, the self and mutual impedances required for the applicable set of equations in Table I are calculated at each frequency contained in a predetermined set which will be described in detail later. Results are obtained in ohms per kilometer.

As indicated in Table I the self and mutual impedances, which now are known, become the coefficients of the unknowns in the simultaneous equations describing a given system. When the disturbing current is known there are as many equations as unknowns; therefore, the induced voltage-to-ground, V_6 , may be calculated for each frequency contained in the predetermined set mentioned above.

The solution of the simultaneous equations is carried out using a procedure referred to as Cholesky's Scheme.⁹ This method was chosen

because it is the simplest and fastest of the known elimination methods and is well adapted to equations with complex coefficients. The procedure is clearly described in the reference; therefore, the details will be omitted herein.

The considerations involved in determining the frequencies and currents to be used depend upon the inductive influence of the power system (the third factor in our list) as discussed below.

INDUCTIVE INFLUENCE^{5,10}

In evaluating noise induction due to harmonics of the fundamental frequency power current, two types of harmonic current must be considered: 1) balanced current and 2) unbalanced or residual current. Balanced components are those components which are confined entirely to the phase conductors of the power line and which add up vectorially to zero. The unbalanced or residual current is the vector sum of the components flowing in the line wires. In grounded neutral systems the residual current includes the current returning in the neutral. In the case of single phase taps from three-phase, four-wire or three-phase, common-neutral circuits, the neutral current is equal to the total current in the phase wire.

On a power transmission system harmonics originate in the generators, transformer banks and loads. A three-phase transmission line usually is well enough balanced to ground so that harmonics originating as balanced components in the equipment or loads essentially are confined to the phase conductors. If, however, grounded neutral generators feed directly to the line or through grounded neutral transformer banks not equipped with tertiary delta windings, odd triple harmonics are generated and are impressed directly on the line as in-phase residual components. These odd triple harmonic residual currents usually are the most significant in exposures involving transmission lines.

Three-phase power distribution lines feed a substantial amount of single phase load; thus, they are inherently more unbalanced to ground than are three-phase transmission lines because of the unequal lengths of line associated with each phase. Moreover, there are substantial numbers of transformers and loads connected to distribution lines all of which are potential sources of harmonics. Power factor correction capacitors also are a potential source of harmonics. The harmonic currents generated by distribution system equipment and loads are not limited to the odd triple harmonics. Depending upon existing conditions the non-triple harmonics (or possibly even harmonics where rectifiers are the source) may be controlling in a given noise situation.

In most practical situations involving an exposure with a three-phase transmission or distribution system it will be necessary to measure the magnitude of, and phase relationships between, the currents in the phase wires. Procedures for making such harmonic analyses will be taken up in the next section. Should obtaining measured data be impractical it still is possible to obtain a reasonable estimate of the expected measured noise in certain specific cases involving parallels with single phase taps from three-phase common neutral and three-phase, four-wire circuits. Information obtained from power system wave shape surveys on a rather large sampling of such systems by the Joint Subcommittee on Development and Research, Bell Telephone System and Edison Electric Institute¹¹ may be used in lieu of measured data.

HARMONIC ANALYSIS

Methods for measuring the single frequency harmonic currents on power transmission lines are described in the literature^{12,13}.

In the case of single phase taps from three-phase common neutral or three-phase, four-wire systems the neutral current is equal to that in the phase wire. Thus, it is only necessary to measure the magnitude of the current in the phase wire at each harmonic frequency. The measured current is recorded on a form similar to that shown in Figure 4 in the column headed I_A .

Calculations of estimated noise from exposure to three phase circuits will require the measurement of: 1) the magnitude of the currents in each phase wire (I_A , I_B and I_C) at the fundamental and harmonic frequencies, and 2) the magnitudes of the vector sums of the currents in two combinations of two phases ($I_A + I_B$ and $I_A + I_C$) at the fundamental frequency. The magnitude of the vector sums of the phase currents can be obtained by paralleling the secondaries of the current transformers in the two phases, with proper attention to polarity. This assumes equal transformation ratios and identical characteristics for the current transformers. The measured data again are recorded on a form as indicated in Figure 4.

The data obtained at 60 Hertz are used to determine the phase relationships existing between the power line currents. The non-triple harmonics are assumed to have the same relationships among themselves as do the fundamental frequency currents, but in the standard sequence for a wye system. The triple harmonic currents are assumed to be in-phase.

TELEPHONE INFLUENCE FACTOR^{13,14}

The inductive influence of a power system often is expressed in terms of a quantity referred to as the "Telephone Influence Factor",

abbreviated TIF, which is a numerical quantity used to rate the wave shape of power system currents and voltages with respect to their influence on communication circuits; there are two types: current TIF and voltage TIF.

The Telephone Influence Factor of a voltage or current wave is defined as "the ratio of the square root of the sum of the squares of the weighted rms values of all the sine wave components (including in alternating waves both fundamental and harmonics) to the rms value (unweighted) of the entire wave."¹⁵

For reasons already mentioned in the section on message weighting not all of the harmonic components in the power system wave form are of equal importance from an influence standpoint. Therefore, the values of the various frequency components must be weighted before calculating the Telephone Influence Factor. As one might suspect the TIF weighting factors presently in use are related to the C-message weighting factors and, in fact, can be obtained from them by the formula,

$$T = 5f \log_{10}^{-1} \frac{C}{20} \quad (14)$$

Where, T = The TIF weighting factor at frequency f

f = frequency in Hertz

C = C-message weighting factor in dB.

The contribution of each harmonic component of current to the TIF is the product of the current at that frequency and the TIF weighting factor at the same frequency. This quantity is designated I·T. A similar calculation can be made at each frequency using the supply voltage, the product being designated V·T. The overall TIF is the square root of the sum of the squares of the I·T products (or V·T products) divided by the rms value of the entire wave. The I·T products and the current TIF are calculated by the computer program using the currents and C-message weighting factors recorded in Figure 4.

The individual frequency I·T products and overall current TIF calculated as described above are the phase current values. Values of I·T and TIF based upon ground return and neutral currents also are significant indicators of the power system influence. Methods for measuring the ground return and neutral current I·T products and the current TIF have been described¹² and are quite simple to apply. One method makes use of a 30.5 meter (100 foot) probe wire placed beneath the power line and connected at each end to driven ground rods. This method is used to measure the magnitude of the ground return currents at each harmonic frequency. A second

method employs a clamp-on current coupling device which may be used to measure the current in the power neutral. In both of these methods the currents are fed to a Western Electric 4A Analyzer or equivalent. The overall TIF can be calculated from the individually measured I·T products or it can be obtained by direct measurements using a Western Electric 3A or Northeast Electronics 37B noise measuring set.

Standard forms for recording the data and for carrying out the computations are described in reference 12. Since the calculation procedure for the ground return and neutral current I·T products and TIF values is relatively simple compared to the noise calculation procedures, it is not included in the computer program.

OTHER CONSIDERATIONS

The equations employed herein assume uniform conditions throughout the length for which a calculation is made. In practical situations the input information seldom will be constant throughout the entire length of the exposure. Distances between the disturbed, disturbing, and shielding conductors may vary; currents in the disturbing conductors may change due to the presence of loads or taps. Thus, it may be necessary to divide the exposure length into sub-lengths in each of which the exposure is approximately uniform. The induced longitudinal voltages are calculated for each section and are added vectorially to obtain the total induced voltage for the entire length of exposure.

The equations are not applicable to situations involving conductors composed of magnetic materials due to limitations on the calculation of the self and mutual impedances. Under these conditions the impedances vary with the amount of current flowing in the disturbing conductor and must be determined experimentally or by trial and error methods.¹⁶

CONCLUSION

This paper has discussed some of the factors relating to noise-frequency induction in communication circuits paralleling power circuits and has described a mathematical procedure which may be programmed on a computer for estimating the noise levels resulting from such exposures. A program has been written for the IBM 1130 system. Figure 6 is an example of the output obtained from the data shown in Figures 3 and 4.

A useful application of the procedure is that of determining, for a given set of coupling and balance conditions, the maximum permissible value of harmonic current at some one frequency

to ensure that a prescribed noise level will not be exceeded, assuming the contribution from other frequencies to be negligible.

ACKNOWLEDGEMENTS

I wish to express appreciation to Eugene J. Uzen for his interest and assistance in the development of the computer program.

REFERENCES

1. "A Prediction of Power System Development, 1968 to 2030", Alexander Kusko, IEEE Spectrum, April 1968, pp. 75-80.
2. "Electrical Interference Aspects of Buried Electric Power and Telephone Lines", F. Woodland, Jr., Proceedings of the Special Technical Conference on Underground Distribution of the IEEE, May 1969, pp. 245-251.
3. "Buried Power and Telephone Distribution Systems - Analysis of Primary Cable Fault Tests and Evaluation of Experience with Random Separation", EET/Bell System Joint Subcommittee on Development and Research, EET Publication 68-62, June 1962.
4. "Solving Picturephone Transmission Problems", D. W. Nast, Erwin Welber, Telephone Engineer and Management, October 1, 1969, pp. 111-116.
5. "Telephone Noise Measurement and Mitigation", Rural Electrification Administration, Telephone Engineering and Construction Manual, Section 451, November 1965.
6. "Directives Concerning the Protection of Telecommunication Lines Against Harmful Effects from Electricity Lines", International Telecommunications Union, (An Agency of the United Nations), 1963, Chapter XII
7. "Wave Propagation in Overhead Wires with Ground Return", J. R. Carson, Bell System Technical Journal, Vol. 5, October 1926, pp. 539-554.
8. "Coupling Factors for Ground Return Circuits - General Considerations and Methods of Calculation", EET/Bell System Joint Subcommittee on Development and Research - Engineering Report, Volume II, April 1932, pp. 121-185.
9. Numerical Methods in Engineering (Book), Mario G. Salvadori and Melvin L. Baron, Prentice Hall, Inc., July 1962, pp. 27-32.
10. "Methods of Investigating Noise Frequency Induction Problems". Bell System Practices, Section AB 63.080, August 1949.
11. "Wave Shape Survey on Operating Power Systems", EET/Bell System Joint Subcommittee on Development and Research - Engineering Reports, Volume II, April 1932, pp. 187 - 290.
12. "Control of Voice-Frequency Noise In Electric Power Circuits", O. W. Zastrow, IEEE Conference Paper no. CP 67-271, May 1967.
13. "Telephone Influence Factor (TIF) and Its Measurement", W. C. Ball and C. K. Poarch, IEEE Transactions Paper no. TP-1195, October 1960.
14. "The Telephone Influence Factor of Supply System Voltages and Currents", EET/Bell System Joint Subcommittee on Development and Research - Engineering Reports, Volume IV, January 1937, pp. 177 - 192.
15. "USA Standard C 42.65 - 1957, Definitions of Electrical Terms, Definition No. 65.12. 069".
16. "Low Frequency Shielding in Telephone Cables" EET/Bell System Joint Subcommittee on Development and Research - Engineering Reports, Volume V, January 1943, pp. 273 - 333.

APPENDIX A

CALCULATION OF SELF AND MUTUAL IMPEDANCES

The self impedance of a conductor n with ground return, designated Z_{nn} , and the mutual impedance between two conductors m and n, designated Z_{mn} , are a function of the geometrical relationships between the conductors and between each conductor and the environment as shown in Figure 5. The equations employed are:

$$Z_{nn} = z_n + 4\omega P_n \times 10^{-4} + j \left[2\omega \log_e \frac{2h_n}{a_n} + 4\omega Q_n \right] \times 10^{-4} \text{ ohms per kilometer.} \quad (15)$$

$$Z_{mn} = 4\omega P_{mn} \times 10^{-4} + j \left[2\omega \log_e \frac{\rho''_{mn}}{\rho'_{mn}} + 4\omega Q_{mn} \right] \times 10^{-4} \text{ ohms per kilometer.} \quad (16)$$

Z_n = Internal impedance of conductor n in ohms per kilometer. Within the range of frequencies considered in this paper Z_n may be assumed equal to the d-c resistance of the conductor in ohms per kilometer.

f = Frequency in Hertz

$$\omega = 2\pi f$$

h_n = Height of conductor n above ground in meters.

a_n = Radius of conductor n in centimeters.

$$\rho'_{mn} = \sqrt{(h_m - h_n)^2 \times 10^4 + (d_{mn})^2} \text{ in centimeters.}$$

$$\rho''_{mn} = \sqrt{(h_m + h_n)^2 \times 10^4 + (d_{mn})^2} \text{ in centimeters.}$$

h_m = Height of conductor m above ground in meters.

d_{mn} = Horizontal separation between conductors m and n in centimeters.

$$P_n = 0.3927 - 0.2357 r_n \cos \theta_n + \frac{r_n^2}{16} \cos 2\theta_n (0.6728 + \log_e \frac{2}{r_n}) + \frac{r_n^2}{16} \theta_n \sin 2\theta_n$$

$$P_{mn} = 0.3927 - 0.2357 r_{mn} \cos \theta_{mn} + \frac{r_{mn}^2}{16} \cos 2\theta_{mn} (0.6728 + \log_e \frac{2}{r_{mn}}) + \frac{r_{mn}^2}{16} \theta_{mn} \sin 2\theta_{mn}$$

$$Q_n = -0.0386 + \frac{1}{2} \log_e \frac{2}{r_n} + 0.2357 r_n \cos \theta_n$$

$$Q_{mn} = -0.0386 + \frac{1}{2} \log_e \frac{2}{r_{mn}} + 0.2357 r_{mn} \cos \theta_{mn}$$

$$r_n = 2h_n \times 10^2 \sqrt{\alpha}$$

$$r_{mn} = \rho''_{mn} \sqrt{\alpha}$$

$$\alpha = 4\pi\lambda\omega$$

$$\lambda = \frac{1}{\rho} \times 10^{-11}$$

ρ = Earth resistivity in meter-ohms.

$$\theta_n = \tan^{-1} \frac{a_n}{10^2(2h_n)}$$

$$\theta_{mn} = \tan^{-1} \frac{d_{mn}}{10^2(h_m + h_n)}$$

Equations 15 and 16 are applicable only for a range of r_n and r_{mn} less than or equal to 0.25. This is sufficient for most practical applications. If the maximum permissible value is exceeded an error message will be printed and the computer output will be suppressed. Suitable approximation may be obtained under these conditions by increasing the assumed value of earth resistivity provided the separation between conductors is not greater than about 30 meters.



Eugene W. Riley
Anaconda Wire & Cable Co.
Comm. Products Div.
North Cross St.
Sycamore, Ill. 60178

Eugene W. Riley was born in Wilmington, Delaware on August 29, 1932. He received the B.E.E. degree from the University of Delaware in 1958 and the M.S. degree in Mathematics from Northern Illinois University in 1968.

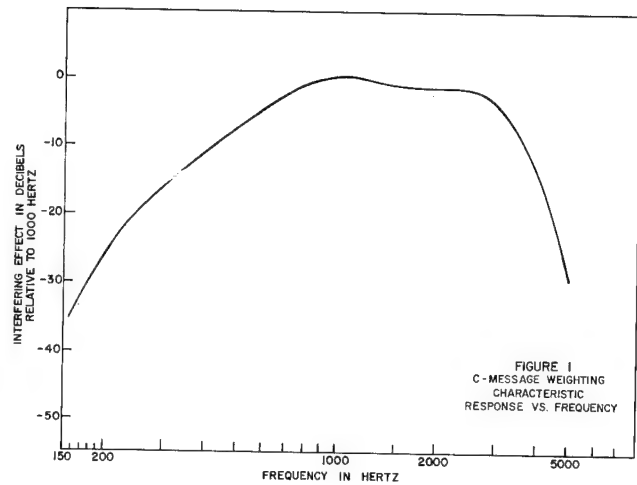
From 1958 to 1960 he was employed by the Rural Electrification Administration as a Staff Engineer in the Outside Plant Branch of the Telephone Engineering and Operations Division. He joined Anaconda Wire and Cable Company in October 1960. Since 1967 he has been in charge of the Transmission Engineering Section of the Communications and Electronics Division.

Mr. Riley is a member of the Institute of Electrical and Electronics Engineers.

TABLE I

EQUATIONS DESCRIBING POWER/COMMUNICATION SYSTEM
COMPLEXES WITH VARYING NUMBERS OF SHIELDING CONDUCTORS

NO. OF SHIELDING CONDUCTORS	EQUATIONS DESCRIBING THE SYSTEM
0	$V_6 = Z_{67} I_7$
1	$Z_{11} I_1 + 0 = -Z_{17} I_7$ $Z_{61} I_1 - V_6 = -Z_{67} I_7$
2	$Z_{11} I_1 + Z_{12} I_2 + 0 = -Z_{17} I_7$ $Z_{21} I_1 + Z_{22} I_2 + 0 = -Z_{27} I_7$ $Z_{61} I_1 + Z_{62} I_2 - V_6 = -Z_{67} I_7$
3	$Z_{11} I_1 + Z_{12} I_2 + Z_{13} I_3 + 0 = -Z_{17} I_7$ $Z_{21} I_1 + Z_{22} I_2 + Z_{23} I_3 + 0 = -Z_{27} I_7$ $Z_{31} I_1 + Z_{32} I_2 + Z_{33} I_3 + 0 = -Z_{37} I_7$ $Z_{61} I_1 + Z_{62} I_2 + Z_{63} I_3 - V_6 = -Z_{67} I_7$
4	$Z_{11} I_1 + Z_{12} I_2 + Z_{13} I_3 + Z_{14} I_4 + 0 = -Z_{17} I_7$ $Z_{21} I_1 + Z_{22} I_2 + Z_{23} I_3 + Z_{24} I_4 + 0 = -Z_{27} I_7$ $Z_{31} I_1 + Z_{32} I_2 + Z_{33} I_3 + Z_{34} I_4 + 0 = -Z_{37} I_7$ $Z_{41} I_1 + Z_{42} I_2 + Z_{43} I_3 + Z_{44} I_4 + 0 = -Z_{47} I_7$ $Z_{61} I_1 + Z_{62} I_2 + Z_{63} I_3 + Z_{64} I_4 - V_6 = -Z_{67} I_7$
5	$Z_{11} I_1 + Z_{12} I_2 + Z_{13} I_3 + Z_{14} I_4 + Z_{15} I_5 + 0 = -Z_{17} I_7$ $Z_{21} I_1 + Z_{22} I_2 + Z_{23} I_3 + Z_{24} I_4 + Z_{25} I_5 + 0 = -Z_{27} I_7$ $Z_{31} I_1 + Z_{32} I_2 + Z_{33} I_3 + Z_{34} I_4 + Z_{35} I_5 + 0 = -Z_{37} I_7$ $Z_{41} I_1 + Z_{42} I_2 + Z_{43} I_3 + Z_{44} I_4 + Z_{45} I_5 + 0 = -Z_{47} I_7$ $Z_{51} I_1 + Z_{52} I_2 + Z_{53} I_3 + Z_{54} I_4 + Z_{55} I_5 + 0 = -Z_{57} I_7$ $Z_{61} I_1 + Z_{62} I_2 + Z_{63} I_3 + Z_{64} I_4 + Z_{65} I_5 - V_6 = -Z_{67} I_7$



DATA SHEET

SAMPLE CALCULATION

SINGLE PHASE EXPOSURE

3 ϕ , 4w, 4Kv FEEDER

LIGHT INDUSTRIAL LOAD

POWER - 2 Awg SOLID Cu.

COMM. - 100/22 ALP on 6M

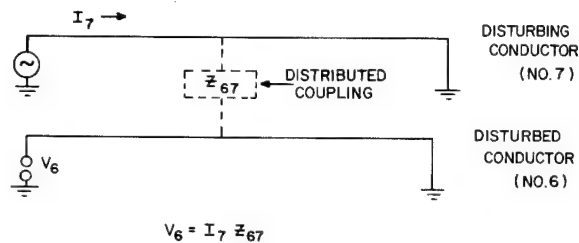


FIGURE 2A

BASIC INTERFERENCE SITUATION - WITHOUT SHIELDING

CONDUCTOR	NO.	HEIGHT METERS	RADIUS CM.	RESISTANCE OHMS/KM.
POWER CABLE OR CONDUCTOR	7	9.1		
COMM. CABLE OR CONDUCTOR	6	6.1		
SHIELDING CONDUCTORS	1	8.2	0.33	0.52
	2	6.1	1.14	1.35
	3			
	4			
	5			

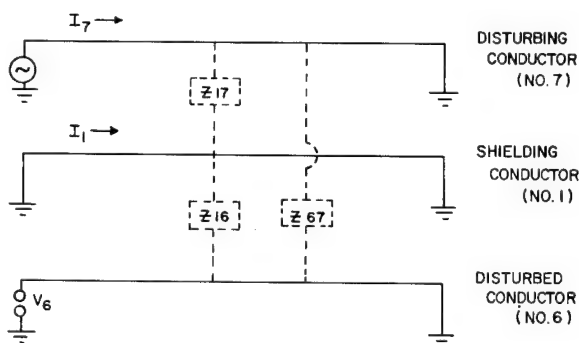


FIGURE 2B

BASIC INTERFERENCE SITUATION - WITH SHIELDING

CONDUCTOR		SEPARATION BETWEEN CONDUCTORS IN CM.					
		POWER	COMM.	SHIELDING CONDUCTORS			
CONDUCTOR	NO.	7	6	1	2	3	4
COMMUNICATION	6	137					
SHIELDING CONDUCTORS	1	137	0				
	2	136	1.14	1.14			
	3						
	4						
	5						

EARTH RESISTIVITY: 100 METER - OHMS

EXPOSURE LENGTH: 3.0 KILOMETERS

FIGURE 3

SAMPLE CALCULATION	LIGHT INDUSTRIAL LOAD
SINGLE PHASE EXPOSURE	POWER- 2 Awg SOLID Cu.
3 ϕ , 4w, 4kV FEEDER	COMM.- 100/22 ALP on 6M

FIGURE 4

SELF RETURN NEAR-END NEAR-END CROSSTALK OF MULTI-PAIR BALANCED TYPE CABLE

by

Toshio Hosono* Hiroshi Kaiden** and Shozo Inao**

The Furukawa Electric Co., Ltd. Tokyo, Japan

SUMMARY

We describe the phenomenon of self return near-end near-end crosstalk of multi-pair cable, investigation of its cause, and means to solve, transmitting high frequency signals of 1 MHz or over.

1. INTRODUCTION

Recently there is a demand for transmission of high frequency bands of 1 MHz or over, such as ITV and high speed pulse, using Multipair cable (Ref. 1) On actually transmitting high frequency signals of 1 MHz or over, we found there came up a conspicuous phenomenon of crosstalk which could not be conceived in case of low frequency. That is Self Return Near-end, Near-end Crosstalk, which is defined here as follows:

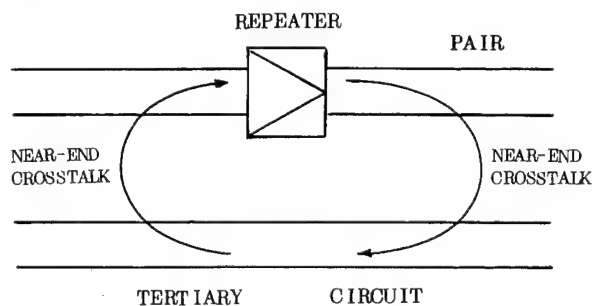


Fig. 1 Path of self-return near-end, near-end crosstalk

In the above figure, the output of repeater at the repeater section of the cable is sent reversely to the input side of the repeater through third circuit because of near-end crosstalk, and this reversely sent cross-talk electric power re-enters, as crosstalk, the repeater input. This is defined here as Self Return Near-end, Near-end Crosstalk. This Near-end, Near-end Self Return Crosstalk, when it worsens still farther and exceeds the repeater gain, will even develop oscillation phenomenon.

This report covers investigations of its cause and studies of remedial measures.

2. METHOD OF MEASURING SELF RETURN NEAR-END, NEAR-END CROSSTALK

To ascertain self return "near-end, near-end cross-talk attenuation" (hereinafter called "S.R.X.T.") quantitatively, the following measuring method is adopted:

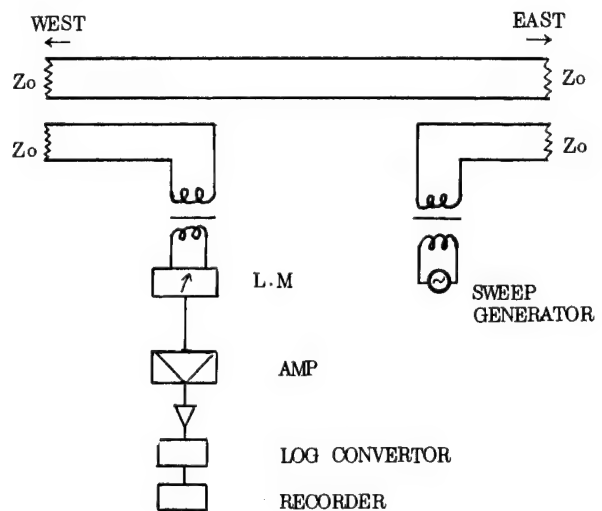


Fig. 2 Schematic diagram of circuit used in measuring self-return near-end near-end crosstalk

* Electric Engineering Department
College of Science and Engineering,
Nippon Univ.

** Tele-communication Laboratory
The Furukawa Electric Co., Ltd.

From the definition described in the Introduction,

$$\text{S.R.X.T.} = 10 \lg \frac{P_o}{P_L}$$

Where P_o : Output power of oscillator

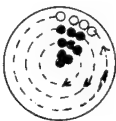
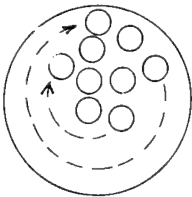
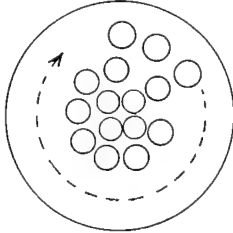



P_L : Input power of level meter

When, in actual practice, L.M. reading is taken of OSC as OdBm, the value obtained represents SRXT.

3. S . R . X . T.

Multipair cable, to which we refer simply as such, is numerous in kind according to wire diameter, insulation, sheath, etc. But we looked into SRXT of the following four deferent kinds of cable. The result is shown in Table 1.

Table 1. Near-end Near-end Self Return Crosstalk from 1 MHz to 10 MHz for four types of cable

Tested cable	No.1			No.2			No.3			No.4	
	0.9 mm, 100-pair PEF Insulated toll cable			0.4 mm, 200-pair, CCP Insulated Ex. cable			0.4 mm, 2400-pair, Paper Insulated Ex. cable			0.65 mm, 32-pair PEF Insulated toll cable	
Freq- uency	m	δ	min	m	δ	min	m	δ	min	m	min
1-2 MHz	70	—	dB	82.3	6.6	dB	87.4	4.1	dB	64.2	50 dB
2-3	69	—	64	81.3	3.5	67	84.8	4.5	75	58.4	50
3-4	68	—	50	78.8	5.9	59	82.5	4.2	75	56.4	45
4-5	65	—	49	76.3	6.3	58	80.8	3.7	71	48.4	30
5-6	61	—	36	73.6	5.3	62	78.5	4.7	71	48.6	35
6-7	61	—	27	73.7	3.6	67	78.2	4.1	72	48.0	35
7-8	60	—	32	71.4	3.3	63	76.6	2.4	67	52.4	43
8-9	59	—	37	69.8	5.5	63	75.7	2.3	67	49.0	45
9-10	56	—	9	69.2	3.4	60	74.8	5.6	67	60.2	45
Number of Samples	16			20			40			5	
Cable Length	500 m			500 m			200 m			1,200 m	
Structure											
Type	Layer type 50 quads			unit type 20 unit			unit type 24 unit			layer type 16 quads	
	----- Stradnign direction ● mark carrier quad o mark voice quad			 5 quad in unit			 50 quad in unit			● mark carrier quad o mark voice quad	

We shall explain particulars of SRXT of the above cables later. Now, from the results of measurement of those cable may be seen the following matters:

- 1) In No. 1 and No. 4 layer type cables with both left-hand stranding and righthand standing there are quads showing very bad SRXT.
- 2) Among No.2 and No.3 unit type cables there are none which show bad SRXT.
- 3) In No. 2 and No. 3 cables there are many which have good SRXT, as compared with PEF insulated cables.

To give a full description of all the cables from No.1 to No.4 will complicate the matter, so that we will pick up No.1 cable as representative examples and expalin them in detail.

Cross sections of No. 1 cable (0.9 mm, 100-pair, PEF insulated) is shown in Fig. 3.

0.9mm, 100-pair, PEF insulated quad and layer type cable

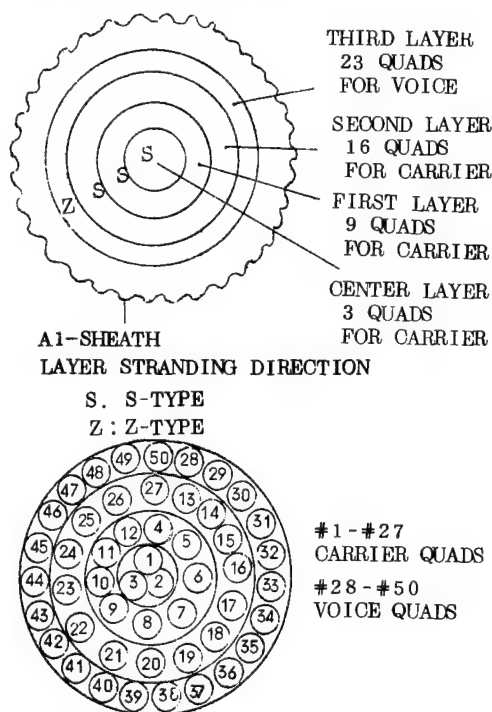


Fig. 3 Structure

When SRXT was measured from 1 MHz to 11 MHz of all quads, by a measuring circuit shown in Fig. 2, in the middle of 500 m No.4 cable, two quads showed SRXT of 30 dB or under. An example of it is shown in Fig. 4.

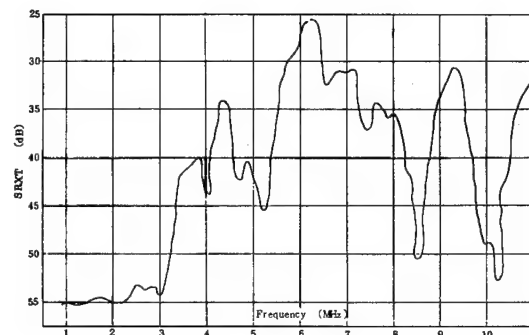


Fig. 4 Example of bad SRXT

Number #17 quad of 0.9 mm, 100-pair, PEF, cable

As can be seen from the above figure, there is a queer phenomenon that the carrier quads, which are generally said to be free from all problems in carrier frequency bands, had pairs of bad SRXT, while there is no such one in voice quads. Also there is a 26.5 dB SRXT in the vicinity of 6.4 MHz. If we take this value by the model of Fig. 1, we can consider that one side NXT is about 13 dB double near end crosstalk.

3.1 Path of SRXT

If, in the model of Fig. 1, to locate circuit corresponding to tertiary circuits, we cut off other quads while measuring SRXT of No. 1 cable #17 quad, we find that, as shown in the Fig. 5 (A) below, there is practically no decrease in SRXT in cutting carrier quad groups. In case of cutting off the voice quads one by one, that is great change in SRXT, so the disturbing signal of this crosstalk passes through voice quads.

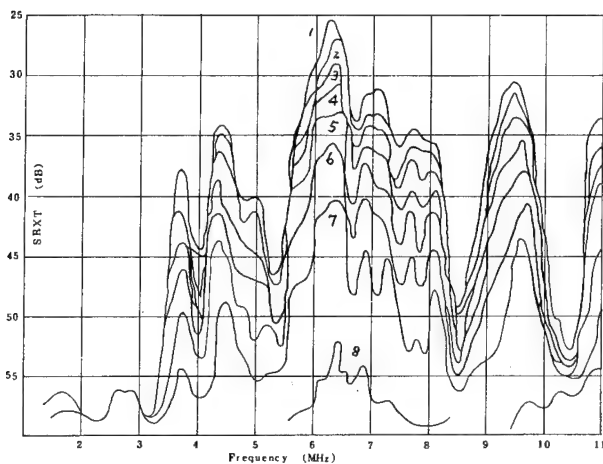


Fig. 5 (A) Decrease of SRXT of #17 quad, in case of cutting voice quads

- CURVE 1 After cutting off carrier quads
(Before cutting off voice quads)
- 2 After cutting 3 voice quads
- 3 After cutting off 6 voice quads
- 4 After cutting off 9 voice quads
- 5 After cutting off 12 voice quads
- 6 After cutting off 15 voice quads
- 7 After cutting off 18 voice quads
- 8 After cutting off 21 voice quads

In the stage of Fig. 5 (A), one of voice quads is connected respectively. If they are further cut off, the result will be as per Fig. 5 (B).

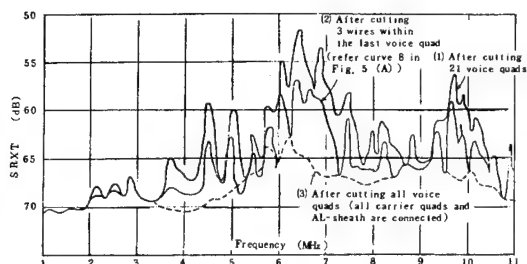


Fig. 5(B) Decrease of SRXT of #17 quad, in case of cutting off all voice quads and jointing all carrier quads

If all of the carrier quads are cut off, the result will be as per figure below. If all sheath is cut off, the result will be as shown by broken line.

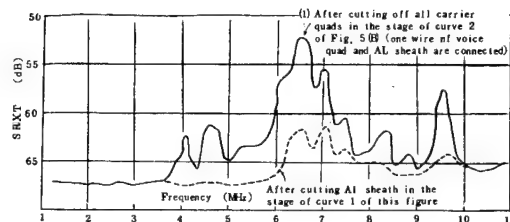


Fig. 5 (C) Decrease of SRXT of #17 quad, in case of cutting off all carrier quads.

From the above experiment we know that path of SRXT of #17 is voice quad, but we do not know.

By similarly cutting off other circuits within voice quads it is known clearly that the third circuit which deteriorates #17 SRXT is not real circuits and phantom circuit within the quads, and it is traced exclusively to the following two paths:

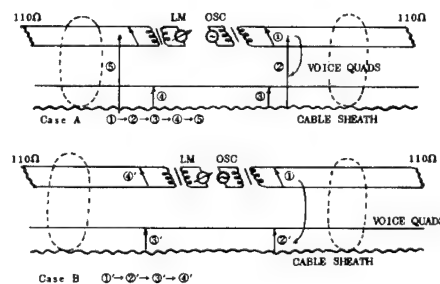


Fig. 6 Schematic diagram of circuit used in looking for path of SRXT

Transmitter and level meter were connected together as per Fig. 6 and near end crosstalk attenuation was measured with a result as shown in Fig. 7. From this figure we know Case (B) of Fig. 6 is the path in question.

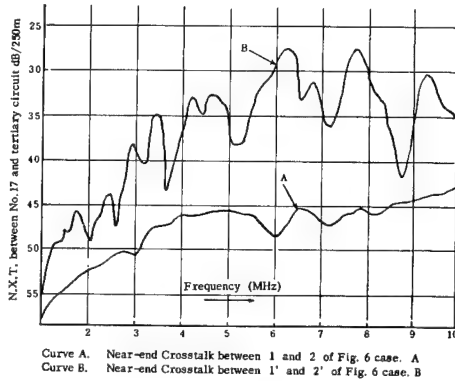


Fig. 7 Near end crosstalk between No.17 pair and tertiary circuit

Curve A. Near-end Crosstalk between 1 and 2 of Fig. 6 Case. A

Curve B. Near-end Crosstalk between 1' and 2' of Fig. 6 case. B

N.X.T. between No.17 and tertiary circuit dB/250

3.2 Sum of SRXT

If, as shown in Fig. 5 of the above, consecutive connection is made of the third circuit, SRXT will gradually increase. If rearrangement is made from that figure in respect of 6 MHz and 6.4 MHz frequencies Fig. 8 may be obtained.

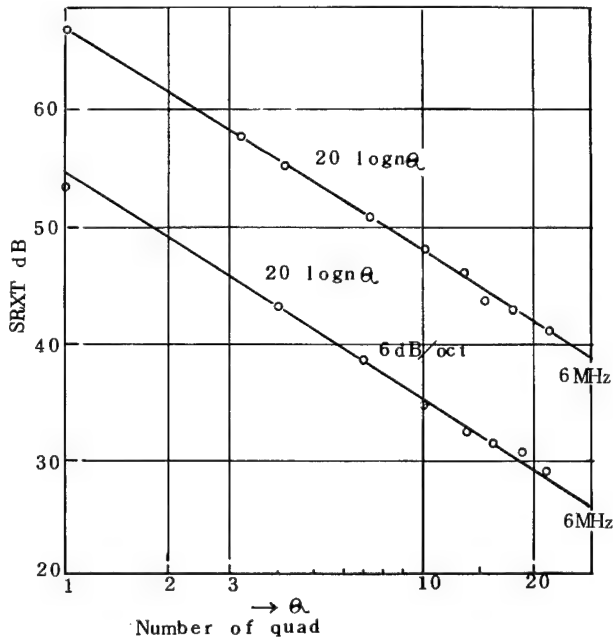


Fig. 8 Sum of SRXT

From Fig. 8 can be introduced the following formula:

$$SRXT = \overline{NXto} + \overline{NXTi} - 20 \log Q + A$$

where \overline{NXto} = near-end crosstalk of the output-side of repeater

\overline{NXTi} = near-end crosstalk of the input-side of repeater

Q = number of tertiary circuits (quads)

A = compensation term

4. ANALYSIS OF SRXT

In the preceding clauses, we have clarified experimentally "path of SRXT", "tertiary circuit", "sum of SRXT", etc. Here we shall make a theoretical calculation of SRXT.

4-1 Single Near-end Crosstalk between Transverse Circuit and Tertiary Circuit

As shown in Fig. 9, an assumption is made of in which electro-magnetic coupling "M(z)" between transverse circuit and tertiary circuit exists when

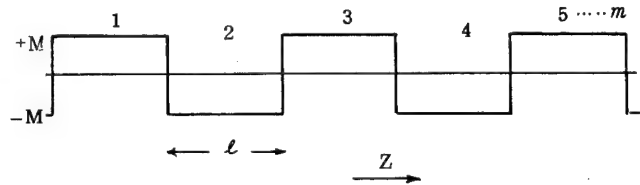


Fig. 9 Mutual inductance between transverse circuit and tertiary circuit

the interval is " l " and the number of intervals is m (even integer). When the near-end crosstalk attenuation is N and when it is assumed that the coupling is located in the middle of the " l ".

$$\begin{aligned} e^{-N} &= \frac{1}{2} \sum_{\nu=1}^m \epsilon_{\nu} \cdot e^{-\gamma(\nu-\frac{1}{2})l} M_{\nu} \\ &= \frac{1}{2} (\epsilon_1 e^{-\gamma l} + \epsilon_2 e^{-2\gamma l} + \epsilon_3 e^{-3\gamma l} + \dots \\ &\quad + \epsilon_{2i-1} e^{-(2i-1)\gamma l} + \epsilon_{2i} e^{-2i\gamma l} + \dots) e^{\frac{\gamma l}{2}} M_{\nu} \end{aligned} \quad (1)$$

where,

$$M_{\nu} \doteq \frac{j \omega M \ell}{\sqrt{Z_1 \cdot Z_2}} \equiv \frac{j \omega M \ell}{Z}$$

$$\epsilon_{2i} = -1 \quad (2)$$

$$\epsilon_{2i-1} = +1$$

$$\gamma = \gamma_1 + \gamma_2 = (\alpha_1 + \alpha_2) + j(\beta_1 + \beta_2) \equiv \alpha + j\beta$$

Z_1 = characteristic impedance of transverse circuit

Z_2 = characteristic impedance of tertiary circuit

$$\omega = 2\pi f$$

f = frequency

γ_1 = propagation constant of transverse circuit

$$= \alpha_1 + j\beta_1$$

γ_2 = propagation constant of tertiary circuit

$$= \alpha_2 + j\beta_2$$

$$e^{-N} = \left| \frac{j\omega M \ell}{2Z} \frac{(1 - e^{-\gamma \ell})}{(1 + e^{-\gamma \ell})} \cdot e^{-\frac{\gamma \ell}{2}} \right|$$

$$= \left| \frac{j\omega M \ell}{2Z} \cdot e^{-\frac{\gamma \ell}{2}} \cdot \sinh \frac{\gamma \ell}{2} \cdot \operatorname{sech} \frac{\gamma \ell}{2} \right| \quad (3)$$

when $\gamma \ell \gg 1$, Eq. (3) becomes

$$e^{-N} = \left| \frac{j\omega M \ell}{2Z} \cdot \operatorname{sech} \frac{\gamma \ell}{2} \right| \quad (4)$$

From Eq. (4), when

$$\frac{\beta \ell}{2} = \frac{\pi}{2}, \frac{3}{2}\pi, \frac{5}{2}\pi, \dots$$

the crosstalk worsens very much.

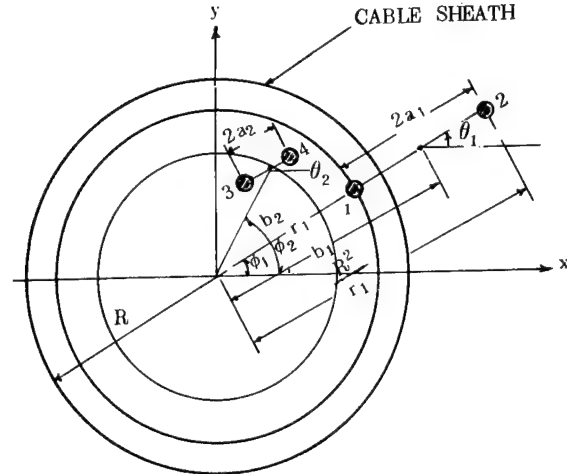
4-2 Mutual inductance M between transverse circuit and tertiary circuits.

In Fig. 11, mutual inductance between transverse circuit and tertiary circuit is calculated. It is assumed that Conductor (2) is located at image point of Conductor (1).

To this is applied

Neuman's formula.

(Reference 2)



3-4 : TRANSVERSE CIRCUIT

1-2 : TERTIARY CIRCUIT
(QUADS EARTH-RETURN CIRCUIT)

Fig. 10 Calculation of mutual inductance

$$TM = \frac{\mu}{4\pi} \int_{S_I} \int_{S_J} \frac{\cos \theta}{\rho} dS_I \cdot dS_J \quad (6)$$

$$TM = TM_{13} + TM_{24} - TM_{23} - TM_{14}$$

Let the coordinates of points each conductor regard as (X_I, Y_I, Z_I) and (X_J, Y_J, Z_J)

$$TM = \frac{\mu}{4\pi} \int_{S_I} \int_{S_J} \frac{dx_I dx_J + dy_I dy_J + dz_I dz_J}{\sqrt{(x_I - x_J)^2 + (y_I - y_J)^2 + (z_I - z_J)^2}}$$

$$= \frac{\mu}{4\pi} \int_{S_I} \int_{S_J} \left(1 + \frac{dx_I}{dz_I} \frac{dx_J}{dz_J} + \frac{dy_I}{dz_I} \frac{dy_J}{dz_J} \right) \frac{dz_I dz_J}{\sqrt{R_{IJ}^2 - (z_I - z_J)^2}}$$

$$\equiv \int_0^L M(z_1) dz_1 \quad (7)$$

$$R_{IJ} = \sqrt{(x_I - x_J)^2 + (y_I - y_J)^2} \quad (8)$$

$$\rho_{IJ} = \sqrt{R_{IJ}^2 + (z_I - z_J)^2}$$

When the rectangular cordiantes (x, y, z) in Eq. (8) are converted into the cylindrical cordiantes (r, θ, z) , R_{IJ} 's become

$$\left. \begin{aligned} R_{13} &= |a_1 e^{j\theta_1} + a_2 e^{j(\theta_2+\pi)} + b_1 e^{j\phi_1} + b_2 e^{j(\phi_2+\pi)}| \\ R_{23} &= |a_1 e^{j(\theta_1+\pi)} + a_2 e^{j(\theta_2+\pi)} + b_1 e^{j\phi_1} + b_2 e^{j(\phi_2+\pi)}| \\ R_{14} &= |a_1 e^{j\theta_1} + a_2 e^{j\theta_2} + b_1 e^{j\phi_1} + b_2 e^{j(\phi_2+\pi)}| \\ R_{24} &= |a_1 e^{j(\theta_1+\pi)} + a_2 e^{j\theta_2} + b_1 e^{j\phi_1} + b_2 e^{j(\phi_2+\pi)}| \end{aligned} \right\} (9)$$

where

$$\left. \begin{aligned} \theta_1 &= \frac{2\pi}{P_1} Z_1 + \alpha_{11} \\ \theta_2 &= \frac{2\pi}{P_2} Z_2 + \alpha_{22} \\ \phi_1 &= \frac{2\pi}{Q_1} Z_1 + \beta_{11} \\ \phi_2 &= \frac{2\pi}{Q_2} Z_2 + \beta_{22} \end{aligned} \right\} (10)$$

- P_1 = Pitch length of tertiary circuit
 P_2 = Pitch length of transverse circuit
 Q_1 = Stranding pitch length of tertiary circuit
 Q_2 = Stranding pitch length of transverse circuit
 α_{11} = Initial phase angle of pair of tertiary circuit
 α_{22} = Initial phase angle of pair of transverse circuit
 β_{11} = Initial phase angle of standing machine of tertiary circuit
 β_{22} = Initial phase angle of standing machine of transverse circuit

In the same manner, Eq. (7) is converted into the cylindrical coordinates, and by the use of computer, numerical integral is made with Z_2 ($dx = 1.0$ cm). Then, numerical integral is made with Z_1 .

When 0.9 mm x 100 pairs PEF toll cable is taken as an example,

- (i) Fig. 11-1A shows the results of calculation of $M(Z)$ between #17 quad with poor SRXT and earth-return circuit of voice quad within the third-layer in cable. TM value is shown in Fig. 11-1B.

As shown in Fig. 11-1B, $M(Z)$ has a large periodicity " $2L$ " ($= 13.2$ m), and TM has a large peak value.

- (ii) Fig. 12-2 shows $M(Z)$ between #15 quad with good SRXT and quad-earth return circuit of voice quad within the third-layer in cable.

$M(Z)$ in Fig. 11-1 has no large periodicity.

- (iii) When "Z" stranding direction of voice quad within the third-layer in cable is changed to "s" stranding (see Fig. 3), Fig. 11-3 shows $M(Z)$ between #17 quad and quad-earth return circuit of voice quad within the third-layer in cable.

As is known from this an ample, if the same stranding direction and the same stranding pitch are used for each layer, the periodicity of $M(Z)$ will become smaller and SRXT better.

- (iv) When the ratio of pair pitch-length P_2 of transverse circuit to stranding pitch-length Q_1 is 11 (odd integer) and Q_2 equals $-Q_1$, $M(z)$ becomes as shown Fig. 11-4.

From Fig. 11-4, as $M(z)$ has a constant value and TM increases linearly with Z as is seen from Fig. 11-4, SRXT becomes worse.

Fig. 11-1A Mutual inductance $M(z)$ between transverse circuit No.17 and quad earth-return circuit. in 0.9 mm, 100-pair PEF insulated Cable

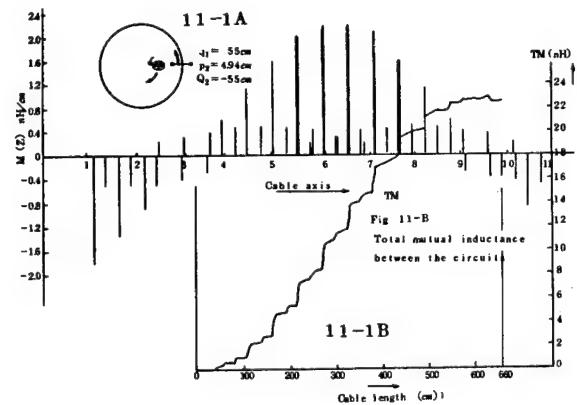


Fig. 11-2 Mutual inductance $M(Z)$ between transvers circuit with good SRXT and quad earth-return circuit within the third layer in 0.9 mm, 100-pair PEF insulated cable

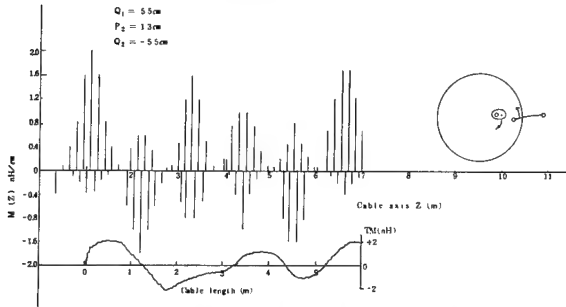


Fig. 11-3 Mutual inductance between transvers circuit No.17 and quad earth-return circuit with "S" stranding direction ($Q_2 = 55\text{cm}$) within the third layer in 0.9 mm x 100 pair, PEF insulated cable.

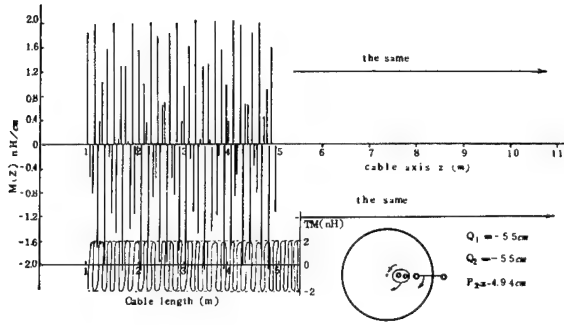
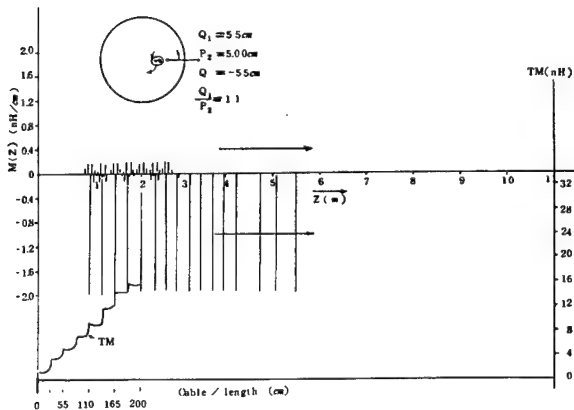


Fig. 11-4 Mutual inductance between transverse circuit under worst condition and quad earth-return circuit within the third layer supposing 0.9 mm, 100 pair PEF insulated cable (refer Fig. 11-1A)



The relation of the mutual inductance $M(z)$ between transverse circuit and tertiary circuit that is shown in Fig. 11-4 as viewed from the interrelated position of cable is as per Fig. 12.

$$Z = 0 \quad Z = \frac{Q_1}{11} \quad Z = \frac{Q_1}{4} \quad Z = \frac{Q_1}{Z} \quad Z = Q_1 \quad Z = 2Q_1$$

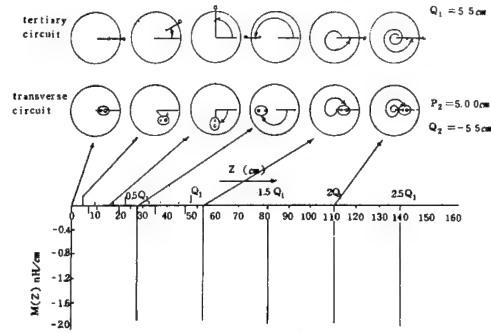


Fig. 12 Schematic explanation of mutual inductance $M(z)$

From Fig. 12, when $z = 0, \frac{Q_1}{2}, Q_1, \frac{3}{2} Q_1$,

$M(z)$ becomes the largest. As a result, total mutual inductance TM linearly increases according to the increase of z .

Now we will look into the extent of the deviation of Q_1/P_2 from odd integer which will cause $M(z)$ to have a function z having a large periodicity "21" as shown in Fig. 11-1.

In Fig. 13, we will obtain the condition under which mutual inductance $M(z)$ shown in Fig. 12 becomes a coupling distribution of $2 = mG_1$ ($m = 12$) as in Fig. 13.

Now, we take $Q_1 = \text{const.}$, $P_2' = P_2 \pm P$, odd number. If transverse circuit having pitch length P_1 and P_2 as an angle $\theta(z)$ or $\theta'(z')$ at Z point

$$\theta(z) = \frac{2\pi}{P_2} z \quad (11)$$

$$\theta'(z) = \frac{2\pi}{P_2'} z$$

Condition's under which $M(z)$ is 0, when $Z = Q_1 \cdot i$,

$$\pi \times (\text{even-number}) = \frac{2\pi}{P_2} Q_1 \cdot i \quad (12)$$

$$\pi \times (\text{even-number} + \frac{1}{2}) = \frac{2\pi}{P_2'} Q_1 \cdot i$$

$$\text{From Eq. (12)} \quad \pm \frac{1}{4} = \left(\frac{1}{P_2} - \frac{1}{P_2'} \right) Q_1 \cdot i$$

$$= \left(\frac{1}{P_2 \pm \Delta P} - \frac{1}{P_2} \right) Q_2 \cdot i$$

where $\Delta = 1$

$$\frac{Q_1}{P_2 \pm \Delta P} = \frac{Q_1}{P_2} \pm \frac{\Delta}{4i} \quad (13)$$

In Eq. (13) scope P_2' cm which satisfied $i \geq 3$, when $Q = 55$ cm, $P_2 = 5$ cm,

$$4.933 \leq P_2' \leq 5.069$$

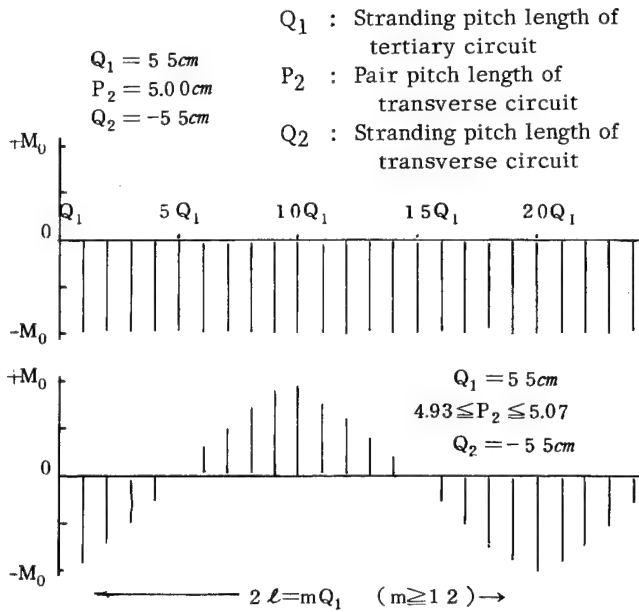


Fig. 13 Bad example of relation between Q_1 and P_2

From the above, the relation between Q_1 , P_2 , Q_2 for total mutual inductance "TM" to increase according to increase of "Z" is:

$$Q_1 = -Q_2$$

$$\frac{Q_1}{P_2} = 1, 3, 5, \dots \text{ (odd integer)} \quad (14)$$

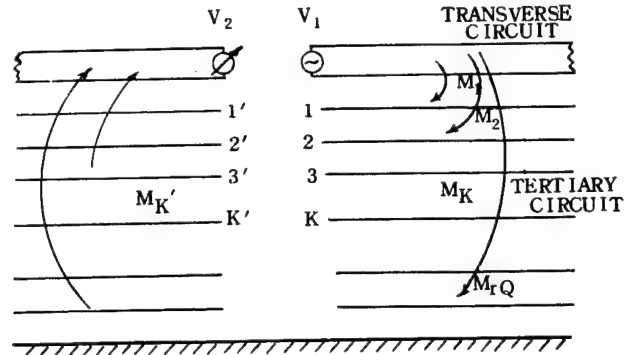
4-3 Sum of SRXT

The total number of tertiary circuits is Q . From Eq. (4), when $\alpha_1 + \alpha_2 \ll \beta_1 + \beta_2$ and $\gamma m \ell \gg 1$, e^{-N} can be written as:

$$e^{-N} = \frac{j\omega M \ell}{2Z} \sec \frac{\beta}{2} \ell \quad (15)$$

As shown in Fig. 14, the near-end crosstalk N_1 from "V₁" to "1" is

$$e^{-N_1} = \frac{j\omega M_1 \ell}{2Z} \cdot \sec \frac{\beta}{2} \ell \quad (16)$$



$$M_K = M_0 \cos \frac{K-1}{Q} \cdot 2\pi$$

Fig. 14 Sum of SRXT

The near-end crosstalk N_k from "V₁" to "K" is

$$e^{-N_k} = \frac{j\omega M_K \ell}{2Z} \cdot \sec \frac{\beta}{2} \ell \quad (17)$$

$$K = 1, 2, 3, \dots, Q$$

Similarly, the near-end crosstalk N_k from K' to V₂ is

$$e^{-N_{k'}} = \frac{j\omega M_{K'} \ell}{2X} \cdot \sec \frac{\beta}{2} \ell \quad (18)$$

Therefore in Fig. 14 SRXT from V₁ to V₂ is

$$\frac{V_2}{V_1} = \sum_{k=1}^Q e^{-(N_k + N_{k'})} = \left(\frac{\omega \ell \sec \beta \ell / 2}{2Z} \right)^2 \sum_{k=1}^Q M_k \cdot M_{k'} \quad (19)$$

From paragraph 4-2 and Fig. 14

$$M_k = M_0 \cos \frac{k-1}{Q} \cdot 2\pi \quad K = 1, 2, 3, \dots, Q$$

(i) in case of jointing k to k', Eq. (19) becomes

$$\frac{V_2}{V_1} = \left(\frac{\omega \ell \sec \frac{\beta}{2} \ell}{2Z} \right)^2 \cdot \frac{M_0^2 \cdot Q}{2} \quad (20)$$

$$S RXT = -20 \log \frac{V_2}{V_1} = 2 \cdot N - 20 \log Q + 6 \quad (21)$$

(ii) in case of random jointing, Eq. (19) becomes

$$\frac{V_2}{V_1} \Big|_{\text{random}} \neq 0 \quad (22)$$

4-4 Example of SRXT calculation

We shall calculate SRXT of No.17 with poor SRXT of 0.9 mm, 100 pairs, PEF cable. From Eq. (4), Single Near-end Crosstalk "N" is, when L is long, as follows:

$$\begin{aligned}
 N &= 20 \log \frac{\omega M \ell}{2Z} + 20 \log \operatorname{sech} \left| \frac{\gamma \ell}{2} \right| \\
 &= 20 \log \frac{2\pi f M \ell}{2Z} - 10 \log \left\{ \cosh \frac{\alpha_0 \sqrt{f} \ell}{2} \cos \frac{\beta_0 f \ell}{2} \right\}^2 \\
 &\quad + \left(\sinh \frac{\alpha_0 \sqrt{f} \ell}{2} \sin \frac{\beta_0 f \ell}{2} \right)^2 \} \\
 &\equiv N_1 + N_2
 \end{aligned} \tag{23}$$

Where

α_0 = sum of attenuation (α_{01}) of transverse circuit and attenuation (α_{02}) of tertiary circuit at 1 MHz: nep/m

β_0 = sum of phase const. (β_{01}) of transverse circuit and phase const. (β_{02}) of tertiary circuit rad/m

$$N_1 = 20 \log \frac{2 f M \ell}{2Z}$$

$$N_1 = 20 \log \frac{2 \pi f M \ell}{2Z}$$

$$N_2 = -20 \log \left\{ \left(\cos^2 \frac{\beta_0 f \ell}{2} \left(1 - \frac{\alpha_0^2 f \ell^2}{4} \right) + \frac{\alpha_0^2 f \ell^2}{4} \right) \right\} \tag{24}$$

When the following values are put into Eq. (24),

$$\alpha_{01} = 1.15 \times 10^{-3} \quad \alpha_{02} = 5.08 \times 10^{-3} \quad \text{nep/m}$$

$$\beta_{01} = 29.0 \times 10^{-3}, \beta_{02} = 39.5 \times 10^{-3} \quad \text{rad/m}$$

$$M \ell = 22.8 \times 10^{-9} \quad (\text{H})$$

$$Z_1 = 100 \Omega$$

$$Z_2 = 40 \Omega$$

$$f = \text{MHz}$$

Fig. 15 is obtained

Fig. 15 Single near-end crosstalk between transverse circuit of No.17 quad and a quad earth return circuit within the third layer

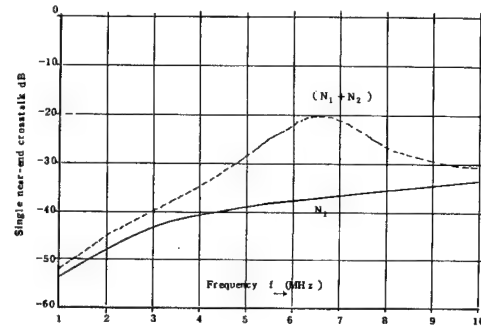
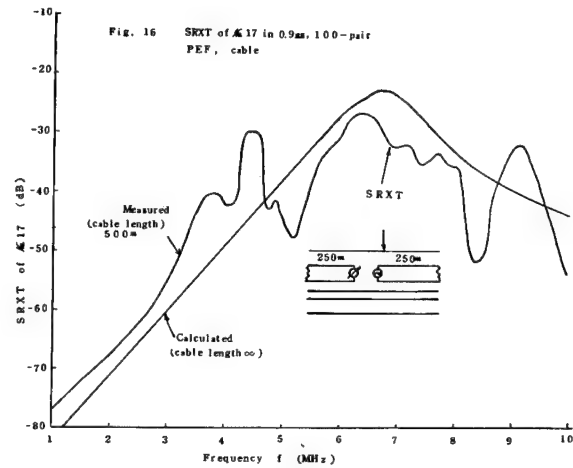


Fig. 16 SRXT of No.17 in 0.9 mm, 100-pair PEF, cable



As mentioned in 4-1, ($N_1 + N_2$) worsen very much when $B\ell = \pi$.

From Eq. (23) and Eq. (21), SRXT is expressed as,

$$\text{SRXT} = 2(N_1 + N_2) - 20 \log Q + 6 \tag{25}$$

In the case of 0.9 mm 100 pairs cable Q is 22 quads in the third layer. Therefore, when Eq. (25) is calculated with $Q = 22$, the results are as shown in Fig.16. Also shown are the measured value. They approximately follow the same tendency.

5. METHOD OF REDUCING SRXT

In the foregoing we have explained how SRXT develops. Here we explain the following two points.

(1) In case very poor SRXT develops in the existing

cable, through a high-frequency signal, what means means can be taken to solve it?

- (2) In case a new multipair cable is designed to pass the high-frequency signal.

5-1 In case poor SRXT develops in the existing cable

- A) As above mentioned, poor SRXT does not occur at random and is regular crosstalk. As shown in Table 1, there are always some with good SRXT in the same cable. Therefore, other circuits must, first of all, be looked for.
- B) In case there is no vacant circuit, the pair at the inlet and the pair at the outlet of the repeater, with different pitches, must be jointed.
- C) In case the above A) and B) are impossible by means tertiary circuits must be short-circuited in high frequency region. As aforementioned, tertiary circuits, which have the relation of Eq. 14, are mostly longitudinal circuits of the layer to which "pairs with poor SRXT" doesn't belong. Therefore, as shown in Fig. 17, in high frequency region short-circuiting is advisable.

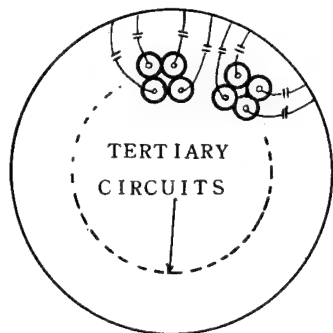


Fig. 17 Method of reducing SRXT by jointing condenser

- D) The following method can also be used. As shown in Fig. 18, tertiary circuits are jointed at random. In the case of Fig. 18

from Eq. (22),

$$\frac{V_2}{V_1} \div 0$$

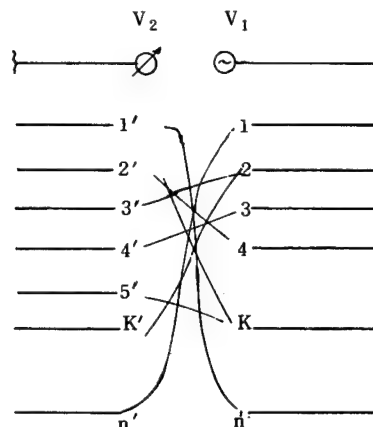
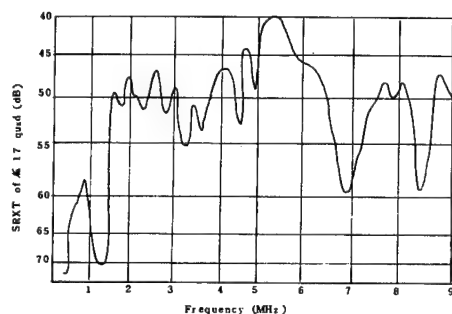


Fig. 18 Method of reducing SRXT by random splicing

Fig. 19 shows the results of measurement taken of SRXT by the method shown in Fig. 18.

Fig. 19 Measuring result of SRXT of No.17 quad in No.1 cable after random splicing



From Fig. 19, it is learned that an improvement of about 15 dB was made at a frequency of 6.4 MHz.

In case a new cable is designed

- A) It is advisable to use the same stranding direction and stranding pitch for each layer. (refer Fig. 11-3)
- B) In case, according to the mechanical requirement, a cable with different stranding direction has to be produced, the conditions of Eq. (14) mentioned in 4-2 must be avoided by all means.
- C) The subunit-type cable is better than the layer-type cable because an additional process of "rope stranding" is used for it and, therefore, the probability of regular summation of mutual inductance lessens very much.

6. CONCLUSION

Above we have described the phenomenon of SRXT, investigation of its cause, and means to solve. Although it had been unbelievable that the cable designed for toll line becomes so great as to oscillate the repeater, such thing really happens under the special conditions mentioned in the foregoing.

When multi-pair cable is used at a high-frequency band, special attention must be paid to SRXT. If possible, SRXT must be measured in the circuit shown in Fig. 2 before cable installation to ascertain whether or not the specified S/N is satisfied.

7. REFERENCE

1. "Problems in ITV transmission by multipair cable" by H. Kaiden, S. Inao and T. Atuya, I.E.C.E.J. April, 1968.
2. "Electro-magnetic coupling between quads of multi-pair cable" by N. Kobayashi. Research Report No. 1563, Oct., 1961.

E.C.L., N.T.T. Japan



H. Kaiden (Speaker)
The Furukawa Electric
Co., Ltd.
6-1 Maronouchi
2 Chome, Chiyoda-Ku
Tokyo, Japan

Hiroshi Kaiden was born on May 1, 1928. Graduated from the Electrical Engineering Department of Yokohama Technical College in March, 1948, and joined the Furukawa Electric Co., Ltd., in April of the same year. At first, he worked for the Production Engineering Section and Inspection Section of Furukawa's Yokohama Communication Cable Plant, during which time he was engaged in design and production engineering of communication cables, especially submarine cables and long-distance carrier cables. Also introduced industrial engineering such as QC and OR into the company and became its consultant.

Upon completion of a new telecommunication laboratory in the Chiba Works in April 1967, became its first head and has since taken charge of the management of research and development.

A LOW CAPACITANCE CABLE FOR THE T2 DIGITAL TRANSMISSION LINE

D. E. Setzer and A. S. Windeler
Bell Telephone Laboratories, Incorporated
Murray Hill, New Jersey 07974

Abstract

The present generation of digital transmission lines operate efficiently on existing multipair cable. However, in developing the new higher speed T2 line, a broader approach was used which included a specially designed cable, the subject of this paper. The cable is characterized by a substantial improvement in attenuation and crosstalk compared to standard plastic insulated cable. A number of design and manufacturing features were developed in order to realize the improvements.

Western Electric Company has manufactured 76,000 feet of 50 pair cable and Bell Telephone Company of Pennsylvania has installed the cable at Willow Grove. The installation is part of the Bell System T2 Digital Transmission Line Field Trial. A summation of the properties of an earlier prototype cable and of the field trial cable is presented.

Introduction

A new cable has been designed specifically for the T2 digital transmission line. Before describing the characteristics and construction of the new cable a few words about the T2 line are in order. The T2 line is a digital transmission system which uses a 6.3 megabit/sec pulse stream to provide 96 two-way pulse code modulated (PCM) telephone channels or alternatively, one two-way PCM PICTUREPHONE® channel on two separated cable pairs. In order to reduce near-end crosstalk, two cables are used. Pairs for opposite directions of transmission are located in separate cables. The system is designed to operate over distances as great as 500 miles. With the new cable the regenerative repeater spacing objective is 13 kilofeet and the power for the repeaters will be sent over the cable from power stations spaced about 18 miles.¹

In designing and developing the new cable for the T2 digital line the major effort was put on producing a cable with both low loss and low far-end crosstalk, critical for pairs transmitting in the same direction. Crosstalk and loss determine, to a large extent, the maximum repeater spacing which can be used in the line. The T2 line can also be used with standard cables, however, as will be discussed later, the new low loss, low

capacitance cable permits much greater repeater spacing and thereby produces a larger system savings in many applications. The low capacitance design will be used wherever it is practical to do so. The expected primary application is in the buried, intercity plant.

The 22 gauge, low capacitance cable has roughly half the capacitance of standard cable; 0.039 compared to 0.083 microfarads per mile. At 3.15 MHz (one half T2 pulse transmission rate) the characteristic impedance is 170 ohms compared to 96 ohms for standard PIC, and the attenuation is nominally 22 dB per mile compared to 46 dB per mile, i.e., approximately half the attenuation of 22 gauge standard PIC. The power sum of far-end, output-to-output crosstalk at 3.15 MHz is in the order of 11 dB better than standard PIC cable. The crosstalk improvement is necessary to attain the low error rate required on the T2 line if 13 kft repeater spacing is to be achieved.

Optimum Mutual Capacitance

Mutual capacitance of 0.039 microfarads per mile is close to the optimum capacitance from the standpoint of lowest cable cost for an attenuation of 22 dB per mile. To be more specific, one can adjust, and therefore trade off either resistance or capacitance to obtain the desired attenuation. This is illustrated in Fig. 1. Figure 1a shows a standard PIC conductor having a relatively large conductor diameter and relatively thin plastic insulation. If the copper conductor diameter is kept constant, and the insulation thickness is increased, as shown in Fig. 1b, the attenuation then goes down, but the cost goes up because of the increase in insulation and sheath material. Figure 1c illustrates a possible method of obtaining reduced attenuation and lower cost by reducing the copper diameter and increasing the insulation thickness. In other words, the trade-off is between the cost of the copper and the cost of the insulation. Since the cable capacitance depends on the ratio of insulation to conductor diameter, the trade-off is called the optimum capacitance concept.

The solid line in Fig. 2 is a plot of material costs versus capacitance for a 50 pair cable with the price of copper at 43¢ per pound, and the price of plastic at

24¢ per pound. These prices do not represent typical current costs. However, they were representative at the time our studies were made and they do serve to illustrate the principle involved. All cables represented by the solid curve have the same attenuation. The right-hand portion of the curve represents cables having relatively heavy gauge conductors and thin wall insulation. Moving toward the left the conductors get smaller and the insulation thicker. For the solid curve, representing 22 dB per mile at 3.15 MHz, the optimum point is slightly below 0.04 microfarads per mile. This is the point where the material costs are least. Labor and installation costs were neglected because they change only slightly with variations in cable capacitance. Note, that the optimum design costs less than one half as much as an 0.083 design having the same attenuation as the low capacitance design, 22 dB per mile.

The optimum capacitance obviously will depend on the relative costs of copper and plastic. In Fig. 2 the upper curve represents results for 53¢ copper and the lower for 33¢ copper; the plastic price remaining fixed at 24¢ per pound. The optimum capacitance becomes slightly lower as the cost of copper increases. For small size cables, containing 50 pairs or less, the change in the optimum capacitance with price of copper is small. With large cables there is a much greater change since the cost of the conductors is greater relative to the cost of the sheath.

The optimum capacitance concept applies for any value of cable attenuation. For a given attenuation there corresponds a capacitance for which the material costs will be minimum. This is illustrated in Fig. 3.

Expanded or foamed plastic insulation was assumed for all cables in this study. As a result of development work extending over a period of years, we are assured of the practicality of expanded insulation, especially with the heavy walls required for low capacitance designs. The savings derived from the use of expanded insulation make the low capacitance design look especially attractive.

Aluminum vs. Copper

For high capacitance designs the cost of cable will be reduced if aluminum conductors are used. This result is a consequence of the comparatively low cost of aluminum and the proportionately high percentage of total cost which is due to conductor material in a high capacitance cable. However, in low capacitance cables the ratio of conductor material to insulating material is considerably smaller,

therefore, diminishing the influence of the lower cost of aluminum. At the time of our studies, we were able to show that the use of copper would result in lower cable costs. Figure 4 illustrates the trade-off between copper and aluminum at that time. To the right of the crossover point aluminum occupies a favorable economic position, but to the left for values of cable capacitance less than 0.042, the economics favor copper. Therefore, copper was chosen as the preferred conductor for the new cable. The present high price of copper makes aluminum appear competitive. However, a switch to aluminum conductors for the new cable is not planned unless the ratio of copper price to aluminum price continues to increase drastically.

Improvements in Crosstalk and Unbalance

In addition to the low attenuation required for the new design, large improvements in other electrical parameters such as crosstalk and unbalance to ground had to be realized in order to achieve the savings resulting from extended repeater spacing. The crosstalk improvement did not come easily. Over the past five years, more than 50 experimental cables based on analytical and experimental models were made and tested. As a result of this work certain design and manufacturing changes, which result in substantial crosstalk improvements, were incorporated. The new design and manufacturing features include: (1) matched conductors for pairs, (2) 7 pair units, (3) combined twisting and stranding, and (4) judicious selection of pair twists. The use of the 7 pair unit, six around one, is especially important because this construction is geometrically stable, that is, the pairs tend to stay in position after stranding. The pair twists can be placed in position according to design requirements and will normally remain there throughout the life of the cable, permitting control of crosstalk via planned physical separation.

Combined twisting and stranding of the pairs is a significant departure from traditional cable manufacturing techniques. The usual procedure is to twist the pairs in one operation and strand in a second operation. With two-operation manufacture, twists are often distorted in going from one operation to the other. Thus, the one-operation process has worthwhile crosstalk advantages.

A total of 22 different pair twists were selected and arranged in such a way as to minimize the crosstalk. Every pair has an exact position in the cable and like or equal twist lengths do not occur within units or in adjacent units. Pair twist selection and arrangement play a very important role in the crosstalk improvement.

The capacitance unbalance to ground, i.e., the difference of direct capacitance to ground of the two wires of a pair, is a measure of the noise susceptibility of the pair. Unbalance to ground improvement was achieved by matching conductors. Conductors are matched by taking conductors of a pair from successive lengths off the same insulating extruder and from the same spool of copper wire. They will then tend to have the same mean conductor and insulation diameters. In addition, the wire is insulated under the control of a capacitance monitor. This method of matching the conductors of a pair results in loss of the familiar tip and ring designation since the wires of a pair will now be the same color. For the T2 line, this presents no problem because differentiation between wires within a pair is not required.

Optimizing System Costs

Having developed the means for substantial crosstalk and unbalance reduction and having determined the cable capacitance which would produce a given attenuation for the least cost, it then became necessary to find the attenuation which would produce the lowest system cost, that is, the lowest cost for a complete T2 line. The T2 line includes installed cables, regenerative repeaters, power stations and associated apparatus. With the crosstalk performance improved, the attenuation of the cable significantly affects the repeater spacing and thus the cost of the repeaters per unit length of line. As the attenuation is increased the number of repeaters required increases and therefore the total cost of repeaters goes up, but the cable cost decreases. Thus, an optimum attenuation exists. Finding the value of this attenuation was the subject of a system economic study. A description of the study is beyond the scope of this paper. However, the curves of cost versus cable attenuation shown in Fig. 5 illustrate some of the principles involved. On the cable cost curve the capacitance remains constant at 0.039 microfarads per mile for all values of attenuation; but, the conductor diameter and the cost decrease as the attenuation increases. The straight line for repeater costs reflects the fact that repeater spacing is inversely proportional to cable attenuation. The total costs show a distinct optimum at approximately 22 dB per mile, which is the nominal attenuation we have chosen for the 22 gauge, low capacitance cable. As mentioned previously, by reducing the repeater spacing and thereby increasing the repeater cost, standard 19 or 22 gauge PIC cable can be used for T2 lines. However, even though the new cable is more expensive than standard 19 and 22 gauge cable, it permits overall systems savings in most T2 applications.

Field Trial

A field trial of the T2 digital transmission line with the low capacitance cable is now in progress. A total of 76 kft of 50 pair cable has been installed aerially in Willow Grove, Pennsylvania. The associated electronic apparatus will be installed as it becomes available. The schedule calls for the line to be fully equipped by Jan. 1971. T2 lines will normally consist of buried cable but in the case of the field trial a strong incentive to observe the line under the large and rapid changes in air temperature dictated the choice of the aerial installation. In this trial, repeater spacings up to 15 kft are being used. The 15 kft represents the present estimate of the ultimate maximum allowable spacing.

Design Features

The insulating compound is expanded or foamed polypropylene copolymer. The expansion is in the order of 50% air by volume. Figure 6 shows a cross section of the conductor insulation. Average wall thickness is 26.5 mils and air cells are normally less than one mil in diameter. Expansion was achieved by using a chemical blowing agent.

The average coaxial dielectric constant, determined from the dimensions and capacitance monitor measurements, was 1.53. Because of the air space in the cable core the cable dielectric constant is somewhat smaller than the above value. Using the measured cable capacitance of 0.0385 microfarads per mile and the capacitance formula given in Reference 2, a cable dielectric constant of 1.35 is obtained. This compares with nominal values of 1.77 for PIC and 1.65 for pulp cable. The average interaxial spacing of the conductors of a pair as determined from low frequency inductance measurements was approximately 0.081 or 3 mils greater than the outside diameter of the wire (DOD).

The cable core consists of seven, 7 pair units and one interstice pair. The lay-up is shown in Fig. 7. Twenty-one different pair twists are used to make up three unique units. A 22nd twist is used for the 50th pair. As pointed out earlier, all pairs in adjacent units and within units have different twist lengths.

The sheath for the new cable was designed to minimize the likelihood of water entering the cable. The sheath is double jacket construction known as ARPAP.3 Starting from the inside then proceeding outward, this acronym signifies: Aluminum-Resinbond-Polyethylene-Aluminum-Polyethylene, Fig. 8. The use of two jackets substantially

reduces the probability of lightning damage. Adhering the inner aluminum tape to the inner jacket increases the moisture permeation time constant to the point where the accumulation of detrimental quantities of water in the cable core is negligible unless the sheath is damaged.^{4,5} This sheath was designed for buried construction.

Electrical Characteristics

Measurements of attenuation, crosstalk, and capacitance unbalance to ground were made on many experimental prototype cables and the field trial cable.

Attenuation characteristics of a typical prototype cable and the field trial cable are shown in Fig. 9. For comparison, the attenuation of standard PIC is also shown. The results indicate that the field trial cable exhibits slightly less attenuation than the experimental cable. Improvement in attenuation over that of standard PIC is due in a large part to the lower capacitance and higher inductance, however, there is also a significant reduction in high frequency resistance as a result of the greater space between conductors in the low capacitance design. The increased space reduces the proximity component of the high frequency resistance. This is an important advantage of the low capacitance design.

As mentioned previously, crosstalk is a function of twist length and physical separation of pairs. The twist arrangements used in the field trial cables are similar to those used in the prototype. However, because of delays in procuring machinery, a two-operation process was used for twisting the pairs and stranding the units for the field trial cable. The results are shown in Fig. 10 which is a plot of the power sum of far-end crosstalk versus the cumulative percentage of the pairs in the 50 pair cables. The power sum of crosstalk is the crosstalk which appears in a given pair as a result of coupling from all other pairs in the cable. The crosstalk characteristics of the field trial cable are not as good as those of the prototype. The field trial cable advantage over standard PIC is approximately 8 dB. The further advantage of the prototype cable may have been due in part to twisting and stranding in a single operation. However, the crosstalk is considered tolerable for the field trial. Work will be continued to meet the original objective of approximately 11 dB improvement over standard PIC.

The capacitance unbalance data are plotted on probability paper in Fig. 11. Note that only 3% of the pairs in the

prototype cable and 8% of the pairs in the field trial cable have capacitance unbalances greater than 100 $\mu\text{F}/1500$ feet, whereas 60% of the PIC cable pairs exceed this level. This means a substantial improvement in noise susceptibility with the low capacitance cable.

Summary

An entirely new cable has been designed for the T2 line. It features one half the attenuation of standard PIC cable, substantial improvement in capacitance unbalance, and approximately 11 dB (8 dB in the field trial cable) improvement in power sum crosstalk. These improvements are the result of the application of a number of new design and manufacturing techniques. Currently, the entire T2 line, including the new cable, is being tested at Willow Grove, Pennsylvania. The trial will last until mid-1971, during which time the cable performance will be continuously evaluated. Limited production for commercial use is expected to begin in 1971.

Acknowledgments

We extend our thanks to the people at Western Electric Company and to our associates at Bell Laboratories who contributed to the development of the cable.

References

1. Davis, J. H., "T2: A 6.3 Mb/s Digital Repeated Line," IEEE International Conference on Communications, June 9, 1969, Boulder, Colorado, No. 34, pp. 9-16.
2. Windeler, A. S., "Design of Polyethylene - Insulated Multipair Telephone Cable," A.I.E.E. Transactions, No. 46, Jan. 1960, pp. 736-739.
3. Bleinberger, W. E., "Aluminum Conductor Telephone Cable - A Reality," Wire Association Congress, Oct. 6, 1969, St. Louis, Missouri.
4. Hladik, W. M., "Accumulation of Moisture in a Plastic Sheathed Cable," Thirteenth Annual Wire and Cable Symposium.
5. Friesen, H. W., and Windeler, A. S., "Moisture Permeation and Its Effect on Communication Cable," Fifteenth Annual Wire and Cable Symposium, Dec. 7, 1966, Atlantic City, New Jersey.



David E. Setzer
Bell Telephone Labs
Murray Hill, N.J. 07974

Mr. Setzer received a B.S.M.E. in 1958 from Lehigh University, a M.S.E.M. in 1960 from New York University, and a Ph.D. in Applied Mechanics in 1964 from Lehigh University. He joined the Bell Telephone Laboratories in 1958 as a Member of the Technical Staff and remained until 1961 when he took a position as an Instructor of Mechanics at Lehigh University. In 1964 he rejoined the Laboratories. Mr. Setzer's early work dealt with the design and construction of the Telstar Earth Stations. Later, he engaged in experimental and theoretical studies of transmission through natural aerosols. He is presently working on improving electrical and mechanical properties of communication cables.

Alfred S. Windeler

Mr. Windeler joined the Bell Telephone Laboratories as a Member of the Technical Staff after his graduation from Rutgers University in 1930. He has been concerned with various aspects of cable design and development, including both multipair and coaxial cables. He was involved in the design and manufacture of the first transatlantic telephone cable. He is presently in charge of the Exploratory Cable Processes Group at the Bell Telephone Laboratories in Murray Hill, New Jersey.

Mr. Windeler is a member of IEEE, a Registered Professional Engineer in the State of Maryland, and a Telephone Pioneer. He is the author of a number of technical papers and articles, and holds five patents in the field of cable design, manufacture and testing.

OPTIMUM CAPACITANCE CONCEPT

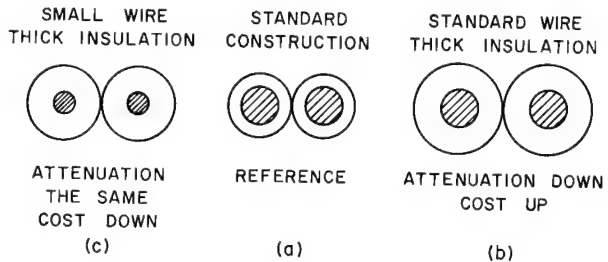


Fig. 1

CAPACITANCE VS COST FOR DIFFERENT COPPER PRICES

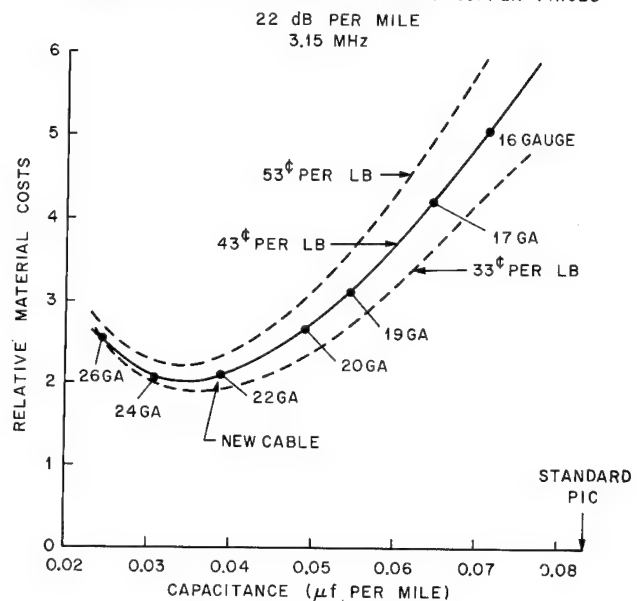


Fig. 2

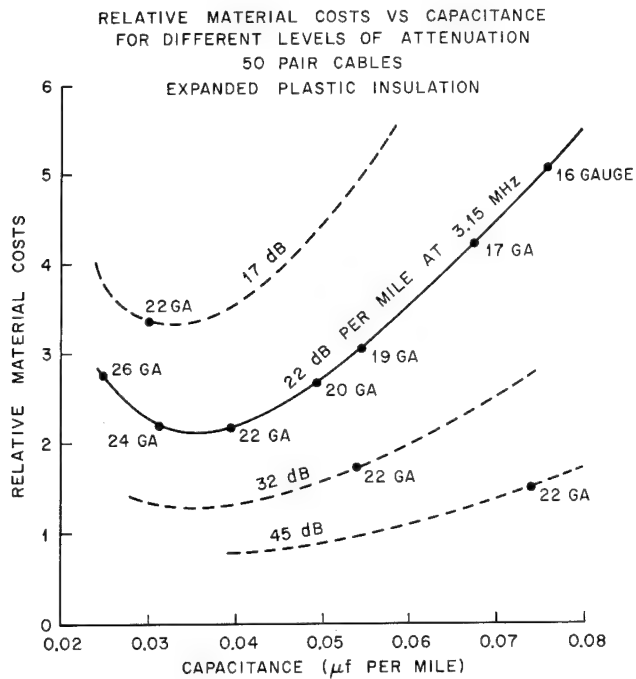


Fig. 3

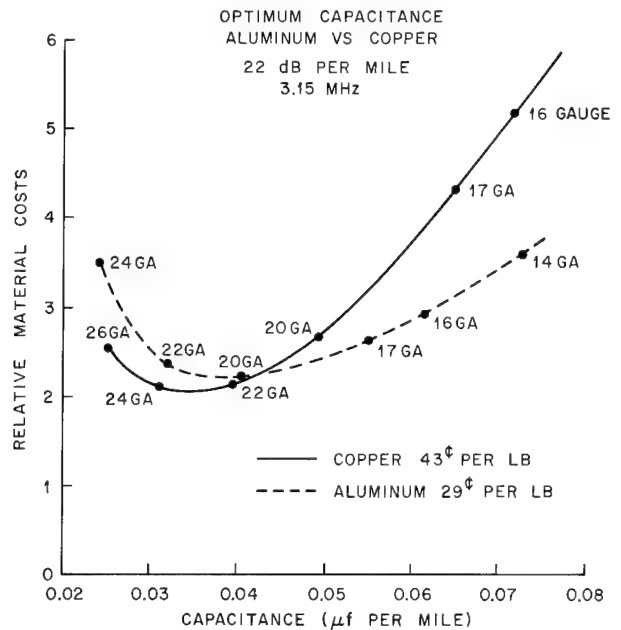


Fig. 4

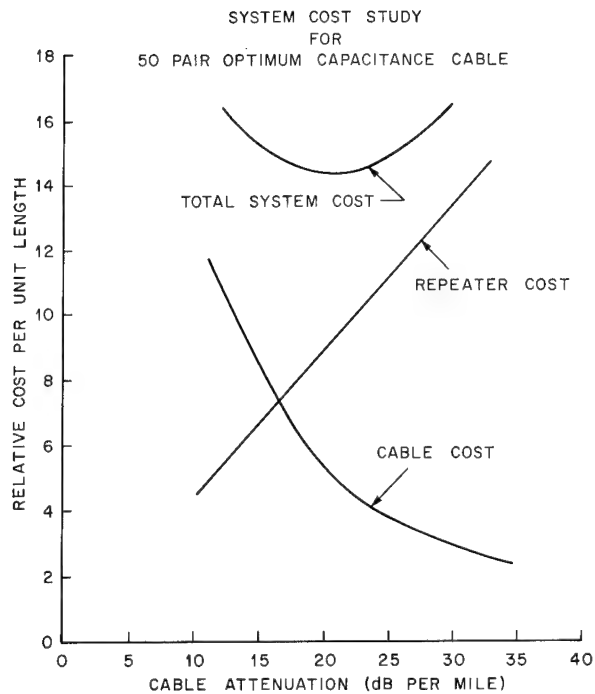


Fig. 5

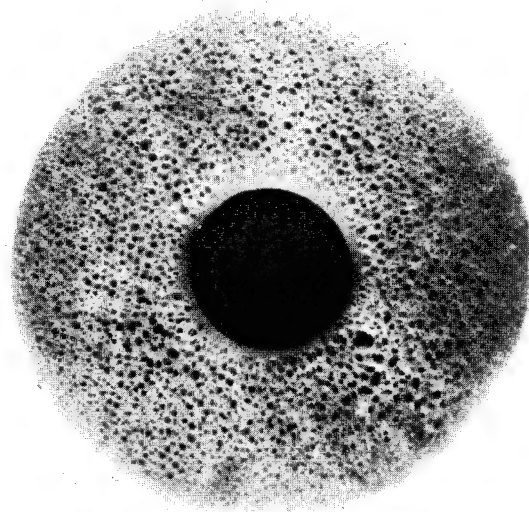


Fig. 6

50 PAIR CABLE DESIGN
EMPLOYING
3 UNIQUE UNITS (A,B,C)

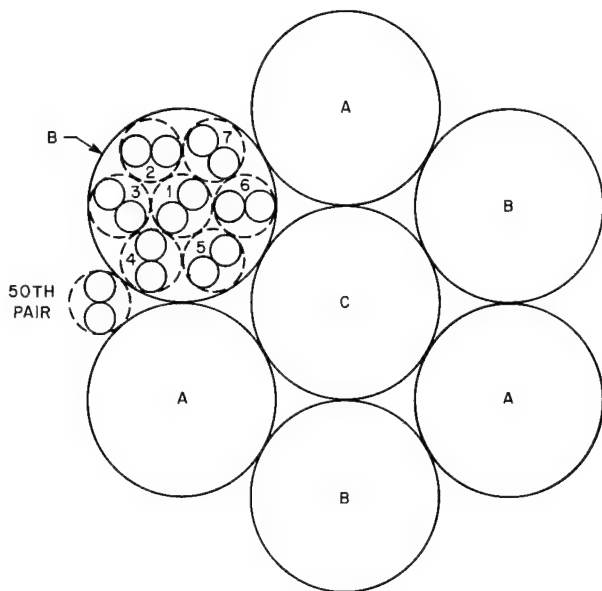
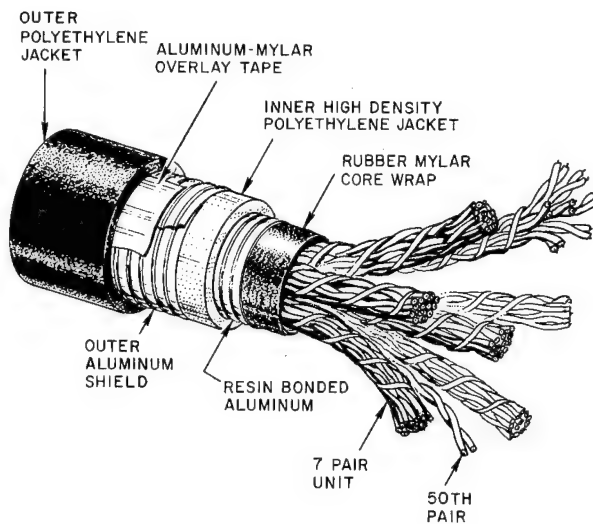


Fig. 7



THE CABLE

Fig. 8

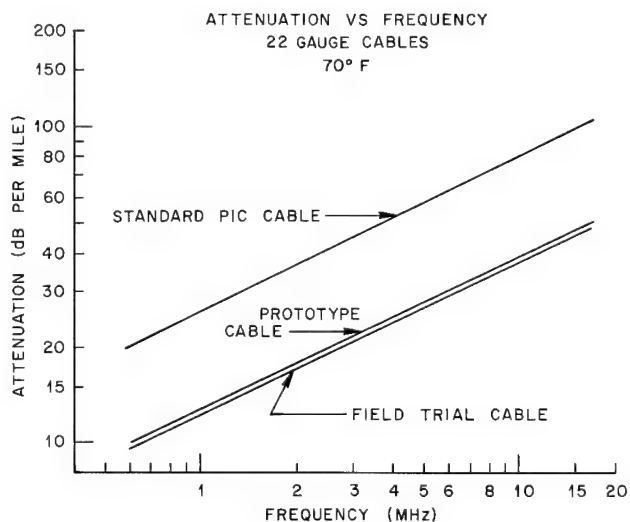


Fig. 9

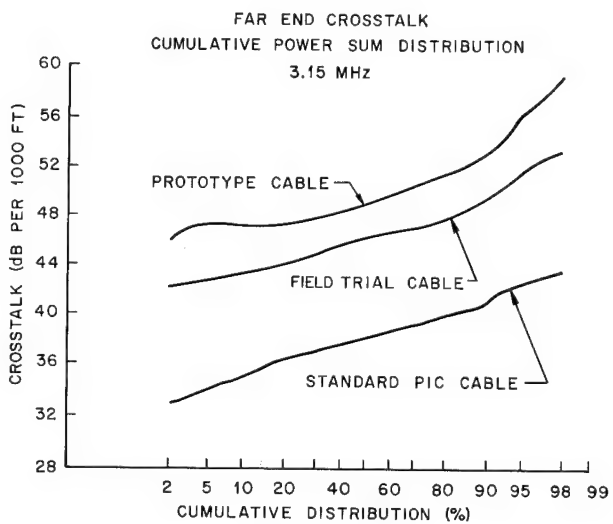


Fig. 10

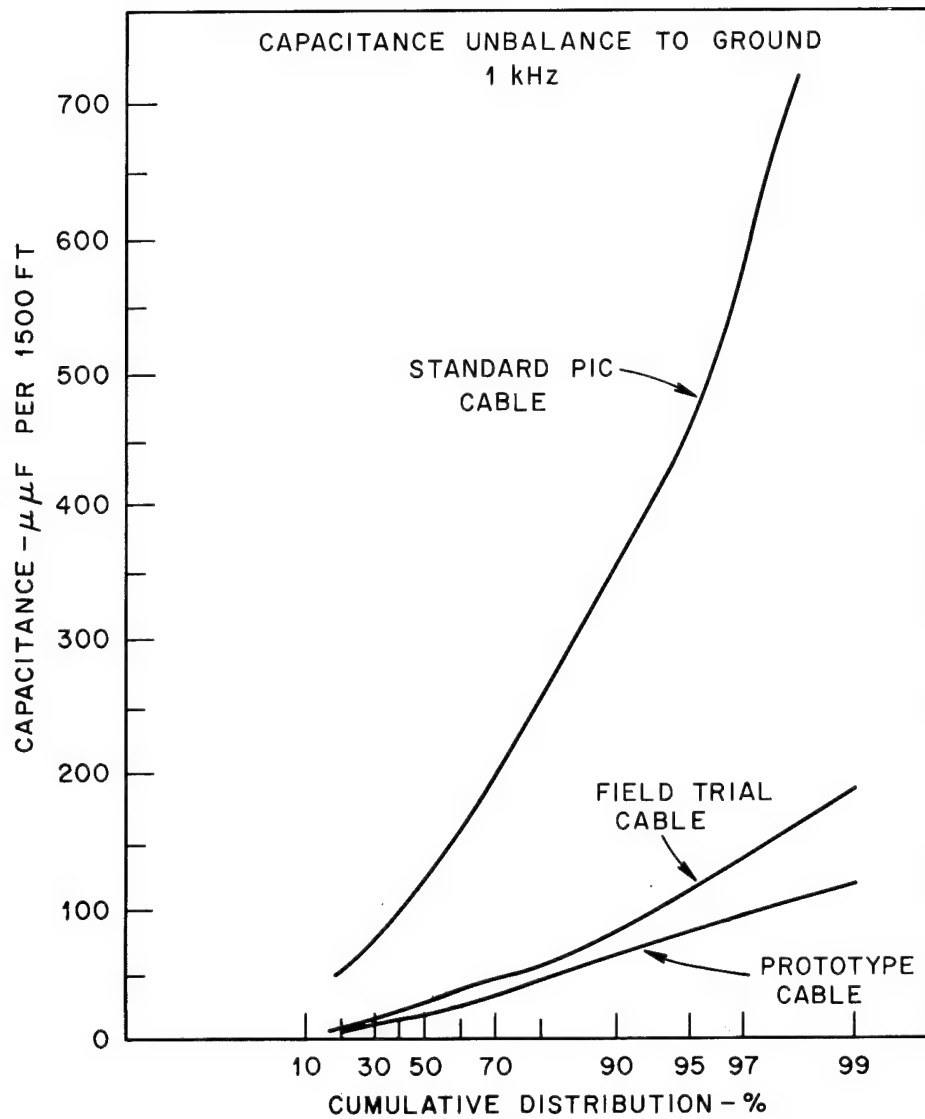


Fig. 11

MULTIPAIR CABLE SHIELDING FOR PCM TRANSMISSION

W. L. Roberts and F. N. Wilkenloh
Superior Continental Corporation
Hickory, North Carolina

The success of the pulse code modulation (PCM) technique, a fact made indisputable during the past several years, has encouraged review and reappraisal of existing cable designs. Operating characteristics of these cables have only been tolerated in conventional transmission system designs. A recent survey¹ projects domestic service by year end 1970 at about 700,000 PCM channels with more than 100,000 channels in operation in other countries.

In U. S. operating companies the terms PCM and T1 (the T1 Western Electric carrier system) have become practically synonymous² and, in the following discussion, this habit is further perpetuated. Where systems other than the T1 type are referenced, specific designations are indicated.

Though the T1 system was designed to operate over existing cable plant, contemplation of systems for new routes encourages cable design concepts offering improved cable performance for the specific application. The shielding concept described in this paper is a direct consequence of such considerations. Complete utilization of PCM systems on a single conventional multipair cable is limited because of near-end crosstalk (NEXT) performance of the cable pairs. Either repeater spacing or maximum number of operating systems (or a combination of the two factors) limits total system utilization. In this paper a method of removing the NEXT limitation on T1 repeater spacing is described in detail. An internal shield, or screen*, provides the performance improvement required for removal of this limitation. Though many shielding methods can provide the necessary circuit isolation, this particular technique achieves the required performance at a very modest cost.

In the following sections are described the experimental steps through which the screen design evolved. Calculation of the NEXT levels required to remove crosstalk limitations, results of measurements taken on various designs, and applications to systems other than T1 PCM are presented in detail.

Required NEXT Performance

Engineering requirements for transmission and crosstalk performance of T1 lines have been developed³ and utilized in "T" system planning.⁴

* Distinction between "shield" and "screen" may not be justifiable technically, but "screen" is used here to denote an electrical partitioning as differentiated from overall electrical protection offered by a "shield".

Error considerations stipulate a 10^{-7} error rate contribution by NEXT sources in a repeater section. Should the near-end crosstalk characteristics of the line be insufficient to assure the 10^{-7} maximum error rate (for more than 1 per cent of the sections), the repeater spacing can be decreased to reduce level differences between the two transmission paths. Taking this into account, along with the effects of multiple system interference, the following repeater spacing (line loss) is allowable:⁵

$$L = (m-\sigma) - 10 \log n - 26 \quad \text{dB} \quad (1)$$

where: L = mean line loss (dB)

m = mean NEXT at 772 kHz (dB)

σ = standard deviation of NEXT at 772 kHz (dB)

n = number of interfering systems

valid to within 0.2 dB for $6 \leq \sigma \leq 14$

In event of uncertainty regarding actual crosstalk performance (when applying a system to existing cable plant, for example), practical systems are designed applying equation (1) with a 6-dB safety margin.⁶

Ideally, the crosstalk performance of a cable would be sufficient to permit use of all of the pairs for "T" systems, while achieving a repeater spacing limited only by line loss considerations. Thus, for a 35-dB repeater spacing (at highest expected operating temperature) and allowing one pair to be reserved for alarm or supervisory use, the following $(m-\sigma)$ value for NEXT would be required:

$$(m-\sigma) \geq 58 + 10 \log (N-1) \quad \text{dB} \quad (2-a)$$

or, if the 6-dB safety margin is invoked,

$$(m-\sigma) \geq 64 + 10 \log (N-1) \quad \text{dB} \quad (2-b)$$

where: N = number of cable pairs

Equation (2-b) is graphed in Figure 1 (line A) showing required $(m-\sigma)$ NEXT performance for cables ranging from 3-pair to 400-pair sizes. If this criterion is met or exceeded, the cable can be operated with essentially 100 per cent T1 system fill and repeater spacing of 32 dB (at 55°F). Obviously, the physical spacing achieved will depend on the loss characteristics of the particular cable involved.

Far-End Crosstalk Considerations

It should be pointed out that far-end crosstalk couplings might limit repeater spacing in some instances. Though far-end couplings do not

limit T1 system spacing in conventional multipair cables, a very low-loss cable might allow such a long section that the total crosstalk coupling would become excessive. Using the method of Cravis and Crater,⁷ it can be estimated that far-end couplings would be limiting for multipair cables with conductors approximately 16 AWG and larger. This depends on the assumption that crosstalk coupling *coefficients* are no worse for coarse-gauge than for fine-gauge cables.

Shielding Improvement Estimates

In Figure 1 typical NEXT values achieved with multipair cable (22-AWG PIC) are shown as curves C and D. As may be noted, improvements in the order of 12 dB or so are necessary to achieve the required NEXT performance level (curve A).

Near-end crosstalk loss between cable pairs may best be considered in terms of the coupling factors resulting from capacitance unbalance and mutual inductance between the involved pairs. These were derived by Campbell⁸ and can be determined from

$$\frac{\Delta I}{I} = - \left[\frac{Y Z_o}{16} + \frac{Z}{4 Z_o} \right] e^{-2Yx} dx \quad (3)$$

where: $\Delta I/I$ = NEXT crosstalk current ratio for an elementary length

Z_o = characteristic impedance of the line

Y = mutual admittance unbalance

Z = mutual impedance unbalance

Y = propagation constant of the line

Near-end crosstalk has been shown by Cravis and Crater⁹ and others¹⁰ to vary with the 3/4 power of frequency (4½ dB/octave; 15 dB/decade). In equation (3) Y can be made practically zero as a result of elimination of pair-to-pair capacitance unbalance through screening. From Eager¹¹ it can be determined that elimination of pair-to-pair unbalance in multipair cable would improve high-frequency NEXT by only 3 or 4 dB, depending on pair combinations considered. The magnitude of the impedance unbalance term of equation (3) is typically in the order of two times the admittance unbalance term.

The attenuation of a magnetic wave passing through a metal shield is given¹² by

$$\alpha = \sqrt{\pi \mu g f} \quad \text{nepers/cm} \quad (4)$$

where: α = attenuation constant

f = frequency

μ = permeability of shield

g = conductivity of shield

Additional reductions should be realized through reflection losses at the screen-dielectric interfaces. The reflection loss depends upon the ratio between the radial impedance of the dielectric to that of the metal shield.¹³ The ratio can

be substantial: for first order magnetic waves, a value of 36 is obtained for aluminum and air at a frequency of 772 kHz where the screen is 0.10 inch from the pair. This would provide a reflection loss of about 18 dB, if the screen is not too thin electrically.

Use of concentric shielding, dividing the cable core into inner and outer groups, is a technique dating back at least to the early 1930's.¹⁴ This shielding technique has the potential of being applied simultaneously with the cable stranding operation, thereby appearing attractive cost-wise. As a first step toward the development of a suitable NEXT screen, experimental designs utilizing a concentric screen were fabricated and measured. A 25-pair 22-AWG PIC cable was selected as a convenient size for experimental purposes. The concentric screen was applied over a 12-pair core while the outer 13 pairs were stranded around the screen. The first versions (#2 and #3 in Table I) employed a 0.002-inch aluminum/0.005-inch polyester laminate screen, #2 being applied longitudinally, #3 wrapped helically. Both versions exhibited 772-kHz NEXT ($m-\sigma$) values about 16 dB better between compartments than the control (non-screened) versions #1 and #4. Reference to Figure 1, curves A and C, shows this improvement provides adequate performance to remove the NEXT limitation for one-cable operation.

Attempts to apply the concentric screen to a variety of cable core sizes revealed certain inflexibilities in design, especially for small pair counts. A method for dividing the cable core cross section into two arbitrary compartments was subsequently conceived and evaluated experimentally (Figure 2). This construction yielded NEXT performance comparable to that obtained with concentric screening. The screen, as viewed from the cable ends, forms an "S" or "Z" in section. The screen can be placed in the core as the pairs (or units) are stranded, dividing the core into any arbitrary grouping. The tape (screen) width is sufficient to allow a fold over at each edge to assure complete separation of the compartments. This concept has been given the commercial designation of T-Screen®. Patent applications on these concepts have been filed.

As may be judged from Table I, a wide variety of materials have been evaluated as candidate screens. An insulated aluminum foil has not only demonstrated a suitable electrical performance but it is also quite pliable and does not interfere with mechanical properties of the cable.

To assure an adequate NEXT performance margin, 0.004-inch aluminum has been made standard for the thickness of the screen material. From equation (4), for aluminum

$$\alpha = 2.63 t \sqrt{f} \quad \text{dB} \quad (5)$$

where: t = shield thickness (mils)

f = frequency (MHz)

An improvement of 9 dB at 772 kHz is predicted from equation (5). Additional reflection loss

improvements and reduction of crosstalk coupling through elimination of pair-to-pair capacitance unbalance accounts for the additional improvement obtained with this design. Pairs having very close proximity to the screen do not benefit from a substantial reflection loss, but elimination of pair-to-pair unbalance does provide several decibels improvement beyond that predicted by equation (5). Those pairs further removed exhibit improvement in crosstalk couplings from both screen attenuation and reflection effects. Reflections between the outer shield and the screen apparently reduce much of the shielding improvement expected from interface reflections. Reflection shielding improvement appears to be about 4 to 6 dB.

Analysis of the contribution of pair-to-pair capacitance unbalance to NEXT was assisted by Design #11 where a 0.006-inch carbon-filled cotton semiconducting tape was used for the screen. This tape would be expected to provide only a capacitive screen and the shielding improvement of only 6 dB (72 *versus* 66 dB [m-σ]) appears to verify the prediction of improvement through elimination of pair-to-pair unbalance.

An experimental design using a video magnetic recording tape screen was fabricated (Design #12). Shielding improvement was not as great as was anticipated, possibly explained by the unknown value of high-frequency relative permeability which, in fact, may not have been substantially greater than unity.

A bare metallic tape interposed between the pairs offers a tertiary path for dielectric breakdown between noncoincident conductor flaws and must therefore be provided with a suitable dielectric covering. This is considered necessary in spite of the fact that the screen is not grounded, but rather "floats" in service.

Further, measurements confirmed that the proximity of the screen to cable pairs affected transmission losses, increases of 5 to 10 per cent being observed in early experimental cables. A method was developed whereby a 0.002-inch embossed (corrugated to about 0.010-inch effective thickness) polyester tape is folded around the aluminum screen, providing both a dielectric barrier and a spacing function to eliminate proximity losses in the pairs. Measurements of mutual capacitance, capacitance unbalances, and high-frequency characteristics have verified that proximity effects are now reduced to 1 - 2 per cent maximum. Measured results taken on more than a million sheath feet of 22-AWG cables (6 pairs to 200 pairs) fit the following empirical equation for (m-σ) NEXT at 772 kHz:*

$$(m-\sigma) = 61 + 15 \log (N-1) \text{ dB} \quad (6)$$

Conservatively (considering the 6-dB margin) the required performance is achieved even for 3-

* These results (particularly on small cables) are slightly better than predicted by an earlier empirical equation taken from internal correspondence $(m-\sigma) = 47 + 23 \log (N-1) \text{ dB}$.

to 6-pair cable sizes (see Figure 1, curve B). At the other pair-count extreme, inclusion of the screen with unit-type cables eliminates the stronger couplings associated with adjacent units. The screen should provide adequate performance for large cables and, in fact, the slope of the T-Screen NEXT curve is steeper than the "NEXT Performance Required" curve (see Figure 1). Operating margin should thus improve for larger cables.

Cost associated with addition of the screen is quite reasonable. The additional cost for a small pair-count cable is about 10 per cent, decreasing to about 3 per cent for large cables. Figure 3 compares first cost for two-cable equivalents and T-Screen[®] relative to standard single-cable cost. These curves have been computed on the basis of cost differentials. It is recognized that anomalies may exist for certain cable sizes. These computations do not acknowledge any such discrepancies. The curves will be found to be a "best fit" to actual cost data even though individual differences may be noted. Initial cost studies generally prove-in T-Screen[®] operation. Annual cost considerations (and the more intangible aspects such as record administration) further favor this approach when repeater spacing comparable to two-cable operation is achieved.

Other Applications

This screening concept may be found useful for providing isolation between dissimilar carrier systems operating under a common cable sheath. It may be desirable, for instance, to operate frequency-division systems such as "N" carrier along with T1 systems either on a temporary or permanent basis. The resulting noise levels on the "N" channels may be intolerable unless additional isolation is available.

Figure 4 shows NEXT performance over a frequency range of 100 kHz to 4 MHz. As may be noted considerable isolation can be achieved over this frequency range.

To determine whether the shielding improvement would be adequate to permit common sheath operation, the interfering level of the PCM pulse stream must be determined. The PCM signal is represented by a probability density function¹⁵ from which the power spectrum can be calculated by use of the Fourier transform appropriate for the pulse. When computed for a 3-kHz noise bandwidth, a useful measure of interfering effect is obtained. Figure 5 is the result of this computation. Consideration of both Figure 4 NEXT levels and Figure 5 power levels allows evaluation of noise interference from T1 PCM signals on any FDM channel.

The repeater receive level on the highest frequency channel of N1 carrier (256 kHz) may be as low as -58 dBm,* with side bands about 12 dB lower. From Figures 4 and 5, the noise power level

* 0 dBm: 1 milliwatt across 600 ohms.

(1 per cent worst) coupled from a single PCM system would be -75 dBm (a signal-to-noise ratio of about 5 dB) on conventional cable. Use of the screen would improve this to -96 dBm ($S/N = 26$ dB). Without compandoring, the S/N ratio on the conventional cable obviously is not adequate. Even with compandoring, the S/N ratio would be questionable at low speech levels. Use of the screen should provide adequate margin, particularly if the compandor advantage is realized. If the interfering effect of the PCM energy can be assumed equivalent to that of white noise (thus 0 dBm = 88 dBm), idle noise levels would be about 13 dBm and -8 dBm respectively.

The method of the preceding example could be used to analyze other FDM/PCM or FDM/FDM combinations to determine if coordination of such systems would be made practical by use of the screened cable. Where crosstalk might arise, attention must be given to margins required to avoid intelligible crosstalk in addition to noise interference considerations.

If the particular application warranted, a core could be divided into more than two compartments by inserting an additional screen during the core unit stranding operation. For example, two PCM compartments and a compartment for FDM might be provided.

Transmission of Picturephone® signals on local exchange cables presents another possible application for the T-Screen® concept: Near-end crosstalk may limit amplifier (equalizer) spacing to intervals about 15 dB less than a full section in many instances.¹⁶ From Figure 4 the improvement in NEXT "1% worst" value for the screened version is greater than 20 dB at 1 MHz, the frequency for which crosstalk coupling would be greatest. Unless other restrictions prevailed, the screen would permit full equalizer spacing if the two transmission paths are kept separated by the screen.

Conclusions

T-Screen® offers a versatile, economical technique for improving PCM performance of multi-pair cable. In particular, NEXT restrictions for T1 operation on one-cable systems are removed.

Several early field trials were carefully monitored from in-process testing through installation and system operation. Operating characteristics in service proved stable and as predicted from measurements taken on factory lengths.

Over 2.5 million feet of cable ranging from 12-pair to 200-pair sizes have been manufactured and are now in service.

The continued growth of telecommunications and the resulting needs for new circuits will impose demands on all cables for transmission service carrying PCM, Picturephone®, data and other classes of signals. Use of the T-Screen® in all new exchange plant would add immeasurable

flexibility for future system planning and utilization.

Acknowledgments

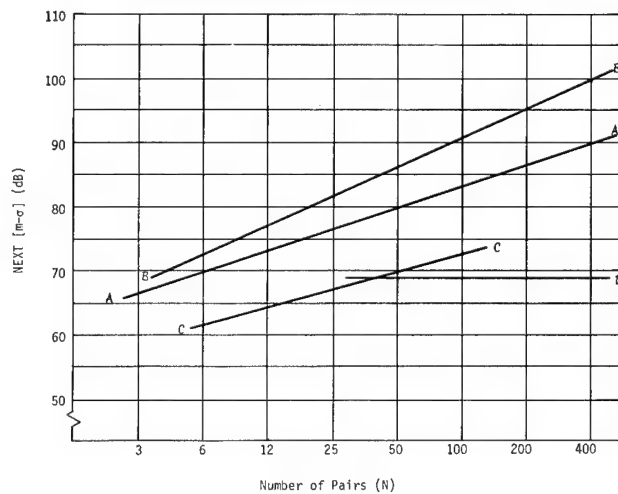
The authors wish to acknowledge the contributions of Messrs. Bruce Blackburn, John Micol, and Paul Wilson for their efforts in preparing experimental cables and compiling test data referenced in this paper.

References

1. W. Bucci, "PCM: A Global Scramble for Systems Compatibility," *Electronics*, pp. 94-102, June 23, 1969.
2. F. Boxall, *Pulse Code Modulation in Telephony*. California: VICOM, 1969, p. 2.
3. H. Cravis and T. Crater, "Engineering of T1 Carrier System Repeatered Lines," *Bell System Technical Journal*, vol. 43, pp. 431-486, 1963.
4. VICOM, "Repeatered Span Line Engineering, Installation and Maintenance," *VICOM T PCM Exchange Trunk Carrier System*, Part II, May 1968.
5. Cravis and Crater, *op.cit.*, pp. 431-486.
6. VICOM, *op.cit.*, p. 207.
7. Cravis and Crater, *op.cit.*, pp. 453-455.
8. G. Campbell, "Dr. Campbell's Memoranda of 1907 and 1912," *Bell System Technical Journal*, vol. 14, pp. 558-566, 1935.
9. Cravis and Crater, *op.cit.*, p. 466.
10. G. Eager, Jr., L. Jachimowicz, I. Kolodny, and D. Robinson, "Transmission Properties of Polyethylene-Insulated Telephone Cables at Voice Carrier Frequencies," *Communication and Electronics*, No. 45, p. 629, November 1959.
11. *Ibid.*, p. 630.
12. S. Schelkunoff, "The Electromagnetic Theory of Coaxial Transmission Lines and Cylindrical Shields," *Bell System Technical Journal*, vol. 13, p. 574, 1934.
13. *Ibid.*, p. 569.
14. H. Nyquist, "Concentric Shield for Cables," U. S. Patent 1,979,402, November 6, 1934.
15. M. Aaron, "PCM Transmission in the Exchange Plant," *Bell System Technical Journal*, p. 126, January 1962.
16. Bell Telephone Laboratories, *Bell Laboratories Record*, vol. 47, p. 172, May/June 1969.

FIGURE 1

Near-end Crosstalk (NEXT) Performance Requirement for 32-dB (at 55°F)
Repeater Spacing and (N-1)/2 Systems (100% Cable Fill)



- A. NEXT performance requirement for 100% T1 system cable fill, including 6-dB margin $[(m-a) = 64 + 10 \log (N-1) \text{ dB}]$
- B. NEXT characteristics 22-AWG T-Screen® type cable
- C. NEXT characteristics 22-AWG standard cable (measurements taken between same pair combinations as for curve B)
- D. NEXT between adjacent 22-AWG cable units

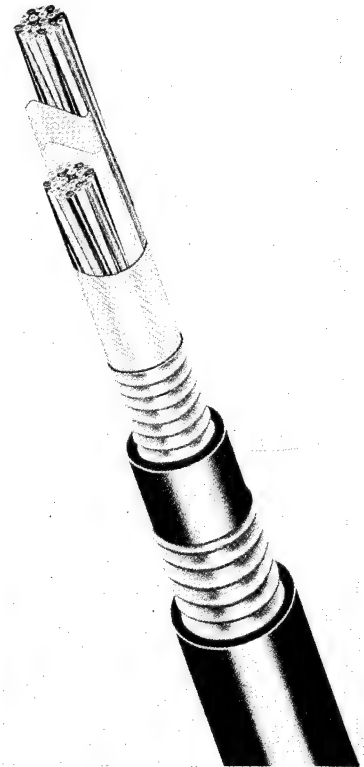
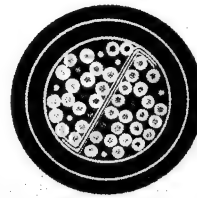


Fig. 2

FIGURE 3
Price Comparison

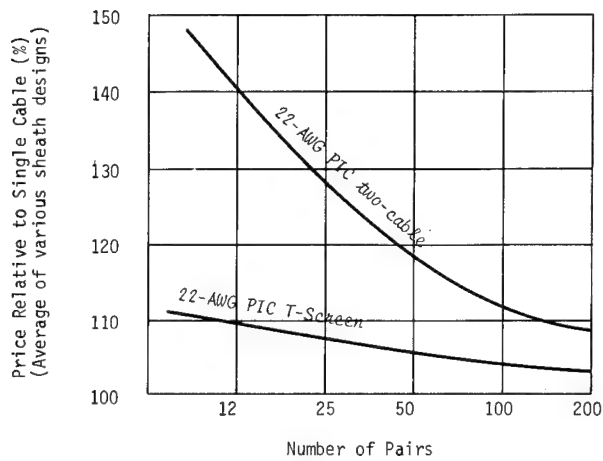


FIGURE 4
Near-end Crosstalk vs Frequency

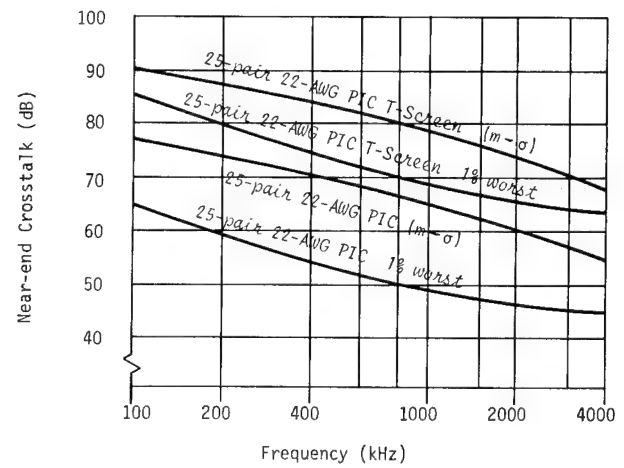
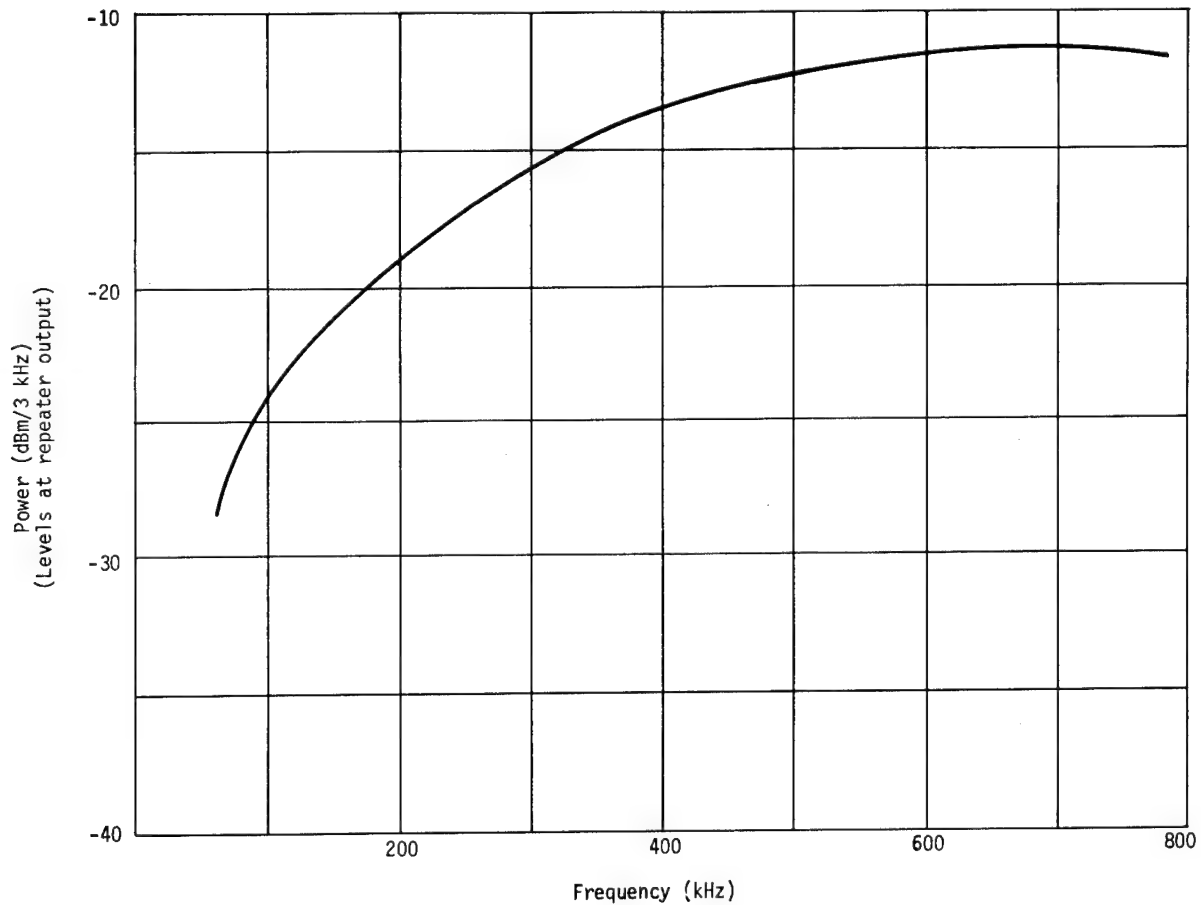


FIGURE 5
T1 POWER SPECTRUM





F. N. Wilkenloh
Superior Continental
Corp.
P.O.Box 489
Hickory, N.C. 28601

patents in the field of communication technology and has authored numerous technical papers for the AIEE, NCTA, IEEE, U. S. Army Signal Corps, and communications trade journals.

Frederic N. Wilkenloh was born in Atlanta, Georgia. He attended Davidson College and Lenoir Rhyne College, Hickory, N. C., where he received the A.B. degree in mathematics and physics.

He served in the U. S. Air Force from 1956 until 1960, when he became associated with Western Electric Company in field engineering assignments. In 1963 he joined Superior Cable Corporation as a laboratory technician, advancing to Research and Development Engineer, and to his present position of Manager, Wire and Cable Development for the Continental Telephone Laboratories.

A member of the Institute of Electrical and Electronics Engineers, Mr. Wilkenloh has authored various technical papers and has patents pending in the field of communication technology.

Walter L. Roberts -

Walter L. Roberts was born in Granite Falls, North Carolina. He was educated at Lenoir Rhyne College, Hickory, N. C., where he received the B.S. degree in chemistry and mathematics in 1956 and, after graduation, also completed requirements for a physics major.

He served in the U. S. Army from 1953 until 1955, when he became a chemist for the Shuford Mills, Inc., in Hickory, N. C. In 1956 he became associated with the Superior Cable Corporation, also in Hickory, as a laboratory technician, advancing to Research and Development Engineer, to Director of Research and Quality, and to Director of Research and Engineering for Superior Continental Corporation.

In January 1969, Mr. Roberts was elected a company officer as Vice President, Research and Engineering, and in May 1970, to the Board of Directors of the company.

A member of the Institute of Electrical and Electronic Engineers, the Society of Plastics Engineers, and the American Society for Testing Materials, Mr. Roberts is currently serving on the advisory board of the National Cable Television Institute. He holds a number of

TABLE I

NEXT Performance at 772 kHz — 25-pair 22-AWG PIC

Design	Description	Length (ft)	NEXT (m-a)
1	Control - no screen	970	66.1 dB
2	Concentric Screen - longitudinal 0.002" aluminum/0.0005" mylar	970	82.0
3	Concentric Screen - helical 0.002" aluminum/0.0005" mylar	1000	82.7
4	Control - no screen	1080	65.4
5	Screen - 1/8" x 0.002" aluminum	1090	76.2
6	Screen - 5/8" x 0.002" aluminum	1000	78.7
7	Screen - 3/4" x 0.002" aluminum	1000	79.7
8	Screen - 5/8" x 0.001" aluminum	1000	77.8
9	Screen - 5/8" x 0.001" aluminum	2000	77.0
10	Screen - 3/4" x 0.004" aluminum	1000	80.3
11	Screen - 5/8" semiconducting tape	2030	72.3
12	Screen - 1/2" video magnetic recording tape	2300	72.2
13	Screen - 5/8" x 0.004" segmented aluminum	1160	79.7
14	Screen - 5/8" x 0.003" copper	2050	80.2
15	Screen - 5/8" x 0.002"/0.001"/0.002" aluminum laminate	1700	81.0

NOTE: To correct NEXT (m-a) level to a limiting value for long lengths, subtract 1 dB from the value shown for 1000-foot lengths and subtract 0.1 dB for 2000-foot lengths.

DESIGN AND APPLICATIONS
OF
COAXIAL CABLE CARRIER SYSTEMS

S. J. Johnson - K. R. Bullock
Canada Wire & Cable Company Limited
Toronto, Ontario

J. D. Adam
Manitoba Telephone System
Winnipeg, Manitoba

SUMMARY

This paper describes the development of coaxial cable carrier systems using Type 174, Type 246 and Type 375 coaxial cables to satisfy a demand by the Canadian telephone industry for a short to medium haul communications facility. A brief history is given and advantages of coaxial carrier systems are reviewed.

Design details of the system are presented including the balloon/welded coaxial tube, hardware, line equipment, installation and splicing. The capabilities and various applications of these systems are discussed.

INTRODUCTION

Coaxial cable is recognized as having the capability to provide both traditional and proposed communications services, whether on long lines or short haul, to accommodate voice, data or television frequency spectrum requirements. The coaxial structure is one of the most versatile facilities that communication engineers have at their disposal in meeting current and future bandwidth requirements.

The full broadband potential of the coaxial cable as first described by L. Espenschied and M.E. Strieby of the Bell Telephone Laboratories¹ in 1934 has yet to be exploited nearly forty years later.

We should realize that the coaxial cable is a transmission medium not just for the present but for the future. Its unique characteristics will allow far greater exploitation than other forms of transmission such as balanced pair.

This paper deals with the development of one type of coaxial cable for use as a short to medium haul facility by Canadian telephone utilities. In writing this paper the authors have presented the combined viewpoints of a telephone operating company, the Manitoba Telephone Sys-

tem and a manufacturer, Canada Wire and Cable Co. Ltd.

COAXIAL SYSTEM EVOLUTION

Many previous papers have dealt with the evolution of coaxial cable systems and we will, therefore, not go into great detail here. However, a brief resume is necessary to provide a more complete picture of the need for our development work.

In North America the first field installation of a coaxial cable carrier system was installed in the United States in 1936 between New York and Philadelphia, by the Bell Telephone System². This cable contained two coaxial pairs of .267 in diameter, and was capable of handling 240 two-way circuits. It is interesting to note that it was over this cable that the first experimental television transmission in the United States was made in 1937. From this initial installation evolved the L1 coaxial system using .375 in coaxial pairs capable of handling 600 two-way circuits.

In the late 1930's European telephone administrations commenced using coaxial cable systems with .375 in coaxial pairs but with different frequency assignments and different repeater spacings than the L1 standardised by Bell Telephone.

At this point European and North American approaches to supplying toll telephone circuits tend to diverge. In North America long haul requirements were satisfied primarily by microwave and newer generations of the L1 system; namely, L3 with a capacity of 1860 channels and L4 with a capacity of 3600 channels, both on two .375 in coaxial pairs. Short to medium haul requirements were handled by carrier systems on open wire or multipair cables.

In Europe, however, because of shorter distances and higher population densities toll facilities have primarily been supplied by cable, in particular,

coaxial cable carrier and consequently, the selection of coaxial systems is more diverse in Europe than in North America.

In addition to the .375 in coaxial pair, a smaller more economical design, .174 in diameter, was developed in Europe to take advantage of the lower cost, lower power requirements and higher reliability of solid state equipment, which was being developed to supercede the original vacuum-tube designs.

The International Telegraph and Telephone Consultative Committee (C.C.I.T.T.) has standardized on 300, 600, 960, 1200 and 2700 channel systems for use with .174 in and .375 in coaxial pairs. All of these systems use one coaxial pair for each direction of transmission.

CANADIAN TELEPHONE UTILITY REQUIREMENT

In Canada in the early 1960's it was recognized that there was a need for a short to medium haul communications facility to provide branch spurs off the main microwave routes and to interconnect the new central dial offices which the telephone administrations were planning.

In the province of Manitoba (Figure 1) the Manitoba Telephone System has full responsibility for both exchange and toll telephone service. Manitoba is about 330 miles east to west and about 760 miles south to north amounting to about 250,000 square miles. The Manitoba Telephone System has 5200 route miles of toll structure and 25,000 miles of exchange plant servicing approximately 426,000 telephones.

In the late 1950's and early 1960's the Manitoba Telephone System similar to other Canadian utilities was forced into a restructuring of their toll networks due to growth requirements and obsolescence of open wire routes. Due to distance, population distribution and economics, this was mainly accomplished with microwave radio. Figure 2 shows the microwave network in Manitoba which totals approximately 2500 miles.

In addition to the main long haul toll reconstruction, many short and medium haul secondary routes and entrance links to new dial offices required expanding. Coaxial cable was chosen as the transmission medium to provide these facilities because:

- a) coaxial carrier systems can interconnect with radio multiplex at

baseband frequencies.

- b) coaxial cable provides a high quality extended bandwidth suitable for future services such as data transmission.
- c) coaxial cable carrier systems can be increased in channel capacity as demand requires.
- d) reliability and performance of coaxial cable carrier systems are very high as a result of solid state electronics, modern cable manufacturing techniques and proper installation practices.

SYSTEM DESIGN

Historical Background

In 1950 the French telephone administrations first studied designs for smaller size coaxial pairs than the .375 in disc-insulated type which had been used for fifteen years. Impetus was given a few years later to this proposed new design due to the economical improvements which could be realized due to the development of transistorized amplifiers. Because of lower cost, better noise performance and higher reliability the number of solid-state repeaters in a system could be increased and the cable size decreased, particularly for systems with small channel capacities.

In 1960 Fuchs and Vergès^{3,4}, described their "Balloon" insulation development and Bélus⁵ described its application to the .174 in coaxial design, which has had such good acceptance in France. In 1961 C.C.I.T.T. Red Book Volume 3 carried recommendation G341 covering a 300 channel coaxial system and G342 specified the basic parameters of the .174 in (1.2/4.4mm) coaxial pair. The British Post Office also proposed a specification in 1961 based on the C.C.I.T.T. recommendation but with tighter impedance tolerances. In 1963 Foord⁶ described another type of .174 in coaxial pair development and in 1964 Allan⁷ outlined the evaluation work conducted by the British Post Office, summarising data on the four different types investigated.

It was in 1966 that Canada Wire and Cable Co. Ltd. adopted the "balloon" type dielectric as developed by Societe Anonyme Télécommunications (S.A.T.) of France in conjunction with the Minewema welding process from Kabelmetal of Germany for seam welding the copper outer

conductor⁸.

In marrying these two processes we believe we have produced a coaxial tube whose characteristics and parameters are ideally suited to North American requirements.

Design Philosophy

The basic philosophy involved in designing composite cables incorporating coaxial tubes centered on the need for a cable construction that would be suitable for Canadian conditions encountered during direct burial, aerial or duct installations. Thus the emphasis has been on constructing a rugged facility with maximum protection against water ingress into the coaxial pairs if sheath damage occurs during or after installation.

In most countries it has been, and still is, the practice to look for maximum moisture protection in the form of extruded lead, extruded aluminum or stalpeth sheaths. By utilizing a seam welded design for the coaxial pair, in contrast to existing types which utilize butted or crimped outer conductors which are not hermetically sealed, we believe that standard plastic telephone sheaths could be utilized as they have a proven history of reliability. More so, in the last few years with the development and application of sheaths consisting of extruded polyethylene jackets bonded to a polymer coated aluminum or copper shielding tapes an even greater degree of reliability from external moisture ingress can be expected.

Another feature of the seam welded coaxial pair is the mechanical reliability which is so important in the cable core assembly stage of manufacture as well as in the ploughing operation associated with direct burial in the ground. Ploughing trials followed by several years of experience gained in installations in many parts of Canada have confirmed these points.

The Type 174 Coaxial Pair

The coaxial pair consists of a centre conductor of solid soft bare copper .047 in diameter, over which is extruded the balloon-type dielectric consisting of a thin (0.015 in) tube of natural low density polyethylene.

The polyethylene tube is crimped down onto the conductor at intervals of about

0.75" by endless belts specially shaped to mold the plastic insulation. The crimps also provide effective seals between balloons and prevent moisture passage along the core.

The excellent uniformity, which is obtained with the crimped polyethylene balloon insulation is obtained as a result of the unique belt design which has been described in previous papers by Fuchs and Verges and by Belus. This results in very close control of the capacitance of the insulated conductor and contributes to the high order of impedance uniformity.

The outer conductor consists of a 0.007 in soft copper tape longitudinally formed in a tube over the dielectric and the butted edges welded. The tape is welded oversize and then swaged down over the dielectric to produce a tight fit. Because the swaging operation can be controlled to very tight diameter tolerances, it is possible to obtain a very high degree of impedance uniformity.

Electromagnetic shielding is provided by two copper-clad mild steel tapes 0.0035 in thick helically applied in opposite directions over the outer conductor. This construction was chosen to provide maximum shielding between the coaxial pairs at the lower carrier frequencies.

Over the shielding tapes either a polyester tape or an extruded polyethylene jacket is applied along with a coloured identification tape.

The choice of protection over the coaxial pair will depend on the dielectric strength requirements stipulated. Figure 3 shows the construction of a typical coaxial pair.

Composite Cable Assembly

The coaxial pairs may be utilized alone in a cable or as is more common in conjunction with a number of polyethylene insulated twisted pairs. Figure 4 shows a typical composite coaxial cable. In designing a composite cable containing coaxial pairs and twisted pairs care has to be exercised in laying up the components so as to obtain a circular core and maximum use of the cable cross-section. Further, placement of components and cabling lays, have to be carefully selected to ensure that the cable can be installed with minimum effect on the electrical characteristics.

To prevent excessive torque damaging the coaxial pairs, cabling of composite cables should be performed with a planetary type of cabler where the bobbins float during rotation in the vertical plane.

Sheath

The sheaths chosen for composite cable constructions containing coaxial pairs are of the standard Alpeth and PAP type incorporating the CPA (coated aluminum tapes bonded to a polyethylene jacket) feature for direct burial applications; where gopher or additional mechanical protection is required a GP sheath consisting of a flooded 0.006 in longitudinal overlapped steel tape and overall polyethylene jacket is applied. Details of the sheath construction are shown in Figure 4.

The Family of Coaxial Cables

Type 375

Following the success of the Type 174 coaxial cable the large bore Type 375 coaxial cable was developed using the balloon/welded technique. The .375 in balloon insulated coaxial was originally developed in France in 1961 and used a folded butted copper outer conductor. We produced the combined design of balloon insulation and seam welded copper outer conductor in 1968.

The Type 375 balloon/welded coaxial cable meets the C.C.I.T.T. recommendation G.334 and in some areas is better. Of particular interest is the impedance tolerance. G.334 recommends an impedance of 75 ± 1 ohm.

The Type 375 balloon/welded coaxial tube has an impedance of 75 ± 0.25 ohms. The smaller impedance deviation does not necessitate stringent matching procedures when splicing cables in the field. Table 1 gives a comparison of CCITT recommendations and the standard electrical characteristics of balloon/welded coaxial tubes.

Type 246

There was also a demand in Canada for a medium bore coaxial cable which led to the development of the Type 246 coaxial pair which allows for optimization of the economics of some coaxial cable carrier systems. The Type 246 coaxial pair is not a C.C.I.T.T. standard but impedance tolerance and impedance regularity are within the C.C.I.T.T. recommendations.

Table 2 gives a comparative summary of the pertinent characteristics of the family of three coaxial pairs. Figure 5 gives the attenuation curves of the three coaxial pairs. Statistical distribution of the impedance deviation and impedance regularity (worst echo) are shown in Figures 6 and 7 respectively.

Splicing of Coaxial Pairs

The Type 174, 246 and 375 coaxial pairs can be spliced length to length with standard accessories developed especially for the purpose. Figure 8 shows a typical Type 375 splice including all components. The conductor splice is made by soldering a split, tinned copper sleeve which is placed over the two butted conductors. Teflon inserts support the outer conductor. A teflon sleeve is slipped over the conductor joint, and overall is placed a tinned sleeve which is soldered to the outer conductor at each end. The steel tapes are restored to position over the joint to maintain shielding between coaxial pairs within.

An important feature of the splice is that by soldering the ends of the solid outer conductor sleeve the coaxial pair splices are made water and moisture proof. Further, the splice is of rugged construction and introduces minimum impedance discontinuity.

Coaxial Cable Splices

Initial installations of these systems were designed to offer ready access at splice points for test and maintenance purposes using surface pedestals. However, experience has indicated that these features are not of great importance and pedestals are susceptible to many forms of damage and water ingress. Although experience to date has been satisfactory, because toll carrier systems require complete security and protection, work is continually progressing on developing improved splices. Buried splices have been used effectively in some systems and provide a means of complete interment of the transmission facility. They are less expensive than pedestal splices and introduce less electrical discontinuities into the transmission path.

Table 1
Electrical Specifications of Coaxial Pairs

	<u>C.C.I.T.T.</u> <u>Recommendations</u> ⁹		<u>Balloon/Welded</u> <u>Specification</u>		
	<u>0.047/0.174 in</u> <u>1.2/4.4 mm</u>	<u>0.104/0.375 in</u> <u>2.6/9.5 mm</u>	<u>Type</u> <u>174</u>	<u>Type</u> <u>246</u>	<u>Type</u> <u>375</u>
<u>Nominal Impedance-ohms</u>	75 *	75 **	75 *	75 *	75 **
<u>Impedance Tolerance-ohms</u>					
Telephony	± 1.5	± 1.0	± 0.5	± 0.5	± 0.25
Video	± 1.0	± 1.0	± 0.5	± 0.5	± 0.25
<u>Impedance Regularity ***-dB</u>					
Telephony					
- 100% better than	45	50	45	45	50
Video					
- 100% better than	48	50	48	48	50
- 95% better than	-	54	-	-	54
- 80% better than	54	-	54	54	-
<u>Dielectric Strength</u>					
Vdc for 1 minute	1500	-	1500	2000	-
Vdc for 2 minutes	-	2800	-	-	3000
<u>Insulation Resistance</u>					
megohm - miles min	3100	3100	8000	8000	8000

* Measured at 1 MHz.

** Measured at 2.5 MHz.

*** Measured with a sine-squared pulse with half-amplitude duration no greater than 100 nanoseconds.

Table 2
Characteristics of Type 174, 246, 375 Coaxial Pairs

<u>Type</u>	<u>Centre</u> <u>Conductor</u> <u>Diameter (in.)</u>	<u>Outer</u> <u>Conductor</u> <u>I.D. (in.)</u>	<u>Outer</u> <u>Conductor</u> <u>Thickness (in.)</u>	<u>Nominal</u> <u>Impedance</u> <u>ohms</u>	<u>Nominal</u> <u>Attenuation</u> <u>dB/1000'</u>
174	.047	.174	.007	75 *	1.61 *
246	.065	.246	.007	75 *	1.14 *
375	.100	.376	.010	75 **	1.15 **

* at 1 MHz

** at 2.5 MHz

Terminating Coaxial Cables

The coaxial and voice frequency pairs are normally terminated in an aluminum gland which is suitable for office terminations or repeater entrances. The coaxial pairs are terminated in BNC coaxial connectors while the voice frequency pairs are terminated in multi-pin connectors. All the connectors are embedded in an epoxy resin filling. This method facilitates direct connection with leads from the repeater or terminal equipment.

Repeater Housing

Repeaters are installed in pre-cast concrete manholes because of the severe climatic conditions and the need for ready access. Work, however, is continuing, on less massive structures to house repeaters such as sub-surface hand-holes.

PRESSURIZATION

It has been standard practice to pressurize composite coaxial carrier cables utilizing the interstices of the core for air passages. The loss of pressure in the cable is used as an indication of sheath damage during and after installation. Repeater housing cabinets have been pressurized using static pressure. At splices; pressure has been carried through, while at pedestals a by-pass has been utilized around the pedestal.

Installation

The Type 174, 246 and 375 coaxial cables have been designed for installation in ducts, trenches, aerially or ploughed directly in the ground. The cables are installed using standard telephone utility practices with some additional precautions particularly during manhandling. Experience to date has indicated that the cables are less susceptible to damage when installed by properly operated equipment such as a plough than when manhandled by construction crews. Most cables for rural toll routes have been ploughed. Depth of ploughing is normally about 3 ft.

The minimum bending radius during installation is 16 times the cable diameter. During any form of installation

the cable should be paid off reels at a steady rate and preferably from trailers which have reel braking devices. This will prevent excessive strain being applied to the cable as well as over-running.

Where buried splices are being used, they should be offset from the main line of the cable so as to minimize strain at the entrance point of the cable into the splice closure.

Line Equipment

Although there were several European sources of line equipment available, it appeared obvious that we should also have a domestic supplier who could design and manufacture the necessary equipment specifically for Canadian climatic conditions, and telephone utility practices and requirements. Numerous North American suppliers had the necessary terminal line equipment which could be used for coaxial wire line entrance links (WLEL) but there was not available a remotely powered repeater capable of being installed underground to operate over Type 174 coaxial tubes.

Equipment for use in Canada has to be capable of operating under the most adverse conditions. Temperatures in the prairie provinces can range between -40°F in the winter and +100°F in the heat of the summer. However, 3 ft. below grade the annual temperature swing is only 25° F to 60°F.

Lightning surges and high voltage potentials from power lines require that both primary and secondary protection be provided on both the coaxial pairs and the twisted pairs.

Lenkurt Electric, Vancouver, took on the project and developed line transmission equipment to complement the Type 174 coaxial cable which they designated 46C. The system uses two coaxial pairs, one for each direction of transmission.

The 46C system is expandable from 300 to 600 to 720 channels and meets the C.C.I.T.T. recommendations and Bell System Specifications. Redundant protection is provided by the use of identical parallel amplifiers for both transmit and receive directions. Remote repeaters are powered over the centre conductors of two coaxial tubes.

Five 60 channel supergroups provide 300 channels in the 60 kHz to 1300 kHz frequency range. Ten or twelve supergroups provide 600 or 720 channels in the

60 kHz to 3084 kHz range. The equipment is also compatible with Type 246 and 375. As the coaxial pair loss curves are parallel (Figure 5) the repeater designed for each system capacity can be used with all 3 coaxial pair sizes.

SYSTEM CONCEPTS

In the preceding section we have dealt with the development of the individual components which make up the system. Behind the process of development of each stage there were several concepts which were used as basic criteria.

Simplicity was of prime importance because of the desire to introduce as few new practices and procedures as possible. For instance, the splicing of the coaxial pairs can be accomplished with the standard tools found in a splicers tool bag with the addition of a small sizing tool. Other than a few precautions related to the manhandling, the cable can be installed in ducts, trenches or ploughed using standard telephone practices.

Quality of materials and manufacture was, of course, always of utmost importance. The copper tape used for the welded outer conductor is an example. The copper is a high conductivity low oxygen content grade produced to very exacting tolerances for chemical composition, thickness, conductivity and surface condition.

Costs of components were, of course, kept to a minimum but often took second place to quality. The concept of simplicity aided in maintaining economical designs.

Versatility and flexibility of components was desired because of the many different applications of the system.

There are several features of the cable design which we feel are important enough to make special note.

1. As a result of welding the copper outer conductor each coaxial tube maintains its own moisture and vapour protection. Studies by Canadian telephone utilities^{10,11} indicate that direct buried cable is susceptible to sheath damage during and after installation with consequential ingress of water into the cable core. As each individual coaxial tube is sealed, carrier transmission characteristics will remain unaffected by water entering the cable core due to external sheath damage.

2. The welded outer conductor provides the coaxial tubes with a high degree of ruggedness and mechanical strength which would not otherwise be obtainable with a non-welded outer conductor. This can prove to be advantageous during the manufacturing process and subsequent installation.

3. Because during the welding process the outer conductor is swaged down onto the dielectric, the inside diameter of the outer conductor can be controlled to very small tolerances. This results in very close control over the transmission parameters of the coaxial pair as evidenced by the impedance distribution given in Figure 6. Matching of lengths of composite cables or individual tubes at splice points is not necessary in order to meet impedance regularity requirements.

One interesting feature of which advantage has been taken by the Manitoba Telephone System is the combination of polyethylene insulated pairs for rural distribution and coaxial pairs for toll requirements within the same cable. Each facility can be used and developed independently of the other. The shielding characteristics of the coaxial pairs also allow rural carrier to be applied to the twisted pairs without the usual concern about conflict with toll carrier.

The combination of facilities within the same cable has made it necessary for the Manitoba Telephone System to develop some new practices with respect to splicing and loading. D66 loading is applied to the twisted pairs every 4500 feet. At these points and at repeater locations the rural distribution pairs are taken to a pedestal of their own via a Y splice. This practice then physically separates maintenance of the rural distribution facility from the more complicated toll facility.

One additional procedure is that rural subscriber services are only extracted at reel ends where there is a splice. It is not realistic to add discontinuities to the coaxial transmission path by looping it in and out of a pedestal just to provide telephone service to a customer en-route. Some paralleling of the main cable from reel ends does result. It follows, that where the density of subscriber requirements is sufficiently heavy, separate toll and rural distribution cables are preferred.

Operating Systems

Since production commenced on the Type 174, 246 and 375 coaxial cables,

close to 1,000,000 feet of route cable has been supplied to systems across Canada. Figure 9 provides a list of the various systems, their channel capacities and length.

The majority of cable, (in the order of 90%) was ploughed directly in the ground. The Baddeck and Shelburne systems are both completely aerial. Portions of other systems are aerial, in duct or installed by trenching.

One system of particular interest was the Neepawa-Eden system in north west Manitoba. The overall length was approximately 40 miles with a capacity of 300 channels. Two Type 246 coaxial pairs were used with the number of voice frequency interstitial pairs varying depending on the local distribution requirements. The equipment was Lenkurt's 46C. Table 3 gives specification and measured system parameters. Figure 10 shows a schematic of this system.

Table 3

Transmission Parameters

Neepawa-McCreary Coaxial Carrier System

	<u>Speci- fication</u>	<u>Actual Test Data</u>	
Nominal Bandwidth-kHz	60-1300	60-1300	
Frequency Response*-dB	±1	+.5	
Maximum		-.6	
Near End Crosstalk-	-60	-62.5	
-dB maximum			
Noise Performance			
pw/km maximum**	3	N-S	S-N
70 kHz		1.4	1.2
534 kHz		2.0	0.6
1248 kHz		1.1	0.6

* Reference level at 700 kHz

** White noise loading level + 9.8dBmO

N-S - North to South

S-N - South to North

Figure 11 shows a repeater housing in a manhole with the cable entrance gland in the foreground.

Other Applications

Originally the Type 174, Type 246 and Type 375 coaxial cables were

developed to meet the demand for short and medium haul 300/600 channel capacity telephone carrier systems. However, the flexibility and versatility of the coaxial structure has allowed many other types of systems and applications to evolve. The equipment manufacturing companies have developed and are producing at present a wide selection of line equipment for a broad range of system capacities. Figure 12 gives a listing of the more popular system capacities with their respective repeater spacings. With 3 coaxial pair sizes to choose from in any complement of 2 to 20 pairs in a cable and numerous equipment capacities available, the communications systems engineer is able to optimize performance and economics for his particular set of conditions.

Further, most systems are capable of expansion by replacing plug-in modules in existing equipment and adding repeaters at the midpoints of those already installed.

For example, referring to Figure 12 by choosing a 300 channel Type 174 system with a repeater spacing of 5.0 miles, the system capacity can be increased to 960 channels by adding repeaters at the midpoints to give a spacing of 2.5 miles. By halving the repeater spacing again to 1.25 miles, the capacity can be increased to 2700 channels.

A 120 channel Type 174 system with a repeater spacing of 7.4 miles can be increased to 300 channels or to 1260 channels by placing additional repeaters at 3.7 mile or 1.85 mile spacings respectively.

This expansion capability of coaxial carrier systems allows for installation of initial capacity as needed and for additional capacity as demand for circuits grows.

Coaxial carrier systems are not restricted to use solely by telephone administrations. The broad selection of system capacities, the versatility and unique advantages of this medium of transmission make possible other applications such as pipeline and railroad communications, signaling and control. Coaxial cable systems are ideally suited as the means of providing communication facilities for these two industries because of the existing right-of-way available for cable placement. On a pipeline the coaxial cable may be placed in the same trench as the pipe with consequential installation cost savings. Or if so desired, the cable can be ploughed directly in the ground a short distance from the pipe, but still on the pipeline company easement. In the case

of the railroad, ploughs are available which can be mounted directly on a flat car allowing for cable placement in the roadbed. If there are too many track-side obstacles, or if the rail line is busy necessitating excessive delays in progress, there is sufficient width in the railroad easement to allow for direct ploughing using a standard tractor-plough arrangement.

Channel extraction units provide a means of access to groups of channels in the coaxial system at any location on the route. Although not available on all types of systems, they provide a simple and economical feature which pipeline and railroad companies can use to great advantage.

One very important feature which is often overlooked is that no government regulatory body authorization is required to install or privately use a coaxial cable carrier system. The owner has complete freedom of choice as to capacity, utilization and expansion.

Future Development

Because of the unique features of coaxial cable carrier systems, the demand for these facilities is on the increase.

Utilization of modern technology has provided improvements in both reliability and cost so that on a per channel cost basis, these systems are proving to be economically competitive with other forms of transmission.

Development of new coaxial systems are already in progress to take advantage of the extended bandwidth and inherent self shielding characteristics of the coaxial structure. In Europe and Japan 60 MHz, 10,800 channel systems are in the process of being developed as well as long haul high capacity Pulse Code Modulation (PCM) systems for telephony and video transmission.

Acknowledgements

The authors would like to acknowledge the assistance of many of their associates in writing this paper. Appreciation is also extended to Lenkurt Electric Co. of Canada Ltd., Vancouver; Cable Communication Systems, Inc., New York and Siemens Canada Ltd., Montreal for their assistance.

References

1. Systems for wide-band transmission over coaxial lines
- L. Espenschied and M.E. Strebby
- Bell System Tech. Journal Vol 13 1934 pp 654 - 679
2. A million cycle telephone system
- M.E. Strebby
- Bell System Tech. Journal Vol 16 No 1 1937
3. Isolation tubulaire balloon de polyéthylène pour câbles téléphoniques
- G. Fuchs et P. Vergès
- Câbles et Transmission Vol 14 No 2 April 1960 pp 113 - 131
4. New low-loss "balloon" type polyethylene insulation for telecommunication cables
- G. Fuchs and P. Vergès
- 9th Wire & Cable Symposium Asbury Park, N.J. Dec. 1960
5. La paire coaxiale de 1.18/4.43mm normalisée pour câbles à grande distance
- R. Belus
- Câbles et Transmission Vol 14 No 4 October 1960 pp 294 - 306
6. Recent development in small-core coaxial cable
- S.G. Foord
- 12th Wire & Cable Symposium Asbury Park, N.J. Dec. 1963
7. Small diameter coaxial cable developments
- S.F.G. Allan
- POEEJ Vol 57 Pt 1 April 1964 pp 1 - 8
8. Application of welded thin metal in new communication cable designs
- J.D.A. Busby, G. Lehnert, L.E. Marrin, J.V. McBride, D.R. Stein
- 15th Wire & Cable Symposium Atlantic City, N.J. Dec. 1966
9. C.C.I.T.T. Recommendation G.331 and G.342 White Book Vol III Mar del Plata 1968
10. Sask Tel Buried Cable Damage Survey 1967
- J.D. Gudmundson
11. Progress and Pitfalls of Rural Buried Cable
- J.D. Kirk, D.G. Saul, R.C. Brooks
- 18th Wire & Cable Symposium Atlantic City, N.J. Dec. 1969

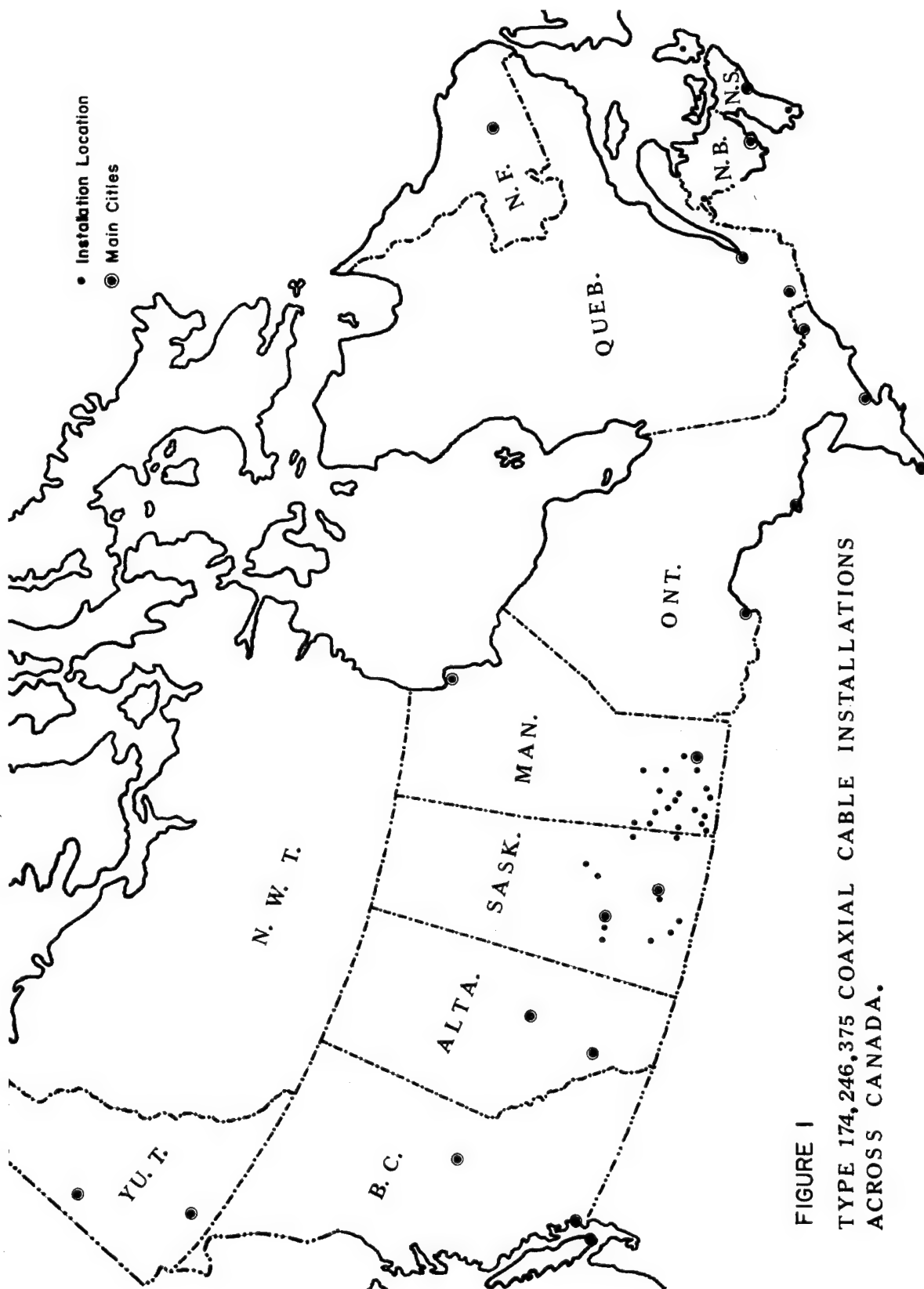


FIGURE 1
 TYPE 174, 246, 375 COAXIAL CABLE INSTALLATIONS
 ACROSS CANADA.

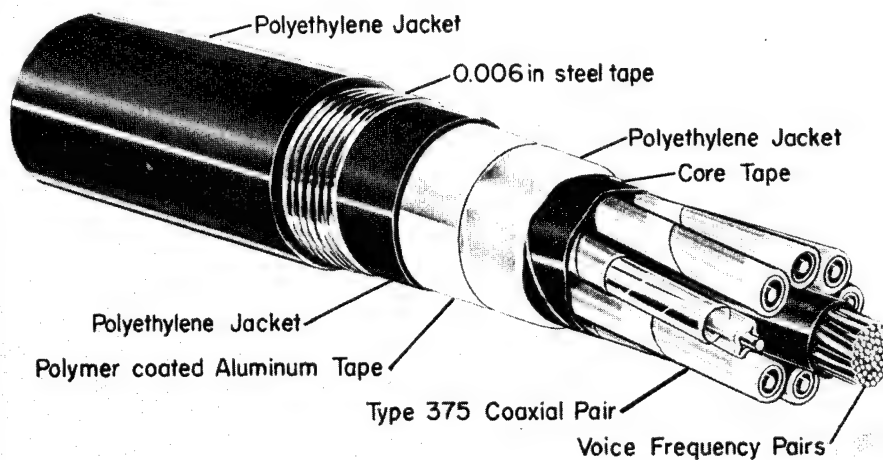
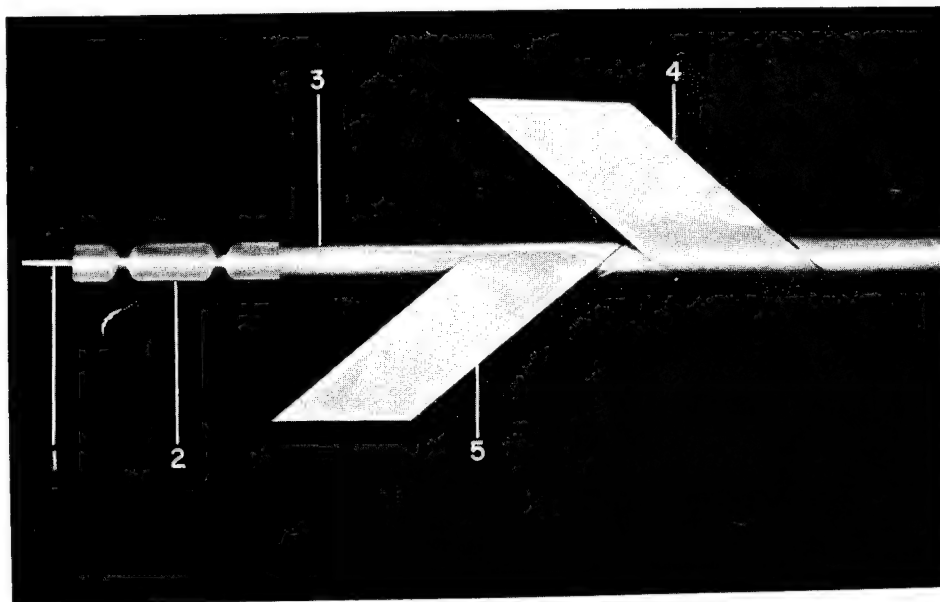


FIGURE 4—COMPOSITE COAXIAL CABLE FOR DIRECT BURIAL
8 TYPE 375 COAXIAL PAIRS
PLUS 25 PAIRS NO. 19 AWG.

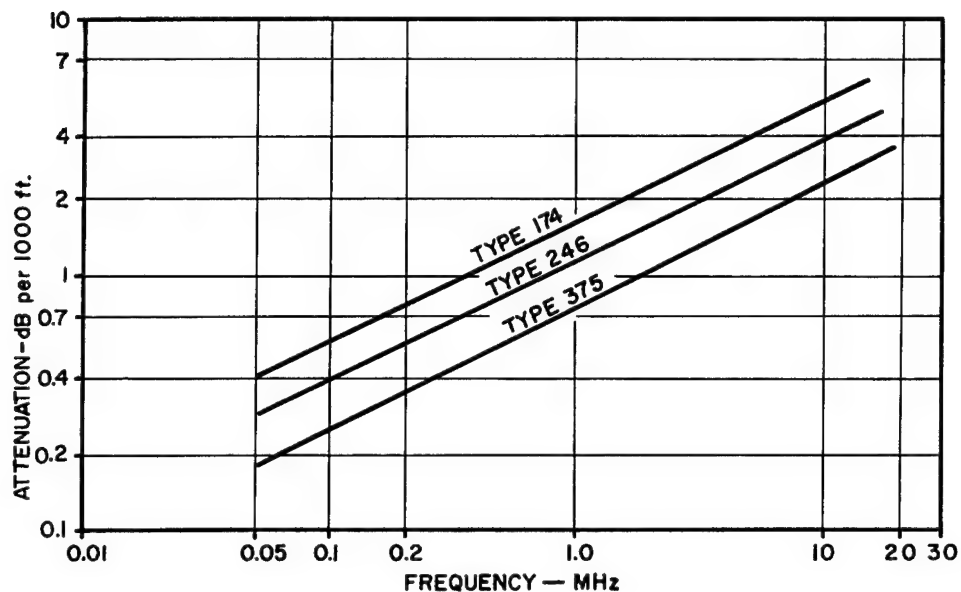


FIGURE 5 — ATTENUATION ν FREQUENCY CHARACTERISTIC AT 10°C FOR TYPE 174, 246, and 375 COAXIAL PAIRS

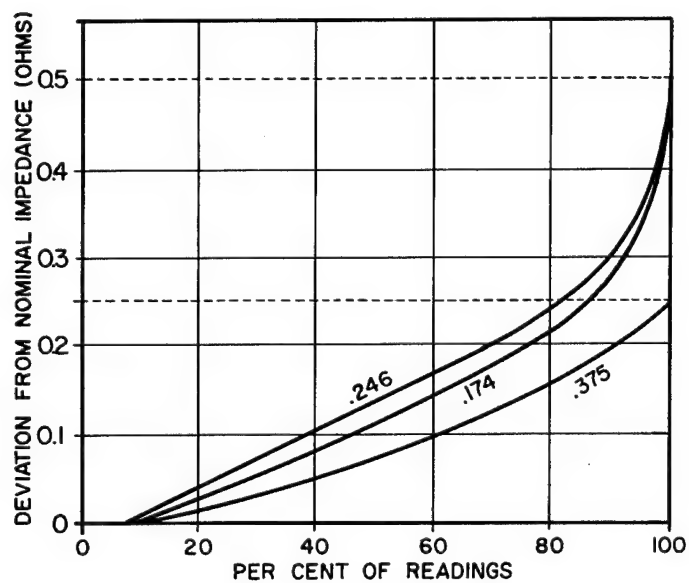


FIGURE 6 — STATISTICAL DISTRIBUTION OF IMPEDANCE DEVIATION FOR TYPE 174, 246, and 375 COAXIAL PAIRS

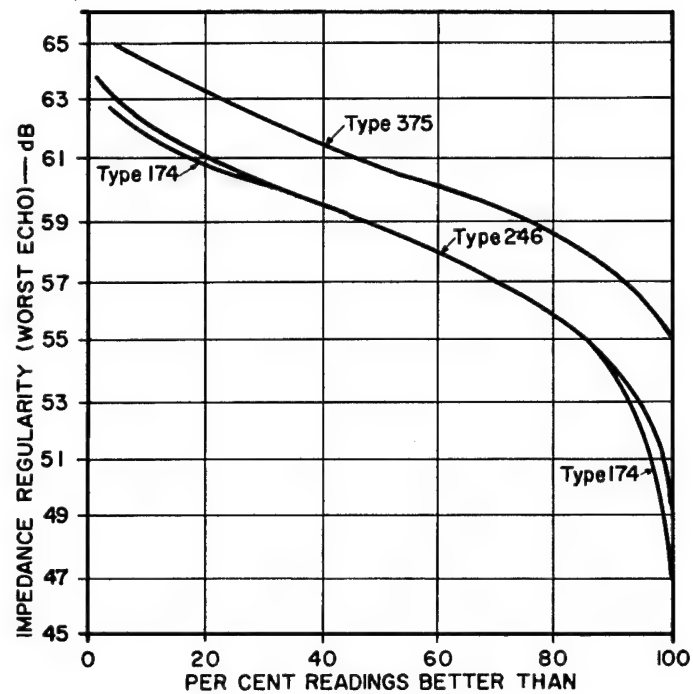
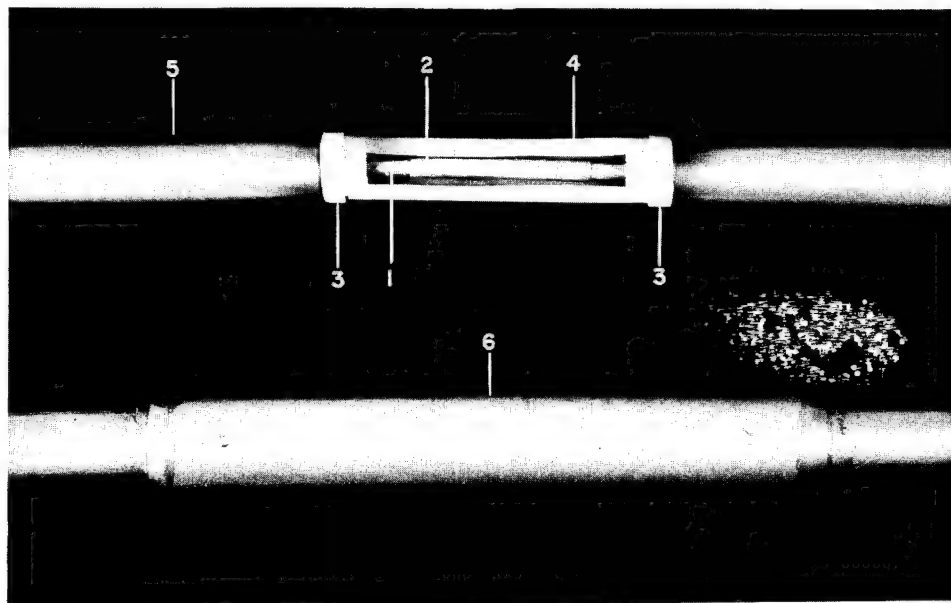


FIGURE 7 — IMPEDANCE REGULARITY READINGS FOR TYPE 174,246, and 375 COAXIAL PAIRS



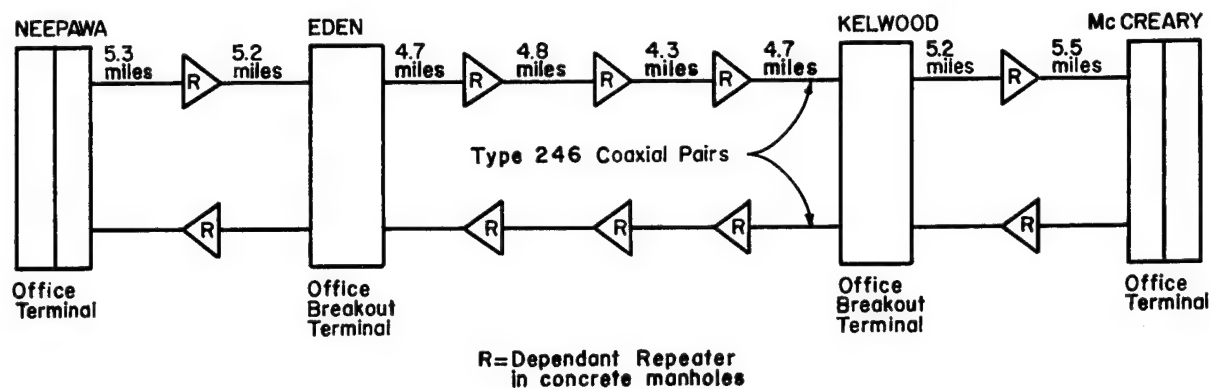
1—Inner copper conductor 3—Teflon insert 5—Outer copper conductor
2—Split tinned copper sleeve 4—Teflon sleeve 6—Tinned copper sleeve
FIGURE 8—TYPE 375 COAXIAL PAIR SPLICE

Figure 9

Coaxial Carrier System Installation 1966-70

<u>Channels</u>	<u>Cable</u>	<u>Length Miles</u>	<u>Administration</u>	<u>Location</u>
960	4 Type 174	6.6	N.B.T	Edmundston, WLEL
300	2 Type 174	3.4	M.T.T.	Baddeck, WLEL
300	2 Type 174	2.4	M.T.T.	Shelburne, WLEL
300	4 Type 174	2.3	Sask Tel	Nipawin, WLEL
300	4 Type 174	2.3	Sask Tel	Melfort, WLEL
300	2 Type 174	4.5	Sask Tel	Moosomin, WLEL
300	2 Type 174	3.4	Sask Tel	Belle Plaine, WLEL
300	2 Type 174	1.1	M.T.S.	Neepawa, WLEL
300	4 Type 174	3.0	M.T.S.	Melita, WLEL
1200	4 Type 246	2.7	M.T.S.	Minnedosa, WLEL
240	2 Type 246	9.3	M.T.S.	Strathclair-Shoal Lake
300	2 Type 246	40.0	M.T.S.	Neepawa-McCreary
240	2 Type 246	5.4	M.T.S.	Deloraine, WLEL
300	2 Type 174	2.0	M.T.S.	Pilot Mound, WLEL
1200	8 Type 174	1.3	M.T.S.	Selkirk, WLEL
600	8 Type 375	4.3	Sask Tel	Swift Current, WLEL
300	2 Type 174	1.5	M.T.S.	Roblin, WLEL
300	2 Type 174	20.0	M.T.S.	Melita-Pierson
300	2 Type 174	8.2	M.T.S.	Belmont, WLEL
300	2 Type 246	21.8	M.T.S.	Carmen-Haywood
300	2 Type 174	1.2	M.T.S.	Verden, WLEL
300	2 Type 246	4.4	M.T.S.	Teulon, WLEL
300	2 Type 174	1.6	M.T.S.	Fisher Branch, WLEL
300	1 Type 375 + 6 Type 174	7.4	C.T.	Riverview, Montana, WLEL
300	2 Type 246	35.4	M.T.S.	Foxwarren-Shoal Lake
300	2 Type 174	19.0	M.T.S.	Melita-Waskada
300	2 Type 174	4.6	Sask Tel	Biggar, WLEL
300	2 Type 174	2.3	Sask Tel	Asquith, WLEL
300	2 Type 375	8.4	Sask Tel	Canora, WLEL
300	2 Type 174	13.7	Sask Tel	Gravelbourg, WLEL
600	2 Type 174	1.3	Sask Tel	Assiniboia, WLEL
300	2 Type 246	.9	M.T.S.	Souris, WLEL

Note: N.B.T. New Brunswick Telephones
M.T.T. Maritime Telephone & Telegraph
Sask Tel Saskatchewan Government Telephones
M.T.S. Manitoba Telephone System
C.T. Continental Telephone Corp.
WLEL Wire Line Entrance Link



NEEPAWA-EDEN-KELWOOD-McCREARY-SCHEMATIC of REPEATER LAYOUT

Figure 10

FIGURE 11- Repeater housing in manhole showing cable entrance gland

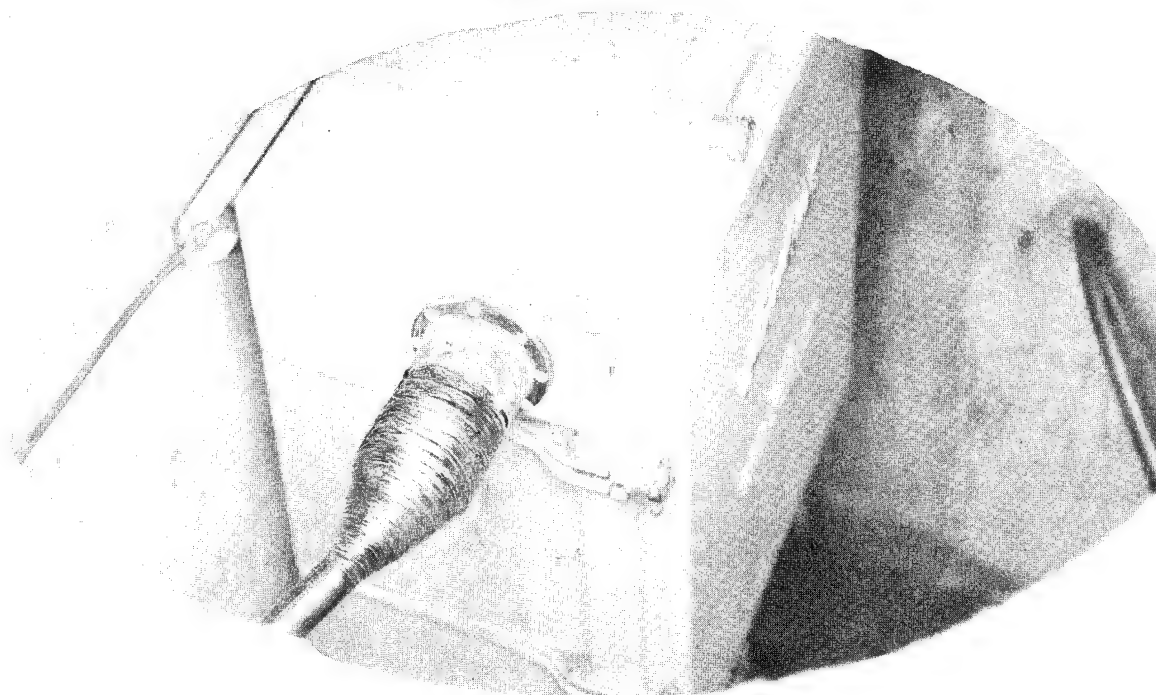


Figure 12

System Data Using Type 174, 246, 375 Coaxial Pairs

<u>Channel Capacity</u>	<u>Frequency Range-kHz</u>	<u>Type 174</u>	<u>Type 246</u>	<u>Type 375</u>
120	60 - 600	7.40	10.00	17.20
300	60 - 1300	5.00 4.35 3.70	6.90 6.00 5.20	11.50 9.30 8.00
600	60 - 3084	2.25	3.20	5.10
720	60 - 3084	2.25	3.20	5.10
960	60 - 4028	2.50	3.50	5.60
1260	60 - 6000	1.85	2.60	3.90
2700	300 - 12,388	1.25 .93	1.75 1.30	2.90 1.92

Note: Repeater spacings are approximate and depend on amplifier gains;
spacings are also in miles.



(Speaker)
K. R. Bullock
Manager - Engineering
& Manufacturing
Communication Products
Canada Wire & Cable
147 Laird Drive
Toronto, 352, Ontario
Canada

Kenneth R. Bullock was born in Portsmouth, England in 1927. He graduated from McGill University in Montreal in 1952 with a B. Eng degree in Electrical Engineering.

He has been in the Wire and Cable Industry for seventeen years having been a Design Engineer with Phillips Cables from 1953-1959, and with Anaconda Wire and Cable from 1959-1965 holding the position of Senior Communication Cable Engineer at the time of his return to Canada. With Canada Wire he has been Senior Projects Engineer, Manager of Process Engineering for all products, and since January 1970 in his present position

He is a Senior Member of IEEE, a Member of IEE (UK) and a Member of Association of Professional Engineer of Ontario.

Stan Johnson -

Stan Johnson was born in Winnipeg, Manitoba in 1938. He graduated in 1961 with a BSc in Electrical Engineering from the University of Manitoba. Since 1961 he has worked with Canada Wire and Cable in their Communications Group. Until 1966 he was Product Development Engineer with this group and between 1966 and 1969 was Manager Engineering, Communication Products. Since 1969 he has been Marketing Manager, Communications Products.

He is a member of the Association of Professional Engineers of Ontario.

Mr. J. D. Adam, P. Eng.
General Staff Engineer
Manitoba Telephone System
489 Empress St.
Winnipeg 10, Manitoba, Canada

"John" adam is a native son of Manitoba, Canada. He was born in Roblin, Manitoba in 1920.

He spent $4\frac{1}{2}$ years in the Royal Canadian Air Force as a wireless electrical mechanic in World War II. $3\frac{1}{2}$ years of this was in Britain, North Africa and Europe.

On his return to Canada he took the Electrical Engineering degree - (Communications Option) at the University of Manitoba graduating in 1949.

He entered the Manitoba Telephone System in 1949 and has held various positions in the Engineering Dept. These include Transmission Engineering, Plant Extension toll planning, Outside Plant Engineer and at present General Staff Engineer. In brief, this position has the responsibility for System standards and general practices for design, construction, installation, maintenance and quality control for all fields-- central office, toll, outside plant and customer equipment.

Memberships - A Member and President of the Association of Professional Engineers of Manitoba for 1970.

Member of the senior technical committees for Part I and Part III of Canadian Standards Association for the Telephone Association of Canada.

LEAKY COAXIAL CABLE AT VHF BAND AND IT'S APPLICATION TO VEHICULAR COMMUNICATIONS

TATSUO YOSHIYASU*, TORU HATTA**, KOICHI MIKOSHIBA**,
SHIGEO OKADA**, TOSHIO HANAOKA**

ABSTRACT

In train wireless-radio systems and vehicular communications, a very important problem is maintaining stable communications at all locations, especially in tunnels and in underground such as subway.

The transmission characteristics and performances of the leaky coaxial cable, effective guided radiation system, with diameter of the outer conductor; 15 mm will be mainly described in order to provide stable VHF vehicular communications in tunnel, subway, for example, subway in Ohsaka city, where radio waves are unable to penetrate.

1. INTRODUCTION

The surface-wave transmission line, parallel conductor line and slitted coaxial cable are well known as the transmission lines which have simultaneously two functions, transmission and antenna. These transmission lines have the following disadvantages:

- (1) The difficulty in controlling the energy leaked from the above transmission lines
- (2) The degradation of the transmission performances due to adhesion of vapors, dust and iron powder to the above lines
- (3) The degradation of the transmission characteristics as the lines approach the earth ground, and due to environments surrounded the lines

The transmission lines, therefore, do not have stable transmission and radiation characteristics generally in the VHF and UHF bands. Electromagnetic field distribution over these transmission systems is not uniform except at very near fields of these lines, thus causing a substandard quality of communication because these lines do not effectively radiate a portion of the radio waves from the lines.

The coaxial line with the outer conductor having periodic slots which act as effective radiating elements,⁽¹⁾ so called leaky coaxial cable presented here, have the following advantages when the design of interval of the slots are made in order to suppress the surface-wave, and to get radiation wave to only one direction:

- (1) Easy control of the energy leaked from the leaky coaxial cable
- (2) The effects of the adhesions of vapors, dust and of the environments surrounding the leaky coaxial cable will be negligible
- (3) The uniformity of leaked energy distribution (electromagnetic field distribution) along the leaky coaxial cable will be effectively improved

These transmission systems will provide new effective means of communications, especially vehicular communications as guided radiation.

The size of coaxial cable is smaller, and the operating frequencies are lower, the effective radiation from the cable will be more difficult. The leaky coaxial cable, however, will be available by using the effectively radiating slots on the outer conductor. The transmission characteristics of the leaky coaxial cable with diameter of the outer conductor; 15 mm, characteristic impedance; 75 ohms are described in order to provide effective VHF wireless communications in tunnel, subway, for example, subway in Ohsaka city, where radio waves are unable to penetrate.

Moreover, the leaky coaxial cable like this are planning to put into practical use at the New Sanyo Line's train wireless communication systems, and will be able to be accepted and utilized in the future in development of new vehicular communication or underground communication systems.

2. THEORETICAL BACKGROUND OF THE LEAKY COAXIAL CABLE

A. Radiation from coaxial transmission line⁽²⁾

In order to obtain radiation from coaxial transmission lines in which TEM waves propagate, slots have to be made in such a way as to distribute the electrical current in the outer conductors, or as not to disturb the current but to be excited by stubs, etc. (see Fig. 1a, b and c). The slot shown in Fig. 1a is suitable for antenna as well known as the slotted cylinder antenna, but a guided radiation system using the slot may be unable to put into practical use because the slot have many difficulties in production of the cable with it.

For coaxial lines having diameters smaller than the condition, $D/\lambda < 0.12$, resonance phenomenon on slot may not be observed. However, electrical performances of nonresonant slots have moderate frequency characteristics, and then by use of these slots the leaky coaxial cable as the guided radiation systems having stable transmission and radiation characteristics in the VHF and UHF bands are realized. Under the nonresonant condition these slots may be unable to radiate effectively as the ratio of the outer diameter to the operating wave-length, D/λ , approaches to zero.

*T. YOSHIYASU is with Ohsaka City Transit Authority, Ohsaka, Japan.

**T. HATTA, K. MIKOSHIBA, S. OKADA, T. HANAOKA are with Hitachi Cable, Ltd., Hitachi, Ibaraki, Japan.

The coupling loss L_c , denoting the difference between the transmitting level and the receiving level with a standard dipole antenna, may be obtained under the following assumptions; the radiated waves are omnidirectional in the circumferential direction and distributed uniformly along the axial direction, and then given by

$$L_c(\text{dB}) = 53.2 - 10 \cdot \log(\lambda^2/r) - 10 \cdot \log \alpha_R \quad (1)$$

where

λ ; operating wave-length, in meters

r ; distance between the cable and dipole antenna, in meters

α_R ; additional attenuation constant due to radiation, in dB/km

Assuming that the additional attenuation constant due to slots contributes only to radiation, the total attenuation constant α of the leaky coaxial cable adds the attenuation constant α_0 of the coaxial cable without the slots to the additional attenuation constant α_R in eq.(1), and then is given by

$$\alpha = \alpha_0 + \alpha_R \quad (2)$$

B. Radiation modes and arrangements of the radiating elements

When realizing the leaky coaxial line using these radiating elements, it is usual to arrange these elements as a periodic array in the axial direction. The direction of radiation from the periodic array, that is, the radiation angle ϕ_m as shown in Fig. 2 is well known to be given as follows:

a case with phase reversal;

$$\cos \phi_m = \beta_m / k_0 \approx \sqrt{\epsilon} + \frac{\lambda}{L} (m + \frac{1}{2})$$

$$(m = 0, \pm 1, \pm 2, \pm 3, \dots) \quad (3)$$

a case without phase reversal;

$$\cos \phi_m = \beta_m' / k_0 \approx \sqrt{\epsilon} + \frac{\lambda}{L} m'$$

$$(m = 0, \pm 1, \pm 2, \pm 3, \dots) \quad (4)$$

where k_0 ; wave number in free space

L ; spacing between periodic elements

ϵ ; equivalent relative permittivity of coaxial line

β ; phase constant of TEM wave in coaxial line

$$\beta_m = \beta + (2\pi m + \pi) / L, \quad \beta_m' = \beta + 2\pi m' / L.$$

From eqs.(3), (4), the conditions for obtaining radiation and surface-wave are shown as follows, respectively

$$\text{radiation condition; } |\beta_m / k_0|, |\beta_m' / k_0| \leq 1$$

$$\text{surface-wave condition; } |\beta_m / k_0|, |\beta_m' / k_0| > 1. \quad (5)$$

The relations between the radiation angle ϕ_m and λ/L are shown in Fig. 2b.

The coaxial lines with slot arrangements under surface-wave region have unstable transmission and radiation performances. Therefore, in order to get the stable performances by surrounding conditions and environments the slot arrangements which satisfy the radiation condition, eq.

(5) have to be chosen. The uniformity of the leaked waves along the leaky coaxial line may be improved by satisfying the radiation condition, but may be unable to be improved very much by interference of radiation waves with different radiation angles even if under the radiation condition. By avoiding the interference of the radiation waves, uniform distribution along the line is achieved. A easy method to avoid the interference is design which chooses the slot arrangements with only one radiation wave, for example, the region of λ/L as shown in Fig. 2b.⁽³⁾

3. ELECTRICAL PERFORMANCES OF LEAKY COAXIAL CABLE AT VHF BAND

A. Physical structure of the leaky coaxial cable

The leaky coaxial cable for VHF band presented here are based on 15-C type coaxial cable using the balloon type insulator, and consists of annealed copper wire as center conductor and of aluminum sheet with periodic radiating slots satisfying the radiation condition with only one radiation wave as outer conductor. The details of physical structure of the line are shown in Fig. 3a, and moreover a photograph of the line with large diameter is referred in Fig. 3b. The equivalent relative permittivity of the insulator is about 1.21.

B. Transmission loss performances

The balloon type coaxial cable has low-loss characteristics compared with other coaxial cable with the same diameter, and the leaky coaxial cable using the balloon type, therefore, may have low-loss, too. According to the discussion in section 2, the transmission losses of the line are affected strongly by the value of the coupling loss L_c as shown in Fig. 4. The calculated curves by eqs.(1), (2) and experimental curves are presented in Fig. 4. From these results, the differences between the calculated and experimental value are made larger as the ratio, D/λ , approaches to zero, for example, the ratio is about 7.5×10^{-3} of Fig. 4a, 6×10^{-2} of Fig. 4b.

It becomes clear that the size of the coaxial line is smaller and operating frequencies are lower, realization of the effective radiation from the line is more difficult.

Approaching the lines to earth ground, the transmission performances of the lines satisfying the radiation condition change slightly as shown in the many experiments.⁽³⁾ Soiling the lines by dust, iron powder, and spreading water on the surface of the lines, the additional transmission losses become larger as the values of the coupling loss are smaller. Adhesion of vapors, dust and iron powder to the lines degrades slightly the

transmission performances as shown in Fig. 5.

C. Coupling loss performances

An estimation of the coupling loss may be difficult by the simple theory expressed in eqs. (1), (2), because the lines with the smaller ratio, D/λ , can not radiate effectively as shown in Fig. 4a. According to the experimental results illustrated in Fig. 4a, the leaky coaxial cable with the required coupling losses over about 68 dB in E_θ component and about 63 dB in E_z component at 150 MHz band can easily be designed.

At coupling loss measurement the leaky coaxial cables are laid 10 cm high on a concrete floor, and the distance between the cable and dipole antenna keeps 2 meters high. Measurements are taken in a lengthwise direction along the lines, and the results are recorded by an automatic recorder.

Distributions of the coupling loss along the line are illustrated in Fig. 7. The deviation of the coupling loss along the line is noticeably smaller than of the ordinary cable of this type⁽⁴⁾ and the uniformity of the coupling loss distribution can be improved by the slot arrangement with only one radiation wave.

4. TRANSMISSION PERFORMANCES IN TUNNEL

It is well known that frequencies in the VHF region commonly used for mobile communications are severely attenuated in tunnel structures⁽⁵⁾, ⁽⁶⁾ and behave as though they are propagating in a lossy waveguide.

The distribution of the coupling loss along the leaky coaxial cables installed in a tunnel may be affected by dimensions of a tunnel cross-section and operating frequency.

It is evident that the fluctuation of field intensity inside a tunnel is little greater than that outside the tunnel through our experiments at the VHF region.

5. WIRELESS COMMUNICATION SYSTEM USING THE LEAKY COAXIAL CABLE IN THE SUBWAY IN OHSAKA CITY

A. Outline of the subway wireless radio system

The network consists of 5 base stations located along the 6th line. The locations of the base station as shown in Fig. 7 are Tenroku, Ohgimachi, Kitahama, Nagahori-bashi and Ebisu-machi base station. These base stations are connected to and controlled by the Dispatcher at Tenroku base station via telephone lines. The leaky coaxial cables with three different values of the coupling loss installed in the right-of-way of the subway tunnel in the rule are used for radio transmission and receptions, as shown in Fig. 8. Communication system, frequencies and transmitter output power used the subway wireless radio system in Ohsaka city are listed up on Table 1.

B. Field strength in the subway installed the leaky coaxial cable

The leaky coaxial cables are feeded the both side simultaneously as shown in Fig. 7, and the lines with three different coupling losses are installed in each section between transmitter and a dummy load, because the distance between base stations is about 2 kilometers and it is necessary to reduce the difference between the maximum and minimum field strength in the above section.

Assuming the value of the field strength in a subway tunnel do not change whether trains are in the subway tunnel or not, the field strength E (dB μ V/meter) in a tunnel installed the leaky coaxial cable is given for 1 watt output power, 150 MHz by

$$E \text{ (dB } \mu\text{V/meter)} = 145.6 - L_c - \alpha Z - L - X$$

where L_c ; coupling loss with a standard dipole antenna in tunnel, in dB⁽⁶⁾
 α ; attenuation constant of the leaky coaxial cable, in dB/km
 Z ; the cable's length from the transmitter, in km
 L ; losses of feeder, distribution circuits, in dB
 X ; additional coupling loss in opposite tunnel installed the leaky coaxial cable, in dB.

The field strength calculated by eq.(6) and measured values by train are illustrated in Fig. 9. The fairly good agreement is shown between the experiment and calculation by eq.(6) at the place where each tunnel are separated perfectly. The positions of the cables at tunnel wall, the structures and the dimensions of tunnel are not more simple than that of the section described above. Therefore, the difference between the experiment and calculation are 5 - 12 dB.

6. CONCLUSION

The leaky coaxial cable as a guided radiation system with an easily and optionally designed radiation power, using a stable coaxial cable with the effective radiating slots is represented here. These lines are effective transmission media not only to a place where radio waves are unable to penetrate, but also to a place where communication services are needed along the lines.⁽⁷⁾ The leaky coaxial cable with wide-band (from 100 MHz to 500 MHz) transmission and radiation performances are investigating, and a combination of cable-multiplex techniques and a guided radiation system using the cable may be suitable for a linear communication such as high speed train communications and highway communications.

REFERENCES

- (1) K. Mikoshiba and Y. Nurita "Guided radiation by coaxial cable for train wireless systems in tunnels" IEEE Trans. Vehicular Technology, Vol. VT-18, pp.66-69. August 1969.
- (2) K. Mikoshiba "Radiation from small-size coaxial lines" Trans. I.E.C. Japan 51-B, 6, pp.279. June 1968 available in English in E.C.J., same date, p.xx.
- (3) K. Mikoshiba, Y. Nurita and S. Okada "Radiation from a coaxial cable and it's application to a leaky coaxial cable" Electronics and Communications in Japan, Vol. 51, 10, pp.61-68 October 1968.
- (4) T. Naito et all "Leaky coaxial waveguid for monorail" Hitachi Review. Vol.46 pp.85 October 1964.
- (5) R.A. Farmer and B.H. Shepher "Guided radiationthe key to tunnel talking" IEEE Trans. Vehicular Communications, Vol.VC-14, pp.93-102 March 1965.
- (6) D.O. Reudink "Mobil radio propagation in tunnels" presented to IEEE Vehicular Technology Group Conference in December 1968.
- (7) W.S. Halstead and K.A. Mazzola "Highway communication using wide-band cable and inductive transmission methods" IEEE Trans. Vehicular Technology, Vol.VT-19 pp.59-68 February 1970.

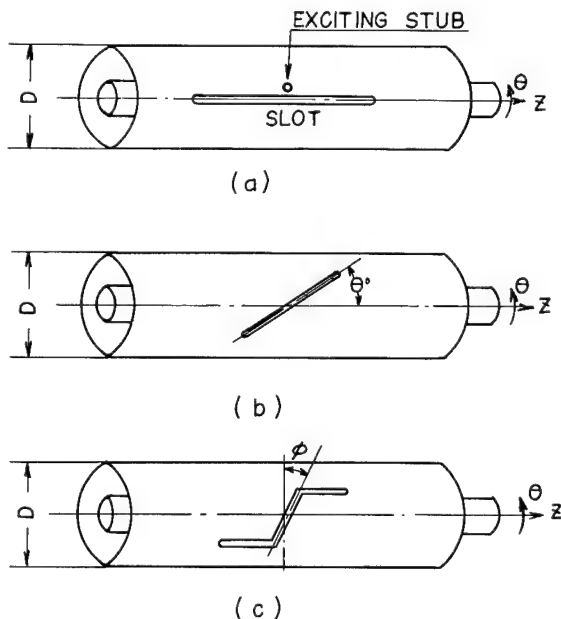
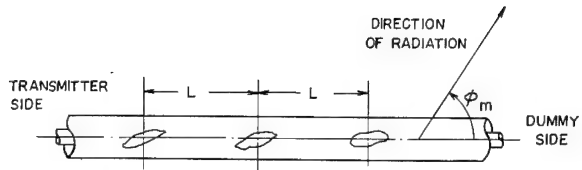


Fig.1 Radiating elements of coaxial transmission line.



(a) SLOT ARRANGEMENT AND RADIATION ANGLE ϕ_m

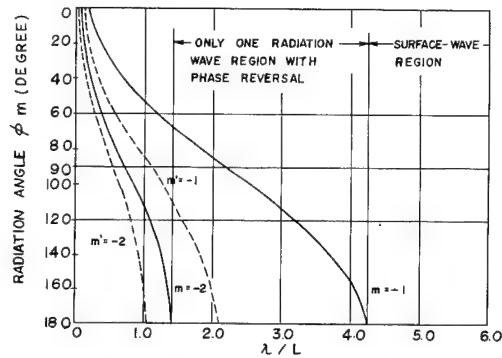
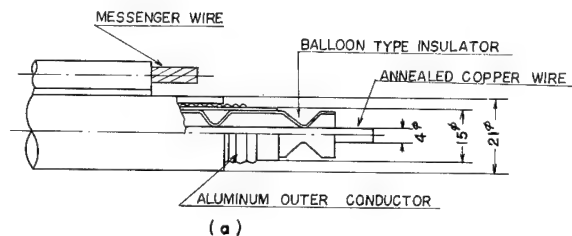
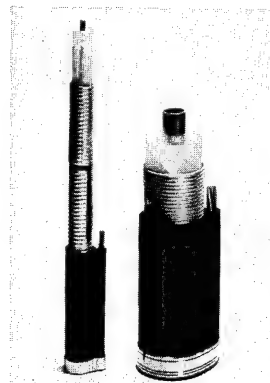


Fig.2 The relations between slot arrangement and radiation angle ϕ_m, m'



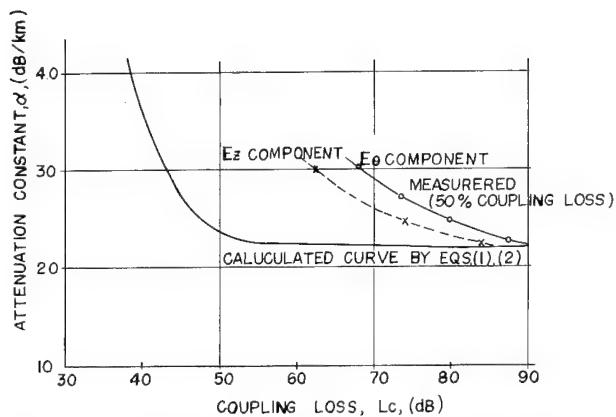
(a)



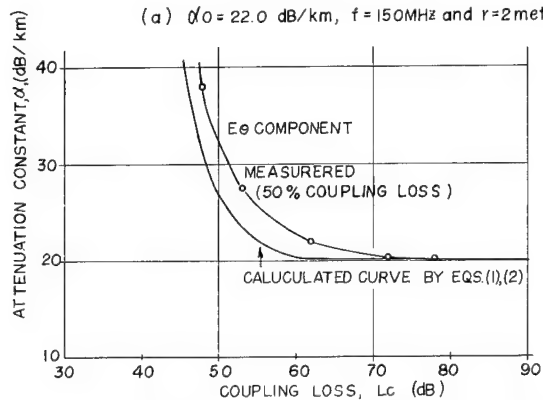
(b)

Fig.3 Physical structures of the leaky coaxial cable

- (a) Physical structures of small size leaky coaxial cable
- (b) Photograph of the leaky coaxial cables with different diameter



(a) $\alpha_0 = 22.0 \text{ dB/km}$, $f = 150 \text{ MHz}$ and $r = 2 \text{ meters}$



(b) $\alpha_0 = 20.0 \text{ dB/km}$, $f = 430 \text{ MHz}$ and $r = 2 \text{ meters}$

Fig. 4 The relations between total attenuation constant and the coupling loss

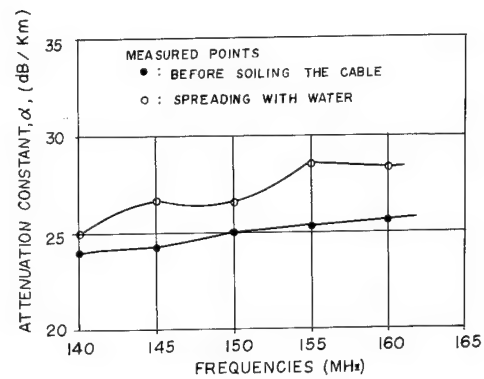
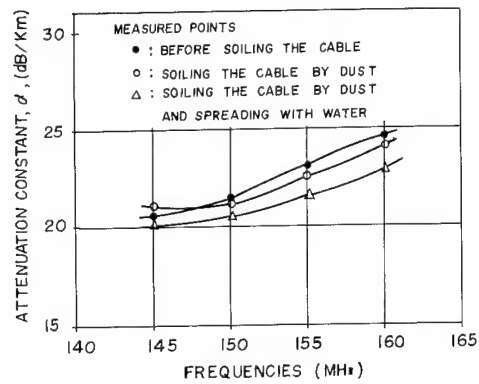


Fig. 5 Transmission loss performances due to soiling the leaky coaxial cable

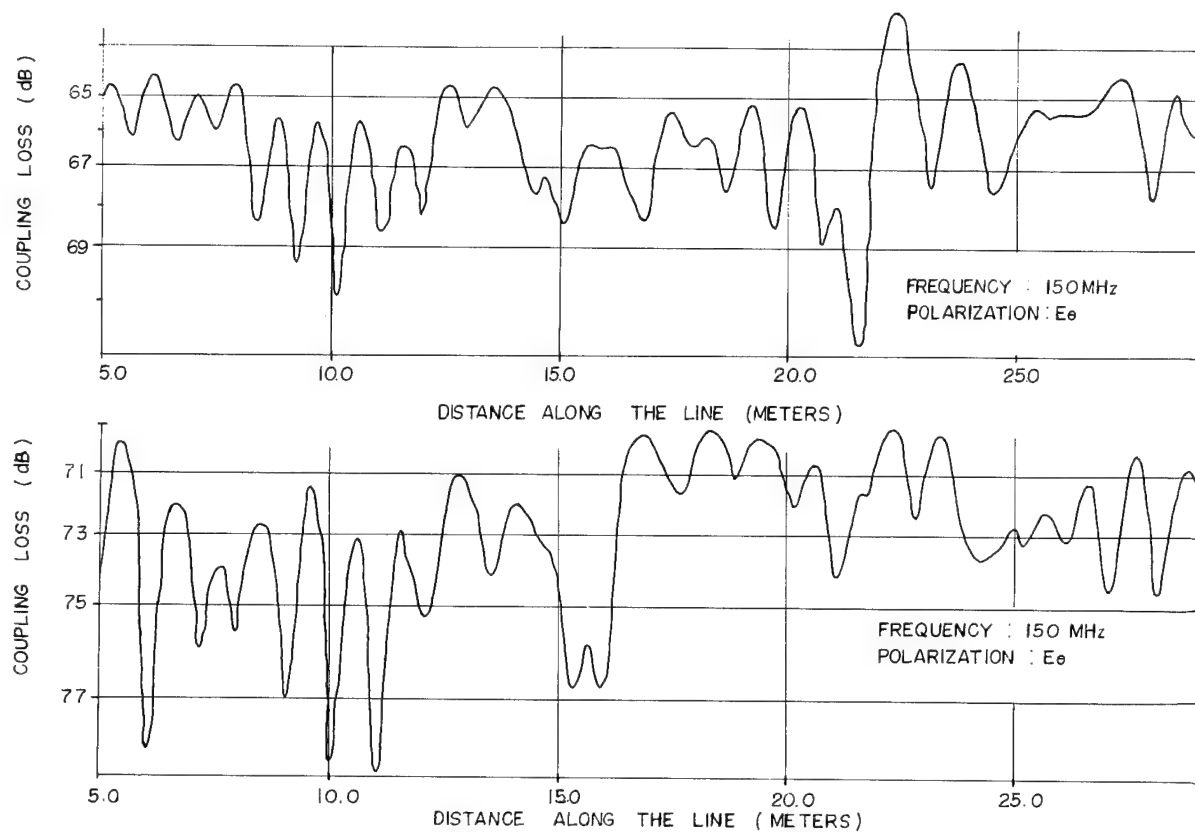


Fig.6 Radiation uniformity along the leaky coaxial line

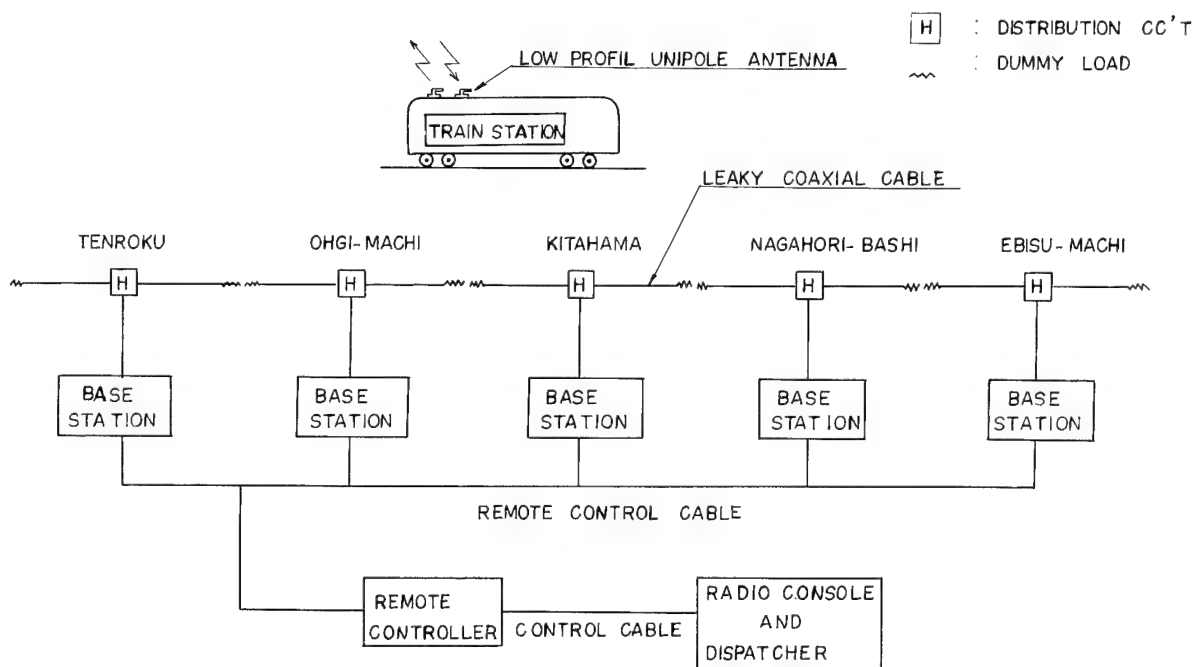


Fig.7 Wireless communication system diagram in subway of Ohsaka city

Table 1. Communication system

STATION	BASE STATION	TRAIN STATION
ITEMS		
COMMUNICATION SYSTEM	TWO-FREQUENCY DUPLEX SYSTEM	
FREQUENCY	147.94 MHz	143.94 MHz
TRANSMITTER OUT PUT	5 WATTS	10 WATTS
TRAIN ANTENNA	LOW PROFILE UNIPOL ANTENNA	

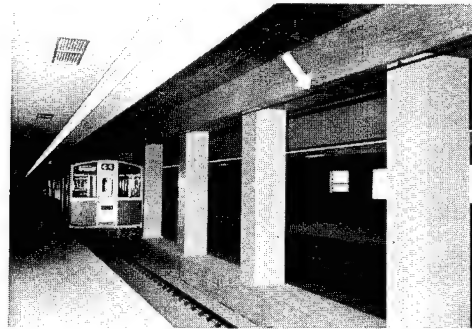


Fig.8 The leaky coaxial cable installed in the subway

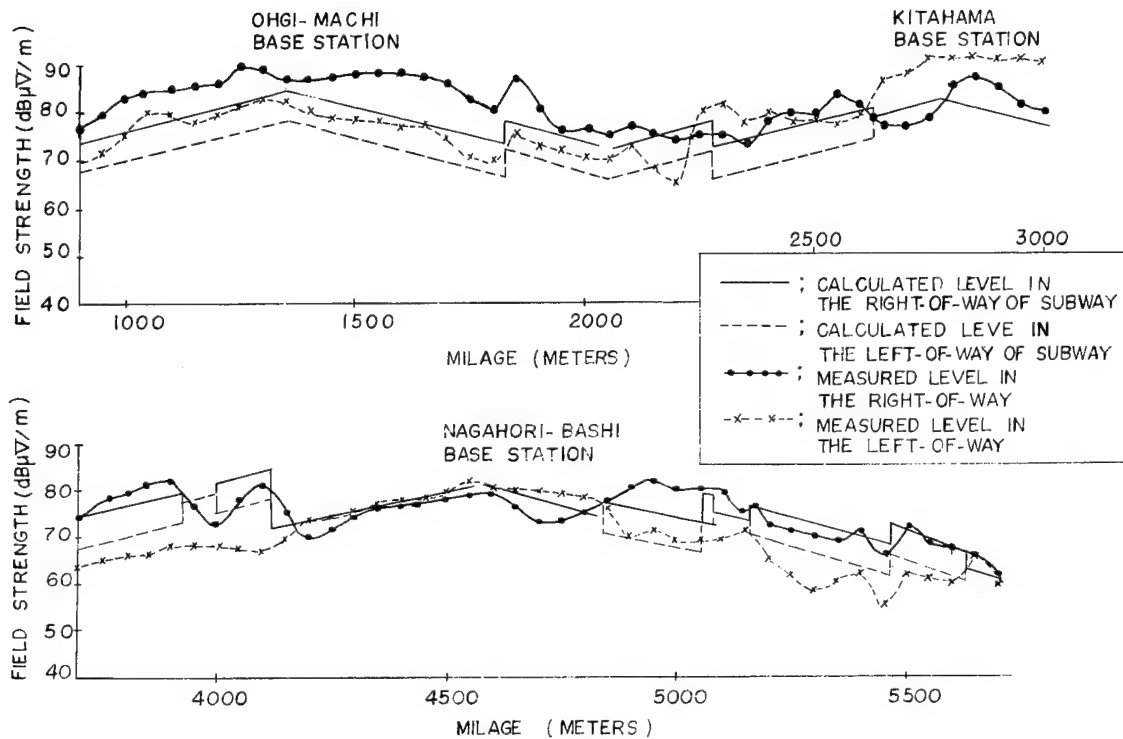


Fig.9 The calculated and measured field strength in the subway



(Speaker)
Koichi Mikoshiba
Hitachi Cable, Ltd.
2-16 Marunouchi
Chiyoda-Ku
Tokyo, Japan

He was born in Matsumoto City, Japan in 1937. He received the B.E. and Ph.D. degrees in electrical engineering from Tohoku University, Sendai, Japan in 1959 and 1967, respectively.

In 1959 he joined Hitachi Cable, Ltd., Tokyo, Japan, where he has been a Research Member of the Research Lab. He has been engaged in the development of millimeter circular waveguides, UHF antenna systems for television broadcasting, and in the research and application of such nonconventional waveguides as surface waveguide, leaky waveguide, beam waveguide and leaky coaxial cable system.

From 1968 to 1969 he was a Post Doctoral Fellow at the MRI of Polytechnic Institute of Brooklyn, Brooklyn, N. Y.

Dr. Mikoshiba is a member of the Institute of Electronics and Communication Engineers of Japan, and IEEE.

Tatsuo Yoshiyasu -

He was born in Gifu Prefecture, Japan in 1930. He received the B.E., M.S., and Ph.D. degrees in electrical engineering from Kyoto University, Kyoto, Japan in 1953, 1955 and 1970, respectively.

In 1955, he joined the Ohsaka Municipal Transportation Bureau. His first assignment was with Electrical Engineering Department, where he worked on the planning of communication system. In 1963, he was assigned responsibility for advanced systems engineering of signal and communication, and he was largely responsible for development of the automatic train control system for the Ohsaka subway. He is now responsible for subway operation Department

Dr. Yoshiyasu is a member of the Institution of Electrical Engineers of Japan and the Institute of Electronics and Communication Engineers of Japan.

Toru Hatta -

He was born in Suwon, Korea, in 1923. He received the B.E. and Ph.D. degrees from Tohoku University, Sendai, Japan, in 1949 and 1960, respectively.

From 1949 to 1953 he was the Assistant of Tohoku University, and joined Hitachi Ltd. in 1953. Since 1956, he has been with Hitachi Cable, Ltd., where he has belonged to the Research Laboratory and studied the telephone cables, the power transmission lines, the transmitting antennas and the feeding equipments for television broadcasting.

Dr. Hatta is a member of the Institute of Electronics and Communication Engineers of Japan.

Shigeo Okada -

He was born in Tokyo, Japan in 1943. He received the B.E. degree in electrical engineering from Tokyo University, Tokyo, Japan in 1967.

In 1967 he joined Hitachi Cable, Ltd., Tokyo, Japan, where he has been engaged in the development of antennas, surface waveguides, and leaky coaxial cables.

Mr. Okada is a member of the Institute of Electronics and Communication Engineers of Japan.

Toshio Hanaoka -

He was born in Nagano Prefecture, Japan in 1934. He received the B.E. degree in communication engineering from Shinsyu University, Nagano, Japan in 1957.

In 1957 he joined Hitachi Cable, Ltd., where he has been engaged in the development of the communication cables. He is now a Senior Engineer in the Communication Cable Design Section.

Mr. Hanaoka is a member of the Institute of Electronics and Communications Engineers of Japan.

A RECENTLY DEVELOPED COMPOSITE INSULATION SYSTEM KAPTON/POLYIMIDE

by

Robert E. Smith

Manager, Engineering

HAVEG INDUSTRIES INC 

SUPER TEMP WIRE DIVISION
WINOOSKI, VERMONT

Presented at the Nineteenth International
Wire & Cable Symposium

Atlantic City, N. J., December 1, 2 and 3, 1970

A RECENTLY DEVELOPED COMPOSITE INSULATION SYSTEM KAPTON/POLYIMIDE

There have been profound developments in recent years in new electric insulation systems with particular emphasis on the reduction of weight and space, as well as improved physical and electrical properties. This has been spurred by the demanding requirements of our space exploration effort and more recently by the military and commercial aircraft industries. A series of composite insulation systems have been developed incorporating materials with a history of long term usage as well as others which have been available for only a few years. Other systems have included the use of established insulations combined with newer materials and more recently developed manufacturing techniques.

One of the more interesting materials which has been successfully used is known generically as "polyimide," and several varieties having similar properties are supplied by different manufacturers usually in the form of an enamel dispersion. One type is supplied by DuPont as a thin film called Kapton® which can be wrapped around a conductor and heat sealed.

Kapton has been used in many space programs and various military and commercial aircraft applications as a tape-wrapped insulation system. Generally this system is overcoated with a dispersion to improve surface smoothness and to facilitate color identification. The most widely used overcoat is a dispersion of FEP Teflon® which is applied in thicknesses between 1/2 to 1 1/2 mils even though it has certain disadvantages that will be discussed later.

Polyimide enamel has been used in a dispersion form as an overcoat on other primary insulation materials most notably TFE and FEP Teflon, to improve mechanical properties while not degrading the fluorocarbon's outstanding electrical and chemical properties.

Recently Kapton with an FEP overcoat was selected by one of the major aircraft manufacturers as the primary insulation system for one of its new aircraft programs. It soon became apparent that a tougher overcoat was desirable in view of the physical abuse experienced by the wire during installation in the airframe.

As a result, the technologies developed to apply polyimide enamel overcoats to extruded

fluorocarbons were utilized in applying a polyimide overcoat over the wrapped Kapton. Many of the outstanding mechanical improvements that have resulted are discussed in this paper.

General

Some of the major problems which have existed with available insulation systems in the past have been their inability to provide temperature stability, mechanical toughness and high dielectric strength consistent with the demand for reduced size and weight. In addition, aircraft manufacturers have always preferred to have wire and cable supplied in relatively long lengths so that a minimum amount of scrap is generated in their assembly processes. Also people responsible for safety have always been concerned with flammability and especially smoke emission as evidenced by present studies underway concerning the insulation systems being used on newly developed commercial aircraft.

Some insulation systems are extremely stable at elevated temperatures and although they do not burn or smoke, they are available only in limited lengths. Other systems available in long, continuous lengths are not stable at elevated temperatures and sometimes burn or cause prodigious volumes of smoke.

Historically, Kapton has proven to be one of the toughest organic insulation materials available with high dielectric strength and marked stability at elevated temperatures. It does not smoke and does not burn. However, it was not available in the long lengths required by the airframe manufacturer.

Recently, improvements have been made by DuPont to provide longer lengths of Kapton tapes. At the same time, the insulators have developed an ability to produce physically and electrically sound splices. This should have resulted in the availability of long, continuous lengths of insulated conductor to the end user. However, the conventional FEP dispersion overcoat often nullified the gains achieved due to the wire processor's inability to consistently apply this system without surface irregularities.

® Registered Trademark of DuPont

The development of techniques necessary to apply polyimide enamel over Kapton has enabled the wire insulator to apply an overcoat without these surface irregularities. In addition, the surface toughness of the insulated wire has been improved over 1000%. The combination of these two insulation systems has provided industry with a system composed of polyimide tapes (Kapton) and a polyimide enamel overcoat resulting in an insulated wire with essentially unlimited lengths and excellent dielectric strength. It is available in the minimum wall thicknesses consistent with present day connector miniaturization efforts. It is extremely light in weight and yet possesses a toughness normally associated with heavier constructions. It is non-flammable and does not smoke. It is available in the long lengths necessary for efficient aircraft assembly operations.

Figure 1 will provide a better understanding of Kapton tape wrapped insulation systems. Two tapes are normally applied in a helical fashion but in reverse direction to each other. Over the wrapped tapes an overcoat is applied to provide surface characteristics such as a base for color identification, smoothness for grommet sealing or bondability for potting. As shown, each tape consists of two or three laminates. The black depicts a polyimide film to provide dielectric strength and toughness. It is sandwiched with FEP Teflon, shown in white, which melts and seals the entire system when subjected to heat during manufacture. Figure 1 also describes the cross-section of each wrap with the conductor shown in cross hatch and the thickness of the various FEP and polyimide laminates in inches.

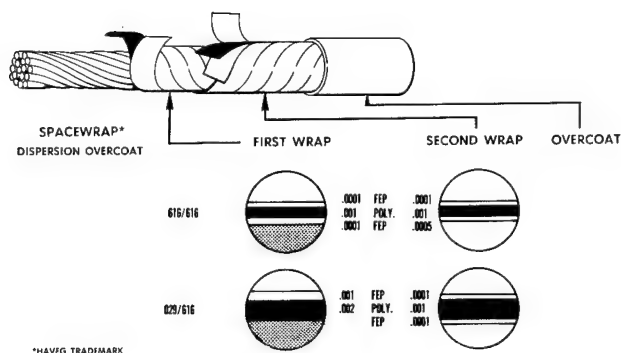


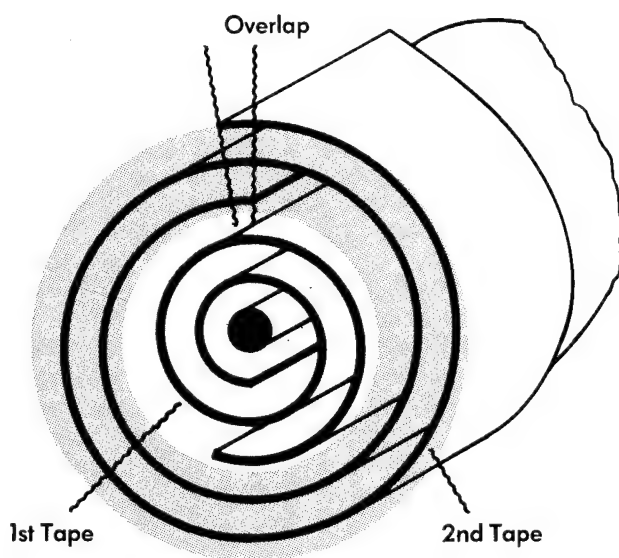
FIGURE 1

Table I describes some of the more significant 20 AWG Kapton insulated wire systems described in this paper which are now in use or under consideration in aircraft applications. The nomenclature describes the construction and typically 019/616F means a two tape construction with an FEP overcoat. The 019 describes the first tape consisting of two laminates, a 1 mil thick polyimide film and a .5 mil FEP adhesive. The 616 indicates a 1 mil polyimide film with a .1 mil FEP adhesive on both sides. The "F" stands for an FEP overcoat.

Figures 2 and 3 typically show wrapping details of all the constructions listed. All incorporate two tapes except the 616-2/3 construction which uses only one. Notice that in Figure 2 the tapes are wrapped using a nominal 50% overlap which provides a minimum of 5 layers while Figure 3 shows a single tape with a 66% overlap but still provides an adequate 4 layers of tape.

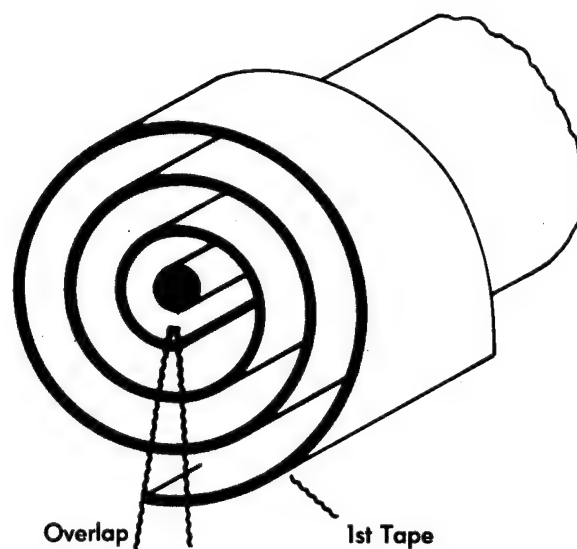
TABLE I
Construction Comparison
Of Kapton Insulated
20¹⁹/₃₂ AWG

Nomenclature	Tape 1 Kapton	Tape 2 Kapton	Dispersion Overcoat Type	Insulation Wall Thickness Nominal	Overcoat Thickness Nominal	Finished O.D. Inches	Finished Weight Lbs/1000 Ft
616 ² / ₃ - F	.1/1/.1	—	FEP	.0036	.0075	.0465	4.13
616 ² / ₃ - H	.1/1/.1	—	Polyimide	.0036	.0075	.0465	4.08
616/616 - F	.1/1/.1	.1/1/.1	FEP	.0050	.0075	.0495	4.31
616/616 - H	.1/1/.1	.1/1/.1	Polyimide	.0050	.0075	.0495	4.27
019/616 - F	0/1/.5	.1/1/.1	FEP	.0055	.0075	.0505	4.39
019/616 - H	0/1/.5	.1/1/.1	Polyimide	.0055	.0075	.0505	4.34
019/919 - F	0/1/.5	.5/1/.5	FEP	.0070	.0075	.0535	4.61
019/919 - H	0/1/.5	.5/1/.5	Polyimide	.0070	.0075	.0535	4.56
029/616 - F	0/2/.5	.1/1/.1	FEP	.0075	.0075	.0545	4.62
029/616 - H	0/2/.5	.1/1/.1	Polyimide	.0075	.0075	.0545	4.57



616/616
50% MIN. OVERLAP

FIGURE 2



616²/₃
66% MIN. OVERLAP

FIGURE 3

Experience has shown that even a one layer tape properly sealed can withstand dielectric breakdown voltages of over 3,000 volts and the additional layers are really added to increase the toughness of the system.

Figure 4 depicts the amount of insulation weight the various tape constructions contribute to the finished wire weight. It tabulates only

those constructions using the polyimide overcoat but are representative for those using the FEP overcoat system.

The 019/919H system is similar in weight and construction to MIL-W-81381/1 and /2. Notice that when the 616-2/3 lap construction is used, approximately 50% of the total insulation

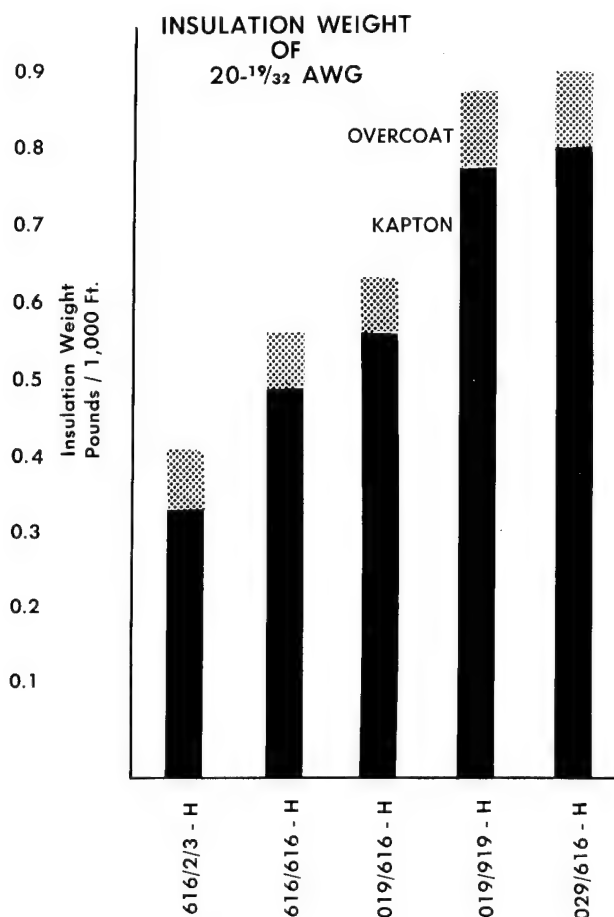


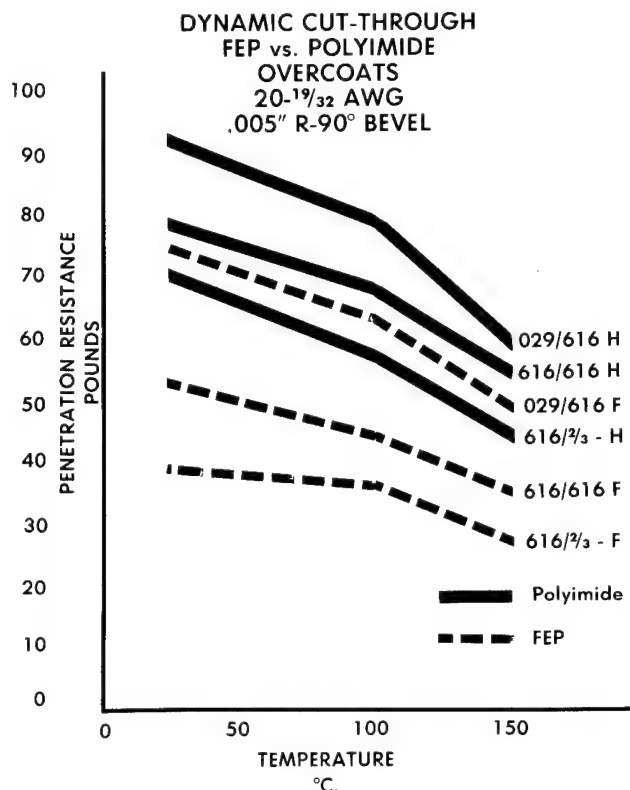
FIGURE 4

weight used on this military specification can be saved. By comparison, in an aircraft using 500,000 feet of wire this would provide a weight savings of approximately 225 lbs. per aircraft by using this lighter weight insulation system. It should also be apparent that the overcoat contributes only a small portion of the total insulation weight but as will be seen later greatly increases the toughness of this insulation system.

The physical toughness of these constructions can be compared by measuring their resistance to dynamic cut-through which is considered as most representative of the conditions seen during installation and operation. Testing performed by subjecting the insulation to an increasing load applied by a .005" radius blade gave results shown in Figure 5. Tests were run

at both room and at elevated temperatures. Notice that the substitution of the polyimide enamel for the FEP topcoat increases the overall insulation cut-through resistance at least 25%. It is apparent that very little change occurs as temperatures are raised. This is significant when compared with other similar insulation systems.

It is interesting to note that the 616-2/3 polyimide provides nearly the same resistance to cut-through as the 029/616 with the FEP overcoat. As previously discussed the insulation used in this construction is approximately 1/2 the weight of that used in the 029/616. This dramatically shows the toughness the polyimide provides when compared to the same thickness of the FEP overcoat.



Historically, an insulation system receives maximum abuse especially during its installation in aircraft. Its durability when being drawn through confined spaces or openings has always been important to the aircraft manufacturer. The polyimide overcoat has proven to be much more durable than the previous FEP system and is tested using a scrape abrading apparatus similar to that shown in Figure 6. The overcoat is subjected to

the abrasion of a .025 inch diameter needle under a 1 lb. load which is moved back and forth over its surface at a rate of 60 times per minute. The abrading is performed until it penetrates the overcoat and the Kapton is exposed. The test is terminated at this point to simulate the scraping which can occur before the electrical integrity of the Kapton is degraded.

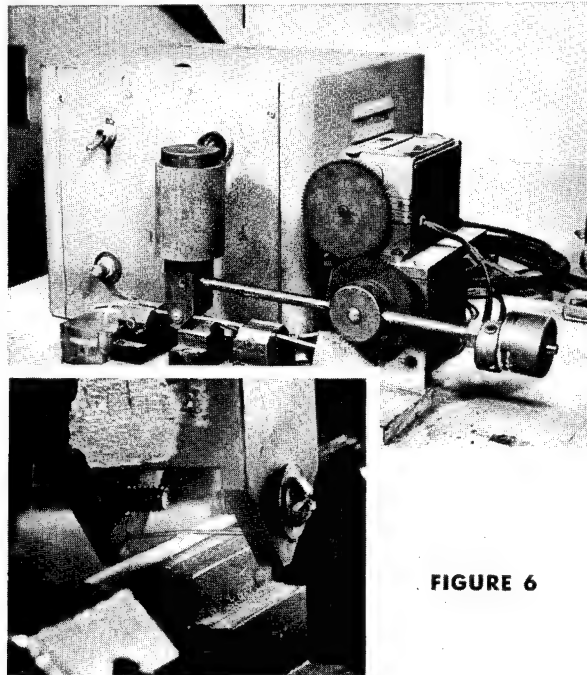


FIGURE 6

Table II presents a comparison of the overcoat durability of the polyimide vs. FEP system and shows the number of scrapes the overcoats will withstand before the Kapton is exposed. Notice that increasing the thickness of the FEP from 1/2 mil to 1 mil improves its durability between 1

and 2 times while replacing the 1/2 mil of FEP with 1/2 mil of polyimide can increase the durability between 10 and 30 times. An additional 1/2 mil of polyimide providing a total thickness of 1 mil can improve it nearly 50 times.

TABLE II

Overcoat Durability
20¹⁹/₃₂ AWG
1# Weight
.025" Diameter Needle

TYPE DISPERSION	OVERCOAT THICKNESS MINIMUM INCHES	NUMBER CYCLES MINIMUM
FEP	.0005	20 - 30
FEP	.0010	30 - 60
Polyimide	.0005	250 - 1000
Polyimide	.0010	500 - 1500

By combining the longer Kapton film available with new splicing techniques and replacing the FEP overcoat with polyimide, significantly longer lengths of insulated conductor were made. Figure 7 shows the length comparison. Notice that the configuration marked 019/919F is the length requirement of the current military specification MIL-W-81381 and that only 30% of the

wire manufactured can be guaranteed over 100 foot long. Compare this with the 029/616H specification where 500 foot long minimum lengths are guaranteed and as much as 50% can be supplied in lengths 5,000 ft. or longer. Actually, experience has shown that 5,000 feet is a conservative minimum.

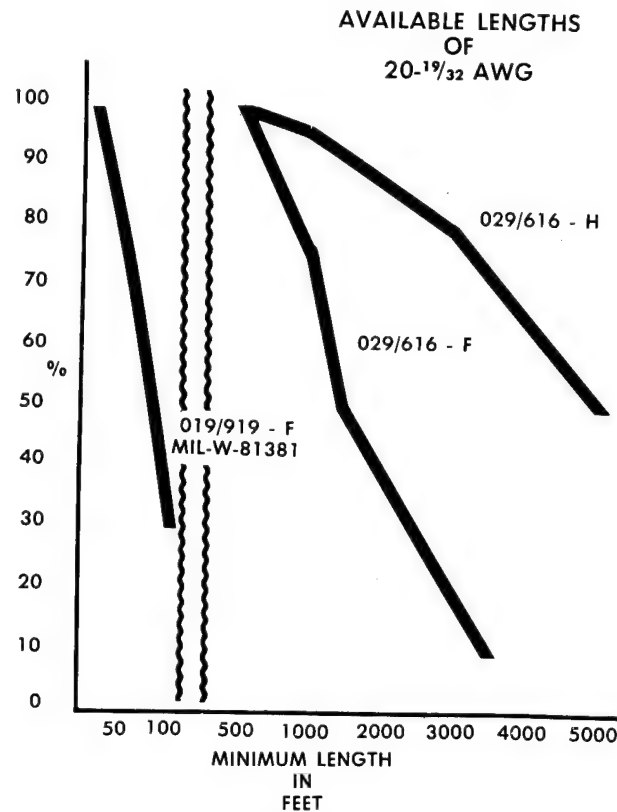


FIGURE 7

Circuit identification is important to the end users and pigmented polyimide overcoat can be color coded with a full range of MIL-STD-104 colors. The utilization of this new overcoat system has yielded outstanding dividends during aircraft installation. This new polyimide insulation system can be marked or identified by procedures similar to that used with the previous FEP overcoats. When identification is applied during the manufacture of the wire, it becomes nearly impossible to remove. This type of overcoat system also acts as an excellent quality control aid to check on any installation damage which might occur. Because the underlying Kapton insulation is a distinctive amber color, it is

readily visible if the overcoat has been scraped away by abusive installation. This can serve as a quick visual warning to operators and inspectors that insulation damage may have taken place.

The new polyimide enamel which makes this overcoat system so attractive requires knowledgeable processing by the insulator in order to be effective. If it is not completely cured on the wire, its performance will be severely downgraded. The material can be applied by the manufacturer with relative ease compared to previously available polyimide materials and may visually appear to be completely cured when actually it is not. To avoid this the manufacturer

must have a sound understanding of the chemical and physical changes taking place when the polyimide is cured. He must establish precisely controlled application and drying processes with appropriate tests to guarantee that the enamel is completely cured. The most significant test used to date is that of subjecting the overcoated wire to a high humidity environment and a 1X

mandrel bend while inspecting for visual cracks. This procedure has been recommended for inclusion in various military specifications and, in fact, is now incorporated in MIL-W-81381. Another quality control test is the needle scrape test described previously. Used together, they will insure the end user of a sound insulation system.

Conclusions

This new composite insulation system combining the improved polyimide tapes (Kapton) with improved polyimide enamel overcoats provides a lightweight insulation with a combination of properties heretofore unavailable. It has the ability to withstand elevated temperatures without smoking or burning. It is mechanically tough and can be installed easily by the end user at a minimum installation cost. It is available in colors, long lengths and uses component materials which have had extensive flight and application history.

Robert E. Smith, Jr.
Manager, Engineering
Haveg Industries, Inc.
Super Temp Wire Division

Mr. Smith graduated from the University of Vermont in 1950 with a B.S. in Mechanical Engineering and from Stevens Institute of Technology with an M.S. in 1960. He served in the U.S. Army Ordnance Corp from 1950 to 1955 with prime assignments in Guided Missiles and was with Curtis Wright during 1955 to 1957 as a Project Engineer on Ram Jet Propulsion Systems. Between 1957 and 1961 he worked as a Project Engineer in Thiokol Chemical Corporation on X-15 rocket propulsion systems. Since 1961 he has been employed by Haveg Industries, Inc., Super Temp Wire Division, a subsidiary of Hercules Inc.

At Haveg Industries he has been Manager of Engineering for a major portion of this time with prime responsibilities of Product Development, Research, Production Engineering and Technical Services. He holds several patents and applications relating to various types of insulation systems. He is a Registered Professional Engineer and a member of various societies including NEMA, SAE, ASTM, SPE and participates in various technical committee activities.

TEFZEL® ETFE FLUOROPOLYMER:
A VERSATILE NEW INSULATION FOR WIRE AND CABLE

E. A. Stecca, E. W. Fasig, Jr., J. C. Chevrier

PLASTICS DEPARTMENT
E. I. Du Pont de Nemours & Co. (Inc.)
Wilmington, Delaware

Summary. Tefzel®* ETFE fluoropolymer is a new high temperature resin for electrical insulation that combines ruggedness with very good dielectric properties and chemical resistance. Tefzel® is a melt extrudable polymer of ethylene and tetrafluoroethylene. Its balance of properties appears particularly well suited for wire and cable insulation, heat shrinkable and spaghetti tubing, and electronic components. Specific properties and performance characteristics for electrical wire and cable insulation are reviewed.

Introduction

In early 1970, the Du Pont Company announced the availability of a new developmental resin for electrical insulation: Tefzel® ETFE fluoropolymer. This paper describes Tefzel®, why it was developed, how it performs as a wire and cable insulation, and why it is believed that Tefzel® will assume a major role among today's many and varied insulating materials.

Trade-Off Dilemma

Today's wire user has many insulations from which to choose. He must, however, frequently face a trade-off in finished properties when selecting a wire construction for a particular application, or when he must have a new wire design created to satisfy some unusual set of operating conditions. This often has been the case when he had to combine high levels of mechanical strength and ruggedness with good electrical properties, to operate reliably under such difficult conditions as thermal cycling, high temperature, chemical spillage,

moisture, overloads, fire, and rough handling.

Designers, manufacturers, and users of wire and cable have resolved this trade-off dilemma by turning to composite wire constructions; i.e., those that use two or more materials to form the finished insulation. These range all the way from nylon-jacketed PVC, on up through Teflon® and its polyimide-coated constructions.

The result often represents a major compromise between what is really wanted, and what is actually available.

Developing New Polymers

The Plastics Department of the Du Pont Company has been close to this problem and has conducted an ongoing program of research on insulating materials, especially on fluorine-containing polymers. It has long been felt that a better way of resolving the trade-off dilemma would be to return to the basic chemistry underlying insulations. The objective would be to fashion a completely new material or, at least, one whose chemical building blocks would be more adept at fulfilling the unique needs of certain applications for wire and cable.

The greatest need seemed to be for an insulation that would be in the gap between "low-temperature" and "high-temperature" insulations; i.e., the temperature range from about 105°C to 200°C without unduly sacrificing whatever mechanical, electrical, thermal, or chemical properties that a good, versatile, reliable wire insulation should have.

What was being sought was a material that had the ruggedness of existing

*Du Pont trademark for ETFE fluoropolymer resins.

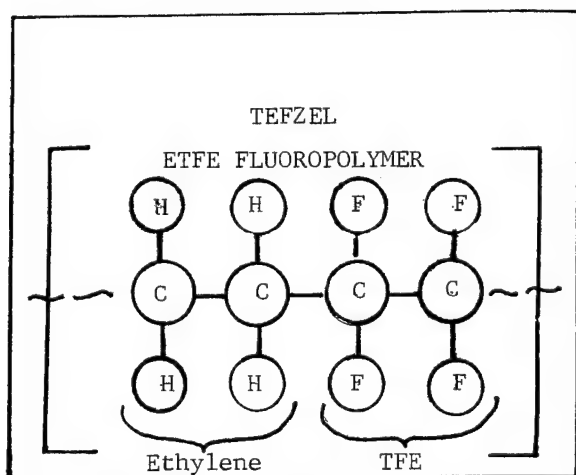
composite insulations, plus the special features of a single high performance polymer.

This goal appears to have been achieved with the new fluoropolymer, Tefzel® ETFE, which is best characterized as being "rugged...plus", because it does offer an unusual blend of mechanical strength and ruggedness, plus a combination of several other very desirable wire insulation properties.

Description of Tefzel®

Tefzel® is chemically a first cousin to Teflon® TFE fluorocarbon resin (Fig.1).

Figure 1 -- Molecular Structure of Tefzel® ETFE fluoropolymer



It is a copolymer of ethylene and tetrafluoroethylene. The TFE part of the molecule accounts for more than 75% of the new polymer's weight. The properties that are expected to derive from each part of the molecule have interacted with each other to produce a synergistic balance of properties for the entire molecule. Table I presents the basic property data for Tefzel® resin.

For example, Tefzel® retains most of the outstanding dielectric properties and chemical inertness of Teflon®; it also has a broad service temperature range and, in addition, has a mechanical ruggedness one would not expect to find in the fluorocarbons.

New Polymer

In every sense, Tefzel® is a com-

pletely new polymer, never before used as an insulation. However, Tefzel® is not just another laboratory curiosity. It already has passed many laboratory and processing screening tests. It is expected to satisfy several immediate needs of the wire and cable industry. There already is a pilot plant on stream with completion of a new, full-scale production facility scheduled for 1972.

Table I -- Properties of Tefzel® ETFE Fluoropolymer Resin

Tefzel® is Rugged
Plus....Very Good Dielectrics
Plus....Very Good Thermal/Cryogenic Performance
Plus....Very Good Chemical Resistance
Plus....Good Printing & Potting
Plus....Elastic Memory

Performance As Wire Insulation

Because Tefzel® is a fluoropolymer, it should first be compared as a wire insulation with the perfluorocarbons, such as Teflon® TFE and FEP, and with the fluorohydrocarbons such as polyvinylidene fluoride (PVF₂). The former have superior dielectric, thermal, and chemical properties; the latter has intrinsically good mechanical strength up to moderate temperatures.

Mechanical Properties

The ruggedness of Tefzel® lies in its tensile strength, stiffness, flex life, and impact strength (Table II). It has a tensile of 6,500 psi, greater than that of Teflon® TFE and equalling PVF₂. Its stiffness is moderate, higher than TFE, but not as high as PVF₂. Its flex life is much greater than PVF₂, and its impact strength is better than either PVF₂ or TFE. Tefzel® also exhibits excellent cut-through and abrasion resistance.

When fabricated as a wire insulation, Tefzel® can therefore withstand an unusual amount of physical abuse both during and after installation.

Table II -- Mechanical Properties of Various Fluorinated Polymers

	TEFZEL®	PVF ₂	TFE
Specific Gravity	1.70	1.78	2.15
Tensile, psi	5-7M	5-7M	3-5M
Elongation, %	100-400	20-400	250-350
Tensile Modulus, psi	125M	120M	50M
Flex Modulus, psi	200M	250M	95M
Flex Life (180°) flexes			
7-9 mil film	30M	5M	TFE > 1MM
3 mil film	190M	75M	--
Izod Impact, ft. - lbs./in.			
@ RT.	no break	4	no break
@ -54°C.	> 20	--	3-4
Hardness Rockwell R	50	--	25
Durometer D	75	75	55
Coefficient of Friction			
1 ft./min., 100 psi	0.4	0.4	0.05

Military Wire Specifications. This mechanical ruggedness may be illustrated by comparing typical military specification wires with constructions having Tefzel® ETFE fluoropolymer as insulation (Table III). The combination of good electrical performance, mechanical ruggedness, and moderate specific gravity (1.7) in Tefzel® leads to lightweight, minimum diameter constructions. Ten mils of Tefzel® provide good tape abrasion, comparable to currently used wires. Moreover, the cut-through resistance is better in Tefzel® than in some thicker constructions--such as MIL-W-81044/9--and approaches that of the polyimide constructions on the market today.

Computer Back-Panel Wire. This improvement in cut-through also is reflected in the performance of Tefzel® as an insulation for computer back-panel wiring. As the data in Table IV show, an AWG #30 wire with five mils of Tefzel® passes penetration tests at both 450 and 700 grams. Tefzel® is better than Teflon® TFE fluorocarbon resin in this respect.

Electrical Properties

Besides being rugged, Tefzel® also is a very good dielectric (Table V). Its low dielectric constant of 2.6 does not vary either with frequency or temperature; its dissipation factor, while higher than Teflon® TFE, is considerably lower than that of most other dielectrics. It has a dielectric strength greater than 2,000

volts per mil in 10 mil wall thickness equalling Teflon® TFE. Its volume and surface resistivities approach those of Teflon® TFE.

Thermal Properties

Other "plus" features of Tefzel® include its very good thermal and low temperature properties, summarized in Table VI. Tefzel® has a broad operating temperature range. In its non-irradiated form, Tefzel® is capable of continuous service at 150°C, as indicated by extensive high temperature testing.

When Tefzel® is cross-linked by radiation, it appears to have extended high temperature capabilities, along with the expected advantages of enhanced solder-iron resistance and current overload protection. It is expected that wire constructions based on radiation cross-linked Tefzel® will be capable of continuous service at 180°C.

Possibly the most impressive of all of the properties of Tefzel® is its low temperature toughness. It does not break in the notched Izod impact test, either at room temperature or at -54°C. This corresponds to a very high impact strength, over 20 ft.-lb./in. The brittleness temperature is below -100°C.

Table III -- Comparison of Wire Insulated with Tefzel® ETFE Fluoropolymer
with Military Specification Wires, AWG #20

	<u>Wire Construction</u>			
	<u>Tefzel® ETFE</u>	<u>MIL-W-22759/13</u>	<u>MIL-W-81044/16</u>	<u>MIL-W-81044/9</u>
Insulation, mils	10	11	10	15
Number of components	1	2	3+	2
Space, o.d., mils	60	61	60	70
Weight, lb./1,000 ft.	4.9	5.5	4.7	5.4
Conductor (above 150°C.)	Sn/Cu (Ag or Ni/Cu)	Sn/Cu	Sn/Cu	Sn/Cu
Tape abrasion, 400-grit, 1/16-in.	40	40	40	60
Cut-through, 5-mil blade, 0.2 in./min.	40	20	65	30

Table IV -- Comparison of Computer Back-Panel Wires, AWG #30
Against Well-Known Industry Standards

	<u>Insulation</u>			
	<u>Tefzel® ETFE</u>	<u>Teflon® TFE Fluorocarbon Resin</u>	<u>Teflon® TFE With Polyimide Coating</u>	<u>PVF₂</u>
Insulation, mils	5	5	5 + 0.75	5
Penetration, 50°C. 450 grams, 36 hr.	Pass	Pass	Pass	Pass
700 grams, 24 hr.	Pass	Fail	Pass	Pass
Shrinkback, 5 sec. over 320°C.-solder iron (max. 1/16-in. shrinkage)	Pass	Pass	Pass	Pass
Bond strength, 0.25 to 1.25 lb.	Pass	Pass	Pass	Pass
Dielectric strength, VRMS	12,000	10,000	10,000	8,000
Dielectric constant @ 1kHz	2.6	2.1	2.1	7.7

Table V -- Electrical Properties of Various Fluorinated Polymers

	Tefzel® ETFE Fluoropolymer	PVF ₂	Teflon® Fluorocarbon Resin
Dielectric Strength-volts/mil			
125 mils	400	250	500
40 mils	900	---	900
10 mils	2000	---	2000
Dielectric Constant @ 10 ² Hz	2.6	8.4	2.1
10 ³ Hz	2.6	7.7	2.1
10 ⁶ Hz	2.6	6.5	2.1
Dissipation Factor @ 10 ² Hz	.0006	.049	<.0002
10 ³ Hz	.0008	.018	<.0002
10 ⁶ Hz	.005	.17	.0002 TFE .0007 FEP
Arc Resistance, sec.	72	60	> 360
Volume Resistivity, ohm-cm	>10 ¹⁶	>10 ¹⁴	>10 ¹⁸
Surface Resistivity, ohms/sq	>10 ¹⁴	--	>10 ¹⁶

Table VI -- Thermal Properties of Fluorinated Polymers

	TEFZEL®	PVF ₂	TEFLON®
Melting Point, °C.	270	172	275 FEP 327 TFE
Service Temp., °C	150	135	200 FEP 250 TFE
Heat Distortion @ 66 psi, °C.	105	145	70 FEP 122 TFE
@ 264 psi, °C.	70	90	51 FEP 55 TFE
Coefficient Linear Expansion x 10 ⁵ in/in °F	7.5-9.5	8.5	8-10
Low Temperature Embrittlement, °C.	<-100	<-80	-82 FEP -100 TFE

Flammability

From a flammability viewpoint, Tefzel® can be rated as either "nonflammable" or "self-extinguishing" in the various tests for flammability (Table VII). It passes both vertical and horizontal flammability tests on insulated wire, both as a single wire and in bundles. By these tests, it is considered

"self-extinguishing"; by ASTM D-635, Tefzel® is rated "non-burning". After-burn following removal of the ignition source varies somewhat with flame temperature but remains within the limits of each specification test for a self-extinguishing material.

The ability of Tefzel® to pass the most severe vertical flame test in air is

Table VII -- Flammability Tests on Tefzel® ETFE Fluoropolymer

<u>Wire Test</u>	<u>No. Wires</u>	<u>Angle</u>	<u>Burn After Flame Removal</u>	<u>Flame Travel</u>	<u>Tissue Burn</u>
1. UL STD 83	1	90°	Pass	Pass	N.S.*
2. MIL-W-81044	1	60°	Pass	Pass	Pass
3. MIL-W-22759	1	60°	Pass	Pass	N.S.*
4. MIL-W-5086	1	0°	Pass	Pass	Pass
5. MIL-W-22759/13	1	90°	Pass	Pass	N.S.*
	7	90°	Pass	Pass	N.S.*

*N.S. Not Specified

confirmed by the General Electric Limiting Oxygen Index (Table VIII). Tefzel® requires an oxygen concentration of at least 30% to sustain combustion. This is higher than the 21% oxygen concentration in normal air by a comfortable margin. Also of importance is the fact that the heat of combustion of Tefzel® is only 5,900 Btu/pound, one-half to one-third that of other commonly used insulating materials. In an emergency situation, Tefzel® would add less to the severity of a fire than do non-fluorinated hydrocarbon insulations.

Smoke Resistance

Although currently there is no industry-wide standard for smoke generated by wire insulations under overload or overheating conditions, tests indicate that Tefzel® most likely will meet any foreseeable industry requirements for smoke generation. It has been established that Tefzel® produces far less smoke under current overload than do PVC/nylon, PVF₂ jacketed polyethylene, or other similar insulations. At its best,

however, Tefzel® is not equal to Teflon® TFE or FEP fluorocarbon resins which are virtually nonsmoking.

Chemical Properties

Tefzel® has much in common with Teflon® resins as far as chemical inertness is concerned. A solvent for Tefzel® at temperatures below 200°C has yet to be discovered. Water absorption is less than 0.1%. None of the representative chemicals listed in Table IX has shown any noticeable effect on Tefzel® when tested at 50°C for one month.

Wire constructions insulated with Tefzel® also have passed compatibility tests for aircraft hydraulic fluids such as "Skydrol"¹ and "Aerosafe"². When wire insulated with Tefzel® was wound on a 1X mandrel and immersed in these fluids at 150°C, it did not crack, even though industry specification requirements seldom are above 70°C.

Table VIII -- Oxygen Index of Heat of Combustion of Various Polymers

<u>Material</u>	<u>Heat of Combustion</u>	<u>Limiting Oxygen Index</u>
TEFLON®	2,200 BTU/lb.	>95% oxygen
TEFZEL®	5,900 BTU/lb.	30% oxygen
PVF ₂	6,400 BTU/lb.	44% oxygen
Coal	14,000 BTU/lb.	
Polyethylene	20,000 BTU/lb.	18% oxygen

Table IX -- Chemical Resistance Data

Tefzel® ETFE fluoropolymer resin samples showed no effect after being immersed in the following chemicals at 50°C. for one month:

acetic acid	dimethyl sulfoxide	"Perclene®"
acetone	hydrochloric acid (conc.)	pyridene
acetophenone	hexane	"Skydrol®" 500A
"Aerosafe®"		
aniline	isooctane	sodium hydroxide (50%)
benzene	kerosene	sulfuric acid (conc.)
butylamine	n-methyl pyrrolidone	"Triclene®"
carbon tetrochloride	ammonium hydroxide (conc.)	water
dimethyl acetamide	nitric acid (conc.)	

Handling Characteristics

For a fluoropolymer containing so high a percentage of tetrafluoroethylene, Tefzel® exhibits a truly unusual printability and pottability as a wire insulation.

Printing. Tefzel® can be readily printed in a standard, one-step, hot-stamp process, using conventional ink foils without any special treatment either before or after printing. The print is very durable and exceeds the industry standards for scrape abrasion, eraser rub, and indentation.

Potting. Potting likewise is easier for Tefzel® than for Teflon® fluorocarbon resin, even though Tefzel® has a low critical surface free energy. It differs enough from completely fluorinated polymers to permit potting and bonding without etching.

When potted directly in a polysulfide compound, Tefzel® has a potting pull-out strength of about 10 lb./in. This equals the pull-out strength for several military specification wires and that of etched Teflon® TFE. Etching the surface of Tefzel® will increase pull-out strength.

Handling. The handling characteristics of wire insulated with Tefzel® are extremely important to the user. Wire insulated with Tefzel® is very flexible, yet takes a set and does not spring back, and is easy to strip. Mechanical or thermal, hand or automatic wire strippers can be used. It also has a very low strip force, nearly the same as that

of Teflon® TFE (Table X).

These combined features should add to the attractiveness of Tefzel® from an assembly viewpoint.

Color Coding

Tefzel® is also easily pigmented for color coding. Color concentrates are presently available in red, yellow, black, white, and blue. The remainder of colors necessary for standard military and industrial color coding will be available by commercialization.

Processing Tefzel®

There are several aspects of Tefzel® that relate, at least indirectly, to finished wire properties and performance.

Melt Extrudable. For one thing, Tefzel® can be fabricated by both melt extrusion and by injection molding. Its extrusion rates are considerably higher than those used commercially for Teflon® FEP. Both Du Pont and commercial wire fabricators have produced wire insulated with Tefzel® at rates ranging from 50 to 400 ft./min. These wires have met all pertinent specification requirements for electrical integrity and shrink-back at elevated temperatures.

Conductors. It is possible to extrude Tefzel® over copper wire plated with tin, nickel, and silver with equal success. Tin should materially improve the costs and soldering ease of many lightweight wire constructions.

Table X -- Strip Force for AWG #20 Wires

<u>Insulation Construction</u>	<u>Strip Force, lbs., 1-in. slug</u>
Tefzel® ETFE Fluoropolymer (10-mil wall)	3
MIL-W-81044/9	14
MIL-W-81044/16	10-16
MIL-W-16878 Type E	1-3

Radiation Cross-linking

A very important feature of Tefzel® is that it can be cross-linked by radiation, despite the high proportion of TFE fluorocarbon resin in the fluoropolymer. The radiation cross-linking treatment renders it no longer plastic, thus providing enhancement of high temperature properties including overload protection.

Solder Iron Resistance. Irradiation also improves solder iron resistance permitting wire insulated with Tefzel® to withstand a 400°C solder iron for over ten minutes without noticeable effect.

Radiation Resistance. A corollary of the ability of Tefzel® to cross-link is its tolerance to large dosages of radiation. How great this tolerance might be has not yet been determined, but it should be significantly greater than that of the perfluorocarbon resins.

Heat Shrinkable Tubing

Tests on oriented films of Tefzel® show a high degree of recoverable strain. The elastic recovery is high enough to yield shrink ratios of 2/1 when Tefzel® is heated well below its melting point--for example, 120°C.

This ratio can be increased significantly by irradiation cross-linking prior to expansion to as much as 5/1 when heated above its melting point. There is every reason to believe that the balance of properties offered by Tefzel®, combined with its elastic memory, should make this new fluoropolymer an excellent candidate for heat shrinkable products, especially for encapsulating, protecting, and identifying irregular shapes.

Conclusion

To summarize the work done on this new fluoropolymer, it has been demonstrated that Tefzel® is an insulating material which offers many intriguing possibilities in wire and cable designs. These stem mainly from the improvements in mechanical properties that Tefzel® resin offers.

To the basic ruggedness of Tefzel®, there also have been added very good dielectric properties, chemical resistance, thermal and low temperature performance, easy printing and potting, the ability to be melt processed, elastic memory, plus the improvements in these properties made possible by radiation cross-linking.

Tefzel® has the balance of properties that should help fill the gap of insulation needs in the wire and cable industry.

Table XI -- Heat Shrinkable Tubing Data for Fluorocarbons

	<u>TEFZEL®</u>	<u>Irradiated TEFZEL®</u>	<u>Irradiated PVE²</u>	<u>TEFLON® FEP</u>
Shrink Ratios	2/1	5/1	4/1	1.6/1
Expansion temperature	120°C.	>270°C.	>200°C.	130°C.

¹Registered trademark, Monsanto Co.
²Registered trademark, Stauffer
Chemical Co.

Eugene A. Stecca, Technical Representative -
"Tefzel", E. I. du Pont de Nemours & Co., Inc.
Plastics Department D-13054
Wilmington, Delaware 19898

June 1956, graduated with B.S. in Chemical
Engineering from Case Institute of Technology,
Cleveland Ohio. Elected to Tau Beta Pi, Alpha
Chi Sigma, Blue Key and Pi Delta Epsilon
Honorary Fraternities. Member of Phi Kappa Psi
Social Fraternity. Graduated with honors.

Commissioned 2nd Lt./USAF.

Joined Du Pont Company, Plastics Department,
Wilmington, Del. Following training program,
assigned Technical Representative for "Teflon"
fluorocarbon resins, Technical Services
Laboratory.

November 1956, called to active duty in Air Force.
Assigned Project Officer at Wright Air Develop-
ment Center. Promoted to 1st Lt. Served three
years.

Responsibilities included writing specification,
evaluating technical proposals and monitoring
government contracts. Prepared technical reports
for Air Force Commands. Completed Toastmaster's
Training. Assisted in presenting monthly
indoctrination courses and delivered technical
speeches to Headquarters Command Personnel and
Installation Engineering Schools.

Returned to Du Pont as Technical Representative.
Engaged in customer service and application and
process development with "Teflon".

February 1962, assigned to Applications Group,
"Teflon" Marketing Section. Activity included
promotion and development in expanding markets
in mechanical and chemical applications.

January 1963, transferred to Chicago District
Office as Field Technical Representative -
Fluorocarbons Division.

September 1966, assigned Field's Sales Marketing
Representative, Chicago District Office. The
territory included Illinois, Wisconsin,
Minnesota, and Iowa.

February 1969, assigned new product development,
Fluorocarbons Marketing Section - development of
"Tefzel" ETFE fluoropolymer.

I have acquired eleven years experience in
processing, marketing, and technical service with
fluorocarbon resins and have also presented
papers to the Society of Aerospace and Processing
Engineers--Chicago--and a joint meeting of
National Association of Corrosion and Lubrication
Engineers--St. Louis.

My wife Caryl and I have five children and are
living in Wilmington, Delaware. Our interests
include music, bridge, and discussion clubs.
Gardening is my avocation.

Edgar W. Fasig, Jr., Technical Representative
"Teflon" FEP

August 1960, graduated with B.S. in Chemical
Engineering and M.S. (Engineering) from the Ohio
State University, Columbus, Ohio. Elected to
Tau Beta Pi and Anchor and Chain (Military)
honorary organizations. Member of Sigma Chi
social fraternity (Treasurer, one year).

Commissioned Ensign, Civil Engineer Corps, U.S.N.
Attended Civil Engineer Corps Officers School,
Port Hueneme, California, and assigned to the
Public Works Department, Naval Support Activity,
Naples, Italy.

November 1963, joined the Du Pont Company,
Plastics Department, Wilmington, Delaware, as
a Research Engineer, Fluorocarbons Division,
at the Experimental Station Laboratories.

February 1965, reassigned to the Research Group,
Fluorocarbons Division, Washington Laboratories,
at Parkersburg, W. Va.

August 1968, transferred to the Marketing Group,
Fluorocarbons Division, as a Technical Representa-
tive, "Teflon" fluorocarbon resins, Technical
Services Laboratory, Wilmington, Delaware.

April 1969, assigned as a Technical Representa-
tive, Market Development Group, with responsibility
for marketing activities associated with "Teflon"
as a wire and cable insulation in the airframe
wire market.

October 1970, assigned product responsibility for
"Teflon" FEP fluorocarbon resin.

My seven years with Du Pont have included research
activities in Wilmington and at a manufacturing
plant site, special assignment during plant start-
up activities in both the U. S. and Europe and
marketing activities in technical, end-use
development and product areas.

My wife Peggy and I have one daughter and live in
Wilmington, Delaware. Our activities include
music (voice groups, opera) and amateur theater.

Jean-Claude J. Chevrier, Technical Representative
Electrical Applications

1960 - B.A. in Physics from George Washington
University in Washington, D. C.

1962 - M.S. in Physics from University of
Virginia.

1964 - Ph.D. in Physics from University of
Virginia.

1964-1966 - Research Associate and Instructor -
Physics Department, University of Virginia.

Field - Mechanical and electrical properties of
metals and alloys.

1966- 1968 - Research Physicist doing new product
development in Research and Development Division.

1968-Present - Electrical Industry Group,
Fluorocarbons Division.

Married and has one son. Interests include
photograph, music, tennis, and scuba diving.

BRITTLE FRACTURE OF POLYETHYLENE AT LOW TEMPERATURES

Masaaki Okada
Atushi Utumi

Research Laboratory,
Dainichi-Nippon Cables, Ltd.
Amagasaki, Hyogo, Japan.

Summary

Polyethylene jacketed cables sometimes show brittle fractures at an unexpectedly higher temperature than is expected from the ASTM Brittleness Temperature Test results. In order to elucidate this phenomenon, brittle fractures of polyethylene at low temperatures were studied by uniaxial tensile tests, brittleness temperature tests, biaxial stress tests, and cable bending tests. It was found that low density polyethylene is more brittle under biaxial stress than under uniaxial stress at low temperatures and that the presence of notch greatly affects the ductile-brittle transition temperature. Tests were also made on other materials which showed different sensitivity to stress polyaxiality and stress concentration. Cable bending tests at low temperatures showed a good correlation with plaque tests, which suggests that the brittleness temperature test with notched specimens and the biaxial stress test are best suited for screening out a cold resistant material for cable jacketing.

Introduction

Low Temperature Brittleness Test specified in ASTM D-746 is most widely used as a standard testing method for determining the low temperature impact resistance of plastics. It has long been recognized that polyethylene has excellent low temperature flexibility. In fact commercial cable jacketing grade polyethylene never loses its toughness even at a temperature of -80°C , according to ASTM results. This is the reason why polyethylene has been largely used as a cable jacketing material for a wide range of applications. However, it is known that polyethylene which is believed to be one of the toughest materials industrially available, sometimes shows brittle fractures at an unexpectedly higher temperature. For instance, there have been unusual cases of polyethylene

jacketed cables showing brittle fractures even at a temperature of -30°C or higher.

From these facts, it is considered that testing by the ASTM test is unsatisfactory for the purpose of grading a cable jacketing material.

With this view point, a series of tests were carried out in our laboratory to study the low temperature impact brittleness of polyethylene, and the results are reported in this paper.

Experimental

Samples tested

Samples were compression molded into plaques according to a standard procedure, after milling by a two roll mill. Specimens were taken from these plaques. Specimens were subjected to the tests as "unannealed" or as "annealed". "Unannealed" specimens were tested after they were molded without being treated, but "annealed" specimens were treated at 110°C for one hour, then cooled at 5°C per hour prior to testing.

Density, Melt Index, and viscosity average molecular weight of the main samples are listed in the Appendix together with the test results.

Testing methods

The following tests were made in this study.

Uniaxial tensile test : Specimens prepared by the use of Die No. 3 as described in JIS K 6301 were tested at the jaw separation speed of 500 mm/min., using an Instron type tensile tester, Autograph (Shimadzu Seisakusho Ltd.).

Notched specimens were tested as well as unnotched ones, whereby the notch was made in the center of the side face with a razor blade held in a controlling jig allowing only that portion of the blade, equal to the desired depth of

the notch, to protrude. This device was also used in the following low temperature brittleness test.

Low temperature brittleness test : This test was made according to the procedure specified in JIS K 6723 which is essentially the same as ASTM D-746.

To eliminate the unfavorable effect of a rough edge by die cutting, about 0.3mm of the side faces of the specimens were cut off using a sharp razor.

In the test with notched specimen, the notch was made to a 0.5mm depth in the side face.

Biaxial stress test : Biaxial stress tests were made using a diaphragm type apparatus.

Fig.1 shows a part of the apparatus. Inner diameter of the diaphragm was 40mm. Nitrogen gas was used as the pressure medium. The specimen was in a disc about 70mm in diameter and about 0.5mm in thickness.

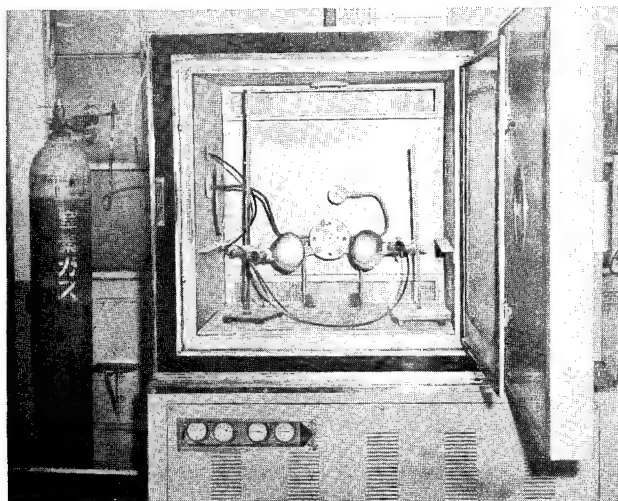


Fig. 1. Apparatus used in biaxial stress test.

In this study two testing procedures were adopted. In one procedure, a constant pressure was abruptly loaded on the specimen to see the transition of the fracture type from ductile to brittle with temperature change. Crossed notch specimens having 0.05mm depth and 10mm length in the center surface were also used.

In the other procedure, the pressure was gradually applied to the specimen, on which was printed 3mm coordinate grids by the silk screen method, and the fracture processes were photographed and analyzed using cine cameras.

Tensile stresses were calculated using the formula, $\sigma = RP/2t$, where R is the radius of buldge, P the pressure, and t is the sample thickness. This procedure is essentially the same one employed by Bell Telephone Labs. investigators.¹ In this experiment, all of the calculations were made using an electronic computer.

Cold bending test : The samples about 1.2m long, were maintained at a fixed low temperature for several hours in a circulating-air oven equipped with a cooling unit.

Each of the samples was abruptly bent around a 40mm diameter mandrel as soon as it was taken out of the oven.

Types of fracture

The fractures of plastic materials are generally divided into two types (Fig.2). One is the ductile fracture which is accompanied by yielding and permanent deformation of the material. The other one is the brittle fracture which is not accompanied by permanent deformation at all. Generally the type of fracture changes from ductile to brittle as the temperature decreases. In our experiments the determination of the transition temperature of fracture type was very important.

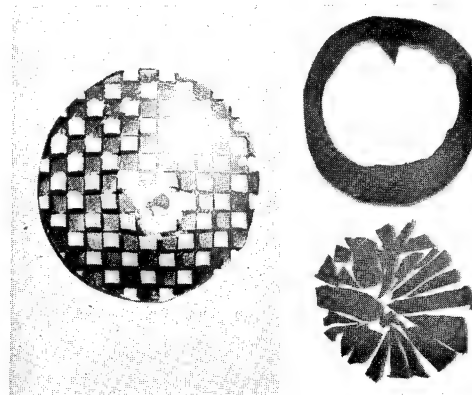


Fig. 2. Ductile and brittle fractures of low density polyethylene in biaxial stress test.

left : ductile

right : brittle

Typical results of the temperature dependence of stress at break in uniaxial tensile tests are shown in Fig.3. In this Figure it is seen that yield stress has a peak at a certain temperature, and sharply decreases at lower temperatures.

It was found that the peak temperature coincided very well with the ductile-brittle transition, according to the observation of the fractured surfaces of the specimens.

Results and Discussion

It has been reported by many investigators that a number of factors affect the low temperature brittleness of polyethylene.³⁻¹⁰ According to our investigation, these factors are classified as follows.

1. Stress concentration
2. Complexity of stress
3. Chemical structure and crystallization state of the material.

The experimental results and discussion will be explained according to this classification.

Stress concentration effects

It has been known since Hoff and Turner reported on this subject in 1957, that polyethylene has a high notch sensitivity on impact.³ Actually in most cable jacket fractured in commercial service, it was proved that the fracture was induced by stress concentration in the presence of a notch. According to our examination, however, another type of stress concentration effect, co-fracture, was found to exist in actual failures.

Here, the co-fracture means a fracture which occurs by a sudden stress concentration caused by the brittle fracture of a poor cold resistant material fused to the jacket substrate. Therefore, experiments on the notch effect and co-fracture were carried out to elucidate the stress concentration effect on polyethylene.

Notch : The effects of notch on the brittleness temperature were studied first.

In Fig.4 is shown the effect of the notch on the brittleness temperatures. This result shows that polyethylene is severely affected by the presence of a notch.

In particular, a notch on the impact surface raises appreciably the brittleness temperature of polyethylene, for instance a notch of 0.1mm depth raises the brittleness temperature to around -20°C.

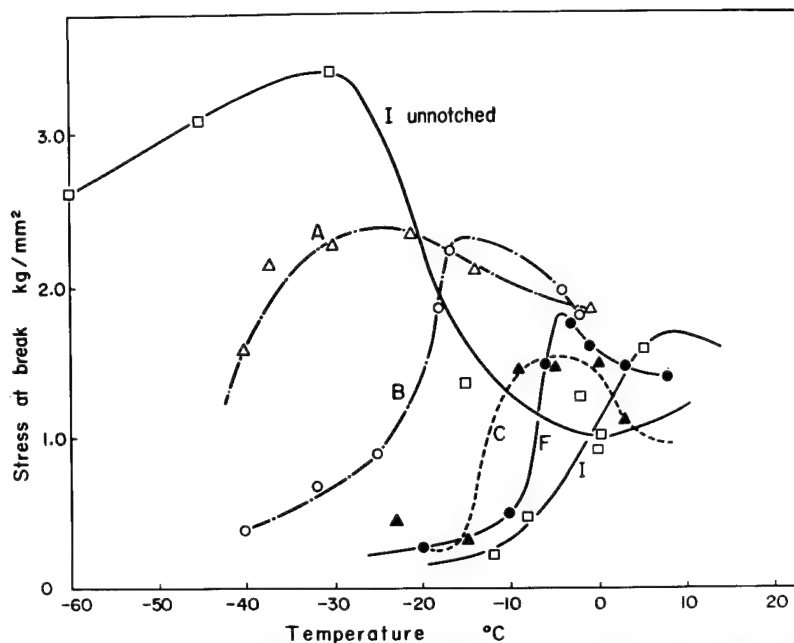


Fig. 3 Temperature dependence of stress at break of low density polyethylene in uniaxial tensile test with notched specimens.

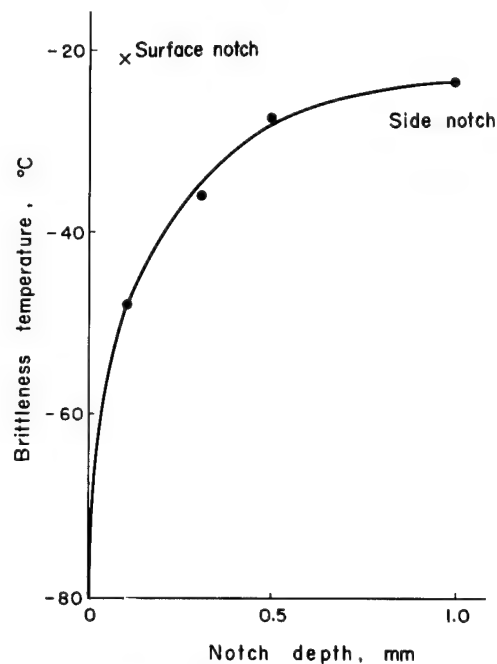


Fig. 4 Effects of notch depth on brittleness temperature.

Sample : Cable jacketing grade low density polyethylene of MI . 0.3 and density 0.930 .

A notch on the side face of the specimen also severely raises the brittleness temperature of polyethylene.

The deeper the depth of the notch, the higher is the brittleness temperature showing a leveling off where the notch is considerably deep.

From this experiment, considering the specimen thickness, it was decided to use a specimen having a 0.5mm side notch as the standard notched specimen.

Co-fracture with other materials : In order to study this phenomenon, specimens were prepared as follows. On a 2mm thick sheet of material, a 0.2mm thick film of another material was heat bonded to make a melt adhesion. Specimens were cut from the composite sheet and subjected to brittleness temperature tests. The characteristics of the materials used in this test and the test results are summarized in Tables 1 and 2.

As is seen in the Tables, polyethylene is a material which is highly susceptible to the effects of co-fracture.

Biaxial stress effect

It is well known that Hopkins and other investigators made fine contributions to the study of the biaxial stress effect on polyethylene.^{1, 2} They showed that polyethylene was more brittle under biaxial stress than under uniaxial stress at room temperatures. From this fact it would be natural to think that polyethylene would also be influenced by the polyaxiality of stress at low temperatures. However, few papers have ever been published on the biaxial effect on polyethylene at low temperatures. Clegg, Turner, and Vincent mentioned the glass-like fracture of polyethylene on impact at low temperatures, but the description contained only a few lines.⁹ Morris made a measurement of the falling weight impact strength of various materials in a wide temperatures range wherein low density polyethylene was not included.¹⁰ Fujioka made puncture measurements on polyethylene at low temperatures, but in his experiments polyethylene was not tested either.¹¹

When a cable is bent, the outer jacket is subjected to a complex polyaxial stress.

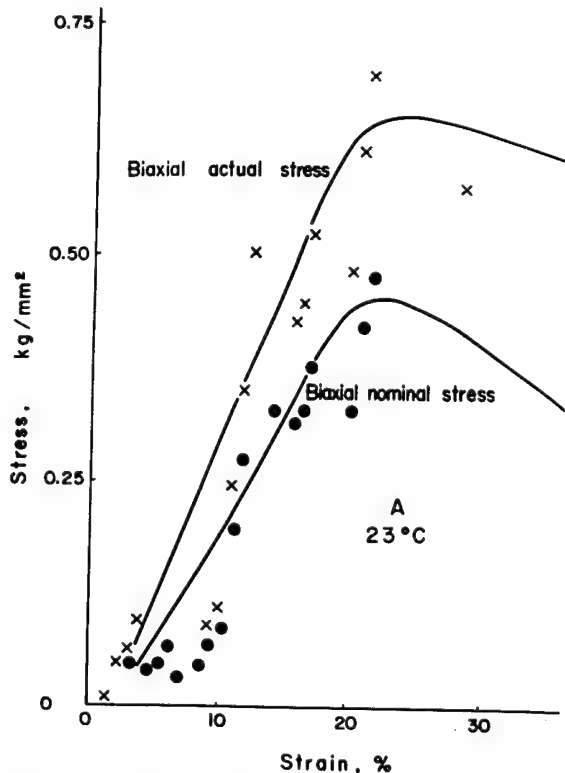


Fig. 5 Stress-strain curves of low density polyethylene. at 23°C

Table 1. Characteristics of the material.

Material	Tb, unnotched	Remarks
LD Polyethylene	< -77°C	Cable jacketing
Plasticized PVC-A	-42°C	Cable jacketing
Plasticized PVC-B	-28°C	Cable jacketing
Plasticized PVC-C	-1°C	Cable insulation
Polypropylene	+5°C	General purpose

Table 2. Cofracture effects on the apparent brittleness temperatures of laminated samples.

Sheet 2mm thick	Film 0.2mm thick	Brittleness temperature, °C	
		impact on film	impact on sheet
LDPE	PP	+2	< -77
PVC-A	PVC-B	-37	-42
PVC-A	PVC-C	-18	-42

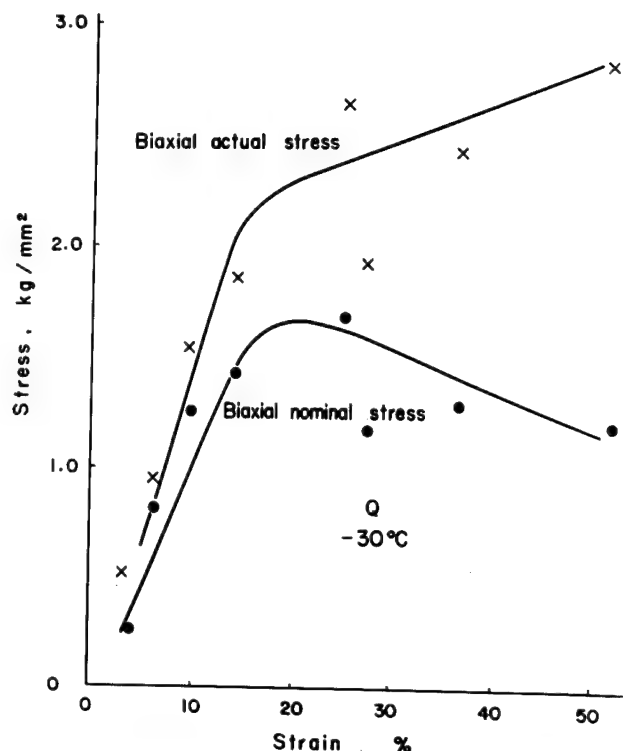


Fig. 6 Stress-strain curves of low density polyethylene. at -30°C

Therefore, as far as the cold bend fracture of a polyethylene jacket is concerned, the behavior of polyethylene under polyaxial stress at low temperatures must necessarily be investigated.

Fig. 5 shows a stress-strain curve at 23°C , and Fig. 6 at -33°C , obtained from the biaxial tensile test. It is noticed that the stress is appreciably lower than that usually obtained in the uniaxial tensile test. These results are opposite to those of the Bell Telephone Labs. investigators who showed that the biaxial stress-strain curve was drawn higher than the uniaxial stress-strain curve.¹ While it is reported by Miklowitz that a polyamide film showed a lower stress-strain curve in a biaxial stress test than in a uniaxial test¹², further study was not attempted at this point in our laboratory.

Fig. 7 shows the change of elongation at yield with temperature determined by the above method with unnotched specimens. Samples were polyethylenes of various Melt Indices with nearly the same density. It is

seen, except for the one polymer with the lowest Melt Index, that the yield elongation decreases rapidly with temperature decrease until brittle fractures occur.

Comparisons were then made of ductile-brittle transition temperatures among biaxial stress tests, impact brittleness tests, and uniaxial tests. In Fig. 8, transition temperatures with unnotched specimens are plotted against the Melt Index of sample polymers having nearly the same density. It is clearly seen that polyethylene without notches is very brittle under a biaxial test. In Fig. 9, similar plots were made with notched specimens where the highest transition temperatures were obtained in the impact brittleness test. This is considered as the manifestation of polyaxiality induced by the notch made in the impact brittleness test specimen.⁹ It should also be noticed that the rate of strain is considerably higher in the impact test than in the present biaxial test.

Effects of chemical structure and crystallization state of the material

More than fifty kinds of polyethylene and ethylene copolymer differing in their molecular weight, molecular weight distribution, density, chemical composition and thermal history were tested to study the effects of these factors on the brittleness temperature.

In the Appendix are shown the characteristic properties of the samples used in this study.

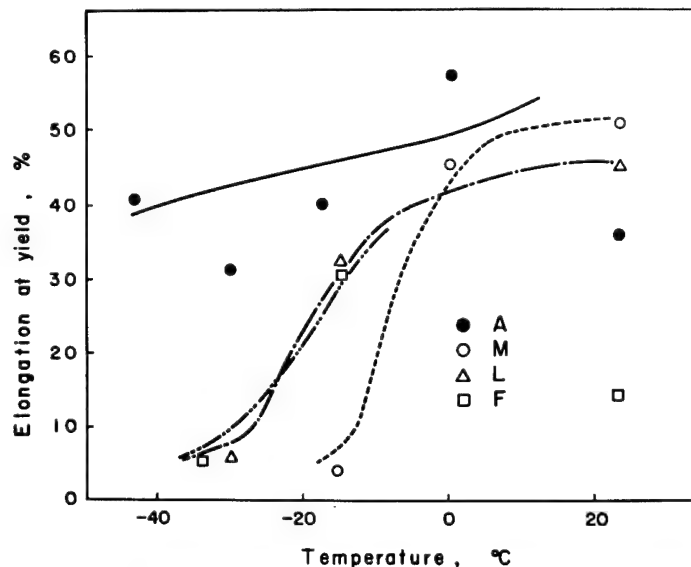


Fig. 7 Temperature dependence of elongation at yield in biaxial stress test of low density polyethylene.

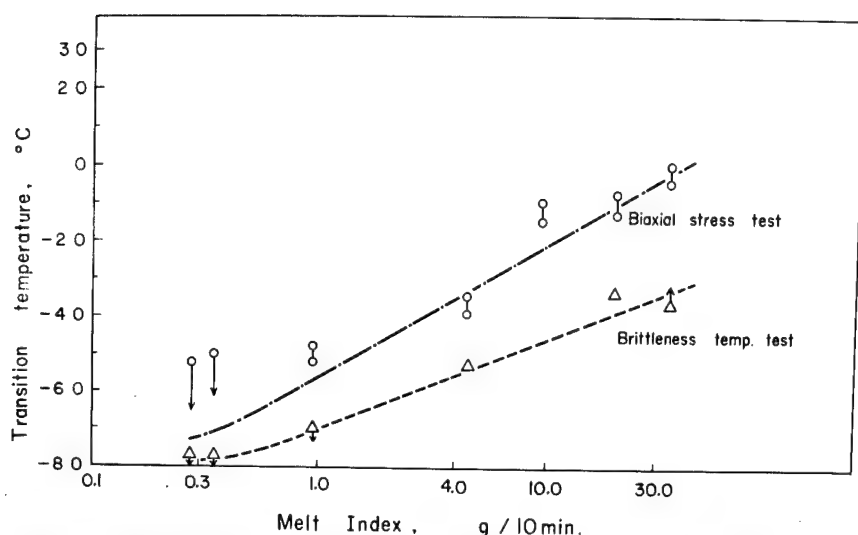


Fig. 8 Comparison of transition temperatures of low density polyethylene between brittleness temperature and biaxial stress tests with unnotched specimens .

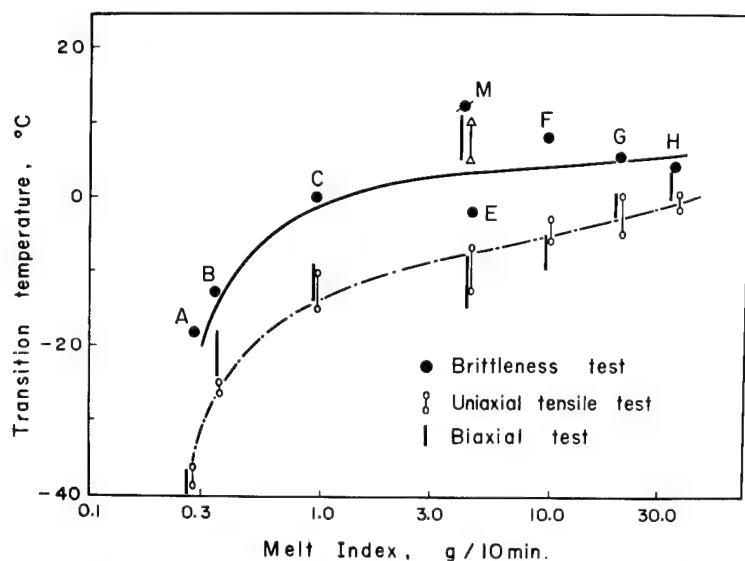


Fig. 9 Comparison of transition temperatures of low density polyethylene among three types of tests with notched specimens .

Molecular Weight : Melt Index is a measure of molecular weight. Melt Index dependence of ductile-brittle transition temperature of polyethylenes was already shown in Figs. 8 and 9. Fig. 10 also plots the data obtained in the brittleness temperature test with notched and unnotched specimens. The increases in transition temperatures of polyethylene with the increases in Melt Index have been reported by many investigators.^{3,5} It is seen in this Figure, that the effects of

Melt Index are less profound as compared with the effect of a notch.

Low molecular weight fraction:

In order to study the effects of molecular weight distribution, especially of the low molecular weight fraction, polymer samples were artificially made by incorporating various amount of Allied Chemical polyethylenes (nominal mol. wt. : 1500) into the polyethylene from which had been extracted its low molecular weight fraction by immersion in boiling chloroform for 24 hours, the original density and Melt Index of the polymer was 0.92g/cm^3 , and 0.25g/10min. , respectively. The samples were notched and subjected to the biaxial stress test, the results of which are shown in Fig. 11. It is seen that the low molecular weight fraction in the polymer has a serious effect on the transition temperature of polyethylene.

Density : Four low density polyethylenes with around the same density but differing in Melt Index, were selected and the brittleness temperatures for annealed and unannealed notched specimens were determined. Results are plotted in Fig. 12. It is seen that the transition temperature is a linear function of the density of the sample polymer. The density of the polyethylene is determined by the short branches of the polymer itself and the thermal treatment, both affecting the crystallization state of the sample. The linearity seen in Fig. 12 suggests that both factors contribute to the ductile-brittle transition in the same way.

On the other hand, a controversial result was obtained with high density polyethylene. From the data of Fig. 12, one might expect that a high density polyethylene would show a highly brittle behavior. However, it was found that high density polyethylene never showed a brittle fracture. Data obtained with high density polyethylene will be explained later.

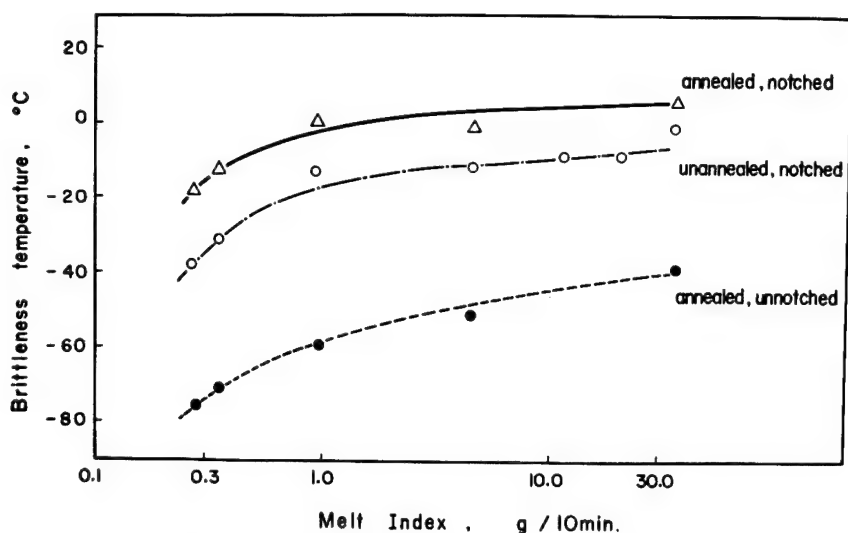


Fig. 10 Effect of melt index of low density polyethylene on brittleness temperatures .

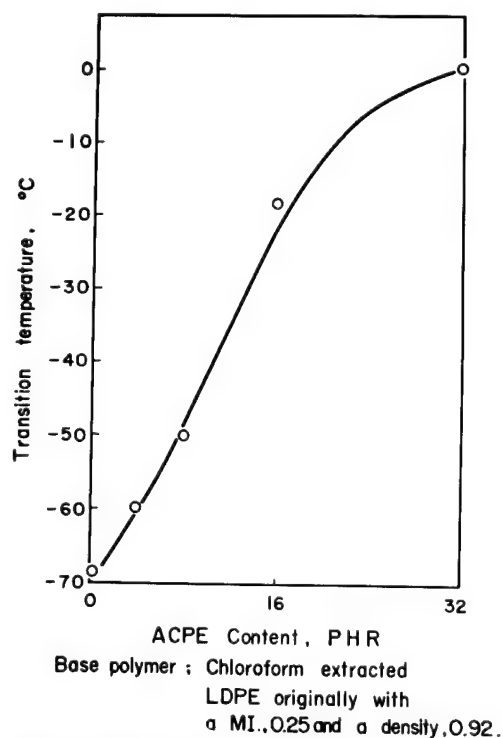


Fig. 11 Effect of low molecular weight fraction on the transition temperature in biaxial tests .

Thermal history : In Figs.10 and 12, the effect of thermal treatment on the transition temperature was clearly indicated. Table 3 shows how brittleness temperature of a cable jacketing

polyethylene is affected by various thermal treatments.

Crosslinking and copolymerization : From the results hitherto mentioned, it would be obvious that the crystallization state of the polymer, especially of the interspherulitic region has a most profound effect on the transition temperatures. Introduction of crosslinking or another constituent into a polymer chain is known to induce a change in the crystallization state of the sample. With this point of view, the following experiments were carried out.

A commercial grade of polyethylene was peroxide-cured to different degrees of crosslinking with various amount of organic peroxide.

The crosslinked polyethylene was then subjected to a brittleness temperature test and a biaxial stress test. Data are plotted in Fig.13 which shows the pronounced effect of crosslinking on the transition temperatures.

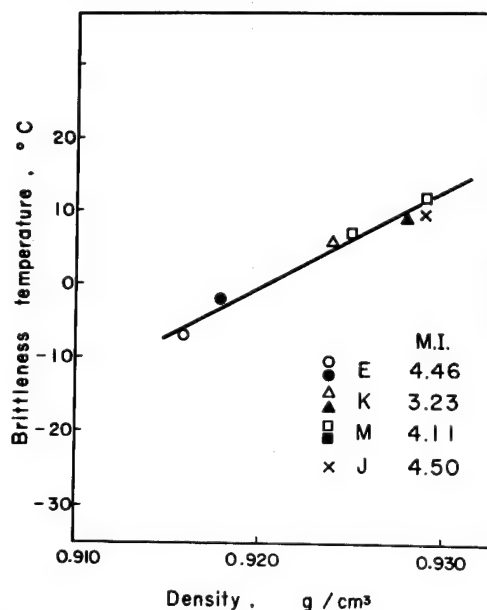


Fig. 12 Effect of density of low density polyethylene on the brittleness temperatures of notched specimens
open symbol : unannealed
closed symbol : annealed

Table 3. Effect of thermal history on brittleness temperature

Treatment	Brittleness temperature, °C	
	notched	unnotched
Quenched	-52	< -77
Standard	-44	< -77
10min. in boiling water	-33	< -77
60min. in boiling water	-31	< -77
300min. in boiling water	-28	< -77
140°C, 1hr then 30°C/hr gradually cooling	-33	< -77
140°C, 1hr then 5°C/hr gradually cooling	-11.5	-60

Sample : Jacketing grade ethylene homopolymer.

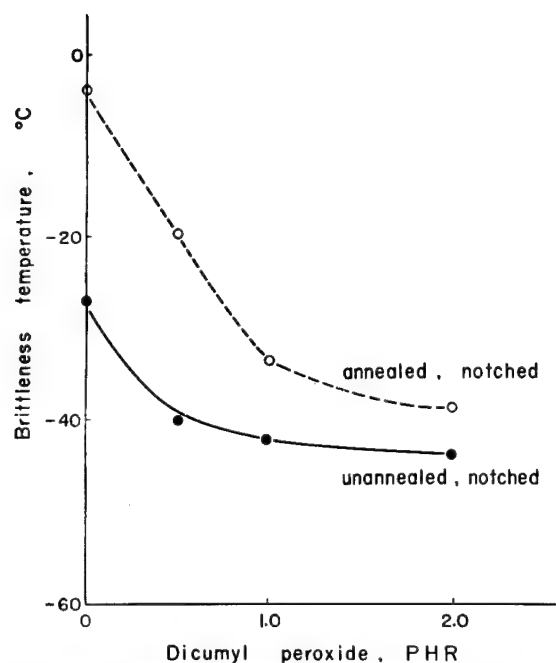


Fig. 13 Effect of degree of crosslinking on brittleness temperatures of low density polyethylene with a M I, 1.0 and a density, 0.92

To see the effects of copolymerization, commercial grade of ethylene vinylacetate copolymers with around the same Melt Index were tested and the results are plotted in Fig. 14. It is seen that the introduction of vinyl-

acetate into the polymer chain has brought about an appreciable improvement in low temperature impact resistance.

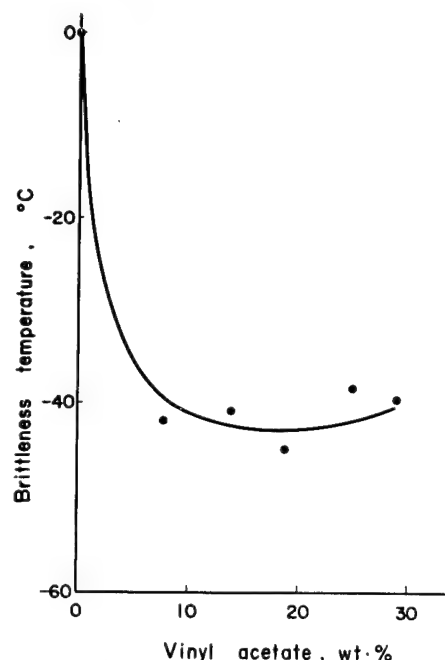


Fig. 14 Effect of vinyl acetate content of ethylenecopolymer on brittleness temperatures of notched specimens. Melt Indices are around 2 .

Table 4 shows the brittleness temperatures and the biaxial stress test transition temperatures obtained with commercial jacketing grade polyethylenes, homo- and co-polymers.

Comparison with other materials

It has been described how seriously the low temperature brittleness of low density polyethylene is affected by stress concentration and complex stressing. In order to study those effects on materials other than polyethylene, brittleness temperature tests and biaxial stress tests were carried out with specimens both notched and unnotched. The results are shown in Table 5.

It is seen in Table 5 that vulcanized chloroprene rubber, ethylene vinylacetate copolymer, and high density polyethylene are hardly affected by either notch or stress biaxiality. On the other hand, plasticized PVC and Nylon 12 are seen to be influenced by the presence of a notch but not by stress polyaxiality. Polytetrafluoroethylene is also influenced by a notch. Biaxial

Table 4. Comparison of transition temperatures of commercial jacketing grade polyethylenes.

Sample	Density ^{*1}	Melt Index	Brittleness Tb, °C ^{*2}		Biaxial Tb, °C ^{*1}		Remarks
	g/cm ³	g/10min.	notched	unnotched	notched	unnotched	
P	0.936	0.22	-33	<-77	ca.-13	ca.-47	homopolymer
Q	0.938	0.23	-31	<-77	ca.-22	<-50	homopolymer
R	0.939	0.25	-30	<-77	ca.-13	<-40	EVA copolymer
S	0.939	0.31	-29	<-77	ca.-21	<-40	EVA copolymer
T	0.942	0.35	-25	<-77	ca.-18	<-40	EVA copolymer
U	0.943	0.25	-51	<-77	<-50	<-50	EVA copolymer
V	0.940	0.30	-44	<-77	ca.-47	<-52	EVA copolymer

* 1. annealed sample

* 2. unannealed sample

Table 5. Transition temperature of various materials

Sample	Brittleness Tb, °C		Biaxial Tb, °C		Remarks
	notched	unnotched	notched	unnotched	
Low density polyethylene	<-18	<-75	ca.-37	<-52	d=0.921 MI=0.28 annealed
High density polyethylene	<-75	<-75	<-60	<-60	d=0.950 MI=0.90 annealed *
High density polyethylene	<-75	<-75	<-60	<-60	d=0.950 MI=0.30 annealed *
Vulcanized chloroprene rubber	-36	-36	ca.-38	<-43	jacketing compound
EVA copolymer	-42	<-75	<-60	<-60	MI=2, VA content=8wt%
Plasticized PVC	-12	-29	ca.-27	ca.-30	jacketing compound
Nylon 12	+5	<-75	<-32	<-63	annealed *
Polytetrafluoroethylene	+5	<-75	—	—	
Polypropylene	-8	-25	ca.+13	ca.+1	d=0.90 MI=0.5 annealed *

* condition : 120°C, 4hrs then 10°C/h gradually cooling

stress tests on this material were almost impossible because of the slippery nature of the material. Polypropylene was found to be susceptible to both notch and stress biaxiality.

The behavior of high density polyethylene is somewhat peculiar. As mentioned earlier (Fig.12), with low density polyethylene, the

higher the density the higher the brittleness temperature. High density polyethylene would not come on this line. At low temperatures it fractures with little deformation, but the type of fracture is ductile, never brittle. In Fig.15 is shown the appearance of a notched specimen of a high density polyethylene fractured at -65°C

under biaxial stress.

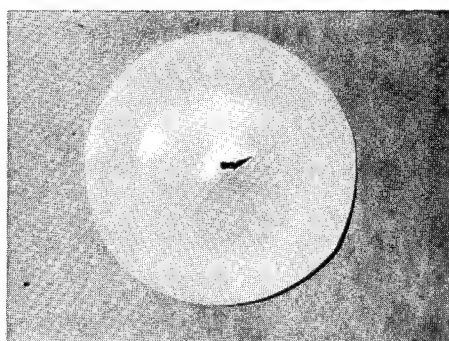


Fig.15. Fractured disc of high density polyethylene in biaxial stress test at - 65°C.

pictures of three successive frames at the moment of fracture of a cable on cold bending. It is seen that the fracture took place in less than 1/2700 second in this case.

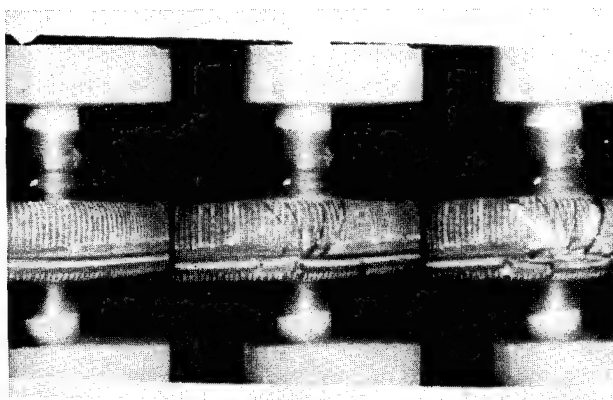


Fig.16. Brittle fracture process in cable bending test at -40°C, photographed by a high speed cine camera at a speed of 2700 frames per second. sample: notched CCP-SS cable.

Cold bending test of cable samples

Cold bending test of polyethylene sheathed communication cables were carried out to see the correspondence between the plaque tests and actual cold bending resistance of the cables. The results in Table 6 show that the brittleness temperatures of notched specimens taken out of the cable sheath correspond well with the percentage of fractures of cables in the cold bending test.

Some of the tests were traced by a high speed cine camera. In Fig.16 are shown

Conclusions

Brittle fractures of polyethylene at low temperature were studied by uniaxial tensile tests, brittleness temperature tests, biaxial stress tests, and cable bending tests. Low density polyethylene was the main subject of the investigation. From the study the following conclusions were obtained.

- (1) The ductile-brittle transition temperature of low density polyethylene is affected by stress concentration, stress polyaxiality, molecular parameters, and the crystalline state of the polymer. Among these factors the stress concentration caused by a notch or co-fracture has the most pronounced effect.
- (2) The polyaxiality of stress also has a profound influence. The transition temperature of low den-

Table 6. Comparison among cable bending test, brittleness temperature test, and biaxial stress test.

Jacketing compound	Brittleness, Tb, °C notched		Biaxial, Tb, °C annealed		Cable - bending test *2 at -50°C
	sheet	jacket *1	notched	unnotched	
EVA copolymer, U	- 51	- 64	< -50	< -50	0/20
EVA copolymer, S	- 29	- 48	ca.-21	< -40	4/20
Homopolymer, P	- 31	- 33	ca.-13	ca.-47	20/20

*1. Tb of the specimens taken from cable jackets.

*2. Number of fractured samples / Number of tested samples.

Sample: 0.5mmØ conductor, 200 p CCP-P-SS cable.

sity polyethylene is higher under biaxial stress than under uniaxial tension.

(3) Chemical modification of the polymer chain by crosslinking or copolymerization brings about an appreciable improvement in low temperature ductility of low density polyethylene.

(4) Materials other than low density polyethylene show different sensitivity to stress concentration and polyaxial stress.

(5) Cable bending tests at low temperatures showed a good correlation with plaque tests, which suggests that the brittleness temperature test with notched specimens and the biaxial stress test are best suited as screening test for a cold resistant material used in cable jacketing.

References

1. I. L. Hopkins, W. O. Baker, and J. B. Howard, J. Appl. Phys., 21, 206 (1950).
2. I. L. Hopkins, and W. O. Baker, "The Deformation of Crystalline and Cross-Linked Polymers", in Rheology, F. R. Eirich, ed., Academic Press, New York, 1960, Vol. III, p. 463.
3. E. A. W. Hoff, and S. Turner, ASTM Bull., 58 (Oct., 1957).
4. W. W. Spohn, and H. J. Frey Jr., AIEE Winter Meeting, New York, Jan. 22, (1957).
5. A. M. Birks, and A. Rudin, ASTM Bull., No. 242, 63 (Dec., 1959).
6. P. I. Vincent, Polymer, 1, 425 (1960).
7. A. Rudin, and J. S. Mackie, J. Polymer Sci., pt. A, 1, 2075 (1963).
8. A. Rudin, "Brittleness" in Crystalline Olefin Polymers, R. A. V. Raff and K. W. Doak, ed., Interscience, New York, 1964, part II. p. 1.
9. P. L. Clegg, S. Turner, and P. I. Vincent, 7th Wire and Cable Symp., Asbury Park, N. J., (1958).
10. A. C. Morris, Plastics & Polymers, 433 (Oct., 1968).

11. K. Fujioka, J. Appl. Polymer Sci., 13, 1421 (1969).

12. J. Miklowitz, J. Colloid Sci., 2, 217 (1947).

Masaaki Okada - Dainichi-Nippon Cables, Ltd.
8, Nishino-cho
Higashimukaimima, Amagasaki
Hyogo-ken, Japan

Masaaki Okada joined Dainichi Electric Wire and Cable Co. in 1957 after he received his BS degree in Industrial Chemistry from Kyoto University. He has been consistently engaged in research and developmental works on plastic materials for Wire and Cable. He is now a senior research engineer in the Research Laboratory of Dainichi-Nippon Cables Ltd.

Atsushi Utsumi -

Atsushi Utsumi received his BS degree in Industrial Chemistry from Kobe University in 1965. That same year he joined Dainichi-Nippon Cables Ltd. He has been working on the research and development of plastic materials for wire and cable in the Research Laboratory of the Company.

Appendix . Characteristics of the main polymers and the results .

Sample	Density		M. I.	\bar{M}_v^*	Uniaxial, Tb, °C				Brittleness, Tb, °C				Biaxial, Tb, °C			
	g /cm ³				notched		unnotched		notched		unnotched		notched		unnotched	
	a	u	η_{10min}	$\times 10^4$	a	u	a	u	a	u	a	u	a	u	a	u
A	0.921	0.920	0.28	5.8	-38	<-60	<-60	<-60	-18	-35	<-77	<-77	-38		<-52	
B	0.919	0.916	0.35	4.8	-21	-55	<-60	<-60	-13	-32		<-77	-25		<-50	
C	0.918	0.920	0.95	5.3	-12		<-60	<-60	0	-14		<-77	-13		-50	
D	0.918	0.916	0.95	5.4			<-60	<-60	0				-13		-44	
E	0.918	0.917	4.5	4.3	-13	-23			-2	-7	-52	-72	-10		-36	
F	0.921	0.918	9.6	3.7	-8				+8				-5		-12	
G	0.921	0.919	20	2.6	-2				+5		-34		-3		-10	>-30
H	0.919	0.916	35	3.6	+1				+4	-3	-30	>-50	-3		-3	
I	0.931	0.920	20	2.5		>0		-37	+18	+10	-22	-55	>+23			
J	0.929	0.926	4.5	4.0	+10		-45		+8		-60		+13	-23	+2	<-33
K	0.928	0.924	3.2	3.3	>+8	-15			+9	+6	>-50	-73	+13		+14	
L	0.929	0.926	4.0	4.2	+3								+13		-14	
M	0.929	0.925	4.1	3.6	>+5		<-60	<-60	+12	+7	-73	<-73	+13	>-30	-10	
O	0.919	0.917	1.0						-4	-27	<-77	<-77				
P	0.936	0.934	0.22							-33	<-77	<-77	-13	-23	-47	
Q	0.938	0.935	0.23			-24				-31	<-77	<-77	-23		<-40	
S	0.939	0.936	0.31							-29	<-77	<-77	-21		<-40	
V	0.940	0.937	0.30						-20	-41	<-77	<-77	-47		<-52	
W		0.950	0.91						<-75	<-75	<-75	<-75	<-65	<-65	<-65	<-65
X		0.951	0.25						-69	-56	<-75	<-75	<-65	<-65	<-65	<-65
Y		0.949	0.31						<-75	<-75	<-75	<-75	<-65	<-65	<-65	<-65

* I : $[\eta] = 1.05 \times 10^{-3} \text{ Mn}^{0.63}$, at 81°C in p - Xylene.

a : annealed specimen

u : unannealed specimen

A NEW SELF-EXTINGUISHING HYDROGEN CHLORIDE BINDING

PVC JACKETING COMPOUND FOR CABLES

Dr. Ottmar Leuchs

Laboratory for High Polymers

Kabel- und Metallwerke Gutehoffnungshuette Aktiengesellschaft

Hannover, West Germany

Summary

Cable jackets of flexible PVC have the advantage of being slow-burning; however, in the event of fire, they also have the disadvantage of releasing corrosive hydrogen chloride in the smoke. Attempts have therefore been made to modify flexible PVC formulations in such a way that they do not emit any HCl in the smoke, while remaining nonetheless self-extinguishing. Our efforts proved successful and HCl compounds were developed which, under typical fire conditions, completely bind the HCl in the ash. An improvement was also achieved with regard to incombustibility as compared to ordinary flexible PVC formulations; this will be demonstrated using a new cable fire test.

Introduction

Flexible polyvinyl chloride (PVC) is used widely in cable where very low combustibility is required and has successfully replaced insulation covered with braided textile fiber, as used heretofore. Although the number of defective contacts has probably remained the same, the number of fires -- and the extent of fire damage -- has been reduced to a small fraction by use of flexible PVC insulation, as was reported in Stockholm in 1969¹.

New forms of corrosion damage have been observed in recent years; these are attributable to the burning of PVC, and are a source of grave concern in view of their massive extent^{2,3}. When PVC is decomposed by high temperatures, it releases HCl in the smoke; this HCl combines with water vapor in the smoke to form a hydrochloric acid fog which in turn attacks bare metals and masonry. This can lead to a sequence of damages, which can exceed the fire damage itself many-fold, especially when large quantities of valuable and easily corroded materials are exposed to the smoke.

The purpose of the present investigation was to overcome this disadvantage. We found that a flexible PVC cable jacket formulation could be so modified that the compound released no HCl on burning while retaining the most important advantages typical of flexible PVC, such as a slow-burning rating. The new compound, on which the Kabelmetal Company has applied for patents is tentatively designated "Chlorostop".

General

Materials commonly used for insulating and jacketing cables include such substances as paper, rubber, or plastics. Most of these are combustible; only a few -- such as PVC or polychloroprene rubber, are slow burning⁴⁻⁸. Safety considerations dictate that electric cables be as fire-resistant as possible. Although we ourselves do live in combustible homes and even sleep in combustible bedding, this is not because we expressly wish to do so but simply only because most of our traditional building materials happen to be combustible.

If a cable jacket of slow-burning flexible PVC becomes heated, it does become softer. A flow region occurs at about $170 \pm 20^\circ\text{C}$ in which the elastic behavior changes to plastic flow. The decomposition region, which is the upper limit for existence of the material occurs at about $250 \pm 50^\circ\text{C}$. The molecules decompose in this temperature region; volatile gases are evolved, starting with HCl. A black, voluminous, porous carbon-rich residue remains after a short time.

The gaseous HCl being split off has the very desirable action of promoting the flame resistance of PVC compounds, since it cools the flame. However, it also has a very unwelcome action in that it is transported away by the ascending smoke

and produces corrosion of metals and masonry; it is thus responsible for another kind of damage which can exceed that due to the fire. We have reduced the fire damage by means of HCl, but have thereby assured the possibly greater damage due to chloride corrosion. The immediate problem is thus how to prevent fire damage without simultaneously causing chloride damage. This could be accomplished theoretically by formulating a slow-burning compound using chloride-free (or, in general, halogen-free) substances; if, nonetheless, a halogen-containing material must be introduced, it is necessary to ensure that no hydrogen halide ends up in the flame or smoke even though it may be split off chemically. Before we present the fundamentals for formulating PVC compounds which release no HCl with the smoke while remaining slow-burning, we will briefly describe the necessary analytical methods used for formulation development.

Binding HCl in the Ash

The analysis of combustion fumes is very difficult and time consuming, if one wishes to prove that the voluminous smoke contains absolutely no HCl. On the contrary, it is simple to determine a larger amount of chloride in a small amount of ash. If the theoretical amount of chloride is found in the ash from a given sample, one can be certain that the smoke was chloride-free. Such a method can also be used in evaluating a fire, if a piece of undamaged cable jacket is available for use in determining the theoretical quantity of chloride. Here one does not only have to determine the chloride content of the ash, but also must ascertain the content -- in the starting material as well as in the ash -- of incombustible mineral filler (or that of some element which does not form a volatile chloride); thus, knowing the fraction of the chloride found in the ash, one can establish how much must have been emitted with the smoke.

The chloride determination can be conducted by calcining in a quartz tube. We used the following conditions:

SAMPLE WEIGHT:

0.5 gram (20 x 4 x 3 mm³) in a 67 mm long porcelain tray

TEMPERATURE ALONG ENTIRE LENGTH OF PORCELAIN TRAY:
650 ± 3°C; controlled by thermocouple at the tray

CALCINATION TIME:
30 minutes

AIR:
Dry or not dried, 50 liters/hour

FURNACE LENGTH:
35 cm

QUARTZ TUBE DIMENSIONS:
60 cm long, 2 cm outer diameter,
1.8 cm inner diameter.

The porcelain tray is rapidly inserted into the heated tube. Temperature is measured with a thermocouple directly in front of the tray (in the direction of air flow). The ash is pulverized under water and taken up in hot water containing some nitric acid, and titrated by the Mohr method following filtration. If troubling elements are present, titration by the Volhard method is made. In this it is assumed that no more chloride is bonded by carbon. At low temperatures or with short ashing times, this must be checked. If necessary, one can perform a peroxide attack according to DIN (Deutsche Industrie-Norm - German National Standard) 53 474, Paragraph 7.1, which can also be used for attacking undecomposed PVC.

Combustibility

Concepts. If a flexible PVC cable jacket is held in a flame, it is rapidly heated well beyond the decomposition region and becomes coked. Temperatures in fires range between 700 and 880°C⁹ or between 700 and 1000°C¹⁰. We ourselves measured temperatures between 700 and 800°C. Flexible PVC is not resistant to heat or fire and can be readily destroyed by high temperatures. The gases evolved during decomposition can color the foreign flame, e.g., yellow-orange due to incandescent particles of soot; this creates the impression that the cable jacket is burning like a candle, i.e., the PVC burns itself. This is certainly not impossible, as will yet be shown, but is generally not the case. Flexible PVC is admittedly combustible but difficult to set afire.

What determines the combustibility of an object? It is not easy to answer this question in a completely definite manner. However, it has been established that the answer depends on at least two factors. On the one hand, the combustibility or oxidizability of the material itself is a factor; external factors are also involved on the other hand, such as thickness, initial temperature, number of objects and their arrangement, fresh air supply, and smoke venting. The factor associated with the material itself is under control of the cable fabricator, and is discussed in greater detail below.

With respect to materials, we can distinguish between "combustible" and "noncombustible" substances as follows: a combustible material is generally any substance which reacts with oxygen with evolution of heat. Thus, a noncombustible substance can be taken to be either one which does not react with oxygen at all, or one which reacts with absorption of heat. This group includes the inert gases and already combusted substances such as oxides, carbonates, sulfates, etc., (like water, sand, chalk, gypsum), as well as such substances as nitrogen and table salt, which require the absorption of heat to combine with oxygen, forming nitric oxide or sodium chlorate, respectively.

Substances regarded as combustible per se can advantageously be subdivided still further. This group contains such matter as paraffin as well as wood and iron. Iron combines with oxygen with evolution of heat. Also, finely powdered "pyrophoric" iron incandesces in air; a steel watch spring burns luminously in pure oxygen. Nonetheless, it is correct to regard iron as virtually noncombustible, as is the normal case when we are dealing with a nail or plate in the air.

Combustible substances per se are therefore further subdivided as follows: (a) those which burn independently and with a hot flame; (b) those in which the flame produces, under favorable circumstances, just enough decomposition gases to maintain the flame, i.e., those materials which burn independently only with difficulty, and (c) those which under normal circumstances (i.e., in air and in ordinary massive form or without pre-heating) do not ignite at all but only become decomposed and coked.

Examples of polymers which are per se "combustible" are:

1. Readily combustible:

Easily decomposable hydrocarbons with high heats of combustion, such as polyethylene, natural rubber, butyl rubber.

2. Slow-burning:

Easily decomposable oxygen-containing polymers with moderate heats of combustion, such as wood and polyamides (nylon).

Mixtures which contain substances having moderate heats of combustion which split out hydrogen halides when heated, such as flexible PVC.

3. Virtually noncombustible in a practical sense or self-extinguishing:

Substances with low heats of combustion, such as Teflon. Substances with moderate heats of combustion which emit HCl profusely, such as rigid PVC. Also, substances like coke which are difficult to set afire.

The flame temperature of the decomposition gases emitted from these substances is unnecessarily high for the first group, it is still sufficiently high in the second group, and it is too low in the last group to maintain decomposition and gas formation.

Ignitability is more a question of the degree of subdivision. Wadding and jute burn rather readily, even with a small igniting flame; books, paper bales, or wooden beams on the contrary are really more difficult to set on fire, i.e., in such a way that they burn completely. Ignitability and flame propagation velocity are related concepts; readily ignitable substances are those which have a high flame propagation velocity.

The decomposability can be described approximately by the magnitude of the ignition temperature¹¹⁻¹³. The heat of combustion is highest when the molecules consist only of carbon and hydrogen¹⁴.

Testing (Oxygen Index). It will be difficult in specific cases to establish boundaries between substances or substance groups. For this purpose we need a numerical measure for combustibility or noncombustibility. Fenimore and Martin¹⁵⁻¹⁸ proposed such a measure. In 1966, they published a method according to which a test specimen mounted vertically was ignited at its upper end and permitted to burn downward slowly. The test variable is the composition of the surrounding atmosphere, i.e., the ratio of oxygen to nitrogen. (Air contains 78% nitrogen, 21% oxygen and 1% argon.) The test determines the lowest possible oxygen content at which the specimen actually continues to burn. This oxygen content in percent is designated the "Oxygen Index". The Oxygen Index is a numerical measure of noncombustibility; the higher the index value, the greater is the noncombustibility. The method is very reproducible.

Fenimore and Martin noted that relatively higher Oxygen Index values would be found under their test conditions since the specimen burns downward. They proposed the following group classifications¹⁶:

Oxygen Index Above 27%: Self-extinguishing substances

Oxygen Index Between 22 and 27%: Slow-burning substances

This classification of "combustible" substances corresponds to the grouping proposed above, namely: virtually noncombustible, slow burning and readily combustible.

We can probably compare all combustible solid substances in a quantitative manner by using the Oxygen Index method. Specifically, we can characterize flexible PVC compounds and establish the effects of plasticizers, fillers and stabilizers; thus we can develop compounds with good noncombustibility. Whenever the desired level of noncombustibility cannot be attained for a substance, some other action must be taken among the remaining conditions^{8,19,20,27}.

Chlorostop

Compound Formulation and Properties

The development of Chlorostop was

based on the concept that the compound should retain all of the HCl in the ash in the event of fire, and that no compromise would be permitted with regard to this requirement. With respect to other physical properties, the compound was to be as noncombustible as possible.

A PVC cable jacket normally consists of about 50 parts PVC (resin), 30 parts plasticizer (makes rigid PVC flexible, since it reduces the second order transition region from +90°C to about -30°C²²), and 20 parts of filler. In addition, small amounts of stabilizer, lubricant, and coloring agents are present.

If a compound releases HCl voluminously in a flame, this partially inhibits the exothermal combustion of carbon monoxide to carbon dioxide^{5,15,23-28}. The flame becomes colder and is extinguished; PVC, chlorinated paraffins and other similar substances cause slow burning in this manner. However, when HCl is bound in the ash, the flame again becomes hotter and the substance becomes combustible. It thus follows that all other compounding aids must be utilized if we are to make the material noncombustible despite this. Consequently, chlorine-containing (or in general, halogen-containing) substances must be almost entirely renounced. All of the compounding ingredients will be thoroughly discussed in this sense.

PVC

PVC is the resin in the compound. It contains about 56.5% chlorine, corresponding to 58.1% HCl. The HCl is split off in a fire, and must be chemically bound by the filler at the same instant. Sufficient filler must be provided to bind all of the HCl. Chlorostop is thus a highly-filled compound. High strength is always difficult to attain under these conditions, especially when good low temperature flexibility (i.e., large amounts of plasticizer) is required simultaneously. Based on these considerations, one tends to use high molecular weight PVC. PVC resins having K values between 70 and 75 are used in practice^{29,30}; higher K values are admittedly desirable, but they make for processing difficulties.

Plasticizer

Ordinary phthalate plasticizers are

combustible. Phosphate plasticizers are slow burning³¹; aromatic phosphate plasticizers are the least combustible among these. They appear to distill unchanged, at least in part, during a fire. The low temperature flexibility of such a compound is known to be limited, and here the standard quality cannot be attained without compromise³².

Figure 1 gives results for diphenylcresyl phosphate (DPK), as compared to diisononyl phthalate (DINP), on combustibility as measured by the Fenimore and Martin Oxygen Index¹⁷.

Both plasticizers reduce the non-combustibility of pure PVC (Oxygen Index = 45). However, self-extinguishing to slow burning compounds can be obtained using the phthalic acid ester; the phosphate ester compound formulations are all in the self-extinguishing region.

Fillers

The fillers are of the greatest importance in our case. They are required to combine with HCl released in a fire, thus binding it by chemical conversion into thermally stable salts. The danger of corrosion is thereby removed. No HCl is formed even when the salt is dissolved by quenching with water. In a fire, fillers in a polymer compound generally behave as ballast, which must be heated but can never function as a heat source. A filler can also function as a cooling agent, for example, by evolving CO₂ or H₂O. One could thus expect the Oxygen Index to increase with filler loading. However, this is not the case; the Oxygen Index applies specifically for coking conditions at the lower limit of the burning rate. If the burning rate is doubled, the increase in Oxygen Index with the filler loading becomes apparent. Some reduction and scattering does occur because highly filled compounds display fewer jets of flame along the sides of the test sample--this leads to improved reproducibility and somewhat lower Oxygen Index.

Fillers may be classified into three groups: chemically inactive fillers, fillers which form volatile chlorides and fillers which form non-volatile chlorides.

Talc and kaolin are examples of chemically inert fillers. They make the

compound somewhat noncombustible at higher burning rates. However, they do not combine with HCl and are thus of no interest here.

Those fillers which form volatile chlorides are also of no interest, since they interfere with retaining all the chlorine in the ash. Thus, compounds of antimony and zinc are thereby eliminated.

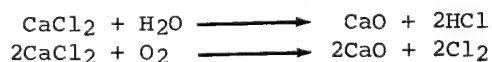
However, those fillers which do not form volatile chlorides are definitely of interest. Alkali and alkaline earth compounds, in particular, are in this group. Table 1 gives melting and boiling points for some chlorides:

Table 1

Melting and Boiling Points for Chlorides of Interest

	NaCl	KCl	MgCl ₂	CaCl ₂	BaCl ₂
Melt.point °C	800	770	712	765	960
Boil.point °C	1465	1407	1418	>1600	1560

Since temperatures between 700 and 1000°C occur in flames^{9,10}, one could expect that all of these chlorides would be sufficiently thermally stable. Unfortunately, this is not the case. They can decompose by reacting with water vapor or oxygen:



Both of these reactions occur concurrently. Table 2 shows the decomposibility of freshly prepared calcium chloride, obtained by ashing a Chlorostop compound; it can be seen that the higher the temperature, the more quickly decomposition takes place. Figures 2a and 2b present the corresponding curves. Ashing in moist air yields scattering values lower than values resulting with ashing in dried air. The highest values are found when ashed in a nitrogen stream. After 60 minutes ashing at 1000°C, we found 96.7% of chlorine in the ash. If one considers that a given point in a fire is exposed to maximum temperatures for only a few minutes at most -- as the flames advance, one realizes that a salt like calcium chloride does offer rather considerable protection. Barium chloride behaves in similar manner; magnesium chloride is significantly

less stable thermally. In view of their water solubility, alkali salts are not even considered for use as fillers. We have worked with calcium and barium fillers, which seem to offer optimum stability.

The fillers may be oxides, hydroxides or carbonates. The latter are preferred since they are the most compatible with PVC.

Figure 3 shows the HCl-binding power of a chalk (average particle size $3.5\ \mu\text{m}$) at various loadings in two PVC compounds. It is known that 90 parts of chalk bind only about 30% of the HCl theoretically possible as calcium chloride. Some 80 parts should be sufficient to bind all of the HCl with an optimally effective chalk. It can also be seen how slightly the combustibility of these compounds is affected by addition of chalk. The type of plasticizer plays no role here.

Figure 4 shows the corresponding action of a considerably more finely divided chalk (average particle size $0.05\ \mu\text{m}$). This chalk binds the HCl in an almost optimum manner. This is probably associated with the fineness of the chalk, which is now generally distributed throughout the compound in such a way as to be available wherever HCl can be released. The noncombustibility of the mixture, as measured by Oxygen Index, does indeed decrease considerably; however, the DPK compounds still remain in the self-extinguishing region above an Oxygen Index of 27.

Stabilization

Only small quantities of stabilizers are added; consequently, they can have little significant effect on noncombustibility and HCl binding. We found that barium-cadmium-epoxide stabilization was superior to lead stabilization; this coincides with the effect on color stability.

Stabilizers have the function, among others, of binding the HCl emitted during working the PVC. In this sense, they should be considered as fillers, i.e., one must judge whether their chloride formed in the fire is sufficiently stable to heat. Despite the presence of chloride-binding fillers, stabilizers are needed,

because they react more quickly with HCl at working temperatures.

Properties of a Chlorostop Compound

Flexible PVC compounds formulated according to foregoing concepts were prepared in any desired color without any difficulties using customary machines. Granulator (pelletizer) throughput was about 20% lower than for a comparable jacketing compound. However, the jacketing extruder output was almost as high as normal.

Table 3 compares properties of a Chlorostop compound with those of a compound commonly used in Germany for jacketing switchboard cables. The data show that the new compound is similar to the previous jacketing compound. It is somewhat harder and denser but is substantially superior in chloride-binding power. A considerable improvement was also achieved with respect to noncombustibility. The fact that the values for tensile strength and low-temperature flexibility are somewhat reduced represents a disadvantage. The low temperature strength can be improved to some extent by increasing the plasticizer content; however, this would further reduce the strength. There is an interaction here, which can (or must) be balanced somewhat depending on the purpose of the cable. There is also a clear inferiority with regard to electrical resistivity which appears to be of fundamental nature; thus, we are not yet in a position to develop an insulating compound meeting the present requirements with adequate low temperature flexibility. The characteristic odor of the aromatic phosphate plasticizers represents another disadvantage.

Properties of a Chlorostop Cable Jacket

The following values were measured (Table 4) on a Chlorostop jacketed S-Y(St)Y 20 x 3 x 0.6 switchboard cable containing wires insulated with flexible PVC. (20 3-conductor units, #22 AWG)

The required values for tensile strength and low temperature impact strength could not be met. One must judge, however, which requirements are really most important in a Chlorostop cable jacket. For the time being,

Chlorostop provides an optimum in which the HCl evolved in a fire is practically completely bound in the ash while the compound remains as noncombustible as possible; i.e., is still self-extinguishing. If one were prepared to accept a somewhat reduced Oxygen Index, the low temperature flexibility could be improved.

In conclusion, it will be shown how slow burning compounds for wire insulation and cable jacketing behave under external conditions.

Chlorostop Jacketed Cable in a Fire

Development of a More Severe Combustibility Test for Cable.

The national and international methods for testing cable for combustibility contain only pass-fail tests and yield no numerical values³³⁻⁴⁰. These tests distinguish between "readily combustible" and "slow burning" materials. Broad latitude in PVC compounding permits innumerable gradations, as already shown in Fig. 1; there are thus PVC cables that are slow burning to perceptibly different degrees.

Combustibility testing of cable by the VDE method³³ can be made significantly more severe, without setting fire to standard commercial cable insulated with flexible PVC. The cable can be hung vertically, a very strong propane gas flame can be used for ignition, and ignition can continue until metals such as copper begin to melt at the igniting end and all other flames are extinguished. PVC cable withstands these conditions if its wire insulation and cable jacket have Oxygen Indices of 27 and 22.5, respectively. Since, however, it is known that PVC insulated cable was actually set afire in the past, and this spread the fire to the upper floors of a structure, more severe test conditions must be established. We therefore ignited 7 commercial cable samples, each 3 m long, simultaneously. These were so arranged that some air could flow between them. One cable was hung in the central position; the other six were suspended around it about 1 cm away, using several spacing supports. The assembly cross-section contained about 40 percent cable and 60 percent free space. The wire insulating compound had an Oxygen Index of 26.6, that of the cable jacket was 23.5.

The combustible gases evolved by heat from the central cable were augmented by gases from the outer cables; heat radiating from the central cable warmed the outer cables, and was re-radiated by them back to the central cable. This open arrangement substantially increased the severity of the test. Some references were found in the literature that cable bundles burn better than single cables^{37,41}; but no references were found as to the danger of the open arrangement.

Figures 5 through 9 illustrate a fire test on commercial PVC cable in three adjacent chimneys. The central chimney contains a single cable about 3 m long. The right-hand chimney contains 7 lengths of the same cable in the open arrangement. On the left, for comparison, are another 7 lengths bundled together so that air and flame could not pass between them. The fire test ran for 23 minutes. The igniting flames remained lit for the entire period, so that individual copper conductors melted. The single wire and the solid cable bundle did not ignite, although the same cable in the open arrangement certainly did.

The test shows that cable insulated with flexible PVC is not readily combustible. It also shows that combustibility is by no means only a matter of the substance used but also depends on the degree of air access and on the thickness of the material, as well as on the material itself. In these chimneys, which were open in front, further tests demonstrated that a strong cross wind halved the burning time. It was also shown that after 15 minutes of exposure to a flame, a solid bundle of 7 cables suddenly caught fire. This can be explained by the fact that in this bundle of cables the copper conductors absorbed the developed heat, resulting in a pre-heating of the entire cable assembly before ignition occurred. By contrast, a single cable, insulated and jacketed with standard PVC never caught fire in any of our tests.

Cable bundles insulated with polyethylene (PE) burn readily, and so do single cables and insulated conductors after a short ignition time. PE has the disadvantage of melting and running, and of permitting burning droplets to fall. The burning velocity of PE cable was

significantly increased in the open arrangement, and was about as large as for the open arrangement of PVC cables.

The degree of air access is evidently a decisive factor affecting flame propagation velocity and ignitability, as has already been demonstrated by the comparison of wadding, jute, baled paper and wooden beams, while the kind of material, on the other hand, seems to be of lesser importance.

Chlorostop Jacketed Cable in the More Severe Combustibility Test

Chlorostop is self-extinguishing and makes the cable not readily combustible. However, one must consider what material was used to insulate the individual conductors, and whether the cable core contains other combustible substances. If the conductors are insulated with PE (Oxygen Index 18.0), a Chlorostop jacket will not protect such cable from igniting in the hazardous open arrangement. The PE melts and wets the Chlorostop ash at the point of ignition; it runs down from above and destroys the Chlorostop jacket in its hot flames. If the ignition point were at the upper end of the cable, Chlorostop generally would hinder the downward advance of the flames.

The compound used in the cable filler shows a corresponding although admittedly more moderate influence. However one can compensate for this by a layer of ground (Ceander)⁴² wires between the filler and cable jacket. On the other hand, if the wire insulation consists of normal PVC (Oxygen Index 26.6), a Chlorostop jacket (Oxygen Index 27.7) protects the cable even in the hazardous open arrangement from catching fire and from continuing to burn (Figures 10 and 11). A coked region some 25 to 35 cm long is formed; furthermore, although the cables do become warm from heat conduction along the copper wires, they do not catch fire and do not spread the fire farther. Flaming remains localized at the point of ignition.

Conclusion

The materials commonly used for cable jackets confront us with an alternative: they are either combustible, or they are slow-burning or even self-extinguishing.

However, in the latter case the danger of corrosion damage through release of HCl vapors is present. The new Chlorostop compound is the result of development work aimed at overcoming both hazards. It is self-extinguishing, i.e., virtually noncombustible, and nevertheless binds HCl. Thus no chloride damage can result except where the material is exposed to unusually high temperatures for a prolonged period of time.

The advantages of Chlorostop as a jacketing compound are to some extent offset by disadvantages: the kind of plasticizers needed lowers the softening range of the PVC less than is the case with standard plasticizers, and it restricts the range of the softening region so that the low temperature flexibility is somewhat reduced. The highly-filled compound has a lower tensile strength than standard PVC compounds, which is not necessarily serious.

It is obvious that a Chlorostop-type material meeting the requirements for a wire insulating compound would be of very great interest. Our development work in this direction has not yet led to the desired success. So far we were able, in one instance only, to meet the insulation resistance requirements laid down in the German specifications. Tests with double layer insulations are under way.

The described more severe fire test for cables makes it possible to evaluate the effect of cable design and material selection on combustibility. This method defines the limit between slow-burning and self-extinguishing, whereas test methods heretofore used for cables merely differentiated between readily combustible and slow-burning. It is hoped that the new test method as well as our new Chlorostop jacketing compound may contribute to the elimination of fire propagation through cables, thereby achieving a higher degree of fire safety in electrical equipment.

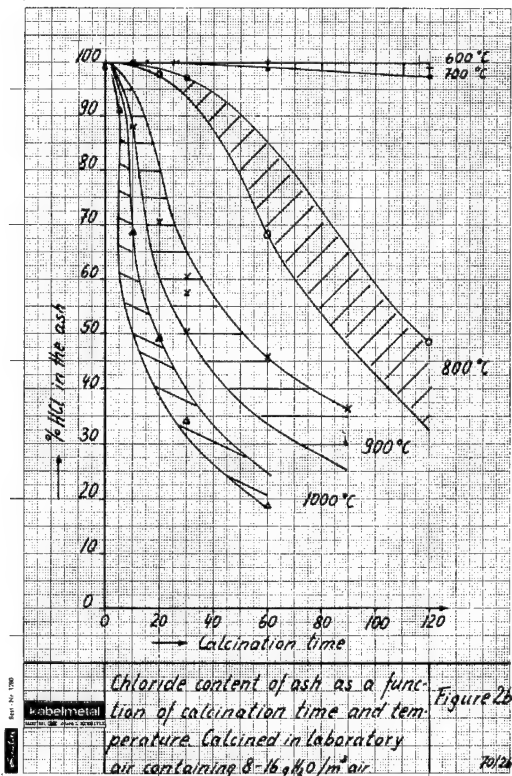
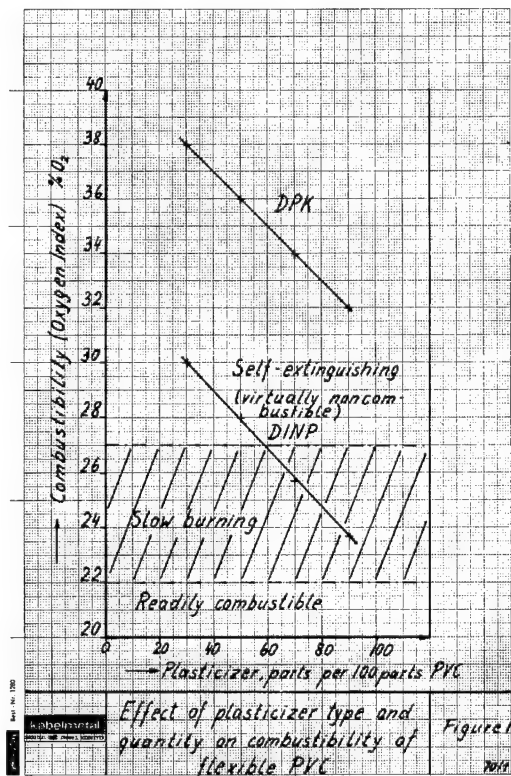
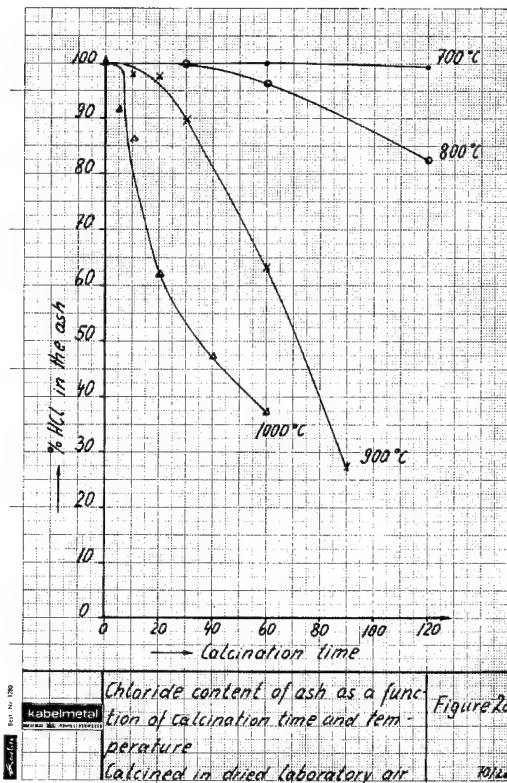
References

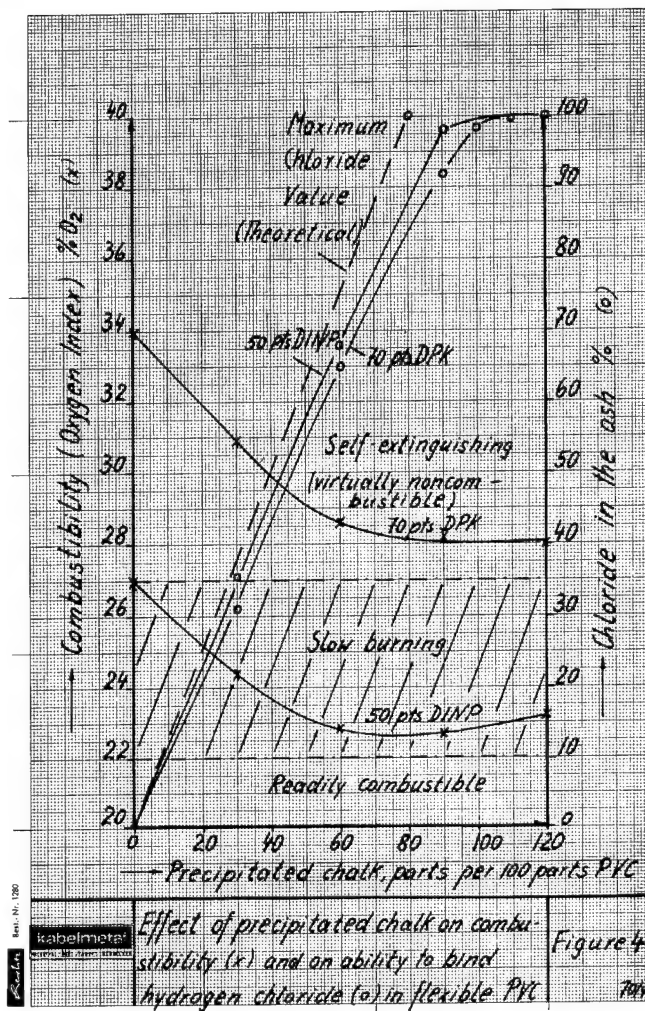
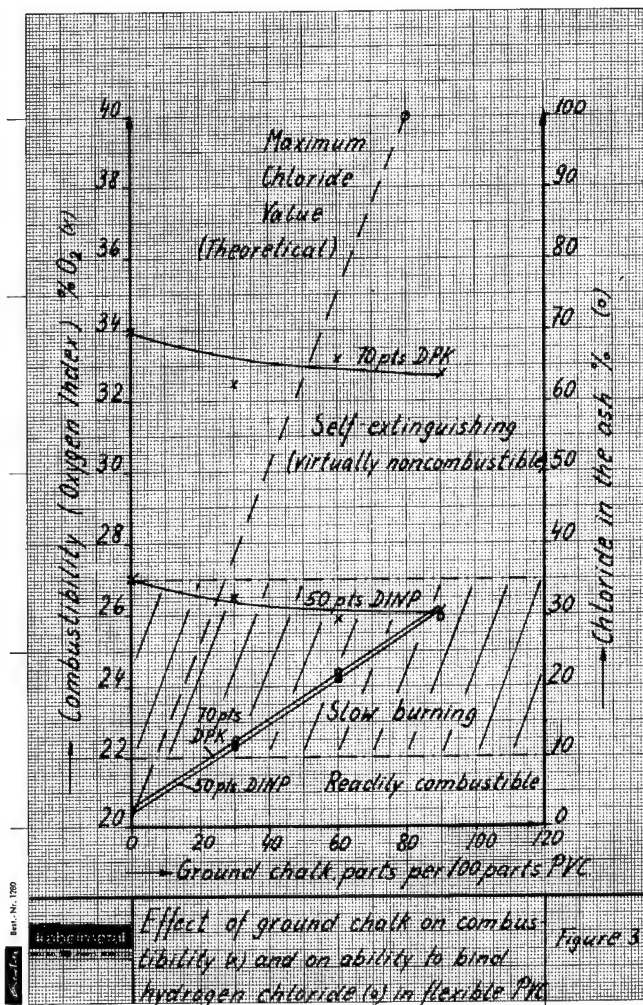
1. International Symposium on Plastics-Fire-Corrosion. Swedish Fire Protection Association, Stockholm, 1969.

2. Muenchener Rueckversicherungsgesellschaft (Munich Reinsurance Assoc.), "Der Abbrand von Kunststoffen und seine Folgen" (The Ignition of Plastics and Its Consequence), Schaden-spiegel, 11, No. 4, pages 33-52, 1968.
3. Purth, G., "Korrosionsgefahr bei PVC-Braenden" (Corrosion Hazards in PVC Fires). Chemie, Anlagen, Ver-fahren, April 1969, pages 79-80.
4. Brundelius, F., "Brandtechnische Eigenschaften von Kunststoffen" (Combustion Properties of Plastics). Brandschutz Deutsche Feuerwehr-zeitung, October 1969, pages 266-67.
5. Friedrich, M., "Untersuchungen ueber die Loeschwirkung halogenierter Kohlenwasserstoffe" (Studies on the Extinguishing Action of Halogenated Hydrocarbons). Forschung und Tech-nik im Brandschutz (Research and Technology in Fire Protection). Zeit-schrift der Vereinigung zur Foerderung des deutschen Brandschutzes, 6, 23-26 and 59-65, 1957.
6. Hilado, C. J., Flammability Handbook for Plastics, Technomatic Publishing Co., Inc., 750 Summer Street, Stamford Conneticut 06902.
7. Thater, R., "Brennverhalten von Plastformstoffen" (Combustion Be-havior of Molded Plastics). VEB Deutscher Verlag fuer Grundstoffin-dustrie (German Publishing House for the Raw Materials Industry), Leipzig 1968.
8. Wood, St., Facing the problems of fire. Modern Plastics 45, No. 6, 82-86, 1968.
9. Fischer, K., "Ueber das Brandver-halten einiger im Bauwesen Verwen-deter, thermoplastischer Kunststoffe" (On the Fire Behavior of Several Thermoplastics Used in Building Con-struction), ZVFB⁵, 13, No. 1, 8-12 and No. 2, 34-46, 1964.
10. Schechl, L., "Brandlehre und chem-ischer Brandschutz" (Theory of Fire and Chemical Fire Protection). Dr. Alfred Huethig Verlag GmbH, Heidelberg 1958.
11. DIN (German National Standard) 51 794/ 7.61, "Pruefung von Mineraloelkohlen-wasserstoffen" (Testing of Petroleum Hydrocarbons). "Bestimmung der Zuend-temperatur" (Determination of Ignition Temperature). Beuth-Vertrieb GmbH, 1 Berlin 15 und Koeln.
12. Nabert, K., and Shoen, G., "Sicher-heitstechnische Kennzahlen brennbarer Gase und Daempfe" (Industrial Safety Data on Combustible Gases and Vapors). Second Edition. Deutscher Eichverlag GmbH, Braunschweig, 1968.
13. Patten, G. A., Ignition Temperatures of Plastics, Modern Plastics, Septem-ber 1961.
14. Kregeler, K., and Klimke, P. M., "Heizwertbestimmung von Kunststoffen gemaess DIN 51 900/Sept. 61" (Deter-mining Heat of Combustion of Plastics Using DIN 51 900/Sept. 61). Kunst-stoffe 55, No. 10, 758-65, 1965.
15. ASTM D-2863: Flammability of Plastics using the Oxygen Index Method., Amer. Soc. Test. Mat., 1916 Race St., Philadelphia, Pa.
16. Fenimore, C. P., and Martin, F. J., Flammability of Polymers. Combustion and Flames, 10, No. 2, 135-39, 1966.
17. Fenimore, C. P., and Martin, F. J., Candle-type Test for Flammability of Polymers. Modern Plastics, November 1966, page 141 ff.
18. Goldblum, K. B., Oxygen Index: Key to Precise Flammability Ratings, SPE Journal, 25, No. 2, 50-52, 1969.
19. Fischer, K., "Brandschutztechnische Beurteilung von Leitungen Niederdruck -Polyaethylen und Polypropylen im Laborbau" (Evaluation of Low Pressure Polyethylene and Polypropylene Wire in Laboratory Construction from the tection). Chemie-Ing.-Technik, 40, No. 24, 1203-09, 1968.
20. Bischoff, B. G., Fire Protexion for Electrical Cable Trays and Associated Facilities. Iron and Steel Eng., 45, No. 6, 107-12, 1968.

21. Becker, K., and Steiniger, E., "Schutz von elektrischen Kabeln und Leitungen gegen aeussere Feuereinwirkung" (Protection of Electrical Cables and Wires Against External Action of Fire). *Industrie-Elektrik und Elektronik*, 14 No. 10, 242-44, 1969.
22. Leuchs, O., Falk, G., Grobusch, W., and Jesse, W., "Schlagfestigkeit von PVC-isolierten Kabeln und Leitungen in der Kaelte" (Low Temperature Impact Strength of PVC Insulated Cable and Wire). *Kunststoffe*, 58, 375-80, 439-46 and 648-54, 1968. See page 378-79.
23. Behrens, H., "Verbrennung und Vergasung des Kohlenstoffs als Kettenreaktionen" (Combustion and Gasification of Carbon as Chain Reactions). *Brennstoff-Waerme-Kraft*, 5, 272-75, 1953.
24. Coleman, E. H., and Thomas, C. H., The Products of Combustion of Chlorinated Plastics. *J. Appl. Chemistry* (London), 4, 379-83, 1954.
25. Jost, W., "Explosions- und Verbrennungsvorgaenge in Gasen" (Explosions and Combustion Processes in Gases). Springer-Verlag, Berlin 1939.
26. Krause, K. H., "Herstellung von feuerhemmenden Polystyrol-Schaum" (Preparation of Flame Retardant Polystyrene Foam). *Kunststoff-Rundschau*, 6, No. 8, 337-39, 1959.
27. Schmidt, W. G., Flame Retardant Additives in Plastics and Recent Related Patents. *Trans. J. Plastics Inst.*, No. 12, 247-55, 1965.
28. Thiery, P., "La resistance des polymeres a la flamme" (Flame Resistance of Polymers). *Plastiques Modernes et Elastomeres*, No. 10, 143-55, 1968.
29. DIN 53 726 "Bestimmung der Viskositätszahl und des K-Wertes von Polyvinylchloriden in Loesung" (Determination of Viscosity Number and K Value for Polyvinyl Chlorides in Solution). Corresponds to 30 below. Beuth-Vertrieb GmbH, 1 Berlin 15 und Koeln.
30. ISO-R 174/1961, Determination of Viscosity Number of Polyvinyl Chloride Resin in Solution. Corresponds to 29.
31. Bell, K. M., McAdam, B. W., and Caesar H. J., "Flammhemmende PVC-Mischungen mit Chlorparaffinen" (Fire Retardant PVC Compounds Containing Chlorinated Paraffins). *Kunststoffe*, 59, No. 7, 419-21, 1969.
32. Leuchs, O., "Zur Weichmachung von Polyvinylchlorid" (Plasticizing Polyvinyl Chloride). *Ibib.*, 46, No. 12, 547-54, 1956.
33. VDE (Verband Deutscher Elektrotechniker - Association of German Electrical Technologists) 0472/6.65, "Pruefungen an isolierten Leitungen und Kabeln" (Testing of Insulated Wires and Cables). Para. 804 VDE-Verlag GmbH, 1 Berlin 12.
34. ASTM Committee D-11, ASTM Specification D 70-56 T, Testing of Rubber- and Plastic-Insulated Wires and Cables. *Am. Soc. Test. Mat.*, 1916 Race St., Philadelphia PA.
35. CEE (International Commission on Rules for Approval of Electrical Equipment) 13 Par. 17, "Feuerbestaendigkeit" (Fire Resistance). VDE-Verlag GmbH, 1 Berlin, 1962. Corresponds to 39.
36. DIN 89 161 (Entwurf. (Draft), Fernmelde Kabel FMXCG, Nennguerschnitt 0.5 mm² (Communication cable type FMXCG, 0.5 mm² conductor cross section) Section 13, "Pruefung auf Flammwidrigkeit" (Testing for Nonflammability). Beuth-Vertrieb GmbH, 1 Berlin 14 und Koeln.
37. IEC (International Electrotechnical Commission) TC (Technical Committee) 20 (Electrical Cable), "Pruefung auf Brennbarkeit" (Testing for Combustibility). 20 Central Office 129, Geneva 1969.
38. NF (Norme francaise) C 32-100/10 12 64 "Conducteurs et cables comportant une enveloppe ou une gaine en caoutchouc" (Conductors and cables with rubber envelope or jacket), Article 25: Verification de la resistance a la propagation de la flamme (Testing resistance against flame propagation), Union Technique de l'Electricite, 20 rue Hamelin, Paris (16e).

39. Semko 8 A - 1957 par. 17, "Feuer-sicherheit der Leiterisolierung und des Mantels" (Fire Resistance of Wire Insulation and Jacket). Schwedische Vorschrift. Corresponds to 35. (Swedish standard).
40. Underwriters Lab., UL 83/1963, Flame Retardant Properties.
41. Hinrichs, B. R., Verhalten der Kunststoffisolation an Kabeln und Leitungen bei Braenden" (Behavior of Plastic Wire and Cable Insulation in Fire). ZVFDB 13, No. 1, 8-14, 1963.
42. "Ceander" is a Kabelmetal trade name for a serving of ground wires applied to electric cables.





Figures 5-9 illustrate a fire test on identical commercial PVC cables showing the influence of the cable arrangement on combustability.

Test Arrangement

The test stand consisted of three chimneys, containing 3 m lengths of a solid bundle of 7 PVC cables (left chimney), a single PVC cable (center chimney) and an open arrangement of 7 PVC cables (right chimney). Note schematic representation of cable assembly configuration at base of each chimney. All three cable groups were ignited with a propane gas burner at the bottom end of the cables and the ignition flame was maintained throughout the test.

Results

The results show that commercially available cables with PVC insulated conductors and a PVC jacket in the single cable or the tightly bundled configuration are slow burning and do not propagate the fire. By contrast, the same cables arranged in an open configuration will burn readily.



Figure 5
4 min
after
ignition

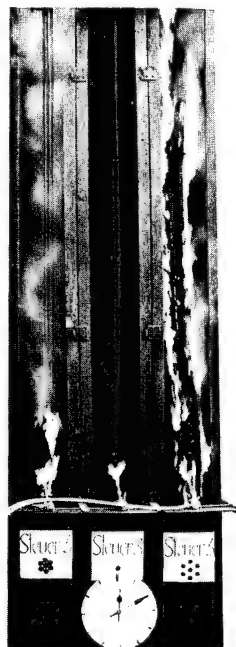


Figure 6
11 min
after
ignition



Figure 7
14 min
after
ignition



Figure 8
19 min
after
ignition



Figure 9
23 min
after
ignition

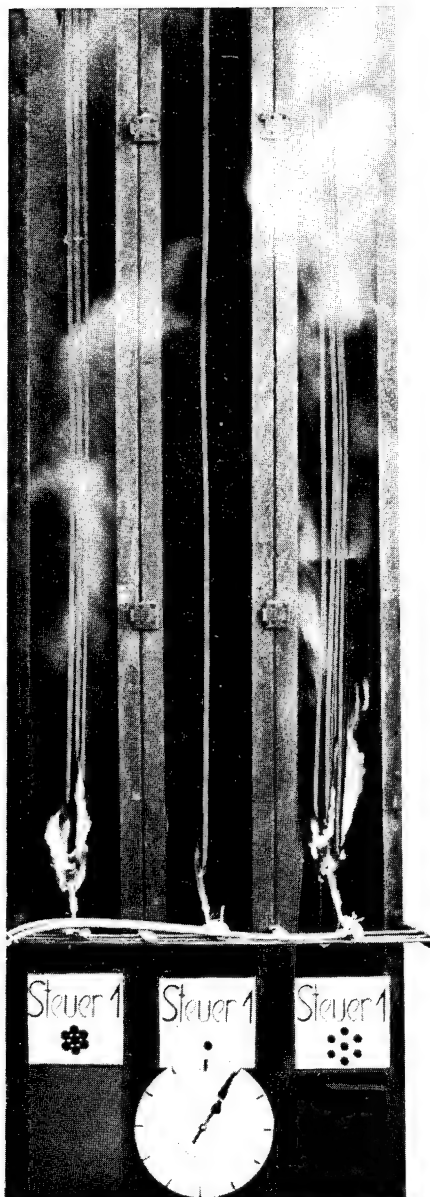


Figure 10
5 min
after
ignition

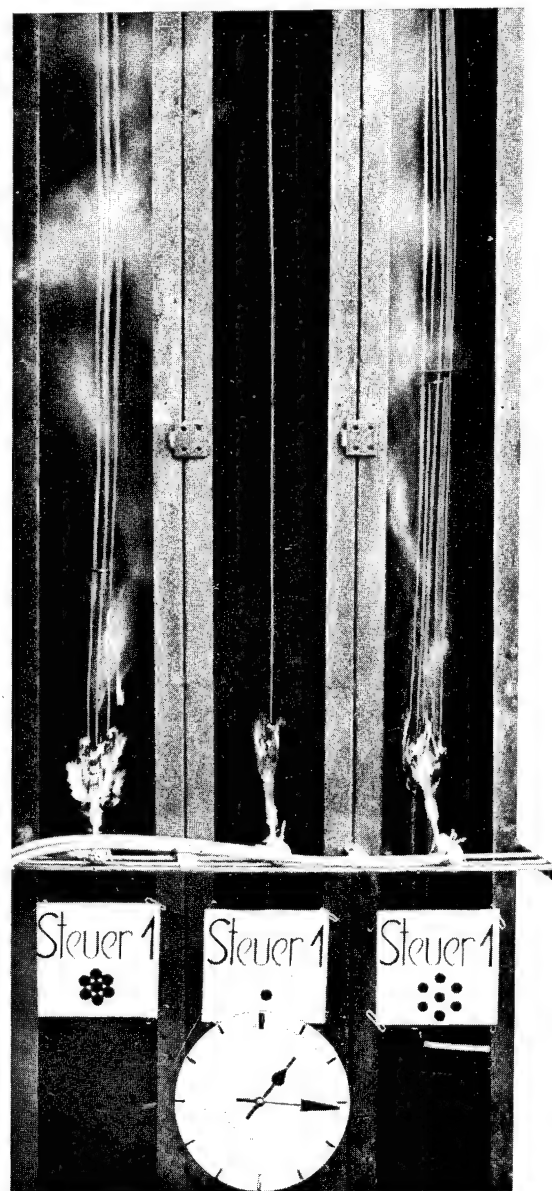


Figure 11
16 min
after
ignition

Test Arrangement

Figures 10 and 11 illustrate a fire test on Chlorostop jacketed cables under the same test conditions used on commercial PVC cables (Figs.5-9).

Results

It is evident that Chlorostop jacketed cables are self-extinguishing even in a most unfavorable configuration and under the most severe fire conditions. In addition, the Chlorostop material does not release HCl.

Table 2

DECOMPOSIBILITY OF CALCIUM CHLORIDE THROUGH ASHING OF A
CHLOROSTOP COMPOUND

Temp °C	Calcination time (min)	Chlorine Content in Ash Calculated as %HCl				
		Ashed with laboratory air				Ashed with dried lab air %HCl
		°C	Relative humidity %	g H ₂ O per m ³ air	% HCl	
600	30	--	--	--	100.0	100.0
	60	--	--	--	100.0	100.0
	90	--	--	--	99.9	-
	120	--	--	--	98.6	-
700	15	24	44	9.6	100.0	-
	30	23	49	10.2	100.0	-
	60	24	48	10.4	98.3	100.0
	120	22	61	11.9	97.1	99.3
800	10	24	53	11.6	100.0	-
	20	24	48	10.5	98.0	-
	30	24	53	11.6	97.0	100.0
	60	25	41	9.4	68.2	96.3
	120	25	38	8.8	48.4	82.3
900	10	23	46	9.5	87.8	98.0
	20	23	52	10.7	70.3	97.7
	30	22	52	10.1	57.6	89.7
		21	59	10.8	50.4	
		27	50	12.8	60.6	
	60	26	55	13.4	45.8	63.3
	90	24	72	15.7	36.4	27.4
1000	5	24	53	11.6	91.2	91.4
	10	24	53	11.6	68.7	86.1
	20	24	53	11.6	49.2	61.8
	30	25	54	12.4	34.2	-
	40	-	-	-	-	47.3
	60	24	49	10.7	18.8	37.2

Table 3

CHLOROSTOP PROPERTIES AS COMPARED TO A STANDARD COMPOUND FOR JACKETING
SWITCHBOARD CABLE

Properties of the Compound	Units	Test Method	YM-1 Compound For Switchboard Cable Jackets		Chlorostop Observed
			Required	Observed	
Tensile strength	kp/cm ²	VDE 0472/6.65 para. 602	≥125	140	125
Tensile strength after 7 days/80°C	kp/cm ²		≥125	140	120
Modulus, 50%	kp/cm ²	Strength at 50% elongation	-	55	76
Elongation	%	VDE 0472/6.65 para. 602	≥125	300	240
Elongation after 7 days/80°C	%		≥125	300	202
Softening or transition temp	°C	"Thaw" test	-	-17	-9
Softening or transition range	°C	"Thaw" test ²²	-	±35	±26
Flow region	°C	Hot pressure test (our own)	-	+162	+165
Decomposition region (DTA, 64°C/min)	°C	Differential Thermal Analysis		260	245
Beginning:				290	300
Knee:				340	340
Maximum					
Density	g/cm ³	DIN 1306/3.67 VDE 0271/3.69	-	1.320	1.630
Thermal stability (HCl evolution at 200°C)	min	para. 17	-	80	85
Shore hardness, A Scale		DIN 53505	-	70	79
Water absorption after 24 hours at 70°C	mg/cm ²	VDE 0472/6.65 para. 802		0.75	1.15
Specific electrical resistance at 20°C	Ωcm	VDE 0472/6.65 para. 502	-	6x10 ¹²	0.1x10 ¹²
Specific electrical resistance at 70°C	Ωcm	VDE 0472/6.65		6x10 ⁹	0.1x10 ⁹
Vaporization loss	mg/cm ²	VDE 0472a/3.69	<2	0.15	0.32
HCl lost in smoke after 30 min at 650°C using 50 liters/hr of dried air	g/kg	Our own method	-	201	<1
HCl lost in smoke after 30 min at 650°C using lab. air with 8.7 g/m ³ H ₂ O	g/kg	Our own method	-	215	<1
Oxygen Index	%	ASTM D 2863	-	23.3	27.7

Table 4

PROPERTIES OF A CHLOROSTOP CABLE JACKET AS COMPARED TO A STANDARD
FLEXIBLE PVC JACKET FOR SWITCHBOARD CABLES

Properties of the Cable Jacket	Units	Test Method	Y M - 1		CHLOROSTOP	
			Required	Observed	Lowest Value	Average Value
Cable diameter	mm	VDE 0472/6.65 para. 401	12.6	13.0	12.7	13.0
PVC jacket thickness	mm	VDE 0472/6.65 para. 402	1.0	1.4	1.3	1.4
Tensile strength	kp/cm ²	VDE 0472/6.65 para. 602	≥125	140	113	123
Strength after 7 days at 80°C	kp/cm ²	"	≥125	140	101	126
Elongation	%	"	≥125	300	210	240
Elongation after 7 days at 80°C	%	"	≥125	300	190	202
Hot compressive resistance	%	VDE 0472/6.65 para. 609	50	35	34	38
Low temperature impact test, 2 hours at -50°C, 3 samples		VDE 0472/6.65 para. 611	3 passed 0 failed	10 passed 0 failed	-	5 passed 5 failed
Same; 2 hours at +5°C		"	-	10 passed 0 failed	-	10 passed 0 failed
Combustibility	mm	VDE 0472/6.65 para. 804	250	130	110	120
Combustibility of 7 vertical 1 m cable lengths hung in a chimney (one in cen- ter, 6 space around it in 1 cm distance); 30 minutes propane gas ignition; after- burn distance	mm	Our own method	-	1000 com- pletely burned	-	400

Dr. Ottmar Leuchs
Kabelmetal, Hannover, Germany

Dr. Leuchs was born in Wuppertal, W. Germany. 1933-39, Study of chemistry. 1949, Entered cable industry. Worked on PVC insulations and published papers on DC strength, osmosis, plastification and cold impact test as well as on classification of polymers. Published a classification and review of nomenclature for polymers. 1959-67, Member: Section on Plastics and High Polymers, International Union of Pure and Applied Chemistry. Presently Director of Laboratory for High Polymers with Kabel- und Metallwerke Gutehoffnungshuette A. G. (Kabelmetal), Hannover, West Germany.

PHOTOMETRIC DETERMINATION OF CARBON DISPERSION QUALITY IN POLYETHYLENE

John B. Howard
Bell Telephone Laboratories, Incorporated
Murray Hill, New Jersey

Some of the problems involved in various possible ways of establishing the quality of carbon black dispersions are discussed, with emphasis on the 100X microscope procedure vs. a simple spectrophotometric method.

It is pointed out that the former, although operating some two orders of magnitude above the particle size range involved, nevertheless provides useful information when properly applied and has served the cause of quality by developing an awareness for the need for very good dispersion.

The newer instrumented approach offers advantages in being non-subjective and quantitative in nature, and in measuring precisely that property for which the black is added, namely, the ability to screen out actinic radiation which can degrade the polymer. Details of the new procedure, included as part of this abstract, are discussed and data demonstrating the relationship of absorption coefficient to actual weathering are reported.

Test Procedure for Determining Absorption Coefficient of Black Polyethylene Plastics

Outline of Method

The transmission of light of a specified wavelength through thin plastic film is measured and the result is used to calculate an absorption coefficient, which is a reciprocal function of transmission corrected for thickness.

Apparatus

Spectrophotometer. An instrument in accordance with ASTM Designation E60 is required.

Note: A Beckman Model B spectrophotometer, with a constant voltage transformer as its power source and the blue sensitive receiver (Beckman No. 12055), has been found suitable. The instrument may be obtained from Beckman Instruments, Fullerton, California.

Mold. A mold in accordance with Fig. 1 and 2. The mold shall be made of Ketos

steel (or equivalent), hardened to Rockwell C45 and the mold surfaces chromium plated to 0.005 mm (0.0002 in.) minimum thickness.

Specimen Holder. Two concentric rings cut from phenolic-paper laminate or other suitable material to the dimensions shown in Fig. 3. These rings should make a snug slip-fit one within the other.

Reference Standard. A reference standard is required having an absorbance value of approximately 1.0 at 375 m μ as measured by the instrument used for testing.

The Kodak Neutral Density Filter No. 5, M-Type carbon, 0.85 density, laminated between cellulose acetate sheets has been found satisfactory. Since this material is furnished as a rigid sheet, it cannot be mounted as described below. Instead, a special mount must be prepared by cutting Ring 1 of Fig. 3 in half around its circumference to give two rings about 1 mm (0.04 in.) thick. Cut a 22 mm (0.87 in.) circle from the laminated filter, sandwich this between the two 1 mm rings, and slide the outer ring (Ring 2 of Fig. 3) over this composite.

An alternative reference standard consisting of an ultra-uniform sample of ASTM Type I polyethylene containing about one percent of a 20 m μ carbon black (either channel or furnace type) may be prepared on a laboratory mill and a uniform film of this material pressed out and mounted, as described below, to meet the above requirements. Reference standards so prepared shall show no more than ± 4 percent variation from the average absorbance value when measured at any point at 375 m μ in the instrument used for testing.

Specimen Preparation

Prepare three test specimens from each lot of material by hot-pressing the plastic at a suitable temperature between highly polished plates, such as those shown in Fig. 1 and 2, using a charge sufficient to yield a specimen 4 to 5 cm in diameter and approximately 0.01 mm in thickness. Preparation of satisfactory specimens may be expedited by double pressing, pressing to approximately 0.05

mm thickness and then pressing a section of that sheet to the required 0.01 mm thickness. Use of a silicone mold release agent is also recommended.

Carefully transfer the specimen to the inner ring of the specimen holder (Ring 1 per Fig. 3). With the specimen positioned concentrically over the inner ring, carefully press the outer ring (Ring 2 per Fig. 3) down over it to complete the mounting operation. The specimen should be firmly mounted, taut, and wrinkle-free. Visually examine the mounted test specimen against a suitable light source. It must be uniform in color and free of clear spots or holes. Mark and identify three points approximately 120 degrees apart on the outer ring of each specimen.

Procedure

After allowing the spectrophotometer to stabilize thermally, with the sensitivity control on position 1 and the shutter open, bring the meter to zero on the absorbance scale by adjusting the slit width. Close the shutter and adjust the dark current control so that the meter reads infinity on the absorbance scale (zero transmittance) at positions 1 to 4 of the sensitivity scale. Repeat the above until stable values are obtained for both zero and dark current.

Place the mounted reference standard in one of the outer positions of the specimen holder of the instrument as close to the receiver as possible. (The reference standard may be left in this position.) Read and record the absorbance value using that setting of the sensitivity control which brings the value nearest to zero on the absorbance scale. With the reference standard still in the beam, and the sensitivity control set at 2, readjust the slit width to bring the meter to zero absorbance. Recheck the dark current value.

Bring the mounted specimen into measuring position using the remaining outer position of the specimen holder, keeping the specimen as close to the receiver as possible. Position the specimen with one of the 120 degree marks at the top. Open the shutter, read and record the absorbance value. The absorbance value recorded is equal to that indicated on the meter plus the measured value for the reference standard.

Close the shutter and recheck the standard. Rotate the specimen to bring the next 120 degree mark to the top and obtain the absorbance value. Repeat the procedure with the third 120 degree mark

at the top. Average the absorbance values for the three positions. If any one value differs from the average by more than 10 percent, discard the specimen and replace it.

Remove the film from the specimen mounting rings by cutting it carefully along the boundary between the two rings, and weigh it to the nearest 0.001 gram. The No. 11 Bard-Parker scalpel blade in a suitable handle has been found very effective for the cutting operation. These are available from most laboratory supply houses. Measure the diameter and calculate the area of the specimen. Determine the equivalent thickness (t) of the specimen from the expression:

$$t(\text{cm}) = \frac{\text{Weight (grams)}}{\text{Density (g/cm}^3\text{)} \times \text{Area (cm}^2\text{)}}$$

Note: The nominal density value for black low-density ethylene plastic is 0.932.

Using the thickness (t), calculate an absorption coefficient (a) at 375 mμ for each specimen from the expression:

$$a = \frac{2.30 \times \text{average absorbance value}}{t(\text{cm})}$$

Average the three values (a) for the three specimens to obtain the value for the sample.

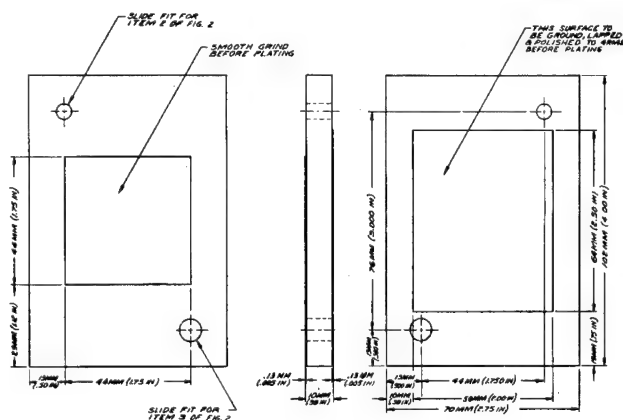


Fig. 1 - Mold, Top Platen

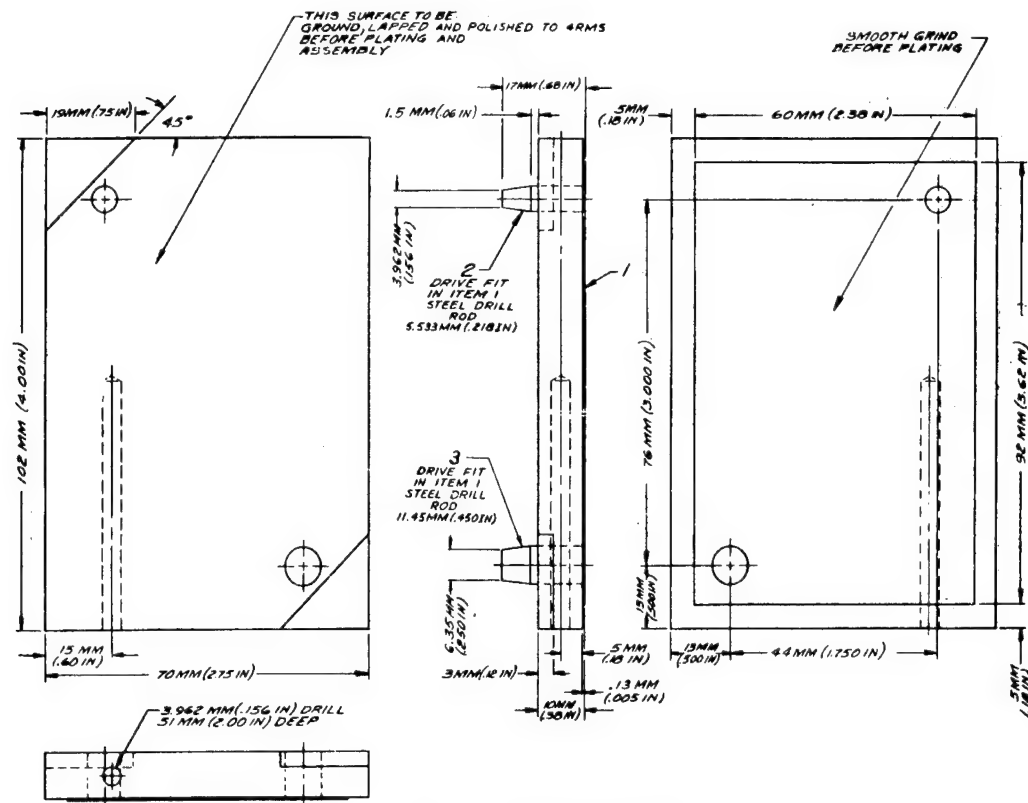


Fig. 2 - Mold, Bottom Platen

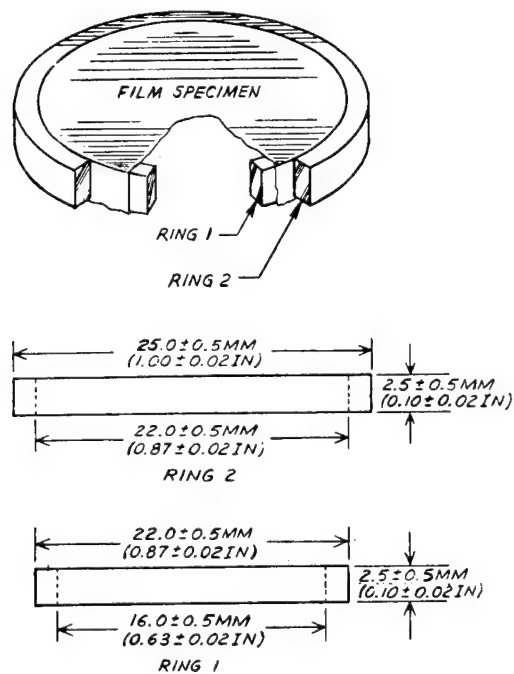


Fig. 3 - Specimen Mounting Rings

A METHOD FOR MANUFACTURING POLYOLEFIN INSULATED COMMUNICATION CABLE BY SOLVENT INJECTION FOAMING PROCESS

M. Jitsukawa, Y. Fujiwara, A. Utsumi and A. Asai
Dainichi Nippon Cables, Ltd. Osaka, Japan

Summary

A novel extrusion technique called the Solvent Injection Foaming Process has been developed by which economical and efficient extrusion of thin wall foamed insulation for telephone cable conductors is attainable at a line speed higher than 1000 m/min. The distinguished features of this process lie in the simplicity of the whole system in which only a solvent injection pump is attached to a conventional extruder. Owing to the lowered melt viscosity of the polymer caused by the solvent injected through the extruder barrel, high speed extrusion of foamed high density polyethylene and polypropylene is possible at temperatures low enough to allow for the selection of chemical blowing agents from a wide range of those commercially available.

By this process, many cable conductors were insulated with high density polyethylene foam. Extrusion conditions were easily controlled so as to produce high quality foamed insulation of 20% expansion at a line speed of 1200 m/min. (4000 ft/min.) for a 0.4mm (26 AWG) conductor with an insulation thickness of 0.1mm (4 mil).

The foamed insulation thus obtained proved to have excellent properties of abrasion resistance, elongation, tensile strength, heat aging resistance and thermal and environmental stress crack resistance. These insulated conductors were assembled into multi-pair exchange area cables of unit type construction. No problems occurred during the twisting and cabling processes by conventional machines.

The finished cables were equivalent in overall diameter and superior in electrical properties to existing paper insulated cables.

Introduction

Notwithstanding the rapid expansion in the use of plastic materials in every field of the wire and cable industry, conventional dry paper tape or pulp is still playing a leading

role in the insulation of the conductors of multi-pair, underground, exchange area telephone cables in Japan.

This predominance of paper insulated cables is maintained primarily by cheaper production costs along with the smaller overall diameter of the cables resulting from the relatively low dielectric constant of the air spaced paper insulation. On the other hand, dry paper has the unavoidable and unfavorable nature of being highly hygroscopic, so that the insulated conductors must be protected by a completely airtight sheath such as lead or stanneth. In addition a gas preservation system as well as other considerations of maintenance are necessary for efficient performance of the cables.

As is well known, plastic materials, in particular polyethylene, are non-hygroscopic and have excellent dielectric properties for use in telephone cables. The uniform thickness of plastic insulation brings about superior cross-talk characteristics even in a cable of star quadded construction. But when polyethylene is used as a solid insulation in the usual way, an unfavorable increase in cable diameter and production costs occur. This is the reason why plastic insulation has not taken a leading place except in smaller cables, of not more than 200 pairs of conductors, which are mostly used in aerial installations for distribution purposes.

These considerations naturally lead to the inference that all insulations of multi-pair telephone cables will be replaced by some plastic material, provided production costs and overall diameter of the plastic insulated cables can be reduced to a level equivalent to that of paper insulated cables.

A most promising plastic insulation to satisfy the above conditions would be a thin foamed polyolefin. Particularly high density, high molecular weight polyethylene or high molecular weight polypropylene seems to be more suitable than conventional low density polyethylene, since the insulation material, in

the form of thin foam, should be tough enough to withstand the abrasion and compressive stress imposed during manufacturing and installation.

The high speed extrusion of these polymers of high melt viscosities into thin foamed insulation is not easy at present and can be attained only at extremely high extrusion temperatures. Unfortunately, there are few chemical blowing agents which will produce fine and well-distributed cells in the foamed insulation at these high extrusion temperatures.

This is the background of our project to develop a new process which will enable high speed extrusion of thin foamed insulation using commercially available materials and existing machines. Our developmental work started in 1966. At the beginning of the work, the so called "Gas Injection Process" was tested in which a gas is directly injected through the barrel wall of an extruder.¹ But this process was found to be very complicated and there were many difficulties in trying to control the extrusion conditions.

Recently we have developed a new version of the gas injection process called the "Solvent Injection Foaming Process (SOFOX Process)" which should contribute greatly to the low cost, commercial production of plastic insulated multi-pair telephone cables.

This paper presents the details of this new process and results obtained by this method.

The Solvent Injection Foaming Process

Outline of the process

The most distinguished feature of the process lies in the fact that a conventional extrusion line can be used without any additional expensive equipment. The only necessary attachment for the extruder is a small plunger type pump, and stable and easy operations are possible with this simple system.

During a series of experimental studies on the earlier gas injection process, it was noticed that a liquid gas had a pronounced plasticizing effect on polyolefin, which did suggest a possibility of high speed extrusion of foamed insulation at reasonably low temperatures, enabling selection of chemical blowing agents from a wide range of those commercially available.

During subsequent experiments, by injecting a solvent into the polyolefin melt through the extruder barrel, a remarkable decrease of internal pressure due to the decrease of the apparent melt viscosity of the polymer was

observed.

The effect of the amount of injected solvent on the crosshead pressure of the extruder is shown in Fig.1. Data is replotted in Fig.2 illustrating the effect of line speed on the head pressure.

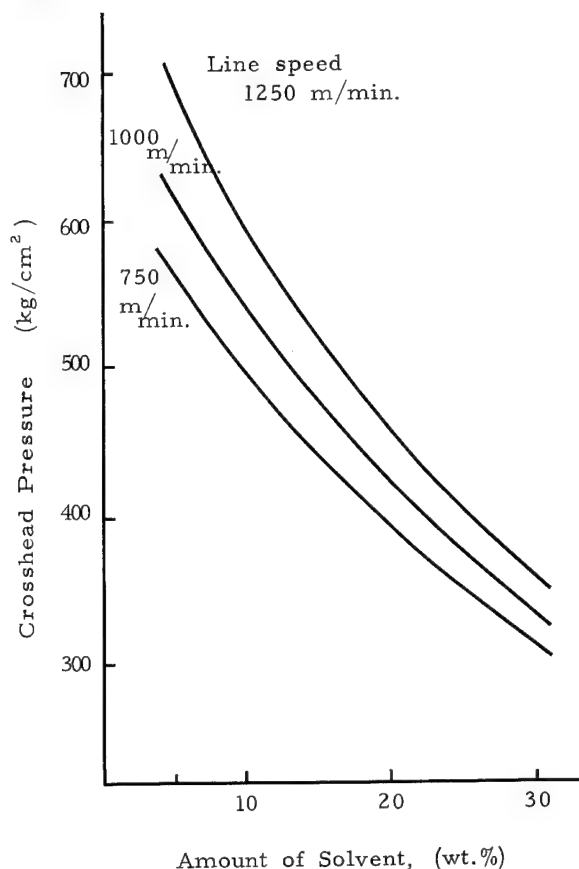


Fig.1 Variations of crosshead pressure with amount of solvent.

Condition of experiment

Material : High density polyethylene
 Density : 0.95, M.I. : 0.25
 Azodicarbonamide content
 0.7 PHR

Extrusion temperature: 190°C (374°F)
 Conductor diameter : 0.4mm(16 mil)
 Wall thickness : 0.1mm(4 mil)

It is evident from these Figures that with a sufficient amount of solvent injected it is possible to extrude a high density polyethylene foam at high speeds under a pressure even lower than that found in the extrusion of conventional low density polyethylene.

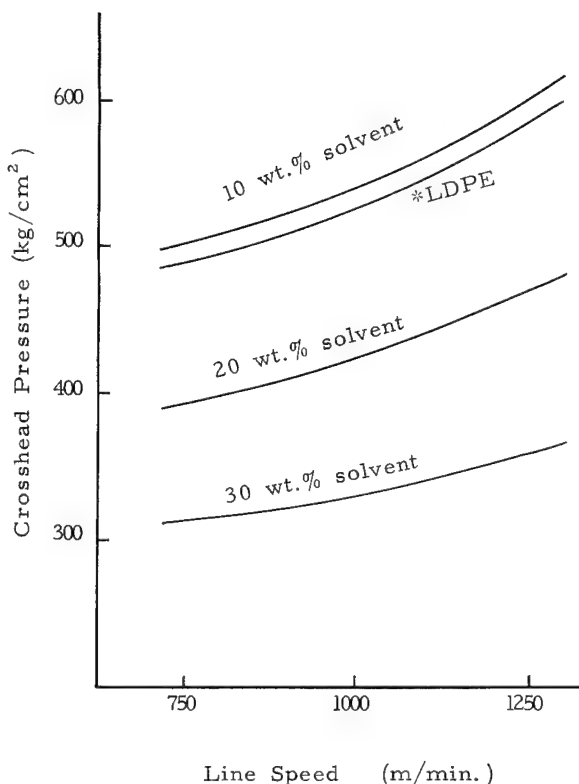


Fig. 2 Variations of crosshead pressure with line speed.

Condition of experiment

Material : High density polyethylene
 Density : 0.95, M.I. : 0.25
 Azodicarbonamide content
 0.7 PHR

Extrusion temperature : 190°C (374°F)
 Conductor diameter : 0.4mm (16 mil)
 Wall thickness : 0.1mm (4 mil)

* Low density polyethylene without injected solvent.

Density : 0.92, M.I. : 0.3

On the other hand, injection of excess solvent is undesirable because in the course of time it causes an unfavorable diametral shrinkage of the extruded insulation as well as a decrease in extruder output of the polymer. According to our experiment, 10 to 20 wt.% solvent injection was found to give the best results for 0.4mm conductors.

Almost all of the organic solvents tested had good plasticizing effects on polyolefins.

However, by the restrictions arising from practical extrusion performance, only a few solvents with high boiling temperatures were found to be useful for this process.

A stable operation can only be achieved under precise control of solvent injection which is made possible by the use of a plunger type pump in the system.

This process is not only useful for foamed insulation but for the low temperature and high speed extrusion of solid insulation.

As is seen in Fig. 3, the injection system is very simple in design and is attached to a conventional extruder without difficulty.

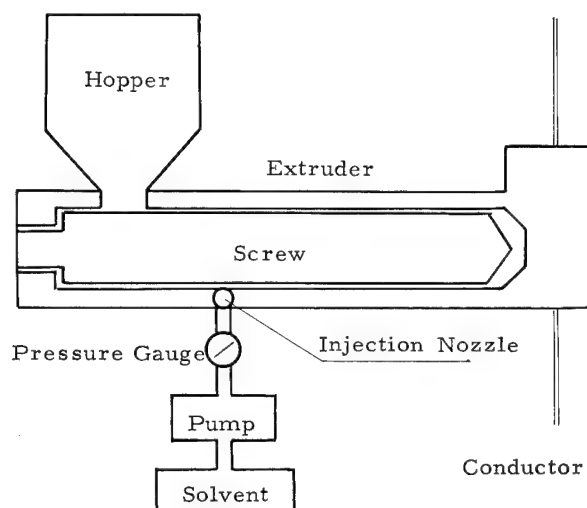


Fig. 3 Schematic diagram of extruder

Details of the process

(1) Extrusion equipment

(a) Extrusion line : Fig. 4 is an illustration of the extrusion line. The studies for this process were carried out on two different lines, extruders of which were 40mm (1.5 inch) and 65mm (2.5 inch) in screw size respectively. The line of the 40mm extruder was chiefly employed for the basic study and the other was for studying the process for use in practical manufacture. The specifications of both extruders are shown in Table 1.

(b) Die : There was no necessity for special consideration of the die design since the injected solvent did much toward smoothing the surface of the insulated wires. A double tapered die with a short land of low flow resistance was used. By virtue of the high melt fluidity

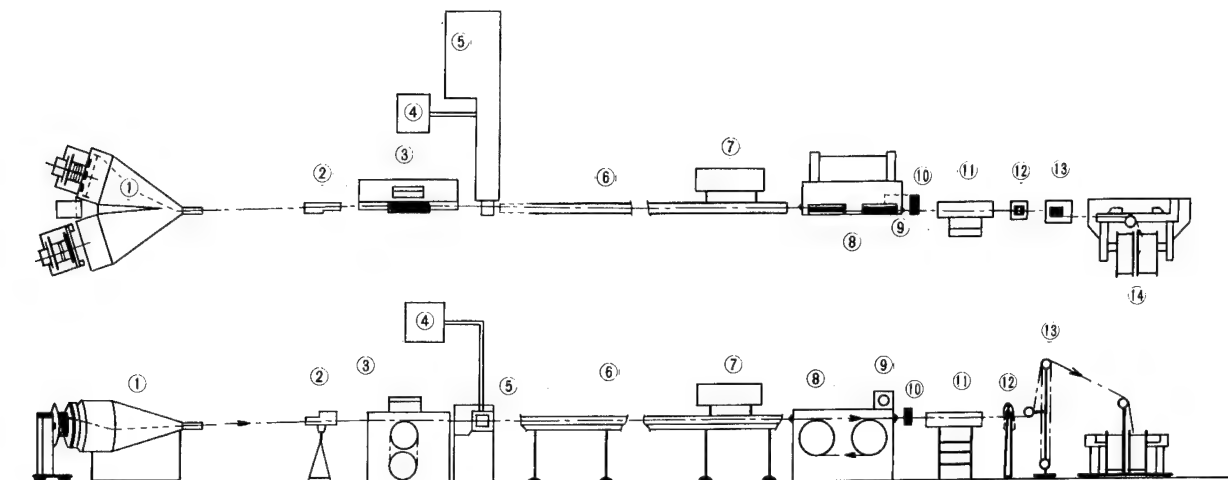


Fig. 4 Extrusion line of the solvent injection foaming process

- 1 Pay-Off
- 2 Wire Straightener
- 3 Preheater
- 4 Injection Pump and Nozzle
- 5 65 mm ϕ Extruder
- 6 Water Trough
- 7 Capacitance Monitor

- 8 Capstan
- 9 Diameter Measuring Recorder
- 10 Diameter Measuring Device
- 11 Spark Tester
- 12 Measuring Machine
- 13 Dancer Roll Assembly
- 14 Take-Up

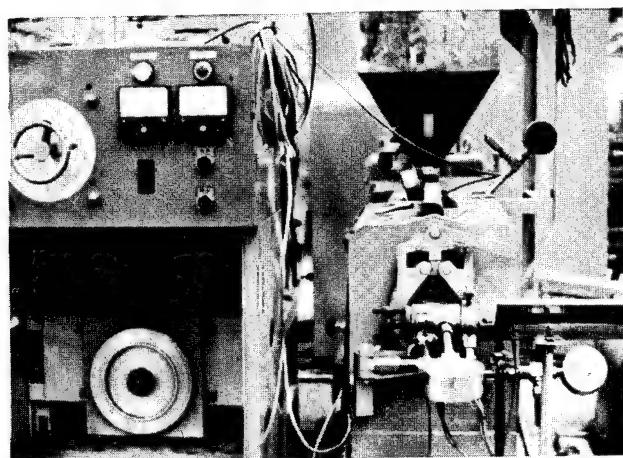


Fig. 5 The extruder and preheater

of the polymer, larger draw-down was allowable to a ratio of about 1.75 for a 0.4mm conductor (26 AWG) and 1.3 for a 0.5mm (24 AWG) conductor.

Table 1 Specifications of the Extruders

Screw Diameter	40 mm	65 mm
Screw Type	Metering Type	Metering Type
L/D Ratio	22.5 : 1	23.5 : 1
Compression Ratio	3 : 1	3 : 1
Flight Pitch	40 mm	65 mm
Pump	Plunger Type	

(2) Materials

(a) Polymer : The types and properties of the polymers used are given in Table 2. The high

Table 2 Characteristics of Materials

Items	Materials	High Density Polyethylene	Polypropylene
Density,	g/cm ³	0.95	0.90
Melt Index,	g/10 min.	0.25	0.90
Tensile Strength,	kg/mm ²	1.8	2.0
Elongation at Break,	%	800	800
Brittleness Temperature,	°C	Below - 80	Below -30

density polyethylene was of electric insulation grade which has excellent environmental and thermal stress cracking resistance, and thermal aging resistance. The polypropylene was a copolymer grade of excellent low temperature characteristics.

(b) Blowing agent: The selection of blowing agent is one of the most important factors necessary for achieving the desired type of foamed insulation. After an extensive study, a special kind of azodicarbonamide was chosen from among a number of commercially available blowing agents in common use for low density polyethylene foamed insulation.

(c) Solvent : Solvent was directly responsible for the satisfactory performance of this process. A few kinds of high boiling point solvents were finally chosen with the view towards plasticizing effect, non-toxic and odorless properties, and causing no damage to the conductor and the other materials in the cable. Economy was also a factor.

(d) Miscellaneous materials : As for the blending of polymer with chemical blowing agent to produce an expandable compound, two methods, dry blending and hot mixing, were examined and both proved to be satisfactory for extrusion.

In relation to polypropylene, the method of dry blending has a specific benefit, since polypropylene can usually be processed by hot mixing only at such a high temperature as to disallow the use of a chemical blowing agent of low decomposition temperature.

Color concentrate was used for the coloring of the insulation, the most suitable pigments being chosen so as not to adversely affect the foaming of the insulation.

Foaming and extrusion conditions

The extrusion and the foaming of the high density polyethylene and polypropylene were made under almost the same conditions as that for standard solid low density polyethylene. The degree of foaming, as required by the

Table 3 Conditions and Results of the Extrusions

Condition	Material Conductor (mm)	High Density Polyethylene Foam			Polypropylene Foam	Low Density Solid Polyethylene
		0.4	0.5	0.9	0.4	0.4
Temperature,	°C	210	210	210	210	210
Line Speed,	m/min.	1200	1200	1000	1000	1200
Crosshead Pressure,	kg/cm ²	495	410	390	520	515
Running Tension,	g	2100	4200	12200	2300	2250
Amount of Solvent,	wt. %	15	10	5	15	-
Wall Thickness,	mm	0.100	0.125	0.240	0.08	0.130
Percentage Expansion,	%	20	25	25	31	-

transmission properties of the finished cable, was controlled by the amount of blowing agent in the compound and by the extrusion temperature.

A stable extrusion operation was achieved at a line speed of up to 1200 m/min. (4000 ft/min.) for an extended period of time. This limitation of line speed was not attributed to the capability of the Solvent Injection Foaming Process but to the speed-rating of the machine employed. In fact, excellent quality foamed insulation was

attained experimentally at a line speed of 1400 m/min. (4700 ft/min.). The conditions of extrusion are shown in Table 3.

Properties of Insulated Conductors

Representative properties of insulated conductors obtained by this process are shown in Table 4.

Table 4 Properties of Foam Insulation Conductors

Items	Materials	High Density Polyethylene Foam		Polypropylene Foam	Solid Low Density Polyethylene *1		Remarks
Conductor Diameter, mm		0.4	0.5	0.4	0.4	0.5	
Wall Thickness, mm		0.10	0.12	0.08	0.13	0.15	
Percentage Expansion, %		20	25	31	-	-	Specific Gravity Method
Cell Size, micron		max. 15	max. 20	max. 20	-	-	Microscopic Observation
Tensile Strength, kg/mm ²		3.1	2.9	2.9	1.8	1.8	JIS K 6760
Elongation at Break, %		375	360	400	over 600	over 600	JIS K 6760
Abrasion Resistance,		120	586	86	42	89	*2
Thermal Stress Crack Resistance		over 1000 hrs	over 1000 hrs	over 1000 hrs	over 1000 hrs	over 1000 hrs	*3
Environmental Stress Crack Resistance		over 1000 hrs	over 1000 hrs	over 1000 hrs	over 1000 hrs	over 1000 hrs	*4
Shrinkback		Passed	Passed	Passed	Passed	Passed	REA, PE-22 *5
Dielectric Strength, kV	Single Conductor	ave. 4.1 min. 3.5	ave. 7.2 min. 5.9	ave. 3.0 min. 2.1	over 13	over 15	*6
	Pair Conductor	ave. 9.1 min. 8.0	ave. 15.2 min. 13.8	ave. 7.6 min. 6.5	over 25	over 25	JIS C 3000 *7

*1 Melt Index, 0.3 g/10 min : Density, 0.920 g/cm³

*2 A rotating cage machine provided with 36 steel rods of 8mm diameter was used. A load of 850g was applied to each conductor specimen.

*3 Conductor specimens were wrapped ten times around their own diameter, and tested at 70°C.

*4 Conductor specimens were wrapped ten times around their own diameter, and tested in an aqueous solution of 10 wt.% Igepal CO-630 at 50°C.

*5 6 inches specimens were maintained at 115°C for 24 hours.

*6 Conductor specimens were immersed in a glycelin bath mixed with sodium chloride and DC voltage was applied between the conductor and the bath.

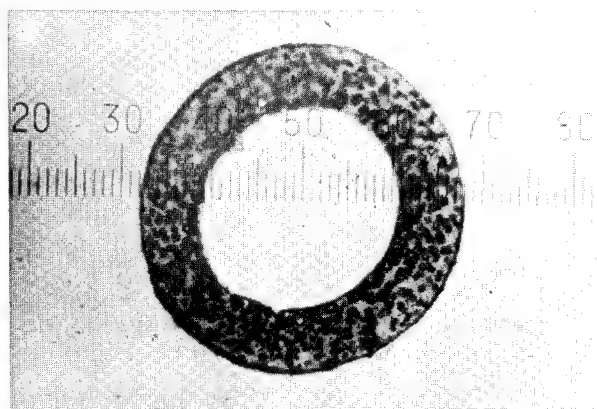
*7 Two conductor specimens were twisted together for a length of 12cm under a tension of 350g (450g in 0.5mm conductor). The number of twists was sixteen times. DC voltage was applied between the two wires.

Appearance

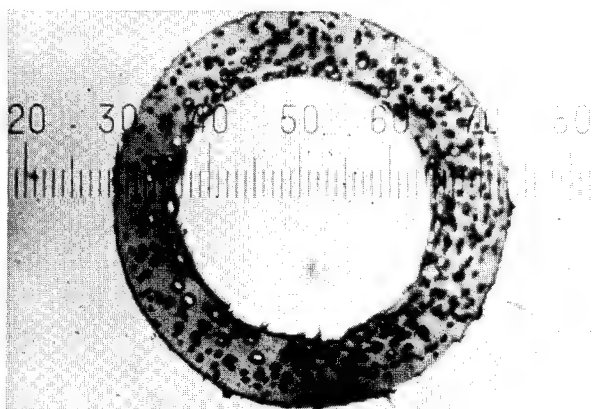
The insulated conductors resulting from this process were smooth in surface and gave satisfactory appearance even though they were extruded at the low temperature of 190 to 220 °C. At this temperature even solid insulation of low density polyethylene produced at the same extrusion speed would not show smooth appearance.

Percentage expansion and foamed structure

The amount of blowing agent and extrusion conditions were adjusted to give a 20% expansion, resulting in a coaxial capacitance of 270 pF/m (83 pF/ft) for a single wire of a 0.4mm (26AWG) conductor with 0.1mm (4 mil) insulation.



conductor diameter : 0.40 mm
wall thickness : 0.100 mm



conductor diameter : 0.50 mm
wall thickness : 0.125 mm

Fig.6 Micrographs of cross section of high density polyethylene foamed insulation

The foamed structure is closely related to insulation appearance, mechanical property, dielectric strength and pin-holes, and a structure consisting of fine, independent and uniformly distributed cells is preferable.

Fig.6 shows micrographs of the cross section of the insulations, illustrating the well distributed fine cells. Average cell size is about 10 microns and the maximum is less than 20 microns.

Abrasion resistance

In addition to the intrinsic strength of the polymer itself, smoothness of insulation surface, percentage expansion, and cell size have an influence on the abrasion resistance of foamed insulation. As is shown in Table 4, the abrasion resistance of insulated wire from this process, when tested in a rotating cage type test machine, is superior to that of solid insulation of low density polyethylene having a greater thickness. As to the results and the evaluation method there may be grounds for some qualification since other test methods such as the cut through type test often bring different results. In any event, an increase of pin-hole defects in the insulated conductors during the subsequent cabling process scarcely occurred, which proved the insulation had sufficient mechanical strength against abrasion.

Tensile properties

Thin wall polyethylene insulation extruded at a high speed by the conventional extrusion method is apt to show low ultimate elongation values of less than 100%. This is considered to be caused by the high degree of molecular orientation in the polymer insulation.

Insulation extruded by the Solvent Injection Foaming Process has sufficient tensile properties as shown in Table 4, and this is the result of preheating of the conductor and reducing crosshead pressure, both of which work well on minimizing orientation.

Shrink Back

Shrink back is a measure of the degree of molecular orientation frozen in the extrudate and, therefore, is closely connected with elongation and tensile strength.

It is seen that the shrink back of the insulation by this method is sufficiently low, which is reflected to the high tensile properties.

Dielectric strength

The insulated conductors by this process,

of which breakdown voltage was above 6 kV in twisted specimens, are superior to existing paper insulated conductors in dielectric strength.

Thermal and environmental stress crack resistance

Thermal and environmental stress crack resistance are very important properties for the insulation of cable. As is shown in Table 4, the conductors from this process show good performance in relation to these properties. These results are considered to reflect both the basic properties of the materials selected and the cushioning effect of the foamed insulation.

Miscellaneous properties

Oxidation resistance, color fading resistance to weathering and dielectric properties of the insulated conductors were studied and all these properties were confirmed to be satisfactory.

Examination of Cables

Cable manufacture

A number of exchange area cables of unit type construction up to 2400 pairs of star-quadded conductors of 0.4mm (26 AWG) to 0.9 mm (19 AWG) were manufactured for practical examination, using the insulated wires produced by this process.

During the period between insulation and quad twisting, diametral shrinkage of 5 to 7 microns was observed in the insulated conductor, which seemed to result from the evaporation of residual solvent in the insulation. But this shrinkage did not cause any problems in subsequent processes or in the electrical properties of the finished cables.

The flow-diagram of the manufacturing process is given in Fig. 7.

The quad-twisting, stranding, cabling and stalpeth-sheathing were carried out by conventional machines under the same conditions as for existing paper tape insulated cables. No problems or increase in pin-holes in the insulations occurred, which proved the insulation had sufficient strength against abrasion and compressive stress during these processes.

Therefore there is no need for considering installation of new and expensive machines to manufacture these cables.

Fig. 8 is a photograph of samples of the finished cables.

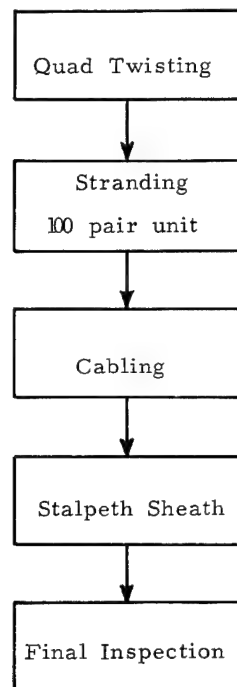


Fig. 7 Flow-Diagram of manufacturing the multi-pair telephone cables

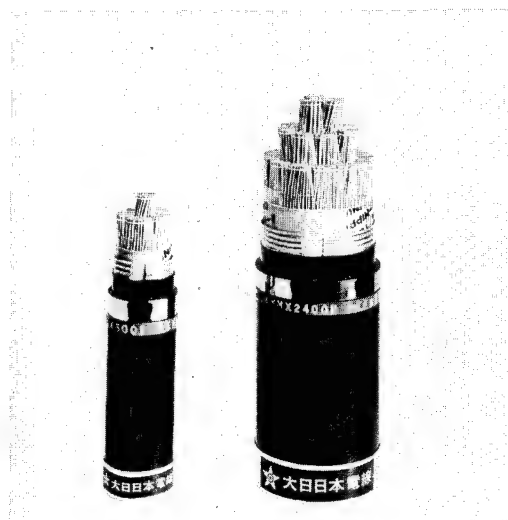


Fig. 8 High density polyethylene foam insulated multi-pair cables

left : 0.4mm, 600 pair
right : 0.4mm, 2400 pair

Properties of finished cables

The electrical properties of a number of finished cables are shown in Table 5 and Figs. 9 and 10. The cables having the plastic insulated conductors were superior to existing dry paper insulated cables in insulation resis-

tance, capacitance unbalance and transmission loss at high frequency. And they satisfactorily fulfilled all the requirements which are specified in the Nippon Telegraph & Telephone Public Corporation's Specification for Polyethylene (solid, low density) Insulated Exchange Area Cable for distribution purpose.

Table 5 Electrical Characteristics of Finished Cables

Items	Cables		High Density Polyethylene Foam		NTT's Specification on 0.40mm Paper Insulated Cable
			0.4mm 600 Pair Cable	0.4mm 2400 Pair Cable	
Conductor Resistance Ω/km	ave.	135.9	ave.	137.5	max. 147.5 nom. 139.0
Insulation Resistance $M\Omega\text{-km}$		210,000		200,000	min. 2,000
Dielectric Strength 500V DC for 1 min.		withstood		withstood	500V DC or 350V AC for 1 minute
Average Mutual Capacitance nF/km		49.8		49.7	50 ± 5
Pair to Pair Capacitance Unbalance within a Quad $\text{pF}/500\text{m}$	ave.	74.5	ave.	30.0	ave. 300
	max.	399.0	max.	94.0	max. 1,600

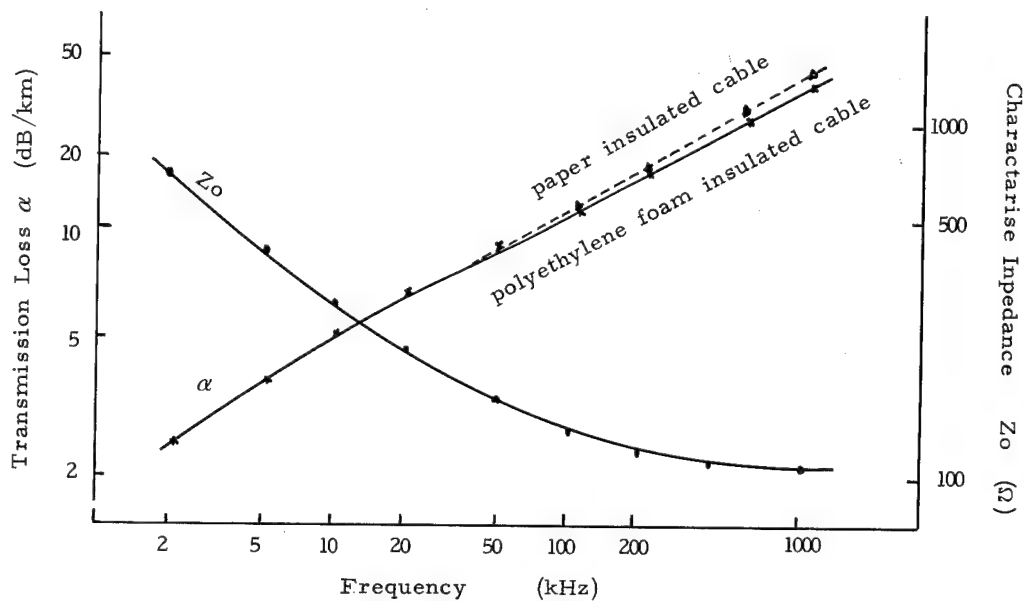


Fig. 9 Propagation constants of the cable

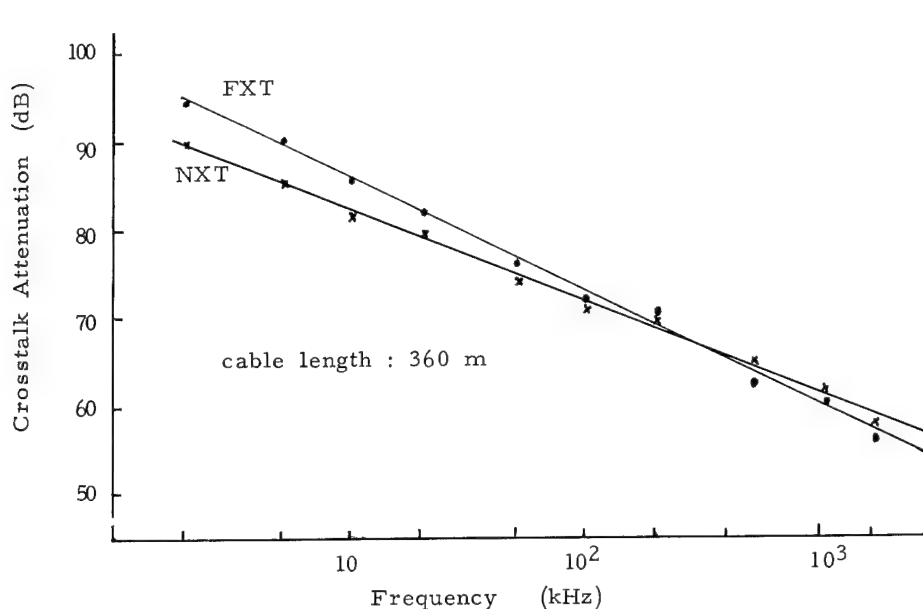


Fig.10 Crosstalk between pairs within a quad

All the overall diameters of the cables were nearly equal to those of existing dry paper insulated exchange area cables.

Conclusion

By this newly developed technique, in which are used chemical blowing agents and a conventional wire extrusion line attached by a solvent injecting plunger type pump, it is now possible to perform high speed extrusion of thin-wall polyolefin foam insulated telephone conductors.

In a series of basic and practical examinations, this process proved to have many advantages as summarized below.

(1) High speed extrusion of thin wall foamed insulation of high density polyethylene and polypropylene is attainable using a commercially available chemical blowing agent.

(2) A conventional extruder, slightly modified by attaching an injection nozzle and a pressure pump to it, is used. Therefore, the whole line is simple in design and equipment cost is reasonable.

(3) The usage of this particular pressure pump allows the precise control of solvent injection so that stable and long operation of the extrusion process is possible.

(4) Owing to the improved extrudability, larger draw-down, lower crosshead pressure and lower running tension were brought about.

(5) Even the use of a polymer such as polypropylene, which is difficult to process by hot mixing, is easily applicable to this process, since the expandable compound may be prepared by dry blending the polymer with the chemical blowing agent.

(6) This process is useful not only for the extrusion of foamed polyolefin but also for the low temperature and high speed extrusion of solid polyolefin insulation or other plastics.

(7) Because of the simplicity of the extrusion line, together with the easy and efficient running of equipment and the small diameter of the cable core, the cost of the cable was reduced to a level equivalent to that of existing paper insulated exchange area cable.

Reference

1. M. Okada, A. Utsumi, Y. Fujiwara, A. Asai, M. Yajima and K. Akasaka, the Annual Meeting of the Institute of Electronics and Communication Engineers of Japan, Tokyo, Oct. 1969.

A. Asai
Dainichi-Nippon Cables, Ltd.,
7-3 Umeda, Kitaku
Osaka, 530, Japan

Akira Asai joined Dainichi-Nippon Cables Ltd. in 1966 after he received his BS degree in Electrical Engineering from Tokyo Institute of Technology. He has been engaged in research and developmental works on communication cables. He is now a staff engineer of the Development Department of Communication Cables in the present company. He is a member of the Institute of Electronics and Communication Engineers of Japan.

Atsushi Utsumi joined Dainichi-Nippon in 1965 after receiving his BS degree in Industrial Chemistry from Kobe University. He has been engaged in research and developmental works on plastic materials for wire and cable. He is now a research engineer in the Research Laboratory of the present company. He is a member of the Society of Polymer Science, Japan.

Yasuaki Fujiwara graduated from Hyogo Technical High School in 1957 majoring in Mechanical Engineering. That same year he joined Dainichi Electric Wire and Cable Co. He has been engaged in the manufacturing engineering works on wire and cable. He is now a staff engineer of the Department of Manufacturing Engineering of the present company.

Masao Jitsukawa graduated from Chiba Technical High School in 1957 majoring in Electrical Engineering. That same year he joined Nippon Electric Wire and Cable Co. He has been engaged in inspection and manufacturing works on wire and cable. He is now a staff engineer in Kumagaya Plant of the present company.

MANUFACTURING WATERPROOF TELEPHONE CABLE

R. A. Conser

T. A. Heim

L. D. Moody

Western Electric Company
Omaha, Nebraska

ABSTRACT

The Western Electric Company - Omaha Works has developed a process for manufacturing waterproof telephone cable on a commercial production basis. The process includes a flooding technique which coats each pair of wires with a filling compound and forms them into a watertight core. The process is also used to provide a coating over the core wrap material and the aluminum which are formed over the filled core. The result is a watertight cable which prevents the entrance and the channeling of water into the core causing degradation of the electrical characteristics of the telephone cable.

INTRODUCTION

With the development of a waterproof cable design by the Bell Telephone Laboratories, Inc., the Western Electric Company was faced with the problem of providing manufacturing technology that could produce the new design in large enough quantities to meet its commercial demand. Manufacturing waterproof cables on a commercial production basis would increase the difficulties associated with manufacturing telephone cables since the large percentage of air space (approximately 47% of the cable core cross section) would have to be replaced with filling compound. Additional facilities would also be required to provide waterproofing of the core wrap material and the aluminum which are formed over the filled core during the sheathing process.

Other problems associated with providing an adequate manufacturing process for the new cable design included:

- (1) Adequate capacity from existing insulating extruders since the new design required a larger diameter over the dielectric (DOD);
- (2) More sophisticated temperature and pressure controls for the insulating extruders which would be running a polypropylene insulating material rather than the standard polyethylene;
- (3) An adequate identification system to distinguish the special wire from regular polyethylene wire as it is processed through the shop;
- (4) Providing handling and melt-down facilities for the polyethylene-petroleum jelly filling compound (PE-PJ); and
- (5) Testing procedures.

DEVELOPMENT OF A FILLING PROCESS

Early Development Work

Many filling techniques were investigated in the early stages of the development of a manufacturing process for filling telephone cables with a waterproof compound. One of the first techniques tried at the Omaha Works involved the use of a small extruder which attempted to force the filling compound into the cable core as it passed through the extruder head much in the same manner that the sheathing compound is extruded over the cable core on a regular cable. The filling compound being used at the time was very tacky and proved to be unacceptable for use with this technique. Unevenness in application, partly attributable to the tacky compound, resulted in unacceptable filling and the technique was abandoned in favor of other techniques with better means of controlling the amount of filling compound being applied to the cable core.

A second technique investigated involved the use of a cavity die through which the wires were drawn and the filling compound injected. The filling compound used was PE-PJ. An air pump was used to inject the compound into the die. Experimental trials using this technique indicated that application of the PE-PJ compound by this method presented undesirable results. Excess filling material squeezed from the cable core by the die and the lack of control of the amount of compound being forced into the core made for adverse characteristics of the system. In addition, the air pump being used proved to be inadequate to handle the PE-PJ compound at room temperature. Thus, other means were sought to fill the cable core.

Development of the Flooding Process

From early experimental waterproof cable productions made for the Bell Telephone Laboratories by Western Electric, valuable information was acquired on filling techniques. This information was used as the basis for the present filling technique used to manufacture waterproof cables at Omaha - the flooding or immersion technique. This technique uses a flooding or immersion process to coat each pair of wires with the PE-PJ filling compound. The process involves pulling the paired wires through a flooding tank containing melted PE-PJ compound at approximately 240°F. As the wires pass through the tank, the PE-PJ adheres to the "cold" wires (76°F as compared with the hot compound). The wires are then formed into a cable core or a primary unit at a bunching die within the tank before the core or unit is coated with a thin film of the compound as it exits from the tank. The

exit die of the flooding tank is usually .02 inches larger than the diameter over the outer layer of the core or unit when measured dry. This allows for about .01 inch build-up from the filling compound within the core itself, and a .01 inch build-up over the outside of the core. This technique provides a built-in "automatic" control of the amount of compound needed to fill the core since the core takes what it needs to replace the air between the pairs. Maintaining the level of the compound above the wires is all that is required to insure an adequate fill of the cable core.

After the cable core exits from the flooding tank, it is covered with a core wrap material which is bound in place by polypropylene ribbon. In the case of the primary unit, as many primary units as are needed to make the size of cable desired are filled in the same manner as mentioned. Instead of the core wrap material being applied to each unit, the units are drawn through a second flooding tank which fills the air space between them. The cable core then receives a thin film of the PE-PJ compound as it exits from the tank. The core wrap material is then applied over the unit type cable and bound in the same manner as the single-unit cable core.

The coating of each pair of wires with the filling compound and the forming of them into a core form within the flooding tank minimizes the possibility of air being present between the pairs within the core. The application of the core wrap to the filled core as it exits from the tank and the drawing down of it tight against the core with the use of polishing dies minimize the amount of air which is encapsulated around the core.

The waterproofing process involves additional application of the PE-PJ compound to the outside of the core wrap material just prior to the longitudinal application of the aluminum, and also over the outside of the aluminum just before the sheath is applied. Flooding tanks similar to those used for flooding the primary units and/or the cable core are used for these applications. Exit dies are usually .02 inches larger than the diameter over the core wrap (DOCW) and the diameter over the aluminum (DOA) to allow for sufficient coating of each with the PE-PJ compound.

MANUFACTURING

Insulating

Since the low density, high molecular weight polyethylene insulation used on the standard PIC cable conductors in the Bell System was replaced with polypropylene, modifications to present insulating equipment were necessary in order to manufacture the conductors for use in the waterproof cables.

Modifications required in the tandem wire insulating process have taken the form of:

- (1) Definitive Product Identification
- (2) Extrusion Tooling
- (3) Extruder Temperature Control
- (4) Wire Temperature Control
- (5) Production Rate Limitations

Definitive Product Identification. Since the polypropylene insulated wire is made in the same colors as polyethylene insulated wire and adjacent to lines manufacturing polyethylene insulated wires (48 insulating lines are in one area), the chances of a product mix-up were significant. Under current designs, if a polyethylene wire were accidentally to get into a waterproof cable, the hot PE-PJ compound would damage its insulation. Ink coding of the polypropylene insulated wire was proposed and development of a compact unit is still in design. The conventional coders will not fit in the manufacturing space available. Product identification has temporarily been accomplished through the use of a definitive reel tag color system. Questionable wire can be isolated based on insulation diameter and elongation. Refer to Table 1 for product parameter limits.

Extrusion Tooling. Extrusion tooling as presently used in our tandem insulating process and adjusted only for the change in insulation DOD could not be used to satisfactorily insulate wire with polypropylene insulation. Processing difficulties first encountered were inability to control the stock temperature in the crosshead and excessive erratic eccentricity. The problem was assumed to be excessive pressure from shear action in the tooling. The material supplier confirmed this as a probable cause and in addition recommended a significant increase in the die orifice diameter. Refer to Table 2, Polypropylene Compound A. From a theoretical point of view, the large amount of pull-down required for polypropylene compound A is undesirable and it is felt a significant factor in the out-of-roundness differences indicated in Table 1.

Pressure transducer instrumentation was installed to assist in evaluation of the difficulties. The pressure instruments revealed a critical head pressure of 2000 psi. Pressures greater than 2000 psi produce eccentricity failures. To correct the difficulties, spacers were added to the core tube or guider tip assembly to increase the gum space, the die orifice diameter was increased, and the minimum die angle was increased. Refer to comparison data in Table 2. Further work with the insulator die indicated that head pressure could be reduced to 1800 psi by increasing the minimum included angle to 10°.

It should be kept in mind that Western Electric uses a fixed center crosshead because of the magnitude of its wire insulating operation and to minimize errors in tooling set up. Also of mention is the material interchangeability requirement of Western Electric. Extrusion settings should not require adjustment from one supplier's material to another.

Extruder Temperature Control. Our development line is equipped with a 2-1/2", 20/1 NRM extruder, air cooled. Development included changing the extruder drive from a V-belt to a timing belt for greater stability of control, and changing the extruder barrel and crosshead to melt control. Because of the close operating tolerances on the plastic temperature and the different melting characteristics of polypropylene and polyethylene, a combination SCR proportional current heating and time proportioning cooling system is used. The close control of the plastic melt is indicated in Figure 1. Since zone melt thermocouples are dual units, the melt temperature in the zones is monitored and found to be performing equal to the master melt record of Figure 1 which is measured in the crosshead. The air capacity of cooling fans is monitored with velocity sensing switches which will turn on indicator lamps when a fan fails to deliver when called upon. Sample operating profiles are presented in Table 3 for the two polypropylenes being used in development.

Wire Temperature Control. Control of wire temperature entering the extruder is of utmost importance since it affects line start-up, eccentricity, adhesion, and insulation elongation. Also of note in operator reaction to processing problems is that the effect of preheat on polypropylene is opposite that of polyethylene. In view of various instruments for measuring wire temperature, we have chosen a temperature sensitive paper as being the most reliable device. The paper is similar to litmus paper in size and shape, and can be purchased in 10°F increments above 100°F. One side of the paper is black, the other white. The white side changes to black in less than 2 seconds when the rated temperature is achieved and is not affected by frictional heat between the moving wire and the paper.

The resistance preheater previously equipped with a tap switch was modified for infinitely variable control because of the affect of wire temperature on insulation parameters. The preheater is automatically turned on as the line speed accelerates through 75% of the assigned line speed. At this point, the extruder drive is made available to the operator. These interlocking features were found necessary to prevent breakdown on start up and eliminate a prime cause of defective product. Figure 2 shows the changed areas of the insulating line.

Production Rate Limitations. Production rates are essentially limited by extruder size, extruder screw design, and cooling capacity.

The 22 gauge polypropylene is manufactured at 2500 fpm as compared to 22 gauge polyethylene at 3500 fpm. Refer to Figure 3. To manufacture the polypropylene at the 3500 fpm speed requires 65% more extruder thru-put than 22 gauge and 16% more than 19 gauge at 2600 fpm. In this consideration, it should be noted in Figure 4 that compounds A & B differ in the extruder rpm required for the same thru-put. Within a given compound, our experience has been to anticipate a 10% to 15% increase in extruder rpm for a given pounds per hour output, and is explainable by a plugging of the screen pack.

Prior to any size up of our extruder, work was begun on an extruder screw design. Initial work with polypropylene compound A looked promising; however, as we began investigating compound B, significant differences in the processing characteristics of the two materials were validated. This was anticipated from published melt flow rates of the two materials as noted in Table 4. Other significant material differences have appeared in terms of required tooling and operating profiles discussed earlier such that screw design work has stopped, pending forthcoming material property changes.

Development of increased cooling within the line length is still in process.

Twisting

No modifications to twisting equipment were necessary to process the special polypropylene conductors through the twisting operation. A reduction in the length of wires wound onto the 534 reel was necessary, however, because of the larger DOD of the polypropylene wire. In the case of 22 gauge wire, 12,500 feet of wire is placed on the 534 reel rather than the 17,700 feet of polyethylene wire.

Stranding and Sheathing

Early experimental waterproof cables were manufactured on a drum strander which was equipped with experimental filling facilities. The cable sizes were limited to 25 pair or less because of the 534 reel capacity of the drum strander. These cables were made with a 24 inch left lay. The filling material and mylar core wrap were applied at the drum strander. The filling material was added to the cable core by pulling the pairs through a separately heated tank containing the material. This experimental tank was approximately 12 inches long, 6 inches wide, and 6 inches deep with heaters mounted on the outside surfaces. The entrance end of the tank utilized a wooden faceplate mounted in a ball bearing so that the faceplate would rotate with the drum of the drum strander. Each opening in the faceplate had sufficient radius to eliminate any sharp corners. At the exit end of the tank,

a wooden sizing die was used with a large radius to provide a smooth and gentle closing action.

As additional and larger experimental waterproof cables were manufactured, new procedures were required to handle the larger pair sizes and to improve manufacturing techniques. The manufacturing procedures fell within two categories, those used for 25 pair cables and smaller and those used for 50 pair cables and larger.

Layless Operation. Waterproof cables 25 pair and smaller are manufactured on a sheathing line equipped with a layless stranding facility and flooding tanks as shown in Figure 5. The polypropylene insulated paired wires are pulled from the supply stand on the left through an oscillating faceplate mounted on the entrance of the core flooding tank. The oscillating faceplate is synchronized with the line speed so that an oscillation of 360° over and back in 9 feet is implanted into the cable core as it is formed within the flooding tank. Since the present layless facility drive system was not capable of maintaining this oscillation rate at the higher line speeds, a new drive system was designed incorporating a Scotch yoke mechanism. A one horsepower adjusto-speed motor with controller was used to drive the assembly at the required speed to maintain synchronization with the line speed.

The pairs are flooded with the PE-PJ compound in the tank and bunched together into core form by a bunching die mounted below the compound level of the tank. An exit die is mounted on the exit side of the tank, and is sized to allow a thin film of the PE-PJ compound to coat the cable core as it exits from the tank. In the case of layless cables, the tube type exit die which is used is about .06 inches larger than the cable core. Float controlled solenoid valves maintain the hot PE-PJ compound at the desired level.

Directly in line with the core flooding tank is the core wrap facility. The core wrap is applied longitudinally over the filled core as it exits from the flooding tank, and is squeezed down tight by means of polishing dies. Oriented polypropylene ribbon is then applied to hold the core wrap in place.

Just prior to the application of the aluminum, a second flooding tank is stationed for applying PE-PJ compound over the core wrap. The entrance and exit dies on this tank are sized to allow for a thin coating of the compound over the core wrap as it passes through the tank. The exit die is usually about .02 inches larger than the core. The entrance die is sized about .01 inches larger to provide for the clearance necessary for the core to pass through the die, yet provide some sealing against leakage of the PE-PJ compound from the opening in the tank.

A third flooding station, located to the left of the extruder as shown in Figure 5, applies PE-PJ compound over the aluminum just before the polyethylene sheath is extruded over the core. Once this sheath is in place, the waterproof cable is handled like an ordinary PIC cable through the remaining processes except for high voltage testing where the filling compound must first be removed from the wires before testing. Various solvents such as naphtha have been used to remove the compound from the test end for high voltage testing.

Stranding and Sheathing Operation. Waterproof cables 50 pair and larger are manufactured in a two operation process. Because of their primary unit construction, these cables must first be processed through the stranding area where each primary unit is filled in the same manner as the 25 pair cable cores. Depending upon the size of the cable, from four to ten primary unit flooding tanks are provided for filling the primary units of the cable before they are formed into a cable core. In the case of a 50 pair cable, four tanks are used as shown in Figure 6. The paired wires are pulled from their supply positions in the supply stands and enter the oscillating faceplates of the four primary unit tanks. Two twelve and two thirteen pair primary units make up the construction of the 50 pair cable. The pairs are oscillated 180° over and back in 125 feet as they pass through the faceplate and into the tank. As they pass through the tank, they are coated with PE-PJ compound and formed into a cable unit. The exit die of the primary unit tank is sized .02 inches larger than the unit so that a thin film of the compound will coat the outer layer of the unit.

Identifying color-coded, polypropylene binder ribbon is applied to each unit after it exits from its flooding tank. This ribbon serves two functional purposes. One is to bind the pairs of the unit together and hold the oscillation in the unit, and the second is to serve as an identification system so that a pair may be distinguished from another pair with the same conductor color combination from another unit within the cable core.

The filled units then pass through a second flooding station called the core flood tank where each primary unit receives an additional coating of PE-PJ compound before being bunched together in core form. It is within this tank that the cable lay is implanted into the cable core by the strander flyer bow or cradle. Implanting the cable lay within the flooding tank insures that no air is left encapsulated between the primary units. The core flood tank's exit die is also sized .02 inches larger than the cable core in order that a sufficient amount of the PE-PJ compound will coat the outer layer of the cable core.

After the unit-type core exits from the core flooding tank, the core is bound with polypropylene ribbon and covered with a core wrap material which is formed longitudinally and drawn down tight over the core. A second binder applicator applies polypropylene binding over the core wrap to hold it in place. The filled core is then wound onto the take-up reel or core truck within the strander take-up.

From the stranding area the filled and covered cable cores are taken to the sheathing line equipped with flooding facilities. The core trucks are loaded into the core truck pay-off stand shown to the left in Figure 7. Since the cable core is already filled and has the core wrap applied, the core flooding tank and core wrap facilities used for the layless operation are not utilized. The stranded core passes directly from the pay-off stand to the core wrap flood tank. From this point on, the stranded core is processed in the same manner as the layless core. The core wrap is flooded, aluminum applied and flooded, and the sheath applied. One additional flooding point is added in this operation, however, to insure adequate filling between the core wrap and the aluminum. PE-PJ compound is injected into the aluminum forming tube which is used when corrugated aluminum is being applied. This forces PE-PJ compound into the ridges and valleys of the corrugated aluminum making a watertight seal between the aluminum and core wrap.

An interesting characteristic of the PE-PJ compound is its ability to act as an insulator. A good example of this is shown in Figure 8. Figure 8 is a plot of the core temperature versus elapsed time from the filling operation. Analysis of the data used in preparing this plot showed that although the temperature of the filling compound in the flooding tank was at about 240°F, it cooled to approximately 150°F by the time the take-up reel was removed from the take-up. Evidently, the insulated copper conductors, at a temperature of 76°F, act as a heat sink and absorb heat from the filling compound resulting in an average core temperature of about 150°F. The temperature of the core decreased from 150°F to about 105°F between the fourth and nineteenth hour after filling. After 48 hours, the temperature of the filling compound was at 82°F while the conductors were measured at 91°F. Ambient room temperatures ranged from 75°F to 78°F during the 48-hour period.

PE-PJ Supply and Distribution System

Since each flooding station consumes large quantities of the PE-PJ compound during the manufacturing process, a central melt-down system and distribution piping system is provided to supply each station. A steam-jacketed melt-down tank with a steam grid melts the PE-PJ compound, which is supplied in 400 pound drums, at the rate of approximately 600 pounds per hour. As the compound melts, it is pumped into a holding tank or reservoir from where it is pumped through the steam-traced pipe distribution system to the flooding stations. The distribution piping is a closed loop system so that the compound can be circulated constantly and be maintained in a molten state. The amount of compound dumped into the flooding tanks is controlled by float operated solenoid valves so that the flooding tanks are maintained at a specified level.

Results

Utilizing the above techniques and facilities, approximately 65 miles of waterproof cable have been manufactured for the Bell Telephone Laboratories for field trial installations in Iowa, Alabama, Mississippi, North Carolina, Missouri, Maine, and California. In addition, approximately 400 miles of the cable have been produced to fill commercial orders. The design is presently available in 22 gauge only, in pair sizes from 11 to 25 pair. Other gauges and larger pair sizes are expected to become commercially available in the near future.

ACKNOWLEDGMENTS

The authors wish to acknowledge R. M. Allen, D. P. Dai, and A. E. Hartman of the Western Electric Omaha Works, R. W. Rake of the Western Electric Phoenix Plant, and D. H. Voss, currently on leave of absence from the Western Electric Omaha Works, for their contributions to the development of the facilities discussed in this paper. They also wish to thank T. S. Dougherty of the Engineering Research Center, Princeton, and E. O. Bauer of the Bell Telephone Laboratories for their assistance in extrusion studies.

TABLE 1
PRODUCT PARAMETER LIMITS

		<u>POLYETHYLENE</u>		<u>POLYPROPYLENE</u>
		<u>19 ga.</u>	<u>22 ga.</u>	<u>22 ga.</u>
Copper Diameter	Nominal	.0360"	.0250"	.0250"
Insulation				
DOD	Nominal	.0600"	.0430"	.0520"
(Ref. Wall Thickness)	Nominal	.0122"	.009"	.0135"
Eccentricity	Nominal	.004"	.003"	.003"
Out of Roundness	Maximum	.0010"	.0008"	.0030"
Elongation	Minimum	300%	300%	600%

TABLE 2
TOOLING REQUIREMENTS

	<u>POLYETHYLENE</u>		<u>POLYPROPYLENE</u>	
	<u>19 ga.</u>	<u>22 ga.</u>	<u>22 ga.</u>	
Ref. Material Code	-----	-----	A	----- B
Ref. Insulation Diameter	.060"	.043"		.052"
Core Tube-Design	A	A	A + Spacer	B
Insul. Die Orifice Dia.	.062"	.045"	.074"	.060"
Pull Down	.002"	.002"	.022"	.008"
"Gum" Space	6/32"	6/32"	11/32"	2/32"
Min. Insul. Die Angle	6°	6°	10°	5°

TABLE 3
SAMPLE OPERATING PROFILE - 22 GAUGE

Process Component	<u>POLYPROPYLENE COMPOUND</u>	
	A	B
Preheater		
Amperage	245	230
Voltage	12	11
Wire Temp	250°F	250°F
Extruder Heats		
Zone 1	400°F	390°F
Zone 2	400°F	410°F
Zone 3	410°F	425°F
Crosshead	410°F	430°F
Pressure		
Breaker Plt.	3000 psi	-----
Crosshead	1800 psi	4700 psi
Screw Speed	88 rpm	117 rpm
Line Speed	2500 FPM	2500 FPM

TABLE 4
SIGNIFICANT PROPERTIES

	<u>NATURAL MATERIAL</u>		
	<u>POLYPROPYLENES</u>		
	<u>POLYETHYLENE</u>	A	B
Specific Gravity grams/cc	0.918	0.900	0.900
Tensile Strength psi	2200	3600	4000
Elongation %	600	600	450
Hardness Rockwell	R 10	R 75	R 75
Dielectric Constant	2.28	2.24	2.24
Softening Point	95°C	140°C	140°C
Melt Flow Rate <u>grams</u> 10 mins.	.3	.7	2.0

MELT TEMPERATURE IN CROSSHEAD VS TIME
&
COAXIAL CAPACITANCE VARIATION VS TIME

A-POLYPROPYLENE COMPOUND A
B-POLYPROPYLENE COMPOUND B

NOTE: CAPACITANCE VARIATION IS THE SAME
FOR BOTH POLYPROPYLENE COMPOUNDS

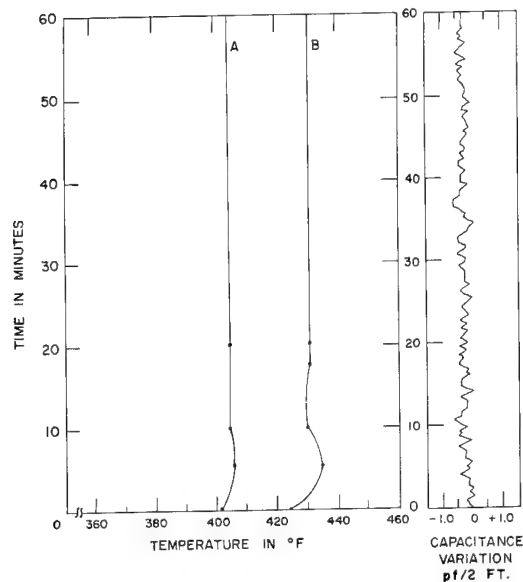


FIGURE 1

EXTRUSION OUTPUT REQUIREMENTS

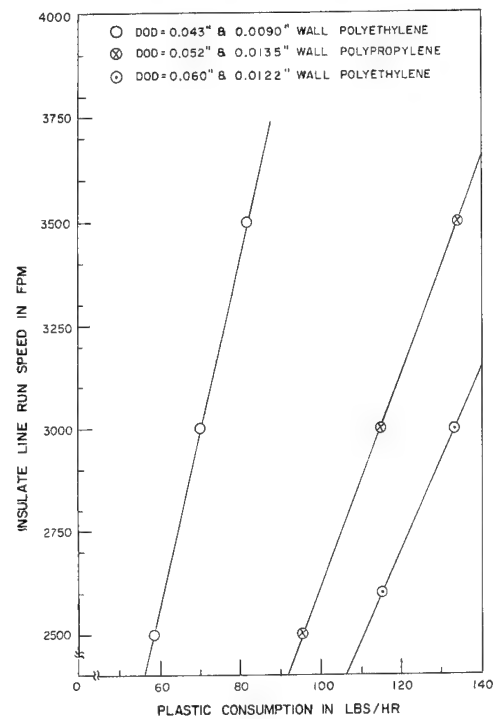


FIGURE 3

EXTRUDER OUTPUT BY MATERIAL
(2 1/2, 20/1 NRM & 0.135 METERING SCREW)

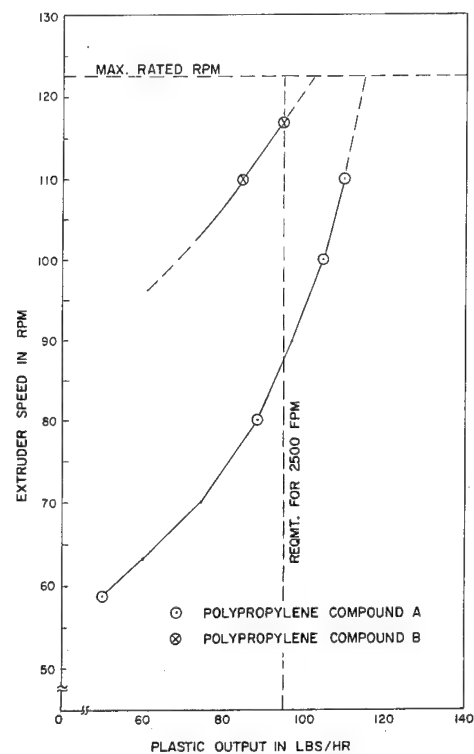


FIGURE 4

POLYPROPYLENE
INSULATING CONTROLS

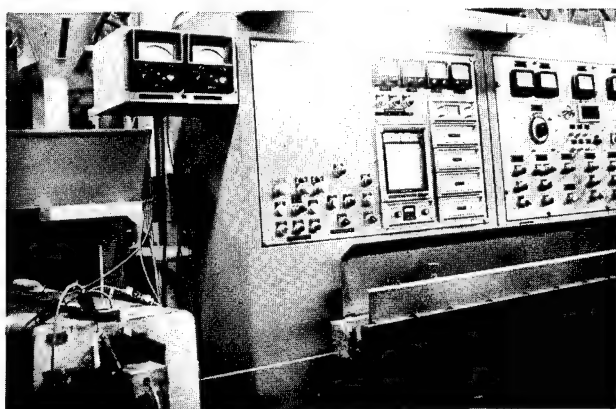


FIGURE 2

FILLED CABLE
LAYLESS-SHEATHING LINE - 6 TO 25 PAIR

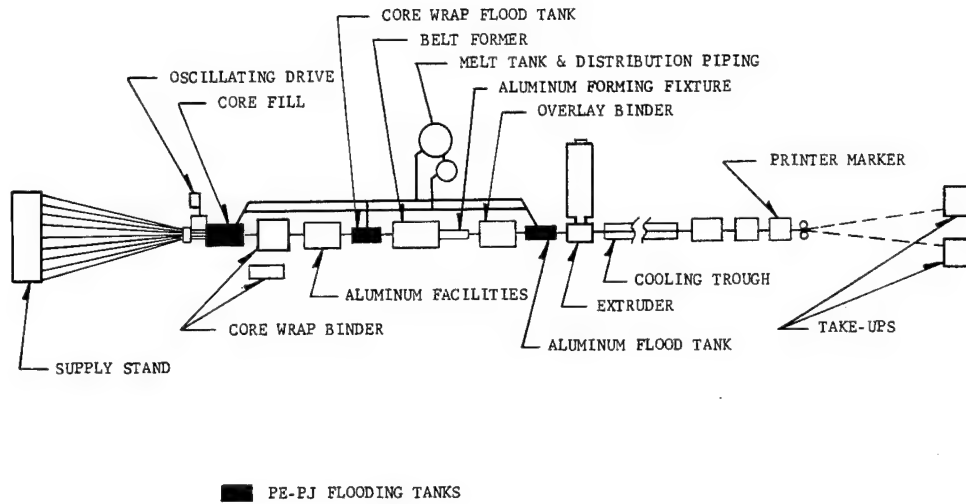


FIGURE 5

FILLED CABLE
STRANDED-FLYER STRANDER-50 PAIR

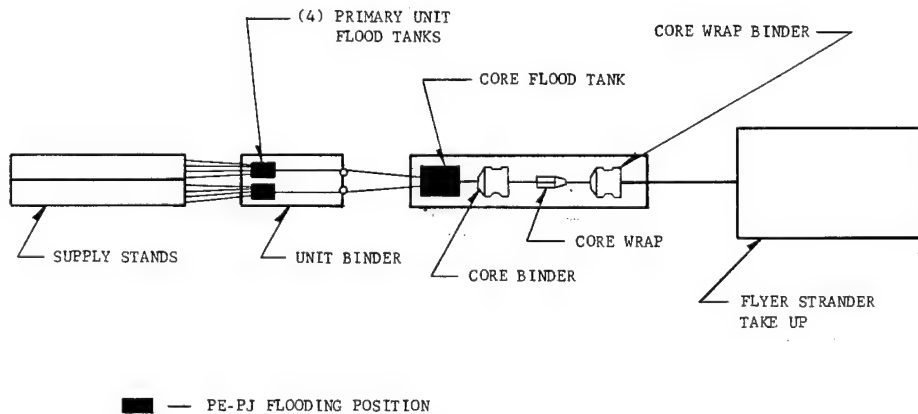
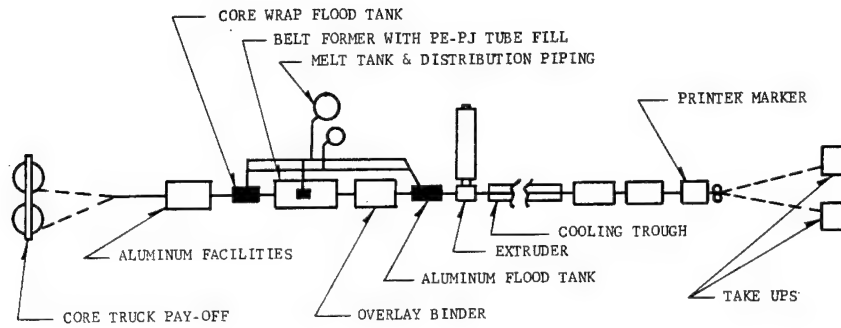


FIGURE 6

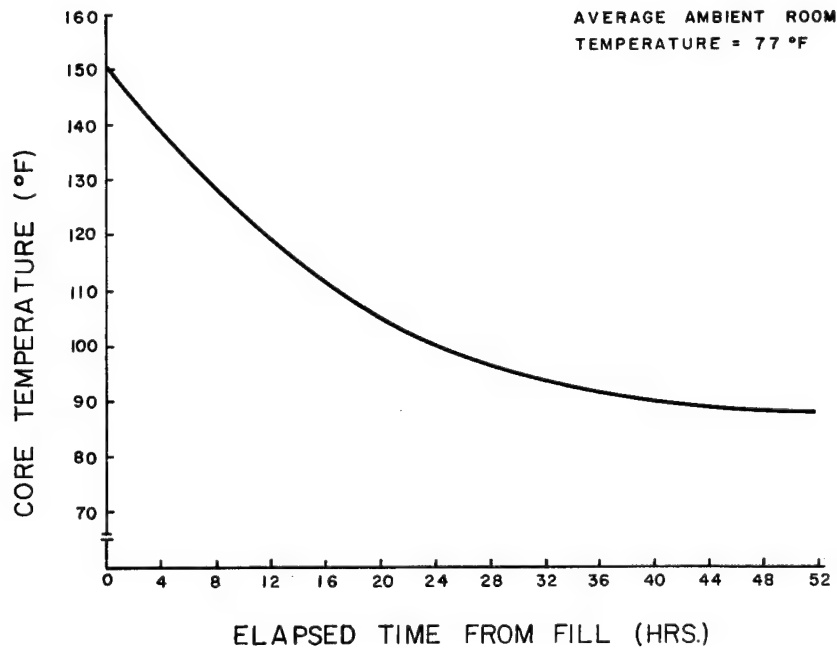
**FILLED CABLE
STRANDED-SHEATHING LINE-50 & 100 PAIR**



THOSE LINE COMPONENTS NOT FUNCTIONAL FOR THIS TYPE OF CABLE NOT SHOWN

■ — PE-PJ FLOODING TANKS

FIGURE 7



**FIGURE 8
WATERPROOF CABLE CORE TEMPERATURE**

T. A. Heim
Western Electric Co.,
Omaha Works
P. O. Box 14000 W. Omaha Sta.
Omaha, Neb. 68114

Thomas A. Heim is a Planning Engineer at the Omaha Works. He graduated from Marquette University with a Bachelor of Science degree in Mechanical Engineering in June, 1965. He joined Western Electric - Omaha in 1966 as an Engineer in the Exchange Cable stranding area where he was responsible for the stranding facilities. He worked on the initial development of the waterproof cable manufacturing facilities and is currently assigned as a Planning Engineer to strander take-ups, core testing and core repair facilities. Mr. Heim is currently pursuing a Master of Business Administration degree at Creighton University and is a registered Professional Engineer in the State of Nebraska.

Larry D. Moody joined Western Electric at the Omaha Works in 1956 and was an apprentice tool and die maker for three years; worked as a journeyman tool and die maker for six years; transferred to the Cable Engineering organization in 1965 where he worked as an Engineering Associate for five years. His assignments included sheathing tooling, cable marking, self-support cable production, bonded sheath development, cable core wrap applications and waterproof cable filling development. In 1970, Mr. Moody received a Bachelor of Science degree in General Engineering from the University of Nebraska at Omaha after attending evening classes for twelve years. His present assignment is Planning Engineering in the Exchange stranding and waterproof cable sheathing areas.

Rodney A. Conser, a Planning Engineer at the Omaha Works, after serving three years as a Radar Operations Officer in the United States Air Force, joined Western Electric in 1959 in the Industrial Engineering organization. After assignments with the majority of the wire and cable manufacturing processes at Omaha, he was transferred to the Operating organization as a first level supervisor and subsequently to his present assignment in the Product Engineering organization. Mr. Conser is responsible for the coordination and development of the tandem wire insulating process for Exchange Area Cable. He graduated from the University of Omaha with a Bachelor of Science degree in Engineering and Business Administration in 1956 and a Bachelor of Science degree in Industrial Engineering in 1965, and is currently a member of the American Institute of Industrial Engineers, the Society of Plastics Engineers, and The Wire Association.



COMPATIBILITY OF POLYOLEFINE INSULATION AND HYDROCARBON FILLERS IN TELEPHONE CABLE

by S. Verne, R. T. Puckowski and J. M. R. Hagger

Central Research and Engineering Division,
British Insulated Callender's Cables Ltd.,
London, England

SUMMARY

Effects of various filling compounds on polyethylene insulation of telephone cores have been further assessed. Providing both the polyethylene and the filler are correctly selected, the insulation retains good physical properties and resistance to cracking in "Wrap Test" after prolonged exposures to 70°C. It is shown that resistance to oxidation of polyethylene insulation is often relatively low due to extrusion conditions and the effect of the copper conductor, but can be radically improved by using certain filling compounds. Some recent improvements in stabilisation of polypropylene for insulation of fully-filled cables are also reported.

INTRODUCTION

The concept of fully filled telephone cable was so important from the outset, that if it required the development of a new insulation, such a new material would have been developed. We did think that the cable required new manufacturing processes and these were developed and reported to this Conference in 1968 and 1969.^{1,2,3}

As far as materials were concerned, we were confident that an adequate control of cable properties could be exercised through selective choice of existing commercial products, polyethylenes and petroleum jelly compounds. There were considerable economic advantages in being able to use these cheap and readily available products, providing that the consequences of their interaction were fully assessed. After six years of service the fully filled cables installed by the BPO continue to give every satisfaction. The laboratory evaluation of both cables and materials is, however, continuing and we are glad once again to present our progress report.

EFFECTS OF FILLER ON INSULATION

When a hydrocarbon impregnating compound is brought into contact with polyolefine insulation, the compound, or some of its ingredients, are absorbed by the polymer, and anxieties have been expressed by some investigators⁴ that in this process the insulation loses its:-

- (a) good mechanical properties;
- (b) resistance to cracking;
- (c) resistance to oxidation
(i. e. to ageing in air).

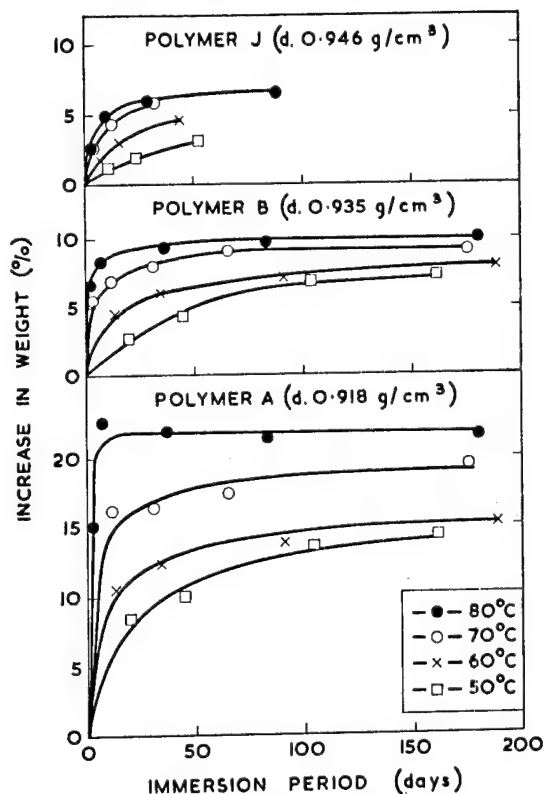


FIG. 1. ABSORPTION OF COMPOUND P
BY DIFFERENT POLYETHYLENES.

Our investigation has attempted to collect evidence on long term interaction effects which may occur in a cable up to maximum service temperature of 70°C.

SWELLING OF POLYETHYLENE

Fig. 1 shows, gravimetrically, the absorption of a petroleum jelly compound, P, by three insulation grades of polyethylene. The higher the temperature, the more rapidly is the apparent absorption equilibrium reached. The effects of temperature and of polymer density are summarised in Table I, which shows that a high density polyethylene absorbs less than a third of the amount absorbed by a typical low density polyethylene. Other aspects of molecular and morphological structure of polyethylene exert only a secondary influence on the amount of absorption, but are decisive in determining the effect of absorption on the mechanical properties of the swollen polymer.

TABLE I

Effect of Polymer Density on Equilibrium Absorption of Compound

Polymer	Density g/cm ³	Equilibrium Absorption % w/w			
		50°C	60°C	70°C	80°C
A	0.918	14.5	15.2	19.4	21.6
B	0.935	7.5	8.0	9.2	10.0
J	0.946	3.1	4.7		6.5

The second important factor in determining the amount of swelling, of any particular polyolefine at a given temperature, is the composition of the filling compound. Table II shows that the gravimetric absorption of a typical polybutene/wax/polyethylene filling compound is substantially lower than that of a typical petroleum jelly compound.

TABLE II

Influence of Compound Type on Absorption by Polymer D

Compound	Equilibrium Absorption % w/w	
	70°C	80°C
S	4.0	4.2
T	7.8	9.3

EFFECT OF ABSORPTION ON MECHANICAL PROPERTIES

For every petroleum jelly compound

(or any other cable filling compound) some of the constituents dissolve in polyethylene more readily than others. In Table III the effect of high petroleum jelly contents on mechanical properties of a low density polyethylene are compared for two sets of samples. In one case, the polyethylene has been allowed to absorb selectively from a large volume of the compound, until an equilibrium value of 16.7% by weight has been reached at 70°C. In the other case, an equivalent quantity of the compound, in its original composition, has been incorporated by milling into the same polyethylene. The effect on the mechanical properties is not the same, but in neither case is there evidence of any significant reduction in elongation at break or in the yield strength. This is further illustrated in Table IV.

TABLE III

Effect of Petroleum Jelly Compound on Mechanical Properties of Polyethylene A

Compound Details	Yield Stress lb/in ²	Elongation at Break %
Control	1380	750
16.7% w/w of Compound Q (incorporated by compounding)	1450	660
16.7% w/w of Compound Q (absorbed by immersion)	1930	500
16.7% w/w of Compound R (incorporated by compounding)	1370	690
16.5% w/w of Compound R (absorbed by immersion)	1980	490

Results obtained on laboratory samples (Table IV) were corroborated by extensive tests on telephone cores. Some of these are shown in Tables V and VI. The figures reported show that no significant deterioration of insulation would occur in at least 4500 hours at 70°C, which would correspond to 6 years of service during which the cable is exposed to 70°C for 8 hours a day for three months of each year.

RESISTANCE TO CRACKING

A typical low density polyethylene insulated core can be wrapped round its own diameter and exposed at 70°C to either air or a petroleum jelly compound without cracking. Anxiety has been expressed, however, that a core which is stressed by wrapping round its own

TABLE IV

Effect of Immersion in Filling Compounds at 70°C on Tensile Properties of Low Density Polyethylenes

Period of Immersion	Property	Polymer A		Polymer C	
		Compound P	Compound Q	Compound P	Compound Q
None	Yield Stress (lb/in ²)	1460	1460	1460	1460
	Elongation (%)	730	730	660	660
7 days	Yield Stress (lb/in ²)	1680	1880	-	-
	Elongation (%)	520	540	-	-
12 days	Yield Stress (lb/in ²)	-	-	1690	1820
	Elongation (%)	-	-	430	550
32 days	Yield Stress (lb/in ²)	1810	2220	1740	1850
	Elongation (%)	510	490	380	480
92 days	Yield Stress (lb/in ²)	1980	2360	1920	2100
	Elongation (%)	550	570	440	510
192 days	Yield Stress (lb/in ²)	1960	2190	-	-
	Elongation (%)	470	540	-	-

TABLE V

Effect of Time and Temperature of Immersion on Tensile Properties of Polymer C in the form of 8 mil Insulation Aged on 24 AWG Copper Conductor

Period of Immersion	Property	70°C		80°C	
		Compound		Compound	
		P	Q	P	Q
None	YS, lb/in ²	1460	1460	1460	1460
	BS, lb/in ²	3240	3240	3240	3240
	EB, %	500	500	500	500
4 days	YS, lb/in ²	1580	1750	1590	1840
	BS, lb/in ²	2430	2750	2300	2690
	EB, %	430	450	420	440
32 days	YS, lb/in ²	1730	1980	1720	2080
	BS, lb/in ²	2560	2780	2330	2720
	EB, %	420	450	400	430
187 days	YS, lb/in ²	1820	2020	1650	2040
	BS, lb/in ²	2270	2720	2070	2620
	EB, %	380	440	390	420

YS = yield stress

BS = break stress

EB = elongation at break

All tensile values are calculated on initial size of core.

diameter after a prolonged exposure to a petroleum jelly compound at 70°C may crack when subsequently re-exposed to the same temperature. The key to controlling this phenomenon is the selection of polyethylene polymer and of the petroleum jelly compound, although adequate control of the manufacturing process is also important. Table VII shows that even with a low density polyethylene, cracking at up to 70°C can be avoided by selecting a "more compatible" petroleum jelly compound. The severity of the test increases with increasing core size and insulation thickness, as shown in Table VIII. For this reason, the data in Table IX are presented for 30 mil insulation on 19 AWG copper wire. Table IX shows that for service at up to 70°C, a few specially selected filling compounds could be used with a range of polyethylenes, or alternatively, selected intermediate density and high density polyethylenes could be used with a wider range of filling compounds. For service at 80°C, both the insulation and the filling compound must be carefully selected, but when this is done, the results are very satisfactory. Core insulation in cellular form has increased resistance to cracking and will pass the "wrap test" at a higher temperature, typically 50-100°C, than the corresponding solid insulation.

RESISTANCE TO AGEING IN AIR

Polyethylene Insulation

At terminations, individual cores of a fully-filled cable are exposed to air. It is therefore important that the core insulation

TABLE VI

Effect of Time and Temperature of Immersion on the Tensile Properties of Polymer A in the form of 8 mil Insulation Aged on 24 AWG Copper Conductor

Period of Immersion	Property	70°C			80°C		
		Compound			Compound		
		P	Q	R	P	Q	R
None	YS, lb/in ²	1540	1540	1540	1540	1540	1540
	BS, lb/in ²	3240	3240	3240	3240	3240	3240
	EB, %	500	500	500	500	500	500
14 days	YS, lb/in ²	2030	2130	2060	1920	2270	2220
	BS, lb/in ²	2800	2990	2780	2500	2850	2720
	EB, %	430	440	400	400	400	400
42 days	YS, lb/in ²	2130	2270	2160	1920	2300	2460
	BS, lb/in ²	2800	3070	2670	2430	2750	2660
	EB, %	420	440	410	410	410	390
84 days	YS, lb/in ²			2350			2560
	BS, lb/in ²			2820			2850
	EB, %			410			400

YS = Yield Stress

BS = Break Stress

EB = Elongation at Break

All tensile values are calculated on initial size of core

should have sufficient resistance to oxidative degradation at the maximum service temperature, which can be as high as 60-70°C in termination boxes exposed to direct sun, in certain geographic locations.

The reasons why a risk of oxidation may occur in the case of dry polyethylene insulated cables are explained by the results in Table X. Polymer A is a typical low density polyethylene used for insulation of telephone cores, both in USA and in Great Britain. The induction period of 20 hours at 180°C, measured on a sheet moulded from granules, confirms that the material, as delivered by the manufacturer, has a good resistance to oxidation (corresponding to a life of at least a year at 105°C, or 20 years at 70°C). When this material is extruded into a thick cable covering there is little loss of stability, but a feature of telephone core manufacture is that the insulation of a high area-to-volume ratio emerges from the extruder at a very high temperature, which results in a large proportion of the antioxidant being lost by oxidation and volatilisation. This was illustrated by extruding a 60 mil diameter filament under conditions similar to those of core extrusion: the resistance to oxidation dropped by 40%. In the case of a less well stabilised polymer, or a greater area-to-volume ratio, the drop can be much larger.

Table X shows that an even greater factor in reducing the resistance to oxidation is contact with copper during extrusion: an 8 mil thick insulation retains only 5-12% of the resistance to oxidation exhibited by the original polymer. Finally the process of ageing of insulation is itself accelerated by the continued contact with the copper conductor. The cumulative result of these three effects is that a typical insulation in the form of an 8 mil covering on a 24 AWG copper conductor will resist oxidative degradation for only a few per cent of the time estimated from tests on the unprocessed polymer. However, even in this form, the conservatively estimated minimum life of the insulation would be at least some 5000 hours at 70°C, or over 12000 hours at an average temperature of 60°C (e.g. 15 years when the average temperature of 60°C is maintained for 8 hours a day, 100 days a year). All the three factors which affect ageing of insulation on copper conductors (loss of antioxidant in extrusion, effects of copper during and after extrusion) depend on area-to-thickness ratio, as is illustrated by the data in Table XI.

Aluminium, unlike copper, has no adverse effect on ageing of polyethylene, as shown in Table XII.

TABLE VII

Effect of Filling Compound on Performance in "Wrap Test"

Filler	8 mil radial insulation on 24 AWG copper conductor	"Wrap Test" after 7 day immersion period and subsequent exposure for 60 days at		
		70°C	75°C	80°C
Compound P	Polymer A	Pass	Fail	Fail
	Polymer C	Fail	Fail	Fail
Compound R	Polymer A	Pass	Fail	Fail
	Polymer C	Pass	Fail	Fail
Compound Q	Polymer A	Pass	Pass	Fail
	Polymer C	Pass	Fail	Fail

Effect of Filling Compounds on Polyethylene

McCann, Sabia and Wargotz⁴ observed that antioxidants which can diffuse out of the insulation cease to be available when the filler is removed in the termination procedure and that, because of this, oxidation stability might be a problem. Data in Table XIII show that contact with filler can either improve or reduce the resistance to oxidation, depending on the composition of the filler. These data refer to

TABLE VIII

Effect of Core Dimensions on Performance in "Wrap Test"

Insulation (Polymer A on copper conductor)	"Wrap Test" after 7 days immersion in Compound Q and subsequent exposure for 60 days at		
	70°C	75°C	80°C
8 mil on 24 AWG	Pass	Pass	Fail
30 mil on 19 AWG	Fail	Fail	Fail

a very well stabilised intermediate density polyethylene and it is observed that even with an insulation thickness of 20 mil, there is no difference between the effects of immersion for periods of 14 and 42 days (at 80°C). Of the two petroleum jelly compounds (both in current use in Great Britain) one has had little effect on resistance to ageing, while the other has improved it. The two fillers of North American origin (one a petrolatum blend, the other a polybutene compound) both had an adverse effect, although even here the effect due to the compound is small as compared with that due to the copper conductor. Data for a thinner, and hence inherently more vulnerable insulation, are shown in Table XIV. The three petroleum jelly compounds, selected from those currently used in Great Britain, confer a major improvement on the insulation. It is interesting to note that cellular insulation benefits even more than the solid of the same thickness, but in either case the result is that the resistance to oxidative ageing of "bare" cores in the termination boxes is many times greater than that required for the maximum service temperature of 70°C.

TABLE IX

Effect of Polymer Type on Performance in "Wrap Test"

30 mil radial insulation on 19 AWG copper conductor	Density g/cm ³	Filler	"Wrap Test" after 7 day immersion period and subsequent exposure for 60 days at		
			70°C	80°C	85°C
Polymer A	0.918	Compound Q	Fail	Fail	-
		Compound R	Pass	Fail	Fail
Polymer F	0.932	Compound Q	Pass	Pass	Pass
		Compound R	Pass	Pass	Fail
Polymer G	0.943	Compound Q	Pass	Pass	Pass
		Compound R	Pass	Pass	Pass

TABLE X

Effect of Extrusion on to Copper Conductor on the Resistance to Oxidation of Various Polymers

Polymer details	Induction Period (hours)		
	180°C	140°C	105°C
Polymer A			
20 mil sheet	20.7	600	1000C
extruded filament	12.9		
8 mil on 24 AWG Cu	0.3	10	250
8 mil off 24 AWG Cu	2.4	100	
Polymer C			
20 mil sheet	6.0	-	-
8 mil on 24 AWG Cu	0.2	5	140
8 mil off 24 AWG Cu	0.3	10	
Polymer B			
20 mil sheet	5.8	-	-
8 mil cellular on 24 AWG Cu	0.2	5	350
8 mil cellular off 24 AWG Cu	0.6	18	

TABLE XI

Effect of Dimensions on the Resistance to Oxidation at 105°C of Polymer A on Copper Conductor

Sample Details	Induction Period (hours) at 105°C
8 mil insulation on 24 AWG copper conductor	250
30 mil insulation on 19 AWG copper conductor	700

TABLE XII

Effect of Extrusion on to Aluminium Conductor on the Resistance to Oxidation of Polymer B

Polymer Details	Induction Period at 105°C (hours)
20 mil sheet moulded from granules	> 3000
8 mil cellular insulation on 24 AWG copper	350
8 mil cellular insulation on 24 AWG aluminium	1400

POLYPROPYLENE INSULATION

The petroleum jelly compounds which increase oxidation resistance of polyethylene insulation do not produce a corresponding improvement with polypropylene. This difference in response is due to different kinetics of auto-oxidation in the two types of polymers. A polyethylene will not suffer any significant oxidative degradation for as long as it contains a few parts per million of an antioxidant. As antioxidant is used up or lost by migration, the resistance to ageing of polyethylene decreases only roughly in proportion to the antioxidant content. With polypropylene, the oxidation resistance falls much more rapidly than in proportion to anti-oxidant content. Moreover, for adequate stabilisation, polypropylene requires the presence of

TABLE XIII

Effect of Different Filling Compounds on Resistance to Oxidation of 20 mil Wall of Polymer D on 19 AWG Copper Conductor

Compound	Immersion Period at 80°C (days)	Induction Period at 105°C (hours)
None		1920
P	14	2800
Q	14	1650
S	14	670
S	42	720
T	14	580
T	42	480

TABLE XIV

Improvement in Resistance to Oxidation of 8 mil thick Polyethylene Insulation on 24 AWG Copper Conductor, after Immersion in Selected Filling Compounds

Compound	Immersion Period at 80°C (days)	Induction Period at 105°C (hours)	
		Polymer	
		A	B
None		250	350
P	14	1800	2400
Q	14	1100	1800
R	14	1450	2300
S	42	160	-

Polymer A = Solid
Polymer B = Cellular

a balanced synergistic mixture of several additives, each of which tends to be extracted by the filling compound at a different rate. For this reason, disappointing results were originally obtained with many commercial grades of polypropylene.

A measure of success was attained by using some of the compounds specially developed for high temperature power cables. Some of the results are shown in Table XV. Polypropylene stabiliser system M was developed for continuous service at 85°C on aluminium conductors and it survived 35 000 hours at 105°C before any significant degradation could be observed. When this material was applied to a copper conductor as 10 mil cellular insulation and then immersed in Compound R, its resistance to oxidation at 105°C was reduced to 300 hours, or less than 1% of the original. In the case of polyethylene,

a material with original stability only one tenth of that of Polypropylene M gave cellular insulation which, after contact with the same compound R, was 8 times more stable. (cf. Table XIV).

Polypropylene stabiliser system N had been developed for insulating power cables with copper conductors rated continuously at 85°C (minimum of 20 years). Table XV shows that N confers 30 times greater stability than M after comparable treatments with the filling compound Q. Polypropylene stabilised with N also retains very high resistance to oxidation, even when extruded as 10 mil insulation on copper conductor. For cases when colour coding of cores is not necessary, Stabiliser O would be a further improvement. Several new, unconventional stabilising systems are currently being evaluated and the results are technically very encouraging. However, the higher material cost and lower extruder outputs will continue to make polypropylene insulation difficult to justify.

TABLE XV

Resistance to Oxidation of Polypropylene Insulation Compounds

Stabiliser	Sample	Time to embrittlement (hours)	
		143°C	105°C
M	20 mil sheet	1200	35000
	ditto, after 7 days in Q at 80°C	30	-
	10 mil cellular insulation on 22 AWG Cu	16	450
	ditto after 14 days in R at 80°C	-	300
N	20 mil sheet	1550	-
	ditto, after 7 days in Q at 80°C	900	-
	ditto, after 127 days in Q at 80°C	280	-
	10 mil insulation on 22 AWG Cu	350	>1700
O	20 mil sheet	1400	-
	ditto after 127 days in Q at 80°C	820	-
O	20 mil sheet, 0.1% fine Cu dust incorporated	850	-
	ditto, after 127 days in Q at 80°C	260	-

ACKNOWLEDGMENTS

The authors wish to express their thanks to Dr. A. L. Williams, Director of Research and Engineering, British Insulated Callender's Cables Ltd., for permission to publish this work.

Due acknowledgment is gladly made to Mr. E. H. Reynolds for his guidance and encouragement and to many units of the BICC Group in Great Britain and Overseas for their assistance.

REFERENCES

1. Seventeenth International Wire and Cable Symposium, "The Development of Fully Filled Cables for the Telephone Distribution Network", N. S. Dean.
2. Eighteenth International Wire and Cable Symposium, "A Report on the further progress made in the application of cellular plastics to telephone cable design and manufacture", N. S. Dean, B. J. Wardley and J. R. Walters.
3. Ibid, "A new process for manufacture of telephone cores with cellular insulation", S. Verne, B. G. Howell and G. A. L. Ward.
4. Ibid, "Characterisation of filler and insulation in waterproof cable", J. P. McCann, R. Sabia and B. Wargotz.

APPENDIX I

MATERIALS EXAMINED

TABLE A

Insulation

Code	Polymer		Melt flow index* (g/10 min)	Antioxidant
	Type	Nominal density (g/cm ³)		
A	PE	0.918	0.15	X-1
B	PE	0.935	1.0	Y-1
C	PE	0.916	0.25	X-2
D	PE	0.934	1.4	Z-1
E	PE	0.927	0.3	X-3
F	PE	0.932	0.3	X-4
G	PE	0.952	0.3	Y-2
H	PE	0.950	0.4	Y-3
J	PE	0.946	0.3	Y-4
M	PP	0.905	0.1**	System I
N	PP	0.909	0.1**	System II
O	PP	0.919	0.1**	System III

Notes: * BS 2782, Method 105C
 ** At 230°C/2.16 kg load

TABLE B

Filling Compounds

Compound	Drop point (°C)		Composition
	IP-31 method	ASTM-D. 127 method (IP-133)	
P	68	76	P.J. of low wax content
Q	75	80	P.J. of high wax content
R	83	-	P.J. of high wax content
S	55	70	Polybutene with some polyethylene and wax
T	76	90	Petrolatum of high wax content
U	52	69	Petrolatum with low molecular weight polyethylene

APPENDIX II

TEST PROCEDURES

A. Absorption of Filling Compound

Compression moulded sheets 0.055 inch thick were kept immersed in the filling compounds at 23°C and at 40°, 50°, 60°, 70° and 80°C using a separate closed container for each polymer composition. The weight ratio of polymer to compound was not less than 1 to 3. Samples were removed at intervals and after conditioning in a desiccator at 23°C for 16 hours and then wiping free of the compound, the gain in weight and changes in dimensions were recorded.

B. Tensile Tests

Dumb-bells (Type "C", BS 903), 0.055 inch thick and lengths of insulated core were kept immersed in the filling compounds as in (A). At intervals samples were removed from the compound, conditioned at 23°C for 24 hours and wiped with a soft cloth. The insulation was stripped from the conductor and its elongation at break and load at break were measured at a rate of extension of 500%/minute. Dumb-bells were tested at a rate of extension of 2000%/minute and yield stress, break stress and elongation at break were measured.

C. Resistance to Oxidation

1. Oxygen absorption test at 140° and 180°C

Specimens 0.020 inch thick were exposed to air at atmospheric pressure and the oxygen uptake was followed manometrically at constant volume. The oxidation induction period was recorded as the time required for the specimen to absorb 2 ml O₂ (NTP)/g.

2. Ageing tests in air at 105°C and 143°C

Sheet samples 0.020 inch thick of each polymer composition were aged in separate glass cells to which pre-heated air was admitted continuously at a rate giving 2-3 changes of atmosphere per hour. Lengths of insulated core were aged in the form of loose helical coils on 2 inch diameter glass tube mandrels. The induction period was recorded as the time to the first signs of physical deterioration (embrittlement in polypropylene, increased loss tangent at 1 MHz in polyethylene).

THE IMPACT OF MELTING THEORY ON SCREW DESIGNS

R. A. Barr, L. Kovacs

Waldron-Hartig Division - Midland-Ross Corporation

Somerset, New Jersey

Introduction

For the past three years, the engineers at Waldron-Hartig have been engaged in an intensive program to improve their accuracy in extruder performance prediction, as well as improve the over-all performance of the extruder.

This work has resulted in a highly advanced computerized prediction capability and, more importantly, in superior configurations for a plasticating extruder screw.

The biggest unknown in extruder performance was in the area of melting. Especially, the mathematical relationships necessary to predict melting rates were unknown. However, as a result of the studies by Tadmor, I. Duvdevani and I. Klein at Western Electric Research in Princeton, New Jersey, a new theory of melting in extruders was formulated and proven.¹ One result of this was a computer program to predict melting rate and uniformity.

The work of these researchers is the most significant in extrusion in recent years. The work done in 1967 and 1968 to develop our own computer program was based on the Western Electric work with improvements by C. I. Chung.² It is our work with this theory, coupled to the daily task of screw design (as well as technical service on screw performance) that has led us to significant new screw configurations.

In order to fully understand these concepts, the melting mechanism as it occurs in a conventional screw will be described.

Conventional Screw Melting Mechanism

The first view is a cross-section taken through the screw and barrel near the throat. The pellets (or powder) are loosely packed and fill the channel. As they move down the screw, they are packed tighter together by frictional drag on the barrel such that a tightly packed "solid bed" of unmelted material is formed. Melting has begun at the surface of the "solid bed" in contact with the barrel forming a thin melt film. It is in this melt film that all of the melting takes place. As soon as the film thickness becomes greater than the screw flight to barrel clearance, the pumping action of the screw begins and the melting mechanism is initiated. This is because at that time the flight begins to scrape melt from the barrel, forcing it down into the channel behind the solid bed. This action is continued throughout the screw

even after melting is complete and it accounts for all the flow in the channel, both cross-channel and down-channel flows.

As melting continues, by virtue of the shear over the solid bed, the bed is forced into the barrel by the effect of the decreasing channel depth in the transition section. This, plus the pressure of the melt on the back of the bed, causes it to become narrower and thinner.

At high rates the melting is not complete when the bed reached the metering section of the screw. At this point the effect of decreasing channel depth is no longer seen and when the bed reached about 10% of its initial width it breaks up into pieces which then are afloat in the channel.

At this instant the high efficiency of melting in the thin film over the bed is lost and the pieces of the bed are afloat in the screw channel where they soon are worked into the center of the channel furthest from the barrel heat and well lubricated by the surrounding melt. To complete the melting of these pieces is very difficult, and is the goal of all of the mixing screws now on the market.

Previous Solutions

Traditionally, residence time has been used to complete the melting of these "iceberg" like pieces of solids. Thus, we have seen the long metering type screws. Also, the mixing of the solids together with some added shear is done with several mixing type of screws. These are all generally long metering types with mixing rings or pins in the metering section to break up the flow pattern and shear the solids to complete the melting.

Another approach, now quite popular, uses a "filtering" method. In this, a two-stage type of screw is seen with a "mixing" section between the stages. The first "stage" is a conventional feed, transition and short metering design. Then the melt enters the "mixing" section which employs a variety of dam or barrier arrangements with small clearances to the barrel. Thus, only very small particles or melted material can enter the second stage. Unfortunately, all of the resin must pass through this section so that material that is already melted prior to the mixing section must also undergo the added shear over the dam or barrier. This results in higher than desired melt temperature at the exit of the mixing section. All of these designs, therefore, depend

upon cooling in the second stage for may applications to achieve low melt temperatures.

Again, unfortunately, barrel cooling introduces temperature variations as we reported in our Antec paper of 1966.³ Although a mixing arrangement in this cooling section can help to minimize fluctuations, the added horsepower and residence time can be a problem.

The real problem with all of the approaches is in residence time at high shear levels. In the long meter, mixing ring, or two-stage types, melting is completed at the middle of the screw. Thus, for a good half of the screw we are adding shear energy after completion of melting. This is a real problem with more resins every day. It reduces the molecular weight of all plastics, but in the case of PVC, Acetals and Polyester it creates problems of excessive melt temperature and even degradation.

Something Better

The question asked is "Why must the melting process be incomplete?"

Our answer was that it need not be and the solution is in a design that can control the melting process to completion. Such a design has been developed at Waldron-Hartig and is called the "Barrscrew".*

Again, follow the design, using the attached cross sectional drawing of the "Barrscrew". (Figure 2)

The feed section of the "Barrscrew" is conventional, allowing the normal formation of the solid bed. However, once the bed is formed, it is, in effect, pushed forward in the channel by making the flight wider in about one turn. The bed is thus trapped in a reduced width channel which continues at a constant width, but decreasing depth to the end of melting. The melting mechanism is exactly the same as in a conventional screw, but as the melt is scraped from the barrel by the screw flight it is pushed into its own channel which we have cut out of the widened flight.

This "melt" channel also has a constant width but an increasing depth until at the end of melting it is deep enough to hold all of the resin. At this point several things can be done. (a) Leave the screw such that the end of melting is the end of the screw. (b) Enter a short metering section for further cooling (usually not necessary or desirable). (c) Enter a second stage for venting, then pumping as in a conventional two-stage screw, or (d) Enter a dispersion section for compounding.

Going back to the melting section, please note that the dam separating the solid and melt

*Patent applied for

has a clearance greater than the melt film thickness. We do not want any shearing over this dam. It is not a filter - it is there to hold the solid bed in place to prevent it from shifting and breaking up.

Advantages

As you can see from the design, there are several obvious advantages.

Low Melt Temperature

Since the resin once melted receives a minimum of further working from shear, lower melt temperature is achieved. This is a big feature of the deep melt channel. Incidentally, this also means that the final melt temperature is the highest the melt sees in the extruder. This is not true of many other types. The two-stage types, for instance, have higher melt temperatures at the exit of the mixing section than at the die.

This is an important point for those who are concerned about degradation within the extruder, as many are.

High Melting Capacity

Since the solid bed width is constant - not decreasing - the total barrel area per turn in the melting section is much greater than others and, since in most cases we do not need a metering section, much more (almost twice) of the length of barrel can be devoted to melting.

Melt Uniformity

Melt uniformity is assured since both the pressure and temperature are guaranteed to be uniform since every grain of resin is melted with the same energy.

Performance Prediction

Performance of larger machines is no problem to predict since there is now full control over the variables affecting performance, "Scale up" to larger machines is much more reliable.

Incidentally, the computer program (as discussed in C. I. Chung's paper) is rewritten for the "Barrscrew" configuration. This is very important since it is now possible to predict the correct design to give the desired performance much more accurately than with a conventional screw. This is true since with the "Barrscrew" many of the troublesome variable seen in a conventional screw are held constant.

Now the Ultimate?

Over the last year or so, development of the "Barrscrew" has continued with various configurations in our laboratory on a wide variety of resins and processes.

In the course of this, it was reasoned - "Why not conduct the melt to the die as soon as possible after it moves off the solid bed, without shearing the melt further?"

Then an idea was born - for a new screw design that did just that. We call it XLK* (LK for Lloyd Kovacs, the inventor). In its simplest version (figure 3) passages are created at the rear of the screw channel through which the accumulating melt pool drains into the core or center bore of the screw. Pressure generated by the solids transport mechanism which is forwarding the solid bed down the screw channel (see Chung's paper - 28th SPE Antec)⁴ forces the melted polymer through these passages into the screw bore (which is open only to the die end) and thus out to the die.

We call this pressure generation by the solid bed transport mechanism - or "Solid State Pumping."

Immediately, there are two great advantages:

1. Low, Low Melt Temperature

Since as soon as the polymer is melted, it leaves the screw channel and the shear forces there, very low melt temperatures are achieved. This is really minimum shear energy input. Just enough to melt - no more.

2. High Output

Now we need not sacrifice channel width to melt pumping either adjacent to the solid bed or in the form of a conventional channel width. Thus the solid bed can occupy nearly all (90%) of the channel width so -- absolute maximum surface area for melting is available. Solid bed area is 90% of channel width and all the way to the end of the screw.

Naturally, solid bed breakup can occur just as it does on a conventional screw (as in figure 1) so to prevent that - we combine the XLK and "Barrscrew" designs by providing a barrier flight or dam (see figure 4) to hold the bed in place and ensure complete melting by the solid bed mechanism.

In addition to this, we included an internal stationary screw supported from the die end of the barrel. This screw has a reverse helix and profile such that it helps to keep resin flowing with out hang-up to the die. Also, in very high head pressure cases it assists the "Solids Transport" in pumping. The complete XLK/Barrscrew is shown on figure 5.

Performance

As would be expected, the best performance of all of these designs has been with the com-

*Patent applied for

bination XLK/Barrscrew. Although the work has just begun, the data to date is significant. The table of figure 6 shows this. The output rates are obviously quite high, but this alone does not tell the whole story. Melt quality, for instance, is excellent, as seen by the melt temperature variation recorded during all of these tests which never exceeded $\pm 2^\circ\text{F}$. The pressure variations are likewise extremely low.

Application of these screw designs to actual production of coated wire is yet to be done. However, we can easily expect to see the same significant improvement in performance as we have in the processes run to date.

References

1. Tadmor, Z., I. Duvdevani and I. Klein, "Melting in Plasticating Extruders, Theory and Experiments", Poly. Eng. & Sci., July (1967).
2. Chung, C. I., "A New Theory for Single Screw Extrusion, Part I and II", Modern Plastics, September and December (1968).
3. Barr, R. A. and C. I. Chung, "Estimating P.E. Extruder Cooling Capacity", Modern Plastics, October (1966).
4. Chung C. I., "The Status of Plasticating Single Screw Extrusion Theory", Tech. Papers, 28th ANTEC, SPE, May, 1970.

ROBERT A. BARR

Presently Mr. Barr is Sales Manager for Extrusion Machinery for the Waldron-Hartig Division - Midland-Ross Corporation. Prior to that position, he was Manager of Applications Engineering and had been Manager of the Research and Development laboratories for the Division. He is a graduate of R.P.I. and resides in Warren, New Jersey with his wife and two children.



LLOYD KOVACS

Presently Mr. Kovacs is Manager, Product Development for the Waldron-Hartig Division - Midland-Ross Corporation. Responsible for development of plastics machinery and techniques. Involved in design and development of plastics machinery for past 10 years. Married; wife and three children residing in Somerset, New Jersey. Education includes B.S.E.E. from Newark College of Engineering and a Master in Engineering Management from the same institution.

Presently Mr. Barr is Sales Manager for Extrusion Machinery for the Waldron-Hartig Division - Midland-Ross Corporation. Prior to that position, he was Manager of Applications Engineering and had been Manager of the Research and Development laboratories for the Division. He is a graduate of R.P.I. and resides in Warren, New Jersey with his wife and two children.

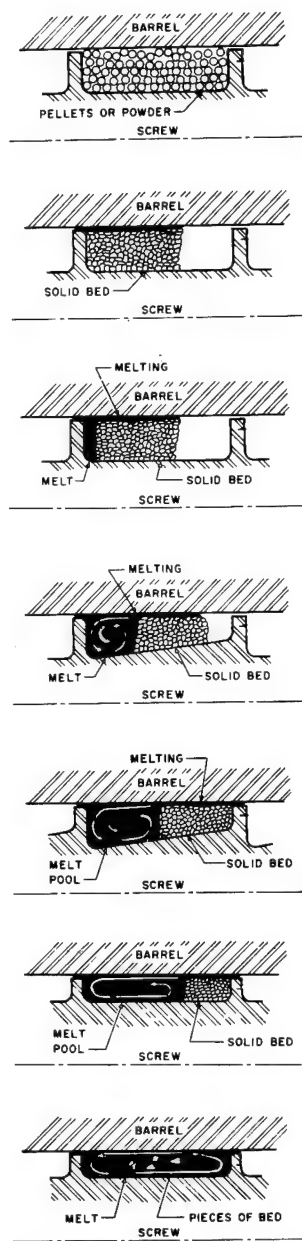
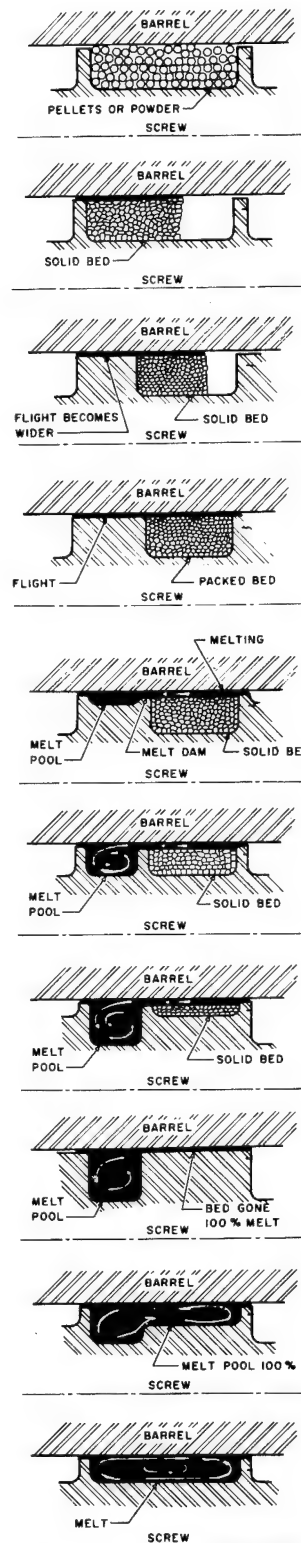


FIGURE 1
CONVENTIONAL SCREW

FEED

TRANS

METER

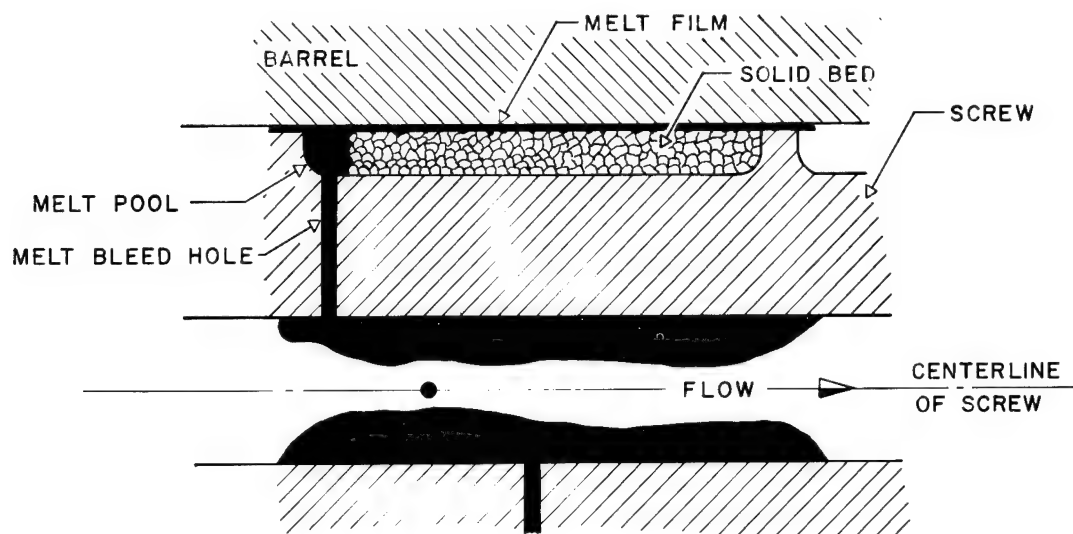


FEED

MELT

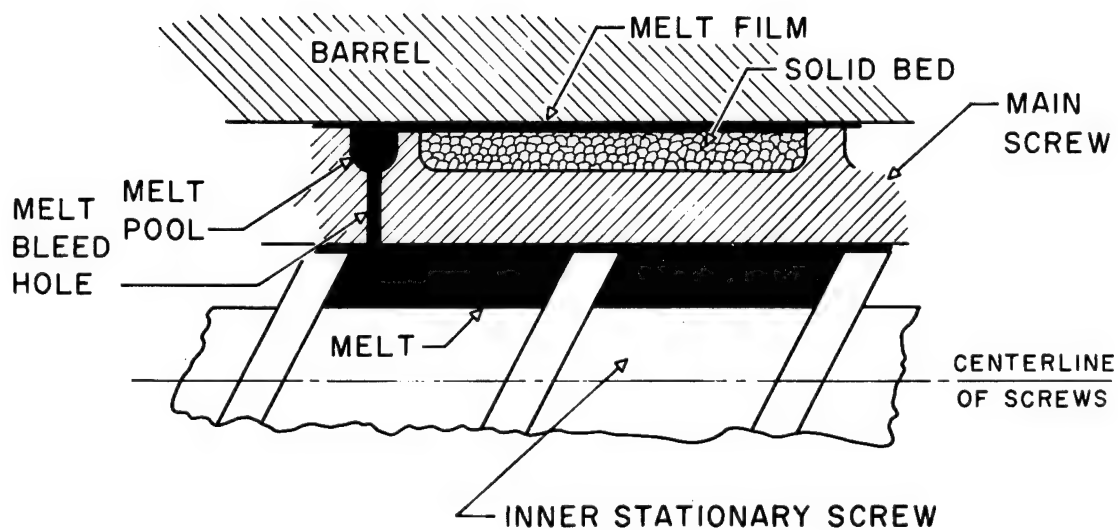
METER

FIGURE 2
"BARR" SCREW



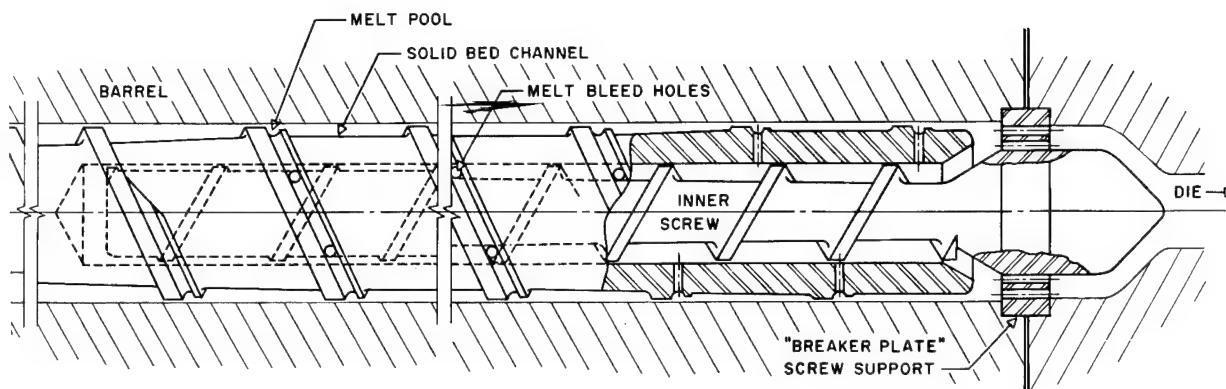
XLK SCREW CROSS SECTION

FIGURE 3



XLK/BARR SCREW CROSS SECTION

FIGURE #4



XLK BARR SCREW

FIG. 5

RESIN	EXTRUDER	LBS/HR	RPM	HP	HEAD PSI	MELT TEMP	REMARKS
.15 M.I./HDPE	2½"-24:1	375	165	55	4000	460	Celanese A60-15
3.5 H.L.W.I./HDPE	"	255	66	43	4900	446	Phillips 55035
6.5 H.L.M.I./HDPE	"	300	122	50	3800	425	Phillips 43065
P.E. Foam (wire)	"	240	100	24	3000	340	2MI + Celogen Agent
P.V.C. - (wire)	"	300	100	23	1200	330	-
.2 M.I. HDPE	4½"-30:1	1320	86	180	3100	465	Koppers - Sheet
3 M.I. LDPE	"	1360	96	180	2400	370	Enjay Film
H.I. P.S.	"	1440	95	138	2350	475	Cosden - Sheet

FIGURE 6

AN ANALYSIS OF COOLING PROBLEMS IN COMMUNICATIONS CABLE INSULATION

R. L. Boysen
Union Carbide Corporation
Bound Brook, New Jersey

Summary

A mathematical model of the cooling process for wire and cable based on a numerical-control volume analysis is described. For routine analysis this model has been programmed in Fortran IV. Several applications of the analysis are illustrated, including a comparison of cooling times required for various polyolefin insulations and a study of the effects of various operating conditions on cooling.

Introduction

Recent developments in communications cable have created insulation cooling problems for cable producers. The tendencies toward use of high density polyethylene, polypropylene and cellular insulations for telephone singles have all tended to create cooling problems because each of these cool at a slower rate than solid low density polyethylene. To compound this problem, changes in cable design have often required heavier wall thicknesses, especially in filled cables.

A mathematical model of the cooling process based on a numerical-control volume analysis has been developed. This model has been programmed in Fortran IV in order to make analyses of the cooling process a routine matter.

The capabilities of the computer program include any heating and cooling problem on axially symmetric constructions with a copper or aluminum core covered with one or two layers of LDPE, HDPE, or Polypropylene or cellular insulations. Inputs to the program include the operating conditions, the cooling set up of the process and the wire construction. Program outputs are temperature and specific gravity profiles of the polymer from the outer surface radially inward to the conductor at several points downstream from the extruder die. The specific gravity profiles are included specifically to assist in analysis of problems involving contraction voids. Voids tend to occur where large, rapid changes in volume (i.e., inverse specific gravity) occur and where the outer regions of the polymer have been case hardened by cooling. Thus suspected areas of void formation can be located by noting where such rapid changes in density occur when the outer surface temperatures are well below

the melting point.

Discussion

Analysis

The control volume approach used in the analysis of the problem is a numerical technique. Although essentially the same results can be attained by using numerical forms of general heat transfer and thermodynamic equations, the route chosen here requires only the equations for the definition of specific heat (at constant pressure) and thermal conductivity. The method used to define each control volume is illustrated in Figure 1. Each rectangular torus shaped volume is defined as fixed in space. The cable passes through the

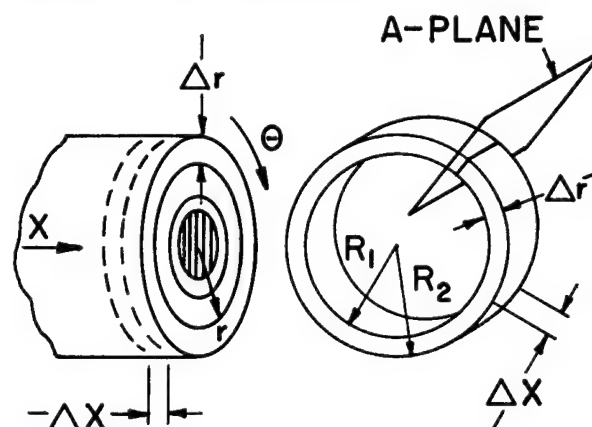


FIGURE 1
Control Volume Definition

volumes thus defined in a steady state condition. Thus the steady state temperature of all control volumes defines the complete temperature profile of the cable. The basic assumption of the analysis is that the temperature throughout a single control volume is constant. The directions used in the analysis are also indicated in Figure 1.

In addition to simplicity of mathematics, advantages of this type of analysis are that no boundary condition or dimensionality assumptions need be made in order to perform the analysis. Thus the potential accuracy is high and the analysis can be easily expanded to include any axially symmetric construction. The major disadvantage of numerical solutions is

that relatively large amounts of computer time are necessary for execution.

Most of the less obvious assumptions which were made were checked out simply by not making the assumption initially. The advantage of assumptions is, of course, simplicity of the analysis. I have listed the most significant assumptions below.

1. In trough areas where line speed is greater than 100 fpm, and the cooling medium is ambient air, the forced convection correlation for turbulent flow over a flat plate is assumed to apply.¹ This is the only assumption which has not been checked. Some assumptions must be made concerning the convection coefficient in air in order to perform the analysis. The only possible way of checking this assumption would be through physical temperature measurement which was deemed impractical at 1000 fpm or higher line speed. The flat plate turbulent correlation is used under the premise that axial flow over the wire surface is a cylindrical analog of one dimensional flow over a flat plate.

2. The surface resistance (i.e., inverse convection coefficient) between water baths (or other liquids) and the insulation is assumed to be zero. This assumption was checked by initially using the coefficients normally used for steam condensers in which pipes are normally coated by condensing steam.² The difference between using the steam condenser values and zero surface resistance was found to be nil.

3. The temperature gradient in the conductor is assumed to be flat. Conductor thermal conductivity is at least 2000 times that of the insulation. Again this assumption was checked by not making it initially. The difference was again nil. This assumption allows treatment of the conductor as a single radial control volume.

4. X-direction heat reansfer is assumed to be negligible. This was found to influence temperature changes by less than 5% in the most severe cases. Again the checking method used was performing the analysis without making the assumption.

Other obvious assumptions are of course made, but these should need no explanation for justification. Among these are, (1) steady state, (2) complete axial symmetry, (3) and no mass transfer in the r or θ directions.

When all these assumptions are made the problem reduces simply to a steady state mass transfer through each control volume in the X direction and heat trans-

fer through each control volume in the r-direction. Figure 2 is a cross section of a typical control volume such as at plane "A" in Figure 1. Since the control

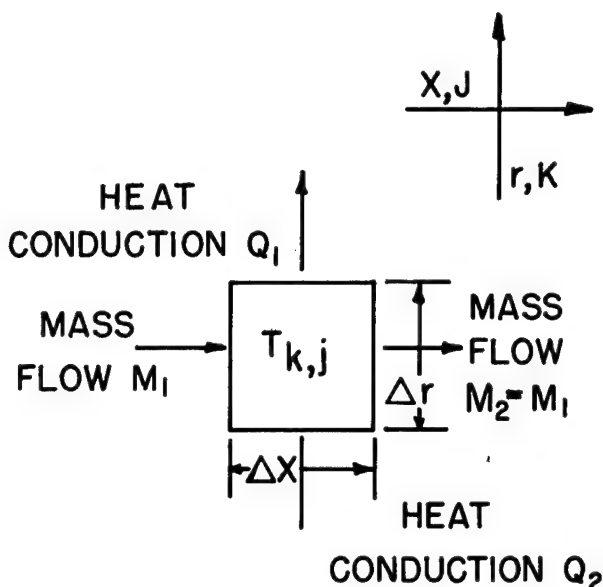


FIGURE 2
Control Volume Cross Section

volume is a steady state system, the energy of the mass within the control volume remains constant, and the energy transfers due to mass and heat flow must add to zero.

$$E_{M1} - E_{M2} + Q_2 - Q_1 = 0 \quad (\text{eq.1})$$

where:

- E_{M1} = internal energy of in-flowing mass
- E_{M2} = internal energy of out-flowing mass
- Q_2 = heat flow into volume
- Q_1 = heat flow out of volume

Since no work is done on the system,

$$E_{M1} - E_{M2} = \Delta E_M = \Delta Q_M \quad (\text{eq.2})$$

where:

- Q_M = change of energy content of the mass flowing through the system

The definition of specific heat at constant pressure can be used to relate ΔQ_M to a change in temperature.³

$$C_P = \frac{1}{M} \frac{dQ}{dT} = \frac{1}{M} \frac{\Delta Q_M}{\Delta T_M} \quad (\text{eq.3})$$

where:

- M = mass flow
- ΔT_M = change in temperature of mass flowing through the system

The definition of thermal conductivity can be used to determine the magnitudes of Q_1 and Q_2 ³

$$Q = KA \frac{dT}{dr} = KA \frac{\Delta T_r}{\Delta r} \quad (\text{eq. 4})$$

where:

K = thermal conductivity
A = area of volume normal to r-direction
 $\frac{\Delta T_r}{\Delta r}$ = radial temperature gradient

Hence,

$$Q_2 = K A_{K,J} \left(\frac{T_{K-1,J} - T_{K,J}}{\Delta r} \right) \quad (\text{eq. 5})$$

$$Q_1 = K A_{K+1,J} \left(\frac{T_{K,J} - T_{K+1,J}}{\Delta r} \right) \quad (\text{eq. 6})$$

And from equation 3,

$$\Delta Q_M = M C_p \Delta T_M \quad (\text{eq. 7})$$

Substituting in equation 1 and 2, and solving for ΔT_M

$$\Delta T_M = \frac{k}{\Delta r M C_p}$$

$$\left[A_{K+1,J} (T_{K,J} - T_{K+1,J}) - A_{K,J} (T_{K-1,J} - T_{K,J}) \right] \quad (\text{eq. 8})$$

From this equation, then the entire temperature profile of the insulation can be determined from

$$T_{K,J+1} = T_{K,J} - \Delta T_M \quad (\text{eq. 9})$$

Individual specific heats and specific volumes are calculated for each control volume based on its calculated temperature. The calculation is based on straight line interpolation between points such as shown on Figure 3 and 4. Accuracy within 2% is attained in this way. The specific heat curves used for low density polyethylene and high density polyethylene are shown in Figures 3 and 4.

Thermal conductivities of the polymers are assumed to be constant. Also density (which is part of the program input) in the case of cellular insulations is considered uniform throughout the insulation except for the effects of temperature.

Computer Program

The analysis just described has been programmed in Fortran IV. The inputs, outputs, and options of the program were chosen for maximum practical versatility and for relatively easy routine investigation of cooling problems. Union Car-

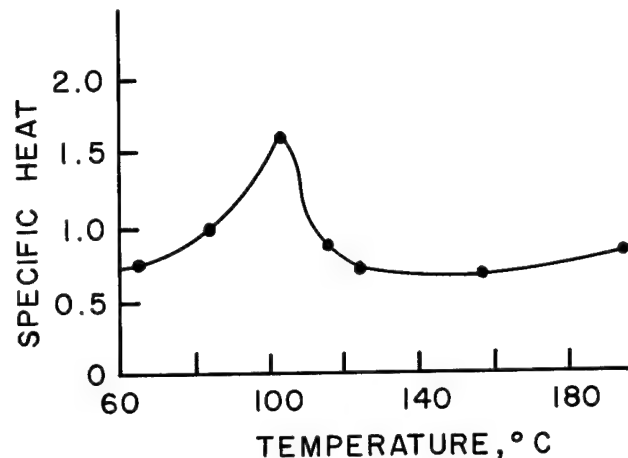


FIGURE 3
Specific Heat of Bakelite® LDPE

bide will shortly offer the use of the computer program to wire and cable producers as a technical service to the industry.

A simplified schematic of the program logic appears in Figure 5. As shown, options of carbon black filled insulations, cellular insulations, and different conductor metals are included. Other capabilities and limitations of the program are as follows.

1. Low density polyethylene, high density polyethylene and polypropylene insulations can at present be analyzed.

2. Any number of cooling sections (or heating sections) up to five can be analyzed.

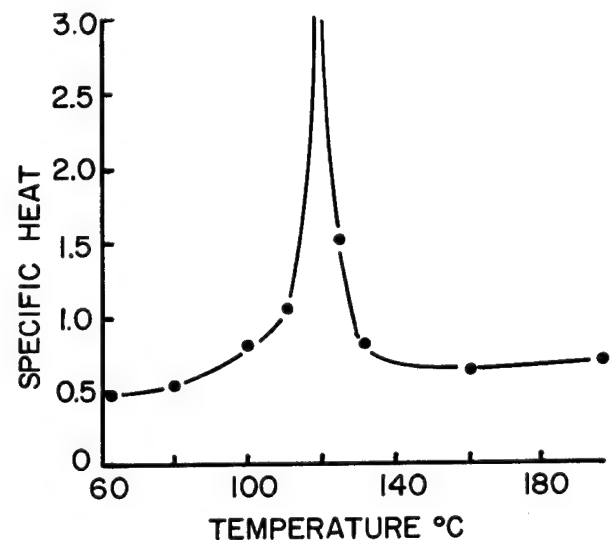


FIGURE 4
Specific Heat of Bakelite® HDPE

3. Only single axially symmetric insulations (no concentrics) are capable of being analyzed.

4. Wire speed in any air cooled section must be at least 100 fpm in order that the turbulent air flow assumption be valid. Only ambient air can be investigated at present.

The program inputs include, of course, the cooling (or heating) sections configuration and temperatures. The initial insulation temperature and conductor temperature and the wire construction are also necessary. Choice on the options mentioned previously is by data switch.

The program output is numerical and includes most of the input data plus a temperature profile and specific gravity profile of the insulation from the outer surface to the inner surface at the end of each cooling section. If a temperature or specific gravity profile intermediate between section terminations is desired, a fictitious section can be included.

The number of points for which a temperature and specific gravity is given depends on the size of control volume (calculation increment) which is chosen. Generally, the thinner the insulation the lesser the number of temperatures and specific gravities calculated.

The purpose of the specific gravity output is to provide a better basis for human judgment on the likelihood of contractural void formation in any particular cooling situation. As we gain more experience in analyzing such problems with this program, it is expected that rules of thumb concerning the relationship of void formation to outer surface temperatures and density gradients will be developed. None are known at present.

Studies of Several Cooling Variables

Each of the present trends in the telephone cable industry tends to increase necessary insulation cooling times. We will show in this section that use of high density polyethylene insulations, and cellular insulations, aluminum conductors, or heavier walls in solid insulation can each significantly increase cooling trough residence time required to cool the finished wire.

The cooling analysis program can be used for general studies of variables such as these as well as for direct comparison of specific cooling cases.

Table I shows a comparison of cooling times required for several different constructions as predicted by our computer program. Each construction listed was

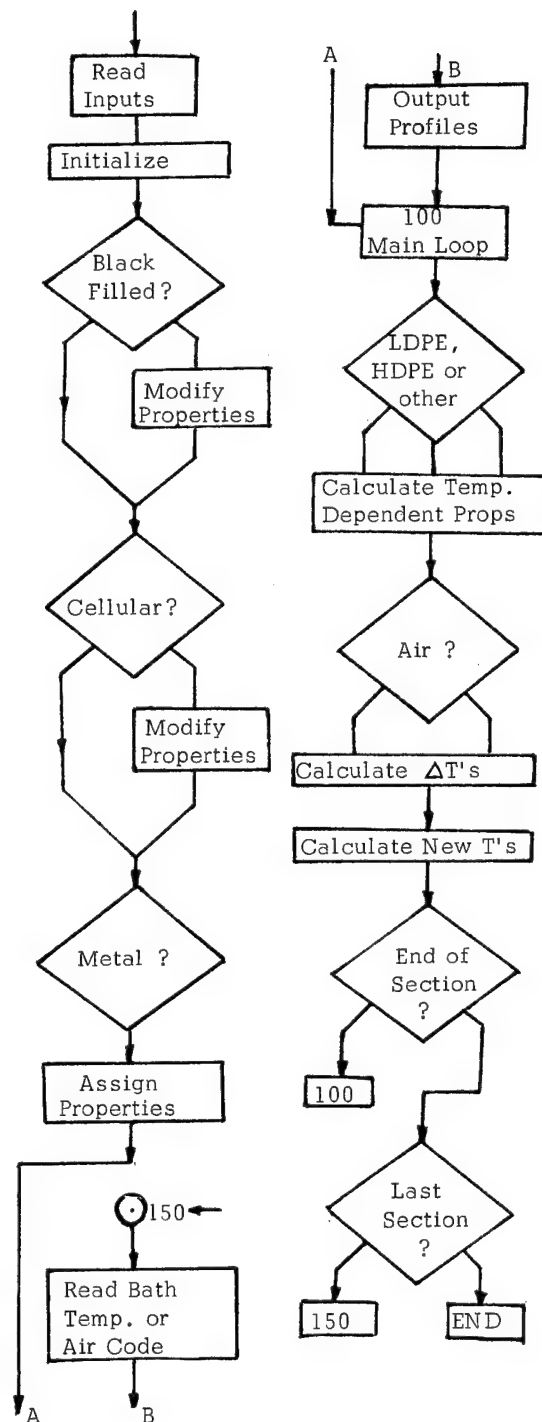


FIGURE 5
Simplified Logic Schematic of
Cooling Analysis Computer Program

designed to arrive at the typical 66 pf/ft. coaxial capacitance. The melt temperatures were chosen as being typical for the type of polymer indicated. Extrusion of cellular compounds usually must be done at temperatures lower than corresponding solid compounds in order to obtain a well-developed cell structure. Thus the temperatures chosen for the cellular constructions is 50°F below typical values used for solid extrusion.

As shown in Table I, to cool solid high density polyethylene to below the melting point (200°F) requires about 35% more time than low density polyethylene of the same construction. The chief reason for this is the much larger heat of fusion of HDPE. Even considering much lower thermal conductivity, the cellular HDPE requires less cooling time than the solid HDPE. This is because the necessary outside diameter is reduced from .036" to .031" to obtain a capacitance of 66 picofarads/foot. Cellular polypropylene is even slower cooling than the corresponding HDPE cellular because of a much lower thermal conductivity and high melt temperature.

Comparison of residence times necessary to reach identical temperatures may be considered unrealistic since the structural character of, for instance, polypropylene is radically different from low density polyethylene at 250°F. This can be a large factor as shown by the fact that the cellular HDPE construction cools to 250°F as fast as the solid LDPE does to 200°F. The necessary time for solid HDPE to cool to 250°F is still signifi-

cantly longer than for LDPE at 200°F. Cellular polypropylene is again much higher.

It is evident that all of the polymers presently being seriously considered for filled telephone cable constructions will cool at a significantly slower rate than low density polyethylene.

Figure 6 shows the effect of aluminum vs. copper conductors and conductor size on cooling speed. The aluminum AWG number is displaced two sizes from the copper on the horizontal axis in order that equal conductivities could be compared. Although aluminum conductors of the same size would tend to cool at a somewhat faster rate than copper, the necessary increase of two conductor sizes significantly increases required cooling times (to about 25% over copper). On decreasing the AWG number, the effect of not only larger conductor size, but also heavier walled insulation is seen in the slower cooling.

The effect of wall thickness while all other variables are held constant is shown in Figure 7. Filled telephone cable constructions will typically require heavier walls than used today in order to arrive at comparable mutual capacitances. The exact thickness required will depend on the dielectric constant of the filler. The effect of wall thickness is, as would be expected, quite large relative to the other variables we have looked at.

Polymers other than LDPE and cellular insulations will require generally high extrusion temperatures and higher conductor preheat temperatures. Extrusion melt

TABLE I

COOLING TIMES FOR VARIOUS TELEPHONE WIRE CONSTRUCTIONS

AWG #24, Copper, 70°F water, 66 picofarad/ft. coaxial capacitance

Construction	Melt Temperature °F	Seconds Residence Time		
		250°F Max.	200°F Max.	150°F Max.
Solid LDPE .036" dia.	400	-	.57	.87
Solid HDPE .036" dia.	500	.66	.87	1.08
Cellular HDPE 0.6g/cc .031" dia.	450	.56	.78	1.02
Cellular Polypropylene 0.6g/cc .031" dia.	500	1.38	1.74	2.40

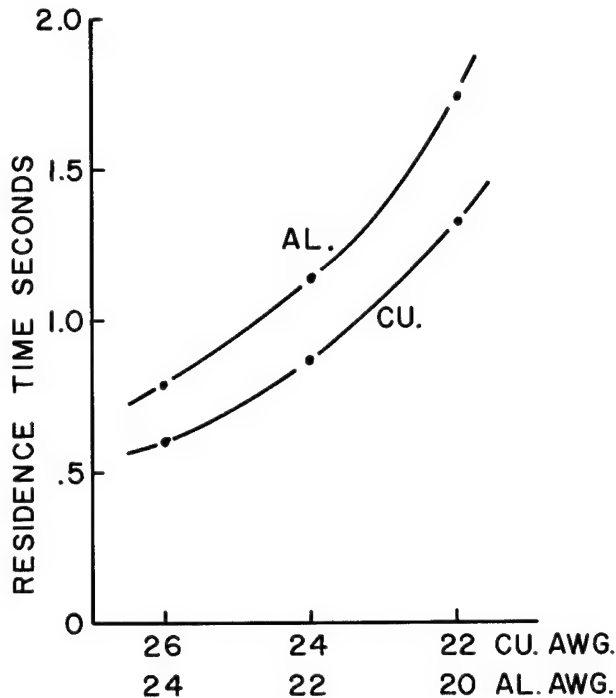


FIGURE 6

Effect of Conductor Size and Metal on Residence Time in 70°F water to Reach 200°F Max. High Density Polyethylene. 500°F Melt Temperature. 400°F Preheat Temperature. Diameter Ratio=1.8

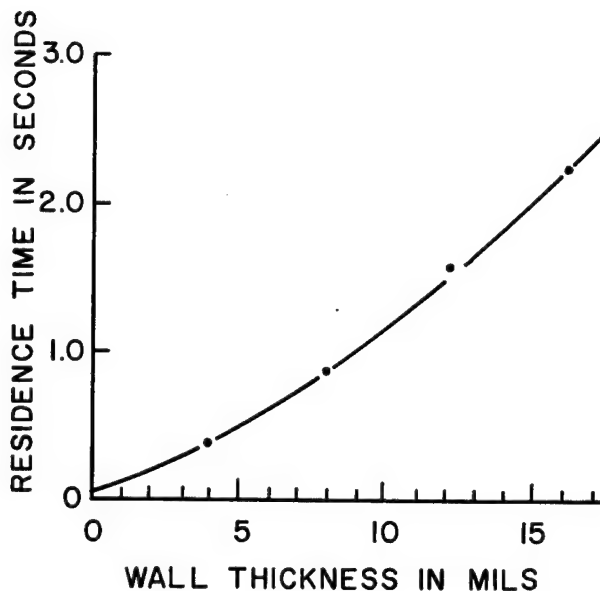


FIGURE 7

Effect of Wall Thickness on Residence Time in 70°F Water to Reach 200°F Max. High Density Polyethylene, 500°F Melt Temperature, 400°F Preheat, Conductor AWG 24 Copper.

temperature effects and copper conductor preheat temperature effects on cooling time are shown in Figures 8 and 9, respectively. A change of 100°F in melt temperature can increase necessary cooling time as much as 20% if all other variables are held constant. The effect of preheat temperature is substantial (12% in 100°F), although somewhat less. These effects will be even larger on constructions larger than AWG #26.

In summary, if the combined effects of aluminum conductors, cellular high density polyethylene (or solid polyethylene of larger wall thickness) with accompanying preheat are taken into account, the potential combined effect on required cooling time could seriously limit outputs from insulating lines which are presently cooling limited or close to being cooling limited.

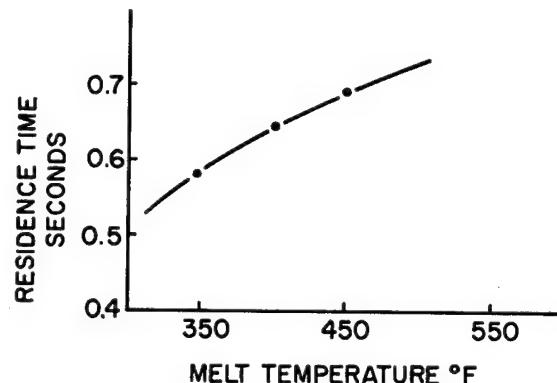


FIGURE 8

Effect of Melt Temperature on Residence Time to Reach 150°F Max. in 70°F Water. AWG #26, Solid HDPE, 400°F Preheat Temperature, Copper.

Another example of a use of the cooling analysis program is shown in Table II. Various cooling trough combinations of air, hot water and cold water cooling have been analyzed for a single AWG #19 copper construction with solid high density polyethylene insulation. The table is explained in detail in the footnotes below. Contraction voids are likely to form when large thermal contractions take place in the insulation interior and the temperature of the outer surface of the insulation is well below the melting point. The second column in the table lists the maximum thermal contractions that take place in .01 minutes for each trough configuration. The maximum insulation temperature after .05 minutes (50' trough, 1000 fpm) is listed in the next column(3). In the fifth column the trough sequence is described with the first section on the

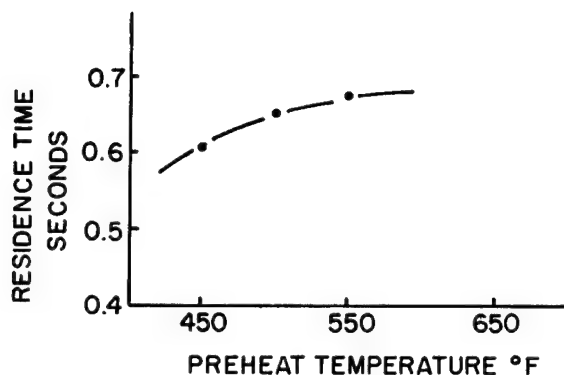


FIGURE 9

Effect of Preheat Temperature on Residence Time to reach 150°F Max. in 70°F Water. AWG #26 Copper. Solid HDPE. 500°F Melt Temperature.

left. Several trough sequences can be eliminated immediately in the search for the optimum configuration. For every run in which the maximum final insulation temperature was above 180°F, a check has been placed in column 4. For every run with greater than 15% contraction in .01 min. an (X) has been placed in column 4. These two classes can be eliminated as

being either too slow a cooling configuration or as being likely to cause contraction voids. Every one of the remaining trough configurations starts with hot water and is followed by cold. An optimum configuration is difficult to choose from these. This type of cooling configuration has, of course, been used successfully for many years.

Each trough configuration in which the hot insulation is immediately immersed in cold water (for .01 minutes) resulted in very large contractions and a low outside surface temperature. Each of these conditions has an (X) in column 4 of the table. Each configuration which did not follow air or hot water with cold water resulted in a high final (after .05 minutes) insulation temperature. The results indicating a hot water to cold water gradient as the best situation suggests that a configuration such as #D6 with air, hot water and cold water would provide an excellent situation as well. Although the 192°F final insulation temperature of #D6 is above our somewhat arbitrary limit of 180°F (see footnote 3), contractions are very low. A configuration with one air section followed by hot and cold water (which was not analyzed in this study) could possibly be a better configuration than D4, D5 and D13 which are the apparent best of this study.

TABLE II

Comparison of Various Cooling Trough Configurations for AWG #19 copper with solid high density polyethylene insulation

Run #	Maximum Thermal ⁽¹⁾	Maximum Insulation	See Note ⁽³⁾	Trough ⁽²⁾
	Contraction in .01 min. %	Temp. at end of .05 min.	Below	Configuration
D1	19.1%	92	X	CCCCC
D2	11.65%	211	✓	HHHHH
D3	5.65%	267	✓	AAAAA
D4	11.65%	145		HHHCC
D5	11.65%	110		HCCCC
D6	8.0%	192	✓	AAHCC
D7	10.9%	251	✓	HAAAH
D8	19.1%	185	X✓	CAAAC
D9	7.25%	259	✓	AAHHH
D10	19.1%	118	X	CACAC
D11	19.1%	198	X✓	CHHHH
D12	19.1%	197	X✓	CHAAA
D13	11.65%	124		HHCCC

1. Maximum change in volume of insulation due to contraction in a 10 ft. section of trough calculated assuming that density changes at any radius have effect equal to density change at average radius.
2. C = Cold water 70°F, H = Hot water 190°F, A - Ambient air only
First section left, each section .01 minutes residence time.
3. X = Maximum contraction over 15%.
✓ = Maximum temperature at trough end over 190°F.

The conclusions of this cooling trough study should certainly not be considered the last word. There are an infinite number of combinations which have not been investigated. This analysis was constricted to only trough sections of .01 minutes residence time, for example. This type of optimization study should be of increasing value if present trends continue in the telephone cable industry.

The absolute accuracy of the cooling analysis program is not yet well known. It is expected that as experience in using the program grows this will become better known and slight adjustments in calculating procedures or assumption will have to be made to conform to reality. For comparison purposes and variable studies such as have just been described, however, the accuracy should be excellent, considering the fact that all major assumptions (except convection coefficients) have been thoroughly checked.

Application of the analysis is, of course, not limited to communications cable. Any cable with a single concentric circular insulation can be analyzed. Extension of the analysis to include pipe and rod cooling is also a simple procedure. Other polymers for which the thermal properties are known can also be analyzed routinely.

References

1. B. Gebhart, Heat Transfer. New York: McGraw-Hill, 1961.
2. T. Baumeister, editor, Marks Mechanical Engineers' Handbook. New York: McGraw-Hill, 1958.
3. P. J. Schneider, Conduction Heat Transfer. Reading, Mass.: Addison-Wesley, 1957.
4. N. C. Wheeler, Jr. and J. R. Wheeler, Jr., Solving Cooling Trough Requirements for a Coaxial Extrusion Line. Paper given at Wire Association Meeting, Providence, Rhode Island, May 13, 1970.



R. L. Boysen
Union Carbide Corp.,
River Rd.
Bound Brook, N. J. 08805

Mr. Robert L. Boysen was born in Princeton, New Jersey on November 18, 1940. He graduated in June 1963 from Rutgers University on completion of a five year liberal arts - engineering program with BA and BS degrees. Mr. Boysen joined Union Carbide Chemicals and Plastics Division at Bound Brook, New Jersey in June 1963. He graduated in 1967 from Newark College of Engineering with a MS in Management Engineering. He is currently in the wire and cable materials group at Union Carbide's Bound Brook Research and Development Center.

Mr. Boysen is a member of Tau Beta Pi and Phi Beta Kappa.

NEW DIELECTRIC TESTING METHODS FOR INSULATED WIRE

Richard S. Thayer
Tensolite Division of Carlisle Corporation
Tarrytown, New York

ABSTRACT

In order to assure that wire insulation provides its most basic function, insulating the conductor from a possible "short circuit", wire is commonly exposed to a 100% overvoltage fault detection test after manufacture. The insulation fault detection essentially consists of a voltage generator coupled to the product under test via a suitable electrode.

The overall effectiveness, however, depends upon which combination of generator and electrode is used, from the 24 or more that are readily available. Our data indicates that the particular combination of an Impulse Generator and a Brush Electrode offers significantly higher levels of reliability than presently obtainable from other combinations now being used or specified.

INTRODUCTION

All insulated wire, with the exception of telephone and magnet wire, must be free from any insulation defects before shipment. This is normally accomplished by dielectric proof testing all wire lengths at voltages several times the normal continuous rating. This is usually done by either of the following two methods or combinations thereof:

1. Wet Tank Test - Spools of wire are immersed in grounded water tanks with high voltage applied to the conductor. If there is a dielectric breakdown or fault path anywhere in the insulation, current will flow through it and the tester will indicate a failure.
2. Sparktest - The wire is passed through an electrode which subjects the insulation to an over voltage, as it passes through. The conductor is maintained at ground potential. When an insulation defect passes through the electrode, current flows to ground via the conductor and a failure is signaled, usually stopping the spark-tester.

Since the Wet Tank test can not indicate the exact location of the failure, it is always used in conjunction with the sparktest, which can detect the fault as it passes through the electrode. The Wet Tank test is commonly used with ac voltages, although dc can be used when permitted.

The sparktest is available with a variety of electrodes and voltage waveforms. The most common is a bead chain electrode with a 60 Hz sinusoidal voltage. Other possible electrodes are brushes, Hipotrodes, annular rings, wet sponges or water. Some of these are shown in Figure 1. In addition to 60 Hz, voltage waveforms may be 3000 Hz sinusoidal, Impulse, or dc. Depending upon the required voltage levels, these four waveforms and six electrodes alone, allow 24 possible waveform/electrode combinations. The Impulse waveform has had greatest acceptance in developing an alternate to the Wet Tank test. Of the electrodes listed, the brush offers the best combination of intimate wire contact, operator safety, and freedom from maintenance.

If the basic sparktest were 100% effective, no other dielectric proof test would be necessary, since the insulation could be verified "fault free" in one operation. However, it is typically found that after the sparktest has been performed, additional failures occur when the wire is subjected to the Wet Tank test. Based on the above, the common procedure is to use the sparktest to locate and remove the most obvious faults, and then use the Wet Tank test as a final verification. The wire lengths that fail the Wet Tank test are again subjected to the sparktest/tank test procedure until no failures are detected.

It can be seen that the sparktest/tank test procedure is a very time consuming and inefficient process. This is especially so when considering that if the Wet Tank test is repeated at the customer's Incoming Inspection, he will usually find still more faults.

The fact that the Wet Tank test detects these additional failures is not sufficient proof that it is more severe or discerning than the sparktest, since some additional failures will usually appear during any subsequent testing. Relative severity may be determined by taking a lot of wire, dividing it into two halves, each tested by one of the two methods being compared, and then determining the failure rate of the tested lots during an additional test, common to both. For example, the Wet Tank test could be compared to the sparktest as follows: half of a wire lot is sparktested while the other half is Wet Tank tested. The two pretested halves are then subjected to an additional test common to both - Wet Tank for example. The failure rate during this second Wet Tank test is then compared for the two halves. The half with the lower failure rate during this second test is the one which had been tested with the more discerning initial test.

As mentioned previously, if a sparktest could be developed that could really assure no additional failures during subsequent testing, the Wet Tank test would no longer be necessary, except perhaps as a sampling test to establish additional confidence. This search for a single sparktest device which will give superior reliability to that provided by the old 60 Hz sparktest/tank test combination is the subject of this paper.

PRESENT TEST METHODS

60 Hz Bead Chain Sparktester

Bead Electrode

Voltage is applied to the wire as it passes through a bead chain electrode, which essentially consists of densely packed fine ball chains hung vertically from a common high voltage plate. Reliable operation depends upon how close the beads come to a wire defect as it passes through. At levels much below 1500 Vrms, little corona is present and the beads must actually contact the wire at the defect for effective fault detection. If the defect happens to be directly at the bottom of the wire as it passes through, detection at lower voltages may not be possible. Dirt and corrosion products which form on the beads, also degrade fault detection performance.

The sparktest only stresses small sections of wire at any one time. This gives rise to relatively small capacitive currents, making it much easier to detect the resistive current flow associated with an insulation defect.

Grounding

The conductor must be properly grounded to the testing equipment in order to maintain a proper return path for the fault current back to the high voltage transformer, through the fault detection circuit. With ac voltages, capacitive coupling is usually sufficient to establish an effective return path in the event that the ground connection has been accidentally broken.

Although the 60 Hz sparktester is the most common dielectric proof tester, its poor performing electrode and usually unsophisticated fault circuitry help to explain its inability to keep failures to a low level upon subsequent Wet Tank testing of the wire.

60 Hz Wet Tank Test

Practical Considerations

Capacitive Current Flow

As opposed to the sparktest, the Wet Tank test applies voltage to the entire spool of wire, rather than one

section at a time. Considering that hook-up wire may have capacitance levels up to 200 picofarads per foot or more, a large spool of wire presents a relatively heavy capacitive load to the high voltage transformer. Capacitive currents of 200 mA are commonly encountered, requiring a transformer of several kVA rating to properly maintain the required voltage. In view of the heavy flow of normal reactive current, the fault sensing device must be properly designed to detect the resistive current associated with an insulation defect, while not reacting to the capacitive current component. Unless special precautions are taken, such as phase sensitive circuits and arc detecting devices, the Wet Tank unit may not be sensitive enough to catch all faults or may be too sensitive and register false faults.

The capacitive current flow also accounts for another drawback of the tank test. The normal flow of reactive current through the insulation attenuates the voltage applied to the wire by a certain percentage, each foot into the spool. This reduction in test voltage, which should properly be measured in db/unit length, results in the middle of the spool seeing a lower voltage than the ends. Indications are that the drop may be as high as 100-200 Vrms. This phenomenon is not present when dc is applied, assuming that a low loss insulation such as Teflon, is being tested.

Use of Water as Ground Electrode

When spools of wire are being Wet Tank tested, one must be certain that the water penetrates down to the inner-most layers on the wire spool, so that all sections of the wire are properly stressed. This is of special importance when working with high surface energy plastics like Teflon. Most specifications require that an anionic wetting agent be added to the water to allow it to more effectively penetrate through the wire layers. A minimum soaking time, typically four hours, is usually specified. Electrical and chemical tests on TFE have shown, however, that full penetration is achieved in 30 minutes or less.

Unfortunately, the wetting solution plays a part in one of the more serious drawbacks of the Wet Tank test - copper/silver galvanic corrosion leading to the formation of cuprous and cupric oxides. Whenever a blowout does occur in the wire, the water tends to flow into the hole and seek its own level. Since the entire spool is submerged, the water, now assisted by the wetting agent, attempts to penetrate the entire spool - setting the stage for later corrosion. Tests have indicated that the water may wick under the insulation for distances of 40 feet or higher, depending on how long it remains in the water bath. If the fault was present before starting the 4 hour soak, penetration may even be further. This was one of the major considerations leading to the military approval of alternate dry tests, in place of the Wet Tank, in such specifications as Mil-C-13777, Mil-W-16878, and Mil-W-

22759.

Economical Considerations

In addition to all of the practical drawbacks discussed above, the Wet Tank test is also very time consuming to perform - for the vendor and especially the end-user. Tensolite utilizes a multiposition (22 separate high voltage transformers) automatic hipot tester which permits us to test close to 350 spools/hour. However, companies with a single high voltage transformer, connected to a multiposition selector switch, may take up to 6 1/2 hours to test the same number of spools. Accordingly, many vendors are especially anxious to eliminate the Wet Tank test if a more economical alternate can be achieved with no compromise on reliability. To further compound the situation, specifications requiring the Wet Tank test typically require that each spool also be tested for insulation resistance. The IR test can take as much time to perform as the Wet Tank, but yields data of questionable significance.

Rate of Voltage Increase and Decrease

Caution must be exercised in the Wet Tank test in reference to the increase or decrease rates of the specified voltage. While general specification requirements set the maximum rate of rise at 500 volts/second, and the set voltage is 2200 Vrms, a 60 second test can become a 2 1/2 minute test. Another facility, also operating within the specification, may have their equipment set at a more reasonable 400 volts/second. In this case, the 60 second test is only extended to 71 seconds. As can be seen, lower rates of rise and fall will tend to increase the severity of the tank test due to the increased exposure time.

Fault Sensitivity

Typical specification requirements state that the unit be able to detect a fault at a voltage at least as low as 50% of the required test voltage. Therefore, if 2200 Vrms is the required test voltage, a unit which is sensitive to faults at 1100 Vrms, but not 1000 Vrms, is acceptable. However, this same unit may blow out the wire at 1000 Vrms, during the voltage decrease portion of the testing cycle, without the equipment signaling the failure. The defect will then be shipped off to the customer, even though specification requirements have been met. In order to overcome this possibility, it has been suggested that specifications be revised to require that the high voltage be automatically cut off at some value just above the minimum workable fault detecting voltage. In this way, voltage will only be applied while the unit is capable of detecting the resulting damage. This problem can also be compensated for by proper use of the insulation resistance test, which commonly follows the Wet Tank test. A low voltage pinhole detector, utilizing neon

lamps, can also be used, prior to removing the spools from the tank.

The Philosophy of Wet Tank Testing

Voltage/Life Relationship

The dielectric performance of a wire insulation can be illustrated by a voltage/life plot. The higher the test voltage, the shorter the life (time to breakdown) of the insulation. Depending upon the insulation involved and the voltage rating assigned to it, it may be possible to predict its long-term performance at rated voltage by insuring that it can meet some high voltage test for a much shorter time. This concept, which also applies to thermal ratings, is basically valid unless the increase in voltage (or temperature, in the case of thermal ratings) brings the insulation into an area where conditions are present which did not exist at rated voltage. Using the temperature rating analogy again, this would be equivalent to having a Mil-W-81381 Life Cycle test temperature too close to the melting point of the FEP adhesive, where a new failure mode is introduced.

Presence of Corona

The above discussion leads to one of the most frequent objections to the Wet Tank test - corona. The effect of corona is graphically demonstrated when referring to a typical voltage/life plot, shown in Figure 2. Below the corona point, insulation life tends to be less sensitive to the voltage level and tends towards extremely long lives. When the voltage level goes beyond the corona point, however, insulation life drops markedly. As presently specified, the Wet Tank test specifies voltage levels that are about 1000 Vrms beyond the corona point. The result is that many potential fault sites, which would never have failed at rated or even above rated voltage where corona is not present, will fail in the Wet Tank test.

Within economic limits, these "extra" faults are not necessarily objectionable as an additional margin of safety is achieved. The problem arises, though, when one considers potential failure sites which can withstand the 60 odd second exposure, but can not pass a slightly extended test of 90 seconds, for example. Since corona damage is accumulative, the result is a wire which may now have an imminent failure within a few seconds and which may only have had a minor insulation defect which never would have failed at sub-corona voltages. If this spool of wire is retested at an end-user's plant, he would most likely find a failure. This tendency of the Wet Tank test to degrade the wire, even though it is detecting the more obvious faults, is one of its most disturbing characteristics.

The above discussion might be interpreted as imply-

ing that the Wet Tank test will not detect failures at voltages below the corona ignition or extinction points. However, as most end-users can corroborate, these failures do occur. The explanation lies mainly in damage to the wire during handling at the vendor's plant and, possibly, damage that the vendor's Wet Tank test has caused but not detected, as explained above.

Dielectric Failure Characteristics of TFE

The "potential failure sites", discussed previously, are found in every insulation, but slightly more so in TFE-Teflon. This is because TFE's extraordinary thermal stability (for a flexible organic insulation) prevents it from being processed in the typical melt extrusion process. Not having a true melt point, it must be paste extruded, similar to some metals and ceramics. In this process the TFE particles are fibrillated and formed at pressures up to 15,000 psi in the presence of a lubricant aid. After extrusion onto the conductor, the insulation is sintered into a solid wall of insulation. Due to the many variables in the TFE extrusion process, dielectric failure sites occur on the average of 1 per 600 to 1200 feet, with occasional lengths up to 10,000 feet. These faults are detected and removed before shipment. However, some marginal failure sites are still present, which should not lead to actual service breakdowns, except during subsequent Wet Tank test.

Impulse Test with Annular Ring Electrode

Impulse/Annular Ring Vs. Wet Tank

The Impulse test was the first to successfully compete with the Wet Tank test as an industry and government accepted alternate. Data was collected by several vendors on millions of feet of wire, which indicated that Impulse tested wire was as good or better than Wet Tank tested wire, in regard to the number of potential faults. The effectiveness of the Wet Tank or Impulse test is usually measured by the ability of the so tested wire to pass a subsequent Wet Tank test - typically at an end-user's Incoming Inspection. Experience has shown that the Impulse tested lot will exhibit fewer dielectric breakdowns. It is very important to realize that present tests can not guarantee that there will be no failures during a subsequent Wet Tank test check - due to the destructive properties of the tank test itself. The goal is to reduce this failure rate to the lowest possible level.

Characteristics of Impulse Tester with Annular Ring Electrode

The basic voltage waveform of the Impulse tester is a sharp peak, in the area of 11,000 to 15,000 volts, followed by a ringing discharge, which decays in about 50 microseconds. The next pulse does not occur for about 4 - 5 milliseconds. This 200 - 250 pulse/second wave-

train applies much higher peak voltages than the spark or tank tests, but the duty cycle is quite low. One of the prime features of the Impulse tester, as described in Mil-W-16878 and Mil-W-22759, is the annular ring electrode. This device is intended to set up a corona discharge active field, so as to act as a conducting fluid which seeks out and detects dielectric faults through the insulation surface. The concept of a conducting fluid was very attractive, when compared to the shortcomings of the 60 Hz bead chain and Wet Tank test.

Although the Impulse tester has now become fairly popular by allowing vendors to finally avoid the 100% Wet Tank and Insulation Resistance tests, unless otherwise advised by their customers, many companies still approach it with great hesitation. The usual objections are summarized below:

1. Although the voltage on the annular rings is known, some question exists as to the voltage actually being seen by the wire surface as it passes through the corona cloud.
2. In comparison to other electrodes, the wire must be centered very accurately within the annular rings, in order to equally stress all sides of the wire and avoid hitting the rings, which are several thousand volts higher in potential than the center of the corona cloud.
3. A range of electrode sizes must be used to properly test wires of different overall dimensions. However, for wires falling into the same range, the larger sizes are closer to the peak voltage electrode rings, resulting in increased stress levels. In general, centering becomes increasingly difficult as the wire size increases. Thin-walled constructions require smaller electrodes which can develop sufficient corona at the corresponding lower voltage settings.
4. Environmental conditions may affect the level of activity of the corona being produced. Such factors as humidity, cleanliness of air, and air velocity in the vicinity of the electrode have been shown to be important variables.
5. The electrode rings rapidly collect dirt and dust and must be cleaned often, in order to avoid introducing another variable into the picture.
6. Since the corona effect is essentially concentrated at the rings, the possibility has been raised that a potential wire defect may come through the electrode at a wire speed which is so related to the impulse frequency that it is always between rings whenever an impulse occurs.

7. There is also the possibility that poorly centered wire could be damaged on the sharp edges of the annular rings.
8. The Impulse tester, utilizing the annular ring electrodes, appears to cause excessive scrap rates when testing AWG 14 and larger TFE insulated wire and filled TFE constructions.

As can be seen, so many objections were raised, some major and some quite minor, that many vendors and end-users were still hesitant to go to Impulse testing. This was so, even though specifications were being revised to allow Impulse testing as an acceptable alternate to the Wet Tank test. In addition, the Wet Tank failure rates on impulsed wire still seemed too high. In view of these objections, many companies continued their search for a better solution, as described in the following sections.

OTHER TESTS BEING PROPOSED

3000 Hz Bead Chain Sparktester

Features

One of the most interesting units that was developed in response to problems with the Impulse tester was the 3000 Hz sinusoidal sparktester. This unit was basically a "super-sparktester", utilizing a small, densely packed bead chain. Higher voltage levels, which also avoided the deficiencies of the bead electrodes, and higher frequencies further increased testing severity. The increased frequency allowed the use of shorter electrodes, while still exposing the wire to the same number of cycles as seen by the wire in longer 60 Hz electrodes. The high frequency also afforded excellent penetration of any accumulated dirt film that may have formed on the beads with time.

3000 Hz Vs. Wet Tank and Impulse/Annular Ring

Initial test results were encouraging. Most of the work was conducted on thin walled TFE insulated solid AWG 30 conductor. Voltage settings were established which reduced the failure rate in a subsequent Wet Tank test to essentially zero. However, when later tests were run on larger size stranded hook-up wire, it was found that failures did occur after subsequent Wet Tank testing, although the rate was lower than obtained with the Impulse tester with annular ring. One encouraging feature was the bead electrode, which overcame almost all of the shortcomings of the annular ring electrode. For example, since the electrode was of the contact type, no question remained as to the actual voltage applied to the wire surface. While some users experienced maintenance problems on the initially introduced models, these were re-

portedly resolved on later designs.

DC Sparktesting

Advantages

While wire inspectors were deep into their evaluations of Impulse and 3000 Hz testers vs. Wet Tank test, proponents of dc sparktesting urged that it be given a fair chance. Due to time and practical considerations, however, little work was expended on evaluating dc sparktesting as compared to the military approved Impulse tester and newly introduced 3000 Hz tester. As a result, little data is now readily available to Tensolite as to the performance of dc sparktesters vs. Wet Tank test, based on testing millions of feet of TFE insulated wire.

Theoretically, the dc sparktester offers several interesting features. The dc fault circuits can be made far more sensitive than ac circuits, and can detect and signal a fault within a matter of microseconds, rather than milliseconds or longer, as compared to ac. The current limiting characteristics of dc are more controllable than ac, and insulation damage, due to localized charring, can be virtually eliminated. Voltage levels are typically increased to 3 - 4 times the usual ac rms levels, without substantially increasing the scrap rate.

Drawbacks

DC sparktesting also exhibits several theoretical drawbacks, which have discouraged some vendors from using it and prevented some end-users from allowing it:

1. One common end-user reaction is that if the wire will be used in an application where ac or high frequency pulses will be present, the dc test may not properly simulate his end use. DC proponents usually argue that the wire will see a pulse as it enters and leaves the high voltage electrode, thus simulating ac or high frequency use. Recent tests indicate that this "pulse" is far more gradual than originally anticipated.
2. While with ac sparktesting improperly grounded conductors may still see enough capacitive reactance to complete the return path to the fault circuit, no such alternate path exists with dc. If the conductor ground is broken and a fault enters the electrode, the conductor may rise to the full test voltage and the unit may not detect the fault.
3. High voltage dc also has the ability to act as a precipitator, causing the electrode to accumulate dirt. In order to minimize this effect, users are encouraged to operate in air conditioned areas, with electrodes in a vertical position.

4. DC sparkers charge up hook-up wires in accordance with their capacitive nature. Unless grounding brushes are used on the wire surface, the completed spool might give someone an annoying, but not dangerous, shock.
5. One interesting property of wire (and conventional capacitors) is that once it has been dc sparktested, it tends to pick up additional charge after being tested. As an example, wire may have been tested at 10 kVdc - 12 kVdc and properly grounded out, after the test, to remove the surface charge. However, after sitting on a rack for a few days, this same spool of wire may actually build up a charge of several hundred volts. This same phenomenon could occur at a customer's plant, after he has received the wire.

I would imagine that with the necessary effort, most of the above theoretical problems could be overcome. However, more data must be gathered on dc sparktesting vs. other available methods before deciding whether it merits further investigation at this time.

DC Wet Tank Test

Eliminate Reactive Current Problem

Although water, with all its drawbacks, is still present in this proposed test, it does offer some important advantages over the ac Wet Tank test. The most significant is the avoidance of reactive current, allowing much more sensitive and low power fault detection. The second, is the less destructive nature of dc corona as compared to ac.

The only available data that we were able to obtain concerning dc Wet Tank testing indicated that it was not sufficiently effective in fault detection as compared to ac Wet Tank testing. We feel, though, that the fault detecting performance would have been markedly improved, if higher voltage levels were used.

TENSOLITE RECOMMENDED TEST METHOD

Impulse Test with Contact Electrode

Transition to Brush Electrode

The first step in our search for an improved spark-tester was the purchase of several Impulse/Annular ring testers, based on the encouraging data that was initially available. After working with these units for six months, though, we found that they were not a suitable alternate to Wet Tank testing. We then looked into the 3000 Hz tester, but still had some reservations as to the failure

rate during subsequent Wet Tank testing.

We then approached Clinton Instruments, a manufacturer of Impulse and 3000 Hz testers, for their recommendations. In view of our relatively large investment at the time in Impulse test equipment, Clinton recommended that we try using our Impulse testers with a contact electrode, instead of the annular ring, corona cloud type. We admitted that most of the Impulse drawbacks were due to the annular ring, but we were doubtful that the different electrode could improve our failure rate during subsequent Wet Tank testing.

The particular contact electrode that was recommended to us was of the brush type, but we were also aware that another company had reported successful results with an Impulse tester coupled to a bead chain electrode. Although we see no theoretical advantage for the brush over the bead, except for large wire sizes, the brush was best for our particular product line. Besides periodic replacement and position adjustment, the brushes were very convenient to use. They completely contacted the entire wire surface, whether we used fine gauge or large TFE insulated 2/0.

Established Voltage Setting

We ran many lots of wire through Impulse/Brush testers in order to establish proper voltage levels. Our criteria for selection was a voltage setting which gave a minimum of failures in subsequent Wet Tank testing, while still yielding a reasonable scrap rate. Appendix A summarizes our latest established values.

By comparing all of the data that we had gathered to date, we found that the Impulse/Brush combination was superior to anything that we had worked with. When Impulse/Brush tested wire was shipped to our customers, we received confirming reports that a significant improvement in Wet Tank test performance was noted as compared to wire tested by all other approaches. Appendix B summarizes our findings, and indicates the apparent superiority of the Brush/Impulse approach over all of the other commonly used methods. It should be stressed that these figures were obtained with extruded TFE and may not be applicable to dissimilar insulations.

Specification Requirements

We advised our customers of our findings and requested permission to use the Impulse/Brush on wire supplied to them. Although we received authorization, we also had to use an Impulse/Annular ring electrode in tandem in order to satisfy military specification requirements. Since the Brush Electrode operates at a lower voltage level than the Annular Ring, we could not connect both electrodes directly to the same impulse generator. We looked into the possibility of using voltage

dropping capacitors and finally decided upon using separate generators. We are hoping that a military specification revision will be made at some future time which will allow the Brush or Bead Electrode as an alternate to the Annular Ring and thus eliminate our need to use both.

Initial work with the Impulse/Brush alone, yielded the same data as with the two in tandem. Thus, we feel that the Impulse/Annular Ring is only needed to meet present specification requirements and makes no contribution, in our set-up, to overall reliability.

Applicability to Kapton Insulated Wire

Although our findings indicated that the best 100% vendor dielectric proof test for TFE is the Impulse/Brush, the question arises as to what would be best for Kapton (DuPont's polyimide/FEP film) insulated wire, another commonly specified insulation for high performance aircraft.

One approach to this question is to consider a reel of wire wrapped with unsealed Kapton film which is then subjected to the Impulse or any other dry sparktest type device, and then to the Wet Tank test. Theoretically, the wire should pass the sparktest as the high voltage arc would not have the ability to travel through the spiral paths necessary to reach the ground potential conductor. When tested in the Wet Tank test, though the water may have the ability to penetrate these layers, shorting out the high voltage conductor and indicating a fault. Based on this example, one might say that, theoretically, a dry test can not replace the Wet Tank test for Kapton insulated wire.

In order to test the validity of the above example, it is first necessary to determine the nature of a dielectric failure when it occurs with Kapton. Based on our experience with Wet Tank testing of Kapton insulated wire, failures fall into two areas: a dielectrically unsound tape splice or insulation damage during handling. Both of these failure types are rare with Kapton, due to improved tape splicing methods and wire handling equipment and procedures. We have never had a failure due to poorly sealed tape. First of all, a completely unsealed tape is obvious to anyone who handles the wire, such as Quality Control Inspectors or Production personnel. Unsealed wire would be rejected even before a sample would be cut for the Lamination Seal Test. On the other hand, poorly sealed Kapton may appear sound at room temperatures and not reveal the defect until reaching the elevated temperatures of the Lamination Seal Test. Since the seal is satisfactory at normal temperatures, there will be no problem during the Wet Tank test.

In order to further determine the dielectric properties of completely unsealed Kapton films, we wrapped an AWG 22 - 19/34 conductor with an 019-919, 50% mini-

mum overlap construction and subjected it to the Wet Tank test. No failure was detected after 60 seconds at 2500 Vrms. The voltage was raised to 5000, 10,000, and 15,000 Vrms, and again no failure was detected. These results further confirmed our findings that Kapton dielectric failures are due to other factors, besides unsealed tapes.

Since Kapton dielectric failures are actual wall punctures, it can be seen that the voltage from a sparktest device could jump the gap just as easily as in the Wet Tank test. However, Kapton would require higher sparktest voltages, in order to develop the necessary stress levels that will break down any existing improper splices or damaged areas. Our initial thoughts are that Brush/Impulse voltage levels in the area of 1000-3000 volts peak beyond our recommendations for TFE, would be sufficient. Depending upon end-user response, a detailed study of the Impulse/Brush with Kapton can be made, to established refined voltage settings.

Wet Tank Test as a Final Inspection Tool

Impulse/Brush Not Recommended for Final Acceptance

Based on the performance of the Brush/Impulse with TFE, we feel that it produces wire with far better dielectric performance than that exhibited by wire tested with the standard sparktest/tank test procedure. Considering the excellent in-service performance of the millions of feet of wire produced under the old method, wire tested with the Impulse/Brush procedure should be even more outstanding.

Regardless of the vendor test method used, the end-user still has the option of running additional tests during his Incoming Inspection. While we recommend the Impulse/Brush as a vendor test, we cannot recommend it as an end-user Incoming Inspection tool. We feel it is a more severe test than the Wet Tank, as shown by the number of potential defects that are detected, and in fact may reject some percentage of perfectly good wire. This latter point may be necessary in order to establish the required margin of safety. However, this characteristic would obviously make it unsuitable as a rejection/acceptance tool. Of course, if any end-user simply desired to give the wire a final check before use, and had no intentions of using it as an acceptance test, I would strongly recommend the Impulse/Brush for this purpose.

Sampling Plan

When the Wet Tank test is used as an Incoming Inspection tool by an end-user, it is recommended that it be done so on a sampling basis in view of the many drawbacks present. Random lengths should be drawn from the inspection lot and subjected to the Wet Tank test. De-

pending upon the results, the entire lot is accepted, rejected, or additional samples are taken.

A recommended sample plan for extruded TFE is shown in Appendix C. These are realistic values based on our internal data for Impulse/Brushed wire and insures, in our opinion, that questionable lots are all rejected. As explained previously, the allowable number of failures shown should not be interpreted as actual defects in the insulation. It is our feeling that the present Wet Tank test, with its specified voltages, is too severe for Teflon and subjects it to conditions that would not be present in actual service. Therefore, these are only Wet Tank test failures and would not necessarily have been service failures.

In the case of Kapton insulated wire, we recommend that samples be drawn from the lot per the indicated plan, but that even one failure would constitute a lot rejection.

Wet Tank Testing - AC Vs. DC

As previously mentioned, the large flow of reactive current in the Wet Tank test is a very real problem. Although suitable adjustments can be made for extruded TFE, a real potential problem exists with Kapton. Due to industry urging, lengths are going to be far longer than ever available before. At the same time, capacitance levels will be substantially higher than for heavier walled, lower dielectric constant, Teflon insulated wire. This will severely compound the reactive current problem and make testing difficult and time consuming, even if the usual precautions are taken. In order to avoid these problems and still allow for convenient testing, it is recommended that when Wet Tank testing is desired for Kapton, dc be investigated to eliminate the reactive current component and allow for sensitive, direct fault detection. Of course, the optimum solution is to use a dry test, such as the Impulse/Brush, to detect faults, thus avoiding the many problems which may arise in properly specifying a practical wet test. In general, dielectric failures in Kapton insulated wire are quite rare.

CONCLUSIONS

If end-users wish to perform an Incoming test to determine the acceptance of a lot of wire based on dielectric performance, we recommend that the Wet Tank test be used, with a realistic sampling plan such as the one recommended herein.

Based on our work to date, Tensolite recommends that vendors of TFE insulated wire be allowed to use Impulse testing, utilizing a brush electrode as an alternate to the presently specified sparktest/Wet Tank test or Impulse with annular ring electrode.

In view of the significant increase in dielectric reliability for Impulse/Brush tested wire, the necessity for an end-user to duplicate any 100% proof test is even less now than in the past.

Because of the practical problems encountered when attempting to Wet Tank test Kapton insulated wire in long lengths, we especially encourage Impulse or other dry testing alternates.

We encourage continued testing of other high voltage test devices, in order to pursue our goal of obtaining the highest level of confidence possible, for insulated wire and cable.

REFERENCES

General

Working Voltage Classification of Insulated Wire

B. F. Lathan. BuWeps Symposium. October 12-13, 1965.

Types of Insulation Breakdown

Murray Olyphant, Jr. Insulation, November 1963.

Insulation Testing: Why Not DC?

Stanley Peschel. Wire and Wire Products, February, 1970.

Dielectric Fault Detection.

Richard Thayer. BuWeps Symposium. October, 1966.

Wet Tank Test

Phase Sensitive Overload Protector

Clinton Electric Company. Henry Clinton.

Oscillation Modes and Transients in Dielectric Testing

J. M. Garg and W. L. Gore, BuWeps Symposium October 14, 1964.

Measuring and Controlling the Destructiveness of the Dielectric Test

D. C. Reagan. Insulation, October 1962.

Impulse Test

Impulse Dielectric Testing Applied to Insulated Wire

D. C. Alexander. Wire and Wire Products

Impulse Dielectric Testing

NEMA Publication No. HPI-1969.

3 kHz Test

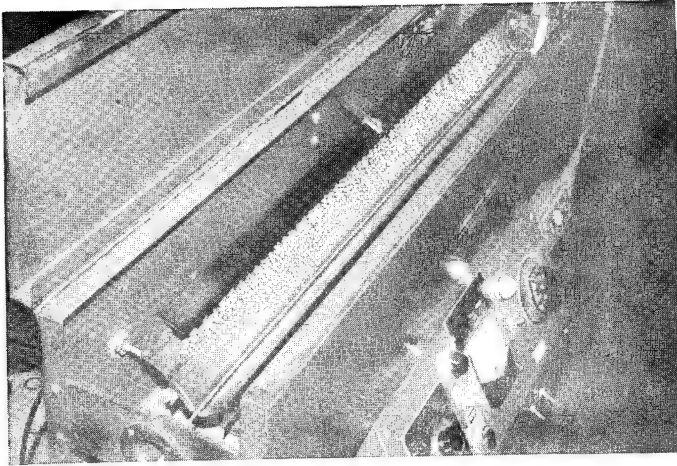
Comparison of Impulse and 3 Kilohertz Sine Wave Sparktesting

H. Clinton and Thomas Stewart, 16th International Wire Symposium, November 1967.

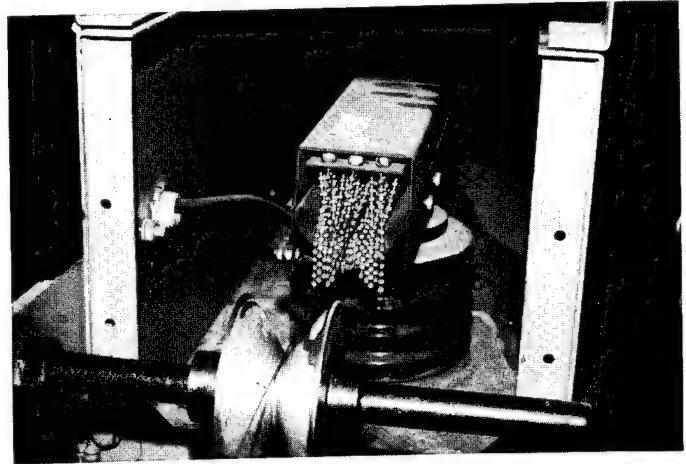
Dielectric Fault Detection with 3 Kilohertz Sinusoidal Sparktester

R. Smith. ASTM Symposium, March, 1969.

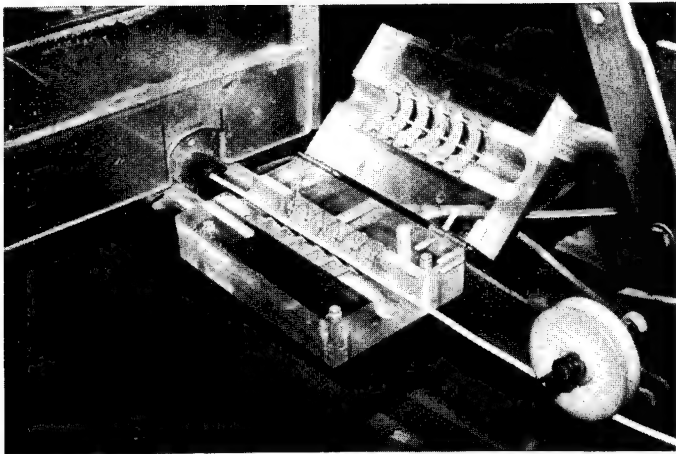
FIGURE 1
SPARKTEST ELECTRODES



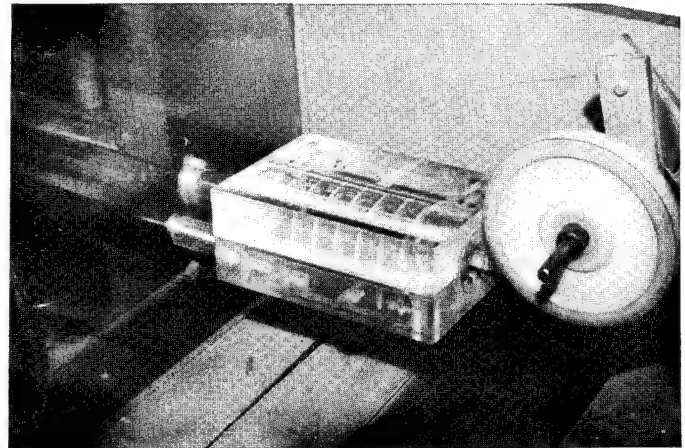
Bead Chain



Bead Chain, End View



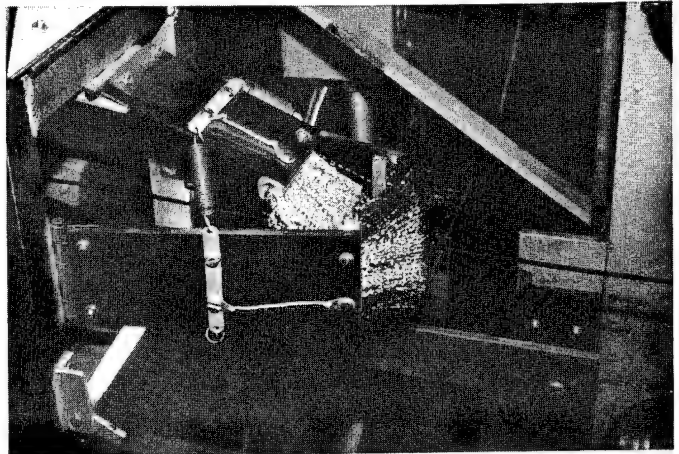
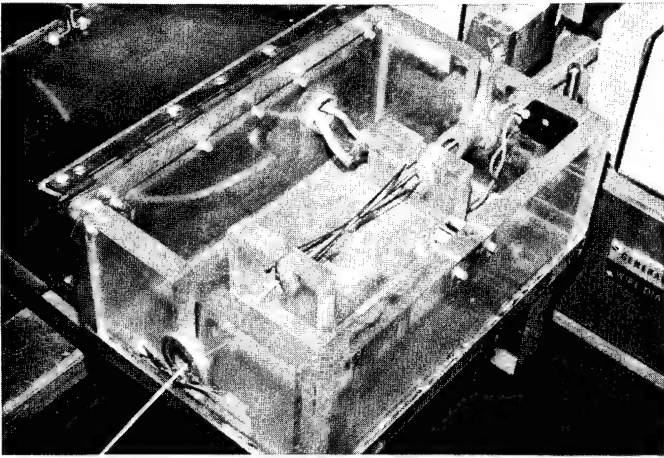
Annular Ring, Open



Annular Ring, Closed

FIGURE 1
(Continued)

SPARKTEST ELECTRODES



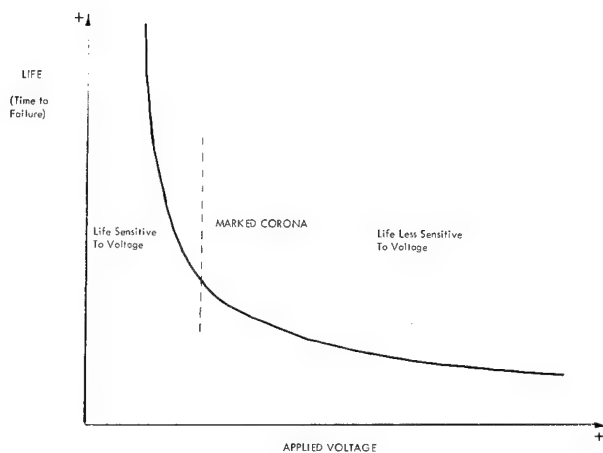
Hipotrode (R)

Brush



Wet Sponge

FIGURE 2
INSULATION LIFE VS. TEST VOLTAGE



APPENDIX A

Recommended Impulse/Brush Voltage Settings

1. Extruded TFE

Voltage Vs. Wall Thickness (inches)

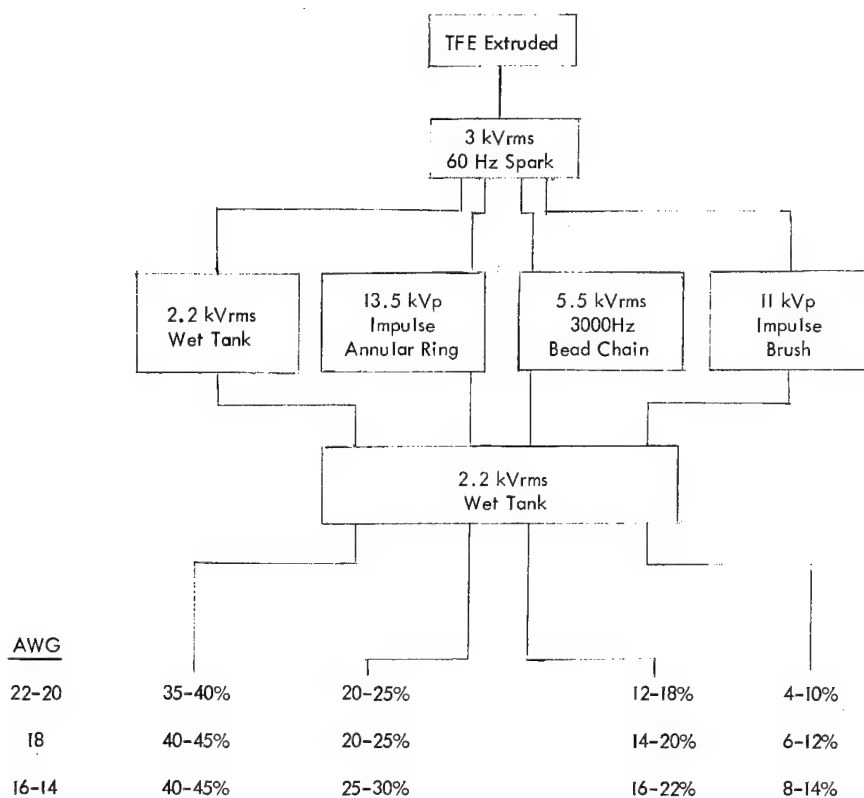
AWG Range	.005-.007	.008-.012	.013-.017
30-22	9kVp	11kVp	12kVp
20-16	9kVp	11kVp	11kVp

2. Filled TFE

AWG Range	MS18000 Medium Wall	MS17411 Heavy Wall
22-18	10KV	11KV
16-12	9KV	10KV
10-6	8KV	9KV

APPENDIX B

Per Cent Wet Tank Failures After Being Pretested



Per Cent of Lengths That Failed Wet Tank Test
(Data based on approximately 10 million ft. of wire)

APPENDIX C

Proposed Wet Tank Test Sampling Plan

TFE

<u>Lot Size (Conductor Ft.)</u>	<u>No. of Random Lengths Selected</u>	<u>Max. No. of Failures for Acceptance</u>	<u>Min. No. of Failures for Rejection</u>	<u>No. of * Failures Requiring Retest</u>
0-9, 999	100%	20%	over 20%	—
10, 000-29, 999	9	1	3	2%
30, 000-64, 999	15	2	4	3
65, 000-100, 000	30	4	7	5-6

* If the number of failures falls into this range, select a new set of samples and retest. If number of failures fall into or exceed this range again, reject lot. If number of failures meet the accepted number, accept lot.

KAPTON

Use the same sampling plan as above, but reject lot if any failures occur.

R. S. Thayer
Tensolite Div., Carlisle Corp.,
W. Main St.,
Tarrytown, N. Y. 10591

Dick Thayer joined Tensolite in 1967 as a Technical Service Engineer, and is now Director of Technical Services. He received his BEE degree in 1964 from the City College of New York.

His background in the field of dielectric testing began at Del Electronics Corporation, as a high voltage design engineer. He joined the former Hitemp Wire Company in 1965 as a product and equipment engineer, where he continued his dielectric testing work with specific reference to wire and cable.

Dick's present paper is based on the latest advances in wire and cable dielectric proof testing, as developed at Tensolite. Most of the data and conclusions were accumulated during the period when Dick headed up the Quality Assurance function as Director of Quality Engineering.



A FOAMING PROCESS FOR WIRE INSULATION

Yoshinori Kato and Hiroshi Ohshima
Electrical Communication Laboratory,
Nippon Telegraph & Telephone Public Corp.
Tokai, Ibaraki, JAPAN

Summary

A fine celled insulation wall suitable for primary wire insulation can be obtained at a high speed by an extrusion of propane and polyethylene mixture fed through a pressure hopper. An attempt is made to analyse the factors which determine the foaming process. It is concluded that the number and the size of the cells depend on the extrusion parameters such as cylinder temperature, L/D ratio and wire speed. They also depend on the pressure of propane, the diffusion coefficient of propane in molten polyethylene saturated with propane, the surface tension and the viscosity of molten polyethylene. In an appropriate condition uniform and closed fine cell of the diameter of less than 15μ can be produced. It is also concluded that certain types of pigments have an effect on the foaming process.

Introduction

Cellular polyethylene has long been used in the communications industry because of the excellent properties for primary wire insulation. Consequently a variety of foaming technique have been devised so far to obtain fine celled insulation.

In general the foaming process may be classified into two categories, the solution coating process and the extrusion coating process. Although fine cells can be obtained by the solution coating technique, its application is confined for several reasons to the insulation of small conductors. On the contrary, extrusion coating process using chemical blowing agent is suitable for the insulation of larger conductors. The wire insulation in the latter case generally results in fairly large cells but can be carried out at a high speed of 1,000 meters per minute or more.

Therefore it has been an intense desire to establish a new insulation technique which enables us to produce highly foamed structure of finer cells even at higher speeds irrespective of the size of conductor. Especially fine celled structure is necessary for thin insulation walls for small conductors to exclude pinholes.

Some years ago a small amount of low density polyethylene was put in an autoclave together with propane and kept at

150°C for an hour to attain equilibrium condition. The pressure in the autoclave was then released instantaneously by opening a valve. It was a surprise to find the expanded polyethylene obtained through this procedure contained extremely fine and uniform closed cells and in addition apparently more than 80% expansion was attained.

On the basis of some preliminary experiments, it was thought that this expansion process might be suitable for a high speed wire insulation. Since then efforts have been concentrated on how to apply it to the primary wire insulation, and the new insulation is now being performed steadily on a 50mm front-end-drive extruder.

In this paper, mainly the results of the analysis of the cell formation are described with the intention to give light on the factors which determine the new foaming process for wire insulation.

Factors determining the foaming process

Extrusion parameters

Preliminary experiments to examine the effect of each extrusion parameter were carried out with a 25mm laboratory extruder. It had a 14:1 L/D ratio and was equipped with a pressure hopper system. The barrel temperature and the temperature of the head assembly were measured by thermocouples. Both were varied between 140°C and 290°C .

The material used was a low density polyethylene DFD-2005 with a melt index of 1.2. Either this type of resin or another low density polyethylene DFD-6005 with a melt index of 0.25 was used in all experiments described in this paper.

Polyethylene pellets were first put into the pressure hopper and then pressurized with propane up to 15 Kg/cm^2 at room temperature followed by a continuous extrusion through a die at an elevated temperature. For simplicity, conductors to be insulated were not used, so that noodle-like extrudates were obtained.

The number and the shape of the cells in the extrudates varied with the amount of propane incorporated in the molten polyethylene in the extruder. Good cellular polyethylene was obtained only when the pressure of propane introduced in the pressure hopper before extrusion exceeded 15 Kg/cm^2 . Variation of the diameter of the die between 0.4 and 1.0mm gave minor

effects on the expansion process while the mixing of propane and polyethylene in the cylinder had significant ones.

Some of the effects of extrusion parameters are shown in Table 1. In the experiment the initial pressure was 15 Kg/cm². The screw speed was 61 rpm and a 0.65mm die was used. The temperature of water in the table stands for that of cooling water bath located at about 15 cm from the outlet of the extruder. As the temperature especially of the cylinder increases, the diameter of the cells decreases while the number increases. When the cylinder temperature is kept at 200°C, a stable foaming can be performed if the temperature of head assembly is higher than that of cylinder.

The diameter of the cells in this case however is about 500 μ on the average.

The cells formed are not spheres but something like prolate spheroids whose major axis being in the extrusion direction. The diameter of a cell is therefore defined as the one measured on the cross-section perpendicular to the major axis.

On the other hand fine cells of the diameter of less than 30 μ are obtained when the temperature of head assembly is kept at about 200°C and besides the cylinder temperature is kept higher than that. The result seems plausible because the cylinder length of the conventional extruder is not long enough, so that the homogeneity of mixing of propane and polyethylene entirely depends on the cylinder temperature which determines the diffusion length of propane into polyethylene. The resultant cell size is probably related to the temperature of the mixture when it is expanded. In principle, the higher the temperature, the larger the cell size becomes. So this may be partly a reason why larger cells are formed under the conditions corresponding to the state C shown in Table 1.

For the purpose of wire insulation the favorable state is obviously the state D. In the experiments with small extruder, however, another assumption may be quite possible to explain the discrepancy between cell sizes corresponding to the states C and D. In the foaming process corresponding to the state C something like microscopic bubbles or condensed spots of propane may still exist among molten polyethylene even at the time of expansion due to insufficient mixing. The larger cells may be originated from these bubbles.

Probably bubbles grow larger at the consumption of the propane dissolved in polyethylene. Therefore, the fact that the densities of the extrudates in both cases are different with each other seems to suggest that not all amount of propane dissolved or trapped in poly-

ethylene have exhausted at least in the foaming process corresponding to the state D. If this is the case and if the other conditions are the same, the resultant cell size, that is the expansion ratio, should increase with the concentration of dissolved propane in polyethylene. Similar conditions represented by the state C are also found in a few experiments with a 50mm extruder having a 24:1 L/D ratio.

The features of the results obtained with the 50mm extruder are fairly similar to those shown in Table 1. Figures 1 and 2 show the effect of the temperature of head assembly on the number and the size of the cells when the cylinder temperature is kept at 180°C. In these experiments a 0.5mm conductor was insulated at a wire speed of 400 m/min. The thickness of insulation wall was about 150 μ .

As shown in Figure 2 there is a tendency that the cell size increases towards the conductor at a lower temperature setting of the head assembly whereas at a higher setting the cell size becomes uniform throughout the insulation wall. The former case may be due to the same reason as the state C described already in connection with Table 1. The reason why the clear-cut tendency was not noticed in the preliminary experiments is that in Figure 2 the tendency near the surface is probably exaggerated by the use of a conductor while in Table 1 almost all the large cells are confined to the inner part where the conductor should occupy in an actual insulation.

Figure 3 shows cross-sections of typical extrudates from 25mm and 50mm extruders.

During the above-mentioned preliminary experiments it was found that the expansion usually caused a temperature drop of some ten degrees in the temperature of extrudate as compared with that of unexpanded extrudate. This adiabatic change taking place near the die may also be one of the essential phenomena not to be overlooked since the decrease of polyethylene temperature results in a rapid increase of the viscosity which hinders the growth of bubbles to be fixed at the final sizes. The temperature drop estimated by a tentative calculation is about 20°C if one assumes the number of cells in the noodle-like extrudate to be 2,000 mm⁻², the δ ($=C_p/C_v$) for propane to be 1.11, and the shape of the cell to be a sphere with a diameter of 20 μ .

Dissolution of propane

As was pointed out in the preceeding section, it appears that the concentration of propane in polyethylene together with the diffusion process plays an important role of the foaming mechanism.

Although propane was believed to be most suitable in many respects, methane and butane were also used in place of

propane in some preliminary experiments.

Figure 4 shows the change of viscosity of molten polyethylenes measured in terms of torque when they are pressurized with butane. Since the viscosity decreases rapidly as the temperature increases the measurement was carried out at 125°C to demonstrate the change very clearly. The difference of the viscosity between these two types of polyethylenes has connection with the fact that a high percentage expansion can be attained more easily with DFD-2005 than with DFD-6005.

Concentration of propane dissolved in molten polyethylene is a matter of great interest so long as one assumes that a cell continues to grow by diffusion of propane from the polyethylene into the cell.

If the pressure of propane obeys Henry's law, it is given by the following equation:

$$P_v = kC, \quad (1)$$

where P_v is the pressure of propane outside the surface of polyethylene, k is a constant and C is the concentration of propane just inside the surface of polyethylene. In order to estimate the constant k the pressure change of propane and polyethylene mixture kept in an autoclave was measured at high temperatures from 120°C to 170°C. The result is shown in Figure 5. The pressure of propane was calculated on the basis of the ideal gas law and the compressibility factor. The value of k is approximately of the order of $10^9 \sim 10^{10}$ (dynes/cm²)(mole/g.PE)⁻¹. In spite of an experimental error due to a condensation of small amount of propane in the pressure gauge and a tendency that the apparent k is slightly increased by the increasing temperature, the value of k thus determined seems to be adequate for our further discussion.

Additives

The number of cells to be formed in a insulation wall depends on various factors in a complicated way. The effects of a variety of materials have been examined by several researchers.^{1,2} Apart from the problem of bubble initiation the effect of certain kind of additive such as pigment usually used for the production of color coded cables needs to be examined from a practical point of view.

The types of pigments studied here and the compositions were listed in Table 2. Each pigment was admixed with the polyethylene prior to the extrusion. The experiments were carried out with the 25mm extruder. A 0.65mm die was used for a conductor of 0.4mm in diameter. The screw speed was in the range from 60 to 63 rpm, the wire speed was 73 m/min, and the cylinder temperature was about 240°C while the temperature of the head assem-

bly was set at 280°C. The pressure of propane in the hopper was adjusted to 15 Kg/cm² at room temperature.

The number and the average diameter of the cells in the insulation walls were measured. The results are illustrated in Figure 6. In general the number of cells decreases as the percentage by weight of pigment increases while the average diameter increases. The degree of the effect considerably depends on the kind of pigment. Among the pigments listed in Table 2 Peony Blue affected the foaming process most. It was not certain whether Peony Red had some effects on the foaming process or not. In each case the degree of expansion was constant within the experimental error and resulted in 30±5%.

It is known that some chemicals which are highly exothermal in their decomposition or rearrangement can create hot spots³ highly effective in initiating bubbles in molten polymer. In this case the number of bubbles initiated increases as the amount of chemical added increases in contrast to the case of insoluble materials such as pigments.

It is likely to assume that the number of bubbles may be decreased by a coalescence of two adjacent bubbles. When the wall of a bubble comes in touch with that of another they coalesce into a large bubble to minimize the surface energy.

If a bubble initiated by the pigment absorbs the neighboring bubbles that are to grow as individual bubbles when the pigment is not added, the resultant number of bubbles should decrease in proportion to the concentration of the pigment added. Furthermore, if the bubbles initiated by the pigment grow large enough to begin to coalesce with each other the relationship between the number of bubbles and the concentration of the pigment added will be changed to a great extent. Since the average distance between two adjacent bubbles is in inverse proportion to the cube root of the number of bubbles in a unit volume, a drastic change in the number of bubbles may be expected to take place at a rather lower concentration of pigment added, on the assumption that the pigment functions as nucleators of fairly large bubbles. Especially this seems to be the case with the Peony Blue.

Analysis of the foaming process

To obtain a desirable cell structure the understanding of the mechanism of the initiation and the growth of a bubble in the extrusion process is quite essential. Above all things the initial period of time after instantaneous release of pressure takes place near the die seems very important.

There are two fundamental steps invol-

ved in the formation of a bubble of visible size in molten polymer saturated with propane. The first is related to the formation of nucleus and the second is related to the growth of this nucleus to a macroscopic bubbles as a result of the decrease in external pressure.

The apparatus shown in Figure 7 was used to study the growth mechanism of a bubble under a simplified condition. There an assumption was made that the temperature in the polymer remained constant in the actual extrusion at least during an initial period of time after the expansion started. So that the experiments were carried out under an isothermal condition where the adiabatic temperature change mentioned before was completely ignored.

A specimen, 10mm X 5mm X 0.8mm, was placed in between two glass plates with a spacer, which were held in a pressure specimen cell having a round window. The specimen cell had a inner volume of 0.5cm X 3cm X 4cm and was connected with a release valve through an 3mm aperture. The oil bath which kept the temperature of the specimen cell constant also had a window through which the specimen cell could be illuminated from the bottom. Any change happened in the specimen could be recorded by the use of an ordinary camera or a high speed camera (HIMAC16M) combined with a photomicroscope.

The cell containing the specimen in it was initially evacuated through the aperture for about an hour at a high temperature and then a known pressure of propane was introduced into the specimen cell. In that case the thin copper pipe connecting the specimen cell with the pressure reservoir was kept at higher temperature to avoid a condensation of propane in it. The pressure and the temperature was kept constant for more than an hour to attain a equilibrium condition in the specimen cell and then the pressure was released by opening the release valve instantaneously. The pictures taken by the high speed camera were shown in Figure 8. In the experiment the temperature and the initial pressure were kept at 280°C and 20 Kg/cm² respectively. Any trace of bubbles were not found in the region within about 0.02cm from the boundary of the specimen. It is probably due to the diffusion of the dissolved propane out of boundary in a time of $2\sqrt{Dt}$, where D is the diffusion coefficient of propane in the molten polyethylene and t is the time period from the beginning of expansion till the end.

It is expected that the pressure inside the specimen cell is approximately given by

$$P = (P_0 - P_a) \exp(-\gamma t) + P_a, \quad (2)$$

where P is the pressure at time t, P₀ is

the initial pressure, P_a is the atmospheric pressure and γ is the characteristic constant which determines the rate of pressure release.

In Figure 9 the change of bubble diameter was plotted against time for two values of γ . The experimental conditions were exactly the same as in Figure 8. Since it was very difficult to determine the time when the pressure release began accurately the origin of the abscissa was chosen arbitrarily.

The value of γ was estimated by picking up the pressure change with a microphone placed against the release valve. For the experiment (B) in Figure 9 the pressure release continued approximately for 15 sec. and about in another 5 sec. bubbles were found to start growing. The value of γ in that case was assumed equal simply to the inverse of 15 sec. In actual extrusions γ must be very large.

Although the depth of focus of the microscope was deep enough to cover almost all the thickness of the specimen the bubbles appeared to come into the focus all of a sudden, in other words, any bubble having a diameter of less than 50 μ could not be detected by this technique.

The effect of the pigment added on the growth velocity of bubbles were also studied and the results were shown in Figure 10. The growth velocity of bubbles was calculated from the change of their diameters in the diameter range from 50 μ to 150 μ . The temperature of the specimen cell was kept at 200°C, the initial pressure of propane was 30 Kg/cm² and the low density polyethylene DFD-2005 was used in the experiments.

It is concluded from Figure 10 that the addition of Peony Red changes the growth velocity of bubbles very slightly whereas Peony Blue and Peony White to a considerable extent. Though the experimental error seems fairly large in the measured velocity the decrease in the rate of growth of a bubble probably means the decrease in the amount of propane around the bubble boundary due to an effect of neighboring bubbles.

Epstein and Plesset³ have treated the growth of a bubble in a liquid-gas solution. They have shown that the ultimate rate of growth is determined by the rate at which heat flows from the surrounding liquid into the bubble.

Here we assume similarly in our propane and polyethylene combination that the mass flow into the bubble per unit time is given by the following equation:

$$\frac{dm}{dt} = \frac{4}{3}\pi \frac{\partial}{\partial r}(R^3 c) = 4\pi R^2 D \left(\frac{\partial c}{\partial r}\right)_R, \quad (3)$$

where m is the mass of the propane in the bubble, c is the concentration, R is the radius of the bubble at time t, D is the diffusion coefficient of propane in molten

polyethylene saturated with propane, and $(\partial c / \partial r)_R$ is the concentration gradient at the bubble boundary. As the bubble grows the pressure within the bubble will decrease resulting in the concentration gradient at the bubble boundary. It causes an inward flow of propane molecules across the boundary, and so the bubble will continue to grow at an ever-increasing rate. In order to estimate the concentration gradient at the bubble boundary we assume that the concentration around the bubble remains C_0 at all times.

Then from a problem of heat conduction of a sphere⁴ it follows that

$$\left(\frac{\partial C}{\partial r}\right)_R = (C_0 - C) \left\{ \frac{1}{R} + \frac{1}{(\pi D t)^{1/2}} \right\}. \quad (4)$$

In reality the drop in concentration from C_0 to C takes place at the bubble boundary in a thin layer surrounding the bubble. If this approximation of a "thin boundary layer" is possible on the basis that D is sufficiently small, the rate of growth of the bubble is

$$\frac{dR}{dt} = \left\{ \frac{BTD}{kM} \left\{ \left(1 - \frac{P_a}{P_0}\right) (1 - e^{-\gamma t}) - \frac{2\sigma}{P_0 R} \right\} \left\{ \frac{1}{R} + \frac{1}{(\pi D t)^{1/2}} \right\} \right. \\ \left. + \frac{\gamma R}{3} \left(1 - \frac{P_a}{P_0}\right) e^{-\gamma t} \right\} \left[\left(1 - \frac{P_a}{P_0}\right) e^{-\gamma t} + \frac{P_a}{P_0} + \frac{4\sigma}{3P_0 R} \right]^{-1}, \quad (5)$$

where M is the molecular weight of propane, T is the temperature, B is the universal gas constant, and σ is the surface tension constant for the propane-polyethylene combination. It is also assumed that the pressure in the bubble, P_v , obeys ideal gas law and is determined by the concentration of propane just outside the boundary through Henry's law

$$P_v = kC, \quad (6)$$

where k is a constant. Integration of Equation (5) using a set of parameters in the following gives a curve which agrees very well with the lower curve in Figure 9. The parameters used are

$$\begin{aligned} \sigma &= 20 \text{ dynes/cm}^2 \\ k &= 10^3 \text{ (dynes/cm}^2\text{)(mole/g.PE)}^{-1} \\ P_0 &= 2.0 \times 10^7 \text{ dynes/cm}^2 \\ D &= 2.6 \times 10^{-3} \text{ cm}^2/\text{sec} \\ \gamma &= 1.43 \text{ sec}^{-1} \\ R &= 4.0 \times 10^{-3} \text{ cm at } t=0.8 \text{ sec.} \end{aligned}$$

More precisely a hydrodynamic equation concerning the flow of molten polyethylene at the bubble boundary should be taken into consideration. The resistance P_R to the flow arising from the viscosity η , for example, is given at the boundary by⁵

$$P_R = - \frac{4\eta}{R} \left(\frac{dR}{dt} \right), \quad (7)$$

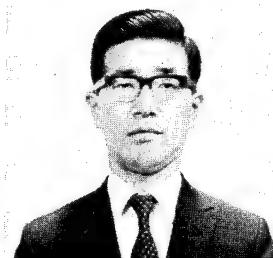
where η is the viscosity of molten polyethylene saturated with propane. The effect of viscosity plays, therefore, an important role near the bubble boundary.

The problem of nucleation in the foaming process in general is not completely

solved as yet. Though it is possible that in some cases the bubbles formed are the result of heterogeneous nucleation, we prefer to assume that the bubbles, when any additives are not used, are originated from nuclei comprising propane molecules.⁶ The size of the nuclei may be estimated from the fact that there is a critical pressure of approximately 15 Kg/cm² in the foaming process. If σ equals 20 dynes/cm² the radius of the nucleus is of the order of 2×10^{-6} cm.

References

- 1) R. H. Hansen, SPE Jour., **18**, 77 (1962).
- 2) R. H. Hansen and W. M. Martin, I&EC Product Research and Development, **3**, 137 (1964).
- 3) P. S. Epstein and M. S. Plesset, Jour. Chem. Phys., **18**, 1505 (1950).
- 4) See for example, H. S. Carslaw, Introduction to the Mathematical Theory of the Conduction of Heat in Solids (Dover Publications, New York 1945), P. 158.
- 5) F. Seitz, Phys. Fluids, **1**, 1 (1958).
- 6) C. W. Stewart, Jour. Polymer Sci., **A-8**, 937 (1970).



Yoshinori Kato
Electrical Communication Laboratory,
Nippon Telegraph & Telephone Public Corp.
Tokai, Ibaraki, Japan

Yoshinori Kato, the speaker, was born in Japan in 1933. He joined Electrical Communication Laboratory of Nippon Telegraph and Telephone Public Corporation in 1957. His early work included studies on properties and structures of high polymers. For several years he was concerned with the weathering studies of polymers. More recently, he turned to cable material research in connection with cable manufacturing. He received his Doctor of Science degree from Tokyo University in 1964.

Hiroshi Ohshima, the co-author, was born in Japan in 1941. After joining Electrical Communication Laboratory in 1965, he has been working on cellular polyethylene insulation. He received his Master of Science degree from Hokkaido University in 1965.

Table 1 The effect of extrusion parameters
obtained with 25 mm extruder

Temp. of cylinder °C	Temp. of head assembly °C	Pressure at head Kg/cm ²	Density gr/cc	Average diameter μ	State of cells
200	140	123	0.61	490	A
200	170	113	0.59	460	B
200	200	107	0.41	340	C
200	230	100	0.40	300	C
200	260	90	0.38	280	C
200	290	83	0.36	240	C
140	200	128	0.62	580	A
170	200	115	0.65	570	A
200	200	108	0.43	550	B
230	200	92	0.67	70	D
260	200	85	0.68	40	D
290	200	77	0.70	20	D

Table 2 The composition of pigments

Pigment	Composition	Per cent by weight
Peony Blue	Cyanin blue	3
	Ultra marin blue	94
	Titanium white	3
Peony Red	Cadmium red	75
	Watchung red	17
	Titanium white	5
Peony White	Titanium white	100

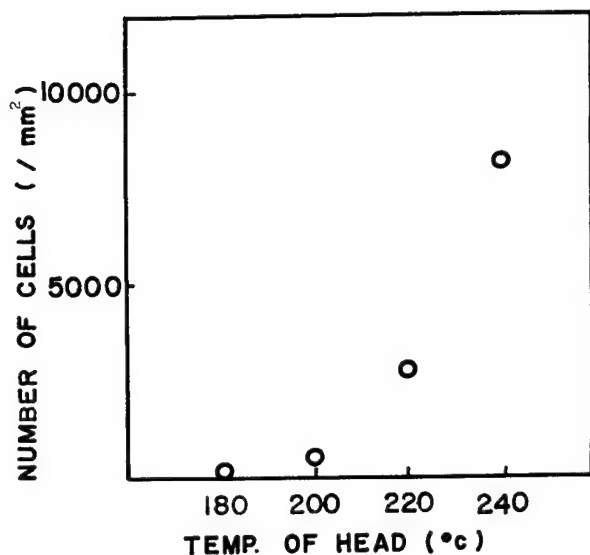


Figure 1. The effect of the temperature of head assembly on the foaming process with 50mm extruder. The cylinder temperature was kept at 180°C.

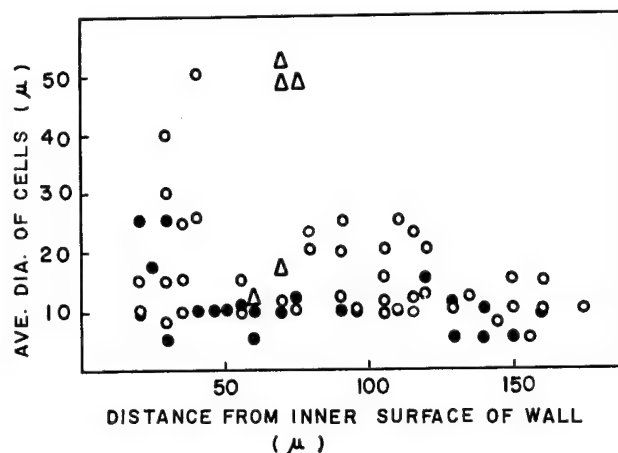


Figure 2. The distribution of cell size in insulation walls.

	Temperature of		
	cylinder	head	die (°C)
Δ	180	200	220
○	180	220	240
●	180	240	240

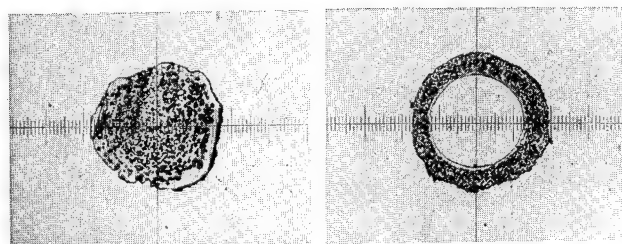


Figure 3. The cross-section of typical cells. The left picture was obtained with 25mm extruder, while the right with 50mm extruder.

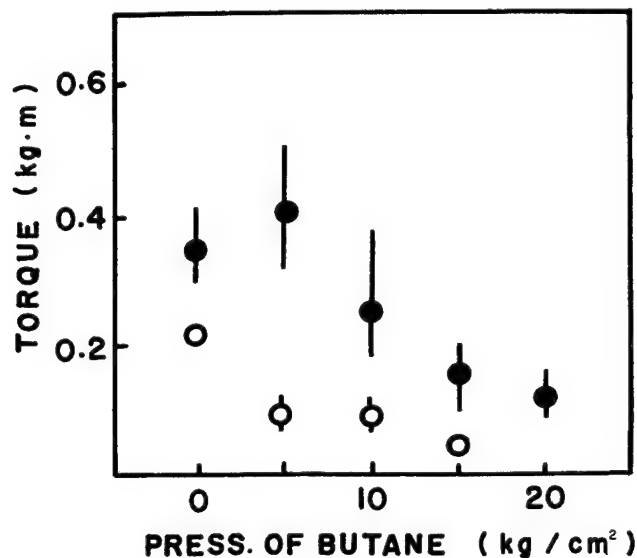


Figure 4. The change of viscosity of molten polyethylenes at 125°C with the pressure of butane.
 ○ DFD-2005 (M.I.=1.2)
 ● DFD-6005 (M.I.=0.25)

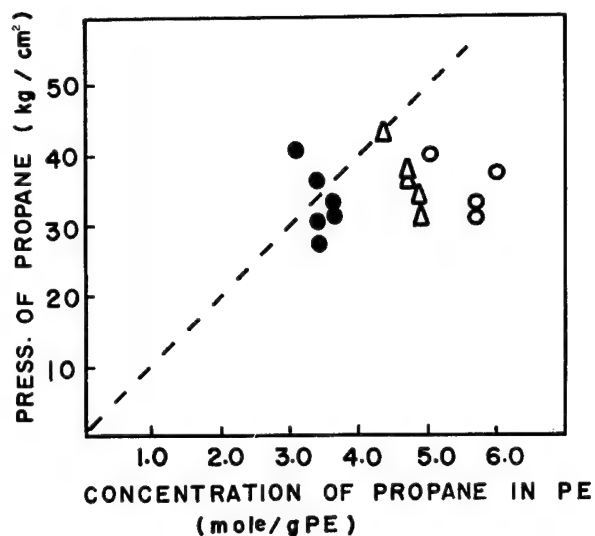


Figure 5. Concentration of propane dissolved in polyethylene.

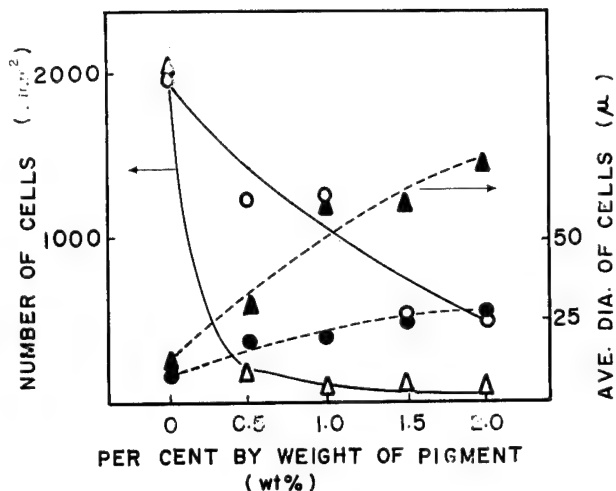
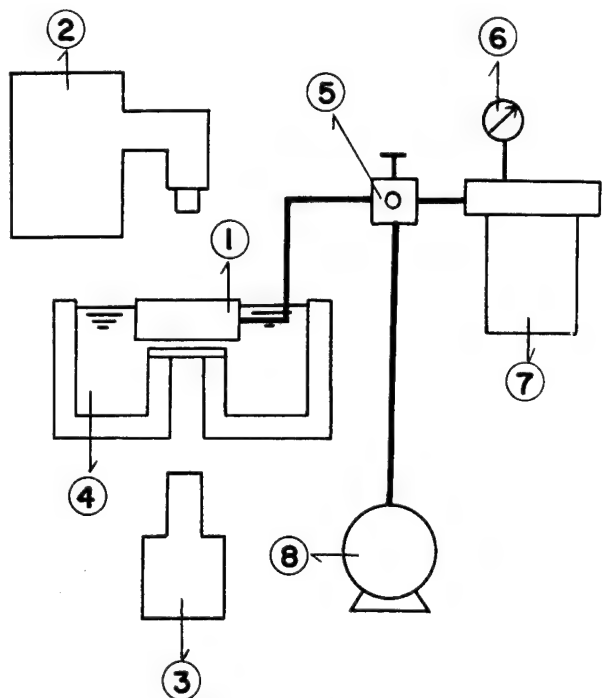
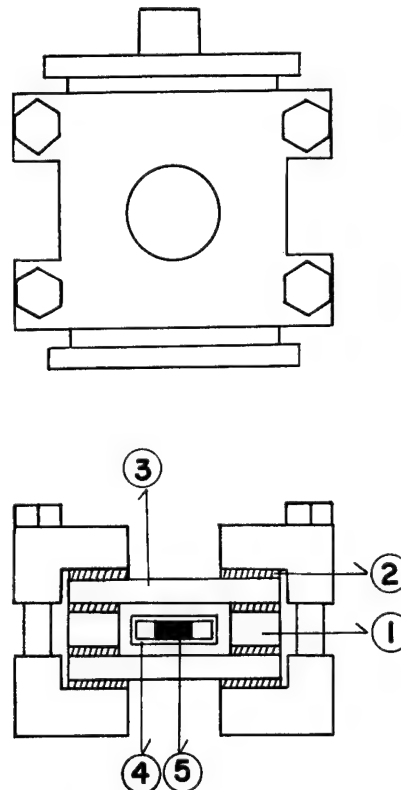


Figure 6 The effect of pigments added on the foaming process.
 ▲, ▲ Peony Blue
 ○, ● Peony White



The left:

- (1) Specimen cell
- (2) High speed camera and photomicroscope
- (3) High pressure mercury lamp
- (4) Oil bath
- (5) Release valve
- (6) Pressure gauge
- (7) Pressure reservoir
- (8) Vacuum pump



The right:

- (1) Spacer
- (2) Teflon packing
- (3) Pressure glass
- (4) Glass plate
- (5) Specimen (PE)

Figure 7. The apparatus for studying bubble growth with a high speed camera and a photomicroscope.

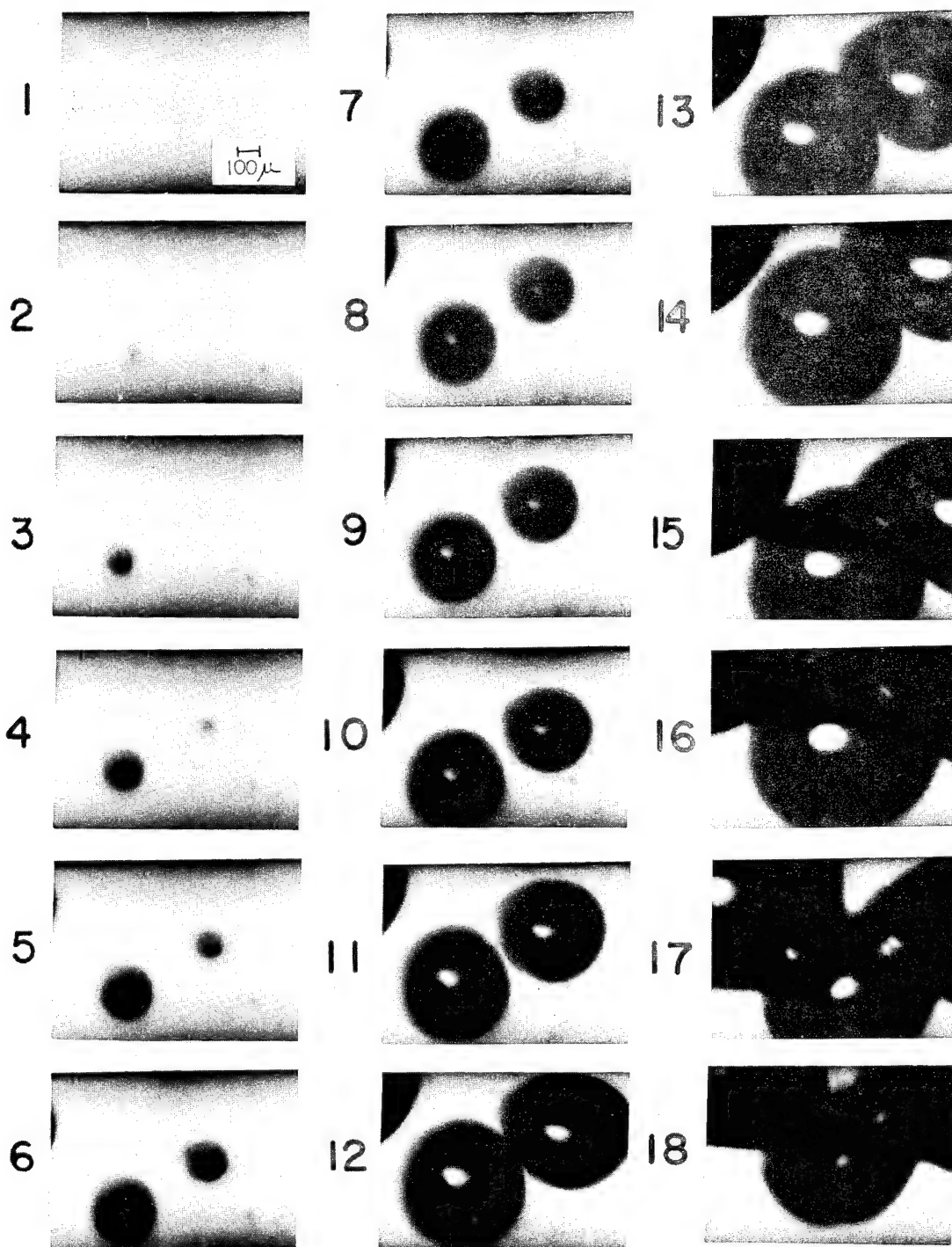


Figure 8. The growth of a bubble.
Time intervals between successive
pictures are 5 msec from 1 to 11
and 9 msec from 11 to 18.

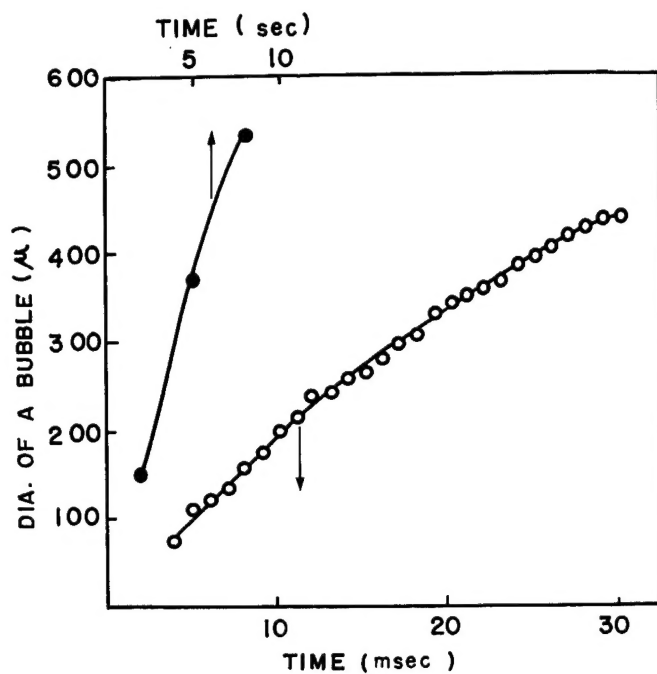


Figure 9. Change of bubble diameter. The temperature was kept at 280°C. The pressure was released from 20 Kg/cm² with $\gamma=1.43$ for the lower curve (experiment (A)) and $\gamma=0.0667$ for the upper (experiment (B)).

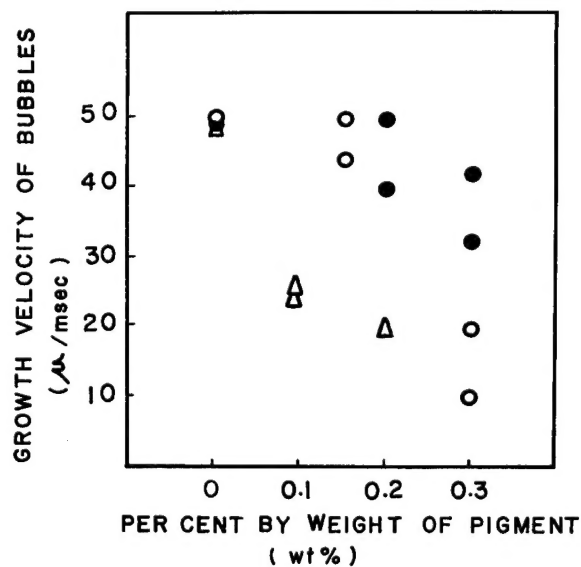


Figure 10. The effect of pigment added on the growth velocity of bubbles.

- Peony Blue
- Peony Red
- △ Peony White

SPONSORS FOR 19th INTERNATIONAL WIRE AND CABLE SYMPOSIUM

ADDISON DIVISION OF MUIRHEAD INC.
ALCAN CABLE
AMERICAN INSULATED WIRE CORP.
AMOCO CHEMICAL CORP. PLASTICS DIV.
AMP INCORPORATED
AMPHENOL CONNECTOR DIV.
ANACONDA WIRE AND CABLE CO.
ANDREW CORPORATION
ANSONIA WIRE & CABLE CO.
ARGUS CHEMICAL CORP.
ARVEY CORP. LAMCOTE DIV.
AVISUN CORPORATION

BELDEN CORPORATION
THE BENDIX CORP.
BOSTON INSULATED WIRE & CABLE CO.
BRAND REX DIV. AMERICAN ENKA CORP.
BURNDY CORP.
BURGESS PIGMENT COMPANY

CABLE CONSULTANTS CORP.
CABOT CORP.
CAMDEN WIRE CO., INC.
CANADA WIRE & CABLE CO. LTD.
CANADIAN INDUSTRIES LTD.
CANADIAN PACIFIC RAILWAY CO.
CARLEW CHEMICALS LTD.
CAROL CABLE COMPANY
R. E. CARROLL, INC.
CDI DISPERSIONS
CERRO WIRE & CABLE
CHASE & SONS, INC.
CHEMPLAST INC.
CIMCO WIRE & CABLE CO.
CHESTER CABLE OPERATIONS
COLEMAN CABLE & WIRE COMPANY
COLONIAL RUBBER WORKS INC.
COLUMBIA CABLE & ELECTRIC CORP.
COLUMBIAN DIV., CITIES SER. CO.
CONTINENTAL HATFIELD
COOKE COLOR DIV. REICHOOLD CHEMICAL, INC.
COPPERWELD STEEL COMPANY
CRESCENT INSULATED WIRE & CABLE CO.

DAVIS ELECTRIC COMPANY
DAVIS-STANDARD/GOULDING
PHELPS DODGE COMMUNICATIONS CO.
DIAMOND SHAMROCK CORP.
DOW CHEMICAL COMPANY
E. I. DUPONT DE NEMOURS & CO. FILM DEPARTMENT
DU PONT PLASTICS DEPARTMENT

EASTMAN CHEMICAL PRODUCTS, INC.
ECONOMY CABLE GRIP CO., INC.
ELCO CORPORATION
ENGELHARD MINERALS & CHEMICALS CORP.
ENTWISTLE COMPANY
ESSEX INTERNATIONAL INC.
EXTRUDO FILM CORP.

FIRESTONE PLASTICS COMPANY
FREEPORT KAOLIN CO.

GAVITT WIRE & CABLE DIVISION
GEM GRAVURE COMPANY INC.
GENERAL CABLE CORP.
G. E. COMPANY SILICONE PRODUCTS DIV.
GEORGIA MARBLE CO., CALCIUM PROD. DIV.
B. F. GOODRICH CHEMICAL COMPANY
W. R. GRACE & COMPANY
GULF OIL CORP.

HARDMAN INC.
HERCULES INC.
HEWLETT PACKARD CO. MFG. DIV.
HUDSON WIRE COMPANY

IBM CORP.
ICI AMERICA INC.
INTERNATIONAL WIRE PRODUCTS DIV.
ITT SURPRENANT DIV.

KENRICH PETROCHEMICALS INC.
KERITE COMPANY

LENZ ELECTRIC MFG. CO.
LOWE ASSOCIATES, J. J. INC.
TAPES & REELS DIVISION

MINNESOTA PAINTS INC.
MINNESOTA MINING & MFG. CO.
MONSANTO CO. H & P DIVISION
MONTGOMERY CO.
SAMUEL MOORE & CO.

NATIONAL LEAD CO.
NATVAR CORPORATION
NONOTUCK MANUFACTURING CO.
NORTHEAST WIRE COMPANY INC.
NORTHERN ELECTRIC CO. LTD.

P. F. & D. PLASTICS CO., INC.
PANTASOTE COMPANY OF NEW YORK INC.
PENNWALT CORP.
PETRO-TEX CHEMICAL CO.
PHALO CORP.
PHELPS DODGE COPPER PRODUCTS CO.
PHILA. INSULATED WIRE CO.
PHILLIPS CABLES LTD.
PHILLIPS PETROLEUM CO.
PLASTIC WIRE & CABLE CORP.
PLASTOID CORP.
PLYMOUTH RUBBER COMPANY INC.
PRODEX DIV. OF KOEHRING CO.

RAYBESTOS-MANHATTAN INC.
RAYCHEM CORP.
REICHOLD CHEMICALS INC.
REVERE ELECTRONICS DIV.
NEPTUNE METER CO.
ROCHESTER CORPORATION
JOHN ROYLE & SONS

SCHLICHTER PRODUCTS CO.
SINCLAIR-KOPPERS CO.
SOLAR COMPOUNDS CORP.
SOUTHWEST CHEMICAL & PLASTICS CO.
SOUTHWIRE CO.
STROMBERG-CARLSON CORP.
SUN CHEMICAL CORP. FACILE DIV.

SUPERIOR CONTINENTAL DIVISION
SYNCRO MACHINE CO.

TEKNOR APEX CO.
TENNECO CHEMICALS INC.
TEXAS INSTRUMENTS INC.
TIMES WIRE & CABLE CO.

UNION CARBIDE CANDA LTD
UNION CARBIDE CORP.
UNIROYAL CHEMICAL
U. S. INDUSTRIAL CHEMICAL

R. T. VANDERBILT CO., INC.
VICTOR ELECTRIC WIRE & CABLE CORP.
VIDEX EQUIPMENT CORP.
THE WALLINGFORD STEEL CO.
WARDWELL BRAIDING MACHINE CO.
WARE CHEMICAL CORP.
WATSON MACHINE CO.
WESTERN ELECTRIC CO.
WESTERN UNION TELEGRAPH CO.
WHITMOR WIRE & CABLE CORP.
WHITNEY BLAKE COMPANY
WILSON PRODUCTS COMPANY
WIRE & TEXTILE MACHINERY CORP.
WYRE WYND INC.
WYROUGH & LOSER INCORPORATED

